TOPSOIL AND SUBSOIL PHOSPHORUS DYNAMICS:

EVIDENCE FROM LONG-TERM EXPERIMENTS

SAMANTHA DOLAN

BSc (Hons) Environmental Chemistry

Thesis submitted to the University of Nottingham

for the degree of Doctor of Philosophy

SEPTEMBER 2018

Abstract

Phosphate rock is the main source of phosphorus (P) in agricultural fertilisers; global stocks are finite and are required for future food security. Long-term use of P fertilisers results in the accumulation of residual P in agricultural soils and utilising these resources will improve sustainability of P use and may lead to environmental benefits. Subsoil P reserves may be an important source of plant-available P however current fertiliser recommendations are based on topsoil P only. Therefore, the aim of this project was to understand topsoil and subsoil P dynamics in long-term experiments and the factors influencing the accumulation (Chapter 3), plant-availability (Chapter 4), solubility (Chapter 5), lability (Chapter 6) and cycling and transfer (Chapter 7) of phosphate in soil. To this end, two long-term field experiments managed by Scotland's Rural College in Craibstone, Aberdeenshire, were utilised. The 'Old Rotation', established in 1922, has a series of plots subject to different NPK fertiliser strategies and the 'pH Rotation', established in 1961, consists of plots in which soil pH is controlled to cover the range 4.5 to 7.5, in increments of 0.5 pH units. Topsoils (0 to 20 cm) and subsoils (20 to 40 cm) were collected in February 2015 post-harvest and prior to tillage and fertiliser application. The effects of soil pH control, fertiliser management strategy and cropping on P dynamics were investigated.

A total element analysis of P (P_{Total}) and associated fertiliser contaminants arsenic (As), cadmium (Cd) and uranium (U) by inductively coupled plasma- mass spectrometry (ICP-MS) in topsoils and subsoils was performed. There were positive correlations between P and As, Cd and U in the topsoils and subsoils which suggested a link between P fertiliser use and increased contaminant levels. In the Old Rotation, subsoils contained higher levels of P_{Total} in plots treated with nitrogen (N) and potassium (K) fertilisers with triple superphosphate (TSP) or ground mineral phosphate (GMP) compared to plots in which no P fertiliser was added and compared to the uncultivated grassland surrounding the trials (Field). Overall, P_{Total} in the topsoils and subsoils of plots in the Old Rotation were depleted relative to the native P_{Total} in the Field which suggested long-term cropping had driven crops to utilise native P_{Total} reserves throughout the profile. The use of TSP or GMP fertilisers reduced the severity of P_{Total} depletion throughout the soil profile compared to restricting P fertilisers. In the pH Rotation, the use of lime to maintain target pH values in the plots resulted in uniform pH profiles in the topsoil and subsoil across the pH gradient. At pH 4.5, topsoil P_{Total} was 1.84x the subsoil compared to 1.40x at pH 6 which suggested P was strongly retained in the topsoil due to adsorption on iron (Fe) and aluminium (Al) oxides at acid pH and was transferred more readily to the subsoil at pH 6 were P is most soluble. Topsoil and subsoil P_{Total}

converged at pH 6 indicating enhanced leaching of P with increasing solubility. The P_{Total} in the pH Rotation topsoils were significantly elevated compared to the Field but subsoils were not. The average net annual P_{Total} accumulation rate in the soil profile, relative to the Field, was 0.86 to 51.5 kg ha^{-1} yr^{-1} although there was no trend with soil pH. The P_{Total} was declining in the Old Rotation at rates between -0.9 to -22.2 kg ha^{-1} yr^{-1} depending on fertiliser management strategy.

The extraction of 'plant-available P' using the Olsen (P_{Olsen}) and Modified Morgan ($P_{MMorgan}$) methods revealed that $P_{MMorgan}$ underestimated P_{Olsen} by 77% (topsoil) and 71% (subsoil). As a fraction of the P_{Total}, P_{Olsen} was 2.53% (topsoil) and 1.84% (subsoil) and $P_{MMorgan}$ was 0.60% (topsoil) and 0.59% (subsoil). In the Old Rotation, topsoil P_{Olsen} was greater than the Field when TSP was used but was depleted under GMP or when P was restricted. Topsoil $P_{MMorgan}$ was greater than the Field when both TSP and GMP were applied. Topsoil P_{Olsen} ranged from 10.2 to 34.2 mg kg^{-1} whereas subsoil P_{Olsen} was approximately half, between 5.90 and 17.4 mg kg^{-1}. In contrast, $P_{MMorgan}$ in the topsoils (3.52 to 7.49 mg kg^{-1}) and subsoils (2.82 and 4.96 mg kg^{-1}) were almost uniform. Subsoil P_{Olsen} was depleted compared to the Field except under TSP where P_{Olsen} was maintained. The $P_{MMorgan}$ in subsoils was elevated compared to the Field when TSP and GMP was applied. When P fertilisers were restricted, P_{Olsen} and $P_{MMorgan}$ in subsoils were depleted which suggest that the crops in rotation had accessed native plant-available P. In the pH Rotation, topsoil P_{Olsen} ranged from 36.4 to 74.5 mg kg^{-1} and subsoil P_{Olsen} ranged from 21.7 to 35.2 mg kg^{-1}. Levels of $P_{MMorgan}$ in the topsoil ranged from 8.73 to 17.1 mg kg^{-1} (topsoils) and 7.03 to 10.2 mg kg^{-1} (subsoils). Fertiliser recommendations would class the P_{Olsen} and $P_{MMorgan}$ in these topsoils (and subsoils) at least optimal (P_{Olsen} Index 2A/B and $P_{MMorgan}$ M) for crop requirements which reveals that these subsoils contain significant levels of plant-available P. The availability of topsoil P was greatest at pH 4.5 and 7.5 and least at pH 6.0. Convergence of topsoil and subsoil P_{Olsen} and $P_{MMorgan}$ at pH 6.0 suggested enhanced leaching due to maximum Ca-phosphate solubility.

Solubility controls were assessed by plotting phosphate potential against lime potential following the resolution of Ca^{2+} and HPO_4^{2-} free ion activities using the Windermere Humic Aqueous Model-VII (WHAM-VII). Comparison of data with equilibrium relations for pure Ca phosphate minerals confirmed that P solubility in topsoils and subsoils plots with a soil pH ≥ 6 was controlled by the relatively insoluble mineral hydroxyapatite (HA). Below pH 5.5, P solubility was likely controlled by strong adsorption to Fe and Al oxide surfaces and plots were under-saturated with respect to HA.

The lability of P was investigated using the Diffusive-Gradients in Thin-Films (DGT) Technique (P_{DGT}). The equilibrium distribution coefficients (K_d) were calculated using P_{DGT} (denominator; mg L^{-1}) and either P_{Olsen} or $P_{MMorgan}$ (numerator; mg kg^{-1}) as estimates of the solid-phase P concentration. The R_{DGT} was calculated using the (dimensionless) ratio of P_{DGT} to the solution P concentration measured by ICP-MS ($P_{Soln-ICP}$). In the pH Rotation, P_{DGT} increased linearly in both the topsoil (70.4 to 108 µg L^{-1}) and subsoil (15.1 to 69.3 µg L^{-1}) with pH. Values of K_d were greater in the subsoil than the topsoil by a factor of 1.07 at pH 7.5, 2.10 at pH 6.5 and 1.21 at pH 4.5 for P_{Olsen}, and by a factor of 1.01 at pH 7.5, 1.82 at pH 6.5 and 2.72 at pH 4.5 for $P_{MMorgan}$ likely due to low concentrations of subsoil P which would be distributed over stronger adsorption sites compared to the topsoil where P would be adsorbed to both weak and strong adsorption sites. The decrease in K_d in both layers between pH 4.5 to 7.5 suggested that (i) P was more strongly adsorbed < pH 5.5 and (ii) the ability of the soil to supply labile P to the soil solution increased with soil pH. The R_{DGT} increased with rising pH in the topsoils (0.324 to 0.549) and subsoils (0.221 to 0.549), confirming that faster resupply occurs at higher pH values. In the Old Rotation, P_{DGT} was elevated in the topsoil when TSP was used (62.2 µg L^{-1}) compared to the Field (48.9 µg L^{-1}) but all other fertiliser treatments in topsoils and subsoils were depleted compared to the Field. The R_{DGT} was greatest in the topsoil of the TSP plot (0.420) compared to GMP (0.299) or the Field (0.335). All subsoils had R_{DGT} lower than the Field subsoil (0.403) with the lowest when P fertiliser was restricted (0.241).

The analysis of stable oxygen isotope ratios (^{18}O:^{16}O) in HCl-extractable phosphate ($\delta^{18}O_P$) showed that topsoils and subsoils across both rotations had $\delta^{18}O_P$ values constrained between 18.1$^0/_{00}$ and 23.0$^0/_{00}$. The isotopic enrichment of duplicate HCl extractions with ^{18}O-enriched spike water revealed minimal incorporation of oxygen from organic sources across the dataset (< 2$^0/_{00}$). Insoluble GMP fertiliser (21.2$^0/_{00}$) persisted in topsoils and was more highly processed towards the soil pore water equilibrium ($\delta^{18}O_W$) range (15.0 to 18.0$^0/_{00}$) before migrating to the subsoil. By contrast, TSP fertiliser (23.9$^0/_{00}$) was rapidly adsorbed to Fe and Al oxides in the topsoil and was slightly processed before leaching to the subsoil. Biological cycling continues in the subsoil. In the pH Rotation, rapid adsorption of TSP in the topsoil was evident at pH 4.5, as was rapid leaching of fresh fertiliser P to the subsoil, as $\delta^{18}O_P$ values (23.0 and 22.5$^0/_{00}$ respectively) were close to the TSP $\delta^{18}O_P$. Uniform topsoil and subsoil $\delta^{18}O_P$ signatures close to soil pore water equilibrium between pH 6.0 and 7.0 suggested maximum P solubility and processing. At pH 7.0 the $\delta^{18}O_P$ of the topsoil (19.3$^0/_{00}$) and subsoil (19.9$^0/_{00}$) $\delta^{18}O_P$ were nearly identical.

The main conclusions of this thesis, based on the evidence described above, is summarised below. Topsoil and subsoil P_{Total}, P_{Olsen} and $P_{MMorgan}$ in the pH Rotation were elevated compared to the (uncultivated) Field across the pH range, with the greatest accumulation at pH 4.5 and least at pH 6.0 where concentrations in topsoils converged with those in the subsoils. A soil pH of 6.0 is optimum for most arable crops and so indicate subsoils may become enriched with fertiliser P due to greater solubility in the topsoil. The fertiliser classifications of 2A/B or M for P_{Olsen} and $P_{MMorgan}$ respectively show the subsoil to contain significant concentrations of plant-available P. However, P_{DGT} and R_{DGT} increased with rising pH as K_d decreased which suggests available-P cannot be considered as a homogeneous fraction and is strongly retained at pH < 5.5 and is more soluble and labile at pH > 6. This highlights the weakness of traditional extraction techniques to assess plant-availability as they do not provide information on desorption kinetics. The underlying mineralogy which controlled P solubility in the experiments were hydroxyapatite at pH > 6 and adsorption to Fe and Al oxides at pH < 5.5. The adsorption of P to Fe and Al oxides pH < 5.5 renders phosphate unavailable for biological processing however there was evidence of rapid redistribution of fertiliser P to the subsoils, effectively by-passing topsoil biological cycling, as evidenced by uniform soil profile $\delta^{18}O_P$ values at pH 4.5 which were close to the $\delta^{18}O_P$ value for TSP. As the pH rises, P becomes more soluble and is thus more likely to be biologically processed before leaching to the subsoil – determined by the extent to which $\delta^{18}O_P$ values had moved towards soil pore water equilibrium (from the original fertiliser values). In the Old Rotation, topsoil and subsoil P_{Total} and P_{Olsen} were lower than in the uncultivated Field when P fertilisers were restricted showing that crops in rotation had utilised subsoil reserves. The TSP maintained P_{Olsen} and $P_{MMorgan}$ levels in the soil profile whereas GMP maintained only the $P_{MMorgan}$. Both TSP and GMP underwent some biological cycling in the topsoil before leaching to the subsoil layers. Finally, elevated As, Cd and U was associated with P fertiliser use, but the levels of contaminants are not concerning as they are below permissible limits according to regulations regarding the application of contaminants via sewage sludge to agricultural land.

Acknowledgements

I would like to thank my supervisors Scott Young, Robin Walker, Martin Broadley, Christine Watson, Anthony Edwards and Neil Crout for their advice, feedback, help and support throughout the PhD.

Thanks to the University of Nottingham and Scotland's Rural College for co-funding the PhD studentship and providing the training, facilities and field-trials necessary to complete this work.

At the University of Nottingham, thanks to Emma Hooley and Sarah Gamba for admin support and to John Corrie, Saúl Vázquez Reina, Laura Holt and Dongfang Li for laboratory support. Thanks to Jim Craigon for advice on statistics and to Rory Hayden for field work support.

At Scotland's Rural College, I would like to thank Audrey Johnstone, Mark Hocart and Fiona Burnett for help and support. Thanks also to Derek Simpson, James Simpson and Michael Coutts at the Aberdeen campus for ongoing field-work support. I would also like to acknowledge the staff past and present who have supported and maintained the long-term experiments at Craibstone over the past c.100 years. The Scottish Government's Rural and Environment Science and Analytical Services Division (RESAS) is acknowledged for providing funding to support the trials.

At Lancaster University, thanks to Hao Zhang, Shane Rothwell, Daniel Menezes-Blackburn and Hannah Wright for advice, training and ongoing support with the Diffusive Gradients in Thin-Films technique.

For the stable oxygen isotopes in soil phosphate work, I would like to thank Andrew Smith and Angela Lamb for support and collaboration throughout. Thanks to everyone at the NERC Isotope Geosciences Laboratory at the British Geological Survey (Keyworth) for laboratory support and the NERC Isotope Geosciences Facilities Steering Committee for funding the isotopic analysis (IP-1700-1116). I am also grateful to Verena Pfahler and Steve Granger at Rothamsted Research (North Wyke) for help and advice on the method.

Finally, I would like to thank my husband Iain for his unconditional support throughout the PhD.

Table of Contents

Abstract I
Acknowledgements V
Table of Contents VI
Table of Tables IX
Table of Figures XII
1 Introduction 1
1.1 Phosphorus and Global Food Security 1
1.2 Phosphorus Dynamics in Soil 2
1.3 Subsoil Phosphorus Research and Long-Term Experiments 4
1.4 Methods to Investigate Phosphorus Dynamics 6
1.4.1 Estimating 'plant-available P' in the Soil 6
1.4.2 Geochemical Modelling of Phosphate Solubility in Soils 7
1.4.3 Labile P and The Diffusive Gradients in Thin-Films Technique 8
1.4.4 Investigating P Cycling and Transfer Mechanisms using the Stable Oxygen Isotope Ratios in Soil Phosphate 9
1.5 Thesis Aim and Objectives 10
2 Materials and Methods 12
2.1 Sample Site and Trial Descriptions – The Woodland's Field Rotations 12
2.1.1 Trial Management 14
2.2 Soil Sampling and Preparation 17
2.3 Crop Sampling and Preparation 20
2.4 Soil pH 20
2.5 Total Soil Carbon (%) and Nitrogen (%) Content 20
2.6 Total Elemental Analysis by ICP-MS 21
2.6.1 Acid Digestion of Soil Samples 21
2.6.2 Acid Digestion of Crop Samples 21
2.6.3 Multi-Element Analysis by ICP-MS 21
2.7 Phosphate Extractions 22
2.7.1 Olsen P 22
2.7.2 Modified Morgan P 22
2.7.3 Colorimetric Determination 23
2.8 Statistical Analysis 24
2.8.1 Dendrogram Cluster Analysis and Pearson Correlation Coefficient Matrices 24
2.8.2 Analysis of Variance 24
2.8.3 Polynomial Regression Analysis of Soil Properties in the pH Rotation experiment 24
2.9 Plot P Balance Calculations 25
2.9.1 Crop P Calculations 25
2.9.2 Plot P Balance and Annual Accumulation Rates 25
3 Topsoil and Subsoil Audit of Phosphorus and Associated Elements in the Woodland's Field Long-Term Experiments 26
3.1 Abstract 26
3.2 Introduction 27
3.2.1 Aims and Objectives 30
3.3 Materials and Methods 31
3.4 Results and Discussion 32
3.4.1 Background Soil Characteristics of Woodland's Field 32
3.4.2 Topsoil and Subsoil Dendrogram Cluster Analyses of Soil Characteristics in the Long-Term Experiments 34
3.4.3 Woodland's Field Old Rotation 39
3.4.4 Woodland's Field pH Rotation 52
3.5 Conclusions 70
4 Topsoil and Subsoil Olsen and Modified Morgan P as Affected by Soil pH and Fertiliser Management in Long-term Experiments 73
4.1 Abstract 73
4.2 Introduction 75
4.2.1 Aims and Objectives 77
4.3 Materials and Methods 78
4.3.1 Sample Site, Trial Description, Soil Sampling, Preparation and Analysis 78
4.4 Results and Discussion 79
4.4.1 Comparison of Extractable P Between the Two Soil P Tests 79

4.4.2 Relationships Between Topsoil and Subsoil Forms of P 81
4.4.3 Effect of Soil pH Management on Topsoil and Subsoil P in the pH Rotation 83
4.4.4 Effect of Crop Rotation on P_{Olsen} and $P_{MMorgan}$ in the Topsoil and Subsoil across the pH gradient of the pH Rotation 88
4.4.5 Effect of Fertiliser Management on the Relationship Between P_{Total} and Extractable-P in the Old Rotation 91
4.4.6 Effect of Crop Rotation on Topsoil and Subsoil P_{Olsen} and $P_{MMorgan}$ across Fertiliser Treatments in the Old Rotation 94
4.4.7 Classifying the Soil P Test Results in the Long-Term Experiments 96
4.5 Conclusions 101
5 Geochemical Modelling of Phosphate Solubility in the Woodland's Rotations using WHAM-VII 104
5.1 Abstract 104
5.2 Introduction 105
5.2.1 Aims and Objectives 107
5.3 Materials and Methods 108
5.3.1 Sample Site, Trial Description, Sample Selection and Preparation 108
5.3.2 Soil ⇌ Solution Equilibration 108
5.3.3 Geochemical Modelling of Phosphate Solubility using WHAM-VII 109
5.4 Results and Discussion 111
5.4.1 Measurement of Soil Solution P (P_{Soln}) 111
5.4.2 Effect of Fertiliser Management and Crop Phase on Soil Solution P 115
5.4.3 Measured vs Target Soil pH in the pH Rotation 117
5.4.4 Effect of Crop and Soil pH on Soil Solution P Concentration in the pH Rotation 119
5.4.5 Topsoil: Subsoil Ratios of P_{Soln} in the pH Rotation 122
5.4.6 Solubility Phase Analysis for the pH Rotation 123
5.4.7 Solubility Phase Analysis of the Old Rotation 129
5.5 Conclusions 132
6 Assessing Labile Soil Phosphorus Using the 'Diffusive-Gradients in Thin-Films' Technique 133
6.1 Abstract 133
6.2 Introduction 134
6.2.1 Aims and Objectives 138
6.3 Materials and Methods 139
6.3.1 Sample Site, Trial Description, Sample Selection and Preparation 139
6.3.2 Diffusive Gradients in Thin-Films Technique 139
6.3.3 Calculating the Concentration of Phosphate-P Measured by DGT (P_{DGT}) 142
6.3.4 Equilibrium Distribution Coefficient Between Solid and Solution phases (K_d) 142
6.3.5 Buffering Capacity (R_{DGT}) 143
6.4 Results and Discussion 144
6.4.1 Repeatability of the DGT Deployment 144
6.4.2 Relationships Between P_{DGT}, P_{Total} and Soil P Extractions 145
6.4.3 Relationship Between Topsoil and Subsoil P_{DGT} 149
6.4.4 Relationship Between P_{DGT} and Soil Solution P 150
6.4.5 Effect of Soil pH Management on P_{DGT} in the pH Rotation 152
6.4.6 Effect of Soil pH on the Equilibrium Distribution Coefficient (K_d) in the pH Rotation 154
6.4.7 Effect of Fertiliser Management on P_{DGT} in the Old Rotation 159
6.4.8 Effect of Fertiliser Management on the Equilibrium Distribution Coefficient (K_d) in the Old Rotation 160
6.4.9 Effect of Fertiliser Management on the Ratio (R_{DGT}) of P_{DGT} to P_{Soln} 163
6.5 Conclusions 165
7 Topsoil and Subsoil $\delta^{18}O_P$ Signatures Following Historical P Fertiliser Use and pH Control 167
7.1 Abstract 167
7.2 Introduction 168
7.2.1 Aim and Objectives 172
7.3 Materials and Methods 173
7.3.1 Sample Site, Trial Descriptions, Sample Selection and Preparation 173
7.3.2 Rainfall, Soil Pore Water and Soil Temperature Sampling and Processing 174
7.3.3 Soil Pore Water Extraction 175
7.3.4 Experimental Procedure for Soil Phosphate Extraction, Purification and Analysis 175
7.3.5 Mass Spectrometry Analysis 180
7.3.6 Calculating Extent of Organic-P Hydrolysis and ^{18}O Incorporation in to Soil Phosphate 182
7.3.7 Calculating % of phosphate *not* exchanged during hydrolysis and O:P ratios 182
7.3.8 Calculating theoretical soil pore water equilibrium 183
7.4 Results and Discussion 184

7.4.1 Pilot Study results 184
7.4.2 Rain and Soil Pore Eater Analysis results for Woodland's Field Rxperimental Site 190
7.4.3 Comparing Equations to Calculate Soil Pore Water Equilibrium $\delta^{18}O_P$ Ranges 193
7.4.4 Oxygen Yields from Standards and Soil Sample Ag_3PO_4 Precipitates 198
7.4.5 The HCl-Extractable P (P_{HCl}) in the Long-Term Experiments 201
7.4.6 Topsoil and Subsoil $\delta^{18}O_P$ in the Long-Term Experiments 208
7.5 Conclusions 225
8 Conclusions 227
9 References 233
10 Appendices 244
Appendix 1 – Pearson Correlation Coefficient Matrices 244
Appendix 2 – Plot P_{Total} Balances and Net Annual Accumulation Rates 248
Appendix 3 – Analysis of Variance Tables 252
Appendix 4 – pH Rotation Polynomial Regression Models and Predictions 256

Table of Tables

Table 2.1. Woodland's Old Rotation fertiliser application rates (1991 – present). The values in parentheses indicate application rates expressed as kg ha^{-1} of P_2O_5 or K_2O. 16

Table 2.2. Woodland's pH Rotation fertiliser application rates (1991 – present). The values in parenthesis indicate application rates expressed as kg ha^{-1} of P_2O_5 or K_2O. 16

Table 2.3. Woodland's Old Rotation fertiliser application rates (1922 – 1991). The values in parenthesis indicate application rates expressed as kg ha^{-1} of P_2O_5 or K_2O. 16

Table 3.1. Selected topsoil and subsoil properties of the uncultivated Woodland's Field grassland area. Values are the average of 9 representative sample auger borings collected from the field, with ± SEM. 33

Table 3.2. Annual P Balance and Net Annual Accumulation Rates in the Old Rotation. No available data is indicated by the symbol (-). 46

Table 3.3. Topsoil P_{Total} (mg kg^{-1}) differences between crops in the pH Rotation topsoil for each target pH. 59

Table 3.4. Topsoil P_{Total} (kg ha^{-1}) differences between crops in the pH Rotation topsoil for each target pH. 59

Table 3.5. Annual P Balance and Net Annual Accumulation Rates in the pH Rotation. 63

Table 4.1. Soil P concentration (mg kg^{-1}) ranges for P_{Olsen} and $P_{MMorgan}$ and the classification systems used. 75

Table 4.2. Mean concentrations of P_{Olsen} and $P_{MMorgan}$ (mg kg^{-1}) in the pH plot topsoils and subsoils of 5 crop phases ± SEM. Soils were classified according to the mean. The P_{Olsen} was assigned a P Index (AHDB, 2017) and the $P_{MMorgan}$ a SAC Status (Sinclair, *et al*., 2013). 98

Table 4.3. Mean concentrations of P_{Olsen} and $P_{MMorgan}$ (mg kg^{-1}) in the topsoil and subsoil for each fertiliser treatment of 5 crop phases ± SEM. The soils were classified according to the mean. The P_{Olsen} was assigned a P Index (AHDB, 2017) and the $P_{MMorgan}$ a SAC Status (Sinclair, *et al*., 2013). 100

Table 5.1. Equilibrium reactions and formation constants (log K^o) for calcium phosphates at 25°C (Lindsay, 1979). 110

Table 7.1. Summary of the sub-group of soil samples in the pilot study. The topsoil and subsoil of one out of three augers per plot were selected and processed and samples were chosen to reflect a range of treatments and P_{Total} concentrations. In addition, one sub-sample of GMP and TSP fertilisers were processed. 174

Table 7.2. Summary of the pilot study results for samples for which enough Ag_3PO_4 was produced for analysis and the data was considered reliable. 188

Table 7.3. Summary of the pilot study results for samples for which the purification stage and precipitate of Ag_3PO_4 was considered unsuccessful and results unreliable. Samples marked * must be treated with caution because only one result was produced from the paired HCl extractions. 188

Table 7.4. Comparison of the pilot study vs main study $\delta^{18}O_P$ values and the ratio between the studies. The pilot study result was of one individual sample; the main study result was the mean of three samples collected per treatment. 189

Table 7.5. Summary of results for the 2017 rainfall and soil pore water analysis for topsoils and subsoils. 190

Table 7.6. Topsoil $\delta^{18}O_P$ equilibrium calculations: Summary of the monthly topsoil pore water $\delta^{18}O_W$ values, the soil temperatures at 10 cm depth (Av, Max Min), the $\delta^{18}O_P$ calculated by both L&N (1973) and C&B (2015) equations for each month using the temperature data. The ratio of the two equations is presented and the difference (multiplied by -1) is also summarised. The average and standard deviation $\delta^{18}O_P$ with the upper and lower limits (average ± 1 SD) of the monthly results combined are shown..... 195

Table 7.7. Subsoil $\delta^{18}O_P$ equilibrium calculations: Summary of the monthly subsoil pore water $\delta^{18}O_W$ values, the soil temperatures at 30 cm depth (Av, Max Min), the $\delta^{18}O_P$ calculated by both L&N (1973) and C&B (2015) equations for each month using the temperature data. The ratio of the two equations is presented and the $\delta^{18}O_P$ difference (multiplied by -1) is also summarised. The average and standard deviation $\delta^{18}O_P$ with the upper and lower limits (average ± 1 SD) of the monthly results combined are shown. 196

Table 7.8. Summary of the average (± SEM) measured soil pH values, P_{Total}, P_{HCl} and % P_{HCl} of P_{Total} for the topsoils and subsoil in all treatments in the long-term experiments and the uncultivated area of the Field. 204

Table 7.9. Summary of $\delta^{18}O_P$ values of the GMP and TSP fertiliser materials and the topsoil and subsoil of the Field (uncultivated grassland); values are mean ± SEM. 212

Table 7.10. Summary of the $\delta^{18}O_P$ analysis for the target soil pH plots in the pH Rotation and also the Field soil profile and TSP fertiliser material for reference. Results are mean of 3 replicates ± SEM except (^{o}) n = 2 and (^{x}) n = 4. 214

Table 7.11. Summary of the topsoil and subsoil mean $\delta^{18}O_P$ (± SEM) for the fertiliser treatments, Field soil profile and the TSP and GMP fertiliser materials used in the Old Rotation. 220

Table 10.1. The Old Rotation Topsoil Pearson Correlation Coefficient Matrix and *p* values 244

Table 10.2. The Old Rotation Subsoil Pearson Correlation Coefficient Matrix and *p* values 245

Table 10.3. The pH Rotation Topsoil Pearson Correlation Coefficient Matrix and *p* values 246

Table 10.4. The pH Rotation Subsoil Pearson Correlation Coefficient Matrix and *p* values 247

Table 10.5. P_{Total} Balance (2015) in the Old Rotation with P fertiliser inputs, crop yields, crop P concentrations and total P offtakes- the (*) roots are in one single split plot..... 248

Table 10.6. Net Soil Profile P_{Total} Accumulation Rates in the Old Rotation over 94 years. 249

Table 10.7. P_{Total} Balance (2015) in the pH Rotation with P fertiliser inputs, crop yields, crop P concentrations and total P offtakes..... 250

Table 10.8. Net Soil Profile P_{Total} Annual Accumulates Rates in the pH Rotation over 53 years. 251

Table 10.9. Old Rotation P_{Total} Analysis of Variance..... 252

Table 10.10. Old Rotation As_{Total} Analysis of Variance..... 252

Table 10.11. Old Rotation Cd_{Total} Analysis of Variance 252

Table 10.12. Old Rotation U_{Total} Analysis of Variance 252

Table 10.13. Old Rotation Ca_{Total} Analysis of Variance 253

Table 10.14. Old Rotation P_{Olsen} Analysis of Variance..... 253

Table 10.15. Old Rotation $P_{MMorgan}$ Analysis of Variance..... 253

Table 10.16. pH Rotation P_{Total} Analysis of Variance 253
Table 10.17. pH Rotation As_{Total} Analysis of Variance 254
Table 10.18. pH Rotation Cd_{Total} Analysis of Variance 254
Table 10.19. pH Rotation U_{Total} Analysis of Variance 254
Table 10.20. pH Rotation Ca_{Total} Analysis of Variance 254
Table 10.21. pH Rotation P_{Olsen} Analysis of Variance 255
Table 10.22. pH Rotation $P_{MMorgan}$ Analysis of Variance 255
Table 10.23. P_{Total} topsoil and subsoil Polynomial Regression Models 256
Table 10.24. As_{Total} topsoil and subsoil Polynomial Regression Models 256
Table 10.25. Cd_{Total} topsoil and subsoil Polynomial Regression Models 256
Table 10.26. U_{Total} topsoil and subsoil Polynomial Regression Models 256
Table 10.27. Ca_{Total} topsoil and subsoil Polynomial Regression Models 256
Table 10.28. P_{Olsen} topsoil and subsoil Polynomial Regression Models 257
Table 10.29. $P_{MMorgan}$ topsoil and subsoil Polynomial Regression Models 257
Table 10.30. P_{HCl} topsoil and subsoil Polynomial Regression Models 257
Table 10.31. Prediction of Field concentration (Model output) using the fitted polynomial models using ‘pH value Input’. If the ‘True Value’ of the Field was within the range of x3 SEM of the Model Output then the conclusion was Not Different; out-with this range is ‘Significantly (Sig.) Different’ to the fitted model. 257

Table of Figures

Figure 2.1. The soil profile of Woodland's Field; the maximum soil depth is just 40 cm due to an indurated (compacted) layer below this. 13

Figure 2.2. The layout of the Old Rotation experiment at the end of the 2014-2015 growing season with sampled plots highlighted in green. 18

Figure 2.3. The layout of the pH Rotation experiment at the end of the 2014-2015 growing season, with sampled plots highlighted in green. 19

Figure 2.4. An example of the linear calibration for the high phosphate standard range of 0 to 50 µg P and typical absorbance values measured at 880 nm. 23

Figure 3.1. Soil characteristics dendrogram cluster analysis for the Old Rotation topsoils and subsoils. 36

Figure 3.2. Soil characteristics dendrogram cluster analysis for the pH Rotation topsoils and subsoils. 38

Figure 3.3. Comparison of the P_{Total} in the topsoil and subsoil in the fertiliser treatments plots and the Field. The mean P_{Total} in the treatment plots is of 5 crop phases (± SEM), and the field means (± SEM) are of 4 sample sites taken across the field. 40

Figure 3.4. Topsoil and subsoil P_{Total}; mean of 3 samples for each crop phase and fertiliser treatment ± SEM. 42

Figure 3.5. Topsoil and subsoil (i) As_{Total}, (ii) Cd_{Total} and (iii) U_{Total} correlations with P_{Total} in the Old Rotation and the Field. Plot values are the mean of 5 crop phases, ± SEM. 48

Figure 3.6.Topsoil: Subsoil ratio of P_{Total}, As_{Total}, Cd_{Total} and U_{Total} for each fertiliser treatment in the Old Rotation, and the Field, compared to a ratio of 1.0 (broken) line. 51

Figure 3.7. Target topsoil pH vs the measured soil pH in the topsoil and subsoil of each target pH plot compared to a 1:1 line. Points are the mean of 5 crop phases with ± SEM. 52

Figure 3.8. Relationship between measured soil pH and Ca_{Total} in the topsoils and subsoils of the pH Rotation and the Field. Trend lines are 2nd order polynomials; each point represents the mean of five crop phases ± SEM. 54

Figure 3.9. The ratio of plot: field (surrounding field natural background) Ca_{Total} in the topsoils and subsoils across the pH plots compared to a 1:1 line. 54

Figure 3.10. Mean P_{Total} in the topsoils and subsoils as a function of soil pH; the trend-lines are 2nd order polynomials; means are of five crop phases ± SEM. 56

Figure 3.11. Soil P_{Total} vs measured soil pH value under each crop phase in the topsoil and subsoil, described as 2nd order polynomials; each point is the mean of three replicates ± SEM. 58

Figure 3.12. Mean As_{Total} in the topsoils and subsoils as a function of soil pH; trend-lines are 2nd order polynomials; means are of 5 crop phases ± SEM. 65

Figure 3.13. Mean Cd_{Total} in the topsoils and subsoils as a function of soil pH; trend-lines are 2nd and 3rd order polynomials for the topsoil and subsoil respectively; means are of 5 crop phases ± SEM. 66

Figure 3.14. Mean U_{Total} in the topsoils and subsoils as a function of soil pH; trend-lines are 2nd and 3rd order polynomials for topsoil and subsoil respectively; means are of 5 crop phases ± SEM. 68

Figure 3.15. Relationship between soil pH and topsoil: subsoil ratios of P_{Total}, As_{Total}, Cd_{Total}, U_{Total} and Ca_{Total} compared to a 1:1 (dashed) line. 69

Figure 4.1. Relationship between topsoil and subsoil P_{Olsen} and $P_{MMorgan}$ for all soil samples analysed in the dataset across both long-term experiments and the Field (n = 348). The linear trend lines are forced through zero. 80

Figure 4.2. Relationship between topsoil and subsoil (i) P_{Total}, (ii) P_{Olsen} and (iii) $P_{MMorgan}$ with linear trend lines forced through zero. 82

Figure 4.3. P_{Olsen} as a function of soil pH for topsoil and subsoil in the pH Rotation; 3rd order polynomials. Each point is the mean of 5 crop phases ± SEM. 85

Figure 4.4. $P_{MMorgan}$ as a function of soil pH for topsoil and subsoil in the pH Rotation; the trend-lines 2nd and 3rd order polynomials respectively; means are of 5 crop phases ± SEM. 85

Figure 4.5. Relationship between the topsoil: subsoil P ratio and target soil pH for P_{Total}, P_{Olsen} and $P_{MMorgan}$ compared to a ratio of 1.0 (broken line). 87

Figure 4.6. Relationship between soil pH and P_{Olsen} for 5 crop phases in the (i) topsoil and (ii) subsoil, with 3rd order polynomials fitted to the data. 89

Figure 4.7. Relationship between soil pH and $P_{MMorgan}$ for 5 crop phases in the (i) topsoil and (ii) subsoil, with 2nd and 3rd order polynomials fitted to the data respectively 90

Figure 4.8. Relationship between P_{Total} and (i) P_{Olsen} and (ii) $P_{MMorgan}$ in the topsoil and subsoil for each fertiliser treatment and the Field; mean fertiliser treatment points are of 5 crop phases ± SEM. 92

Figure 4.9. Topsoil: subsoil ratios for P_{Olsen}, $P_{MMorgan}$ and P_{Total} in each of the fertiliser treatments of the Old Rotation compared to a ratio line of 1 (dashed) and compared to the Field topsoil: subsoil ratio. The average soil pH was 6.12 (topsoil) and 6.19 (subsoil) across the four fertiliser treatments and the field topsoil pH was 5.66 and the subsoil pH was 5.98. 93

Figure 4.10. Effect of crop phase within each fertiliser treatment for P_{Olsen} in (i) topsoils and (ii) subsoils and $P_{MMorgan}$ in (iii) topsoils and (iv) subsoils. Each bar is the mean of 3 soil replicates ± SEM. 95

Figure 5.1. Relationship between $P_{Soln-ICP}$ and $P_{Soln-Col}$ compared to a 1:1 line (samples with non-detectable $P_{Soln-Col}$ were excluded). 112

Figure 5.2. Relationship between $P_{Soln-Diff}$ and P_{DOM} in the dataset compared to a 1:1 line (samples with undetectable $P_{Soln-Col}$ were excluded and one outlying point in the topsoils was also excluded). 114

Figure 5.3. Effect of fertiliser treatment and crop phase on the mean $P_{Soln-Col}$ (± SEM, n = 3) in the solutions (0.005 M Ca(NO3)2) equilibrated with (i) topsoil and (ii) subsoil of the Old Rotation. 115

Figure 5.4. Effect of fertiliser treatment and crop phase on the mean $P_{Soln-ICP}$ (± SEM, n = 3) in solutions (0.005 M $Ca(NO_3)_2$) equilibrated with the topsoil and subsoil of the Old Rotation. 116

Figure 5.5. Relationship between target and measured soil pH in the topsoil and subsoil for (i) grass year 2 and (ii) spring oats of the pH Rotation compared to a 1:1 line. 118

Figure 5.6. Comparison of measured soil pH for grass year 2 and spring oats in the pH Rotation compared to a 1:1 line. 118
Figure 5.7. Effect of soil pH and crop phase on $P_{Soln-Col}$ in the Grass Y2 topsoils (r = 0.838) and subsoils (r = 0.549) and Spring Oats topsoils (r = 0.828) and subsoils (r = 0.805). 120
Figure 5.8. Effect of soil pH and crop phase on the $P_{Soln-ICP}$ in the topsoils and subsoils. 121
Figure 5.9. Topsoil: subsoil ratios for $P_{Soln-Col}$ and $P_{Soln-ICP}$ in the grass year 2 and spring oats crop phases across the target pH plots in the pH Rotation is shown compared to a 1.0 (broken) line. 122
Figure 5.10. Solubility phase diagram for topsoils and subsoil across the pH plots for grass year 2 and spring oats using $P_{Soln-ICP}$ to determine $H_2PO_4^-$ ion activity. Also shown are the Field topsoil and subsoil and the GMP fertiliser as references (although GMP is not applied to the pH Rotation). 124
Figure 5.11. Solubility phase diagram for topsoils and subsoil across the pH plots for grass year 2 and spring oats using $P_{Soln-Col}$ to determine $H_2PO_4^-$ ion activity. Also shown are the Field topsoil and subsoil and the GMP fertiliser as references (although GMP is not applied to the pH Rotation). 126
Figure 5.12. Solubility phase diagram for soils using $P_{Soln-ICP}$ (± SEM 3 auger borings) were measured pH value was greater than pH 6 (measured in 0.005 M $CaNO_3$ soil suspension). Labels indicate which pH plots are shown. 128
Figure 5.13. Solubility phase diagram for soils using $P_{Soln-Col}$ (± SEM 3 auger borings) were the measured pH value greater than pH 6 (measured in 0.005 M $CaNO_3$ soil suspension). Labels indicate which pH plots are shown. 128
Figure 5.14. Solubility phase diagram for the topsoils and subsoils of the Old Rotation using $P_{Soln-ICP}$ data for the grass year 3 and spring oats phases in the rotation: each point represents one of the fertiliser management strategies (± SEM 3 auger borings). Included are the Field topsoil and subsoil and the GMP fertiliser as reference values. 130
Figure 5.15. Solubility phase diagram for the topsoils and subsoils of the Old Rotation using $P_{Soln-Col}$ to estimate PO_4 activity for the grass year 3 and spring oats phases in the rotation: each point represents one of the fertiliser management strategies (± SEM 3 auger borings). Included are the Field topsoil and subsoil and the GMP fertiliser as reference values. 131
Figure 6.1. Agreement between P concentrations for repeated DGT deployments compared to a 1:1 (broken) line; intercepts are forced through zero. 144
Figure 6.2. Relationships between P_{Total} and P_{DGT} in the Field topsoils (r = 0.370) and subsoil (r = 0.981), pH Rotation topsoils (r = -0.340) and subsoils (r = 0.695) and the Old Rotation topsoils (r = 0.612) and subsoils (r = 0.541). One outlier with suspected P_{DGT} contamination is excluded from the pH Rotation subsoil data. 146
Figure 6.3. Relationship between P_{DGT} and P_{Olsen} in the Field topsoils (r = -0.997) and subsoils (r = 0.263), pH Rotation topsoils (r = -0.748) and subsoils (r = 0.302) and the Old Rotation topsoils (r = 0.911) and subsoils (r = 0.691). 147
Figure 6.4. Relationship between P_{DGT} and $P_{MMorgan}$ in the Field topsoils (r = 0.232) and subsoils (r = 0.433), pH Rotation topsoils (r = -0.024) and subsoils (r = 0.593) and the Old Rotation topsoils (r = 0.840) and subsoils (r = 0.700). 148

Figure 6.5. Relationship between topsoil and subsoil P_{DGT} in the Field (r = 0.991), pH Rotation (r = 0.451) and Old Rotation (r = 0.424). One soil core with suspected P_{DGT} contamination in the pH Rotation subsoil was excluded. ... 149
Figure 6.6. Relationship between P_{DGT} and $P_{Soln-Col}$ in Field topsoils (r = 0.653) and subsoils (r = 0.936), pH Rotation topsoils (r = 0.552) and subsoils (r = 0.709) and Old Rotation topsoils (r = 0.550) except (i) one outlier in the pH Rotation subsoils and (ii) Old Rotation subsoils have been excluded due to un-detectable $P_{Soln-Col}$. 151
Figure 6.7. Relationship between P_{DGT} and $P_{Soln-ICP}$ in the Field topsoils (r = -0.801) and subsoils (r = 0.920), pH Rotation topsoils (r = 0.010) and subsoils (r = 0.838) and the Old Rotation topsoils (r = 0.949) and subsoils (r = 0.285). One outlier has been excluded. 151
Figure 6.8. Relationship between P_{DGT} and measured soil pH in topsoils (r = 0.904) and subsoils (r = 0.687) of the pH Rotation; points are mean of 3 replicates ± SEM (except * where 1 replicate was excluded due to suspected contamination). 153
Figure 6.9. Relationship between measured soil pH and $K_{d(Olsen)}$ in the pH Rotation and the Field (mean 3 replicates ± SEM except * were mean 2 replicates ± SEM); 3rd order polynomials are fitted to the data. 155
Figure 6.10. Relationship between measured soil pH and $Kd_{(MMorgan)}$ in the pH Rotation and the Field (mean 3 replicates ± SEM except * were mean 2 replicates ± SEM); 2nd (topsoil) and 3rd (subsoil) order polynomials are fitted to the data 156
Figure 6.11. Ratio of P_{DGT}: $P_{Soln-Col}$ with soil pH in the topsoils (r = 0.001) and subsoils (r = 0.456) of the pH Rotation. 158
Figure 6.12. Ratio (R_{DGT}) of P_{DGT}: $P_{Soln-ICP}$ with soil pH in the topsoils (r = 0.640) and subsoils (r = 0.839) of the pH Rotation. 158
Figure 6.13. Effect of fertiliser treatment (and Field) on topsoil and subsoil P_{DGT} in the Old Rotation; results are mean of 3 replicates ± SEM. 160
Figure 6.14. Relationship between fertiliser treatments and $K_{d(Olsen)}$ in the Old Rotation plots and the Field (mean 3 replicates ± SEM). 162
Figure 6.15. Relationship between fertiliser treatments and $Kd_{(MMorgan)}$ in the Old Rotation plots and the Field (mean 3 replicates ± SEM). 162
Figure 6.16. Ratio of P_{DGT}: $P_{Soln-Col}$ in the topsoils of the fertiliser treatments in the Old Rotation compared to the Field. No $P_{Soln-Col}$ was obtained for the subsoils. 164
Figure 6.17. Ratio (R_{DGT}) of P_{DGT}: $P_{Soln-ICP}$ in the topsoils and subsoils of the fertiliser treatments in the Old Rotation compared to the Field. 164
Figure 7.1. Comparison of $\delta^{18}O_W$ and $\delta^{2}H_W$ values for the monthly rain water samples and the topsoil and subsoil pore waters against the GMWL line. 181
Figure 7.2. Relationship between the mass of Ag_3PO_4 crystals and total CO peak area (oxygen yield) for the Alfa-2 standards and a selection of samples (H_2O_2 treated and non-treated) in the pilot study. Linear trend lines shown are forced through zero. Samples were the purification process was unsuccessful are excluded. 185

Figure 7.3. Pilot vs main study $\delta^{18}O_P$ values compared to a 1:1 line. 190
Figure 7.4. The variation in $\delta^{18}O_W$ ($^0/_{00}$) results for rainfall, topsoil pore water and subsoil pore water throughout 2017. 192
Figure 7.5. Monthly topsoil: subsoil $\delta^{18}O_W$ ratios throughout 2017 compared to a 1:1 line. 192
Figure 7.6. The relationship between rainfall and the topsoil and subsoil soil pore waters $\delta^{18}O_W$. 193
Figure 7.7. Relationship between the monthly $\delta^{18}O_P$ calculated by the two equations in the 9 additional topsoils (red circles) and subsoils (yellow circles) of the uncultivated feld, using maximum, minimum and average temperatures for each month. 197
Figure 7.8. Relationship between the mass of Ag_3PO_4 and total CO peak area (oxygen yield) for the samples, Alfa-2 standard (r = 0.356) and B2207 standard. 199
Figure 7.9. Relationship between the total nitrogen peak area and the sample % oxygen yield relative to the Alfa-2 standard for 236 analyses (r = 0.325) where both data sets were available. 200
Figure 7.10. Relationship between sample P_{HCl} extracted by the non-enriched HCl vs $H_2{}^{18}O$ enriched HCl solutions: data is forced through zero and compared to a 1:1 (dashed) line. 201
Figure 7.11. Relationship between P_{Total} and P_{HCl} in the topsoils (r = 0.987) and subsoils (r = 0.964) of the long-term experiments. 202
Figure 7.12. The effect of fertiliser treatment on the average (± SEM) P_{HCl} in the topsoils and subsoils of the Old Rotation compared with the soil profile of the Field (uncultivated grassland). 206
Figure 7.13. Effect of soil pH control on the mean (± SEM) topsoil and subsoil P_{HCl} in the pH Rotation compared to the soil profile of the Field (uncultivated grassland). Topsoil and subsoils are fitted with 3rd order polynomials. 208
Figure 7.14. Comparison of the non-enriched and enriched HCl extractable $\delta^{18}O_P$ for the plots compared to a 1:1 line in topsoils (red circles) and subsoils (yellow circles). 209
Figure 7.15. Effect of soil pH target on the corrected $\delta^{18}O_P$ for topsoils and subsoils in the pH Rotation (n = 3, mean ± SEM except for pH 4.5 subsoil (n=2)). Upper and lower soil pore water equilibrium ranges for topsoil and subsoil are calculated using the mean temperature (± 1 SD). TSP fertiliser corrected $\delta^{18}O_P$ is included for reference (mean ± 1 SD). Field topsoil and subsoil corrected $\delta^{18}O_P$ values are plotted against their measured soil pH values. 218
Figure 7.16. Effect of fertiliser treatment on corrected $\delta^{18}O_P$ in the topsoil and subsoil compared to the uncultivated grassland (Field), the TSP and GMP $\delta^{18}O_P$ and the topsoil and subsoil $\delta^{18}O_P$ equilibrium ranges. The upper and lower limits of the $\delta^{18}O_P$ equilibrium ranges, TSP and GMP fertilisers, are set as the mean ± 1 SD. 224

1 Introduction

1.1 Phosphorus and Global Food Security

The world population is projected to increase to 9.8 billion by 2050 (United Nations, 2017) which will put pressure on agricultural soil systems and the environment to provide sustainable food production for global food security (Godfray & Garnett, 2014; George, *et al*., 2016). Phosphorus (P) is an essential element for life and is a fundamental component of molecules and biological processes, serving unique functions that cannot be replaced by any other element. In some circumstances, therefore, it can be a limiting nutrient (Elser, 2012). The ability of soils to provide enough P to meet crop P nutritional requirements and maintain food production for increasing human dietary demands (Metson, *et al*., 2012) is sustained through the application of mineral P fertilisers (Cordell, *et al*., 2009). However, the main source of P fertiliser is phosphate rock which is a finite resource and is concentrated mainly in Morocco where more than 75% of global phosphate rock reserves are located (Cooper, *et al*., 2011). It is estimated that, at current phosphate rock extraction rates, reserves in China and the United States of America will be depleted in 60 years resulting in an increase in the proportion of global reserves controlled by Morocco (Cooper, *et al*., 2011). The reduction of globally available sources of phosphate rock may cause market prices to become more volatile and threaten global food security (Cordell & White, 2015). The European Union has no phosphate rock reserves of its own and relies solely on imports (86% of which is used for fertiliser production) (Matthieux, *et al*., 2017) and over half of the P imported by the European Union ends up accumulated in agricultural soils (van Dijk, *et al*., 2016). More research is therefore needed to determine the role of residual P fertiliser in soils to address the sustainability issues surrounding P use (Sattari, *et al*, 2012).

Phosphorus fertilisers contain trace element contaminants including arsenic (As), cadmium (Cd) and uranium (U) that may accumulate in soils as a consequence of extended periods of fertiliser additions (i.e. Hartley, *et al*., 2013; Schipper, *et al*., 2011; Ahmed, *et al*., 2014). Cadmium contamination is of particular concern because its mobility is controlled by pH and it can accumulate in plants (i.e. wheat) (Liu, *et al*., 2015) and enter the human food chain. In the European Union there is ongoing debate with proposals to limit Cd concentrations in P fertilisers to 60 mg kg^{-1} before implementing a further two reductions to 40 mg kg^{-1} and then 20 mg kg^{-1} (Ulrich, 2019). Maintaining or reducing current Cd levels in European soils by limiting their introduction from fertiliser is considered important for future food production safety (Tóth, *et al*., 2016). Overall European-wide trends show that Cd inputs to soils are currently decreasing due to an

overall reduction in P fertiliser use, however, regional variations exist (Six & Smolders, 2014). There are no UK guidelines on restricting Cd (or As) additions to agricultural soils from phosphate fertilisers. However, Sludge (Use in Agriculture) Regulations (1989) limit the amount of Cd and As which can be introduced to agricultural soils from sewage sludge application with limits for Cd and As of 3 mg kg^{-1} (arable soils > pH 5.0) and 50 mg kg^{-1} respectively (The Sludge (Use in Agriculture) Regulations 1989). These are useful benchmark reference values for assessing soil Cd and As levels in agricultural soils were the main source is likely to be P fertilisers.

Historical use of P fertilisers in the UK has resulted in an estimated accumulation of 1000 kg ha^{-1} in agricultural topsoils (Withers, *et al*., 2001) although this figure is less than the estimated figure of 1700 kg ha^{-1} of P accumulation in arable topsoils (< 15 cm) worldwide (Menezes-Blackburn, *et al*., 2017). Total P fertiliser application rates in the UK have steadily declined from 40 kg ha^{-1} since the 1980's by approximately 50% to 20 kg ha^{-1} in 2017 (The British Survey of Fertiliser Practice, 2018). However, the chemical nature and dynamics of 'legacy' residual P in topsoils arising from the historical accumulation must be better understood in order to inform future P management strategies which aim to utilise current stocks of P that have built up in topsoils and subsoils (Stutter, *et al*., 2012; Sharpley, *et al*., 2013). It is estimated that the subsoil may hold up to 70% of a crop's nutrient requirements (Kautz, *et al*., 2013). However, relatively less is known about subsoil P dynamics (Andersson, *et al*., 2013) and the factors influencing subsoil P availability to crops are poorly understood (Bauke, *et al*., 2018). Therefore, in order to meet the aim of improving the efficiency of agricultural P use for long-term food security (George, *et al*., 2016) a greater understanding of both topsoil and subsoil P dynamics is required. In particular, we currently lack an understanding of the agronomic significance of subsoil P and the conditions under which subsoil P stocks may be utilised by crops.

1.2 Phosphorus Dynamics in Soil

Agricultural crops meet their P requirements through root uptake of the inorganic phosphate (P_i) anions ($H_2PO_4^-$ and HPO_4^{2-}) from the soil solution (Kruse, *et al*., 2015). The main process by which crops obtain P is diffusion through the soil solution to the root surface (Degryse, *et al*., 2009). Typically, the P_i pool which is available to plants is less than 2% of the total P in the soil (Fisher, *et al*., 1998). The forms of P in soils, and the availability to crops, depends on soil properties such as soil pH and the concentrations of iron (Fe), aluminium (Al) and calcium (Ca), which influence the lability of P in terms of its exchange between the soil solid and solution phases (Hinsinger, 2001). The adsorption of P_i on to positively

charged Fe and Al oxide surfaces is the dominant reaction determining solubility at acidic pH values (< pH 5.5) (Weng, *et al*., 2011). As the soil pH increases, P is less strongly held and becomes more labile due to a decrease in positive charges on the oxide surfaces following proton dissociation and a rise in humic and fulvic acid competition for surface binding sites (Weng, *et al*., 2011; Perassi & Borgnino, 2014). Increasing soil pH causes desorption of P from variable charge minerals such as goethite (Antelo, *et al*., 2005). Above pH 6, the precipitation and dissolution of Ca-phosphate minerals becomes important (Weng, *et al*., 2011). The optimum pH range for crop production and acquisition of $H_2PO_4^-$ is between pH 6.0 and 6.5 (Goulding, 2016) which is also the range associated with maximum P solubility (Lindsay, 1979). Many UK soils are acidic and crop production could benefit from the application of lime to raise the pH (Holland, *et al*., 2018). However, it has been argued that the optimum pH for crops acquiring P may be lower at soil pH values between 4.0 and 6.0 (Barrow, 2017). Soil texture is also important to P dynamics as soils with a higher clay content may retain more residual P in the topsoil whereas sandy soils will be more susceptible to P losses to the subsoil (Pizzeghello, *et al*., 2011; Pizzeghello, *et al*., 2014). The concentration of P in soil is also important; Fortune, *et al*., (2005) found that, in long-term field experiments, the concentrations of P in both field-drainage water and the soil solution (0.01M $CaCl_2$ soil extractable P), were positively correlated with increasing soil Olsen P levels, suggesting a link between rising Olsen P levels in soils, and dissolved P in water. The movement of P dissolved in soil water throughout the soil profile could therefore be an important mechanism of transfer from topsoil to subsoil. Differences in soil management are also important for P dynamics. Abdi, *et al*., (2014) observed that in plots which had been ploughed, concentrations of different P species were uniform to a depth of 20 cm under fertilised and non-fertilised treatments due to mixing of the soil. In contrast, in plots which were not tilled, reactive inorganic phosphate accumulated in the top 5 cm of soils whereas organic P appeared to leach further down the profile (to a depth of 15 cm), compared to ploughing when uniform profiles of P species were observed (Abdi, *et al*., 2014).

Organic forms of phosphorus (P_o) can constitute more than 50% of the total amount of P in soils (Nash, *et al*., 2014). The most common forms are phosphomonoesters (Menezes-Blackburn, *et al*., 2016; McLaren, *et al*., 2017), phosphodiesters, phosphonates and organic polyphosphates (Turner, *et al*., 2005). Organic P may be more labile in soil and bioavailable to crops than P_i but may also pose a greater risk to the wider environment through leaching (Darch, *et al*., 2014). Phosphorus dissolved in the soil solution may also undergo rapid biological cycling (Paytan, *et al*., 2002) which may result in the immobilisation or mineralisation of P in the organic fraction. Despite recent advances in techniques for quantifying and

characterising organic P, more research is needed in this area in order to understand the contribution from this fraction to plants (Haygarth, *et al*., 2018). A standard test to assess the availability of organic P to plant requirements would be useful to allow comparisons between studies (Turner, *et al*., 2005). This is important because it known that farm yard manure application may increase soil organic P levels by up to 180% over time but there is limited understanding of the mechanisms of organic P cycling in agricultural soils (Dodd & Sharpley, 2015). In the first study to try and isolate the effect of pH on P_o across an established pH gradient in a long-term field experiment, Turner & Blackwell (2013) concluded that soil pH was not an important factor controlling the concentration of P_o in topsoils, but it was important for P_i. Topsoils are typically higher in organic matter than subsoils, however the long-term application of farm yard manure can cause subsoils to become enriched in organic-P (Pizzeghello, *et al*., 2014).

In comparison to the topsoil, less is known about subsoil P (Andersson, *et al*., 2015; Barej, *et al*., 2014). More research is required to understand subsoil P dynamics and the conditions under which crops may access and utilise P potentially stored in the subsoil (Bauke, *et al*., 2018).

1.3 Subsoil Phosphorus Research and Long-Term Experiments

The accumulation of residual P fertiliser in agricultural topsoils due to inputs of P exceeding outputs by crop removal is well known (Withers, *et al*., 2001). However, compared to the topsoil, relatively less is known about the amount and forms of P in the subsoil (Barej, *et al*., 2014). Agricultural subsoils were previously identified as a potentially important source of plant available P (Kuhlmann & Baumgärtel, 1991). The factors influencing the distribution and accumulation of reactive P throughout the soil profile can be investigated using long-term experiments, field trials and agricultural fields which have known fertiliser use and crop removal histories.

In Denmark, the total P in agricultural soil profiles has increased due to the long-term application of P fertilisers (c. 100 years) which has resulted in P enrichment of the soil profile down to 75 cm when compared to other land uses such as forestry (Rubæk, *et al*., 2013). Rubæk, *et al*., (2013) also found that the accumulation rate of P (25 kg ha^{-1}) in Danish soils was comparable to the Danish national surplus of c. 20 kg ha^{-1}. In the UK, Ahmed, *et al*., (2014) showed that, in arable soils where P fertiliser has been used long-term (c. 100 years), the soil profile may become enriched in P compared to woodland areas adjacent to the field on the same parent material. The total P content in the arable soil profile was greater

than the woodland by up to 200 mg kg^{-1} down to a depth of 50 cm (Ahmed, *et al*., 2014). In addition, the uranium concentration was enriched in the arable soil to a depth of 30 cm and was thought to have been introduced as a P fertiliser contaminant (Ahmed, *et al*., 2014). The over application of P fertiliser in excess of crop requirements in a 25-year experiment resulted in increased leaching of P and the accumulation of reactive P in the subsoil to depths of 300 cm in China (Khan, *et al*., 2018). Long-term experiments (44 yr) have also been used to show that the re-distribution of P fertilisers (such as mineral and farm yard manure) from the topsoil to the subsoil in field trials is related to soil type and results in an increase of both total P stocks and labile P in the subsoil layers (Pizzeghello, *et al*., 2014). When manure was applied to soils, P was enriched to a depth of 50 cm in a clay soil and down to 80 cm in sandy and peaty soils and the increase in P concentration with depth occurred whether the P balance was positive or negative (Pizzeghello, *et al*., 2014). In particular, the use of farm yard manures may result in the accumulation of water soluble and labile P forms throughout the soil profile which is a particular concern for sandy soils with a low capacity to retain P (Pizzeghello, *et al*., 2011). In two long-term field trials on silt loam soils, Vanden Nest, *et al*., (2016) showed that the availability and leaching of P was greater in soils where farm yard manure had been applied compared to a range of organic waste composts but was not greater than the soil treated with sewage sludge. The conclusion was that P leaching was related to adsorption due to the significant correlations between P leaching and the distribution coefficient of P between the soil solid and solution phases (Vanden Nest, *et al*., 2016).

The retention of P throughout the soil profile is important when considering the transport of P from topsoil to the subsoil. Andersson, *et al*., (2013) showed that the leaching of dissolved reactive P in lysimeter soil profiles was least in soils where there was a high P sorption capacity in the soil and when subsoils were not measurably enriched in P. In particular, clay soils have higher sorption capacities for P than sandy soils due to the higher concentrations of Fe and Al to which P may be adsorbed (Andersson, *et al*., 2013). In clay soils, P was found to be adsorbed to both Fe and Al oxides but in calcareous soils, P was associated as the Ca-phosphate mineral hydroxyapatite (HA) (Eriksson, *et al*., 2015). Phosphorus may be rapidly transported to the subsoil in sandy soils, particularly if the topsoils are saturated with P, causing an increase in subsoil saturation of between 14 and 55% (De Bolle, *et al*., 2013). As subsoils may intercept P leaching from the topsoils, they are an important consideration in fate-transport models that are concerned with understanding the re-distribution of soil P to groundwater (Kleinman, *et al*., 2015).

Low subsoil P availability and acquisition are cited as common challenges for deep rooting crops (Lynch & Wojciechowski, 2015). However, the research which has been reviewed has shown that subsoils may intercept and contain significant amounts of reactive (available) P. Research has shown that deep rooting crops may be able to access the subsoil through biopores (Barej, *et al*., 2014). The application of nitrogen (N) and potassium (K) fertilisers also promotes crop utilisation of subsoil P and the cycling of subsoil P by microbial enzymes, although subsoils can also contain significant amounts of native, older P minerals (Bauke, *et al*., 2018). However, changing the land-use from grassland to arable or fallow can cause soil organic carbon (C) and nitrogen (N) stocks to be reduced by 13 to 78% throughout the soil profile (60 cm depth) (Gregory, *et al*., 2016). This is significant because there are likely to be implications for changes in subsoil P amounts and forms because P is strongly associated with C in organic matter at a ratio of 0.0016 in nutrient-rich (arable) soils (Tipping, *et al*., 2016). Clearly the subsoil contains significant amounts and forms of P and analysing the topsoil alone is not sufficient for improving P use efficiency in agriculture (Andersson, *et al*., 2013). Further research is required to understand subsoil P dynamics and so by applying analytical techniques to both the topsoil and subsoil, P dynamics throughout the soil profile can be investigated.

1.4 Methods to Investigate Phosphorus Dynamics

There is a range of traditional methods and innovative analytical techniques available to study soil P dynamics (Kruse, *et al*., 2015; Leinweber, *et al*., 2018). The application of these techniques, combined with samples and data from long-term field trials produces datasets that could be used to inform models of P dynamics in soil, help optimise P management strategies, and therefore improve agricultural P use efficiency and sustainability (Chen, *et al*., 2017). The classical experiments at Rothamsted Research (UK) for example demonstrate the value of long-term experiments for assessing the sustainability of agricultural management and the impact of management strategies on maintaining crop yields (Johnston & Poulton, 2018).

1.4.1 Estimating ‘plant-available P’ in the Soil

In the UK, two advisory soil P extraction methods are typically used to estimate plant-available P in the topsoil, but these methods are not routinely applied to subsoils due to the costs associated with the additional analysis (Barraclough, *et al*., 1997). In Scotland, the Modified Morgan’s extraction (McIntosh, 1969) is used, which is a buffered ammonium acetate/ acetic acid extraction (Sinclair, *et al*., 2013). In England and Wales, the Olsen method (Olsen, *et al*., 1954) is recommended and is based on an alkaline

sodium bicarbonate extraction (AHDB, 2017). In both cases, the concentration of P is usually measured by colorimetry using the blue molybdate-reactive phosphate method (Murphy & Riley, 1962). Although soil extracts may contain organic-P, it can be assumed that most of the P extracted is inorganic (Adesanwo, *et al*., 2013). The results of these tests are used to estimate fertiliser requirements for optimising crop production (AHDB, 2017; Sinclair, *et al*., 2013). The optimum soil 'Olsen P' concentration ranges from 16 to 25 mg kg^{-1} and soils within this range are designated as 'Index 2A/B' in the advisory notes (AHDB, 2017). For crops grown under optimal conditions, an average concentration of 20 mg kg^{-1} is thought to be ideal (Poulton, *et al*., 2013). However, the critical topsoil concentration for winter wheat to obtain a 95% maximum yield was found to be lower at an average of 9 mg kg^{-1} (Index 0) in the long-term Exhaustion Land Experiment at Rothamsted Research (UK) (Bollons & Barraclough, 1999). Soil Olsen Indices greater than 2 increase the risk of P leaching to the wider environment and recent reviews recommend lowering the critical soil P level in order to utilise residual P in soils (Withers, *et al*., 2017). The optimum concentration of 'Modified Morgan P' in soil ranges from 4.5 to 13.4 mg kg^{-1} and would be given a soil status of 'M' (Sinclair, *et al*., 2013). A recent study showed that more than half of Scottish soils fell within the optimum range while 30% were below, and 14% were above, the recommended level (Edwards, *et al*., 2016). It was also reported in this study that a reduction in P fertiliser applications to reduce the positive P balance in soil was not met with a reduction of plant-available P levels in soils indicating the extent to which soils are able to buffer changes in extractable P (Edwards, *et al*., 2016). In a recent analysis of soil fertility in the UK, it was suggested that more research is required to try and lower the advisory critical level of P in soil to reduce environmental losses (Withers, *et al*., 2017). This aim may be achieved by further research in to understanding the availability of subsoil P for crop requirements and the potential contribution of the subsoil, as it has long been understood that subsoil P reserves may be an important source of plant-available P (Kuhlmann & Baumgärtel, 1991).

1.4.2 Geochemical Modelling of Phosphate Solubility in Soils

More research is required to understand the impact of mineral phases in long-term agricultural soil systems on the availability and solubility of P (Simonsson, *et al*., 2018). Geochemical speciation models such as the Windermere Humic Aqueous Model-VII (WHAM-VII) (Tipping, *et al*., 2011) can be used to investigate the possible Ca-phosphate minerals phases that control P solubility in soils. This is achieved by speciation modelling to determine the activity of pH, Ca^{2+} and $H_2PO_4^-$ in soil solution phases in order to obtain the lime potential and Ca-phosphate potential; these can then be compared to known solubility

products of common calcium-phosphate minerals to infer which minerals are exercising solubility control over phosphate (Lindsay, 1979). All known ionic interactions (complex and ion pair formation), such as interactions between phosphate anions and the major soil cations (Na, Mg, K, Ca, Al, Mn and Fe), must also be considered in the speciation model to resolve free Ca^{2+} and $H_2PO_4^-$ free ion activities. Geochemical speciation modelling has shown that the solubility of P may be controlled by relatively stable calcium-phosphate minerals such as hydroxyapatite (HA) in soils which have received long-term applications of phosphate fertilisers (Zhang, *et al*., 2014). This is especially likely in soils with a pH > 6, where Ca-phosphate minerals are dominant, whereas in soils which have an acidic pH value, the P solubility is likely to be controlled by adsorption to Fe and Al oxides (Weng, *et al*., 2011). Several calcium phosphate minerals may co-exist to control phosphate solubility between pH 6.0 and 6.5 (Lindsay, 1979) which is also the pH range at which crop production and P acquisition is expected to be greatest (Goulding, 2016). Soils with a pH value less than 6 are likely to be under-saturated with respect to calcium phosphate minerals (Larsen & Court, 1961). However, the solubility of P in soil solution may be influenced by simultaneous interactions with Al, Fe and Ca (McDowell & Sharpley, 2003) and the presence of organic acids (such as fulvic acid) may inhibit the formation of calcium phosphates (Alvarez, *et al*., 2004). Goechemical speciation modelling can therefore be used to elucidate the dominant minerals controlling the solubility of P in solution throughout the soil profile – or suggest that surface adsorption is the controlling mechanism if all candidate P minerals are under-saturated.

1.4.3 Labile P and The Diffusive Gradients in Thin-Films Technique

Labile phosphorus, which is reversibly exchangeable between the solid and solution phase (Menezes-Blackburn, *et al*., 2016), is important for maintaining soil solution P following removal by crops. The Diffusive Gradients in Thin-Films (DGT) technique can be used to study labile P dynamics in soil (Zhang & Davison, 2015) and can be used to obtain information on (i) the apparent distribution coefficient (K_d) of P between the solid and solution phases and (ii) the rate (R_{DGT}) at which the solid phase can re-supply P to the solution (Harper, *et al*., 2000). Briefly, a plastic DGT device containing a diffusive layer, filter membrane and an Fe-oxide layer for binding P is applied to a saturated soil. The DGT method thereby mimics the uptake of P by plant roots (when uptake is limited by diffusion) by inducing a concentration gradient at the surface of the device by removing P from solution through binding to the Fe-oxide layer; this induces a flux and re-supply of P from the solid phase (Degryse, *et al*., 2009). The DGT method can be a better predictor of plant-available P when compared to traditional extraction techniques (Six, *et al*.,

2012) which is most likely if the uptake flux of P by the DGT device and plants is similar (Zhang & Davison, 2015). Because of its mechanistic basis, the DGT technique should represent an improvement over determination of an 'available' pool of P by chemical extraction. However, the literature is quite variable on this question. Burkitt, *et al*., (2016) found that traditional soil P tests performed better (than DGT) at predicting pasture response to P. In a study of temperate soils across Europe, Nawara, *et al*., (2017) found that DGT and traditional extraction techniques were comparable in predicting the response of crops to P and concluded that no single test was superior in the soils of their study. Therefore, it is important to research the soil mechanisms which affect the lability of P in both topsoil and subsoil as this may indicate the underlying soil mechanisms which influence correlations between DGT and plant uptake of P (Degryse, *et al*., 2009). Menezes-Blackburn, *et al*., (2016) recommended that future studies should investigate the effect of soil pH, for example, as it would be useful to compare the lability of P across a pH gradient. Therefore, it would be useful to apply the DGT method to both topsoils and subsoils in order to investigate labile P dynamics.

1.4.4 Investigating P Cycling and Transfer Mechanisms using the Stable Oxygen Isotope Ratios in Soil Phosphate

In order to further understand re-distribution in the soil profile, it would be useful to understand the pathways whereby fertiliser P is cycled and transferred throughout the soil profile. These could include (i) simple rapid leaching of inorganic P in solution (De Bolle, *et al*., 2013) perhaps shortly after the application of soluble mono-calcium phosphate (superphosphate), (ii) the translocation of P to deeper roots which subsequently decompose in situ post-harvest (de Miranda & Rowell, 1987) or (iii) colloidal transfer down the soil profile of P adsorbed to Fe-oxides (Baken, *et al*., 2016). The extent, rate and mechanisms of P fertiliser transport into the subsoil are currently very difficult to quantify. The analysis of stable oxygen isotope ratios (^{18}O: ^{16}O) in soil phosphate extracted by acid dissolution of inorganic P with HCl ($\delta^{18}O_P$) (Tamburini, *et al*., 2010) could be a useful approach for indicating biological transformations and P cycling and transfer in the soil profile (Tamburini, *et al*., 2014). The $\delta^{18}O_P$ signatures of mineral P fertilisers are usually close to the source phosphate rock ($19.6^0/_{00}$ to $23.1^0/_{00}$) and are unaffected by the processing to more soluble forms (Gruau, *et al*., 2005). In contrast, $\delta^{18}O_P$ signatures of farmyard manures may be much lower, between 12 and $15^0/_{00}$ (Amelung, *et al*., 2015; Granger, *et al*., 2017a). Research has shown that the $\delta^{18}O_P$ signatures of agricultural topsoils range from 15 to $18^0/_{00}$ (Bauke, *et al*., 2018) and subsoils may range between 12 and $17^0/_{00}$ (Bauke, *et al*., 2018; Amelung, *et al*., 2015). Measured $\delta^{18}O_P$

values close to, or within, the soil pore water $\delta^{18}O$ equilibrium range indicates intensive cycling of P through biological processes whereas $\delta^{18}O_P$ values closer to source materials indicate a lack of biological cycling possibly due to abiotic soil processes, such as absorption into soil mineral phases, rendering P unavailable for biotic processing (Gross & Angert, 2015). Thus, the stable oxygen isotope ratios in soil phosphate could provide valuable insights in to the extent and rate of cycling, and the transfer pathways of P from topsoils to subsoils under a range of soil management regimes.

1.5 Thesis Aim and Objectives

The aim of this thesis was to understand topsoil and subsoil P dynamics in long-term experiments. The hypothesis was that the long-term application of P fertilisers, soil pH control and rotational cropping would result in the accumulation of P in the topsoil which could have migrated to the subsoil over the long-term and be observed in the soil profiles of long-term field experiments. The aim and objectives are achieved using two long-term field experiments which are managed by Scotland's Rural College (SRUC) and located in SRUC's Woodland's Field, Craibstone Estate, Aberdeen campus. The Old Rotation was established in 1922 and is a six-course crop rotation, fertiliser management trial. The pH Rotation was established in 1961 and is an eight-course crop rotation trial consisting of plots covering a range of target soil pH values between 4.5 and 7.5 in 0.5-unit increments. The objectives, and the experimental results chapters in which they are addressed, are listed below.

Chapter 3. Audit and characterise the total elemental profile of the long-term experiments and the Field surrounding the trials and investigate the effect of soil pH control, crop rotation and P fertiliser management strategy on the distribution of residual P fertilisers and associated contaminants (As, Cd and U) in topsoils and subsoils.

Chapter 4. Investigate the effect of soil pH control, crop rotation and P fertiliser management strategy on the capacity of topsoils and subsoils to provide available-P for crops in rotation using traditional UK soil P extraction methods.

Chapter 5. Investigate the effect of soil pH control and P fertiliser management strategy on the solubility and speciation of P in the soil solution of topsoils and subsoils using (i) the geochemical modelling (WHAM-VII) and (ii) phosphate-lime potential calculations to determine the dominant calcium phosphate mineralogy controlling the solubility of P throughout the soil profile.

Chapter 6. Investigate the effect of soil pH control and P fertiliser management strategy on the lability and distribution of P in topsoils and subsoils and also the ability of the soil to buffer and re-supply P from the solid phase to maintain equilibrium with the solution phase following depletion using the Diffusive Gradients in Thin-Films (DGT) technique.

Chapter 7. Investigate the cycling and pathways of P from the topsoil to the subsoil as affected by soil pH controls and P fertiliser management strategies through analysis of the stable oxygen isotope ratios (^{18}O: ^{16}O) in HCl-extractable soil phosphate ($\delta^{18}O_P$).

2 Materials and Methods

2.1 Sample Site and Trial Descriptions – The Woodland's Field Rotations

The Woodland's Field experimental site on Scotland's Rural College (SRUC), Craibstone Estate, Aberdeen, Scotland, UK (GPS: 57°11'08.6"N 2°12'44.6"W) currently has two on-going long-term rotational (ley/arable) experiments that were originally designed as demonstration trials for local farmers. Both experiments are representative of historical, and current, ley/arable farming systems in the area. The site is managed by SRUC and the plots are maintained through funding from The Scottish Government's Rural and Environment Science and Analytical Services Division (RESAS).

The 'Woodland's Old Rotation' was established in 1922 and compares the effect of six fertiliser treatments on the yield and productivity within a six-course rotation. The fertiliser treatments include: NP without K, PK without N, NK without P, NK plus TSP, NK plus GMP and a zero fertiliser treatment which acts as a control treatment. The order of crops in the rotation is: grass/clover (year 1), grass/clover (year 2), grass/clover (year 3), barley under-sown (year 4), root crops (split plot of potatoes, swedes, turnips) (year 5) and finally, spring oats under-sown with grass/clover (year 6). In all cases, the grass-clover mix used in these two trials consists of perennial ryegrass and white clover. The dimensions of the plots are approximately 7.5 m by 5 m. In total, at the end of the 2014 – 2015 growing season, the rotation had completed 15.5 crop cycles over a 93-year span of continuous rotation, except for a period during World War 2 for which yield data is not available.

The 'Woodland's pH Rotation' was established in 1961 and demonstrates the effect of seven pH values on the health and productivity of an eight-course crop rotation. The pH gradient increases in increments of 0.5 units over the range pH 4.5 to pH 7.5. The order of crops in the rotation is: grass/clover (year 1), grass/clover (year 2), grass/clover (year 3), winter wheat (year 4), potatoes (year 5), spring barley (year 6), swedes (year 7) and finally spring oats under-sown with grass/clover (year 8). The dimensions of the plots are approximately 6.5 m by 5 m. In total, at the end of the 2014 – 2015 growing season, the rotation had completed 6.75 crop cycles over a 54-year period of continuous rotation.

The local soil is of the Countesswells Association, which is a free-draining sandy loam containing coarse fragments; there is an indurated layer at around 40 cm depth (Glentworth & Muir, 1963). The parent material consists of glacial till and drift. The soil profile is shown in **Figure 2.1**: the topsoil (< 20 cm) is relatively more organic than the subsoil (20 to 40 cm) which is sandy, and the orange colour suggests the deposition of secondary iron oxides. Roots were evident throughout the profile.

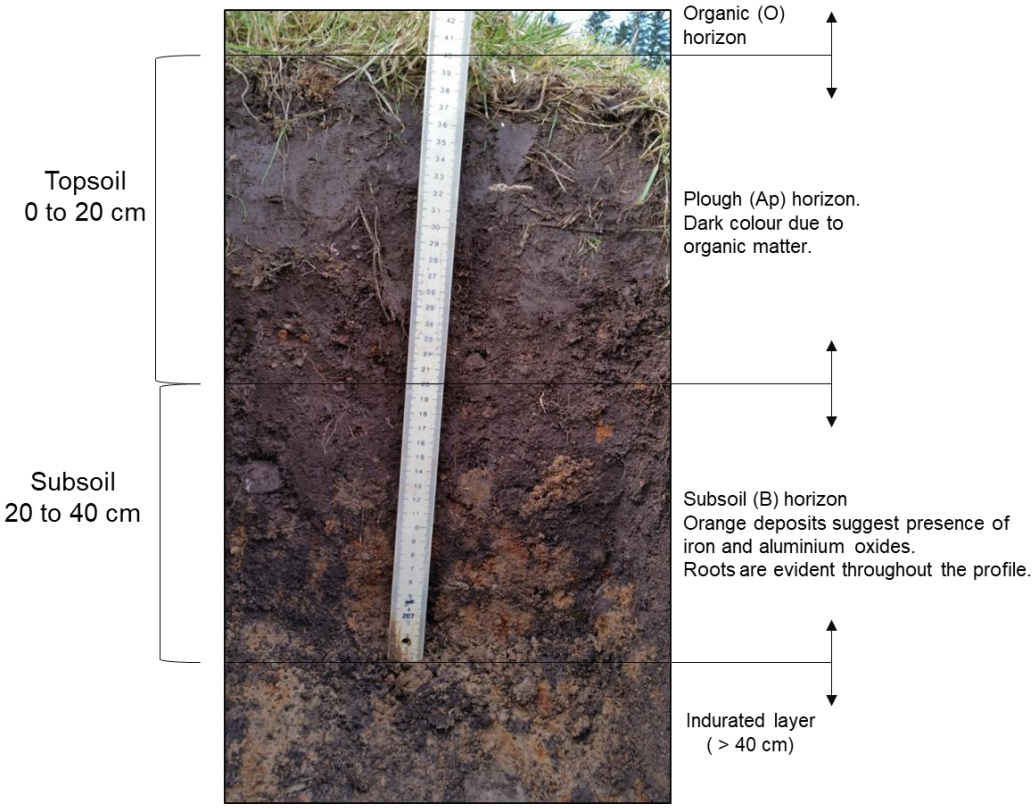


Figure 2.1. The soil profile of Woodland's Field; the maximum soil depth is just 40 cm due to an indurated (compacted) layer below this.

There is a Meteorological Station in Woodland's Field (Craibstone) which records daily air temperature, precipitation and soil temperatures (10 cm, 30 cm and 100 cm depths). For the period January 2013 to December 2017, the average annual rainfall was 878 mm and the average annual maximum and minimum temperatures were 12^{o}C and 6^{o}C respectively.

2.1.1 Trial Management

Routine Soil Analysis

Every 4 to 6 years, plots undergo routine soil analysis by SRUC's SAC Consulting Analytical Services Department (Edinburgh) for Modified Morgan P, K and Mg and, occasionally, loss on ignition. Broad spectrum analysis is rarely performed. Annually, soil pH is assessed in-house in the Aberdeen SRUC Crop and Soil Systems Research Group laboratory to determine if corrections are required where there are deviations from the target soil pH values. Six soil samples are bulk collected in a W-shaped transect from each plot to a depth of 15 cm, within an area 50 cm from the plot boundaries, in either January or February each year, before ploughing and farm yard manure applications. Adjacent plots of the same treatment under different crops may be paired and analysed to save on analytical costs.

Target pH Maintenance

In the Old Rotation, all plots are maintained at pH 6. In the pH Rotation, plots are maintained at their target value, with soils sampled and tested for pH annually and adjusted as necessary. Plots with a pH target lower than pH 5.5 are adjusted using ferric sulphate, and calcium carbonate is used to maintain targets above pH 5.5. Plots at pH 5.5 require minimal adjustment.

Ploughing, Planting and Harvest Operations

Plots are ploughed across treatments, along the line of each crop to a depth of 20 cm, using a two-furrow plough. In alternate years the ploughing direction is reversed to reduce soil creep across the plot. Stalks, roots and plant debris are reincorporated using this approach. All plots except the grass leys are ploughed each year before the new crop is sown or planted. Ploughing time depends on the crop: winter wheat (October), spring cereals (January/February) and root crops (March). Harvest time also differs for each crop: cereals (September or October), potatoes (October), Turnips (October/November) and swedes (November/January). All crops, except the winter wheat, are spring-sown. Cereals are typically sown in early-to-mid April, potatoes are planted late April and swedes and turnips are planted in late May. Potatoes are harvested by hand and with a mechanised one-drill potato lifter. The first-year grass/clover (hay) is cut and removed around July with the remaining sward cut and mulched at the end of the year. The 2nd and 3rd year grass/clover sward is cut and mulched 3 – 5 times throughout the season, with a final cut around October with all material left on the plots to mulch down.

Crop Disease, Pests and Nutrient Deficiencies

Some level of disease occurs most years and severity depend on the season. Crops growing in acid pH values, in the pH Rotation experiment, suffer from a higher incidence of disease. The most common diseases are: *Septoria tritici* in wheat; *Rhynchosporium commune* and mildew in barley; mildew and rust in oats; blight and common scab in potatoes and swedes. Herbicides are applied to cereals and root crops, pre- or post-sowing depending on the crop, and plots may receive a follow up application. Potatoes routinely receive fungicides to treat potato blight. Pesticide application to cereals is limited because the varieties grown are chosen based on earliness of maturity and disease resistance ratings and so cereals may only receive fungicide applications if a disease is observed. Molluscicides are applied to wet and cloddy ground after sowing or planting as a deterrent to slugs, until crops are larger. Manganese and copper deficiencies are the most commonly observed deficiencies across both trials, particularly in oats and barley. Occasionally there may be instances of sulphur deficiency. If trace element deficiencies are observed, all plots receive supplements by foliar spray.

Fertiliser Application Rates

The fertiliser application rates for both experiments are based on the next crop about to be drilled or planted in the rotation. Fertilisers are pre-weighed for the plot area and distributed evenly by hand and are usually applied prior to planting (P & K), with N applied either at planting or, in the case of winter wheat, in the spring. Fertiliser application type and rates were originally based on 1920's recommendations and so in 1991, nutrient inputs were increased to the lower end of current fertiliser recommendations. Currently, all plots receive fertilisers applied as ammonium nitrate (NH_4NO_3), muriate of potash (KCl) and triple superphosphate ($Ca(H_2PO_4)_2$) (TSP). The present fertiliser and farm yard manure (FYM) applications rates are shown for the Old Rotation in **Table 2.1**, and the pH Rotation in **Table 2.2**, with the values in parenthesis indicating application rates expressed as kg ha^{-1} of P_2O_5 or K_2O. There are some exceptions in the Old Rotation where the fertiliser application rate depends on the fertiliser scheme and the rock phosphate plot receives P as Gafsa ground mineral phosphate (GMP). The rotations receive 25 t ha^{-1} cattle FYM at the beginning of every root crop phase of the rotation with an NPK equivalent composition of 143, 42 and 148 kg ha^{-1} respectively. Prior to 1991, ammonium sulphate and superphosphate were used as the sources of N and P; the historical fertiliser rates for the Old Rotation are shown in **Table 2.3**. The original application rates for the pH Rotation, between 1961 and 1991, are not known.

Table 2.1. Woodland's Old Rotation fertiliser application rates (1991 – present). The values in parentheses indicate application rates expressed as kg ha^{-1} of P_2O_5 or K_2O.

Crop	N kg ha^{-1}	P kg ha^{-1}	K kg ha^{-1}	FYM kg ha^{-1}
Grass 1st Year	80	20 (45)	58 (70)	0
Grass 2nd & 3rd Year	80	0	0	0
Cereals	80	20 (45)	58 (70)	0
Roots	80	66 (150)	83 (100)	25

Table 2.2. Woodland's pH Rotation fertiliser application rates (1991 – present). The values in parenthesis indicate application rates expressed as kg ha^{-1} of P_2O_5 or K_2O.

Crop	N kg ha^{-1}	P kg ha^{-1}	K kg ha^{-1}	FYM t ha^{-1}
Oats & Barley	60	22 (50)	58 (70)	0
Swedes	70	35 (80)	83 (100)	25
Potatoes	100	66 (150)	100 (120)	25
Winter Wheat	100	28 (65)	71 (85)	0
Grass 1st Year	70	13 (30)	42 (50)	0
Grass 2nd & 3rd Year	0	0	0	0

Table 2.3. Woodland's Old Rotation fertiliser application rates (1922 – 1991). The values in parenthesis indicate application rates expressed as kg ha^{-1} of P_2O_5 or K_2O.

Crop	N kg ha^{-1}	P kg ha^{-1}	K kg ha^{-1}	FYM t ha^{-1}
Grass 1st Year	26	20 (45)	32 (38)	0
Grass 2nd & 3rd Year	26	0	0	0
Cereals	26	20 (45)	32 (38)	0
Roots	26	39 (90)	62 (75)	25

Sample Archiving and Historical Data

Soil and plant samples have not been routinely archived throughout the history of the Woodland's Field Rotations. However, since 2010, some plant samples have been archived, such as grain and tuber material and, occasionally, straw and tops from root crops. Plant samples are preserved by drying and milling with a titanium blade and stored in 50 g pots, in a vermin-proof room. There is extensive data on fertiliser inputs, crop yields and offtakes, and crop varieties used on the trials. Historical meteorological data is archived from the on-site Met Office weather station.

2.2 Soil Sampling and Preparation

Soil samples were collected in February 2015, prior to any fertiliser or FYM applications or ploughing of the soil in preparation for the 2015-2016 growing season. Three replicate auger borings were sampled from within each plot using a 'Dutch' hand auger (5 cm x 20 cm blade). Two soil layers were collected, designated as topsoil (0 to 20 cm) and subsoil (20 to 40 cm), based on a visual appraisal of horizons in the profile and the presence of an indurated layer at 40 cm depth which precluded sampling at greater depth.

The limitation when using a Dutch auger for soil sampling of sequential horizons is that topsoil tends to contaminate the subsoil sample by falling into the base of the first auger boring and by adhering to the sides of the subsoil sample during retrieval. This had the potential to compromise the primary aim of the project which was to clearly differentiate between P status in the topsoil and subsoil. Therefore, with the aim of obtaining pristine topsoil and subsoil samples, several measures were put in place to reduce the contamination of the subsoil with topsoil: (i) separate augers were used for topsoil and subsoil samples; (ii) the outside and the top section (c. 2 cm) of the subsoil sample were removed and discarded; (iii) the augers were brushed clean between each sample and washed between each treatment plot. Samples were initially retrieved from the field in sealable plastic bags.

In the Old Rotation, soil samples were collected from five out of six crop rotational phases: 1st year grass, 2nd year grass, 3rd year grass, under-sown barley and under-sown spring oats (**Figure 2.2**). Plots with root crops were not sampled. Soil samples were collected from the NK with GMP, NK with TSP and NK without P plots. The zero fertiliser plot is a soil nutrient exhaustion plot (that receives FYM additions at the beginning of the root phase in the rotation) and was also sampled. In total, 120 soil samples were collected.

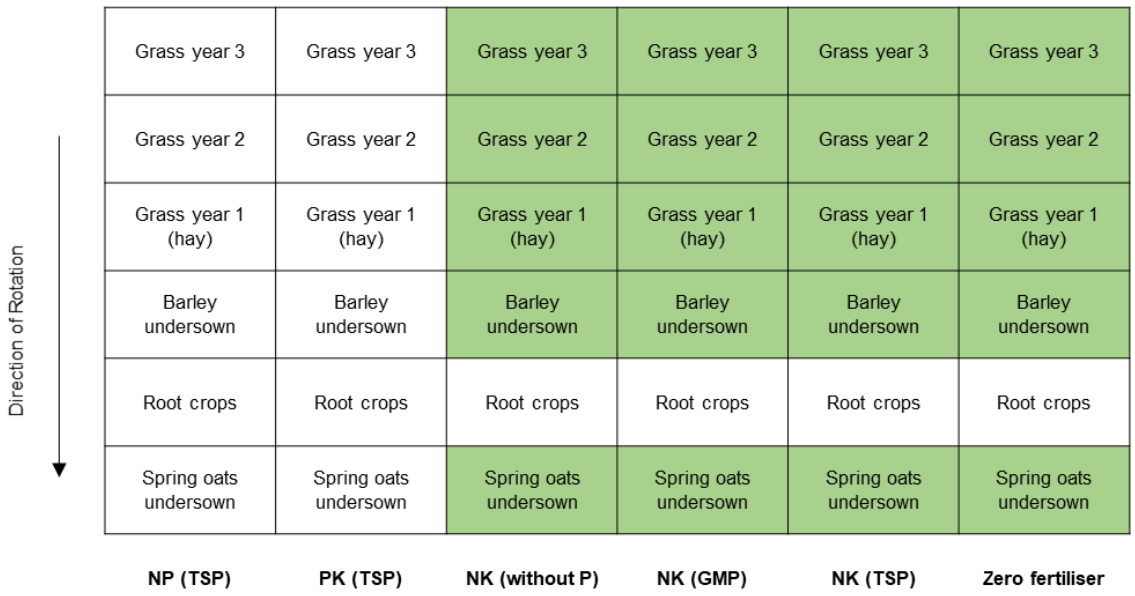


Figure 2.2. The layout of the Old Rotation experiment at the end of the 2014-2015 growing season with sampled plots highlighted in green.

In the pH Rotation, soil samples were collected from every pH increment within five out of the eight crop treatments: grass year 1, grass year 2, winter wheat, under-sown spring barley and under-sown spring oats (**Figure 2.3**). Third year grass was excluded because the plots had been ploughed and the winter wheat for the next growing season had already been sown. The two root crop treatments were also excluded. In total, 210 soil samples were collected.

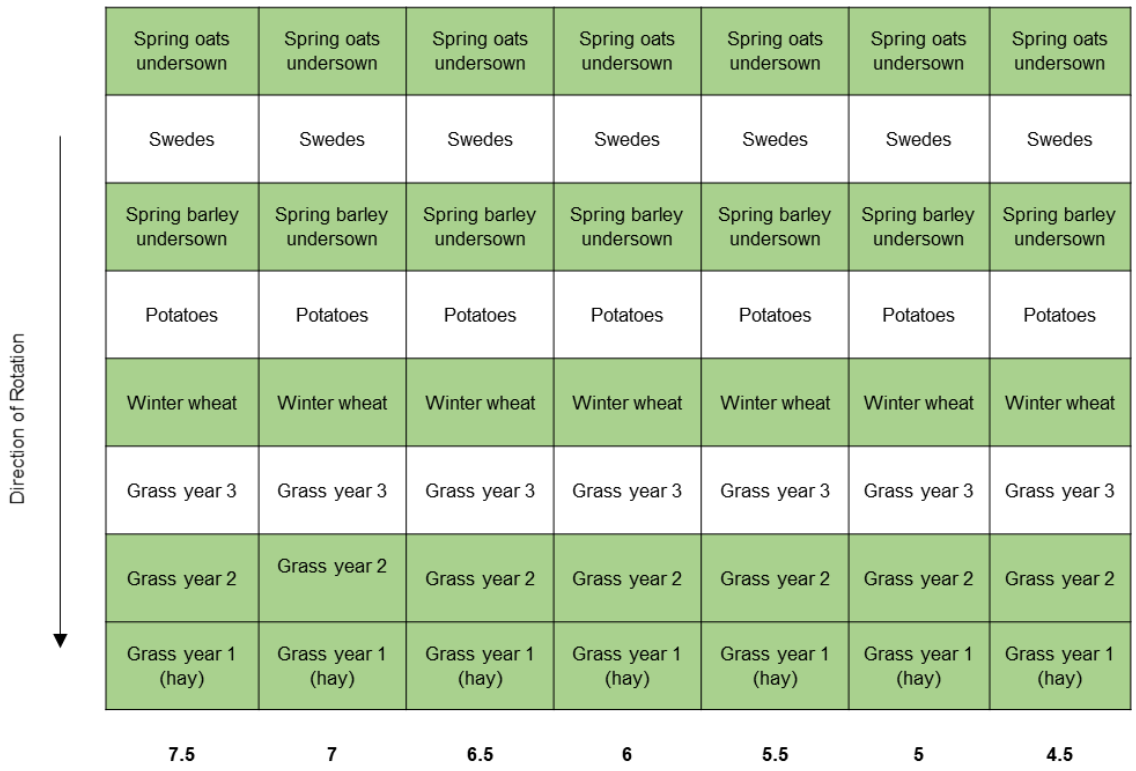


Figure 2.3. The layout of the pH Rotation experiment at the end of the 2014-2015 growing season, with sampled plots highlighted in green.

Additionally, three topsoil and three subsoil samples were collected from within Woodland's Field in an area not under agricultural management. These samples are assumed to represent soil conditions and nutrient status without the impact of long-term agricultural practice. In total, from native soil and both trials combined, 336 soil samples were collected. Later, in Decemer 2015, an additional six topsoil and six subsoil samples were collected from around Woodland's Field to get a more representative sample of the field as a whole, and to assess any spatial variability across the field, bringing the total soil samples collected to 348.

Soil samples were air-dried, sieved to < 2 mm and stored in re-sealable polythene bags. Sub-samples (c. 10 g) were finely ground in an agate ball mill (Planetary Ball Mill, PM400, Retsch GmbH, Haan, Germany) at 300 rpm for 6 minutes and stored in separate plastic sample bags for total carbon (%), total nitrogen (%) and total elemental analysis.

2.3 Crop Sampling and Preparation

Straw samples from wheat, oats and barley were collected from most plots following the 2014-2015 rotation. Crop samples were also obtained from most plots following the 2015-2016 rotation, including: hay (grass year 1); sward (grass year 2); grain (oats, wheat and barley) and tubers (swedes, turnips and potato). Some samples from acid (pH 4.5) or alkaline (pH 7.5) plots in the pH Rotation were unobtainable due to crop failure. Grab samples of the crops were randomly taken from within each plot and bulked together to obtain a heterogeneous mix of material.

Grain was threshed internally within the combine and sampled from the sampling spout of the combine as it was harvested. Swedes, turnips and potatoes were peeled and a core (approx. 1 cm diameter) was sampled and diced before drying. No above-ground leaves or haulms were sampled. Hay samples were a mixture of perennial ryegrass and clover with a minor component of weeds. Cereal and root/tuber samples were placed on foil trays and oven-dried at 80^{o}C (Gallenkamp, accuracy ± 2^{o}C). Grass and straw samples were oven-dried in plastic mesh bags, also at 80^{o}C. Grain, grass and straw samples were dried for 24 hours. Potatoes, swedes and turnips were dried for 48 hours and biomass measurements made on these. A heterogeneous sub-sample (c. 50 g) of all crops were milled using a titanium bladed Retsch mill (Grindomix GM200 knife mill) and stored in labelled 50 g plastic pots. The entire sample in each 50 g pot was finely ground by centrifugal milling (Ultra Centrifugal Mill ZM 200, Retsch) at 10,000 rpm.

2.4 Soil pH

Soil pH was determined in a suspension of 10 g soil: 25 mL de-ionised water (1:2.5), after shaking end-over-end (26 rpm) for 30 minutes. Measurement was with a combined glass electrode and a bench top pH meter (Hanna Instruments, product pH 209) calibrated at pH 4.01 and pH 7 with temperature compensation set to 24^{o}C.

2.5 Total Soil Carbon (%) and Nitrogen (%) Content

Total carbon and nitrogen content were determined by combustion of 20 mg of finely ground soil in tin cups (FlashEA 1112 NC Analyzer, Thermo-Fisher Scientific).

2.6 Total Elemental Analysis by ICP-MS

2.6.1 Acid Digestion of Soil Samples

Total elemental concentrations in soil were determined following digestion of 200 mg of finely ground soil with HF (40%), HNO_3 (70%), $HClO_4$ (70%) and 2.5 mL H_2O in a block digester (Model A3, Analysco Ltd, Chipping Norton, UK). All digestion reagents were either Analytical Reagent grade or, more commonly, 'Trace Analysis Grade' (e.g. Primar). Two mL HNO_3 plus 1 mL $HClO_4$ were added to the soil samples and run overnight for 8 hr at 80^{o}C and 2 hr at 100^{o}C. The following day, 2.5 mL HF was added and run overnight with a temperature ramp consisting of 1 hr at 120^{o}C, 3 hr at 140^{o}C and 4 hr at 160^{o}C. The digests were cooled the next morning before dissolving in 2.5 mL HNO_3 and 2.5 mL H_2O and heated for a final 1 hr at 50^{o}C. Digests were cooled, diluted to 50 mL in plastic volumetric flasks with Milli-Q water; an aliquot was stored at room temperature in a universal tube prior to multi-element analysis by ICP-MS.

2.6.2 Acid Digestion of Crop Samples

Duplicate sub-samples of ground plant material (c. 20 mg) were acid-digested in 6 mL nitric acid (70 %) at 140^{o}C using a Microwave Reaction System (Multiwave Pro; Anton Paar). Plant digests (6 mL) were then diluted to 20 mL with Milli-Q water, for storage, and finally diluted 1-in-11 with Milli-Q water prior to elemental analysis by ICP-MS (iCAPQ; Thermo Scientific).

2.6.3 Multi-Element Analysis by ICP-MS

Multi-element analysis of diluted solutions was undertaken by ICP-MS (Thermo-Fisher Scientific iCAP-Q; Thermo Fisher Scientific, Bremen, Germany). The instrument was run employing three operational modes, as appropriate, including: (i) a collision-cell (Q cell) using He with kinetic energy discrimination (He-cell) to remove polyatomic interferences, (ii) standard mode (STD) in which the collision cell is evacuated and (iii) hydrogen mode (H_2-cell) in which H_2 gas is used as the cell gas. Samples were introduced from an autosampler (Cetac ASX-520) incorporating an ASXpress™ rapid uptake module through a perfluoroalkoxy (PFA) Microflow PFA-ST nebulizer (Thermo Fisher Scientific, Bremen, Germany). Internal standards were introduced to the sample stream on a separate line via the ASXpress unit and included Ge (10 µg L^{-1}), Rh (10 µg L^{-1}) and Ir (5 µg L^{-1}) in 2% HNO_3 or 1.5% H_2SO_4. External multi-element calibration standards (Claritas-PPT grade CLMS-2 from SPEX Certiprep Inc., Metuchen, NJ, USA) included Ag, Al, As, Ba, Be, Cd, Ca, Co, Cr, Cs, Cu, Fe, K, Li, Mg, Mn, Mo, Na, Ni, P, Pb, Rb,

S, Se, Sr, Tl, U, V and Zn, in the range 0 – 100 µg L^{-1} (0, 20, 40, 100 µg L^{-1}). A bespoke external multi-element calibration solution (PlasmaCAL, SCP Science, France) was used to create Ca, Mg, Na and K standards in the range 0-30 mg L^{-1}. Phosphorus, boron and sulphur calibrations utilized in-house standard solutions (KH_2PO_4, K_2SO_4 and H_3BO_3). In-sample switching was used to measure B and P in STD mode, Se in H_2-cell mode and all other elements in He-cell mode. Sample processing was undertaken using Qtegra™ software (Thermo-Fisher Scientific) utilizing external cross-calibration between pulse-counting and analogue detector modes when required. Soil acid digests were diluted 1 in 2 (5 mL sample:5 mL Milli-Q water (18.2 MΩ cm)), instead of the 10 or 100-fold dilutions normally employed at this stage, in order to maximise P concentrations in solutions introduced to the instrument. Data were corrected for blanks which were run on a 1-in-3 (2.5 mL:5 mL) dilution. Quality of analysis was assessed by inclusion of certified reference materials (Montana soil NIST 2711A and Tomato leaves NIST 1573A) and re-analysis of P standards. The average recovery of the certified reference materials was > 90% (n = 23, standard deviation ± 10%). Phosphorus data was measured in KED mode using Rh and Ir as the correcting internal standard. For soil analysis, Ge could not be used as a standard due to high soil Ge concentrations arising from the minimal sample dilution employed.

2.7 Phosphate Extractions

2.7.1 Olsen P

Soil samples were extracted with a modified version of the Olsen method using a soil to solution ratio of 1 g: 15 mL compared to the original ratio of 1 g: 20 mL (Olsen, *et al*., 1954). This modification could potential result in an overestimation of the Olsen extractable-P concentration. Air dried, sieved (< 2 mm) soil (c. 2.0 g) was weighed into a 50 mL centrifuge tube and suspended in 30 mL of 0.5 M $NaHCO_3$ with half a teaspoon of 'low-phosphate' activated charcoal. Samples were shaken end-over-end (30 minutes, 26 rpm), centrifuged (1500 ***g***, 15 minutes) and an aliquot of the supernatant was removed for colorimetric determination of phosphate. Typically, samples were run in triplicate.

2.7.2 Modified Morgan P

Air dried, sieved (< 2 mm) soil (c. 6.0 g) was weighed into a 50 mL centrifuge tube and suspended in 30 mL of ammonium acetate/acetic acid (pH 4.5) solution containing 5 mL L^{-1} 0.05% w/v polyacrylamide solution. Samples were shaken end-over-end (26 rpm, 30 minutes), centrifuged (1500 ***g***, 15 minutes) and an aliquot of the supernatant was removed for colorimetric determination of phosphate.

2.7.3 Colorimetric Determination

The amount of phosphate in soil samples, extracted as Olsen P and Modified Morgan P, was determined by spectrophotometric analysis of the blue phospho-molybdate complex using an adapted version of the method of Murphy & Riley (1962) on a spectrophotometer (Ce1011, Cecil Instruments, Cambridge, UK). Calibration standards covered the range 0, 10, 20, 30, 40, 50 µg P (in 50 mL volume) were produced using 0, 1, 2, 3, 4 and 5 mL of a working phosphate standard (10 mg L^{-1}) combined with 4 mL ascorbic acid and 4 mL of acid molybdate reagent (AMR) and diluted to a total volume of 50 mL with Milli-Q water in volumetric glassware. The colour was allowed to develop for 20 minutes and absorbance was measured at 880 nm in a 1 cm path-length cuvette. The calibration line was linear in the range of P standards used and a typical example for the high phosphate standard range is shown in **Figure 2.4**. For samples, an aliquot (c. 5 to 20 mL) was added to 50 mL volumetric flasks. Where an alkaline (bicarbonate) extraction was performed, samples were diluted slowly with 4 mL of AMR and left for a few minutes to de-gas. Once the solution was no longer effervescent it was diluted further with 4 mL of ascorbic acid and then to 50 mL with Milli-Q water. With non-alkaline extractants, the method was the same but without the need to wait for the solution to de-gas.

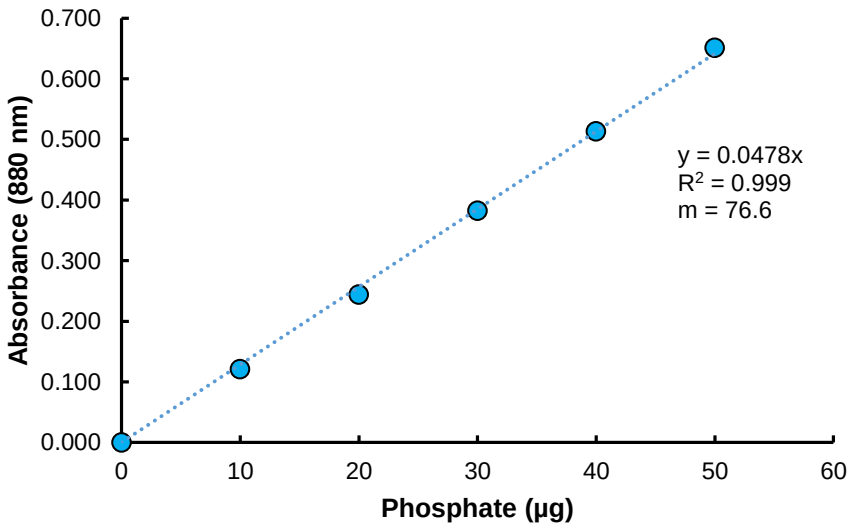


Figure 2.4. An example of the linear calibration for the high phosphate standard range of 0 to 50 µg P and typical absorbance values measured at 880 nm.

2.8 Statistical Analysis

2.8.1 Dendrogram Cluster Analysis and Pearson Correlation Coefficient Matrices

For topsoil and subsoil from each of the two field experiments, Dendrograms were produced using Minitab® 17 Statistical Software to investigate elemental relationships arising from the underlying soil geochemistry and from management practices. The Dendrograms also provided an overview of significant correlations between individual soil properties. Pearson Correlation Coefficients for the total elemental analysis and other soil characteristics were conducted on the dataset, using all unique samples, with no exclusion of soil layer or crop phase. Linear relationships between data were measured and assessed by Pearson Correlation Coefficients.

2.8.2 Analysis of Variance

The Woodlands Field Rotations were originally set up as demonstration trials for local farmers and the Old Rotation was set up before statistical procedures were established before the classical works of Fisher in 1926 and 1935 and so the plot layouts were not designed for statistical analysis purposes. However, the sampling strategy used in this study was designed to overcome some of the statistical limitations. First, each unique plot was assigned a number, with each auger given the value 1, 2 or 3. Second, topsoil and subsoil samples were taken from the same auger boring and separated, being assigned a layer factor of either topsoil or subsoil. These measures allowed an analysis of variance to be conducted using a Blocking structure of plot/auger in GenStat® (17^{th} ed.), and a Treatment combination of (crop*plottreatment)*layer to get the residual mean square for the plot treatment and the soil layer, followed by a second analysis of variance (crop+treatment)*layer to achieve an assessment of the crop phase effect.

2.8.3 Polynomial Regression Analysis of Soil Properties in the pH Rotation experiment

Polynomial regression analysis was applied to soil data from the pH Rotation experiment. The aim was to determine whether long-term soil pH management had resulted in changes in topsoil and subsoil elemental concentrations compared to the (unmanaged) surrounding area. The objectives were (i) to fit a model that best described the trend in P and element concentrations with soil pH in both topsoil and subsoil through a series of polynomial equations at 95% confidence and analysis of the accumulated analysis of variance of crop x measured pH; (ii) to use the optimised polynomial equation to predict what

the natural field concentration of a soil property would be based on the measured pH of the field topsoil and subsoil, from the model using the measured soil pH values of the pH plots and excluding the crop as a group; (iii) to determine whether the measured value in the field was significantly different to the predicted value, using 3 times the standard error of the mean output produced by the prediction as confidence limits (± standard error of the mean (SEM) of the predicted value from the model output). If the measured value fell within this range, the conclusion was that there was no effect of soil pH on the natural concentrations in the soil; if the measured value fell out with this range, this suggested a significant effect of long-term soil pH management on the soil characteristics tested across the pH range (see **Table 10.31** in **Appendix 4**).

2.9 Plot P Balance Calculations

2.9.1 Crop P Calculations

To calculate crop removal of P, crop yield data were first converted to 100% dry matter yield (t ha^{-1}), and then to kg ha^{-1} by multiplying by 1000, to obtain the weight of crop removed (kg ha^{-1}). The crop P concentration (mg kg^{-1}) was multiplied by the weight of crop removed (kg ha^{-1}) and divided by 10^6 to obtain the weight of P removed by the crop (kg ha^{-1}). These results were compared to P fertiliser inputs (kg ha^{-1}) and P remaining in soil (kg ha^{-1}) for a simple P balancing exercise for total and available P concentrations.

2.9.2 Plot P Balance and Annual Accumulation Rates

To calculate differences between P inputs and offtakes in soil and crop samples, soil concentrations (mg kg^{-1}) were converted to kg ha^{-1} by multiplying by 2.4, assuming that soil bulk density was 1.2 g cm^{-3} and soil depths for each layer was 20 cm (based on the depth of sampling) to give 2400 t ha^{-1} in each layer. To calculate net accumulation rates in the soil, the concentration of P (kg ha^{-1}) in the field surrounding the trials was subtracted from the total concentrations in the plot (topsoil plus subsoil) within treatments plots (also in kg ha^{-1}) and divided by the number of years the trial had been running (54 years for pH Rotation and 93 years for Old Rotation).

3 Topsoil and Subsoil Audit of Phosphorus and Associated Elements in the Woodland's Field Long-Term Experiments

3.1 Abstract

The effect of soil pH control, crop rotation and P fertiliser use on the accumulation and distribution of total P stocks (P_{Total}) and associated P fertiliser contaminants (As, Cd and U) in the topsoils and subsoils of two long-term field experiments was investigated. In the Woodland's pH Rotation, topsoil pH was managed through the use of lime and this resulted in a subsoil pH value which matched the plot target value (pH 4.5 to 7.5 in 0.5 increments). The total calcium (Ca_{Total}) increased from 7000 to 13,000 mg kg^{-1} between pH 4.5 and 7.5. The long-term application of TSP fertiliser resulted in total P stocks (P_{Total}) in the topsoil becoming significantly elevated compared to the uncultivated grassland (Field) surrounding the plots. Subsoils were not significantly elevated. The topsoil P_{Total} was greatest at pH 4.5 and least in the subsoil at the same pH, with a topsoil: subsoil ratio of 1.84. As the soil pH increased, topsoil and subsoil P_{Total} converged at pH 6 resulting in a topsoil: subsoil ratio of 1.40. This showed that P_{Total} was more readily re-distributed in the optimum pH range for arable crops and also where P is most soluble compared to the acid plots < pH 5.5 were P is adsorbed and retained on to Fe and Al oxides. The average net annual P_{Total} accumulation rate in the soil profiles of the pH Rotation plots ranged from 0.86 to 51.5 kg ha^{-1} yr^{-1} with no particular pH trend. In the Old Rotation, regardless of fertiliser treatment strategy (NK with TSP or GMP or without P, and zero fertiliser application), the soil profile P_{Total} was depleted compared to the Field, with net annual P_{Total} depletion rates ranging from -0.9 to -22.2 kg ha^{-1} yr^{-1} depending on fertiliser management strategy. The extent of depletion was less when TSP and GMP fertiliser were applied and both fertilisers maintained similar topsoil P_{Total} levels. These results show that crops in long-term rotation accessed native subsoil P_{Total} reserves. Finally, elevated As, Cd and U levels were associated with fertiliser use: Cd with GMP and U with TSP. Across both long-term experiments, the maximum of As_{Total} (7.75 mg kg^{-1}) found was five times less than the limit that can be applied from sewage sludge to agricultural land. The maximum Cd_{Total} (0.295 mg kg^{-1}) was ten times less than the limit from sewage sludge use. Both As_{Total} and Cd_{Total} levels arising from long-term P fertiliser use are not concerning in these trials.

3.2 Introduction

Improving phosphorus (P) use efficiency in agriculture is important for food security (George, *et al*., 2016) and reducing demand on globally finite resources (Cordell & White, 2015). Long-term use of P fertiliser in agriculture has led to the accumulation of surplus P in arable soils (Withers, *et al*., 2001) with P inputs generally exceeding P removal by crops (Sattari, *et al*., 2012). Furthermore, extended P fertiliser use may also result in the accumulation of contaminants such as As, Cd and U throughout the soil profile (Bigalke, *et al*., 2017; Hartley, *et al*., 2013; Schipper, *et al*., 2011; McDowell, 2012; Hao, *et al*., 2011; Kuo, *et al*., 2007). Efficient management and utilisation of residual 'legacy' P in agriculture is expected to improve P fertiliser use efficiency and provide economic benefits as well as wider environmental benefits (Withers, *et al*., 2014) such as improving water quality by reducing diffuse pollution to water resources (Sharpley, *et al*., 2013). Further research and innovative solutions are required to sustainably manage residual soil P stocks (Menezes-Blackburn, *et al*., 2017). However quantifying topsoil P stocks alone is insufficient for understanding the distribution of P in agricultural soils, and more research is required to understand subsoil P dynamics (Andersson, *et al*., 2013).

Studies utilising long-term experiments have shown that a significant proportion of the overall soil P content may be stored in the subsoil layers (Barej, *et al*., 2014). Agricultural subsoils have been shown to accumulate P where there is an extended history of P fertiliser application (Ahmed, *et al*., 2014; Rubæk, *et al*., 2013; Pizzeghello, *et al*., 2014) and P may be rapidly transferred to subsoil layers particularly when topsoils are saturated in P (De Bolle, *et al*., 2013). The interaction between phosphate fertiliser type and soil texture can have a significant influence on the distribution of applied P throughout the soil profile, with P re-distribution to deeper soil layers more likely in sandy or peaty soils compared to clay soils where P is retained more in the topsoil (Pizzeghello, *et al*., 2014). Furthermore, the solubility and lability of P fertiliser applied affects the transfer of P; farm-yard manure may be more labile and susceptible to leaching (Pizzeghello, *et al*., 2011) but mineral fertiliser may also migrate to deeper soil layers (Pizzeghello, *et al*., 2014). The restriction of P in the topsoil may drive crops to utilise subsoil P reserves, explaining 'unaccounted for' P in crop P offtake, in which P outputs exceed inputs (Richards, *et al*., 1995). However, deficiencies of topsoil P do not necessarily promote uptake of subsoil P and the acquisition of P from the subsoil by crops may be more efficient when there is a sufficient supply of P in the topsoil (Bauke, *et al*., 2018). Short-term cropping has been shown to have no effect on subsoil P uptake where topsoil P supplies were considered ideal (Barej, *et al*., 2014). However, subsoil P accumulation was evident in soil profiles following 24 years of P fertiliser application in double cropping systems in China (Khan, *et al*.,

2018). Decomposition of deep crop roots in the subsoil is also thought to contribute to an increase in subsoil P levels in long-term crop rotation experiments (Campbell, *et al*., 1993). Under various fertiliser regimes across field experiments in Switzerland (no P fertiliser, P fertiliser input to match output by crop offtake, and P fertiliser in excess of crop requirements), significant reductions in total and inorganic P stocks in the subsoil (30 to 50 cm depth) were only observed in one of seven field sites when P fertiliser was restricted over a 9-year period (Gallet, *et al*., 2003).

The activity of phosphate in soil solution, and thus the potential for topsoil to subsoil transfer is mainly controlled by soil pH. The maximum solubility of P is observed between pH 6 and 7 (Lindsay, 1979) which is also the target pH range for arable crops (AHDB, 2107) and so the likelihood of P leaching to subsoil may be greatest within this range. However, many UK arable and grassland soils are below the optimum soil pH (Goulding, 2016) and this has implications for the accumulation or transfer of P in the soil profile. Furthermore, crops experience aluminium stress and toxicity at acidic pH values (Sade, *et al*., 2016) which could result in low P use efficiency due to poor crop production and low yield compared to the more optimal pH values between pH 6 and 7 (Walker, *et al*., 2011). However, few field-based studies have investigated the effect of long-term pH management on the distribution of P in the topsoil and subsoil across a pH gradient. In the UK, a study on the Hoosefield acid strip at Rothamsted Research showed that total topsoil P concentrations did not vary significantly across a pH gradient (pH 3.73 to 7.83) after an extended period (c. 150 years) without P fertilisation (Turner & Blackwell, 2013). Using a long-term crop rotation experiment in Germany, von Tucher, *et al*., (2018) showed that crop yields of sugar beet and winter barley may be lower at sub-optimal pH levels (pH 4.7 to 5.3) compared to raising the soil pH to a target range (pH 6.0 to 6.4) but found that winter wheat yields were more resilient to sub-optimal pH values. Furthermore, von Tucher, *et al*., (2018) showed that liming the soil to raise the pH improved crop growth at soil P test values below recommended levels however, the authors noted that they did not analyse the subsoil layers but suggested future research should consider subsoil P in field experiments. Therefore, more field-based studies are required to understand the effect of a range of soil pH values on soil P distribution. Trace contaminants found in P fertilisers can be elevated in agricultural soils as a consequence (Ahmed, *et al*., 2014; Schipper, *et al*., 2011; Hartley, *et al*., 2013) and soil pH is important in determining the bio-availability of these trace contaminants i.e. Cd (Gray, *et al*., 1999) which is more strongly adsorbed as soil pH rises from acid to neutral (Evans, *et al*., 2003). The sorption of U is influenced by soil pH as UO_2^{2+} interacts with carbonates and increasing the soil pH results in U being less strongly adsorbed on soil surfaces (Echevarria, *et al*., 2001). The interaction between As and P is also

influenced by soil pH because arsenate and phosphate ions compete for binding sites particularly at acidic pH values (Deng, *et al*., 2018). Currently, there are no guidelines or limits on the introduction of contaminants to agricultural soils specifically through P fertiliser use in the UK. However, there are limits to the concentrations of As and Cd in agricultural soils arising from sewage sludge application (The Sludge (Use in Agriculture) Regulations, 1989). For As, the limit is 50 mg kg^{-1} and for Cd it is 3 mg kg^{-1} in arable soils maintained at a soil pH greater than pH 5.0. (The Sludge (Use in Agriculture) Regulations 1989). Baseline levels of contaminants in soils and herbage have also been established for As, Cd and U at a national and country scale in the UK and provide another reference (UK Soil Herbage and Pollutant Survey Report (No. 7); Ross, *et al*., 2007). In rural Scotland, background concentrations of As range between 0.5 and 143 mg kg^{-1}, for Cd it is between 0.10 and 1.80 mg kg^{-1} and the average U concentration is 0.653 mg kg^{-1} (UK Soil Herbage and Pollutant Survey Report (No. 7), Ross, *et al*., 2007).

There are two unique and underutilised long-term experiments based at SRUC's Craibstone Estate, Aberdeen where the effect of long-term pH control, fertiliser management and ley/arable rotational cropping on the distribution of P and associated contaminants could be investigated. The 'Old Rotation', established in 1922, has a series of plots with different NPK fertiliser strategies. The 'pH Rotation', established in 1961, consists of plots in which soil pH is controlled to cover the range 4.5 to 7.5, in increments of 0.5 pH units.

3.2.1 Aims and Objectives

The aims of this chapter were to understand the effects of continuous pH management, rotational cropping and fertiliser use on the distribution of P reserves and associated elements in the topsoil and subsoil of the Woodland's Field long-term experiments. The hypothesis was that long-term application of P fertilisers, soil pH control and rotational cropping results in the accumulation of P and fertiliser contaminants i.e. arsenic, cadmium and uranium in the topsoil. Furthermore, if reactive P from fertilisers accumulates in the topsoil over the long-term, this could result in the migration of P to the subsoil. Fertiliser type may influence this as soluble fertilisers are more likely to be transferred to the subsoil compared to insoluble P fertilisers. Differences in the P distribution throughout the soil profile as a result of pH control is anticipated to result in greater P retention in acidic topsoils (< pH 5.5) due to adsorption with increased movement to the subsoil anticipated to occur at c. pH 6 where calcium P minerals are most soluble. The experimental objectives are listed below.

1. Audit and contrast the concentration of P in topsoil and subsoil (P_{Total}), and concentrations of other elements, in the Woodland's 'Old Rotation' in order to examine the impact of historical crop rotation and fertiliser management strategies on P distribution within the soil profile.
2. Audit and contrast the concentration of P in topsoil and subsoil, and concentrations of other elements, along the pH gradient in the Woodland's 'pH Rotation' to examine the impact of crop rotation, soil pH control and TSP fertiliser use on P distribution within the soil profile.

3.3 Materials and Methods

Full details of the long-term experiments used in this study are described in **Chapter 2 Materials and Methods** which outlines the sample site and description of the trials (**section 2.1**), trial management (**section 2.1.1**), soil sampling and preparation (**section 2.2**), crop sampling and preparation (**section 2.3**) and various soil analyses such as soil pH (**section 2.4**), total carbon and nitrogen (**section 2.5**), total element analysis (**section 2.6**) and the statistical analysis (**section 2.8**). In this study, air-dried, sieved (< 2 mm) topsoil and subsoil samples from all three replicate auger borings in each treatment plot were selected from all seven target pH plots (pH 4.5 to 7.5 in 0.5 unit increments) under five crop phases in the pH Rotation (grass (1^{st} and 2^{nd} year), winter wheat, spring oats and spring barley) and also from the four fertiliser treatment plots (NK with GMP, NK with TSP, NK without P and zero fertiliser) under five crop phases in the Old Rotation (grass (1^{st}, 2^{nd} and 3^{rd} year), spring oats and spring barley). All of the soil samples from the uncultivated grassland field (Field) surrounding the trials (9 topsoil and 9 subsoil) were also analysed. For P balancing between fertiliser inputs and crop offtakes (**section 2.9**), crop samples were obtained for most plots in the pH Rotation including samples of root crops (these plots were not sampled for soil). Furthermore, crop samples were obtained for most plots in the Old Rotation and the three root crops in the split root plots were sampled (i.e. one third of the plot was potatoes, one third turnips, one third swedes). Crop samples from the two fertiliser treatment plots which were not sampled for soil were also obtained (P, N without K and P, K without N where the source of P was TSP in both cases). The calculations of the annual P accumulation rates for (i) the P balances in the crop offtakes vs P fertiliser application and (ii) the net annual accumulation rates of P in the soil profiles differences in the plots vs the Field surrounding the trials are explained in **section 2.9**.

3.4 Results and Discussion

3.4.1 Background Soil Characteristics of Woodland's Field

Selected soil characteristics and total element concentrations of the uncultivated, grassland area of Woodland's Field surrounding the trials (Field) are shown in **Table 3.1**. The soil contaminants commonly associated with P fertiliser use are As, Cd and U and so are presented in addition to P, Ca and pH, to assess the effect of fertiliser treatment, and pH control in the trials by comparison with native levels of As_{Total}, Cd_{Total} and U_{Total} in the Field. The 'native, background' soil properties in the Field are thus used as a reference to characterise the effect of the long-term experiments under the assumption that the soil characteristics have not changed for the duration of the experiments (54 and 93 years). The caveat to this assumption is that the total elements in the field may be affected by their proximity to the long-term experiments which receive high concentrations of elemental inputs from lime and fertiliser application or the application of trace element sprays. Furthermore, aerial inputs from dust or animal excrement may contribute to raising total elemental concentrations. For example, woodland areas adjacent to arable fields may be enriched from the excrement of roosting birds which likely consume the grain from the crops grown in the experiments (Ahmed, *et al*., 2014) and may also feed on insects which feed on the crops. The grass in the field is cut and left to mulch which would allow for the process and mechanisms of slow accumulation and turnover to occur.

The Counteswells Association is a naturally acidic soil; the topsoil and subsoil pH values in the field were pH 5.66 and 5.98 respectively (**Table 3.1**). The average P_{Total} in the topsoil was 1380 (± SEM 136 mg kg^{-1}) and the subsoil P_{Total} was 1100 (± SEM 123 mg kg^{-1}); the topsoil: subsoil P_{Total} ratio was 1.25. These levels exceed the total P in mineral soils (aqua regia) of Scottish topsoils which are reported to have a mean of 896 mg kg^{-1} (n = 291) and a median of 813 mg kg^{-1} (n = 291) (Paterson, *et al*., 2011). Throughout the profile the Ca_{Total} was fairly uniform with a topsoil: subsoil ratio of 0.96 and an average topsoil Ca_{Total} of 7880 mg kg^{-1} (± SEM 117 mg kg^{-1}) and subsoil Ca_{Total} of 8240 mg kg^{-1} (± SEM 290 mg kg^{-1}). These values were 1.78x (topsoil) and 1.86x (subsoil) the reported mean total Ca (aqua regia) in mineral topsoils in Scotland (4439 mg kg^{-1}, n = 291) (Paterson, *et al*., 2011). The As_{Total} was greater in the topsoil (6.69 mg kg^{-1} ± SEM 0.34 mg kg^{-1}) than the subsoil (5.94 mg kg^{-1} ± SEM 0.26 mg kg^{-1}) with a topsoil: subsoil ratio of 1.13 likely due to the direct application of P fertiliser to the topsoil. The topsoil and subsoil As_{Total} values fell within the expected 'background' As concentration range of 0.5 to 143 mg kg^{-1} for rural soils in Scotland and were less than the mean (10.9 mg kg^{-1}) and median (7.1 mg kg^{-1}) values

(SD ± 17.2 mg kg^{-1}) reported in the UK Soil Herbage and Pollutant Survey Report (No. 7) (Ross, *et al*., 2007, p. 23). The Cd_{Total} was also greater in the topsoil (0.23 mg kg^{-1}) than the subsoil (0.17 mg kg^{-1}) with a topsoil: subsoil ratio of 1.34. Both topsoil and subsoil Cd_{Total} were within the expected 'background' Cd concentration range of 0.10 to 1.80 mg kg^{-1} for Scottish rural soils as reported by the UK Soil and Herbage Pollutant Survey (Ross, *et al*., 2007, p.6). The Cd_{Total} was also significantly less than the maximum permissible limit of 3 mg kg^{-1} for arable soils receiving sewage sludge (The Sludge (Use in Agriculture) Regulations, 1989). Topsoil and subsoil U_{Total} were near identical with an average of 1.89 mg kg^{-1} (SEM ± 0.01 mg kg^{-1}) and a topsoil: subsoil ratio of 1.00. The U_{Total} was above the average background U_{Total} of 0.653 mg kg^{-1} in Scottish rural locations (Ross, *et al*., 2007, p.118). The N_{Total} was 0.38% (± SEM 0.01%) in the topsoil and 0.23% (± SEM 0.02%) in the subsoil, with a topsoil: subsoil ratio of 1.67. The C_{Total} was 5.50% (± SEM 0.25%) and 4.14% (± SEM 0.15%) in the topsoil and subsoil respectively with a topsoil: subsoil ratio of 1.33. The results for N_{Total} and C_{Total} suggested that the topsoil contained more organic matter than the subsoil. The C_{Total} in Woodland's Field appeared rather high at 5.5% (topsoil) and 4.14% (subsoil) compared to the organic carbon (%) in the long-term experiments at Rothamsted Research which contain less than 4% (Poulton, *et al*., 2018). However, Woodland's Field has been under permanenent grassland and receives moe rainfall whereas the data from the Rothamsted Research experiments reflect agricultural soils over a range of treatment conditions such as fertiliser management or restriction strategies (mineral fertilisers, farm yard manure, sewage sludge, composts for example) and different cropping strategies.

Table 3.1. Selected topsoil and subsoil properties of the uncultivated Woodland's Field grassland area. Values are the average of 9 representative sample auger borings collected from the field, with ± SEM.

	Topsoil	Subsoil	Topsoil: Subsoil Ratio
pH	5.66 ± 0.09	5.98 ± 0.10	0.95
N_{Total} (%)	0.38 ± 0.01	0.23 ± 0.02	1.67
C_{Total} (%)	5.50 ± 0.25	4.14 ± 0.15	1.33
P_{Total} (mg kg^{-1})	1380 ± 136	1100 ± 123	1.25
As_{Total} (mg kg^{-1})	6.69 ± 0.34	5.94 ± 0.26	1.13
Cd_{Total} (mg kg^{-1})	0.23 ± 0.02	0.17 ± 0.02	1.34
U_{Total} (mg kg^{-1})	1.89 ± 0.08	1.90 ± 0.08	1.00
Ca_{Total} (mg kg^{-1})	7880 ± 117	8240 ± 290	0.96

3.4.2 Topsoil and Subsoil Dendrogram Cluster Analyses of Soil Characteristics in the Long-Term Experiments

A multivariate cluster analysis was performed on the total element concentrations (and soil pH values) in the topsoils and subsoils of the Old Rotation (**Figure 3.1**) and pH Rotation (**Figure 3.2**). Generally, there are several main groupings expected in soils, arising from mineralogical and management considerations:

(i) C, N, P and S are associated with the organic matter fraction of soil (Tipping, *et al*., 2016);

(ii) alkali metal cations K, Cs and Rb are associated with clay minerals, especially illitic or micaceous aluminosilicates (Zaunbrecher, *et al*., 2015);

(iii) the exchangeable alkali and alkali-earth cations Na, K, Mg, Ca and Ba may also be linked with clay minerals, especially those with a high cation exchange capacity, such as smectite and vermiculite (Vieillard, *et al*., 2011);

(iv) Cr and V are associated with oxides of Fe as Cr^{3+} and V^{3+} can substitute for Fe^{3+} (Schwertmann & Pfab, 1996) and vanadate (VO_4^{3-}) is adsorbed strongly on Fe oxides (Larsson, *et al*., 2017; Wisawapipat & Kretzschmar, 2017);

(v) Mn and Co may be associated because Co^{3+} substitutes for Mn^{4+} in Mn oxides (Burns, 1976);

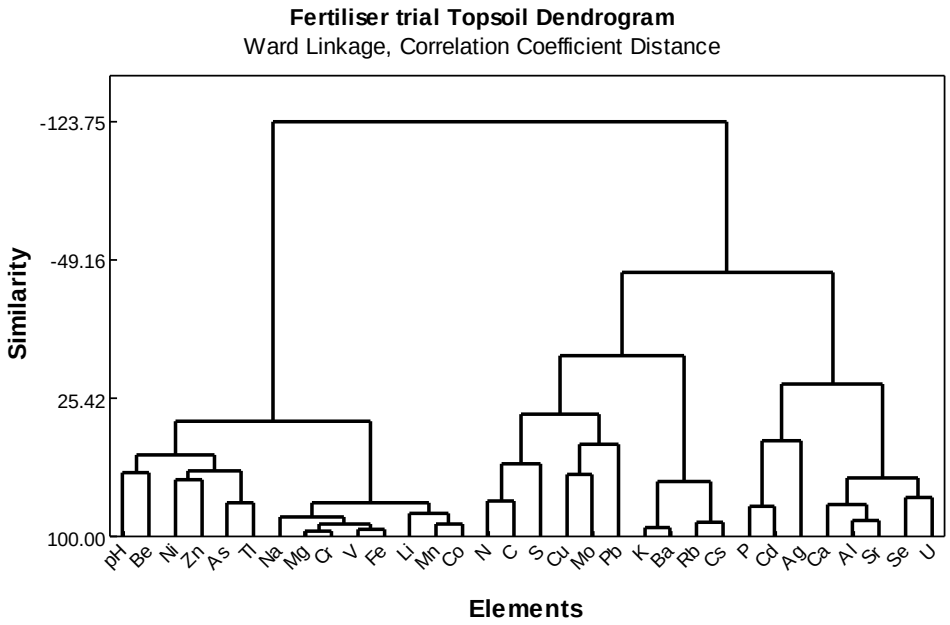
(vi) Sr and Ca often occur in a conservative ratio as Sr^{2+} isomorphically substitutes for Ca^{2+} in $CaCO_3$ (Capo, *et al*., 1998) reflecting either the soil parent material or sustained lime application;

(vii) several trace element associations may arise from prolonged phosphate fertiliser applications, most notably Cd (Kuo, *et al*., 2007; McDowell, 2012), U (Schipper, *et al*., 2011) and As (Hartley, *et al*., 2013).

As the topsoils and subsoils of both long-term experiments are taken from within the same Field and soil association, there may be little variation in background elemental associations. However, there may be treatment effects such as P fertiliser use or pH management which might result in anomalies or may produce new elemental associations. Differences between topsoil and subsoils may also be expected depending on mobility of applied soil amendments. For example, UO_2^{2+} solubility increases in the alkaline pH range through formation of complexes with carbonate (Elless & Lee, 1998). The significance of the main elemental associations is summarised in the Pearson Correlation coefficient matrices in **Appendix 1**

as follows - The Old Rotation topsoils (**Table 10.1**) and subsoils (**Table 10.2**) and also the pH Rotation topsoils (**Table 10.3**) and subsoils (**Table 10.4**).

The dendrograms for the Old Rotation topsoils and subsoils (**Figure 3.1**) confirm the main elemental associations expected in the soils. The soil organic matter fraction is reflected in the link between C, N and S throughout the soil profile. It was also confirmed that Rb and Cs are linked together throughout the profile. In the topsoil and subsoil exchangeable cations were not linked to Al; K and Ba were linked throughout, but Na and Mg were only grouped in the subsoils. The link between V and Fe in both topsoil and subsoil was found with broad links to Cr. Finally, there was a clear link in both topsoil and subsoil between Mn and Co. There was a clear effect of trial management in the link between Ca, Sr and U in the topsoil and Ca and Sr only in the subsoil. The main source of Sr will be through lime as Sr is included within $CaCO_3$. Furthermore, there was a strong association between P and Cd in the topsoils, likely due to phosphate fertiliser application (Kuo, *et al*., 2007; McDowell, 2012) to half of the treatment plots. This grouping was also broadly associated with U, Ca and Sr. Uranium is another soil contaminant potentially introduced in P fertiliser (McDowell, 2012; Ahmed, *et al*., 2014) but the solubility is likely to be strongly affected by soil pH and Ca content. The subsoil revealed a strong link between P and Cd suggesting that P fertiliser use may also have introduced Cd as a contaminant, and the Cd was quite mobile, which warrants further investigation.



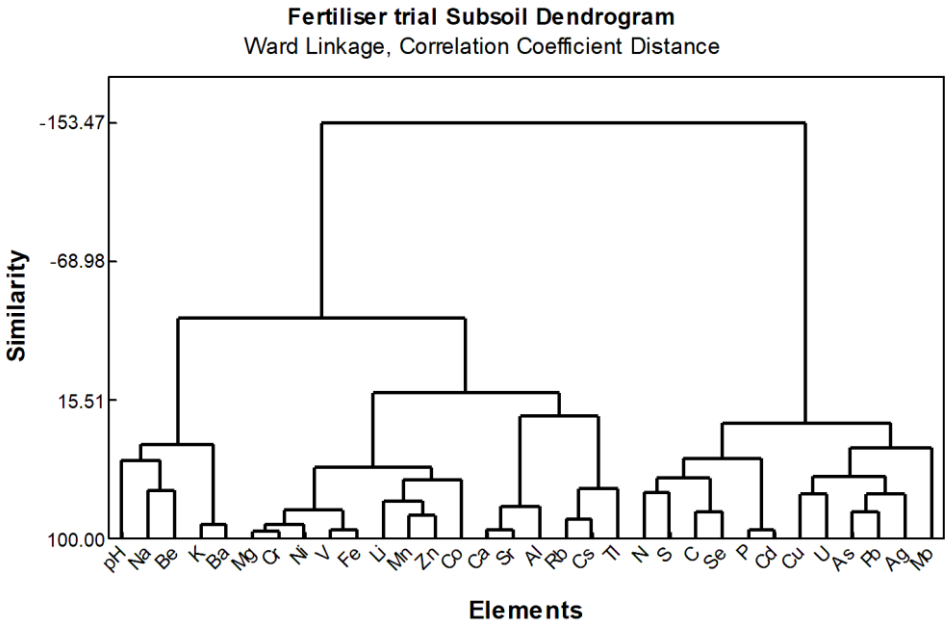


Figure 3.1. Soil characteristics dendrogram cluster analysis for the Old Rotation topsoils and subsoils.

The dendrograms in **Figure 3.2** show the main relationships between elements (and soil pH) in the topsoils and subsoils of the pH Rotation. The main element associations expected in the soil profile were confirmed in the dendrograms. First, the soil organic matter fraction was reflected in the link between N, C and P in the topsoil and subsoil. The alkali metals Cs and Rb were linked throughout the profile as expected and were closely related to both Al and Fe mineralogy in the topsoil and only Al in the subsoil. The exchangeable cations often associated with clay mineralogy were paired as Na and K in both topsoil and subsoil and then a pairing of Ba with Be only in the subsoil. There was a link between V and Cr in the topsoil and then V with Fe in the subsoil (due to the substitution of V with Fe in Fe oxides). Finally, in terms of what is expected, it was not clear why Mn and Co were unrelated in the pH Rotation soil profile. There was a clear, strong link between soil pH management due to a close association between pH, Ca and Sr throughout the topsoils and subsoils of the pH Rotation. The use of lime in the pH trial likely explains the association between pH, Ca and Sr in the topsoil and subsoil. Furthermore, the use of triple-superphosphate (TSP) in the pH Rotation did not seem to cause a link between P with contaminants in the topsoils – possibly due to the lack of contrasting application rates. However, P was closely linked to As, U and Cd in the subsoils which may reflect the use of phosphate fertilisers. The stronger association in the subsoil rather than the topsoil is unexpected but certainly suggested some degree of mobility to accumulate in the subsoil layer; subsoil accumulation of Cd and U has been observed previously (McDowell, 2012).

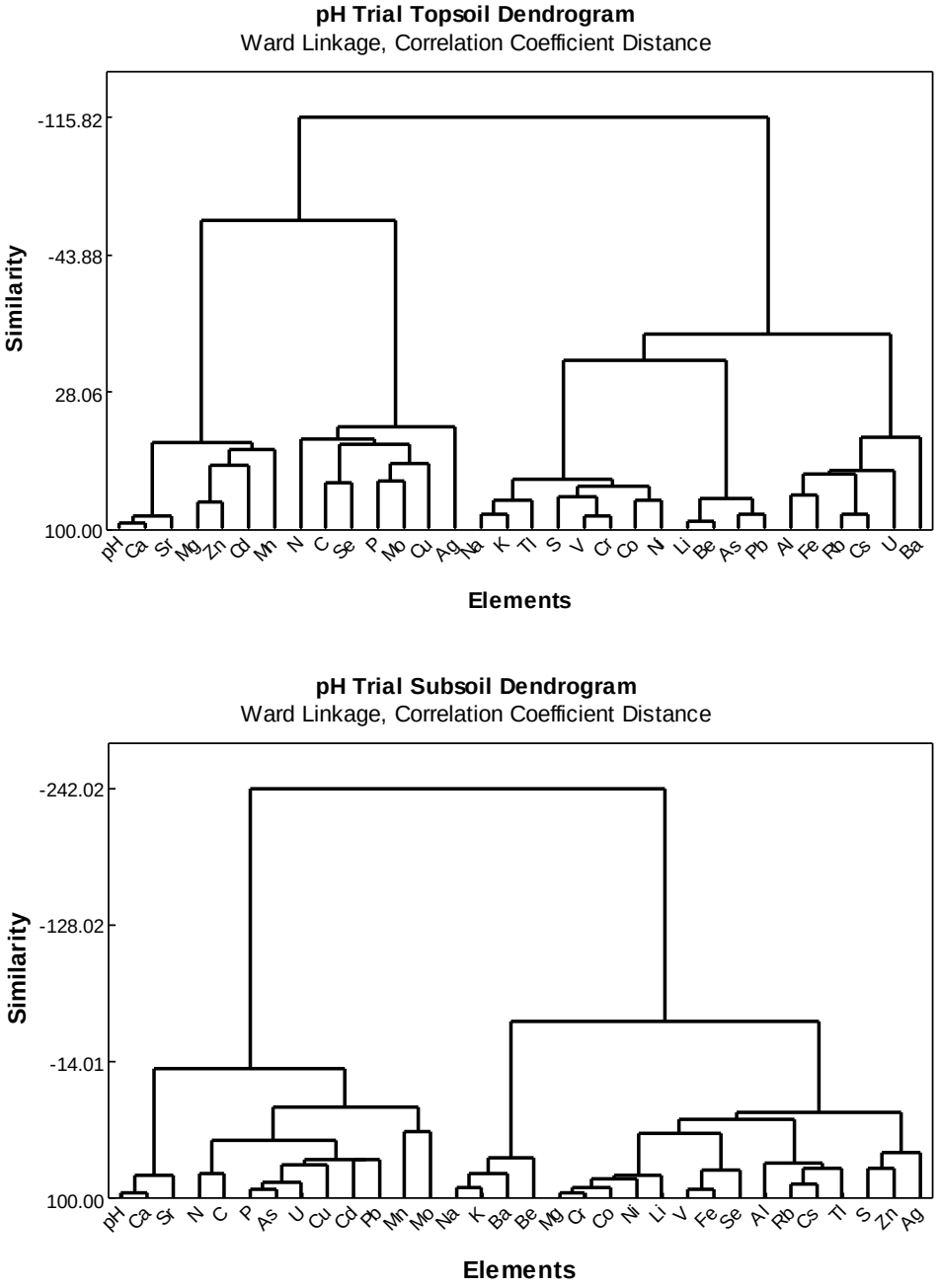


Figure 3.2. Soil characteristics dendrogram cluster analysis for the pH Rotation topsoils and subsoils.

3.4.3 Woodland's Field Old Rotation

3.4.3.1 Effect of Fertiliser Management on Topsoil and Subsoil P_{Total} in the Old Rotation

The relationship between fertiliser treatment and P_{Total} in the topsoils and subsoils of the Old Rotation and the Field is shown in **Figure 3.3**. The mean P_{Total} was equal in the topsoils treated with NK and either TSP (1290 mg kg^{-1} ± SEM 37.9 mg kg^{-1}) or GMP (1290 mg kg^{-1} ± SEM 36.8 mg kg^{-1}). When P fertiliser was restricted, the topsoil P_{Total} was slightly greater in the zero fertiliser plots (976 mg kg^{-1} ± SEM 26.4 mg kg^{-1}) than the NK without P plots (931 mg kg^{-1} ± SEM 13.4 mg kg^{-1}). The difference between the P_{Total} in the NK plus phosphate fertiliser plots and the NK without P plots was 359 mg kg^{-1}, equivalent to 862 kg ha^{-1} (see calculations in **section 2.9**). Continuous cropping without P fertiliser applications could have resulted in a depletion of native P stocks over time whereas the use of P fertilisers may have somewhat maintained the P levels in the soil relative to the Field which overall contained more P than the treatment plots. The average P_{Total} in the Field topsoil was 1380 mg kg^{-1} (± SEM 136 mg kg^{-1}), which was 90 mg kg^{-1} (or 216 kg ha^{-1}) greater than the P_{Total} in the topsoils of the TSP and GMP treated plots. The highest P_{Total} in the subsoils of the Old Rotation was in the NK with GMP plot at 1020 mg kg^{-1} (± SEM 49.9 mg kg^{-1}). The P_{Total} in the NK and TSP plot was on average 982 mg kg^{-1} (± SEM 45.1 mg kg^{-1}). The average subsoil P_{Total} in the zero fertiliser plots was 754 mg kg^{-1} (± SEM 26.7 mg kg^{-1}) and the average subsoil P_{Total} in the NK without P was 793 mg kg^{-1} (± SEM 30.6 mg kg^{-1}). The average P_{Total} in the Field subsoil was 1100 mg kg^{-1} (± SEM 123 mg kg^{-1}). The greatest difference in P_{Total} across the treatment plot subsoils was between the NK and GMP and the zero fertiliser plots at 266 mg kg^{-1} which was equivalent to 638 kg ha^{-1}. Compared to the P_{Total} in the subsoil of the Field, the NK and GMP plot was 80 mg kg^{-1} less whereas a difference between the Field and the zero fertiliser was 346 mg kg^{-1} (equivalent to 830 kg ha^{-1}). The relative decline of P_{Total} in the subsoils under all treatments compared to the Field subsoil suggested that that long-term cropping utilised subsoil P stocks under a variety of treatment and crop conditions, assuming that the Field represents native P and had not received significant inputs of P due to its proximity to the trials. The lack of P fertiliser input for 93 years in the NK without P plot, and the zero fertiliser plot, may have driven crops to utilise subsoil P reserves to meet P requirements to a greater extent than in plots receiving P as TSP or GMP. However restricting P fertiliser does not necessarily drive crops to utilise subsoil P and subsoil utilisation may be better when there are sufficient topsoil P levels (Bauke, *et al*., 2018). Short-term cropping is not shown to affect subsoil P removal (Barej, *et al*., 2014), but if the crops are accessing subsoil P it would explain why P offtakes through crop harvest (Richards, *et al*., 1995) continue when no P fertiliser has been applied for 93 years. In the phosphate fertiliser treated

plots, it is less clear to what extent crops relied on and/or supplemented P requirements from the subsoil, and whether long-term re-distribution of fertiliser P from the topsoil replenished and maintained the subsoil P that was depleted by crops. The mechanisms of topsoil to subsoil transfer are also not clear and require further investigation. Inputs to the subsoil may include rapid leaching of soluble P fertiliser (De Bolle, *et al*., 2013) or bacterial transport which could account for between 0.3 and 7.9% of total P leached (Glæsner, *et al*., 2016). Decomposition of plant roots in situ may also contribute to subsoil P reserves (Campbell, *et al*., 1993). Physical soil management strategies influence the distribution of available and organic species of P throughout the soil profile. Abdi, *et al*., (2014) showed that, in crop rotation systems, long-term ploughing and mixing of the topsoil resulted in uniform P species in the topsoil compared to no tillage practices, which resulted in uneven distribution of P to a depth of 15 cm. The authors found that Mehlich-3 extractable (inorganic) phosphate was concentrated in the top 5 cm of the profile due to a lack of soil mixing (compared to ploughing). Furthermore, some labile organic species were found to have migrated and accumulated deeper in the soil under no tillage conditions, likely due to leaching (Abdi, *et al*., 2014). The potential accumulation of reactive fertiliser P in the subsoil through leaching under contrasting P fertiliser management systems warrants further investigation to determine the availability of topsoil and subsoil P and understand the potential contribution of the subsoil to crop P requirements (see **Chapter 4**).

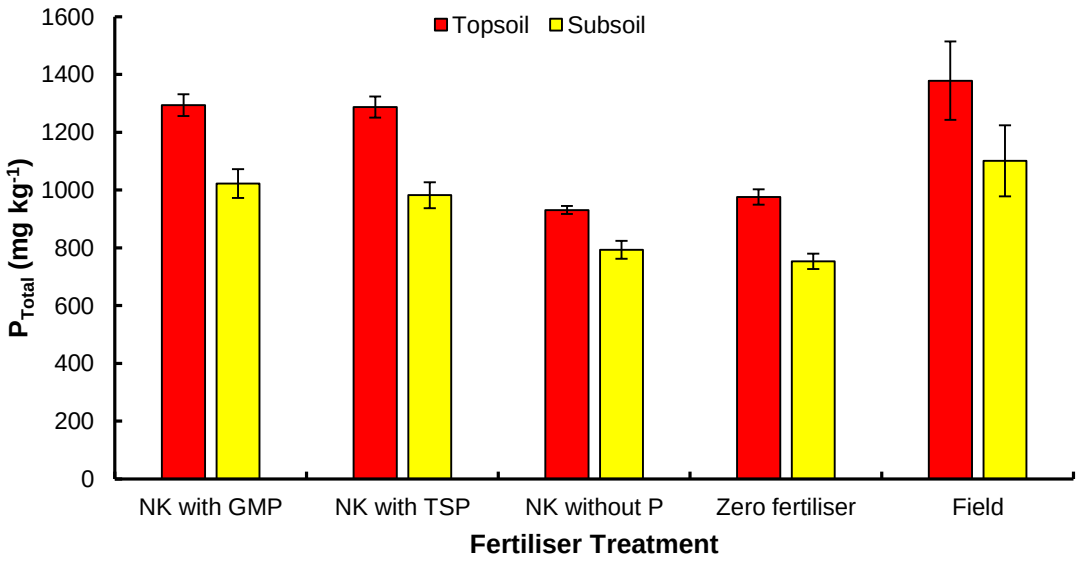


Figure 3.3. Comparison of the P_{Total} in the topsoil and subsoil in the fertiliser treatments plots and the Field. The mean P_{Total} in the treatment plots is of 5 crop phases (± SEM), and the field means (± SEM) are of 4 sample sites taken across the field.

3.4.3.2 Effect of Crop Phase on Topsoil and Subsoil P_{Total} in the Old Rotation

The effects of crop phase on P_{Total} in the topsoils and subsoils of the treatments plots in the Old Rotation are shown in **Figure 3.4**. A combination of fertiliser treatment and crop phase significantly influenced the P_{Total} in the soil layers (crop x treatment x layer, d.f. = 12, p = 0.002) across the plots (**Appendix 3**, **Table 10.9**). There was no obvious difference in P_{Total} in the topsoils attributable to crops in the zero fertiliser and NK without P plots. Under the NK with TSP treatment the P_{Total} appeared to increase under barley and oats which may reflect accumulation of residual fertiliser P in these crop phases (P fertiliser is applied at the beginning of these phases) compared to the lack of P inputs during the grass years. In plots treated with NK and GMP the P_{Total} was fairly uniform across the crops except for a slight elevation in grass year 2 plot which may be residual P fertiliser in that particular row of plots from previous cropping years. There did not appear to be a consistent effect of crop on subsoil P_{Total} in the zero fertiliser or NK without P plots. However, subsoil P_{Total} was elevated under oats and barley where the phosphate fertilisers TSP and GMP were applied. This suggested that residual P fertiliser may be migrating to the subsoil layers at these points in the crop phase. However, the difference of 200 mg kg^{-1} P_{Total} (480 kg ha^{-1}) between grass year 3 and oats in the TSP subsoil cannot be explained by an annual accumulation of P fertiliser between grass (0 kg ha^{-1}) and oats (20 kg ha^{-1}). Nor can the difference be explained by the accumulation of P fertiliser applied during one full rotation cycle (168 kg ha^{-1}) (**section 2.1.1**). Therefore, the accumulation is likely due to long-term accumulation over the years. Under grass year 3 the subsoil P_{Total} appeared to be consistently lower than the other crop phases possibly due to grass roots reaching the subsoil after three years of growing. It appeared that fertiliser treatment had a greater influence over P_{Total} in topsoils and subsoils than the crop phases. This was expected because the continuous annual application of a given management strategy (either adding or restricting P) would be the main influence over P stocks throughout the soil profile, with the annual crop offtake, at any one point in the rotation cycle, having only a secondary influence. Short-term cropping has been shown to have no effect on subsoil P uptake where topsoil P levels are sufficient for crop requirements (Barej, *et al*., 2014). However, the accumulation of P in soil profiles in long-term double cropping trials (Khan, *et al*., 2018) suggested that crop effects may be part of a longer-term influence on subsoil P stocks.

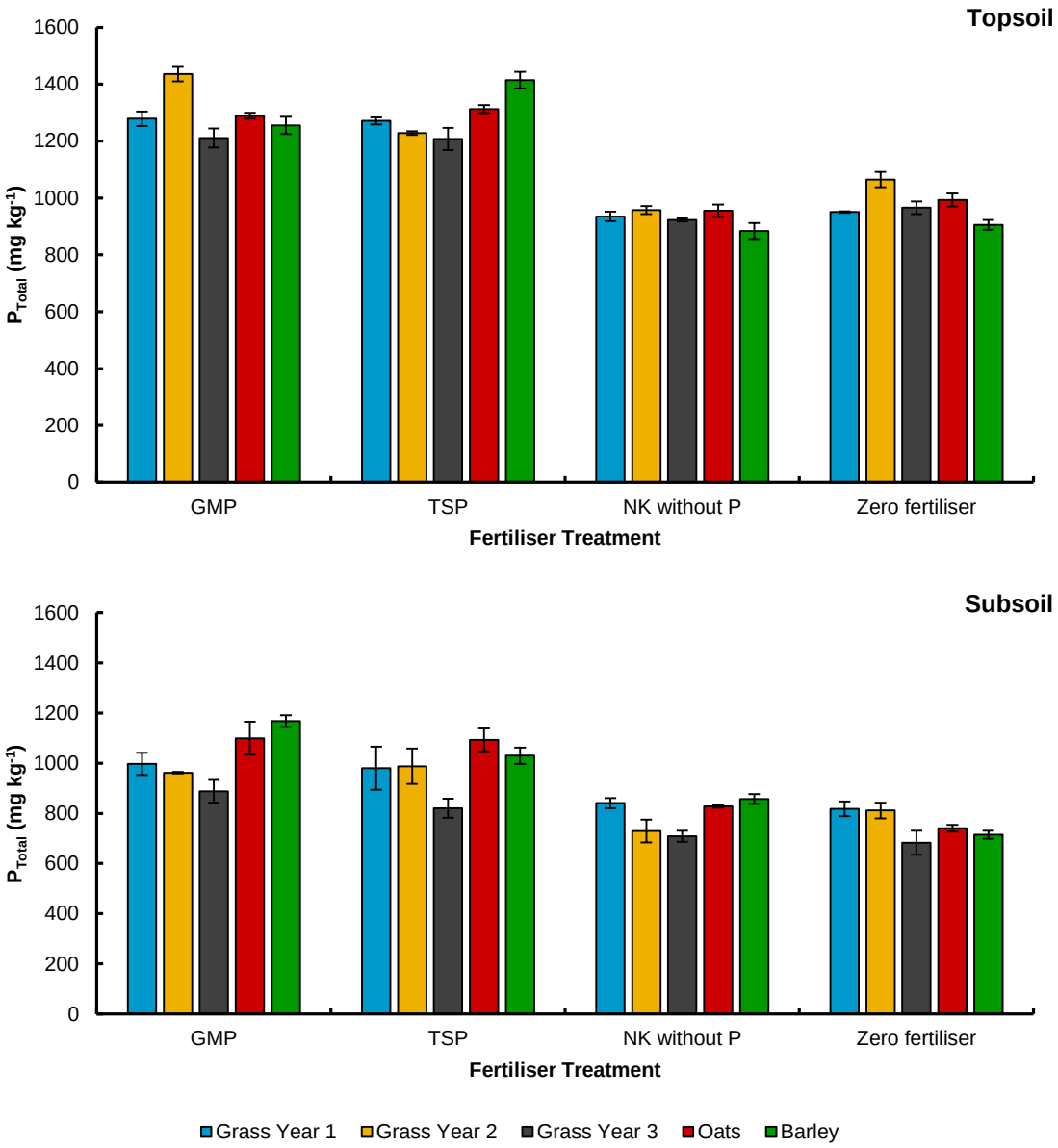


Figure 3.4. Topsoil and subsoil P_{Total}; mean of 3 samples for each crop phase and fertiliser treatment ± SEM.

3.4.3.3 Annual P Balance and Net Annual Accumulation Rates in the Old Rotation

The annual P balance in the Old Rotation between fertiliser inputs and crop offtakes of P, and the net soil profile P_{Total} annual accumulation rate (topsoil and subsoil data combined) are shown in **Table 3.2**. Further details including crop P concentration and yield data, can be found in expanded tables in **Appendix 2**. The net annual P_{Total} accumulation rate was calculated by subtracting P_{Total} in the soil profile of the Field from the treatment plot soil profile P_{Total} before averaging the result over the 93 years duration of the trial to get an estimate of net annual P accumulation (see calculations in **section 2.9**). Annual P balances reflect the difference between inputs and offtakes in a particular plot for 2014/2015 only and reflect the combination of crop and fertiliser treatment that growing season alone. It may be reasonably expected that the annual P balance and the net annual accumulation rates across fertiliser treatments would be similar and thus be reflective of net annual accumulation rate across the individual plots in the Old Rotation regardless of crop phase.

The grass year 1 (Y1) phase varied in the annual P balance from a minimum of -5.69 kg ha^{-1} in the NK without P treatment to a maximum of 15.5 kg ha^{-1} in the PK without N plot (**Table 3.2**). The use of P fertiliser in the grass Y1 plot across four of the six plots showed an accumulation of residual P fertiliser in the annual balances. The P balances were similar at 9.61 kg ha^{-1} (NK with GMP), 9.76 kg ha^{-1} (PN without K), 10.5 kg ha^{-1} (NK with TSP) and 15.5 kg ha^{-1} (PK without N) and indicated the accumulation of P fertiliser in all cases. Crop offtakes of P continued despite the restriction of P fertiliser use resulting in negative annual P balances in the NK without P (-5.69 kg ha^{-1}) and zero fertiliser (-2.69 kg ha^{-1}) treatments, with more P removed when N and K was applied. The net annual P_{Total} accumulation rate in the soil profiles of the three grass phases were all negative and varied depending on the fertiliser treatment and were similar to one another in the amount of P depletion. The greatest depletion rate occurred when no P fertiliser was applied. From 1st to 3rd year, the net soil profile P_{Total} annual depletion rate in the zero fertiliser plot was -18.3 kg ha^{-1} yr^{-1}, 15.6 kg ha^{-1} yr^{-1} and -21.5 kg ha^{-1} yr^{-1} respectively. In the NK without P plot, the grasses showed similar depletion rates of -18.2 kg ha^{-1} yr^{-1} (Y1), -20.5 kg ha^{-1} yr^{-1} (Y2) and -21.9 kg ha^{-1} yr^{-1} (Y3). The use of N and K did not increase the overall net depletion rate by a large amount compared to withholding all fertilisers. The net annual P_{Total} depletion rates were less when P fertiliser was applied, and the extent of depletion did not vary greatly between TSP and GMP fertiliser use. When TSP fertiliser was applied the rates were -5.90 kg ha^{-1} yr^{-1} (Grass Y1), -6.81 kg ha^{-1} yr^{-1} (Grass Y2), -11.7 kg ha^{-1} yr^{-1} (Grass Y3) and when GMP was used the rates were -5.26 kg ha^{-1} yr^{-1} (Grass Y1), -2.12 kg ha^{-1} yr^{-1} (Grass Y2) and -9.83 kg ha^{-1} yr^{-1} (Grass Y3). The net soil profile P_{Total} annual

accumulation rates were within the same magnitude (-21.9 to -2.12 kg ha^{-1} yr^{-1}), but not the same range, as the annual P balances across the fertiliser treatments in the 2014/2015 growing season (-5.69 to 15.5 kg ha^{-1}).

The annual P balance for the two cereal phases showed similarities between treatments but differences between oats and barley (**Table 3.2**). In the zero fertiliser treatment plot, there was a negative P balance of -12.5 kg ha^{-1} in the oats plot and a smaller negative balance of -3.51 kg ha^{-1} in the barley plot. The restriction of P but the application of N and K showed a negative balance of -16.2 kg ha^{-1} in the oats plot and -3.76 kg ha^{-1} in the barley plot. These results were similar within treatments under the same crop but different between the two cereals. The annual P balance showed that P accumulated under barley by 8.75 kg ha^{-1} (NK with TSP) and 14.2 kg ha^{-1} (NK with GMP). In contrast in the oats plots, some plots had a negative P balance of -1.18 kg ha^{-1} (PK without N) and -0.09 kg ha^{-1} (NK with TSP) and a positive P balance in others of 1.14 kg ha^{-1} (NK with GMP) and 4.33 kg ha^{-1} (PN without K). The annual P balances were within the same scale as the net soil profile annual P_{Total} accumulation rates which were all negative for oats and barley. The greatest depletion was found in plots were P fertiliser was restricted at rates of -22.2 kg ha^{-1} yr^{-1} and -19.3 kg ha^{-1} yr^{-1} (zero fertiliser, barley and oats respectively) and -19.1 kg ha^{-1} yr^{-1} and -18.0 kg ha^{-1} yr^{-1} (NK without P, barley and oats respectively). The net annual P_{Total} accumulation rates were close to zero when TSP was applied at rates of -0.90 kg ha^{-1} yr^{-1} (barley) and -1.93 kg ha^{-1} yr^{-1} (oats) or when GMP was applied the P balances -1.46 kg ha^{-1} yr^{-1} (barley) and -2.36 kg ha^{-1} yr^{-1} (oats). These results suggested that, relative to the Field, the use of P fertiliser over the long-term (93 years) reduced the rate at which P may be depleted by cropping, which supports the results seen previously in **section 3.4.3.1**. However, this also suggests that the current TSP and GMP fertiliser rates are not adequate for crop P requirements.

There was a clear, large accumulation of P_{Total} in the annual P balance of the root phase compared to the grass and cereal phases (**Table 3.2**). No soil data is available from the root phase plots to estimate the net profile P_{Total} annual accumulation rate however the P balance data for the root phases provides some idea of the amount of residual P that can remain in the plots when crop yields are lower than average. The amount of P remaining in the plots was significant: plots receive 108 kg ha^{-1} in this phase from a combination of mineral P fertiliser and farm yard manure. Therefore, positive P balances of 75.1 kg ha^{-1} (NK TSP) and 88.3 kg ha^{-1} (NK GMP) meant that 69.5% and 81.8% of the P applied that year remained in the soil respectively. Large P balances were also found for treatments with PK without N (63.7 kg ha^{-1}, 58.9%) or PN without K (71.2 kg ha^{-1}, 66.0%). The annual P balances were positive and lower when mineral P was restricted but farm yard manure was applied for the zero fertiliser (24.2 kg ha^{-1}) and NK without P (24.5 kg ha^{-1}) treatments. However, these plots receive 42 kg ha^{-1} of P in FYM regardless of the restriction of P and so these residual P balances are 57.7% and 58.4% of the P_{Total} added respectively. These annual P balances do not match up with the net soil profile P_{Total} annual accumulation rates in the grass and cereal phases. However, the yields were particularly low for 2014/2015 for root crops and because the annual P balance for the other crops is within the same order of magnitude as the net soil profile P_{Total} annual accumulation rate, this year may be viewed as anomalous to the usual balance. The accumulation of P fertiliser in the topsoil of the root phase would be a source of P for the oncoming crop (oats) and may be a potential source of P which could migrate to the subsoil.

Table 3.2. Annual P Balance and Net Annual Accumulation Rates in the Old Rotation. No available data is indicated by the symbol (-).

Crop	Treatment	Annual P Balance (kg ha^{-1})	Net Soil Profile P_{Total} Annual Accumulation Rate (kg ha^{-1} yr^{-1})
Grass Y1 (Hay)	**Zero fertiliser**	-2.69	-18.3
	NK TSP	10.5	-5.90
	NK GMP	9.61	-5.26
	NK without P	-5.69	-18.2
	PK without N	15.5	-
	PN without K	9.76	-
Grass Y2*	**Zero fertiliser**	0.00	-15.6
	NK TSP	0.00	-6.81
	NK GMP	0.00	-2.12
	NK without P	0.00	-20.5
	PK without N	0.00	-
	PN without K	0.00	-
Grass Y3	**Zero fertiliser**	-	-21.5
	NK TSP	-	-11.7
	NK GMP	-	-9.83
	NK without P	-	-21.9
	PK without N	-	-
	PN without K	-	-
Barley	**Zero fertiliser**	-3.51	-22.2
	NK TSP	8.75	-0.9
	NK GMP	14.2	-1.46
	NK without P	-3.76	-19.1
	PK without N	14.3	-
	PN without K	9.27	-
Roots	**Zero fertiliser**	24.3	-
	NK TSP	75.1	-
	NK GMP	88.3	-
	NK without P	24.5	-
	PK without N	63.7	-
	PN without K	71.23	-
Oats	**Zero fertiliser**	-12.5	-19.3
	NK TSP	-0.09	-1.93
	NK GMP	1.14	-2.36
	NK without P	-16.2	-18
	PK without N	-1.18	-
	PN without K	4.33	-

** Values for P_{Crop} were obtained for Grass year 2 but because there are no inputs and offtakes the annual P balance results in a value of 0.00 kg ha^{-1}*

3.4.3.4 Contaminants Associated with P Fertiliser Use in the Old Rotation

Long-term P fertiliser inputs may result in the accumulation of As, Cd in agricultural soil profiles (Schipper, *et al*., 2011; Ahmed, *et al*., 2014; Hartley, *et al*., 2013). The relationships between P_{Total} and As_{Total}, Cd_{Total}, and U_{Total}, for each fertiliser treatment, in the topsoils and subsoils of the Old Rotation compared to Field are shown in **Figure 3.5**. The results for the treatment plots were averaged across the five crop phases analysed in this study. Across the treatments the As_{Total}, Cd_{Total}, and U_{Total} increased as P_{Total} increased in the topsoil and subsoil, with greater concentrations of soil contaminants associated with plots receiving P fertiliser application. A greater decline in topsoil and subsoil As_{Total}, Cd_{Total}, and U_{Total} relative to the Field was observed in plots were P fertiliser was restricted. The Pearson Correlation Matrix Coefficients (**Appendix 1**) for the Old Rotation topsoils (**Table 10.1**) and subsoils (**Table 10.2**) indicated that As and P were significantly correlated in the subsoil ($r = 0.527$, $p < 0.001$) but not the topsoil ($r = 0.165$, $p = 0.208$) however only half of the plots receive P fertiliser and the treatments likely had an effect on the correlations. Significant correlations between P and Cd in both the topsoil ($r = 0.681$, $p < 0.001$) and the subsoil ($r = 0.902$, $p < 0.001$) were found. Finally, U and P were also significantly correlated in the topsoil ($r = 0.613$, $p < 0.001$) and subsoil ($r = 0.473$, $p < 0.001$).

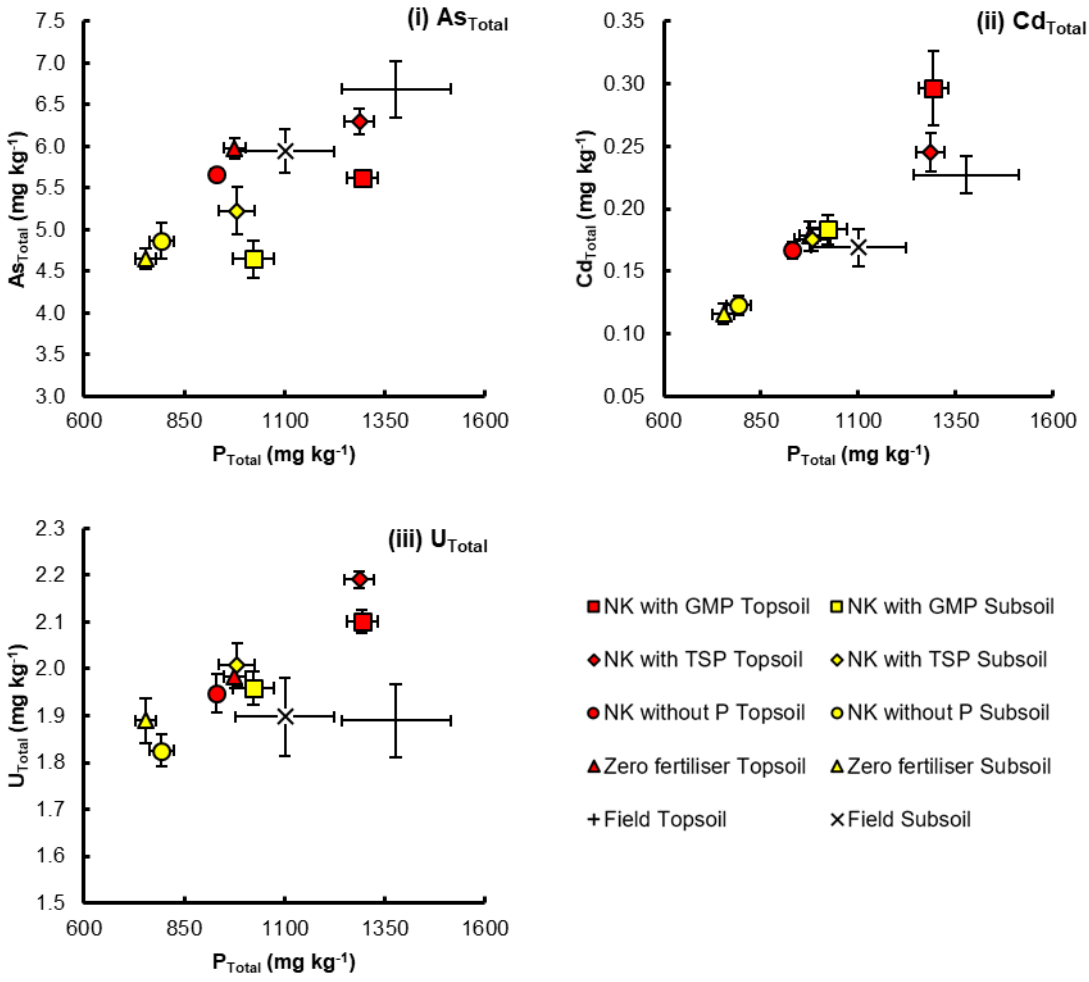


Figure 3.5. Topsoil and subsoil (i) As_{Total}, (ii) Cd_{Total} and (iii) U_{Total} correlations with P_{Total} in the Old Rotation and the Field. Plot values are the mean of 5 crop phases, ± SEM.

Arsenic

The analysis of variance revealed a significant effect of cropping and fertiliser treatment combined on As_{Total} throughout the soil profile (crop x treatment x layer, d.f. = 12, p = 0.008) (**Appendix 3**, **Table 10.10**). The differences between the topsoil and subsoil were the most significant (layer, d.f. = 1, p < 0.001) and fertiliser treatment had a lesser, but significant, effect on As_{Total} (treatment, d.f. = 3, p < 0.001). Across the four fertiliser treatments As_{Total} was on average 5.89 mg kg^{-1} (± SD 0.31 mg kg^{-1}) with the minimum As_{Total} observed in the NK without P plot (5.67 mg kg^{-1} ± SEM 0.06 mg kg^{-1}, n = 5) and the maximum in the NK with TSP plot (6.30 mg kg^{-1} ± SEM 0.15 mg kg^{-1}, n = 5) (**Figure 3.5 (i)**). Subsoil As_{Total} was on average 4.85 mg kg^{-1} (± SD 0.27 mg kg^{-1}) across the four fertiliser treatments, with minimum As_{Total} observed in the plots where NK and GMP were applied (4.65 mg kg^{-1} ± SEM 0.04 mg kg^{-1}, n = 5) and a maximum under NK and TSP treatment (5.23 mg kg^{-1} ± SEM 0.15 mg kg^{-1}, n = 5). This suggested a potential link between topsoil and subsoil As_{Total} associated with TSP fertiliser use with less soluble GMP persisting in the topsoil for longer and leaching more slowly. In the field surrounding the

trials the average As_{Total} in the topsoil was 6.69 mg kg^{-1} (± SEM 0.34 mg kg^{-1}) and the average subsoil As_{Total} was 5.94 mg kg^{-1} (± SEM 0.0.26 mg kg^{-1}). The As_{Total} across all treatments were less in comparison with the plots treated with NK and TSP closest to the native field levels. Overall the treatment plots and the field surrounding the trials had As_{Total} levels which were significantly less than the 50 mg kg^{-1} soil limit in the guideline values for agricultural land to which sewage sludge has been applied (The Sludge (Use in Agriculture) Regulations, 1989). The average As_{Total} values in the treatment plots were on average less than the natural levels in the field surrounding the trials (assuming the field has no inputs of As from other sources) and therefore net accumulation rates in the treatment plots are negative over the 93 year duration of the experiment and are not concerning to the accumulation limit from sewage sludge applications.

Cadmium

The analysis of variance revealed no significant effect of cropping and fertiliser treatment combined on the Cd_{Total} throughout the soil profile (crop x treatment x layer, d.f. = 12, p = 0.299) however there was a significant effect of treatment (treatment x layer, d.f. = 3, $p < 0.001$) with differences between the topsoil and subsoil being highly significant (layer, d.f. = 1, $p < 0.001$) (**Appendix 3**, **Table 10.11**). Topsoil Cd_{Total} was on average 0.22 mg kg^{-1} (± SD 0.06 mg kg^{-1}, n = 4) across the four treatment plots, with a maximum topsoil Cd_{Total} where NK with GMP was applied (0.30 mg kg^{-1} ± SEM 0.03 mg kg^{-1}) and a minimum Cd_{Total} in the topsoil of the NK without P treatment (0.17 mg kg^{-1} ± SEM 0.01 mg kg^{-1}) (**Figure 3.5 (ii)**). Topsoil Cd_{Total} in the NK with TSP treatment was 0.25 mg kg^{-1} (± SEM 0.02 mg kg^{-1}) and the Cd_{Total} of the zero fertiliser treatment was 0.18 mg kg^{-1} (± SEM 0.01 mg kg^{-1}). The use of phosphate fertilisers, in particular the use of GMP, had enriched the topsoil with Cd compared to the Field Cd_{Total} (0.23 mg kg^{-1} ± SEM 0.02 mg kg^{-1}). The average subsoil Cd_{Total} was 0.15 mg kg^{-1} (± SEM 0.04 mg kg^{-1}) with a minimum of 0.12 mg kg^{-1} (± SEM 0.01 mg kg^{-1}) in both the zero fertiliser and NK without P treatment and a maximum of 0.18 mg kg^{-1} (± SEM 0.01 mg kg^{-1}) in both the NK with GMP or TSP treatments. Long-term P fertiliser use did not seem to raise the subsoil Cd_{Total} levels in the plots compared to the background Cd_{Total} in the Field (0.17 mg kg^{-1} ± SEM 0.02 mg kg^{-1}) but restricting P fertiliser seemed to result in a decline in the subsoil Cd_{Total} level compared to the Field. This suggested over the long-term, crops may have accessed subsoil Cd perhaps due to (limited) uptake from deep rooting crops between pH 5 and 6 where Cd bio-availability decreases (Gray, *et al*., 1999). These results also suggest a link between P fertiliser application to the topsoil and Cd_{Total} persistence with Cd possibly moving to the subsoil in P fertilised plots. The maximum Cd_{Total} for application of sewage sludge to arable soils is 3 mg kg^{-1} > pH 5.0 (The Sludge (Use in

Agriculture) Regulations, 1989). The greatest Cd_{Total} found in the treatment plots was ten-fold less than this limit, at a maximum of 0.30 mg kg^{-1} in the topsoil of the plot receiving NK and TSP fertilisers. Most of the soils contained less than 0.20 mg kg^{-1} in the Old Rotation following 93 years of continuous management. The difference between the topsoil Cd_{Total} in the TSP plot and the Field is small at 0.07 mg kg^{-1}, equivalent to a total net Cd_{Total} of 0.168 kg ha^{-1} over the 93-year history of the trial. The maximum accumulation rate permitted over 10 years is 0.15 kg ha^{-1} (The Sludge (Use in Agriculture) Regulations, 1989) and therefore the accumulation rate in this plot was almost ten-fold less than this limit which shows Cd accumulation in the plots are not concerning. Finally, the limit for Cd_{Total} in allotment soils used for food production is 1.80 mg kg^{-1} and despite the historical use of P fertiliser in these plots, this lower limit was not exceeded (Ross, *et al*., 2007).

Uranium

The analysis of variance revealed no significant combined effect of cropping and fertiliser treatment on the U_{Total} in the soil profile (crop x treatment x layer, d.f. = 12, $p = 0.569$) however the differences between the topsoil and subsoil were significant (layer, d.f. = 1, $p < 0.001$) (**Appendix 3**, **Table 10.12**). Topsoil enrichment of U_{Total} relative to the Field (1.89 mg kg^{-1}) was associated with TSP (2.19 mg kg^{-1} ± SEM 0.02 mg kg^{-1}) and GMP (2.10 mg kg^{-1} ± SEM 0.02 mg kg^{-1}) fertiliser use (**Figure 3.5 (iii)**). Topsoil U_{Total} in the zero fertiliser (1.98 ± SEM 0.01 mg kg^{-1}) and NK without P plots (1.94 ± SEM 0.01 mg kg^{-1}) were slightly higher than the background U_{Total} in the Field. The Field subsoil U_{Total} was nearly identical to the topsoil at 1.90 mg kg^{-1} (± SEM 0.08 mg kg^{-1}). The use of P fertiliser was associated with slightly elevated U_{Total} in the subsoil: more so with TSP (2.00 mg kg^{-1} ± SEM 0.05 mg kg^{-1}) than GMP use (1.96 mg kg^{-1} ± SEM 0.02 mg kg^{-1}) with the zero fertiliser plot (1.89 mg kg^{-1} ± SEM 0.05 mg kg^{-1}) comparable to the Field. Only the subsoil of the NK without P was relatively lower than the Field (1.83 mg kg^{-1} ± SEM 0.03 mg kg^{-1}). The results suggest a link between TSP and GMP fertilisers and minor U_{Total} accumulation in the topsoil and subsoil. The analysis of U_{Total} in UK industrial soils revealed that U_{Total} in rural areas of Scotland was on average 0.653 mg kg^{-1} with urban areas of Scotland reaching an average 2.0 mg kg^{-1} (Ross, *et al*., 2007). The U_{Total} across the Old Rotation ranged between a minimum of 1.83 mg kg^{-1} in the NK without P subsoils and a maximum of 2.20 mg kg^{-1} in the topsoils of the NK and TSP treatment plots and were therefore greater than the background U_{Total} levels reported for rural areas.

3.4.3.5 Topsoil: Subsoil Ratio of P and Contaminants in the Old Rotation

The topsoil: subsoil ratio of P_{Total}, As_{Total}, Cd_{Total} and U_{Total} in each fertiliser treatment compared to a ratio of 1.0 line is shown in **Figure 3.6**. All ratios were greater than 1.0 indicating that concentrations were greater in the topsoil (where P is directly applied) than in the subsoil, where the main input of these elements would be from downward migration processes from the topsoil. The ratios for Cd_{Total} followed the trend NK and GMP (1.62) > zero fertiliser (1.54) > NK and TSP (1.39) > NK without P (1.36) > Field (1.34). It was surprising that the ratio in the zero fertiliser treatment was greater than the TSP treated plot as P fertiliser use is associated with elevated Cd levels (McDowell, 2012). It was not surprising however that the ratio was greatest in the GMP plot because Cd is released slowly from GMP whereas Cd solubility is greater in TSP fertiliser which itself is highly soluble (Kuo, *et al*., 2007). Therefore, GMP may have persisted in the topsoil longer (and be less susceptible to leaching) therefore increasing the topsoil: subsoil ratio of Cd under GMP compared to the highly soluble TSP which may leach more rapidly to subsoil layers and produce a more even distribution. The ratios for P_{Total} (1.17 to 1.31), As_{Total} (1.13 to 1.29) and U_{Total} (1.00 to 1.09) were similar across all treatments with U_{Total} ratios close to 1.0 suggesting an even distribution throughout the soil profile. The similarity in topsoil: subsoil ratios for P_{Total} and As_{Total} suggested a link to P fertiliser use but also P and As display similar chemistry across the pH range and compete for the same surface binding sites (Deng, *et al*., 2018). The treatment plots are maintained around pH 6 which is within the range of maximum P solubility and potential for transfer to the subsoil.

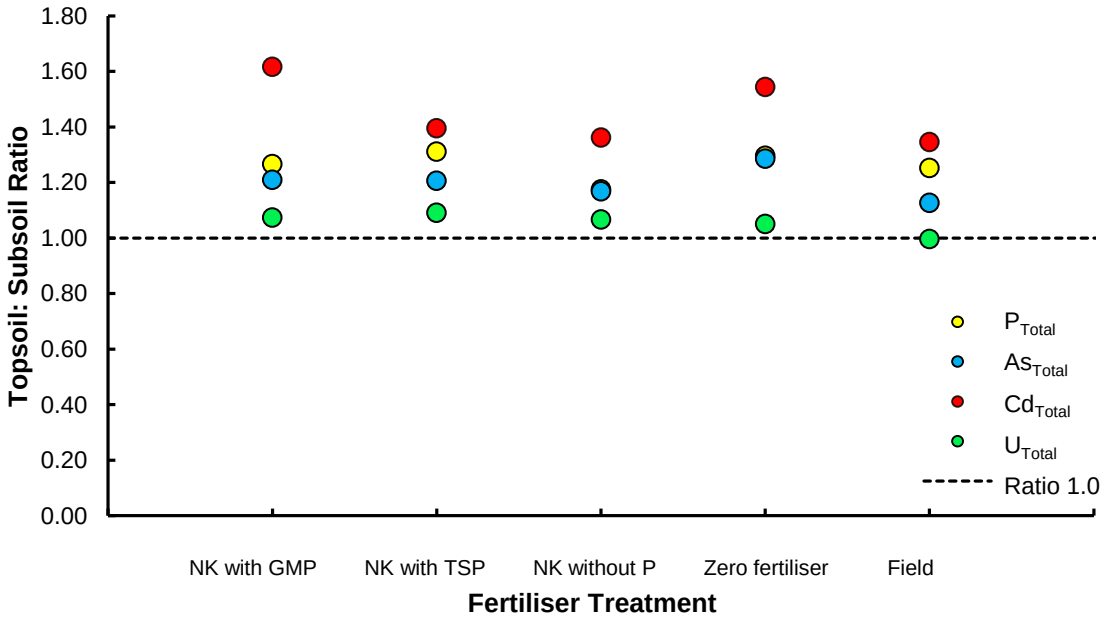


Figure 3.6.Topsoil: Subsoil ratio of P_{Total}, As_{Total}, Cd_{Total} and U_{Total} for each fertiliser treatment in the Old Rotation, and the Field, compared to a ratio of 1.0 (broken) line.

3.4.4 Woodland's Field pH Rotation

3.4.4.1 The Effect of Liming on Topsoil and Subsoil pH Values

Topsoil measured pH values were close to the target pH values for the plots in the pH Rotation (**Figure 3.7**). Surprisingly, measured pH values in the subsoil were also close to target pH values, instead of the pH of the Field (pH 5.98). This indicated that the extended use of lime had created a uniform soil profile pH in each of the target plots. At acidic pH values, the measured soil pH values were greater than the target, tending towards the natural soil values between pH 5.5 and 6. Above pH 6 the measured values again tended slightly towards the natural soil pH, suggesting a resilient buffering capacity in the soil. An increase in Ca in solution and leaching from topsoil to subsoil was the likely mechanism controlling the distribution of Ca_{Total} in the profile. Calcium deficiency and Al toxicity in subsoils are two common challenges for crops (Lynch & Wojciechowski, 2015) and these issues may be alleviated in the plots that have become enriched with Ca because liming improves crop growth and reduces the uptake of Al (de Miranda & Rowell, 1987). The alleviation of subsoil acidity may also have implications for As transport in the profile as shown in the Park Grass experiment where subsoil P and As concentrations were greater under limed conditions than those without lime or P fertiliser applications (Hartley, *et al*., 2013). The re-distribution of Ca_{Total} between the topsoil and subsoil, and the resulting increase in subsoil Ca_{Total} would likely have an impact on P solubility and availability of P throughout the soil profile which will be investigated in more detail in **Chapter 5** and **Chapter 4** respectively.

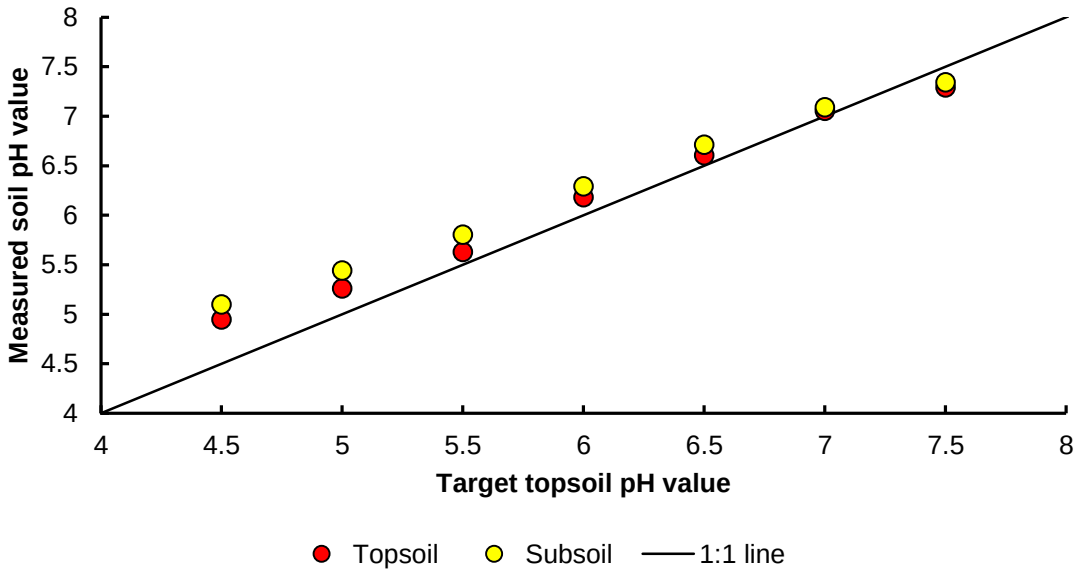


Figure 3.7. Target topsoil pH vs the measured soil pH in the topsoil and subsoil of each target pH plot compared to a 1:1 line. Points are the mean of 5 crop phases with ± SEM.

The Ca_{Total} in topsoil and subsoil were similar and increased as the soil pH values increased from pH 6 towards pH 7.5, which was expected as long-term liming was used to maintain these target plots (**Figure 3.8**). There was not a significant combined effect of crop and pH control on topsoil and subsoil Ca_{Total} as expected (crop x treatment x layer, d.f. = 24, p = 0.386) (**Appendix 3**, **Table 10.20**) because liming is the main source of Ca and so crops would not be expected to have a significant effect compared to the effect of maintaining a target pH (i.e. 'treatment'). However, the average Ca_{Total} for the soil profile in the pH 7.5 plot (12600 ± SD 978 mg kg^{-1}) was 1.75x that of the soil profile Ca_{Total} in the pH 4.5 plot (7290 ± SD 121 mg kg^{-1}). The Field Ca_{Total} was 7880 mg kg^{-1} in the topsoil and 8240 mg kg^{-1} in the subsoil: target pH plots at pH 5.5 and above were enriched in Ca_{Total} in comparison. The prediction analysis using the 2^{nd} order polynomials fitted to the trend in topsoil and subsoil Ca_{Total} with soil pH (**Appendix 4**, **Table 10.27**) suggested that on balance across the pH plots, the topsoil and subsoil Ca_{Total} was not significantly elevated compared to the Field topsoil and subsoil Ca_{Total} (**Appendix 4**, **Table 10.31**). The ratio of Ca_{Total} in each pH plot to the Field CaTotal for both topsoils and subsoils are shown in **Figure 3.9** where the plot Ca_{Total} becomes increasingly enriched as the target pH increases for both layers relative to the background Ca_{Total} in the Field. The topsoil to subsoil ratios ranged from 0.95 at pH 4.5 to a maximum of 1.12 at pH 7.5 with an average ratio of 1.03 across all of the plots. Below pH 5.5, the ratios were around 1 which was expected because no lime was added to these plots and the Ca_{Total} in the plots would be close to background levels. Above pH 5.5, the ratio between the plot and the background increased linearly for both topsoil and subsoil as the target pH increased. In the topsoil, the ratio in the pH 7.5 plot showed that there was 1.75x more Ca_{Total} in the plot than the background, whereas in the subsoil, the maximum amount was around 1.5x more than the background subsoil Ca_{Total}.

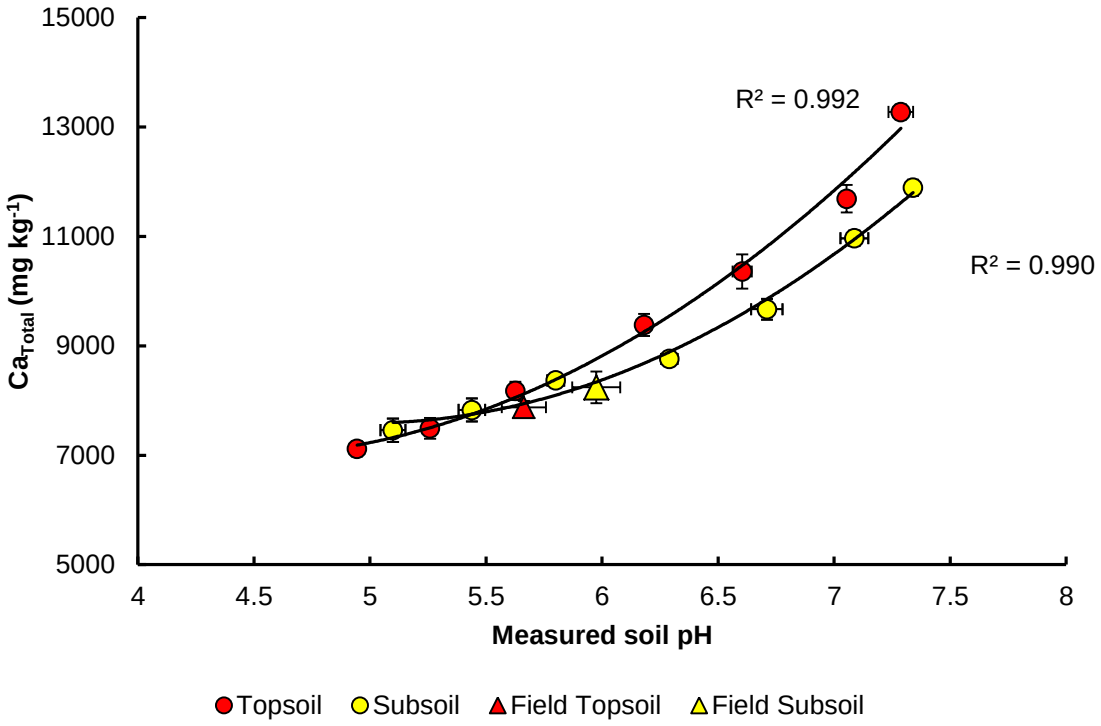


Figure 3.8. Relationship between measured soil pH and Ca_{Total} in the topsoils and subsoils of the pH Rotation and the Field. Trend lines are 2nd order polynomials; each point represents the mean of five crop phases ± SEM.

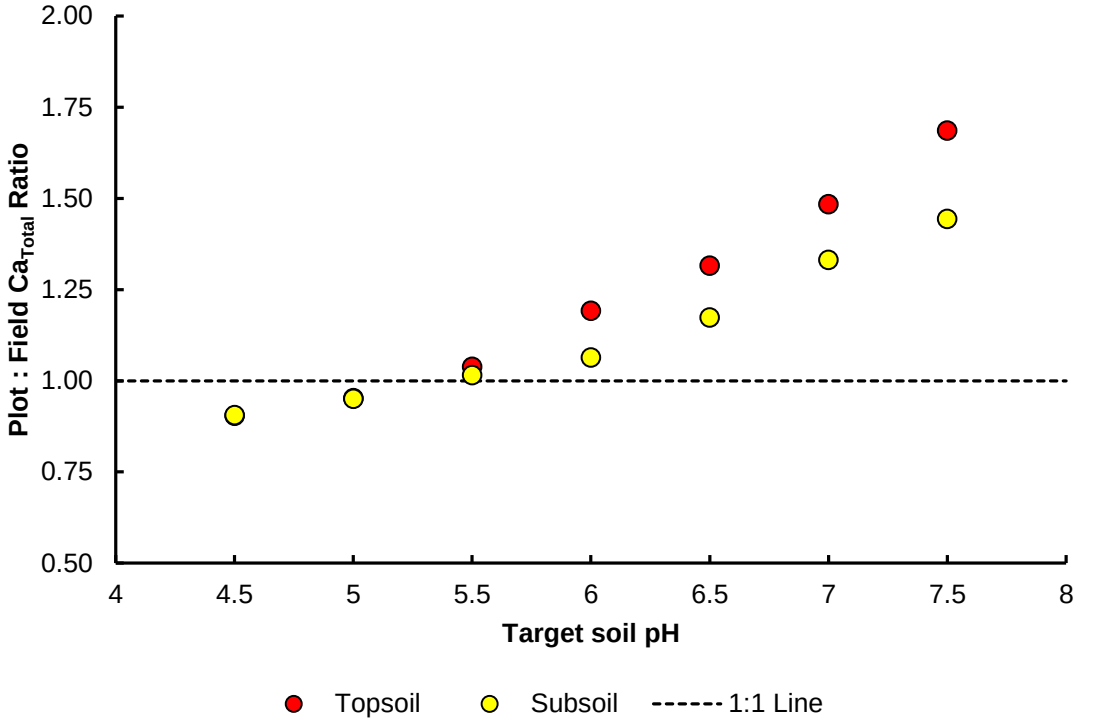


Figure 3.9. The ratio of plot: field (surrounding field natural background) Ca_{Total} in the topsoils and subsoils across the pH plots compared to a 1:1 line.

3.4.4.2 Effect of Soil pH Control on P_{Total} Distribution in the Soil Profiles of the pH Rotation

The relationship between soil pH and P_{Total} in the topsoil and subsoil in the pH Rotation and the Field is shown in **Figure 3.10** with each point in the pH Rotation representing mean P_{Total} data over the five crop phases. Topsoil P_{Total} decreased from a maximum of 1930 mg kg^{-1} (± SEM 55.0 mg kg^{-1}) at pH 4.5 to a minimum of 1770 mg kg^{-1} (± SEM 64.9 mg kg^{-1}) at pH 6 and then increased towards 1870 mg kg^{-1} (± SEM 52.9 mg kg^{-1}) at pH 7.5. Subsoil P_{Total} increased from a minimum of 1050 mg kg^{-1} (± SEM 58.2 mg kg^{-1}) at pH 4.5 and increased by approximately 250 mg kg^{-1} at pH 6 (1260 mg kg^{-1} ± SEM 33.6 mg kg^{-1}) where the topsoil and subsoil tended towards convergence before diverging towards pH 7.5. The subsoil P_{Total} remained fairly uniform between pH 6 and 7.5. The decline in P_{Total} from pH 4.5 towards pH 6 and the rise towards pH 7.5 suggested that topsoil P_{Total} accumulation occurred at both acidic pH (adsorption on Fe/Al oxides) and alkaline pH (precipitation as Ca-phosphate) (Weng, *et al*., 2011). The convergence of topsoil and subsoil P_{Total} between pH 6 and 6.5 suggested that topsoil P_{Total} was more mobile and was transferred to the subsoil in the zone where P solubility is greatest (Lindsay, 1979). Furthermore, this is the target pH for arable crops (AHDB, 2017) and so is significant in agronomy for optimum crop production; this evidence of movement of P from topsoil to subsoil may have implications for phosphorus fertiliser use efficiency and management strategies.

Second order polynomials were a good fit to the data in the topsoil (R^2 = 0.948) and subsoil (R^2 = 0.873) (**Appendix 4**, **Table 10.23**) (**Figure 3.10**) and were used to predict whether the P_{Total} across the pH gradient was significantly altered in comparison to the Field P_{Total} (**Appendix 4**, **Table 10.31**). The analysis revealed that topsoil P_{Total} across all pH plots had significantly increased beyond the 'native' levels in the Field topsoil P_{Total} (1380 mg kg^{-1} ± SEM 136 mg kg^{-1}) whereas subsoil P_{Total} in the plots was not significantly changed relative to the Field subsoil P_{Total} (1100 mg kg^{-1} ± SEM 123 mg kg^{-1}). This could have implications for similar cropping systems on acidic soils in the North East Scotland because it shows that P accumulates in the topsoil particularly at acidic pH values, likely by adsorption to Al and Fe oxides (Weng, *et al*., 2011) such as goethite (Antelo, *et al*., 2005). In the UK, most arable and grassland soils are below the optimum pH range of 6 to 7 (Goulding, 2016) and crop production (and thus removal of P) can be reduced at acidic pH levels which has been observed previously in this Rotation (Walker, *et al*., 2011). Walker, *et al*., (2011) showed that grain weights of spring barley and spring oats grown in the pH Rotation were significantly reduced in the pH 4.5 plot. Later, Walker, *et al*., (2015) showed that dry matter yield of various crops in the pH Rotation were least at pH 4.5 and greatest between pH 5.5 and 6. The rise in topsoil P_{Total} between pH 6 and pH 7.5 suggest that the precipitation of insoluble calcium phosphates

retained P in the topsoil. In contrast to the results described here, there was no variation in P_{Total} observed across the pH range 3.73 to 7.83 of the Hoosfield acid strip (Rothamsted Research, UK) where P fertiliser was restricted for c.150 years (Turner & Blackwell, 2013). Turner & Blackwell (2003) showed that organic forms of P such as inositol phosphate, DNA and phosphonates constitute between 34 and 38% of P_{Total} in the soil across the pH range. Furthermore, the trend in organic P compounds with soil pH in the study by Turner & Blackwell (2013) was similar to that of the topsoils in the pH Rotation shown in **Figure 3.10** which suggested organic P compounds may form a significant proportion of P_{Total} in the pH Rotation. When dairy slurry is applied to agricultural soils, bacterial P may contribute between 0.3 and 8% of P_{Total} and so bacterial transport of P may be an important component of leachate transferring organic P from the topsoil to the subsoil (Glæsner, *et al*., 2016). Although organic P species were not investigated in this study, they may be an important component of the P stocks in the soil profile.

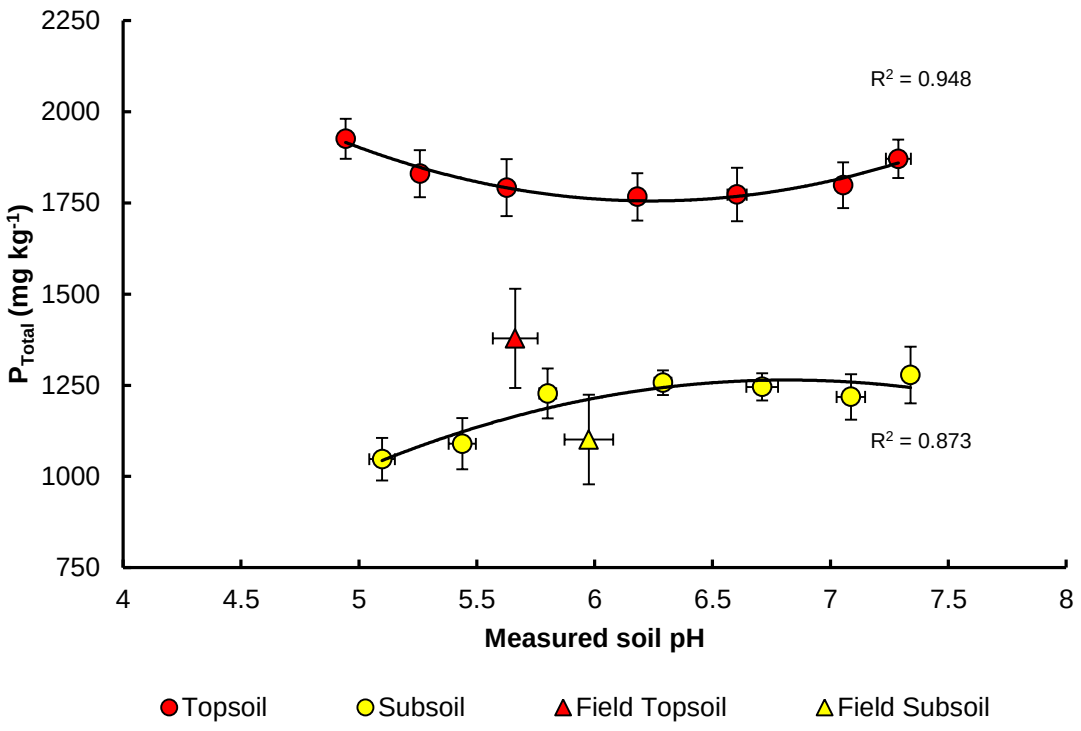


Figure 3.10. Mean P_{Total} in the topsoils and subsoils as a function of soil pH; the trend-lines are 2nd order polynomials; means are of five crop phases ± SEM.

3.4.4.3 Effect of crop on P_{Total} distribution in the soil profile of the pH plots

An analysis of variance indicated that a combination of crop phase and target soil pH significantly influenced P_{Total} in the topsoil and subsoil of the pH Rotation (crop x pH x layer, d.f. = 24, p = 0.007) (**Appendix 3**, **Table 10.16**). Fertiliser application rates depend on the crop and this may explain why there could be a significant effect of crop on the P_{Total} in the pH plots. Walker, *et al*., (2011) showed that crop productivity and yield of winter wheat and spring barley was greatest between pH 5.5 and 6.0 and least at pH 4.5. In contrast, the yield of spring oats was similar between pH 4.5 and 6.0 but declined towards pH 7.5. Therefore, it may be expected that more P fertiliser would accumulate at acid or alkaline pH plots compared to the plots between pH 5.5 and 6.5 due to differences in crop yield thus affecting P_{Total} in the plots.

The relationship between P_{Total} and measured soil pH of the topsoil and subsoil for all crop phases is shown in **Figure 3.11**. There was no apparent effect of crop on subsoil P_{Total} which was expected. However, in the topsoil there was a clear distinction between the spring oats and winter wheat, which were offset from the cluster of barley and the two grass phases (1st and 2nd year). It was thought that this could be due to differences in fertiliser application rates between the crop phases leading to differences in the residual P_{Total} from fertilisers in the topsoil. The average P_{Total} across the pH gradient of the 'grasses plus barley' was 1810 mg kg^{-1} ± SD 60.3 mg kg^{-1}, the spring oats average P_{Total} was 2037 mg kg^{-1} ± SD 44.2 mg kg^{-1} and the winter wheat was 1640 mg kg^{-1} ± SD 89.6 mg kg^{-1} (**Table 3.3**). The difference between the average of the 'grasses plus barley' and the spring oats across the pH plots was 227 mg kg^{-1} (± SD 31.5 mg kg^{-1} n = 7) and the difference between the 'grasses plus barley' and the winter wheat was 170 mg kg^{-1} (± SD 47.6 mg kg^{-1}, n = 7). These differences equate to 545 P_{Total} kg ha^{-1} (spring oats) and 408 kg ha^{-1} (winter wheat) (**Table 3.4**) based on a soil depth of 20 cm and an assumed bulk density of 1.2 g cm^{-3} (see **section 2.9**). The difference in P between spring oats and winter wheat was thus 953 kg ha^{-1}. Annual P application rates amount to 65 kg ha^{-1} at the beginning of the wheat phase and 50 kg ha^{-1} at the beginning of the oats phase (see **section 2.1.1**). Therefore, the differences in P_{Total} observed in these plots were not due to a single annual effect of fertiliser accumulation but likely a result of extended P fertiliser use and rotational cropping (54 years) which is explored next in **section 3.4.4.4**.

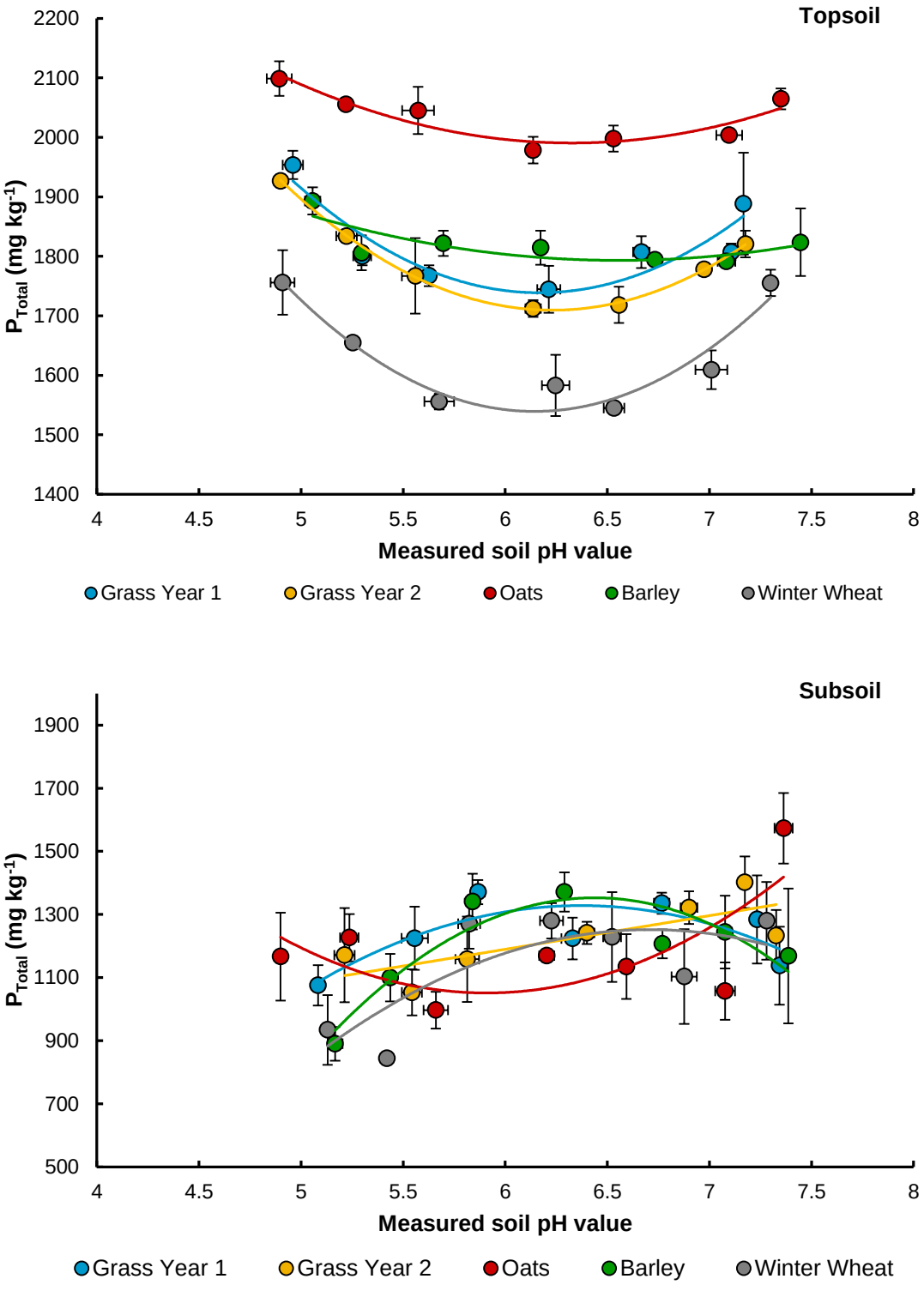


Figure 3.11. Soil P_{Total} vs measured soil pH value under each crop phase in the topsoil and subsoil, described as 2nd order polynomials; each point is the mean of three replicates ± SEM.

Table 3.3. Topsoil P_{Total} (mg kg^{-1}) differences between crops in the pH Rotation topsoil for each target pH.

pH	P_{Total} (mg kg^{-1})				
	Average ('Grass + Bar')*	Oats	Wheat	Oats – 'Grass + Bar'	'Grass + Bar' - winter wheat
7.5	1840	2070	1760	230	80
7	1790	2000	1610	210	180
6.5	1770	2000	1550	230	220
6	1750	1980	1580	230	170
5.5	1780	2050	1560	270	220
5	1810	2060	1660	250	150
4.5	1930	2100	1760	170	170
Average	1810	2037	1640	227	170
SD	60.3	44.2	89.6	31.5	47.6

**'Grass + Bar represents the average of grasses years 1 and 2 and barley altogether because they showed similar concentrations in Figure 3.11.*

Table 3.4. Topsoil P_{Total} (kg ha^{-1}) differences between crops in the pH Rotation topsoil for each target pH.

pH	P_{Total} (kg ha^{-1})				
	Average ('Grass + Bar')*	Oats	Wheat	Oats - 'Grass + Bar'	'Grass + Bar' - winter wheat
7.5	4416	4968	4224	552	192
7	4296	4800	3864	504	432
6.5	4248	4800	3720	552	528
6	4200	4752	3792	552	408
5.5	4272	4920	3744	648	528
5	4344	4944	3984	600	360
4.5	4632	5040	4224	408	408
Average	4344	4889	3936	545	408
SD	145	106	215	76	114

**'Grass + Bar represents the average of grasses years 1 and 2 and barley altogether because they showed similar concentrations in Figure 3.11.*

The possibility of an analytical error which could explain the discrepency in P_{Total} between the oats and wheat was investigated through re-analysis by ICP-MS. Acid digestates were re-analysed following 7 months of storage at room temperature; the original and re-analysed P_{Total} values showed a reasonable fit to the 1:1. On average the oats P_{Total} was within 6.18% (± SD 2.42%, n = 42) and the wheat P_{Total} was within 4.62% (± SD 2.33%, n = 42) of the original P_{Total} result. Furthermore, there was a 98% recovery of the P in the certified reference material (Montana soil, NIST 2711A) using KED mode, where polyatomic interferences were eliminated and so the original results in the database were accepted.

3.4.4.4 P balance in the pH Rotation

The annual P balance between fertiliser inputs and crop offtakes, and the net soil profile P_{Total} accumulation rate over the 53 years of the trial is shown in **Table 3.5**. Further details including crop yields, crop P content and removal can be found in **Appendix 2**. Annual P balances reflect the difference between inputs and offtakes in a particular plot for 2014-2015 only and reflect the combination of crop and pH treatment on the annual P balance for that year alone. However, the net soil profile P_{Total} annual accumulation rate is averaged over the 54 years and each pH plot is therefore the result of *long-term* crop rotation and thus a combination of 54 years of P balances from the cycling of crops. It may be reasonably expected then, that the net annual accumulation rates do not match the crop for that year but on average, the annual accumulation rates across all plots would be within an order of magnitude of one another and reasonably similar in net accumulation rates and thus reflect a constant net annual accumulation rate across the individual plots in the pH Rotation regardless of crop phase.

Soil samples were not collected from the potato or swede plots and so there is no net soil profile P_{Total} annual accumulation rate to compare to the annual P balance (**Table 3.5**). However, the annual P balances were largely positive for both potatoes and swedes which receive 108 kg ha^{-1} and 77 kg ha^{-1} P fertiliser applications respectively. The annual P balance for potatoes across the pH plots had high accumulation rates but with no pH effect resulting in a restricted range of 75.1 to 85.5 kg ha^{-1}. The average annual P balance of 88.3 kg ha^{-1} (± SD 3.66 kg ha^{-1}, n = 7) across the plots was 81.8% of the P fertiliser input for this crop phase. This shows poor P fertiliser use efficiency and is due to unusually low crop yields for the 2014-2015 season which may have been partly affected by poor control of pests and weeds, as was the case in the Old Rotation. The annual P balance in root phases of the pH Rotation was comparable to the range in the Old Rotation when TSP fertiliser was applied (75.1 kg ha^{-1}). There was also a restricted (positive) annual P balance range for swedes across the pH plots from a minimum of 64.2 to 79.5 kg ha^{-1}. The average P balance in the swede plots across the pH gradient was 54.7 kg ha^{-1} (± SD 4.32 kg ha^{-1}, n = 7) which was 71.0% of the total P fertiliser applied to this phase. Swede yields also suffered in 2014-2015 which explains the accumulation of P. The accumulation of residual TSP fertiliser (and FYM) in these plots is a source of highly reactive P which may be a source of P for future crops in the rotation. Furthermore, residual TSP in the topsoil could be susceptible to leaching and therefore may be intercepted in the subsoil where it may accumulate.

The remaining crop phases in **Table 3.5** have annual P balance and net soil profile P_{Total} annual accumulation rates which are comparable and within an order of magnitude of one another. This suggested that the use of the plot soil profile P_{Total} minus the Field P_{Total} gives a fair indication of the average accumulation rate in the soil profile over the 54-year duration of the pH Rotation. There was no evidence to suggest that soil pH had a significant effect on the accumulation of residual P_{Total} in the soil profile of the grass phases. The net annual P_{Total} accumulation rates in the soil profiles of grass year 1 plots were positive within a restricted range of 21.7 to 29.5 kg ha^{-1} yr^{-1}. The annual P balance for grass year 1 was also restricted to a narrow, and lower, range of -1.61 to 4.19 kg ha^{-1}. Grass year 2 does not receive P fertiliser and the grass is cut and left to mulch so there was no 'annual P balance' for these plots. However, the soil sample analysis could be used to estimate a net soil profile P_{Total} accumulation rate. This analysis revealed positive accumulation rates across the pH gradient ranging from 18.1 to 31.1 kg ha^{-1} (pH 7). These rates were comparable to those in the grass year 1 plots which is expected due to the presumed steady-state P_{Total} in the profiles of the plots across the rotation. Annual P balances for wheat however, showed greater variation with pH, falling from a rate at 25.4 kg ha^{-1} at pH 4.5 to a minimum of 4.00 kg ha^{-1} at pH 6.0 before rising to 25.8 kg ha^{-1} at pH 7.5. The P balance for wheat suggested that crop uptake of P was greatest between pH 5.5 and 6.5 which is the ideal pH range for arable crop production (Goulding, 2016). The net soil profile P_{Total} annual accumulation rate in the soils under wheat was comparable to the annual P balances and was reasonably comparable to the rates in the grass phases, but with an observable effect of pH. The annual P balance for barley followed a similar trend to wheat, varying with pH and with all plots accumulating fertiliser P. There was a maximum accumulation of 22.0 kg ha^{-1} (pH 4.5) which decreased to a minimum of 4.04 kg ha^{-1} at pH 6 before increasing to 13.0 kg ha^{-1} at pH 7.5. The net P_{Total} accumulation rates showed an opposite trend with pH for barley and ranged from a minimum of 13.5 kg ha^{-1} (pH) to a maximum of 31.4 kg ha^{-1} (pH 6) which possibly reflects variations in P balances over the 54-year lifetime of the trial. Furthermore, these accumulation rates were comparable to the grass phases in terms of amount of P accumulating. Finally, for the oat plots, all plots accumulated P, but the annual P balance revealed a decline from pH 7.5 (22.0 kg ha^{-1}) to pH 4.5 (9.80 kg ha^{-1}) with a minimum rate observed at pH 5.5 (2.56 kg ha^{-1}). Net soil profile P_{Total} accumulation rates for the oat plots was high, ranging from 25.0 kg ha^{-1} yr^{-1} (pH 5.5) to double that at a rate of 51.5 kg ha^{-1} yr^{-1} (pH 7.5). These high net annual accumulation rates may explain the relatively higher P_{Total} observed in the topsoils of the oat plots across the pH Rotation as observed in **Figure 3.11**.

Annual P balances generally ranged from minor depletion rates of -1.91 kg ha^{-1} to an accumulation of up to 92.3 kg ha^{-1} in the root phases (**Table 3.5**). If there was repeated poor crop performance and annual P balances up to 92.3 kg ha^{-1} in plots over the 54-year period of the trials, this may go some way to explaining the discrepancy in the topsoil P_{Total} between wheat and oats of 953 kg ha^{-1} in the previous section (see **section 3.4.4.3**). It could also be that in some of these plots, crop P use efficiency has generally been ok over the lifetime of the trial, and so a spectrum of accumulation rates can be expected across the crop phases. The average net soil profile P_{Total} annual accumulation rates over the 54 years was 23.9 kg ha^{-1} (± SD 8.89 kg ha^{-1}, n = 35 plots) suggesting that the net annual accumulation rates of P_{Total} in the soil profile across the plots was fairly consistent, and plots were generally accumulating the same amount of P_{Total} in the soil profile each year regardless of the target pH. The range of accumulation rates from 0.86 kg ha^{-1} to 51.5 kg ha^{-1} were reflective of the range of P balances observed in the plots.

Table 3.5. Annual P Balance and Net Annual Accumulation Rates in the pH Rotation.

Crop	Treatment	Annual P Balance (kg ha^{-1})	Net Soil Profile P_{Total} Annual Accumulation Rate (kg ha^{-1} yr^{-1})
Grass Y1 (Hay)	**4.5**	4.19	24.4
	5	1.14	24.2
	5.5	1.59	29.3
	6	-1.48	21.7
	6.5	0.54	29.5
	7	0.96	27.2
	7.5	-1.61	24.3
Grass Year 2	**4.5**	0	27.5
	5	0	18.1
	5.5	0	19.8
	6	0	21.1
	6.5	0	24.9
	7	0	31.1
	7.5	0	25.5
Wheat	**4.5**	25.4	9.36
	5	17.2	0.86
	5.5	4.63	15.4
	6	4.00	17.0
	6.5	6.52	13.1
	7	23.0	10.4
	7.5	25.8	24.7
Potato	**4.5**	92.3	-
	5	81.1	-
	5.5	86.4	-
	6	89.3	-
	6.5	88.2	-
	7	90.8	-
	7.5	89.7	
Barley	**4.5**	22.0	13.5
	5	20.9	18.9
	5.5	9.25	30.4
	6	4.04	31.4
	6.5	5.42	23.2
	7	8.09	24.7
	7.5	13.0	22.8
Swede	**4.5**	61.2	-
	5	59.4	-
	5.5	53.7	-
	6	53.2	-
	6.5	49.5	-
	7	50.7	-
	7.5	55.0	-
Oats	**4.5**	9.80	34.9
	5	6.57	35.7
	5.5	2.56	25.0
	6	6.47	29.7
	6.5	8.94	29.0
	7	18.4	25.8
	7.5	22.0	51.5

3.4.4.5 The Effect of Soil pH on Contaminants Associated with P Fertiliser Use

The effect of soil pH on Arsenic

The analysis of variance (**Appendix 3**, **Table 10.17**) showed that there was a significant effect of cropping and pH control on As_{Total} in the soil profile (crop x treatment x layer, d.f. = 24, p = 0.011) and that only pH control significantly influenced As_{Total} (treatment x layer, d.f. = 6, p = 0.027) while cropping did not (crop x layer, d.f. = 4, p = 0.722). The Pearson Correlation Coefficient Matrix showed that As_{Total} was positively, significantly correlated with soil pH in the subsoils (r = 0.407, p < 0.001) but not in the topsoils (r = 0.154, p = 0.116) (**Appendix 1**, **Table 10.4** and **Table 10.3** respectively).

The relationship between As_{Total} and soil pH in the topsols and subsoil of the pH Rotation is shown in **Figure 3.12**. Topsoil As_{Total} declined from 7.75 mg kg^{-1} at pH 4.5 to a minimum of 7.27 mg kg^{-1} at pH 6 before rising again to 7.65 mg kg^{-1} at pH 7.5. Subsoil As_{Total} increased from 4.98 mg kg^{-1} at pH 4.5 towards 6.05 mg kg^{-1} at pH 6 (were the subsoil converged with the topsoil) before levelling off at 6.37 mg kg^{-1} at pH 7.5. The second order polynomials fitted to the topsoil (R^2 = 0.921) and subsoil (R^2 = 0.841) As_{Total} respectively (**Appendix 4**, **Table 10.24**) were used to predict whether the As_{Total} was significantly elevated relative to the Field topsoil or subsoil As_{Total} (**Appendix 4**, **Table 10.31**). Only the topsoil was significantly elevated which suggested a link between P fertiliser application to the topsoil and As_{Total} elevations. The sorption of As_{Total} on amorphous Al and Fe-oxides as arsenate (Goldberg & Johnston, 2001) in the topsoil represents a potential source in excess of the natural concentrations. The maximum permissible concentration of As in agricultural soils to which sewage sludge has been applied is 50 mg kg^{-1} dry soil (The Sludge (Use in Agriculture) Regulations, 1989) and the contamination of As throughout the soil profile of the pH Rotation is 5x less than the limit and so after 54 years of continuous TSP application these limits are not exceeded. The reasons for the decline in subsoil As_{Total} at low pH could be due to less leaching of P fertiliser to the subsoil and more uptake and removal by deep rooting crops.

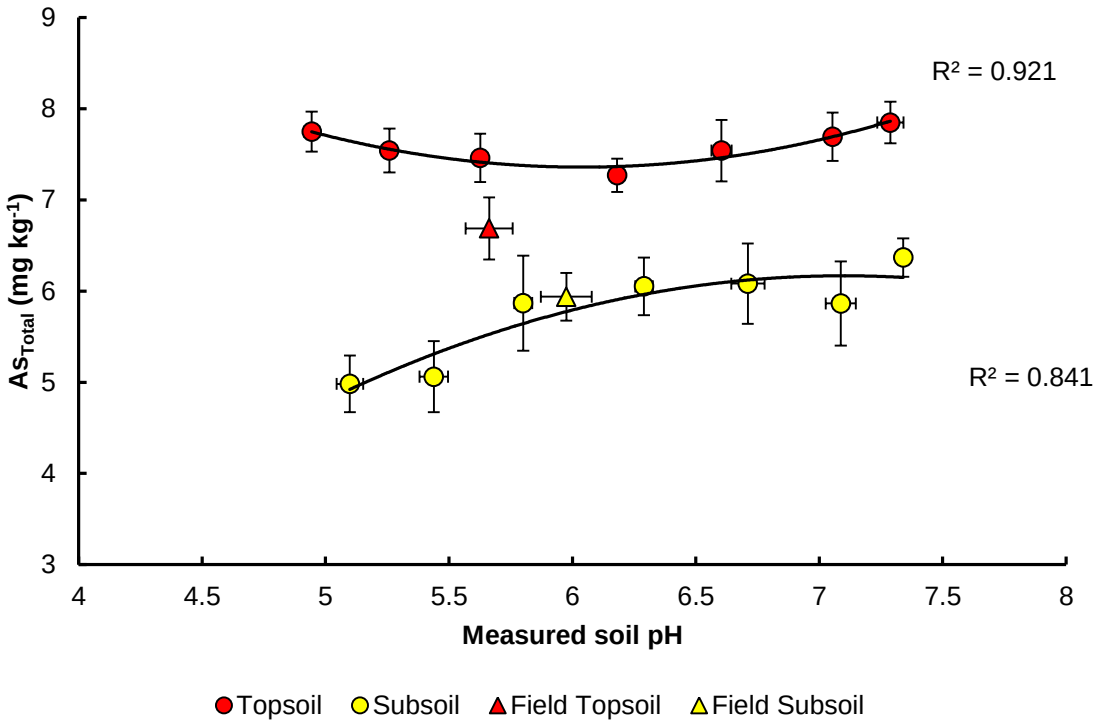


Figure 3.12. Mean As_{Total} in the topsoils and subsoils as a function of soil pH; trend-lines are 2nd order polynomials; means are of 5 crop phases ± SEM.

The effect of soil pH on Cadmium

The analysis of variance revealed that there was not a significant effect of cropping with soil pH on Cd_{Total} throughout the soil profile (crop x treatment x layer, d.f. = 24, p = 0.086) (**Appendix 3**, **Table 10.18**). However, there was a significant effect of pH control on topsoil and subsoil Cd_{Total} (treatment x layer, d.f. = 6, p = 0.028). The Pearson Correlation Coefficient Matrix revealed that Cd_{Total} was positively, significantly correlated with soil pH in the topsoils (r = 0.436, p < 0.001) and subsoils (r = 0.251, p = 0.010) (see **Appendix 1**, **Table 10.3** and **Table 10.4** respectively).

The relationship between soil pH and Cd_{Total} in the topsoils and subsoils of the pH Rotation and the Field surrounding the experiment is shown in **Figure 3.13**. Topsoil Cd_{Total} increased from a minimum of 0.236 mg kg^{-1} at pH 4.5 to a maximum of 0.295 mg kg^{-1} at pH 7.5. A 2nd order polynomial (R^2 = 0.923) was fitted to the data (**Appendix 4**, **Table 10.25**) and was used to predict that the Cd_{Total} across the pH gradient was not significantly elevated compared to the background Cd_{Total} (0.227 mg kg^{-1}) in the Field (**Appendix 4**, **Table 10.31**). In the subsoil, Cd_{Total} increased from 0.144 mg kg^{-1} (pH 4.5) to a maximum of 0.191 mg kg^{-1} at pH 6 where there was a convergence with topsoil Cd_{Total}. A 3rd order polynomial was fitted to the data (R^2 = 0.881) (**Appendix 4**, **Table 10.25**) and predicted that the pH plots were significantly elevated compared to the Field subsoil Cd_{Total} (0.169 mg kg^{-1}) (**Appendix 4**, **Table 10.31**). The increased

accumulation of topsoil Cd_{Total} above pH 5.5 may also be a result of the decrease in phyto-availability and a subsequent decrease of crop uptake of Cd as soil pH increased (Gray, *et al*., 1999). Stronger adsorption of Cd^{2+} as the pH rises is due to an increase in negatively charged surfaces of humic material and oxides along with a reduction in H^{+} competition (Evans, *et al*., 2003). The retention of Cd_{Total} in the topsoil may explain the relatively stable Cd_{Total} in the subsoil above pH 6 however below this pH, Cd is more mobile and may have been easily transferred to the subsoil. There are no guidelines as to the permissible limit of Cd contamination in soils from fertilisers in UK agriculture, however 3 mg kg^{-1} is the limit in soils which have received applications of sewage sludge (The Sludge (Use in Agriculture) Regulations, 1989). The greatest Cd_{Total} in this trial was ten-fold less than this limit, at a maximum of 0.295 mg kg^{-1} at pH 7.5 in the topsoil after 53 years of continuous TSP fertiliser application. Therefore, this limit is unlikely to be exceeded in the long-term. Both topsoil and subsoil Cd_{Total} were within the expected 'background' Cd concentration range of 0.10 to 1.80 mg kg^{-1} for Scottish rural soils as reported by the UK Soil and Herbage Pollutant Survey (Ross, *et al*., 2007, p.6) a value which is also unlikely to be exceeded in the pH Rotation.

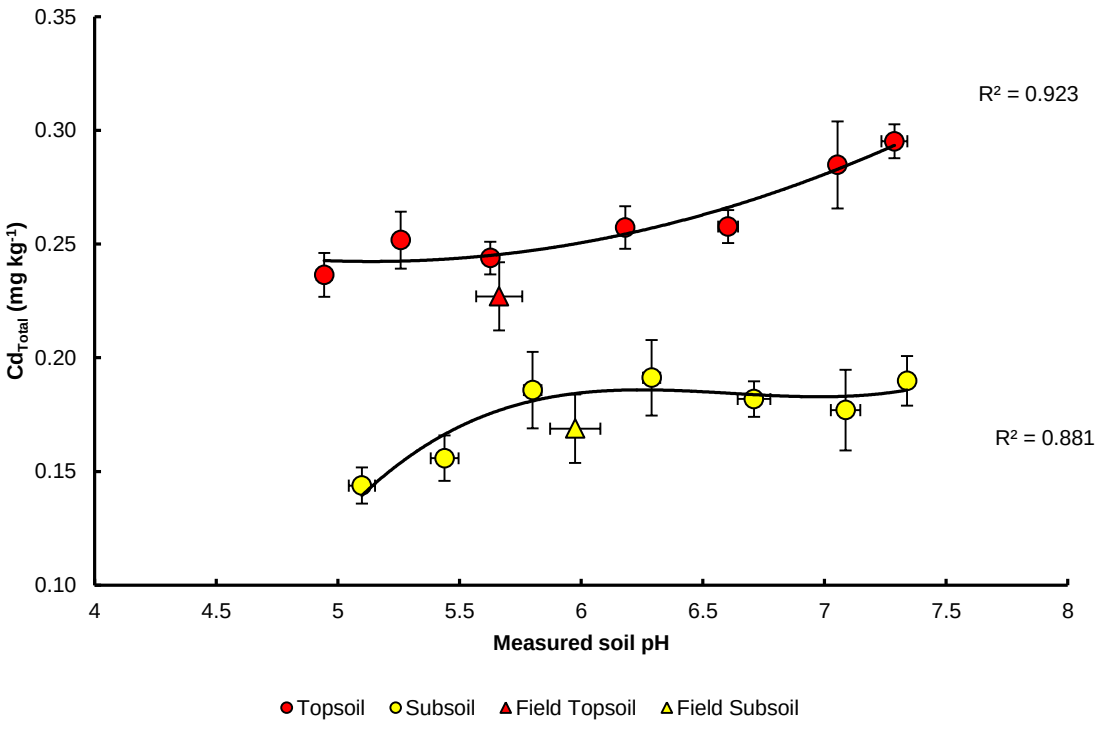


Figure 3.13. Mean Cd_{Total} in the topsoils and subsoils as a function of soil pH; trend-lines are 2nd and 3rd order polynomials for the topsoil and subsoil respectively; means are of 5 crop phases ± SEM.

The effect of soil pH on Uranium

The analysis of variance (**Appendix 3**, **Table 10.19**) indicated that there was no a significant combined effect of cropping and pH control on topsoil and subsoil U_{Total} (crop x treatment x layer, d.f. = 24, p = 0.647) however there was a significant effect of pH control (treatment x layer, d.f. = 6, $p < 0.001$) but not cropping (crop x treatment, d.f. = 4, $p = 0.433$). The Pearson Correlation Coefficient Matrix showed significant correlations between U_{Total} and pH in the topsoils (r = -0.466, $p < 0.001$) and the subsoils (r = 0.327, $p < 0.001$) (**Appendix 1**, **Table 10.3** and **Table 10.4** respectively).

The relationship between the average U_{Total} and soil pH in the topsoils and subsoils of the pH plots in the pH Rotation is shown in **Figure 3.14**; data are compared to those of the Field. The topsoil U_{Total} decreased steadily from 2.44 mg kg^{-1} at pH 4.5 to 2.32 mg kg^{-1} at pH 7.5. Subsoil U_{Total} increased from 1.99 mg kg^{-1} at pH 4.5 to a maximum of 2.18 mg kg^{-1} at pH 6 which remained fairly uniform towards pH 7.5. The decrease in topsoil U_{Total}, and increase in subsoil U_{Total}, between pH 4.5 and 6 suggested that the U_{Total} was perhaps adsorbed by organic matter and Fe/ Mn oxides (Ahmed, *et al*., 2014) at acid pH and became increasingly mobile through desorption as the pH rose. Uranium is more soluble with increasing soil pH and becomes less strongly adsorbed on to soil surfaces due to UO_2^{2+} interactions with carbonates (Echevarria, *et al*., 2001) and this may explain increased movement to the subsoil as the soil pH increases. Furthermore, U may also be associated with Ca and P in arable soils (Ahmed, *et al*., 2014) as a result of liming and phosphate fertiliser use. It is possible that, in the pH Rotation, U associated with Ca or P was leached to the subsoil between pH 6 and 7.5. The Pearson Correlation Coefficient Matrix revealed that U_{Total} and Ca_{Total} were significantly correlated in the topsoil (r = -0.344, $p < 0.001$) and subsoil (r = 0.355, $p < 0.001$). Correlations between P_{Total} and U_{Total} in the topsoil (r = 0.223, $p = 0.022$) and subsoil (r = 0.784, $p < 0.001$) were also significant, and strong, particularly in the subsoil. These correlations suggested that U_{Total} was linked to Ca_{Total} (due to liming) and P_{Total} (due to TSP fertiliser use) and suggest a link between topsoil and subsoil, with U possibly being transferred in association with P and Ca through leaching. The topsoil data was fitted to a 2nd order polynomial ($R^2 = 0.987$) and in the subsoil a 3rd order polynomial was fitted ($R^2 = 0.938$) (**Appendix 4**, **Table 10.26**); both were used to predict the topsoil and subsoil U_{Total} across the pH plots and both were significantly elevated compared to the Field topsoil and subsoil U_{Total}, likely due to long-term TSP fertiliser use (**Appendix 4**, **Table 10.31**). The U_{Total} in this experiment was greater than concentrations found in the soil profiles (100 cm) of the arable and woodland soils (1.2 to 1.6 mg kg^{-1}) reported by Ahmed, *et al*., (2014) however the P_{Total} in their study for the arable soil was less than 1000 mg kg^{-1}, compared to the 1200 to 2200 mg kg^{-1} reported in

this chapter. Schipper, *et al*., (2011) reported U_{Total} of between 1.07 and 2.80 mg kg^{-1} over a range of soil depths (75 cm) and P fertiliser application rates in the same soil investigated over a 23-year period. The results presented here are within the same scale as those reported by Ahmed, *et al*., (2014) and Schipper, *et al*., (2011) and agreed with the other authors in that U_{Total} is likely elevated in the soil profile due to long-term P fertiliser use.

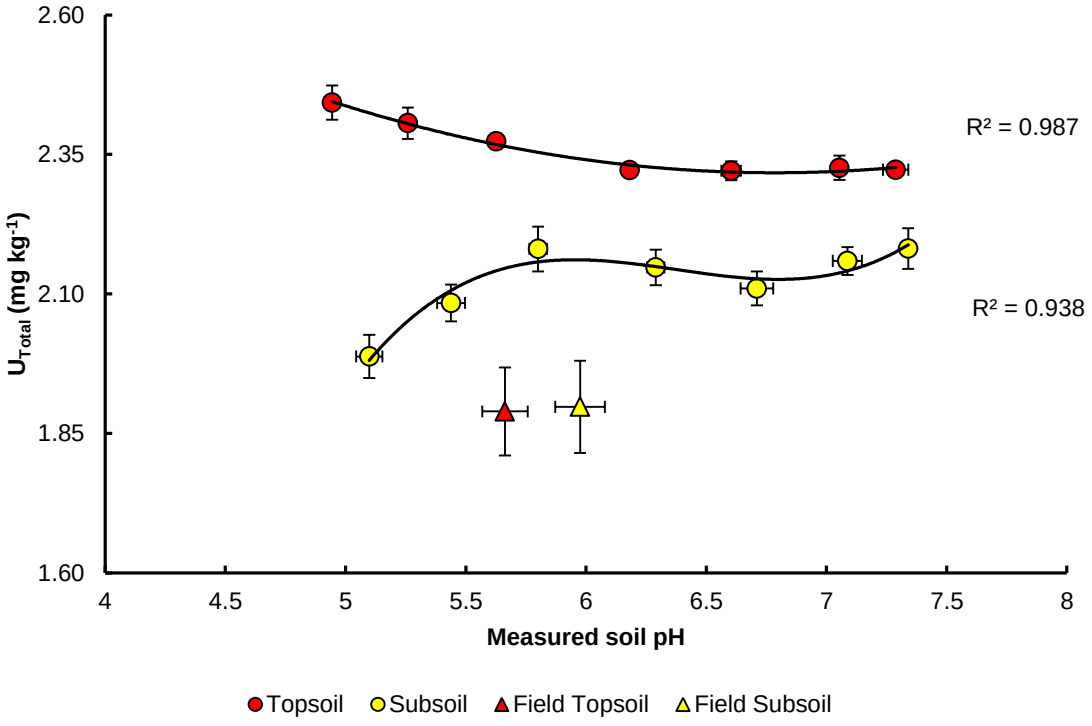


Figure 3.14. Mean U_{Total} in the topsoils and subsoils as a function of soil pH; trend-lines are 2nd and 3rd order polynomials for topsoil and subsoil respectively; means are of 5 crop phases ± SEM.

3.4.4.6 Topsoil: Subsoil ratios of P, As, Ca, Cd and U with Soil pH

The trends in topsoil: subsoil ratio for P_{Total}, As_{Total}, Cd_{Total} and U_{Total} showed clear similarities across the target soil pH range as shown in **Figure 3.15** while the topsoil: subsoil ratio for Ca_{Total} was consistently uniform across the pH gradient (i.e. close to 1.0). Topsoil: subsoil rates were greatest at pH 4.5 for P_{Total} (1.84), Cd_{Total} (1.64), As_{Total} (1.56) and U_{Total} (1.23). The rise in soil pH from pH 4.5 resulted in an overall decrease in the ratios towards a minimum at pH 6 for P_{Total} (1.41), As_{Total} (1.20) and U_{Total} (1.08) and a minimum at pH 5.5 for Cd_{Total} (1.31). The topsoil: subsoil ratio for U_{Total} appeared to plateau towards pH 7.5 where it reached a minimum of 1.06, whereas a second peak at pH 7 was observed for P_{Total} (1.48), Cd_{Total} (1.61) and As_{Total} (1.31). Soil pH appeared to be an important soil characteristic controlling the fate and re-distribution of residual P fertiliser from topsoil to subsoil, following well-known P solubility trends with pH (Lindsay, 1979). The topsoil: subsoil ratio for P_{Total} and Cd_{Total} were very similar across the pH range suggesting a link in P fertiliser use and movement to the subsoil (McDowell, 2012). There were near identical trends between P_{Total} and As_{Total}, which was expected as phosphate and arsenate are controlled similarly by soil pH and compete for adsorption sites (Manning & Goldberg, 1996).

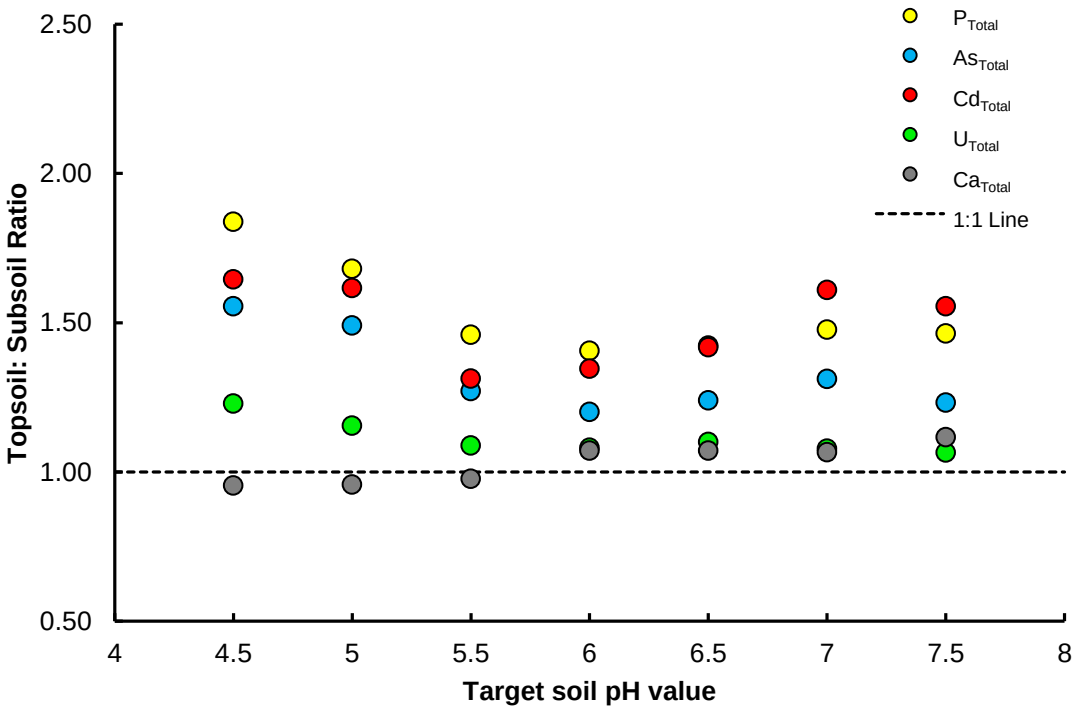


Figure 3.15. Relationship between soil pH and topsoil: subsoil ratios of P_{Total}, As_{Total}, Cd_{Total}, U_{Total} and Ca_{Total} compared to a 1:1 (dashed) line.

3.5 Conclusions

The objectives of this chapter were to investigate the effect of soil pH, crop rotation and P fertiliser management strategy on the distribution of residual P fertilisers and associated contaminants (As, Cd and U) in long-term experiments between topsoils and subsoils. An audit of total elemental concentrations in topsoils and subsoils was performed for the first time in the history of the site. Correlations were found between P and associated P fertiliser contaminants As, Cd and U in topsoils and subsoils. Furthermore, soil pH, Ca and P were also significantly correlated which reflected the maintenance of the target pH values using lime in the pH Rotation.

The effect of fertiliser treatment and cropping on P dynamics, As, Cd and U in the Old Rotation

Topsoil and subsoil P_{Total} were related to P fertiliser use in the Old Rotation. Regardless of fertiliser strategy, topsoil and subsoil P_{Total} in the fertiliser management plots was depleted compared to the native P_{Total} in the Field surrounding the trials (which is presumed to be unaffected by the proximity to the trials). The greatest P_{Total} depletion observed when P fertilisers were restricted and the use of TSP and GMP fertilisers appeared to reduce the rate at which the native soil profile P_{Total} in the Field had declined. This suggested long-term rotional cropping had depleted native P_{Total} stocks as crops utilised topsoil and subsoil P_{Total} reserves. Annual P balances using fertiliser application rates and crop P offtake with yield data, and net soil profile P_{Total} accumulation rates calculated relative to the native stocks in the Field were similar in scale and supported the conclusion that P_{Total} in the plots are under a gradual long-term decline. Contaminants Cd_{Total} and U_{Total} were associated with P fertiliser, as was As_{Total}, but to a lesser extent. Cadmium was more elevated when GMP was applied whereas U was more elevated in TSP treated plots. The maximum Cd_{Total} (0.30 mg kg^{-1}) was 10x less than the permissible limit for Cd applied to agricultural land following sewage sludge applications (The Sludge (Use in Agriculture) Regulations (1989)). Subsoil Cd_{Total} and U_{Total} were elevated compared to the Field when TSP and GMP fertiliser was applied, suggesting a link between P fertiliser application to the topsoil and the possible transfer of fertiliser and contaminants to the subsoil.

The effect of soil pH on P dynamics, As, Cd and U in the pH Rotation

Residual P fertiliser accumulated in the topsoils across the pH plots with the greatest P_{Total} levels found below pH 5 and above pH 7. The retention of P_{Total} in the topsoil at low pH was attributed to strong adsorption to Fe and Al oxides. The differenc between topsoil and subsoil P_{Total} around pH 6 was least, suggesting that residual P was transferred more readily to the subsoil which agrees with known maximum

solubility conditions for P in soil. As the pH rose towards pH 7.5, P_{Total} was retained more in the topsoil but not to the same extent as the acid plots and was possibly controlled by the precipitation of calcium phosphates. Long-term liming to maintain the target pH values increased topsoil and subsoil Ca_{Total} and resulted in almost uniform topsoil and subsoil pH values close to the target values. The P accumulation was greatest at pH 4.5 and 7.5 and least around pH 6, which is the optimum pH for crop production. However, there was also a significant crop effect which was revealed in the annual P balance for 2014-2015 growing season which varied between -1.91 and 92.3 kg ha^{-1} yr^{-1}, with particularly high residual P balances in the potato and swede phases, due to unusually low yields. Net soil profile P_{Total} annual accumulation rates across the pH plots ranged from 0.86 to 51.5 kg ha^{-1} yr^{-1} which was comparable to the annual P balance rate. Finally, contaminants associated with P fertiliser use were elevated in the topsoil and subsoil across the pH range; As_{Total} had a similar trend to P with pH. The convergence of topsoil and subsoil As_{Total}, Cd_{Total} and U_{Total} around pH 6 suggested a link between P fertiliser use and the accumulation of contaminants in the subsoil. The Cd_{Total} in the topsoil increased from pH 4.5 to 7.5 while subsoil Cd_{Total} increased between pH 4.5 and 6 and remained at a steady concentration towards pH 7.5. This suggested that Cd_{Total} was retained in the topsoil > pH 6 likely due to stronger adsorption of Cd^{2+} on to negatively charged surfaces such as oxides and humic materials (Evans, *et al*., 2003). Across the pH range topsoil U_{Total} declined between pH 4.5 and 7.5 while subsoil U_{Total} increased between pH 4.5 and 6. This could be a result of increased UO_2^{2+} solubility with rising pH due to the formation of soluble carbonate complexes (Echevarria, *et al*., 2001) which resulted in U becoming more mobile to the subsoil.

These results are significant because they show that long-term P fertiliser use, pH management and rotational cropping have a significant impact on topsoil and subsoil P dynamics. At agronomically significant pH values (pH 6 to 7) subsoil P is elevated where P fertiliser is most soluble. However, when the soil pH is sub-optimal (< pH 5.5), residual P fertiliser may accumulate in the topsoil resulting in poor fertiliser use efficiency for the farmer and economic losses if the accumulated fertiliser is lost to the wider environment. Furthermore, high soil P levels, such as those found in the pH Rotation, are thought to be linked to increased soil water and field-drainage P concentrations (Fortune, *et al*., 2005) and may have consequences for nearby surface water bodies. This finding is significant because these rotations represent past and present rotational cropping practices in the North East of Scotland and if farmers are targeting this pH range for their rotational cropping systems, then P may be leaching to the subsoil over time, resulting in poorer P use efficiency and an accumulation of resource in the subsoil which crops may or may not be able to access (i.e. shallow rooting crops such as 1st year grass leys compared to deep

rooting wheat crops). Arable subsoils could (i) become enriched in P_{Total} from fertiliser use between pH 6 and 7 which is optimum for crop growth and may continue to accumulate residual (potentially reactive) P fertiliser transferred from the topsoil under similar conditions or (ii) be under long-term depletion due to utilisation of reserves by crops, regardless of fertiliser management strategy or P fertiliser type applied (i.e. TSP or GMP). Where P depletion is occurring in both topsoil and subsoil, fertiliser application rates should be increased in order to improve crop productivity, particular were P deficiencies are observed in the plant material during crop walking.

4 Topsoil and Subsoil Olsen and Modified Morgan P as Affected by Soil pH and Fertiliser Management in Long-term Experiments

4.1 Abstract

The effect of historical phosphate fertiliser use and soil pH management on topsoil and subsoil Olsen (P_{Olsen}) and Modified Morgan ($P_{MMorgan}$) extractable P in the long-term 'Woodland's Rotation's experiments (Scotland's Rural College, Craibstone Estate, Aberdeen) was investigated. In a comparison of the methods, significant, positive correlations were found between Olsen and Modified Morgan in both the topsoil and subsoil however $P_{MMorgan}$ underestimates P_{Olsen} by 77% (topsoil) and 71% (subsoil). Differences were attributed to the extraction mechanisms: Modified Morgan's (pH 4.5) likely causes greater dissolution of calcium phosphates > pH 6 but the agreement between methods < pH 6 suggested that P was extracted by a similar mechanism, thought to be anion competition with phosphate for adsorption sites. There were also significant correlations between the topsoil and subsoil P_{Total}, P_{Olsen} and $P_{MMorgan}$ with subsoil P increasing as topsoil P increased by a factor of 0.681 (P_{Total}), 0.645 ($P_{MMorgan}$) and 0.503 (P_{Olsen}) which suggested a link between topsoil and subsoil P fractions. It was likely that P_{Olsen} overestimated the amount of available-P in the topsoil that is non-transferrable to the subsoil i.e. strongly bound to organic matter or Fe/ Al oxides. Topsoil P_{Olsen} was 2.53% and $P_{MMorgan}$ was 0.60% of P_{Total} whereas in the subsoil, P_{Olsen} was 1.84% and $P_{MMorgan}$ was 0.59% of the P_{Total}.

Soil pH strongly influenced the distribution of extractable P throughout the soil profile in the pH Rotation with evidence of unused, reactive P being retained in the topsoil due to adsorption with Fe and Al oxides at acidic pH (< pH 5.5) for both P_{Olsen} and $P_{MMorgan}$ resulting in (i) greater topsoil: subsoil distribution ratios and (ii) elevated soil P test classifications optimal for crop requirements in rotations that include potatoes. Topsoil P_{Olsen} was Index 4 or 3 and $P_{MMorgan}$ was SAC Status H or M±. The convergence of topsoil and subsoil P_{Olsen} and $P_{MMorgan}$ between pH 5.5 and 6.5 (where phosphate solubility is greatest) suggested greater transfer of P through leaching mechanisms as topsoil: subsoil ratios were close to 1.0 (i.e. uniform distribution) between the two layers. $P_{MMorgan}$ showed a distinct 'U' trend with pH with a minimum between pH 6 and 7 and this was reflected in SAC Status decreasing from 'H' at pH 4.5 through to 'M–' at pH 6 and rising towards 'H' again at pH 7.5. Subsoils were enriched across the pH gradient at levels suitable for the requirements of arable crops in rotations (P_{Olsen} at Index 2B & 3; $P_{MMorgan}$ Status M-), demonstrating that the subsoil has a strong potential to contribute available-P. There was a statistically significant effect of crop and pH control on P_{Olsen} and $P_{MMorgan}$ in the soil profile which was later shown to

be significant in topsoils but not subsoils. However, the effect of crop phase on P_{Olsen} or $P_{MMorgan}$ along the pH gradient in the topsoil was not clear and the main differences were attributed to changes in soil pH.

In the Old Rotation fertiliser treatment effects were evident; P_{Olsen} and $P_{MMorgan}$ increased with P_{Total} due to P fertiliser use: P_{Olsen} and $P_{MMorgan}$ was greater under (highly soluble) TSP fertiliser use than GMP treatments. This was confirmed in the soil P test classifications which showed that P_{Olsen} in the topsoil of the TSP treatment (Index 3) was greater than the GMP treatment (Index 2B). A link between topsoil and subsoil P was suggested by the elevated subsoil P_{Olsen} when TSP was applied (Index 2A). When compared to the Field, depletion of subsoil available-P was evident were N and K without P, or where no fertiliser was applied, with P_{Olsen} indices of 1 or zero, and $P_{MMorgan}$ status of L indicating deficiencies in P status. The topsoil: subsoil ratios of P_{Total}, P_{Olsen} and $P_{MMorgan}$ in the Field were similar suggesting the field had reached a steady-state across the P fractions. There was no consistent effect of crop on P_{Olsen} or $P_{MMorgan}$ across the fertiliser treatments. However, subsoil P_{Olsen} appeared to increase as the crop rotation progressed from grass phases through to oats reflecting increased P fertiliser use and possible leaching from the topsoil. $P_{MMorgan}$ appeared elevated under the grass phases in the topsoil and subsoil which was not revealed in the P_{Olsen} analysis. It was unclear why but was thought to be due to differences in the solubility of P in the contrasting reagents. These results provide unique, field-based evidence that long-term soil pH control and fertiliser management had a significant impact on topsoil and particularly subsoil P dynamics, enriching subsoils with plant-available P which demonstrate a strong potential for supplying P for crop requirements.

4.2 Introduction

Agricultural soils must be able to provide sufficient concentrations of plant-available phosphorus in order to sustain optimum crop yields and productivity. This is achieved through the use of phosphate fertiliser which is manufactured from phosphate rock, a finite resource, and one which is subject to volatile market prices and increasing demands (Cordell, *et al*., 2009). Furthermore, effective soil pH management is critical for optimising the plant-availability of P and for maintaining the health and productivity of crops (Holland, *et al*., 2018). In the UK there are two operationally defined 'soil P tests' which are used to quantify plant-available P concentrations in the soil and (thereby) estimate topsoil P fertiliser requirements. In Scotland, 'Modified Morgan P' ($P_{MMorgan}$) is extracted with an ammonium acetate/ acetic acid solution (McIntosh, 1969) and an optimum result would yield a 'SAC P Status' classification of Moderate (M ±) (Sinclair, *et al*., 2013; Edwards, *et al*., 2016) (**Table 4.1**). By contrast, in England, Wales and Northern Ireland, 'Olsen P' (P_{Olsen}) is extracted with sodium bicarbonate solution (Olsen, *et al*., 1954) and a soil 'P Index' of 2A or 2B would normally be considered ideal (AHDB, 2017) (**Table 4.1**). Recommendations from one test cannot be inferred from the results of the other (Sinclair, *et al*., 2013) and so it is important to use the appropriate test for the soil being analysed. Furthermore, these tests are normally applied to topsoil samples only and are not routinely used to determine how much plant-available P is in the deeper subsoil layers. One reason for this is the extra cost associated with the analysis (Barraclough, *et al*., 1997). However, it has long been understood that subsoil P reserves may be an important source of plant-available P (Kuhlmann & Baumgärtel, 1991) and it has recently been estimated that subsoils may contribute between 10 to 70% of a crop's nutrient requirements (Kautz, *et al*., 2013).

Table 4.1. Soil P concentration (mg kg^{-1}) ranges for P_{Olsen} and $P_{MMorgan}$ and the classification systems used.

P_{Olsen}	P Index*	$P_{MMorgan}$	SAC P Status**
0 to 9	0	0 to 1.7	Very Low (VL)
10 to 15	1	1.8 to 4.4	Low (L)
16 to 20	2A	4.5 to 9.4	Moderate - (M -)
21 to 25	2B	9.4 to 13.4	Moderate + (M +)
26 to 45	3	13.5 to 30	High (H)
>45	4+	> 30	Very High (VH)

*P Index: classification system for P_{Olsen} used by AHDB (previously DEFRA) in the RB209 Fertiliser Manual (AHDB, 2017)
**SAC P Status: classification system for $P_{MMorgan}$ used by Scotland's Rural College (Sinclair, *et al*., 2013)

Long-term experiments can be used to investigate the impact of historical agricultural management on crop and soil systems (Johnston & Poulton, 2018) and provide field-based evidence that is used to assess the agronomic factors that influence the accumulation and availability of P throughout the soil profile. Crops in long-term crop rotation experiments were able to utilise available P resources in low P status soils more effectively in plots were the soil was limed to raise the pH from acidic to near-neutral values (von Tucher, *et al*., 2018). Long-term use of farm yard manure in arable/fodder and wheat/maize rotations increases available- P which can be more readily leached in soils with the same texture (Vanden Nest, *et al*., 2016). Residual P in the soil could be a potential resource for crops but utilising it effectively remains a challenge (Withers, *et al*., 2017). However, consideration for the topsoil alone is not sufficient and consideration must be given to the subsoil (Andersson, *et al*., 2013). For example, subsoils can become enriched in P following long-term P fertilisation (Pizzeghello, *et al*., 2014; Rubæk, *et al*., 2013). Different soil textures can also influence the re-distribution of P from topsoil to subsoil where reactive P may accumulate (Andersson, *et al*., 2013; Pizzeghello, *et al*., 2014). Compared to the topsoil, relatively little is known about the amount and forms of P in the subsoil (Andersson, *et al*., 2015; Barej, *et al*., 2014) and therefore further research is required to understand subsoil P availability (von Tucher, *et al*., 2018), the factors influencing subsoil P dynamics and the conditions under which crop utilisation of subsoil P may be driven (Bauke, *et al*., 2018).

4.2.1 Aims and Objectives

The aims of this chapter were to investigate the availability of topsoil and subsoil phosphate after long-term pH management, rotational cropping and fertiliser use, and determine the potential significance of subsoil P availability to crop P requirements under the influence of these factors. The hypothesis was that long-term P fertiliser use, soil pH control and rotational cropping results in reactive, potentially plant-available P accumulation in both topsoil and subsoil. Migration of P to the subsoil would depend on (i) P fertiliser management strategy with soluble P fertilisers migrating to the subsoil, (ii) pH influencing P solubility in soil solution, and (iii) crop rotation as different crops require different P fertiliser application rates and crop utilisation of P varying depending on the crop. This was achieved by utilising the Woodland's Field long-term experiments. The objectives are listed below.

1. Investigate topsoil and subsoil P availability using the two main UK soil P tests (P_{Olsen} and $P_{MMorgan}$).
2. Discuss the effect of soil pH control, fertiliser use strategy and long-term ley/arable rotation on the availability of P in the soil profile.
3. Discuss the implications of the topsoil and subsoil available P result classifications and the potential contribution to crop requirements.

4.3 Materials and Methods

4.3.1 Sample Site, Trial Description, Soil Sampling, Preparation and Analysis

Full details of the long-term experiments used in this study are described in **Chapter 2 Materials and Methods** which outlines the sample site and description of the trials (**section 2.1**), trial management (**section 2.1.1**), soil sampling and preparation (**section 2.2**) and various soil analyses such as soil pH (**section 2.4**), total element analysis (**section 2.6**), the extraction of P by Olsen (**section 2.7.1**) and Modified Morgan reagents (**section 2.7.2**), the colorimetric determination of extracted P (**section 2.7.3**) and the statistical analysis (**section 2.8**). In this study, air-dried, sieved (< 2 mm) topsoil and subsoil samples from all three replicate auger borings in each treatment plot were selected from all seven target pH plots (pH 4.5 to 7.5 in 0.5-unit increments) under five of the eight crop phases in the pH Rotation (grass (1st and 2nd year), winter wheat, spring oats and spring barley). This was also undertaken from four of the six fertiliser treatment plots (NK with GMP, NK with TSP, NK without P and zero fertiliser) under five of the six crop phases in the Old Rotation (grass (1st, 2nd and 3rd year), spring oats and spring barley). All of the soil samples from the uncultivated grassland field surrounding the trials (9 topsoil and 9 subsoil) were also analysed and are hereafter referred to as Field.

4.4 Results and Discussion

4.4.1 Comparison of Extractable P Between the Two Soil P Tests

The relationship between P_{Olsen} and $P_{MMorgan}$ in the topsoil and subsoil for all soil samples (n = 348) measured in the long-term experiments and the Field is shown in **Figure 4.1**. There were significant, strong, positive linear relationships between the two methods for the topsoil (r = 0.783, $p < 0.001$) and subsoil (r = 0.753, $p < 0.001$): as P_{Olsen} increased $P_{MMorgan}$ also increased. There was vertical scatter in 29 topsoil extractions between 30.6 and 51.0 mg kg^{-1} P_{Olsen} and 10.0 to 22.3 mg kg^{-1} $P_{MMorgan}$. All of these topsoils were from the pH Rotation plots 7.5 (15/29), 7 (8/29), 6.5 (2/28) and 6 (6/28). Furthermore, there was also vertical scatter in 19 subsoils between P_{Olsen} 15.5 to 34.5 mg kg^{-1} and $P_{MMorgan}$ 10.2 and 18.8 mg kg^{-1} which were attributed to a broader range of pH plots: pH 4.5 (3/19), 5 (3/19), 6 (2/19), 6.5 (2/19), 7 (3/19) and 7.5 (6/19). The majority of plots showing this scatter were > pH 6 which reflects the effect of acid Modified Morgan reagent (pH 4.8) reacting with the neutral and alkaline soils that are limed, resulting in the dissolution of calcium phosphate and an increase in available-P, in contrast to the effect of the alkaline Olsen method reducing Ca concentration in solution to promote phosphate solubility (Wuenscher, *et al*., 2015). As the majority of scatter is explained by plots > pH 6, where the dissolution of calcium phosphates is the main mechanism controlling available-P, so the majority of the remaining data which is well correlated between the two methods for topsoil and subsoil is likely to be pH plots < 6 and the plots in the Old Rotation are generally < pH 6 also. The two methods may have a similar mechanism for extracting P in the acidic pH range such as competition between anions and phosphate which compete for binding sites on to Fe and Al oxides. The Modified Morgan reagent (pH 4.5 ammonium acetate/acetic acid) may promote desorption of P from Fe and Al oxides through competition between phosphate and acetate (CH_3COO^-) in the more acidic plots despite phosphate having a higher affinity than CH_3COO^- (van Hees, *et al*., 2003) because of the large concentration of CH_3COO^- introduced by the reagent. In contrast the Olsen reagent introduces a high concentration of bicarbonate (HCO_3^-) which will compete with phosphate for Al and Fe oxide surfaces (such as goethite) and also cause a change in the surface charge of Fe oxides thus weakening the adsorption strength of phosphate (Rahnemaie, *et al*., 2007). The Modified Morgan method extracted 23% and 29% of the P extracted from the topsoil and subsoil by the Olsen method respectively which indicated the differences in the mechanisms of the two methods applied across the range of soils analysed. These results suggest that the estimate of 'available P' between the two methods was not directly comparable in topsoils or subsoils and this agreed with the conclusion from the $P_{MMorgan}$ fertiliser recommendations (Sinclair, *et al*., 2013). Soil P tests are operationally defined and

have been shown to extract different amounts and forms of P species in a given soil (Neyroud & Lischer, 2003) and so it is unsurprising that these two contrasting methods (acid Modified Morgan vs alkaline Olsen reagents) are not comparable in the amount of P removed from the soil covering a broad range of soil pH values.

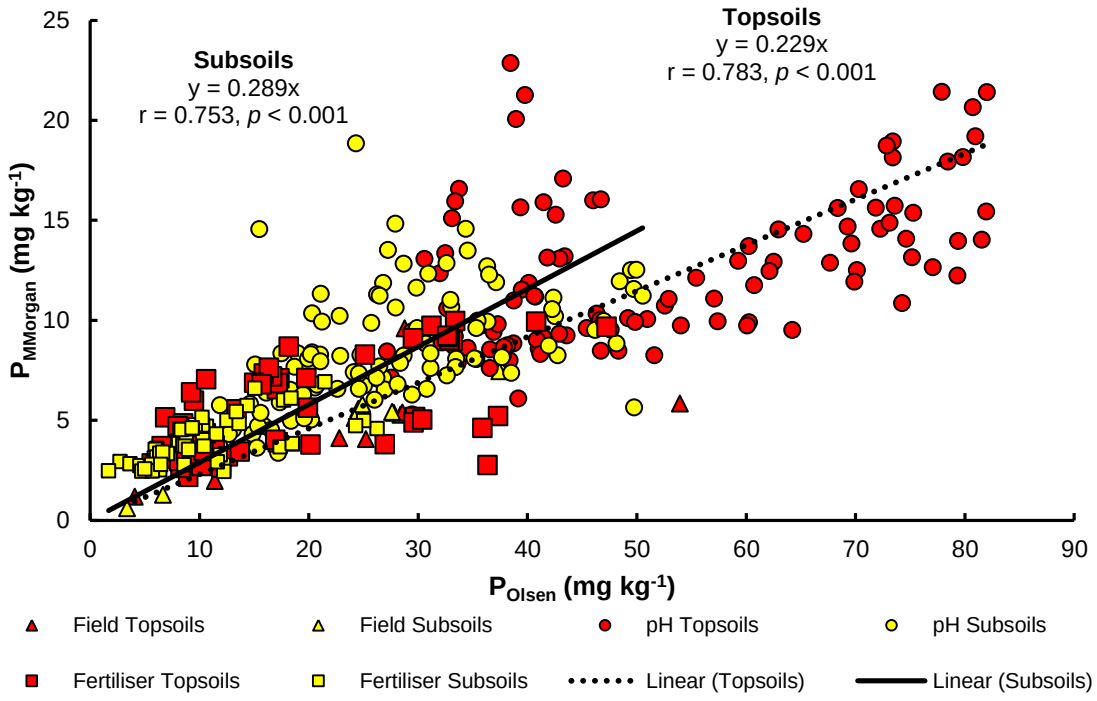


Figure 4.1. Relationship between topsoil and subsoil P_{Olsen} and $P_{MMorgan}$ for all soil samples analysed in the dataset across both long-term experiments and the Field (n = 348). The linear trend lines are forced through zero.

4.4.2 Relationships Between Topsoil and Subsoil Forms of P

The relationship between topsoil and subsoil (i) P_{Total}, (ii) P_{Olsen} and (iii) $P_{MMorgan}$ for all individual soil cores (n = 174) is shown in **Figure 4.2**. There was a significant correlation between topsoil and subsoil P_{Total} (r = 0.629, $p < 0.001$) and as the topsoil P_{Total} increased, the subsoil P_{Total} increased by a factor of 0.681. There was also a strong, significant correlation between topsoil and subsoil P_{Olsen} (slope = 0.503; r = 0.718, $p < 0.001$) and a similar significant correlation was also observed between the topsoil and subsoil $P_{MMorgan}$ data (slope = 0.645; r = 0.683, $p < 0.001$). Subsoil increased with topsoil P; in the order of the largest to smallest increases the subsoil increased with topsoil P_{Total} (0.681) > $P_{MMorgan}$ (0.645) > P_{Olsen} (0.503) which suggested that reactive forms of P, likely from the application of P fertilisers to the topsoil, were being transferred from topsoil to subsoil. The topsoil and subsoil P_{Total} had the strongest correlation between because P_{Total} represents all of the P in the soil, followed by $P_{MMorgan}$ and then P_{Olsen} respectively. On average, over the entire dataset (n = 174 soil cores), $P_{MMorgan}$ was 0.60% (± SD 0.22%) and P_{Olsen} was 2.35% (± SD 1.05%) of topsoil P_{Total}. In the subsoil, $P_{MMorgan}$ was 0.59% (± SD 0.23%) and P_{Olsen} was 1.84% (± SD 0.93%) of the subsoil P_{Total}. Of the three P fractions, the subsoil P_{Olsen} increased the least with increasing topsoil P_{Olsen} suggesting that the Olsen reagent extracts P in the topsoil that is not readily transferable to the subsoil such as organic bound P, strongly adsorbed P or insoluble Ca-P. The reagent may extract unavailable forms through anion competition resulting in a change in surface charge and subsequent desorption of strongly bound P on Fe and Al oxides (< pH 5.5) and increasing the solubility of phosphate through dissolution of calcium phosphates (> pH 6) thus contributing to the lowering of the ratio at which the subsoil appears to increase with the topsoil P_{Olsen}. It is possible that the application of the Modified Morgan method to naturally acidic soils results in less un-available P from being extracted i.e. the Olsen method can access fractions of P that the Modified Morgan reagent cannot in these soils, and the fractions extracted by Modified Morgan are more likely to be transferred to the subsoil. These relationships may also be the result of reactive fertiliser P being transferred from the topsoil to the subsoil by leaching for example, where it is then retained by the subsoil in a reactive form (Andersson, *et al*., 2013) and contributes to the trend where subsoil increases with increasing topsoil P_{Total}.

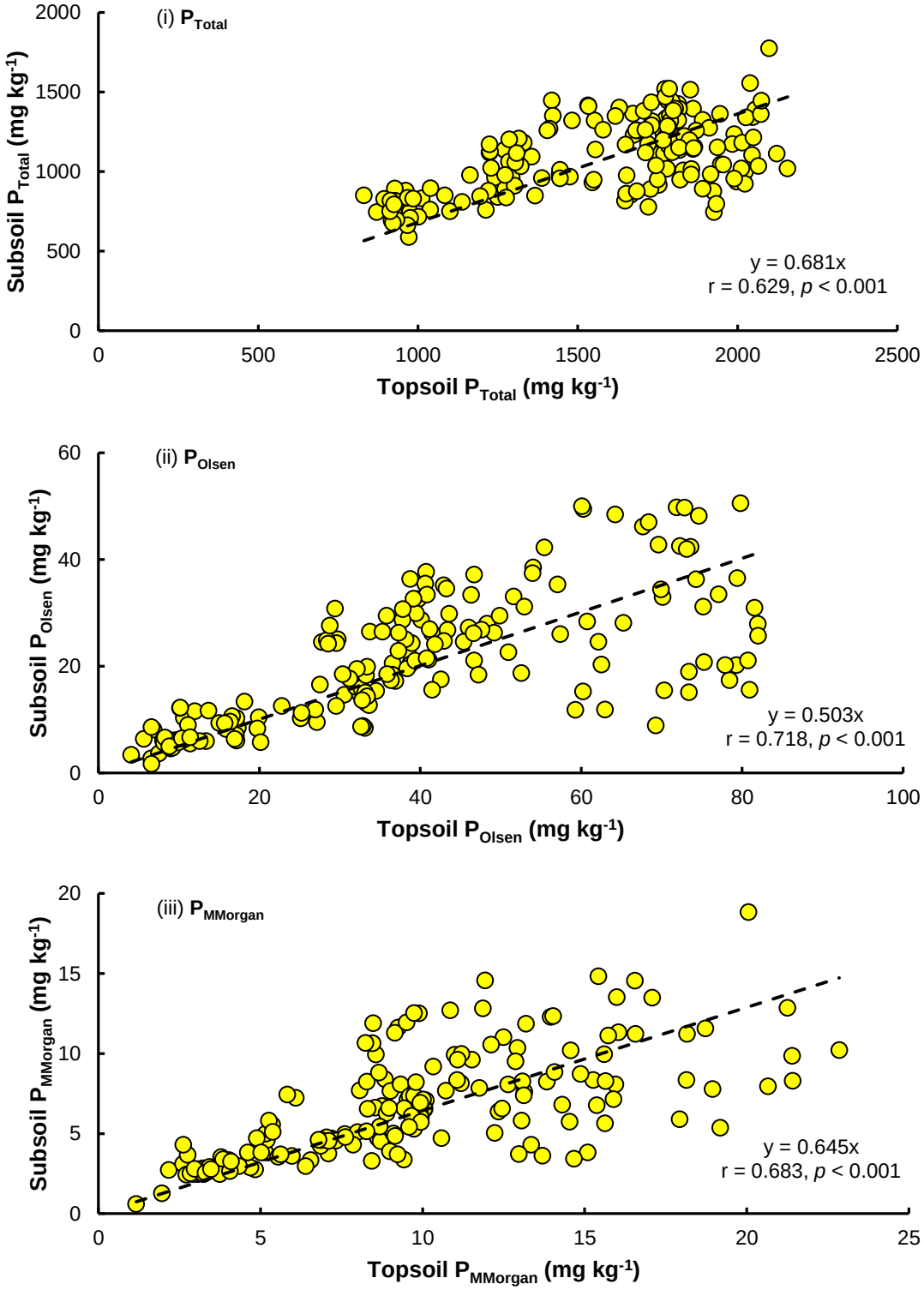


Figure 4.2. Relationship between topsoil and subsoil (i) P_{Total}, (ii) P_{Olsen} and (iii) $P_{MMorgan}$ with linear trend lines forced through zero.

4.4.3 Effect of Soil pH Management on Topsoil and Subsoil P in the pH Rotation

The relationships between P_{Olsen} and $P_{MMorgan}$ trends with soil pH for the topsoils and subsoil of the pH Rotation are shown in **Figure 4.3** and **Figure 4.4** respectively. There was a marked decrease in topsoil P_{Olsen} from 74.5 mg kg^{-1} at pH 4.5 towards a minimum of 36.4 mg kg^{-1} at pH 6.5 before an upturn of P_{Olsen} to 40.1 mg kg^{-1} at pH 7.5. In contrast, the topsoil $P_{MMorgan}$ showed a distinctive 'U' trend with soil pH with $P_{MMorgan}$ greatest around pH 4.5 (17.1 mg kg^{-1} ± SEM 1.26 mg kg^{-1}) and pH 7.5 (16.4 mg kg^{-1} ± SEM 1.42 mg kg^{-1}) with a minimum of 8.73 mg kg^{-1} (± SEM 0.41) between pH 6 and 6.5. The relationships between pH and subsoil P_{Olsen} and $P_{MMorgan}$ were broadly similar to each other. Extractable-P increased as soil pH increased from pH 4.5 as the difference between topsoil and subsoil was least between pH 5.5 and 6 at subsoil P_{Olsen} of 35.2 mg kg^{-1} (± SEM 3.65 mg kg^{-1}) and $P_{MMorgan}$ of 8.72 mg kg^{-1} (± SEM 1.03 mg kg^{-1}). Minimum concentrations were observed between pH 6.5 and 7 where P_{Olsen} was 21.7 mg kg^{-1} (± SEM 1.45 mg kg^{-1}) and $P_{MMorgan}$ was 7.03 mg kg^{-1} (± SEM 1.07 mg kg^{-1}). There was an upturn in P_{Olsen} to 23.4 mg kg^{-1} (± SEM 1.53 mg kg^{-1}) and $P_{MMorgan}$ to 10.2 mg kg^{-1} (± SEM 1.11 mg kg^{-1}) at pH 7.5. Fortune, *et al*., (2005) found that field-drainage P levels (molybdate-reactive P) and 0.01 M $CaCl_2$ extractable-P increased linearly with rising soil P_{Olsen} concentrations. In particular, linear correlations were found at P_{Olsen} greater than 20 mg kg^{-1} and up to 100 mg kg^{-1}, which is the range of P_{Olsen} found in the pH Rotation. The results of Fortune, *et al*., (2005) suggest that there could be a 'Change-Point', or a link between soil and water P, at which high soil P_{Olsen} levels result in increased P dissolved in soil water, that is susceptible to leaching. Dissolved P could potentially accumulate in the subsoil and may explain increased P_{Olsen} levels in the subsoils in the pH Rotation due to the high P_{Olsen} levels found in the pH plots. The retention of P below pH 5.5 in the topsoil may indicate that less leaching occurred due to stronger adsorption to Fe and Al oxides (Hartikainen, *et al*., 2010) despite the greater concentrations of extractable-P. The difference between topsoil and subsoil P_{Olsen} and $P_{MMorgan}$ was least between 5.5 and 6 which may suggest that this was the optimum pH range for P leaching and the topsoil and subsoil dynamics > pH 6 are likely a result of calcium phosphate mineralogy and soil pH controlling the fate of P (Tunesi, *et al*., 1999).

The Modified Morgan extractant may increase P availability at acidic pH through competition between CH_3COO^- and phosphate for adsorption sites promoting phosphate desorption (van Hees, *et al*., 2003) which would explain the high availability at pH 4.5. Furthermore, acetic acid can increase the solubility of P through the dissolution of calcium phosphates (i.e. highly soluble monocalcium phosphate) (Bolan, *et*

al., 1994) thus explaining the second maximum P availability at > pH 6. In contrast, P_{Olsen} shows a maximum only at pH 4.5 reflecting the difference in the mechanisms of the Olsen method across the pH range towards pH 7.5. Competition between HCO_3^- from the Olsen reagent and phosphate bound to Fe and Al oxides releases the maximum amount of P_{Olsen} in the pH range. Furthermore, as the pH increases, Ca^{2+} in solution increases due to liming, so the effect of the Olsen reagent on reducing Ca in solution is less with rising pH. The subsequent dissolution of calcium phosphates due to the lowering of solution Ca is less pronounced thus the available-P is not observed to be as high i.e. the precipitation of calcium phosphates following liming may be one reason for the decline in P_{Olsen} with increasing pH (Sorn-srivichai, *et al*., 1984).

The 3rd order polynomials describing the data in **Figure 4.3** fitted the P_{Olsen} data well in both topsoil (R^2 = 0.998) and subsoil (R^2 = 0.956) (**Appendix 4**, **Table 10.28**). The 3rd order polynomial models fitted for the $P_{MMorgan}$ topsoil (R^2 = 0.917) and subsoil (R^2 = 0.817) data shown in **Figure 4.4** were also a good fit (**Appendix 4**, **Table 10.29**). There appeared to be elevations in P_{Olsen} and $P_{MMorgan}$ across the pH plots in both the topsoil and subsoil, compared to the 'background level' of P_{Olsen} and $P_{MMorgan}$ in the Field. The models used for P_{Olsen} and $P_{MMorgan}$ were used to predict (**section 2.8**) and confirm that topsoils and subsoils were significantly elevated in P_{Olsen} and $P_{MMorgan}$ compared to the Field (**Appendix 4**, **Table 10.31**). Long-term applications of P fertilisers have been shown to increase P_{Total} and P_{Olsen} throughout the soil profile in double cropping systems (Khan, *et al*., 2018) and so a combination of pH management and TSP fertiliser (and FYM) application likely contributed to the build-up of reactive P in this ley/arable rotation. Therefore, these results suggested that P was transferred from the topsoil to the subsoil, despite strong retention of P in the topsoil, which resulted in the enrichment of the subsoil with P across the pH gradient. Liming improves crop productivity and health (Holland, *et al*., 2018) and so the distribution of topsoil P to the subsoil via translocation to deeper roots in crops (de Miranda & Rowell, 1987) may also have contributed to the increased subsoil extractable-P even where P was retained in the topsoil. Furthermore, liming can enhance P solubility as shown in long-term experiments (Simonsson, *et al*., 2018) and therefore soluble P may have been readily leached from topsoil to subsoil at agronomically significant pH values (pH 6 to 6.5). Leaching is another mechanism for topsoil to subsoil transport of P; the pH Rotation is of the Counteswells Association, which is a sandy loam texture and phosphorus leaches rapidly to subsoil layers in sandy textured soils (De Bolle, *et al*., 2013).

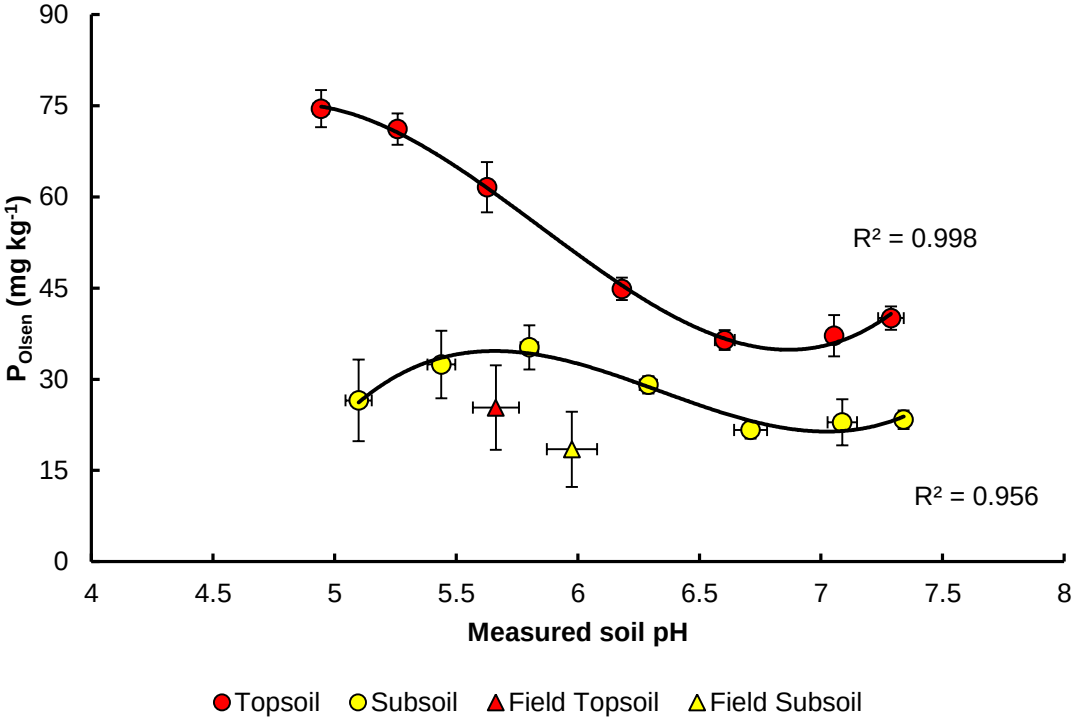


Figure 4.3. P_{Olsen} as a function of soil pH for topsoil and subsoil in the pH Rotation; 3rd order polynomials. Each point is the mean of 5 crop phases ± SEM.

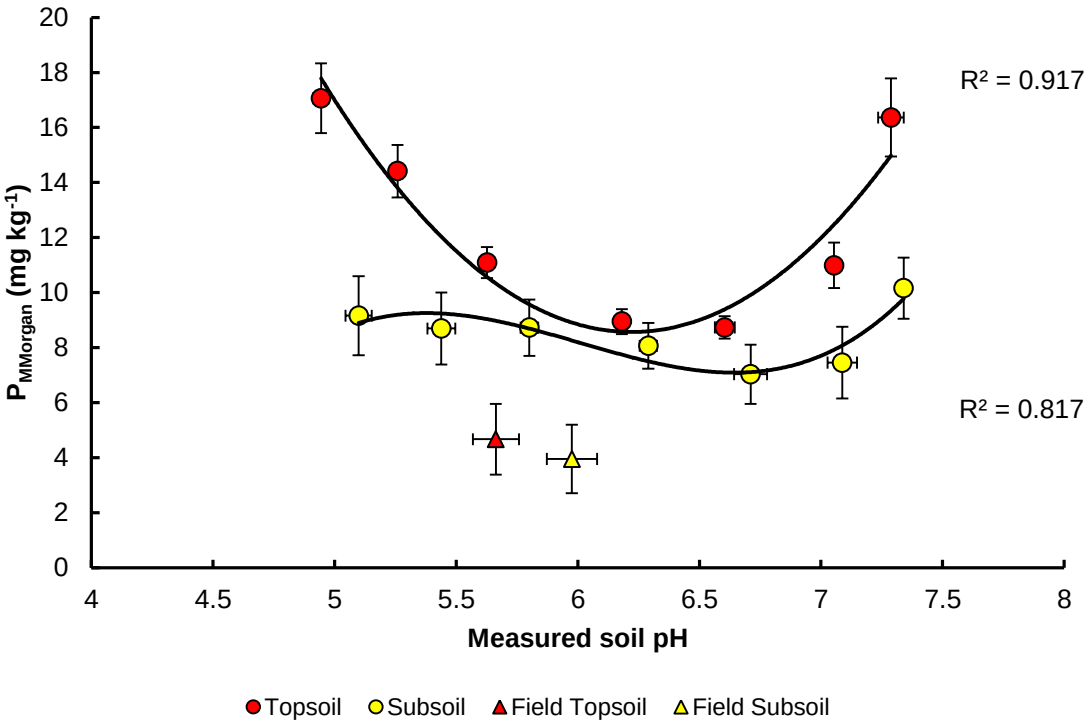


Figure 4.4. $P_{MMorgan}$ as a function of soil pH for topsoil and subsoil in the pH Rotation; the trend-lines 2nd and 3rd order polynomials respectively; means are of 5 crop phases ± SEM.

4.4.3.1 Effect of pH on the Topsoil: Subsoil P Ratio

The relationships between the target soil pH value and the topsoil to subsoil ratio for P_{Total}, P_{Olsen} and $P_{MMorgan}$ are shown in **Figure 4.5**. Topsoil: subsoil ratios were greatest at pH 4.5 for P_{Total} (1.84), P_{Olsen} (2.81) and $P_{MMorgan}$ (1.86). The rise in soil pH from pH 4.5 resulted in an overall decrease in all three ratios towards a minimum P_{Total} (1.41), P_{Olsen} (1.54) and $P_{MMorgan}$ (1.11) at pH 6 before a slight rise towards pH 7.5 to 1.46 for P_{Total}, 1.72 for P_{Olsen} and 1.46 for $P_{MMorgan}$. The P_{Total} ratios showed a fairly conservative trend with pH. Values fall in the range 1.4 to 1.9 reflecting (i) accumulation as oxide-bound P at low pH, (ii) Ca phosphate precipitation at high pH and (iii) accumulation of organic P across the range of soil pH values. There was a minimum value close to pH 6 due to maximum P availability for crop uptake and greater solubility at this point on the pH scale.

Ratios for $P_{MMorgan}$ were similar to those of P_{Total} but showed greater variation with pH. There was a pronounced minimum close to 1.0 at pH 6.0 and consistently lower values (than for P_{Total}) in the pH range of 5.5 to 6.5. The $P_{MMorgan}$ values close to 1.0 around pH 6 may reflect the greater solubility of fertiliser P and increased transfer to subsoil. This was not so pronounced in the P_{Total} ratios because of additional transformation of fertiliser P to organic P forms in topsoil, in the pH zone of optimum plant growth which are not assayed by the Modified Morgan's extractant. Beyond pH 6 the $P_{MMorgan}$ values rose steeply and consistently up to pH 7.5 in marked contrast to ratios for P_{Total} and P_{Olsen}. This is most likely a result of Ca phosphate dissolution in neutral and alkaline topsoil samples by the acidic Modified Morgan reagent (pH 4.5) in contrast to the alkaline Olsen extraction. There was almost complete convergence of $P_{MMorgan}$ and P_{Olsen} ratios at pH 7.5.

The ratios of P_{Olsen} were uniformly higher than those of P_{Total} and $P_{MMorgan}$ across the pH range and the difference increased as pH falls below pH 5.5. It is apparent that the Olsen extraction method (**Figure 4.3**) dissolves more P than the Modified Morgan reagent (**Figure 4.4**) in both topsoil and subsoil. However, it is also clear that the P fractions accessed by the Olsen reagent, but not by the Modified Morgan's reagent, are more prevalent in the topsoil. This could indicate alkaline hydrolysis of organic-P by sodium bicarbonate (Hamdan, *et al*., 2012) mainly in the topsoil. The air-drying of soil samples may have increased the bicarbonate extractable organic-P content of the soil which is greatest at pH 4.5 and declines towards pH 6 (Turner & Haygarth, 2003). However, it is also possible that oxide-bound forms of P are more prevalent in the topsoil and their suspension in a $NaHCO_3$ solution dissolves substantially more than is solubilised in the Morgan's reagent. The pH adsorption envelope for phosphate showed a

sharp decline in adsorption strength close to the second pKa value of 7.2. Dissolution of oxide bound P in the Olsen reagent is therefore most likely to be greatest in soils with pH values < 5 which will have accumulated strongly adsorbed P. This could explain not only the separation of the P_{Olsen} ratio from those of P_{Total} and $P_{MMorgan}$ but also the divergence shown in **Figure 4.5** in the pH range 4.5 to 5.0.

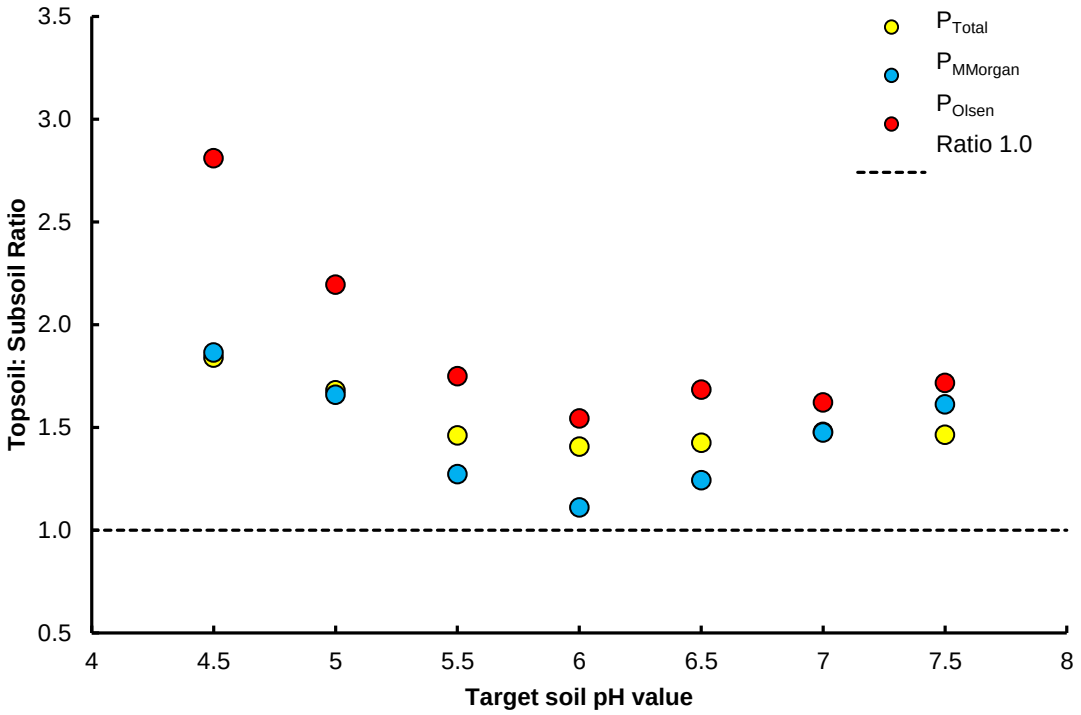


Figure 4.5. Relationship between the topsoil: subsoil P ratio and target soil pH for P_{Total}, P_{Olsen} and $P_{MMorgan}$ compared to a ratio of 1.0 (broken line).

4.4.4 Effect of Crop Rotation on P_{Olsen} and $P_{MMorgan}$ in the Topsoil and Subsoil across the pH gradient of the pH Rotation

An analysis of variance (**section 2.8**) indicated that P_{Olsen} in the topsoil and subsoil varied significantly due to a combination of both crop and soil pH (crop x pH x layer: d.f. = 24, $p < .001$) (**Appendix 2**, **Table 10.21**). The same was found for $P_{MMorgan}$ (crop x pH x layer: d.f. = 24, $p < .001$) (**Appendix 2**, **Table 10.22**). It was expected that there would be an effect of cropping on phosphate availability as the annual (net positive) P balance between fertiliser P input and crop P offtake varied between crops across the pH gradient (**Chapter 3**).

The relationship between measured soil pH value and P_{Olsen} in the topsoil and subsoil for the five crop phases investigated is shown in **Figure 4.6**. The 3rd order polynomial regression analysis indicated a significant interaction between the crop phase and soil pH in the topsoil (pH x crop, d.f. = 12, p = 0.008) (**Appendix 4**, **Table 10.28**) however the differences in topsoil P_{Olsen} between crop phases were not clear. The topsoil P_{Olsen} decreased under all crop phases between pH 4.5 and pH 6.5 indicating greater crop productivity and P_{Olsen} uptake as the soil pH increased within the range optimum for crop production (Goulding, 2016). There was not a significant effect of crop and pH on subsoil P_{Olsen} (pH x crop, d.f. = 12, $p = 0.275$) as shown by the 3rd order polynomial analysis, suggesting that the annual rotation of crop phase had little influence on subsoil P_{Olsen} and the main influence was likely soil pH control as discussed previously (**section 4.4.3**). The topsoil receives fertiliser inputs which varies depending in the crop. Therefore, significant differences in the amount of P in the topsoil for each crop phase is expected whereas the subsoil relies on redistribution of P from topsoil. The subsoil may not be influenced by crop factors such as crop demand or fertiliser application rates based on crop demand.

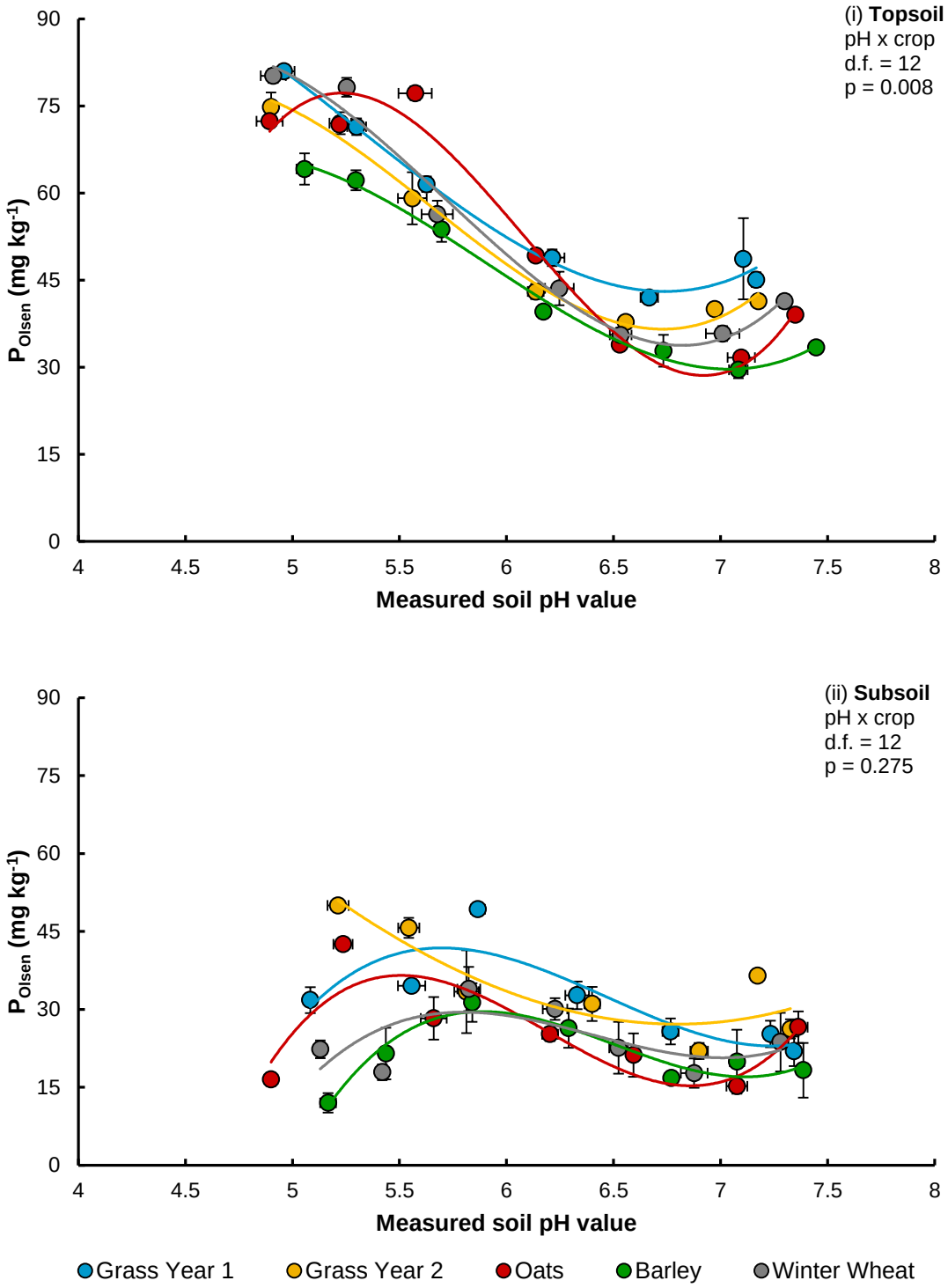


Figure 4.6. Relationship between soil pH and P_{Olsen} for 5 crop phases in the (i) topsoil and (ii) subsoil, with 3rd order polynomials fitted to the data.

The relationship between the measured soil pH value and the topsoil and subsoil $P_{MMorgan}$ for the five crop phases investigated is shown in **Figure 4.7**. The 2nd order polynomial regression analysis revealed a statistically significant relationship in the topsoil $P_{MMorgan}$ between crop phase and target soil pH value (pH x crop, d.f. = 8, *p* = 0.031) (**Appendix 4**, **Table 10.29**) however pH appeared to be the overriding factor controlling $P_{MMorgan}$ (**section 4.4.3**). There was no significant relationship between the measured soil pH values and the crop phase on subsoil $P_{MMorgan}$ as indicated by the 3rd order polynomial model fitted to the data (pH x crop, d.f. = 12, *p* = 0.154) which suggested that subsoils were not heavily influenced by annual changes in crop phase but were influenced by more by soil pH and potentially buffered from significant annual changes due to the long-term nature of the experiments.

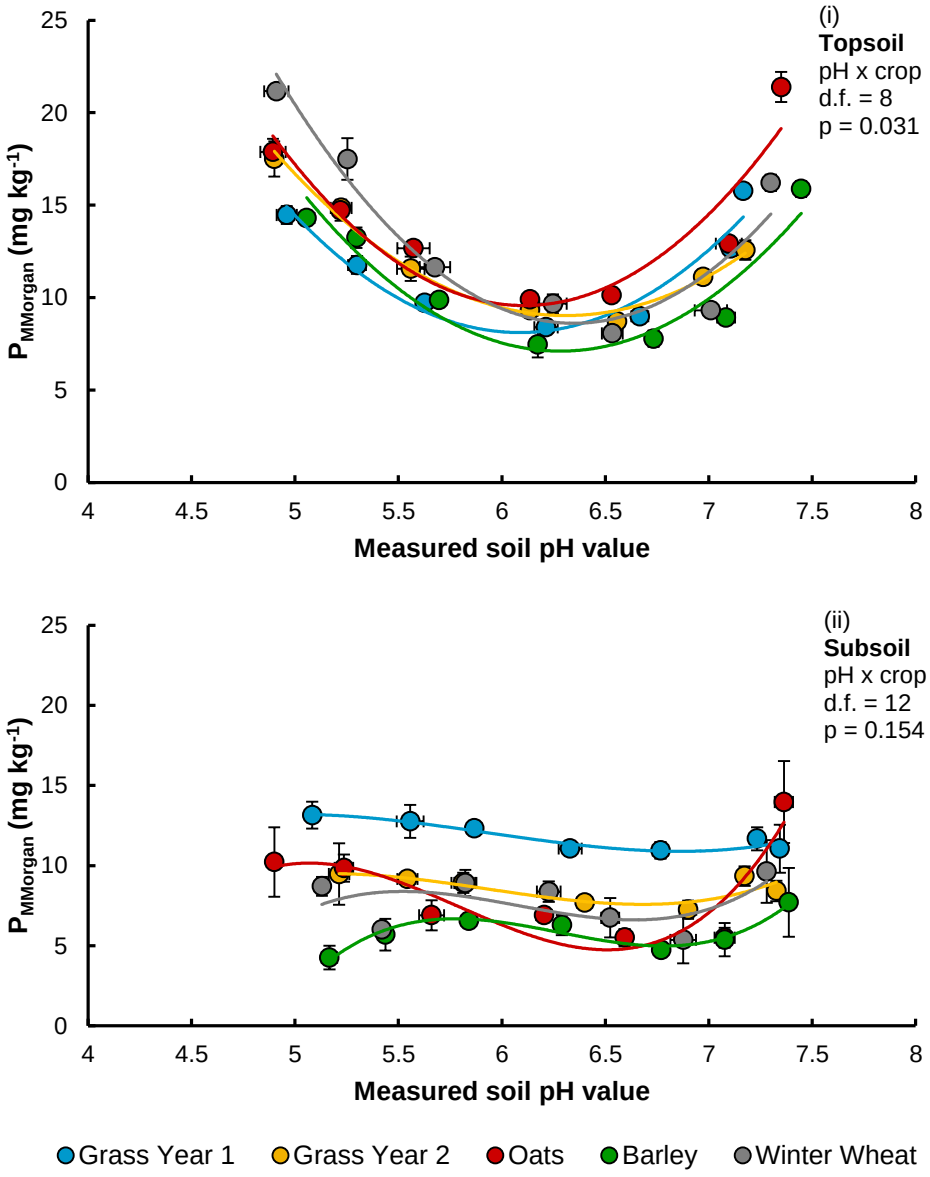


Figure 4.7. Relationship between soil pH and $P_{MMorgan}$ for 5 crop phases in the (i) topsoil and (ii) subsoil, with 2nd and 3rd order polynomials fitted to the data respectively.

4.4.5 Effect of Fertiliser Management on the Relationship Between P_{Total} and Extractable-P in the Old Rotation

The relationships between P_{Total} and P_{Olsen} and $P_{MMorgan}$ (**Figure 4.8**) in the treatment plots and Field topsoils and subsoils were broadly similar. As P_{Total} increased, so P_{Olsen} and $P_{MMorgan}$ increased across the fertiliser treatments. The lowest concentrations of P_{Olsen} and $P_{MMorgan}$ were in the subsoils of plots that received NK without P and the zero fertiliser plots, and the greatest concentrations were observed in the topsoils of the TSP and GMP treatments. There was variation across the Field with an average topsoil P_{Olsen} of 25.3 mg kg^{-1} (± SEM 6.93 mg kg^{-1}) and subsoil P_{Olsen} of 18.5 mg kg^{-1} (± SEM 6.18 mg kg^{-1}) with a topsoil: subsoil ratio of 1.37. The average topsoil $P_{MMorgan}$ in the Field was 4.67 mg kg^{-1} (± SEM 1.28 mg kg^{-1}) and the subsoil $P_{MMorgan}$ was 3.95 mg kg^{-1} (± SEM 1.25 mg kg^{-1}) with a topsoil: subsoil ratio of 1.18. Both methods revealed that there was more variation in P_{Olsen} and $P_{MMorgan}$ in the background Field compared to the individual treatments plots. Assuming that the field concentrations represented native P levels (that were relatively unchanged over the length of the trial), these results suggested that long-term experimental conditions (cropping and fertiliser treatments) had reduced the natural P variation in the soil profile of the experimental plots.

The effect of restricting P but maintaining N and K applications on P_{Olsen} and $P_{MMorgan}$ was comparable to restricting NPK completely. This effect was not observed where P fertilisers (TSP and GMP) were applied; topsoil and subsoil P_{Olsen} and $P_{MMorgan}$ were comparable to the natural field, falling borderline around the limits of the field variation, and suggested that subsoil P may have been maintained through leaching of reactive fertiliser P from the application of TSP and GMP in the topsoils. Despite similar P_{Total} for TSP and GMP in the topsoil, there was a difference in P_{Olsen} of 18 mg kg^{-1}, which reflected the differences in solubility between the two fertilisers. Furthermore, the subsoil P_{Olsen} was greater under TSP than GMP treatment, with a difference of 7 mg kg^{-1} which indicated leaching of relatively more soluble P from the topsoil. In contrast, the average topsoil $P_{MMorgan}$ was 7.49 mg kg^{-1} (± SEM 1.19 mg kg^{-1}) under TSP and 5.96 mg kg^{-1} (± SEM 0.95 mg kg^{-1}) under GMP treatments. The subsoil $P_{MMorgan}$ in the TSP treatment was 4.96 mg kg^{-1} (± SEM 0.46 mg kg^{-1}) and GMP treatment subsoil $P_{MMorgan}$ was 4.21 mg kg^{-1} (± SEM 0.37 mg kg^{-1}). The Modified Morgan reagent (containing acetic acid) may extract more phosphate from highly soluble monocalcium phosphate (i.e. TSP) than from less-reactive phosphate fertilisers (i.e. GMP) (Bolan, *et al*., 1994). These results suggested that more soluble P from the TSP fertiliser was transferred from topsoil to subsoil, than from the slow-release of P from GMP. The reduction in subsoil P

variation suggested that P fertiliser use reduced the natural variation in the TSP and GMP plots suggested that the treatments had the effect of reducing the natural variation. Crop utilisation of subsoil P resources is enhanced through adequate provisions of other nutrients such as N and K (Bauke, *et al*., 2018) and could explain the reduction in natural soil P levels.

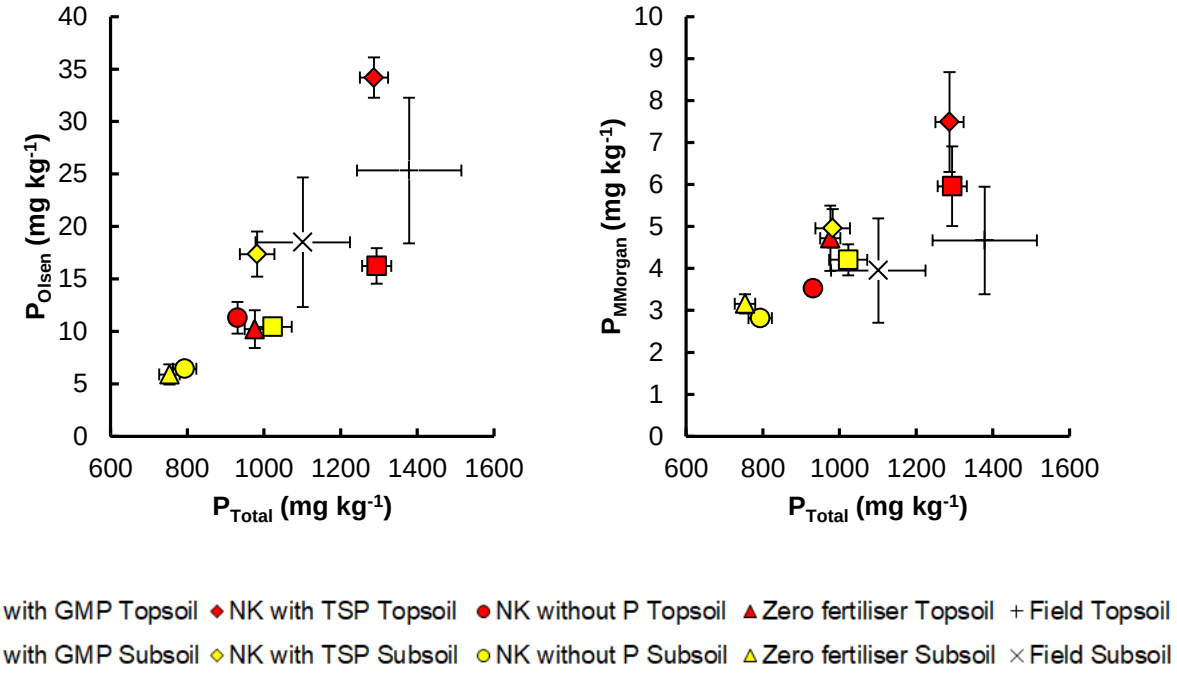


Figure 4.8. Relationship between P_{Total} and (i) P_{Olsen} and (ii) $P_{MMorgan}$ in the topsoil and subsoil for each fertiliser treatment and the Field; mean fertiliser treatment points are of 5 crop phases ± SEM.

4.4.5.1 Topsoil: Subsoil Ratios of P_{Olsen}, $P_{MMorgan}$ and P_{Total} in the Old Rotation

The topsoil: subsoil ratio of P_{Total}, $P_{MMorgan}$ and P_{Olsen} in each of the fertiliser treatments of the Old Rotation compared to a distribution ratio of 1.0 is shown in **Figure 4.9**. The average topsoil pH value was 6.12 and the average subsoil pH value was 6.19 across all four treatments. The Field soil pH was slightly lower at pH 5.66 (topsoil) and 5.98 (subsoil). The P_{Olsen} topsoil: subsoil ratios were 1.55 (NK with GMP), 1.97 (NK with TSP), 1.75 (NK without P), 1.73 (zero fertiliser) and 1.37 (Field). The $P_{MMorgan}$ ratios were 1.41 (NK with GMP), 1.51 (NK with TSP), 1.25 (NK without P), 1.49 (zero fertiliser) and 1.18 (Field). Finally, the P_{Total} topsoil: subsoil ratios were 1.27 (NK with GMP), 1.31 (NK with TSP), 1.17 (NK without P), 1.30 (zero fertiliser) and 1.25 (Field). The topsoil: subsoil ratios for P_{Olsen}, $P_{MMorgan}$ and P_{Total} in the Field were similar and relatively close to 1.0 (between 1.0 and 1.50) suggesting a fairly even distribution of P stocks through the native soil profile at pH values where adsorption of P to Fe and Al oxides likely control the availability of P to crops (i.e. < pH 6). The similarity of the three ratios for the Field soil compared to the treatment plots may also suggest that the Field soil is closer to a profile equilibrium between the various soil P

fractions that contribute to the P_{Total}, P_{Olsen} and $P_{MMorgan}$ operational fractions – although this will also depend on the composition of the topsoil and subsoil. The ratios for P_{Olsen}, $P_{MMorgan}$ and P_{Total} under the NK with GMP treatment showed slight enrichment in the topsoil compared to the ratios that were in the Field but the greatest topsoil enrichment was in the NK with TSP treatment: P_{Olsen} was almost double that of the subsoil suggesting that TSP may have been rapidly adsorbed and strongly bound to Fe and Al oxides which the Olsen method was able to assay at these soil pH values but the Modified Morgan and total P analysis could not, thus leading to values that suggest that the topsoil was enriched in P_{Olsen}. The soil pH in the Old Rotation is maintained around pH 6 and the soil pH values in the fertiliser treatments plots reflect the restriction of the soil pH to the zone where P is most soluble i.e. pH 6.12 in the topsoil and pH 6.19 in the subsoil. In the pH Rotation which receives TSP fertiliser, the topsoil: subsoil ratios at target pH 6 were (in the order of largest to smallest): 1.54 (P_{Olsen}) > 1.41 (P_{Total}) > 1.11 ($P_{MMorgan}$). The ratios in the Old Rotation were comparable to the ratios of the pH Rotation except for P_{Olsen} which was much more enriched in the topsoils of the Old Rotation. This is possible due to the long-term nature of the trial (93 years) where subsoil P resources are possibility depleted more than in the pH Rotation subsoils and are not replenished thus leading to an enriched topsoil P_{Olsen} across the different treatments.

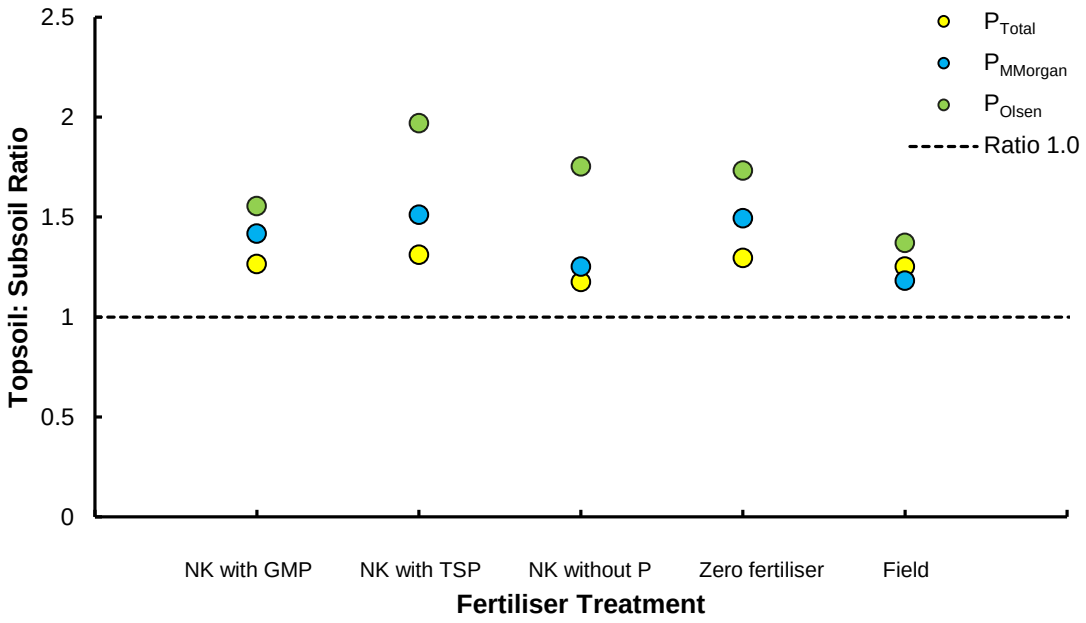


Figure 4.9. Topsoil: subsoil ratios for P_{Olsen}, $P_{MMorgan}$ and P_{Total} in each of the fertiliser treatments of the Old Rotation compared to a ratio line of 1 (dashed) and compared to the Field topsoil: subsoil ratio. The average soil pH was 6.12 (topsoil) and 6.19 (subsoil) across the four fertiliser treatments and the field topsoil pH was 5.66 and the subsoil pH was 5.98.

4.4.6 Effect of Crop Rotation on Topsoil and Subsoil P_{Olsen} and $P_{MMorgan}$ across Fertiliser Treatments in the Old Rotation

An analysis of variance indicated that the main differences between topsoil and subsoil P_{Olsen} across the treatment plots could have been affected by the crop phase (crop x treatment x layer: d.f. = 12, $p = 0.002$) (**Appendix 3**, **Table 10.14**) and the same was found for $P_{MMorgan}$ (crop x treatment x layer: d.f. = 12, $p < 0.001$) (**Appendix 3**, **Table 10.15**). The effect of crop rotation on P_{Olsen} in (i) topsoils and (ii) subsoils and $P_{MMorgan}$ in (iii) topsoil and (iv) subsoils across the fertiliser treatments are shown **Figure 4.10**. There did not appear to be a consistent effect of crop phase on the relationships between P_{Olsen} and fertiliser treatment in each of the crop phases in the (i) topsoils and (ii) subsoils. The main differences seemed to be due to fertiliser management strategy; P_{Olsen} was greatest under TSP and then GMP fertilisers. Under the use of TSP, subsoil P_{Olsen} appeared to increase as the crop rotation progressed from grass through to oats which reflects increased fertiliser use and possibly increased leaching as the rotation moves through the phases. In contrast, the $P_{MMorgan}$ in the (iii) topsoils and (iv) subsoils was affected by crop across the fertiliser treatment. The $P_{MMorgan}$ tended to be higher under the grass phases than the cereal phases in the topsoil (and subsoil) under the NK plus TSP or GMP, and the zero fertiliser strategies. This may be reflective of unused fertiliser P accumulating in the grass plots from previous crop phases. There is no annual removal of P from grass phases which are cut and left to mulch except for one removal of hay in the grass year 1. It was unclear why $P_{MMorgan}$ was elevated under the grass phases across all treatments but not P_{Olsen}- it was thought to be linked to the differences of P solubility in the contrasting reagents.

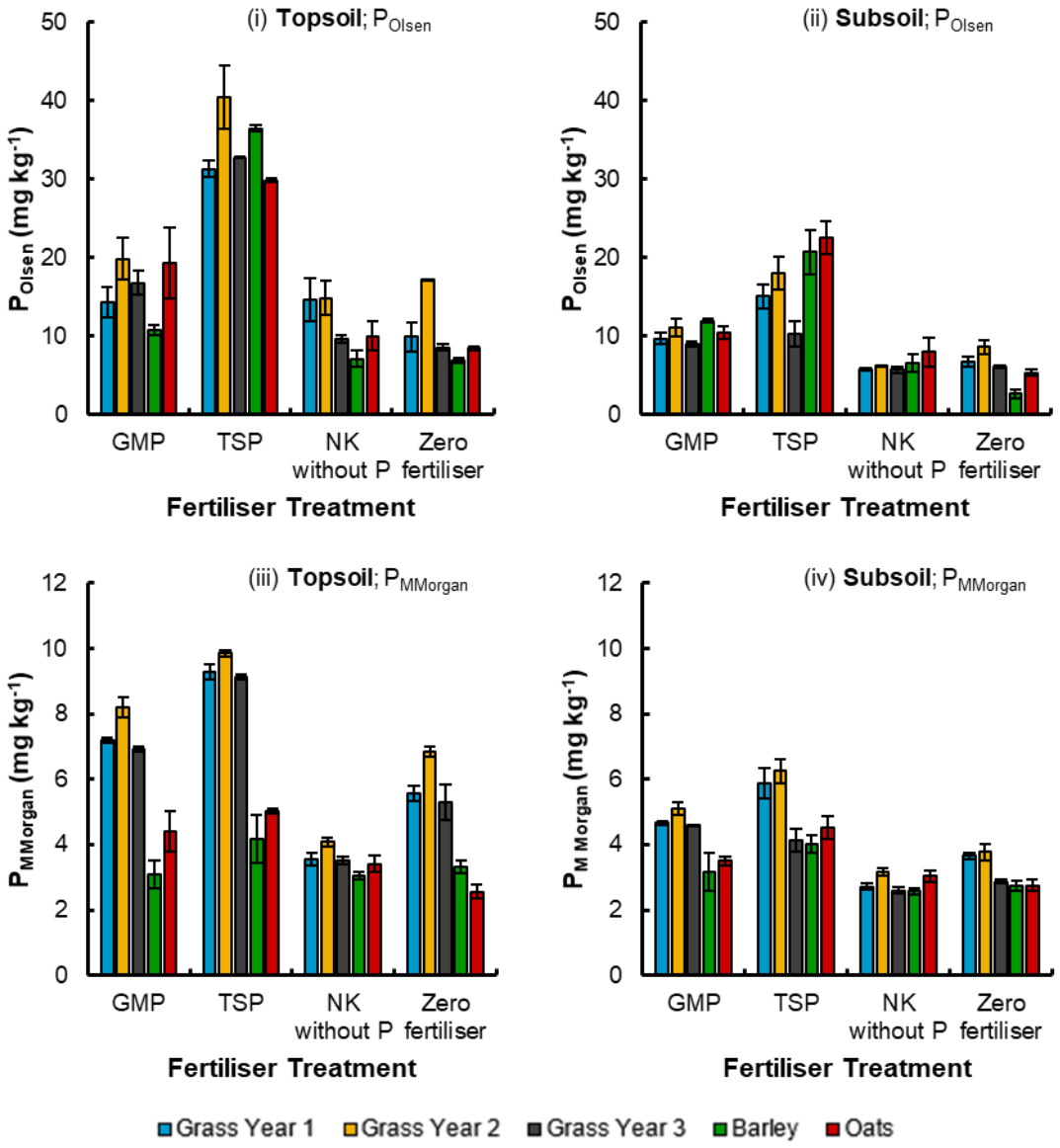


Figure 4.10. Effect of crop phase within each fertiliser treatment for P_{Olsen} in (i) topsoils and (ii) subsoils and $P_{MMorgan}$ in (iii) topsoils and (iv) subsoils. Each bar is the mean of 3 soil replicates ± SEM.

4.4.7 Classifying the Soil P Test Results in the Long-Term Experiments

The results of the soil P tests in the pH Rotation and Old Rotation are presented in this section along with their soil test result classifications: Olsen 'Index' (**Table 4.1**, AHDB, 2017) and Modified Morgan 'Status' (**Table 4.1**, Sinclair, *et al*., 2013). The P_{Olsen} in the Field topsoil was 25.3 mg kg^{-1} (± SEM 6.93 mg kg^{-1}) and the subsoil P_{Olsen} was 18.5 mg kg^{-1} (± SEM 6.18 mg kg^{-1}). These were given Index values of 3 and 2A respectively. The $P_{MMorgan}$ in the Field topsoil was 4.67 mg kg^{-1} (± SEM 1.28 mg kg^{-1}) and in the subsoil it was 3.95 mg kg^{-1} (± SEM 1.25 mg kg^{-1}); these were classified as Status M- and L respectively. The P_{Olsen} classifications indicated that the Field contained sufficient levels of plant-available P for crops whereas $P_{MMorgan}$ suggested sub-optimal levels which may need fertiliser inputs to support crops in a rotational setting. The wider Field is uncultivated and not used for agriculture but the results act as a reference point for the effect of pH management, fertiliser use and crop rotation on the natural availability of P within the field site. The grass is cut regularly in the Field but left to mulch and thus P is not removed from the Field. The only P input likely on the Field is deposition from wildlife and birds passing over the field. The plots used to be surrounded by a large woodland area which was removed for construction of the Aberdeen Western Peripheral Route (expected completion 2018) and only a small woodland adjacent to the field remains. This resulted in the loss of habitat for local wildlife such as deer which, despite fencing, have occasionally managed to access the field and destroy some of the crops and affect the yields (i.e. of swedes).

Classifications between 2A and 3 for P_{Olsen} and M± for $P_{MMorgan}$ in the treatment plots would be considered sufficient for crops; those that are lower would require additional P fertiliser to maintain expected crop yields whereas results greater than these would be more than enough for crops, may pose a pollution risk to the wider environment and further P fertiliser applications may not be recommended.

The pH Rotation

The Olsen and Modified Morgan soil P tests in the pH Rotation plots are described with their test classification in **Table 4.2**. The topsoil P_{Olsen} indices did not fall below '3' and showed the highest rating of '4' below pH 5.5. In contrast, the Modified Morgan Status in the topsoils varied with soil pH: plots were designated as 'H' at either end of the pH scale (pH 4.5 and 7.5) and decreased from both ends of the scale to a minimum status of 'M-' between pH 6 and 6.5. Most of the plots had soil test result classifications at levels higher than, or equal to, the classifications awarded to the Field topsoil P_{Olsen} ('3') and $P_{MMorgan}$ ('M-') which is due to the accumulation of unused fertiliser P. The P concentrations in the subsoils were generally lower than the topsoils, with P_{Olsen} ranging from index 2B (pH 7.5 to 6.5) to 3 (≤ pH 6) and $P_{MMorgan}$ typically classed as status M- except for the subsoil of pH 7.5 which was M+ which could be expected because P fertiliser is applied directly to the topsoil. In all cases, the subsoils were enriched relative to the Field P_{Olsen} (2A) and $P_{MMorgan}$ (L) which suggested reactive fertiliser P may have been re-distributed to the subsoil in all pH plots. The results of the subsoil P tests indicated that there were sufficient levels of plant-available P in the subsoil which could be utilised by crops.

Fertiliser recommendations for cereals grown in the pH Rotation (based on topsoils) would be to apply no P fertiliser where the Modified Morgan status was M ± and for treatments with a status of H, it would be recommended that attempts be made to allow the P status in the soil to decline in order to mitigate harmful effects to the quality of nearby surface waters and save on fertiliser costs (Sinclair, *et al*., 2013). Following the potato phase of an arable rotation, excess P may remain which is ideal for maintaining an M ± status for the following phases (Sinclair, *et al*., 2013). The topsoil P_{Olsen} indices may also warrant the restriction of P fertiliser until optimum Olsen indices of 2 are achieved (RB209, AHDB, 2017) due to the increased risk of leaching to the wider environment (Withers, *et al*., 2017).

Table 4.2. Mean concentrations of P_{Olsen} and $P_{MMorgan}$ (mg kg^{-1}) in the pH plot topsoils and subsoils of 5 crop phases ± SEM. Soils were classified according to the mean. The P_{Olsen} was assigned a P Index (AHDB, 2017) and the $P_{MMorgan}$ a SAC Status (Sinclair, *et al*., 2013).

	pH plot	P_{Olsen} (mg kg^{-1})	P Index	$P_{MMorgan}$ (mg kg^{-1})	SAC Status
Topsoil	**7.5**	40.1 ± 1.92	3	16.4 ± 1.42	H
	7	37.2 ± 3.39	3	11.0 ± 0.83	M +
	6.5	36.4 ± 1.63	3	8.73 ± 0.41	M -
	6	44.9 ± 1.85	3	8.95 ± 0.45	M -
	5.5	61.6 ± 4.11	4	11.1 ± 0.57	M +
	5	71.1 ± 2.56	4	14.4 ± 0.95	H
	4.5	74.5 ± 3.05	4	17.1 ± 1.26	H
Subsoil	**7.5**	23.4 ± 1.53	2B	10.2 ± 1.11	M +
	7	22.9 ± 3.77	2B	7.45 ± 1.30	M -
	6.5	21.7 ± 1.45	2B	7.03 ± 1.07	M -
	6	29.1 ± 1.42	3	8.07 ± 0.83	M -
	5.5	35.2 ± 3.65	3	8.72 ± 1.03	M -
	5	32.4 ± 5.54	3	8.70 ± 1.31	M -
	4.5	26.5 ± 6.74	3	9.16 ± 1.44	M -

Overall the data reflect differences in the extractants. The trend in the Olsen P Indices with pH shows the effect of suspending an acidic soil in the alkaline pH Olsen reagent. The weakened adsorption strength of phosphate occurs when the soils with pH 4.5 to 5.5 are shaken in the alkaline sodium bicarbonate reagent, due to a decrease in positive charge surfaces for adsorbing P (Antelo, *et al*., 2005), producing a high P index result. By contrast, the increase in SAC status from pH 6 to 7.5 possibly reflects the dissolution of calcium phosphates in the acidic Modified Morgan reagent. This potentially represents a flaw in both extraction systems as indicators of phosphate availability and a comparison against P lability using the Diffusive Gradients in Thin Films technique (DGT) may reveal this (see **Chapter 6**).

The Old Rotation

The topsoil and subsoil P_{Olsen} and $P_{MMorgan}$ classifications for the range of fertiliser treatments in the Old Rotation are shown in **Table 4.3**. The topsoil P Indices for the P_{Olsen} in plots treated with TSP (34.2 mg kg^{-1}) or GMP (16.2 mg kg^{-1}) were at optimal levels for crops (3 and 2A respectively). There was an average P_{Olsen} of 11.3 mg kg^{-1} where NK was applied without P and this was comparable to applying zero fertilisers (10.2 mg kg^{-1}); both treatments being classed as P_{Olsen} Index 1. Values of P_{Olsen} in the subsoils produced lower P indices- plots treated with TSP or GMP (1 and 2A) were not entirely deficient in P, with average concentrations of 17.4 and 10.4 mg kg^{-1} respectively and suggested a link between P fertiliser use and subsoil P_{Olsen}. The P_{Olsen} in the subsoils of plots treated with either NK without P (6.44 mg kg^{-1}) or zero fertilisers (5.90 mg kg^{-1}) had P Indices of 0 which was relatively lower than the Field subsoil ('2A'), indicating a depletion of native available-P which is not replenished in these plots due to lack of P fertiliser input. Fertilisation would be recommended in arable rotations were the topsoil P Indices were as low as Index 1 however, spring barley and winter wheat (two crops which feature in the Old Rotation) may require lower levels of P_{Olsen} in the soil if there is an adequate provision of nitrogen (N) (Johnston, *et al*., 2013) (such as in the plots were NK is applied without P). Generally, an average P_{Olsen} of 20 mg kg^{-1} (P Index 2) is ideal for arable crops grown in ideal soil conditions (Poulton, *et al*., 2013). In the Exhaustion Land field experiments (Rothamsted Research, UK) the critical topsoil P_{Olsen} for winter wheat (to achieve 95% of the maximum yield) was found to be an average 9 mg kg^{-1} (P Index 0) over a three-year period (Bollons & Barraclough, 1999) which may explain why there was continued production of cereals in the Old Rotation despite low concentrations of available P in the P restricted plots. This means that topsoil conditions under TSP and GMP are ideal for the rotation although maintenance applications of P fertiliser could help to ensure crop yields do not fall (RB209, Section 4, AHDB, 2017). Three years of the Old Rotation are under grass and clover ('ley') and so if this were a grassland system, P fertiliser recommendations for the plots under the first year grass phase (one removal of hay) would be 55 kg ha^{-1} for the NK without P and zero fertiliser treatment plots, 30 kg ha^{-1} in the plots treated with NK and GMP, and no inputs would be required in the NK with TSP plot (RB209, Section 3, AHDB, 2017). The phosphate fertiliser recommendations for a soil with an index of 3 with a crop rotation containing potatoes would be expected to provide enough P to maintain an index of 2, optimum for cereal crops planted after accounting for the offtake from the potato harvest (RB209, Section 5, AHDB, 2017).

According to the status system for $P_{MMorgan}$, the topsoils under TSP (7.49 mg kg^{-1}), GMP (5.96 mg kg^{-1}) and zero fertiliser (4.72 mg kg^{-1}) treatments had the same status (M-) which was not expected because P

fertilisation is expected to increase extractable-P and restricting P fertiliser is expected to reduce soil P status (**Table 4.3**). The restriction of fertilisers for 93 years (with the exception of intermittent FYM additions) was expected to result in a lower status because crops would have depleted any available P in the soil to meet requirements and so the plant-available P would not be comparable to plots receiving highly soluble TSP fertiliser. Soils with a stratus ‘’M-’ would require top-up applications of P fertiliser in order to reduce the risk of cereal yields suffering from root and seed development issues (Sinclair, *et al*., 2013). In crop rotations with root crop phases including potato, a minimum status of ‘M+’ is recommended (Edwards, *et al*., 2016) and so the topsoils in this trial would require P fertiliser additions which should be applied at the beginning of the root phase to have the greatest impact on crop development and maintain yields (Sinclair, *et al*., 2013). Further research is needed to understand the extent to which subsoil P is acquired by crops and to assess the significance of any contributions particularly for results such as these where there was evidence of TSP movement from topsoil to subsoil. This would help improve fertiliser use efficiency, reduce costs to farmers if a consideration was made for subsoil P and improve the sustainability of agriculture.

Table 4.3. Mean concentrations of P_{Olsen} and $P_{MMorgan}$ (mg kg^{-1}) in the topsoil and subsoil for each fertiliser treatment of 5 crop phases ± SEM. The soils were classified according to the mean. The P_{Olsen} was assigned a P Index (AHDB, 2017) and the $P_{MMorgan}$ a SAC Status (Sinclair, *et al*., 2013).

Layer	Fertiliser Treatment	P_{Olsen} (mg kg^{-1})	P Index	$P_{MMorgan}$ (mg kg^{-1})	SAC Status
Topsoil	**NK with GMP**	16.2 ± 1.68	2A	5.96 ± 0.95	M -
	NK with TSP	34.2 ± 1.92	3	7.49 ± 1.19	M -
	NK without P	11.3 ± 1.52	1	3.52 ± 0.16	L
	Zero fertiliser	10.2 ± 1.81	1	4.72 ± 0.78	M -
Subsoil	**NK with GMP**	10.4 ± 0.52	1	4.21 ± 0.37	L
	NK with TSP	17.4 ± 2.16	2A	4.96 ± 0.46	M -
	NK without P	6.44 ± 0.41	0	2.82 ± 0.12	L
	Zero fertiliser	5.90 ± 0.97	0	3.16 ± 0.23	L

4.5 Conclusions

The effect of soil pH control, crop rotation and P fertiliser management strategy on the capacity of topsoils and subsoils to provide available-P for crops in rotation using traditional UK soil P extraction methods (Olsen and Modified Morgan) was investigated in long-term experiments. Significant, positive correlations were found in the topsoils and subsoils between P_{Olsen} and $P_{MMorgan}$ across the dataset. Plots with a soil pH > 6 tended to have greater $P_{MMorgan}$ suggesting the dissolution of calcium phosphates by the acidic reagent (pH 4.5) whereas the good agreement between methods at plots < pH 6 suggested some similarity in the mechanism of extracting P, probably involving anion competition for surface binding sites (acetate in the Modified Morgan's reagent and bicarbonate in the Olsen extractant competing with phosphate). Concentrations of P_{Olsen}, $P_{MMorgan}$ and P_{Total} correlated positively with the topsoil suggesting a link between P fertiliser application to the topsoil and the accumulation of reactive P in the subsoil. Of the P_{Total} in all of the soil profile cores, $P_{MMorgan}$ was less than 0.75% and P_{Olsen} was approximately 2.5%.

Soil pH management had a significant impact on the distribution of P_{Olsen} and $P_{MMorgan}$ in the topsoil and subsoil over the pH gradient of 4.5 to 7.5 (0.5 increments), with the topsoil and subsoil P elevated compared to the 'native' P in the Field. Both P_{Olsen} and $P_{MMorgan}$ in the topsoil were greatest < pH 5.5 and converged with the subsoil between pH 6.0 and 6.5. High topsoil: subsoil ratios < pH 5.5 suggested most 'available-P' was retained in the topsoil, consistent with strong adsorption of P to Fe and Al oxides. The decline in topsoil: subsoil ratios towards 1.0 between pH 6.0 and 6.5 suggested plant-available P was more evenly distributed between the topsoil and subsoil in the zone of maximum solubility of P (calcium phosphates). There was a significant crop effect for topsoil P_{Olsen} and $P_{MMorgan}$ which was not seen in the subsoils and suggested that subsoil P_{Olsen} and $P_{MMorgan}$ is buffered against the differences in annual applications of P to the topsoils. The crop effect could be an artefact of differences in annual P application rates and P balances as opposed to differences in availability post-harvest to any one crop, as the plots may have reached steady-state P_{Olsen} and $P_{MMorgan}$ early in the history of the trials. Average soil P test classifications for the Field P_{Olsen} topsoil (3) and subsoil (2A) and $P_{MMorgan}$ topsoil (M-) and subsoil (L) revealed ''native'' levels of plant-available P were optimal for P_{Olsen} but sub-optimal for $P_{MMorgan}$ for crop requirements. Topsoils across the pH gradient were enriched in P_{Olsen} (Index 3 and 4) and $P_{MMorgan}$ (M± & H) was also enriched relative to the Field. Classifications of subsoil P_{Olsen} were 2B or 3 and $P_{MMorgan}$ were mostly M- for all plots. These classifications suggest subsoils contain optimal levels of available P for crops and would be considered sufficient enough for crop nutrient requirements in fertiliser recommendation assessments if these were topsoil results.

In the Old Rotation, topsoil and subsoil P_{Olsen} and $P_{MMorgan}$ increased with P_{Total} across the fertiliser treatments suggesting a link between P fertiliser management and rising subsoil P levels. Despite comparable P_{Total} levels in plots treated with NK and either TSP or GMP, topsoil P_{Olsen} was greater when TSP was applied and $P_{MMorgan}$ was reasonably similar in both treatments. This suggested that Olsen may have extracted P which Modified Morgan's could not: soluble TSP may be strongly bound to the solid phase following dissolution in soil solution and rendered 'unavailable' but can be extracted by Olsen's reagent. This was supported by the topsoil: subsoil ratios which revealed elevated P_{Olsen} in the topsoil when TSP was used whilst P_{Total} and $P_{MMorgan}$ ratios remained fairly similar across all treatments. In the Field, topsoil: subsoil ratios revealed that P_{Olsen}, $P_{MMorgan}$ and P_{Total} were similar, suggesting steady-state between the P fractions. In plots where P was restricted, subsoil P_{Olsen} was depleted more so than $P_{MMorgan}$ (relative to the Field levels) but was elevated in plots were P was applied. A significant effect of cropping was indicated in the topsoil but not the subsoil for P_{Olsen} and $P_{MMorgan}$ again suggesting that subsoils are buffered from annual inputs of P fertiliser. Subsoil P_{Olsen} increased across the crop rotation phases which suggested that when TSP was applied, P transfer to the subsoil is greater. Topsoil P_{Olsen} classifications for TSP (3) and GMP (2A) treated plots were optimal, with higher availability index attributed to use of more soluble P fertiliser. When P was restricted topsoils were classed as Index 1 and subsoils Index 0. A link between topsoil and subsoil due to soluble P fertiliser use was indicated in the subsoils of the TSP plots ('2A'). This link was less obvious in the $P_{MMorgan}$ results although the TSP subsoil had the highest award ('M-') compared to the other treatments ('L'). Compared to the Field, the classifications in the fertiliser treatment plots were lower, suggesting long-term cropping resulted in the depletion of subsoil available-P which is only relatively maintained when TSP fertilisers are used.

These results provide unique, field-based evidence on the effect of long-term fertiliser management strategy, soil pH control and ley/arable crop rotation on topsoil and subsoil extractable-P dynamics in long-term experiments that are representative of historical and modern farming practices in the North East of Scotland. Future work may investigate the relative contribution of subsoils with high P availability indices to crop nutrient requirements. An assessment of the potential contribution of subsoil available-P to crop requirements, through quantification of the amount stored in the subsoil, could help farmers improve their P fertiliser use efficiency. It could also reduce impact on the wider environment as subsoil P can be either a sink or a source of P leaching (Andersson, *et al*., 2015), Utilising subsoil P reserves could therefore protect or improve water quality in surrounding surface waters where diffuse agricultural pollution is an issue. The biological cycling and topsoil to subsoil transfer of P may be elucidated through

tracer studies such as the new stable oxygen isotope ratios of soil phosphates technique (see **Chapter 7**). The factors controlling the solubility and lability of topsoil and subsoil P across the fertiliser treatments and pH gradient may also be of interest (see **Chapter 5** and **Chapter 6** respectively).

5 Geochemical Modelling of Phosphate Solubility in the Woodland's Rotations using WHAM-VII

5.1 Abstract

The factors controlling phosphate (PO_4^{3-}) solubility in the two Woodland's long-term experiments based at SRUC's Craibstone Estate Aberdeen were investigated. In the Old Rotation, it seems likely that PO_4^{3-} solubility in both the topsoil and subsoil was controlled by adsorption to Fe and Al oxides regardless of fertiliser treatment (NK with GMP, NK with TSP, NK without P and zero fertiliser application). In the pH Rotation, the data (pH, (Ca^{2+}) and $H_2PO_4^-$)) was consistent with forms of hydroxyapatite controlling the PO_4^{3-} solubility in the topsoils and subsoils of plots maintained at pH 6.5 and greater. This was thought to be a result of long-term liming to maintain the target pH values and the accumulation of Ca throughout the soil profile which resulted in uniform soil pH profiles. In all plots with pH values less than pH 6, the solubility data indicated soil systems which were *under-saturated* with respect to hydroxyapatite and it was concluded that the main control of PO_4^{3-} solubility in soil solution was HPO_4^{2-} and $H_2PO_4^-$ interactions with Fe/ Al hydroxide surfaces. Finally, soil solution P may have contained a significant amount of organic P (P_o). These results provide field-based evidence and insight into the long-term effects of pH management and fertiliser use on PO_4^{3-} solubility and are a useful reference for studies and advisory notes that consider the underlying mechanisms (such as sorption and precipitation/dissolution reactions) that control PO_4^{3-} in soil solution.

5.2 Introduction

Understanding the soil processes and mechanisms that control phosphate (P) solubility in agricultural soil systems, such as identifying phosphate minerals present in soils (Zhang, *et al*., 2014) may help improve P fertiliser use efficiency, reduce P losses and mitigate the impact on water quality (Sharpley, *et al*., 2015). Crops acquire inorganic orthophosphate ($H_2PO_4^-$ and HPO_4^{2-}) from the soil solution but the speciation and activity of orthophosphate ions varies with pH (Lindsay, 1979). At acidic pH (< 6), mechanisms of adsorption and desorption of P associated with Fe and Al oxides are the main controls of P solubility in soil (Weng, *et al*., 2011). As soil pH increases, there is a reduction in positive surface charges on Al and Fe oxides (Weng, *et al*., 2011) leading to the desorption of P, for example desorption of P from goethite (Antelo, *et al*., 2005). The precipitation or dissolution of calcium phosphates become the main controls over solubility of P at pH values greater than 6 (Weng, *et al*., 2011). The analysis of estuarine sediments covering a range of pH values indicated that P speciation was more strongly associated with calcium at alkaline pH (pH 7) and then Al/Fe at acidic pH (pH 4) (Oxmann & Schwendenmann, 2015). The optimum pH range for crops acquiring phosphate (mainly as $H_2PO_4^-$) is between pH 6 and 6.5 (Goulding, 2016) which is where several calcium phosphate minerals co-exist to control phosphate solubility (Lindsay, 1979). Di-calcium phosphate (monetite) and di-calcium di-hydrate (brushite) are the most soluble calcium phosphates in soil and wheat yields may be optimal when PO_4^{3-} solubility is controlled by these minerals (Esmail, 2012). This was also found by Jalali & Jalali, (2016), where unstable monetite, brushite and magnesium-P minerals were thought to be the main suppliers of P in soil solution in important crop production areas of Iran. However, a combination of interactions with Al, Fe and Ca can simultaneously control the solubility and release of P in soil (McDowell & Sharpley, 2003).

Geochemical speciation modelling of pH, Ca and phosphate anion activities using models such as the Windermere Humic Aqueous Model-VII (WHAM-VII) (Tipping, *et al*., 2011) and Visual MINTEQ3 (Gustafsson, 2011) can aid investigations into the possible solubility controls by a range of calcium phosphate mineral phases in soil systems. Geochemical speciation models have been used to show that the solubility of PO_4^{3-} is controlled by stable calcium-phosphate minerals, such as hydroxyapatite, which can form in calcareous soils that have received long-term applications of phosphate fertilisers (Zhang, *et al*., 2014). The precipitation of calcium phosphates following the application of phosphate fertilisers can occur relatively quickly (within 1 week) in calcareous soils (Al-Tameemi, *et al*., 2015). Furthermore, the solubility of P in soil increases as the rate of fertiliser application increases (Al-Tameemi, *et al*., 2015; McDowell & Sharpley, 2003). Regelink, *et al*., (2015) showed that solubility increased with concentration

of P in the soil. They also concluded that because the interaction of P with Fe/Al oxide surfaces decreased due to competition with increasing amounts of soil organic carbon (SOC) then surface complexation models must consider the role of organic matter to avoid underestimating phosphate bioavailability. Similarly, organic matter can also compete with arsenate adsorption to Fe/Al oxides as shown through geochemical modelling (Verbeeck, *et al*., 2017), with arsenate being another important competitor for phosphate binding at low pH (Deng, *et al*., 2018).

It is widely accepted that elevating soil pH to between pH 6 and 6.5 in agriculture, through the use of lime, increases crop production by increasing the solubility and availability of P for crop uptake (Holland, *et al*., 2018). Recently, Barrow (2017) argued that raising the soil pH does not increase phosphate availability to plants and argues that the optimum pH should be between pH 4 and 5, rather than between pH 6 to 7 however many crops would fail to grow below pH 5 due to greater incidences of disease, pests and weeds and also aluminium toxicity at increasingly acidic pH values. However, Simonsson, *et al*., (2018) showed that, in long-term liming experiments over a range of soil textures with a pH range of 5.0 to 6.0, liming to raise the soil pH increased PO_4^{3-} solubility of fertiliser P and crop uptake of P increased. Furthermore, it is suggested that the production of 40% of arable soils and 57% of grasslands systems in the UK could benefit from the application of lime to alleviate natural acidity by increasing the soil to pH 6.5 (arable) and pH 6 (grassland) although this figure is based on limited data that was not representative of all farming systems (Goulding, 2016). The introduction of Ca to the soil through liming may increase the concentration of Ca in soil solution and subsequent additions of P may be rapidly precipitated as calcium phosphates which reduces the solubility and availability of P (Tunesi, *et al*., 1999). Pure phosphate minerals are rarely found in soil systems, with crystalline structures altered by the incorporation or substitution of carbonate and magnesium ions for example, resulting in the formation of amorphous mineral phases and incomplete precipitation of hydroxyapatite (Cao, *et al*., 2007; Cao & Harris, 2008). Liming may introduce soluble silica into the soil system which can prevent fertiliser P from forming insoluble precipitates (Simonsson, *et al*., 2018). Furthermore, surface adsorption of humic acid can inhibit calcium phosphate precipitation and may increase the amount of P in the soil solution (Cao, *et al*., 2007; Perassi & Borgino, 2014). Overall, more research is required to understand the impact of mineral phases in long-term agricultural soil systems on the availability and solubility of P (Simonsson, *et al*., 2018).

In this study, a field-based investigation into the effects of soil pH control and fertiliser use on PO_4^{3-} solubility across an established pH gradient (pH 4.5 to 7.5) and fertiliser management experiment in the

topsoils and subsoils of the Woodland's long-term experiments contributes to the ongoing discussion surrounding PO_4^{3-} solubility controls in an agricultural setting.

5.2.1 Aims and Objectives

The aims of this chapter were to investigate the factors controlling the solubility of PO_4^{3-} in the topsoils and subsoils of the Woodland's Field long-term experiments and, specifically, to understand the effects of continuous pH management, rotational cropping and fertiliser use on the mineralogy controlling PO_4^{3-} solubility. The hypothesis was that P solubility in the topsoil was controlled by calcium phosphate mineralogy above pH 6 due to the long-term effects of liming to control soil pH. The subsoil may be affected by liming to control topsoil pH, thus affecting P solubility in the subsoil. Furthermore, P solubility in plots < pH 6 is likely to be controlled by adsorption because the native soil pH is acidic. Using geochemical modelling (WHAM-VII) of free ion activities (H^+, $H_2PO_4^-$, Ca^{2+}), the experimental objectives are listed below.

1. Investigate topsoil and subsoil PO_4^{3-} solubility across the pH gradient under two crop rotation phases in the Woodland's 'pH Rotation'.
2. Investigate the effect of fertiliser management strategy on topsoil and subsoil PO_4^{3-} solubility and compare between two crop phases in the Woodland's 'Old Rotation'.

5.3 Materials and Methods

5.3.1 Sample Site, Trial Description, Sample Selection and Preparation

Full details of the long-term experiments used in this study are provided in **Chapter 2 Materials and Methods** which outlines the sample site and description of the trials (**section 2.1**), trial management (**section 2.1.1**), soil sampling and preparation (**section 2.2**) and various soil analyses such as soil pH (**section 2.4**) total element analysis (**section 2.6**) and colorimetric determination of P (**section 2.7.3**) and finally the statistical analysis of linear relationships by Pearson Correlation Coefficients (**section 2.8**). Briefly, for this study, air-dried, sieved (< 2 mm) soil samples from all three auger borings in each treatment were selected from all seven target pH plots (pH 4.5 to 7.5 in 0.5 unit increments) that had been under spring oats and grass year 2 (pH Rotation) and four fertiliser treatment plots (NK with GMP, NK with TSP, NK without P and zero fertiliser) that had been under spring oats and grass year 3 (Old Rotation). All of the soil samples from the uncultivated grassland field surrounding the trials ('Field') (9 topsoil and 9 subsoil) and three sub-samples of the GMP fertiliser applied in the Old Rotation were also selected.

5.3.2 Soil ⇌ Solution Equilibration

Air-dried, sieved (< 2 mm) soil (c. 3 g) and 20 mL 0.005 M calcium nitrate ($Ca(NO_3)_2$) solution were shaken end-over-end (26 rpm) in 50 mL capacity centrifuge tubes for 48 hrs. The pH of the soil suspensions was measured, and the samples centrifuged (1500 *g*, 15 mins) and syringe-filtered (0.22 µm PES). An aliquot of supernatant (c. 5 mL) was immediately acidified with 0.2 mL of 50% HNO_3 in ICP tubes and stored at room temperature prior to the determination of total element concentrations (including P, Zn, Ca, Na, K, Mg, and S) by ICP-MS (**Chapter 2**, **section 2.6.3**). The remaining supernatant (c. 10 mL) was stored at 4^oC for no longer than 24 hours before determination of molybdate-reactive P by colorimetry (**Chapter 2**, **section 2.7.3**). Finally, 0.2 mL of supernatant was diluted with 18 mL of Milli-Q water and stored at 4^oC before determining total organic carbon (TOC = TC – IC) following the analysis of inorganic carbon (IC) and total carbon (TC) by combustion catalytic oxidation at 680^oC (Shimadzu TOC-VCPH with auto-sampler ASI-V; Shimadzu, Japan).

5.3.3 Geochemical Modelling of Phosphate Solubility using WHAM-VII

The geochemical model WHAM-VII (Tipping, *et al*., 2011) was used to calculate the ion activities of Ca^{2+} and $H_2PO_4^-$ in the soil suspension supernatant to test for possible solubility control by a range of calcium phosphate mineral phases (**Table 5.1**). The master variables included (i) the measured pH of the soil suspension in 0.005 M $Ca(NO_3)_2$ (ii) total organic carbon (TOC in mg L^{-1}) as a proxy for fulvic acid which may inhibit the formation of calcium phosphates and complexes Ca (Alvarez, *et al*., 2004), (iii) the major cations (Na, Mg, K and Ca in mg L^{-1} and Al, Mn and Fe in µg L^{-1}) as determined by ICP-MS and (iv) the major anions (NO_3^-, SO_4^{2-}, CO_3^{2-} and PO_4^{3-} in mol L^{-1}). The following assumptions were made for the major anions: NO_3^- was assumed to be 0.02 M for all samples, while SO_4^{2-} and PO_4^{3-} (M) were calculated from total S and P determined by ICP-MS (in mg L^{-1}), and finally, CO_3^{2-} (M) was assumed from the measured inorganic carbon (IC) concentration (mg L^{-1}). The output included the free ion activities (M) for the following species: (Ca^{2+}), (CO_3^{2-}), (PO_4^{3-}), (HPO_4^{2-}), ($H_2PO_4^-$) and ($H_3PO_4^0$). The samples were then plotted on a solubility phase diagram based on the measured pH value, the activities of (Ca^{2+}) and ($H_2PO_4^-$) with the X-axis ('lime potential') defined as (pH + ½log(Ca^{2+}) and the Y-axis ('calcium phosphate potential') defined as (log$(H_2PO_4)^-$ - ½log(Ca^{2+})). Thus, the solubility of selected Ca phosphates can be represented as straight-line relationships as the X and Y axes represent factorised logarithmic forms of the solubility equations.

Table 5.1. Equilibrium reactions and formation constants (log K^o) for calcium phosphates at 25°C (Lindsay, 1979).

$CaHPO_4.2H_2O$ Brushite (DCPD)	**log K^o = 0.63**
$CaHPO_4.2H_2O + H^+ \rightleftharpoons Ca^{2+} + H_2PO_4^- + 2H_2O$	
$(Ca^{2+})\ (H_2PO_4^-) / (H^+) = 10^{0.63}$	
$\log(Ca^{2+}) + \log(H_2PO_4^-) + pH = 0.63$	
$\log(H_2PO_4^-) + ½\log(Ca^{2+}) = 0.63 - (pH + ½\log(Ca^{2+}))$	

$CaHPO_4$ Monetite (DCP)	**log K^o = 0.3**
$CaHPO_4 + H^+ \rightleftharpoons Ca^{2+} + H_2PO_4^-$	
$(Ca^{2+})\ (H_2PO_4^-) / (H^+) = 10^{0.63}$	
$\log(Ca^{2+}) + \log(H_2PO_4^-) + pH = 0.3$	
$\log(H_2PO_4^-) + ½\log(Ca^{2+}) = 0.3 - (pH + ½\log(Ca^{2+}))$	

$Ca_4H(PO_4)_3$. $2.5H_2O$ Octocalcium phosphate (OCP)	**log K^o = 11.76**
$Ca_4H(PO_4)_3.2.5H_2O + 5H^+ \rightleftharpoons 4Ca^{2+} + 3H_2PO^-_4 + 2.5H_2O$	
$(Ca^{2+})^4\ (H_2PO_4^-)_3 / (H^+)^5 = 10^{11.76}$	
$11.76 = 4\log(Ca^{2+}) + 3\log(H_2PO_4^-) = 5pH$	
$3\log(H_2PO_4^-) + ½\log(Ca^{2+}) = 11.76 - 5(pH - ½\log(Ca^{2+}))$	
$\log(H_2PO_4^-) + ½\log(Ca^{2+}) = 3.92 - 1.667(pH - ½\log(Ca^{2+}))$	

$Ca_3(PO_4)_2$ β-tricalcium phosphate (β-TCP)	**log K^o = 10.18**
$\beta\text{-}Ca_3(PO_4)_2 + 4H^+ \rightleftharpoons 3Ca^{2+} + 2H_2PO_4^-$	
$(Ca^{2+})^3\ (H_2PO_4^-)^2 / (H^+)^4 = 10^{10.18}$	
$10.18 = 3\log(Ca^{2+}) + 2\log(H_2PO_4^-) + 4pH$	
$2\log(H_2PO_4^-) + ½Ca^{2+} = 10.18 - 4(pH - ½Ca^{2+})/2$	
$\log(H_2PO_4^-) + ½Ca^{2+} = 5.09 - 2(pH - ½\log(Ca^{2+}))$	

$Ca_5(PO_4)_3OH$ Hydroxyapatite (HA)	**log K^o = 14.46**
$Ca_5(PO_4)_3OH + 7H^+ \rightleftharpoons 5Ca^{2+} + 3H_2PO_4^- + H_2O$	
$(Ca^{2+})^5\ (H_2PO_4^-)^3 / (H^+)^7 = 10^{14.46}$	
$14.46 = 5\log(Ca^{2+}) + 3\log(H_2PO_4^-) + 7pH$	
$3\log(H_2PO_4^-) + ½Ca^{2+} = 14.46 - 7(pH - ½Ca^{2+})/3$	
$\log(H_2PO_4^-) + ½Ca^{2+} = 4.82 - 2.33(pH - ½\log(Ca^{2+}))$	

5.4 Results and Discussion

5.4.1 Measurement of Soil Solution P (P_{Soln})

Comparing soil solution P as measured by colorimetry and ICP-MS

The relationship between the concentration of PO_4^{3-} in the soil solution (P_{Soln}) measured by colorimetry ($P_{Soln\text{-}Col}$) and the total P concentration in soil solution measured by ICP-MS ($P_{Soln\text{-}ICP}$) for the topsoils and subsoils of the Field, pH Rotation and Old Rotation is shown in **Figure 5.1** (samples with un-detectable $P_{Soln\text{-}Col}$ have been excluded). The $P_{Soln\text{-}Col}$ ranged from 0 to 100 µg L^{-1} whereas $P_{Soln\text{-}ICP}$ covered a wider range of 0 to 250 µg L^{-1}. The highest values of $P_{Soln\text{-}Col}$ were typically found in the pH Rotation topsoils (13.9 to 97.0 µg L^{-1}) spread over a wide range of $P_{Soln\text{-}ICP}$ (126 to 229 µg L^{-1}). The Old Rotation topsoils covered a lower range of $P_{Soln\text{-}Col}$ (1.99 to 30.3 µg L^{-1}) and $P_{Soln\text{-}ICP}$ (105 to 154 µg L^{-1}). Not all subsoil $P_{Soln\text{-}Col}$ was detectable but where results were obtained the Old Rotation subsoils ranged from 2.02 to 8.087 µg L^{-1} (n = 6) and were mainly from plots which had received TSP and GMP fertilisers. The $P_{Soln\text{-}ICP}$ results for these 6 results ranged from 59.0 to 102 µg L^{-1}. Compared to the Old Rotation, in the pH Rotation, the subsoils had higher $P_{Soln\text{-}Col}$ values ranging from 1.99 to 51.5 and $P_{Soln\text{-}ICP}$ from 36.5 to 156 µg L^{-1}. Across the entire dataset $P_{Soln\text{-}Col}$ was on average 20.0% (± SD 1.86%, n = 132) of the $P_{Soln\text{-}ICP}$ and ranged from 1.86% to 53.3% of $P_{Soln\text{-}ICP}$. These results showed that P_{Soln} was, overall, greater in the pH Rotation topsoils and subsoils than in the Old Rotation. This certainly reflects the differences in P fertiliser management between the two trials where, in the Old Rotation, only half of the plots receive P fertilisers. The spread of P_{Soln} in the pH Rotation may be reflective of soil characteristics controlling P solubility across the pH range (4.5 to 7.5). There was a strong and significant correlation between $P_{Soln\text{-}Col}$ and $P_{Soln\text{-}ICP}$ ($r = 0.684$, $p < 0.001$, n = 132) across the entire dataset which was markedly displaced from the 1:1 line towards the x-axis ($P_{Soln\text{-}ICP}$). The slope of $P_{Soln\text{-}Col}$ against $P_{Soln\text{-}ICP}$ was 0.335; at zero $P_{Soln\text{-}ICP}$ the $P_{Soln\text{-}Col}$ was 50.0 µg L^{-1}. This suggested that either the colorimetric method was not sensitive enough to determine all of the inorganic P present or that the $P_{Soln\text{-}ICP}$ was quantifying other forms of P in the soil solution such as organic P- or possibly both. Organic-P was likely present in $P_{Soln\text{-}ICP}$ but was not quantified by the colorimetric assay for $P_{Soln\text{-}Col}$, where it can be assumed that most PO_4^{3-} determined was inorganic P (Adesanwo, *et al*., 2013). Other studies have also found that the amount of P quantified by ICP is greater than colorimetric determinations (Ziadi, *et al*., 2009; Ivanov, *et al*., 2012; Adesanwo, *et al*., 2013). Soil organic carbon and nitrogen clearly decrease with depth (to 30 cm) in agricultural systems (Gregory, *et al*., 2016). Phosphorus is strongly associated with C in nutrient-rich (arable) soils with an approximate C: P ratio of 0.016 (Tipping, *et al*., 2016) so it is reasonable to expect that the topsoil solution

would contain more organic P. Farm yard manure is directly applied to the topsoils in both rotations during root crop phases and crop residues are integrated when the plots are ploughed and these practices should increase soil organic matter. Phosphorus which is extractable in dilute salt solutions such as calcium chloride extractable-P, is elevated in soils which receive farm yard manure (Vanden Nest, *et al*., 2016). This may explain why the $Ca(NO_3)_2$ extractable P in the Woodland's long-term experiments could be elevated in organic P. Calcium chloride extractable-P may be permanently elevated for over one year (Vanden Nest, *et al*., 2016) and so it may be assumed that, because farm yard manure is applied once every 6 years in the Old Rotation and twice every 8 years in the pH Rotation, organic P levels may be elevated in subsequent crop rotation phases.

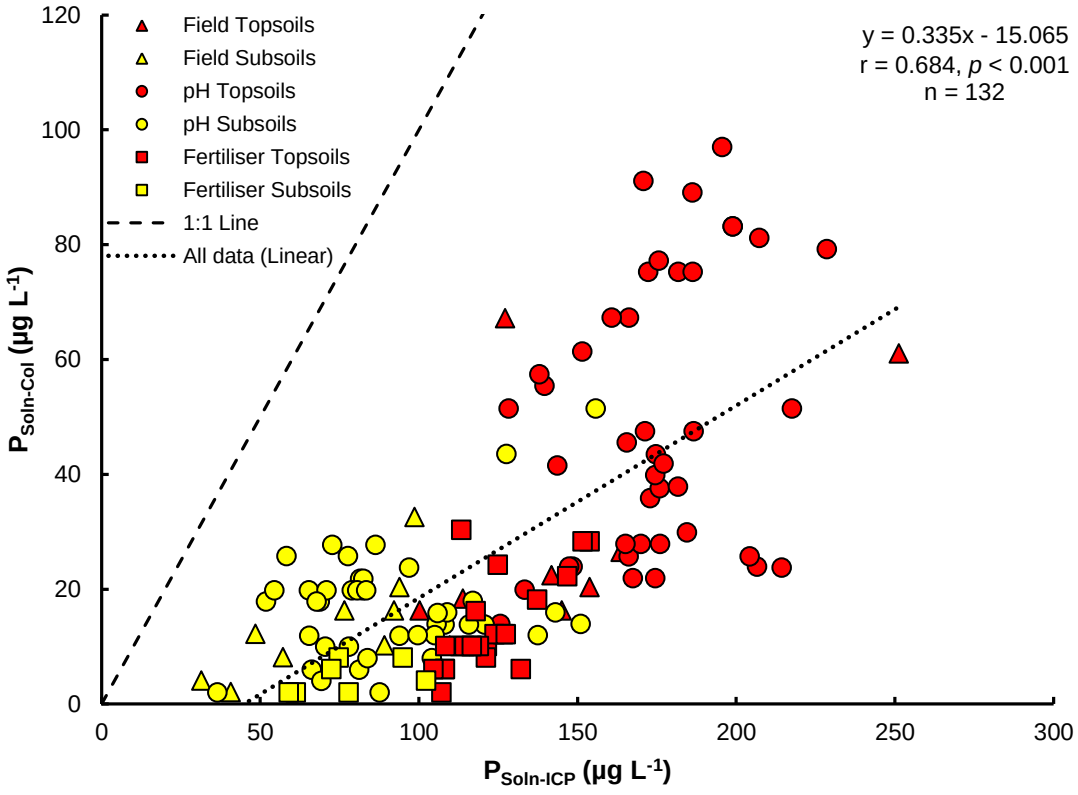


Figure 5.1. Relationship between $P_{Soln-ICP}$ and $P_{Soln-Col}$ compared to a 1:1 line (samples with non-detectable $P_{Soln-Col}$ were excluded).

Estimating P associated with dissolved organic matter (P_{DOM}) in P_{Soln}

Assuming the long-term experiments contain "nutrient-rich soil organic matter", the phosphorus: carbon ratio (P: C) of 0.016 as determined by Tipping, *et al*., (2016) could be used to provide an estimate of the amount of P associated with organic matter (P_{DOM}) by multiplying the dissolved organic carbon by 0.016. The relationship between P_{DOM} and the organic P in the supernatant, which is the difference between total P measured by ICP-MS and inorganic P measured colorimetry ($P_{Soln-Diff}$) (i.e. $P_{Soln-ICP} - P_{Soln-Col}$) for all the samples compared to a 1:1 line is shown in **Figure 5.2**. There was a strong correlation across all samples between P_{DOM} and $P_{Soln-Diff}$ ($r = 0.676$, $p < 0.001$, $n = 132$) but all the data fell below the 1:1 line towards $P_{Soln-Diff}$. P_{DOM} increased by a factor of 0.171 as $P_{Soln-Diff}$ increased, with a displacement of 23.8 µg L^{-1} P in $P_{Soln-Diff}$ when P_{DOM} was zero. $P_{Soln-Diff}$ ranged from 27.4 to 191 µg L^{-1} with an average value of 97 µg L^{-1} (± SD 34.9 µg L^{-1}). In contrast, P_{DOM} covered a narrower range from 19.9 to 70.7 µg L^{-1}. The average P_{DOM} (40.5 ± SD 8.84 µg L^{-1}) was less than half the $P_{Soln-Diff}$ average. The lack of agreement between the results could be due to a number of reasons. First, analytical errors and low limits of detection in the $P_{Soln-Col}$ analysis would influence the difference between $P_{Soln-ICP}$ and $P_{Soln-Col}$ resulting in an overestimate of P_o in P_{Diff}. Second, it is possible that there are errors in P_{DOM} which is estimated based on a P: C ratio which itself is an estimate of the relationship between P and C in nutrient-rich soil organic matter covering a global range of soil samples over a range of soil horizons, with a lot of variation (Tipping, *et al*., 2016). Finally, there may be errors associated with the estimate of P_{DOM} due to low dissolved total organic carbon levels in the soil solutions.

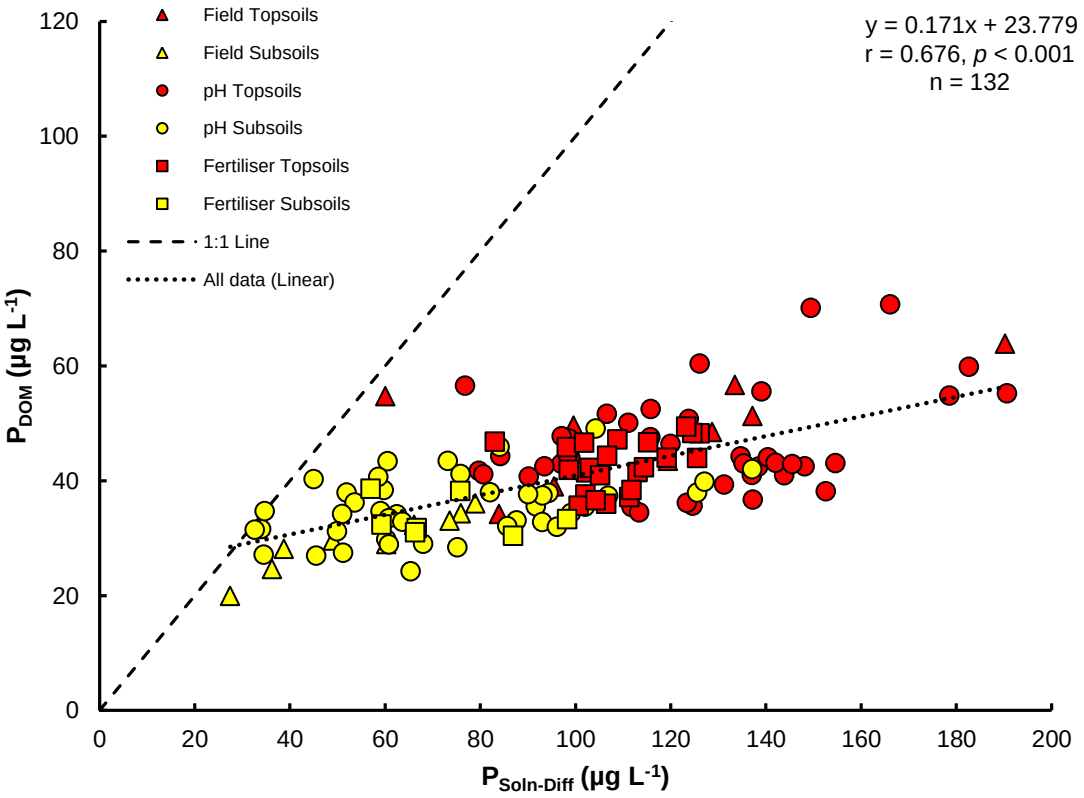


Figure 5.2. Relationship between $P_{Soln-Diff}$ and P_{DOM} in the dataset compared to a 1:1 line (samples with undetectable $P_{Soln-Col}$ were excluded and one outlying point in the topsoils was also excluded).

5.4.2 Effect of Fertiliser Management and Crop Phase on Soil Solution P

The effects of fertiliser treatment and crop rotation phase on the (i) topsoil and (ii) subsoil $P_{Soln-Col}$ in the Old Rotation are shown in **Figure 5.3**. There were variations in topsoil $P_{Soln-Col}$ across the crop phases and fertiliser treatments which ranged between 6.05 and 78.1 µg L^{-1} with an average of 20.5 µg L^{-1} (± SD 24.01 µg L^{-1}, n = 8). There was large standard error in the topsoil under spring oats (51.9 µg L^{-1}) possibly due to contamination in the analysis. Excluding the topsoil spring oats $P_{Soln-Col}$, there was an average $P_{Soln-Col}$ of less than 20 µg L^{-1} across all treatments. Subsoil $P_{Soln-Col}$ were lower compared to the topsoil, and almost undetectable in most cases, with an average $P_{Soln-Col}$ of less than 1.35 µg L^{-1} (± SD 2.28 µg L^{-1}, n = 8) over the four treatments and two crop phases.

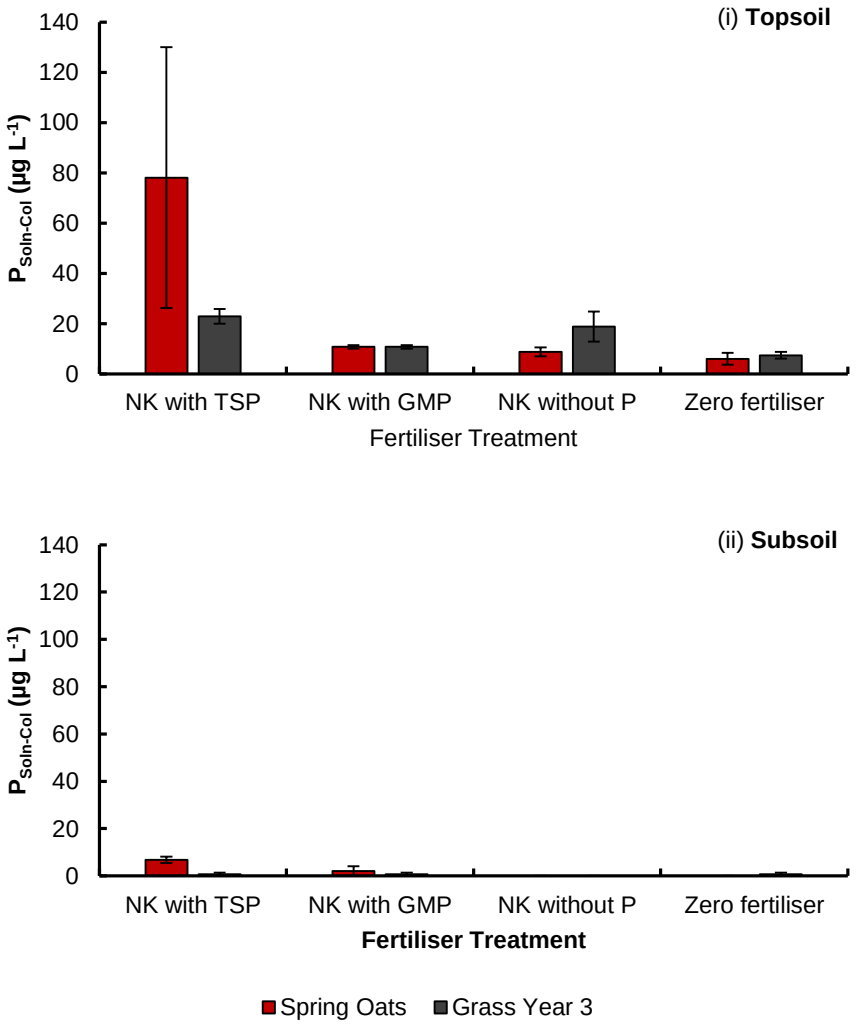


Figure 5.3. Effect of fertiliser treatment and crop phase on the mean $P_{Soln-Col}$ (± SEM, n = 3) in the solutions (0.005 M Ca(NO3)2) equilibrated with (i) topsoil and (ii) subsoil of the Old Rotation.

The effects of fertiliser treatment and crop phase on $P_{Soln-ICP}$ in the topsoil and subsoil of the Old Rotation are shown in **Figure 5.4**. The $P_{Soln-ICP}$ in the spring oats topsoils ranged from 112 µg L^{-1} (zero fertiliser) to 137 µg L^{-1} (NK with TSP), with an average $P_{Soln-ICP}$ of 121 µg L^{-1} (± SD 11.1 µg L^{-1}, n = 4) across all of the fertiliser treatments. Similarly, the $P_{Soln-ICP}$ under grass year 2 ranged from 113 µg L^{-1} (NK without P) to 145 µg L^{-1} (NK with TSP) with an average $P_{Soln-ICP}$ of 124 µg L^{-1} (± SD 14.3 µg L^{-1}, n = 4) across all fertiliser treatments. The combined average of the $P_{Soln-ICP}$ measured in all treatments across both crops was 123 µg L^{-1} (± SD 12.0 µg L^{-1}, n = 8). The $P_{Soln-ICP}$ in the subsoil under spring oats was on average 69.1 (± SD 13.3 µg L^{-1}, n = 4), with the minimum $P_{Soln-ICP}$ of 61.6 µg L^{-1} in the zero fertiliser treatment, and the greatest $P_{Soln-ICP}$ was 90.6 µg L^{-1} when TSP was applied. The subsoil $P_{Soln-ICP}$ under grass year 2 ranged from 56.5 µg L^{-1} (zero fertiliser) to 65.1 µg L^{-1} (NK with GMP) with an average $P_{Soln-ICP}$ of 61.3 µg L^{-1} (± SD 3.66 µg L^{-1}, n = 4). Across both crop phases and all treatments, the average $P_{Soln-ICP}$ in the subsoil was 67.9 µg L^{-1} (± SD 11.5 µg L^{-1}, n = 8). The topsoil: subsoil $P_{Soln-ICP}$ ratio in the spring oats was an average 1.65 whereas it was 2.03 for grass year 2.

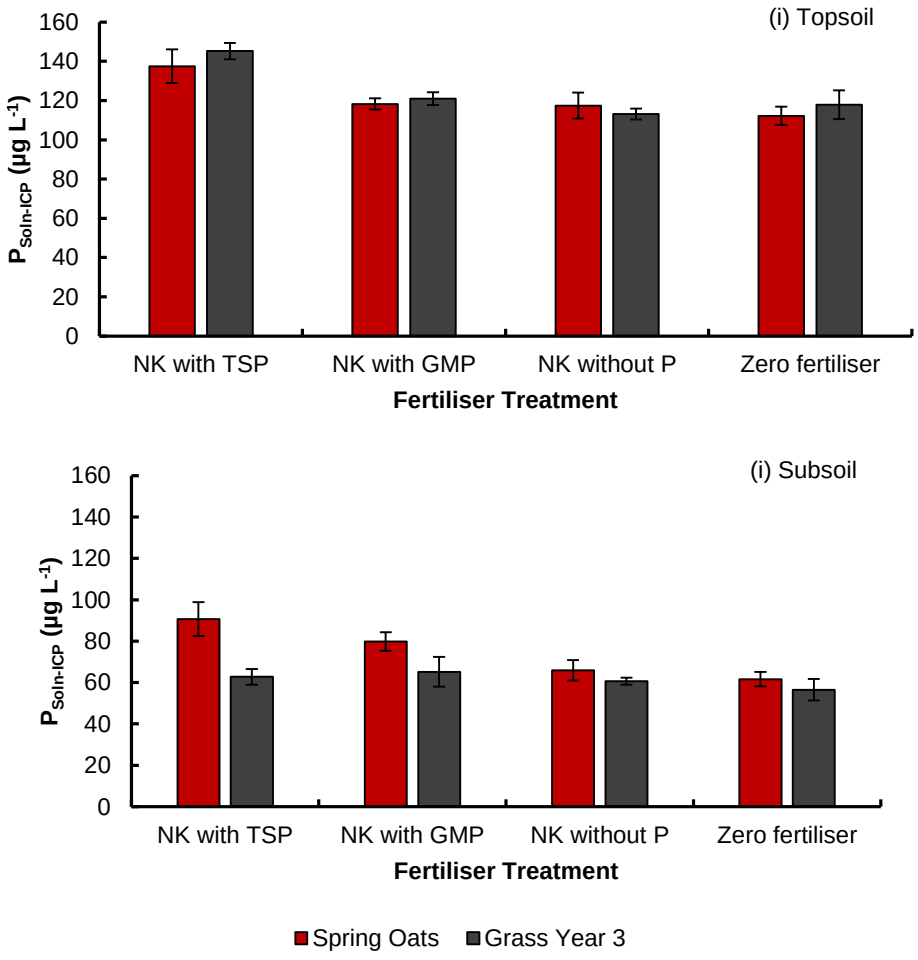


Figure 5.4. Effect of fertiliser treatment and crop phase on the mean $P_{Soln-ICP}$ (± SEM, n = 3) in solutions (0.005 M $Ca(NO_3)_2$) equilibrated with the topsoil and subsoil of the Old Rotation.

The $P_{Soln-ICP}$ (**Figure 5.4**) data were thought to be more reliable than the PO_4^{3-} data measured by $P_{Soln-Col}$ (**Figure 5.3**). Assuming that $P_{Soln-Col}$ was entirely inorganic PO_4^{3-} and $P_{Soln-ICP}$ was the total P combining inorganic and organic P, then an approximation of the P species distribution could be made. Topsoil $P_{Soln-Col}$ was between 6.29% and 15.8% of the $P_{Soln-ICP}$ as inorganic PO_4^{3-}, whereas in the subsoil, this was much lower, up to 1.19% of the $P_{Soln-ICP}$ was $P_{Soln-Col}$. These results suggested that much of the P in the soil solution was organic P, with the topsoil solution consisting of between 83.3% and 93.7% organic P and the subsoil solution consisting of between 98.8% to 100% organic P. The colorimetric method does not appear to be sensitive at low concentrations, so it may not be appropriate to infer the speciation of P present in the samples using the $P_{Soln-Col}$ as an approximation of inorganic P. However, it was also shown previously that the $P_{Soln-ICP}$ was likely to include significant amounts of organic-P in the soil solution based on the P: C ratio of Tipping, *et al.*, (2016). Therefore, it may be useful to perform the geochemical speciation modelling twice using both $P_{Soln-ICP}$ and $P_{Soln-Col}$ to infer the molarity of PO_4^{3-} in solution despite the uncertainty in the analysis and distribution of P species.

5.4.3 Measured vs Target Soil pH in the pH Rotation

The relationship between measured and target soil pH values under both crop phases (spring oats and grass year 2) in the topsoil and subsoil of the pH Rotation deviated slightly below the 1:1 line for both the topsoil and subsoil (**Figure 5.5**). This was expected because all plots are maintained at the same target pH values regardless of crop phase and topsoils are corrected annually for deviations in the target pH. The soil pH of the Field was pH 4.81 (SD ± 0.22) in the topsoil and pH 5.02 (SD ± 0.21) in the subsoil. This explains the deviation of the measured values below the 1:1 line as the soil tended back towards its natural pH value due to its buffering capacity resisting the imposed change in pH (Goulding, 2016). Furthermore, the relationship was similar under both the spring oats and grass year 2, which are four years apart in the rotational cycle, which suggested that long-term pH management had created a uniform pH profile above the indurated layer in the plots. The similarity of topsoil and subsoil measured pH values across the crop phases was confirmed as shown in **Figure 5.6**, where the topsoil and subsoil pH relationship between spring oats and grass year 2 showed a strong 1:1 relationship across the pH gradient.

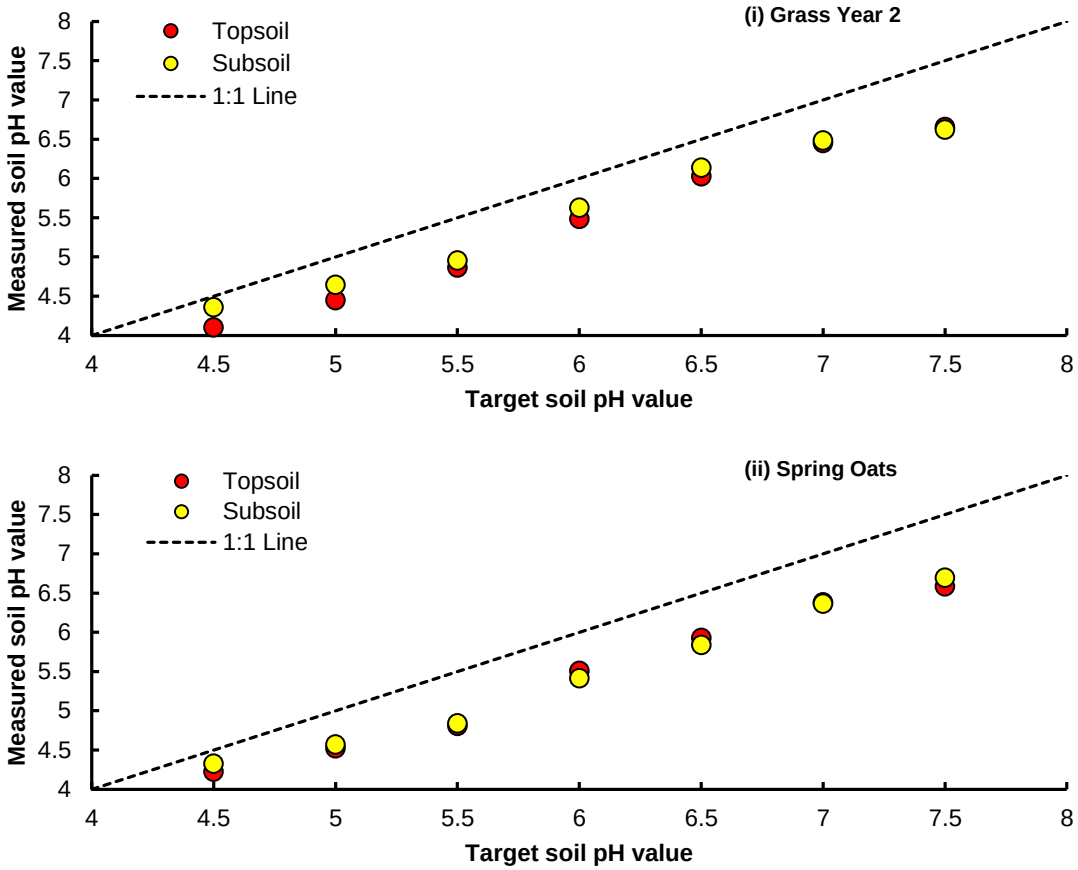


Figure 5.5. Relationship between target and measured soil pH in the topsoil and subsoil for (i) grass year 2 and (ii) spring oats of the pH Rotation compared to a 1:1 line.

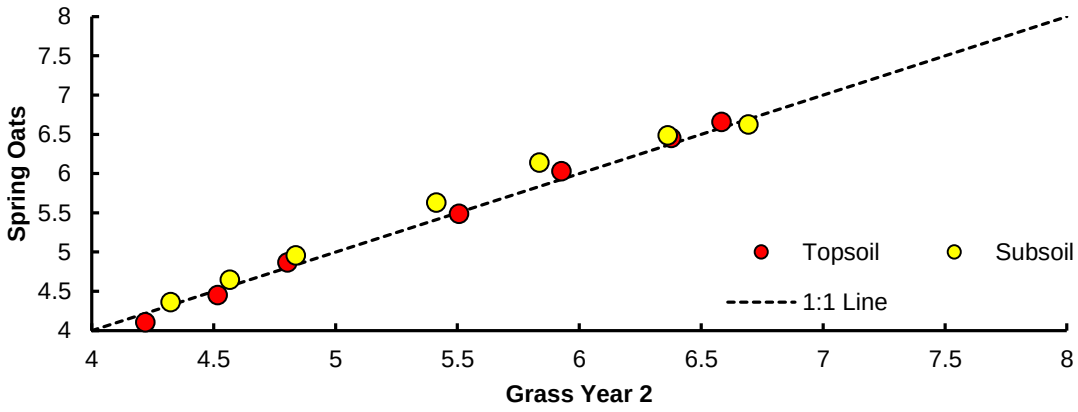


Figure 5.6. Comparison of measured soil pH for grass year 2 and spring oats in the pH Rotation compared to a 1:1 line.

5.4.4 Effect of Crop and Soil pH on Soil Solution P Concentration in the pH Rotation

The effect of target soil pH value and crop phase on $P_{Soln-Col}$ is shown in **Figure 5.7**. The topsoils of the grass year 2 plots had an average $P_{Soln-Col}$ value of 29.3 µg L^{-1} (± SD 7.43 µg L^{-1}, n = 7) whereas $P_{Soln-Col}$ in the topsoils of spring oats topsoils was 2.7 times greater at an average value of 80.6 µg L^{-1} (± SD 4.73 µg L^{-1}, n = 7). In the subsoil, the average $P_{Soln-Col}$ in the spring oats plots was 23.3 µg L^{-1} (± SD 7.69 µg L^{-1} n = 7) which was approximately double that in the grass year 2 plots (10.6 µg L^{-1} (± SD 4.17 µg L^{-1}, n = 7)). Overall $P_{Soln-Col}$ rose with soil pH for all treatments with an average r value of 0.755 across the four treatments reflecting an increase in P solubility with rising soil pH. It was expected that $P_{Soln-Col}$ may have shown greater variation with pH with an initial increase between pH 4.5 and 6.0 as P solubility would increase with rising pH (Weng, *et al*., 2011). Above pH 7, the precipitation of calcium phosphates was expected to cause a decrease in $P_{Soln-Col}$ (Weng, *et al*., 2011). There also appeared to be an effect of crop phase on the $P_{Soln-Col}$ in the topsoils and subsoils. The main reason for the differences between spring oats and grass year 2 topsoils were thought to be a result of differences in recent fertiliser application history. Phosphate fertiliser is not applied to grass year 2 and the last application was TSP at the beginning of the previous phase (grass year 1 ley phase) whereas the spring oats plots received TSP fertiliser at the beginning of the crop phase and prior to that, the root crop phase had received farm yard manure and TSP. The solubility of P increases with frequency of P fertiliser use (McDowell & Sharpley, 2003) and so this may be a persisting effect of on $P_{Soln-Col}$ due to recent fertiliser history. This may also explain the relatively greater values of $P_{Soln-Col}$ in the spring oats plots topsoils with residual, labile P fertiliser remaining in the soil solution. These results suggested that $P_{Soln-Col}$ in this study were not influenced by crop phase but more likely by soil pH and recent fertiliser history. It was expected that there would be differences in $P_{Soln-Col}$ across the pH range due to differences in the main factors controlling P_{Soln}: adsorption and desorption of from Al and Fe oxides (such as goethite) at low pH (Antelo, *et al*., 2005) and the dissolution and precipitation of calcium phosphates controlling P solubility above pH 6 or 7 (Weng, *et al*., 2011). These results therefore raise doubts as to whether the $P_{Soln-Col}$ was a reliable indicator of P_{Soln} due to the lack of variation with pH.

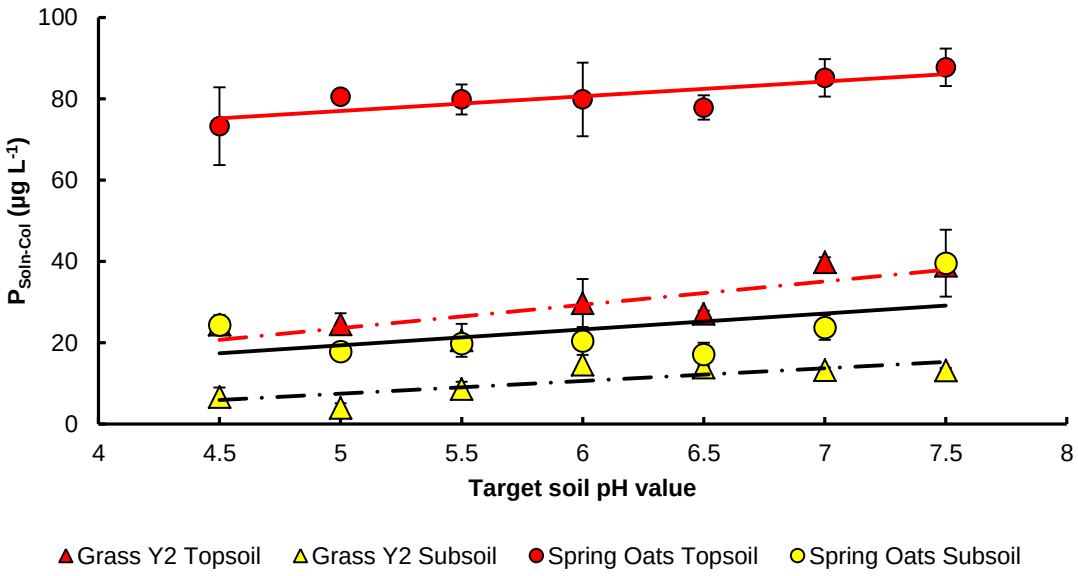


Figure 5.7. Effect of soil pH and crop phase on $P_{Soln-Col}$ in the Grass Y2 topsoils (r = 0.838) and subsoils (r = 0.549) and Spring Oats topsoils (r = 0.828) and subsoils (r = 0.805).

The effect of target soil pH value and crop phase on $P_{Soln-ICP}$ is shown in **Figure 5.8**. Across the pH range the average $P_{Soln-ICP}$ in the topsoil of the grass year 2 plots was 171 µg L^{-1} (± SD 22.2 µg L^{-1}, n = 7) and in the spring oats the average topsoil $P_{Soln-ICP}$ was 177 µg L^{-1} (± SD 24.2 µg L^{-1}, n = 7). The average $P_{Soln-ICP}$ in the subsoils for grass year 2 in the pH Rotation was 99.2 µg L^{-1} (± SD 23.6 µg L^{-1}, n = 7) and in the spring oats $P_{Soln-ICP}$ was 81.6 µg L^{-1} (± SD 21.1 µg L^{-1}, n = 7). There appeared to be elevated values of $P_{Soln-ICP}$ around pH 4.5 in the topsoil under grass year 2 (208 µg L^{-1} ± SEM 3.06) and spring oats (218 µg L^{-1} ± SEM 6.15 µg L^{-1}). Subsoil $P_{Soln-ICP}$ was lowest at pH 4.5 under grass year 2 and spring oats (63.6 µg L^{-1} ± SEM 14.08 µg L^{-1} and 66.4 µg L^{-1} ± SEM 10.0 µg L^{-1} respectively). Topsoil and subsoil $P_{Soln-ICP}$ converged at pH 5.5 which suggested that topsoil $P_{Soln-ICP}$ was desorbed into solution with rising soil pH and became more susceptible to leaching as the pH increased in the zone of maximum P solubility. Topsoil and subsoil $P_{Soln-ICP}$ under grass year 2 increased by approximately 30 µg L^{-1} between pH 6 and pH 7 from 147 µg L^{-1} to 178 µg L^{-1} (topsoil) and 101 µg L^{-1} to 131 µg L^{-1} (subsoil) which suggested the PO_4^{3-} solubility increased as a result of increasing calcium phosphate solubility within this range. Topsoil $P_{Soln-ICP}$ continued to rise between pH 6 and 7.5 (161 to 198 µg L^{-1}) under spring oats but subsoil $P_{Soln-ICP}$ declined slightly between pH 6 and 7 (81.2 µg L^{-1} to 67.4 µg L^{-1}) before rising to a maximum $P_{Soln-ICP}$ of 127 µg L^{-1} at pH 7.5. In contrast to the $P_{Soln-Col}$, there was little variation in the average $P_{Soln-ICP}$ between the two crops across the pH gradient but there was variation in $P_{Soln-ICP}$ with soil pH which was originally expected. The P_{Soln} in the topsoil likely includes more organic-P than the subsoil solution which explains the difference between the topsoils and subsoil $P_{Soln-ICP}$ for both crop phases. The rise in subsoil $P_{Soln-ICP}$

with rising pH for grass year 2 (r = 0.874) and spring oats (r = 0.536) reflects the adsorption strength in the subsoil but also reflects the greater solubility of P as the pH rises. The general rise in subsoil $P_{Soln-ICP}$ concentrations between pH 4.5 and pH 6 may reflect increased leaching of $P_{Soln-ICP}$ from topsoils to subsoil which had desorbed from Fe/Al oxides into the soil solution. However, the continued rise in subsoil $P_{Soln-ICP}$ from pH 4.5 to 7.5 may signal a change in the control of P solubility in the soil solution. The uniformity of topsoil and subsoil pH across the plots may contribute to the solubility of P and it could be that calcium phosphate mineralogy became the controlling factor affecting the solubility of P throughout the soil profile in plots at measured pH values of 6 and greater.

The $P_{Soln-ICP}$ were greater than the $P_{Soln-Col}$ which suggested that the soil solutions may have contained a greater proportion of organic P than inorganic P, as the $P_{Soln-ICP}$ would consist of all sources of P compared to the presence of (assumed) inorganic PO_4^{3-} only in $P_{Soln-Col}$. However, because the colorimetric method may not have been sensitive enough at low $P_{Soln-Col}$ concentrations, it may not be appropriate to infer the forms of P present in the samples from these measurements using $P_{Soln-Col}$. For the geochemical modelling it was thought that $P_{Soln-ICP}$ would be a more reliable indicator of inorganic PO_4^{3-} activity but would likely produce an overestimate due to the presence of organic P. Therefore, the geochemical modelling of the pH Rotation data was also performed using both $P_{Soln-ICP}$ and $P_{Soln-Col}$ to infer the activity of PO_4^{3-} in the soil solution.

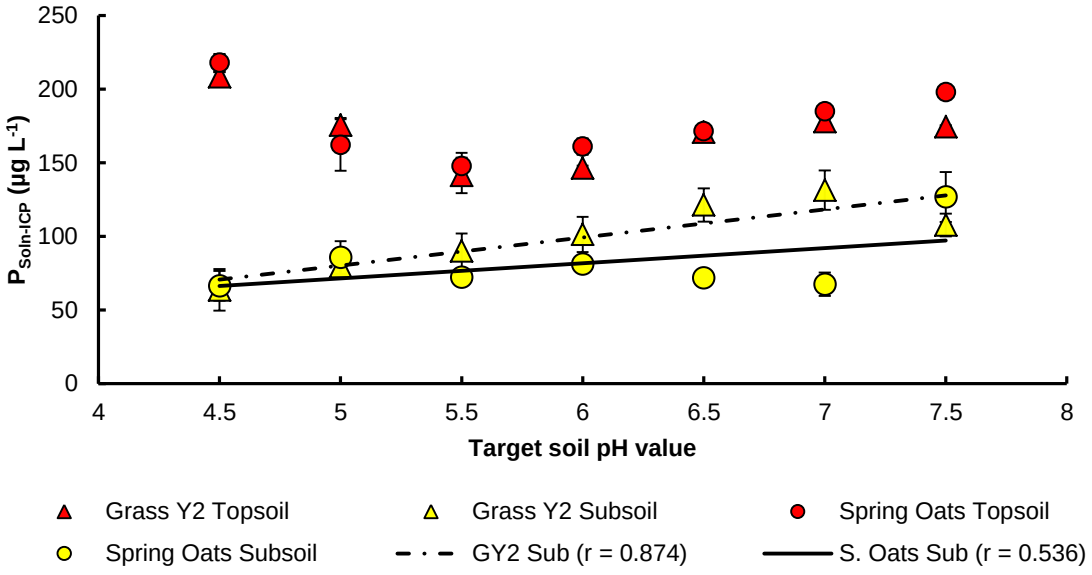


Figure 5.8. Effect of soil pH and crop phase on the $P_{Soln-ICP}$ in the topsoils and subsoils.

5.4.5 Topsoil: Subsoil Ratios of P_{Soln} in the pH Rotation

The topsoil: subsoil ratio of $P_{Soln-ICP}$ and $P_{Soln-Col}$ across the pH gradient in the pH Rotation for grass year 2 and spring oats crop phases is shown in **Figure 5.9** and compared to a topsoil: subsoil ratio of 1.0 (dashed line). The topsoil: subsoil ratio for the grass year 2 $P_{Soln-ICP}$ and $P_{Soln-Col}$ and the spring oats $P_{Soln-ICP}$ showed similar variations with soil pH. Approximately topsoils contained between 3 and 4x the amount of $P_{Soln-ICP}$ and $P_{Soln-Col}$ in the topsoils and subsoils, with the ratio decreasing towards a minimum close to 1.0 at pH 6, before showing a slight rise towards pH 7. The exception was the topsoil: subsoil $P_{Soln-Col}$ ratio under at pH 5 where there was seemingly six times the amount of P in the topsoil than the subsoil, but this was likely due to the 'outlier' contaminated sample discussed previously. These patterns were consistent with retention of P in the topsoil < pH 5.5 adsorbed on to Fe and Al oxides and the increase in solubility of P with rising soil pH. The even distribution of colorimetric (grass year 2) and ICP-MS (grass year 2 and spring oats) determined P between the topsoil and subsoil indicating that topsoil solution P was leached to the subsoil. However, the colorimetric topsoil: subsoil P under spring oats suggested retention of P in the topsoil 4x that of the subsoil between pH 5 and 7, with decreases in the ratios to 3.0 (at pH 4.5) and 2.0 (at pH 7.5) which was not consistent with what was expected across the pH range. It was thought that analytical error in the colorimetric analysis may have resulted in the lack of trend with pH for the spring oats colorimetric data (and also for the outlier grass year 2 colorimetric ratio at pH 5). The ICP-MS P consists of both organic and inorganic P- the colorimetric data should follow a similar trend to that of the ICP-MS with pH as a constituent of the total P.

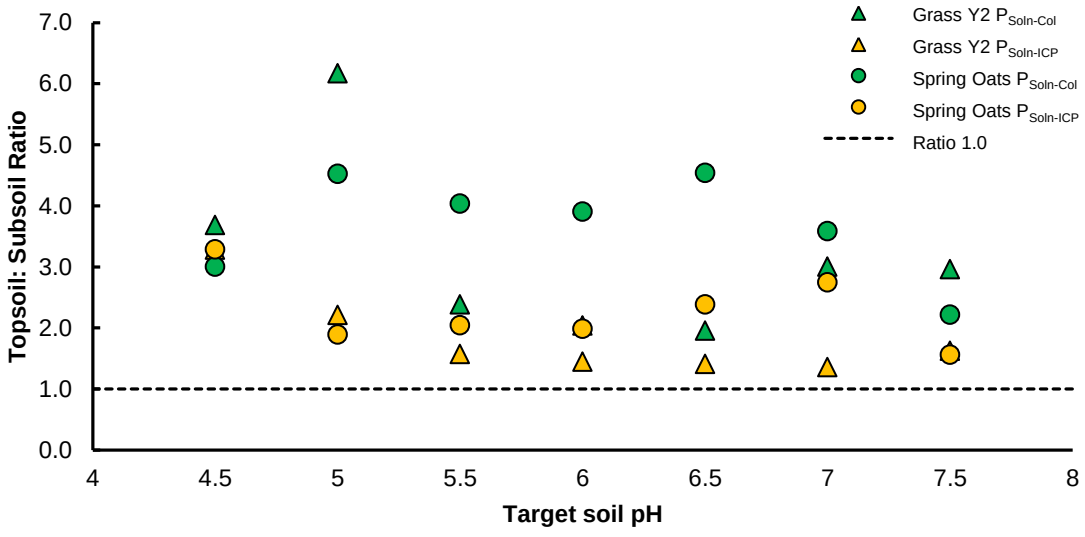


Figure 5.9. Topsoil: subsoil ratios for $P_{Soln-Col}$ and $P_{Soln-ICP}$ in the grass year 2 and spring oats crop phases across the target pH plots in the pH Rotation is shown compared to a 1.0 (broken) line.

5.4.6 Solubility Phase Analysis for the pH Rotation

The solubility phase diagram for all topsoils and subsoils analysed in the pH Rotation using the $P_{Soln\text{-}ICP}$ data to model $H_2PO_4^-$ is shown in **Figure 5.10**. There was a marked effect of soil pH control on the lime and phosphate potentials in the plots across the dataset. Only a sub-group of treatment plots close to the HA line could be explained by the solubility phase diagram: soil samples with a measured soil pH greater than pH 6 showed a solubility product which was between HA and TCP, and those soil samples with a measured pH less than 6 were under-saturated with respect to HA (Larsen & Court, 1961). The treatment plots that were to the left of the HA solubility line were likely controlled by adsorption to Fe and Al oxides, as HA is not expected to be present at soil pH values less than 6, and so were under-saturated relative to HA (Larsen & Court, 1961). The main P fertiliser used in these plots is highly soluble monocalcium phosphate i.e. TSP (farm yard manure is applied in addition to TSP twice out of eight crop cycles) which is not modelled in the phase diagram because the solubility line is outwith the limits of the phase diagram. The ground mineral phosphate (GMP) fertiliser fell between the HA and TCP lines as expected and confirmed the validity of this approach. The phosphate activity in the Field topsoil and subsoil could not be explained by the solubility phase diagram which was expected because the soil is naturally acidic (pH 4.81 and 5.02 in the topsoil and subsoil respectively) and P solubility is likely controlled by adsorption below pH 6. It was expected that pH plots with target less than pH 6 would be more influenced by Al and Fe oxides whereas the solubility of P plots above pH 6, where increasing amounts of lime are used to maintain the soil pH values at alkaline targets, were expected to be influenced by calcium phosphates (Weng, *et al*., 2011). However, $P_{Soln\text{-}ICP}$ likely contains organic forms of P and using these data to assume $H_2PO_4^-$ activity may be overestimating the inorganic phosphate ion activity.

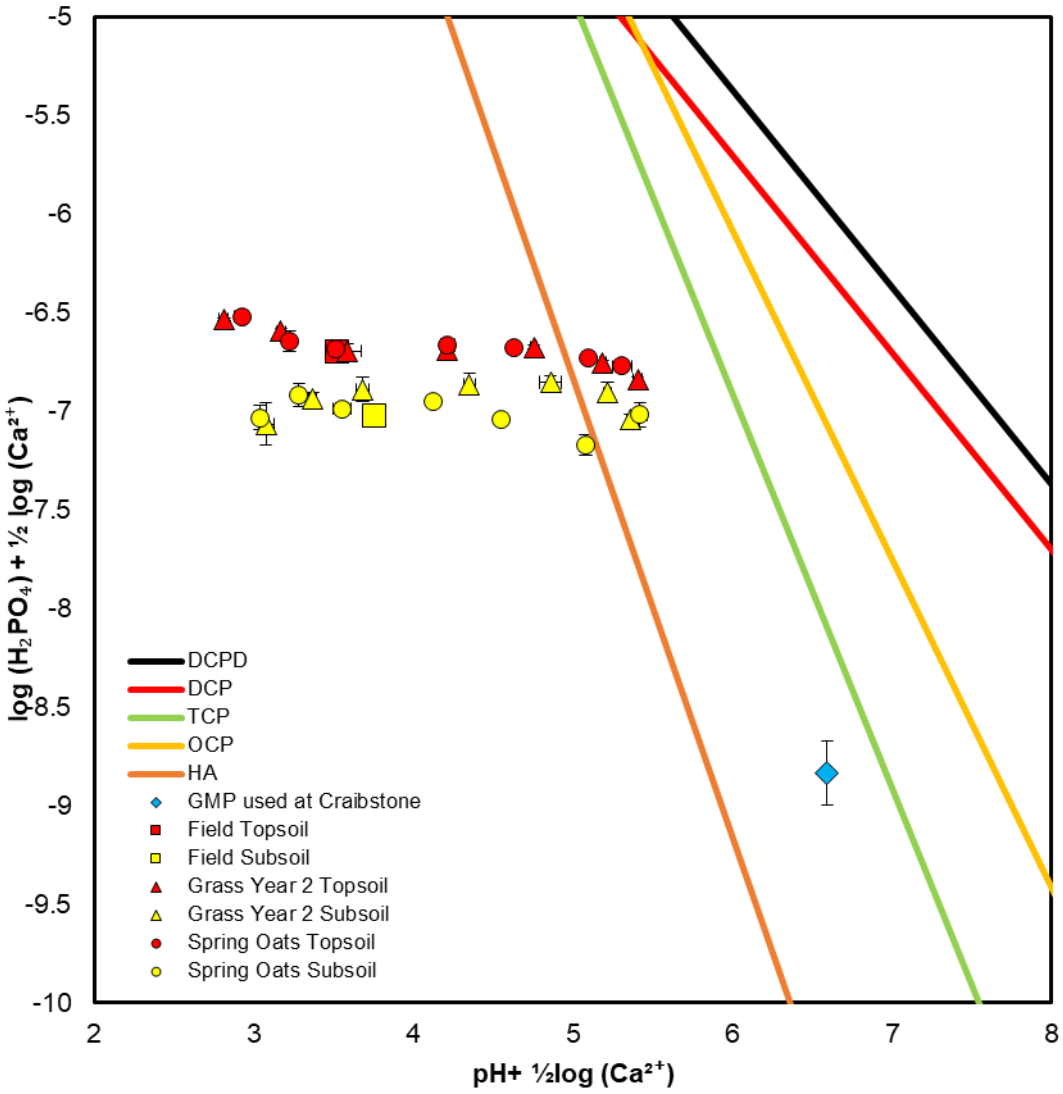


Figure 5.10. Solubility phase diagram for topsoils and subsoil across the pH plots for grass year 2 and spring oats using $P_{Soln-ICP}$ to determine $H_2PO_4^-$ ion activity. Also shown are the Field topsoil and subsoil and the GMP fertiliser as references (although GMP is not applied to the pH Rotation).

The solubility phase diagram for all topsoils and subsoils analysed in the pH Rotation using the $P_{Soln\text{-}Col}$ data to model $H_2PO_4^-$ is shown in **Figure 5.11**. There was a similar marked effect of soil pH on the solubility, again showing variation in the lime and phosphate potentials for each treatment plot. The use of lime can have a positive effect on the solubility of applied and residual P fertiliser as demonstrated by Simonsson, *et al*., (2018) who utilised long-term liming experiments to show that P availability was increased due to liming by preventing the occlusion of P into more stable (less soluble) forms. There was however, a larger degree of separation between treatment plots across the dataset and between crops suggesting differences in ion activity between the crop phases. Overall there was a distinct shift in the data to the left of HA in the solubility diagram, with more treatment plots shifting to the left of the HA line indicating that more soils were under-saturated with respect to HA (Zhang, *et al*., 2014). If $P_{Soln\text{-}Col}$ provides a reliable estimate of inorganic phosphate then these results suggest that the $P_{Soln\text{-}ICP}$ was overestimating $H_2PO_4^-$ activity due to the contribution of organic P. A general conclusion would be that whilst $P_{Soln\text{-}ICP}$ may overestimate the main control of PO_4^{3-} solubility due to the presence of organic P forms, and $P_{Soln\text{-}Col}$ may be underestimating it due to analytical error, it is likely that above pH 6, calcium phosphate mineralogy is dominant and below pH 6, adsorption reactions with Fe and A oxides are likely controlling PO_4^{3-} solubility in the pH Rotation.

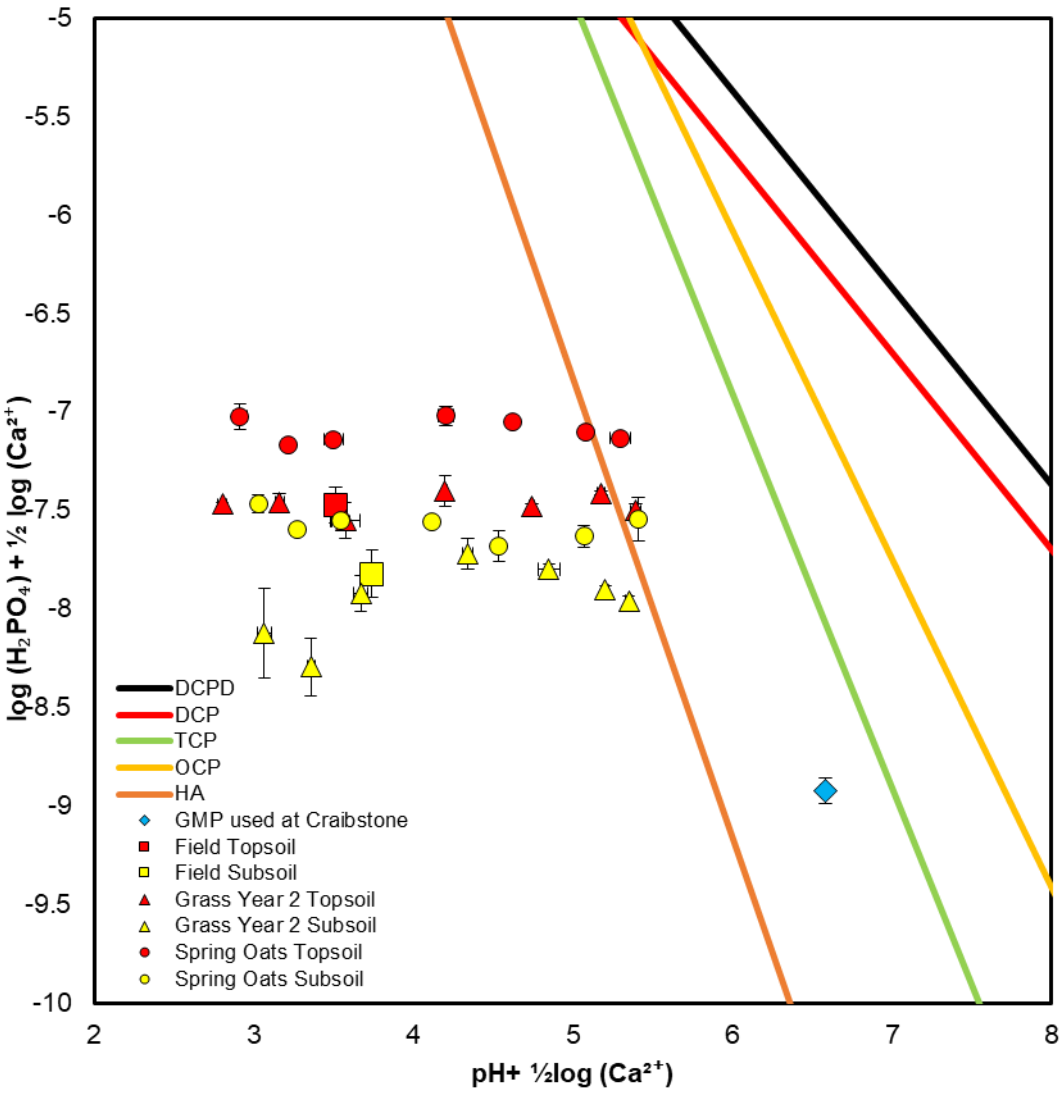


Figure 5.11. Solubility phase diagram for topsoils and subsoil across the pH plots for grass year 2 and spring oats using $P_{Soln\text{-}Col}$ to determine $H_2PO_4^-$ ion activity. Also shown are the Field topsoil and subsoil and the GMP fertiliser as references (although GMP is not applied to the pH Rotation).

Excluding all plots with soil pH values less than 6 (measured in 0.005 M $Ca(NO_3)_2$ soil suspension) showed that only plots with target pH values between 6.5 and 7.5 were controlled by calcium phosphate mineralogy when the $P_{Soln\text{-}ICP}$ data was used to model phosphate ion activity (**Figure 5.12**). The three treatment plots to the left of the HA line in this diagram were likely artefacts of systematic error in the experimental procedure because HA is expected to be present in the soils with a pH of 6 and greater (Larsen & Court, 1961). However, the diagram labels indicated that the topsoils and subsoils of a limited number if plots were controlled by calcium mineralogy and these tended to be where the target soil pH was 6.5 or greater. This was expected because calcium phosphates precipitate as soil pH increases towards alkaline with increasing pH (McDowell & Sharpley, 2003).

The solubility phase diagram for the same soils using $P_{Soln\text{-}Col}$ to model phosphate ion activity is shown in **Figure 5.13**. The shift of the pH plots centred around the HA line when using the $P_{Soln\text{-}Col}$ compared to the $P_{Soln\text{-}ICP}$ suggested that the phosphate ion activity in **Figure 5.10** (and **Figure 5.12**) was overestimated by the contribution of organic P in $P_{Soln\text{-}ICP}$, however the uncertainty in the $P_{Soln\text{-}Col}$ may still be under-estimating the activity. The concentration of soil samples centred around the HA line suggested this was the dominant calcium phosphate controlling P solubility (Zhang, *et al*., 2014). It could reasonably be said that the samples were in transition from TCP to HA, which is the least soluble, and most stable form of calcium phosphates in soil. However, it is unlikely that pure HA would ever be achieved as the presence of surface contaminants such as organic acids (Alvarez, *et al*., 2004,) are likely to interfere with crystal formation, resulting in impurities and isomorphic substitutions impacting the size, structure and morphology of the HA mineral. Generally, soil P solubility with measured pH values above pH 6 were likely influenced by HA which may not supply optimum levels of P for crop requirements, which is more likely to be achieved when minerals such as di-calcium phosphate (monetite) and di-calcium di-hydrate (brushite) (Esmail, 2012; Jalali & Jalali, 2016). Therefore, it appears that residual P in these soils is in a poorly soluble form- either as HA or even less soluble forms, probably adsorbed with Fe oxides, and none of the data suggests that more soluble forms of P are present.

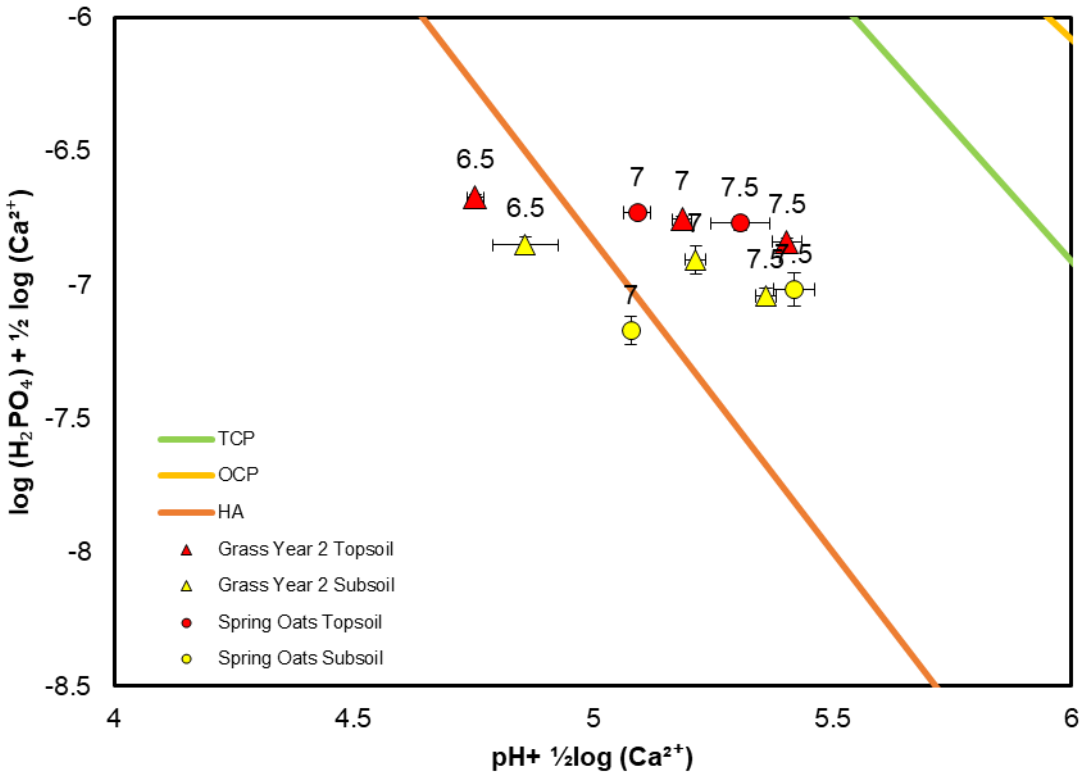


Figure 5.12. Solubility phase diagram for soils using $P_{Soln-ICP}$ (± SEM 3 auger borings) were measured pH value was greater than pH 6 (measured in 0.005 M $CaNO_3$ soil suspension). Labels indicate which pH plots are shown.

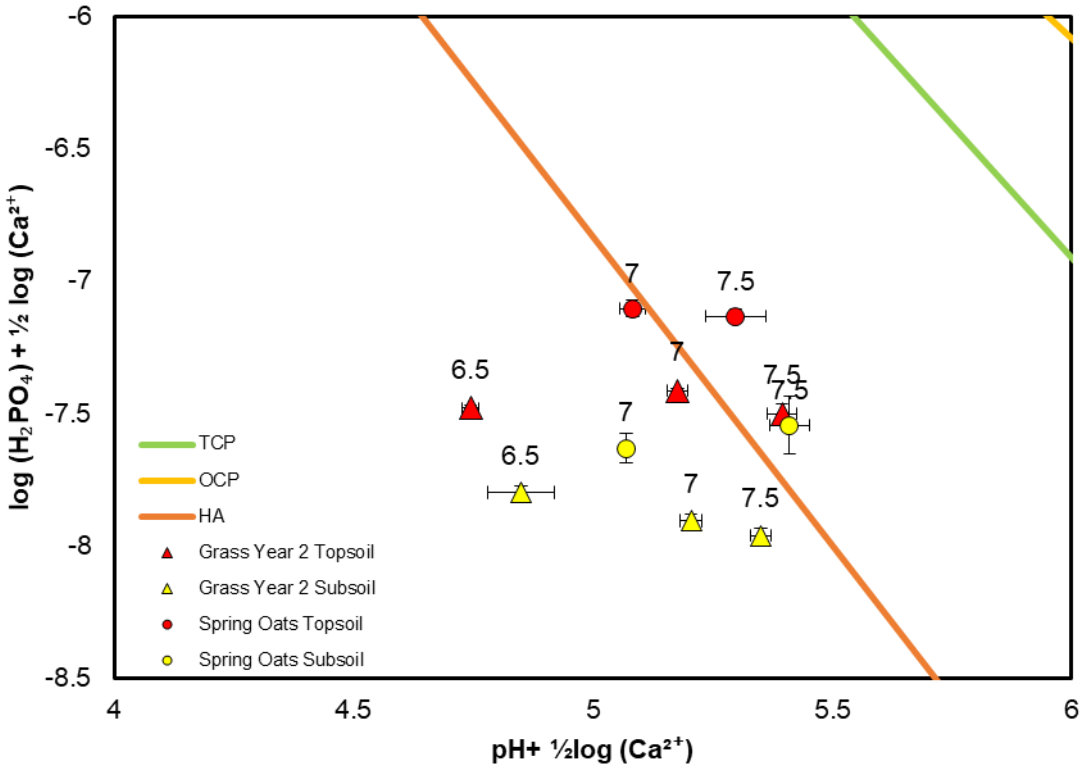


Figure 5.13. Solubility phase diagram for soils using $P_{Soln-Col}$ (± SEM 3 auger borings) were the measured pH value greater than pH 6 (measured in 0.005 M $CaNO_3$ soil suspension). Labels indicate which pH plots are shown.

5.4.7 Solubility Phase Analysis of the Old Rotation

The solubility phase diagram for the grass year 3 and spring oats crop phases for each fertiliser treatment in the Old rotation, and also the data for the field surrounding the long-term experiments, using $P_{Soln\text{-}ICP}$ to calculate PO_4 is shown in **Figure 5.14**. The data was not distinguished by each fertiliser treatment because the results showed very little variation between treatments and were tightly clustered together with small standard errors. It was clear that in the Field, and within the Old Rotation, that PO_4^{3-} solubility in all plots, regardless of soil layer, crop phase or fertiliser management strategy, was not controlled by calcium phosphate mineralogy. All soil samples presented had measured pH values (in 0.005 M $Ca(NO_3)_2$) that were less than pH 6. This result was expected as these plots are maintained towards a target of pH 6 with minimal inputs of lime, but the soil is naturally acidic, and these results further show that the soil has a resilient buffering capacity which counteracts the pH modification in the plots. Zhang, *et al*., (2014) showed that stable calcium phosphate minerals were formed in farmed calcareous soils following long-term fertiliser application. However, the phosphate solubility in these soils is probably controlled by adsorption to Fe and Al oxides regardless of the fertiliser management strategy, even though increased frequency of P fertiliser has been shown to increase P solubility (Al-Tameemi, *et al*., 2015; McDowell & Sharpley, 2003).

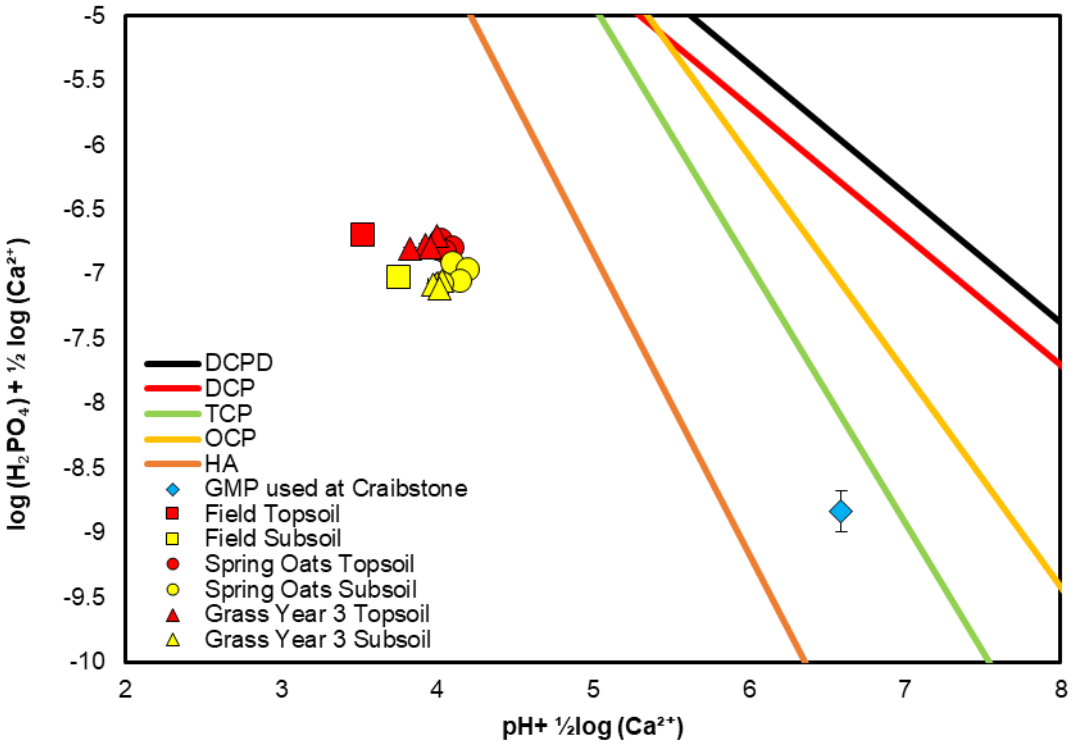


Figure 5.14. Solubility phase diagram for the topsoils and subsoils of the Old Rotation using $P_{Soln-ICP}$ data for the grass year 3 and spring oats phases in the rotation: each point represents one of the fertiliser management strategies (± SEM 3 auger borings). Included are the Field topsoil and subsoil and the GMP fertiliser as reference values.

The $P_{Soln-Col}$ data was also used to investigate ion activities and to plot a solubility phase diagram for the grass year 3 and spring oats crop of each fertiliser treatment in the Old Rotation experiment and the Field as shown in **Figure 5.15**. Due to analytical errors in the $P_{Soln-Col}$ analysis, fewer results were obtained, particularly for the subsoils where $P_{Soln-Col}$ was undetectable and so some samples could not be modelled. The soils were not distinguished in the solubility phase diagram between fertiliser treatments because all soils were under-saturated with respect to HA regardless of crop phase, fertiliser treatment and soil layer. The data however did show slightly greater variation compared to **Figure 5.14** possibly the result of errors associated with measuring low (and almost undetectable) $P_{Soln-Col}$ data. Regardless of the analytical technique used to determine PO_4^{3-} solubility it was clear calcium phosphate minerals did not control PO_4^{3-} solubility in the Old Rotation. Adsorption to Fe and Al oxides was expected to be the main factor controlling the solubility of P in the soil solution because the measured pH values (in 0.005 M $Ca(NO_3)_2$) that were less than pH 6.

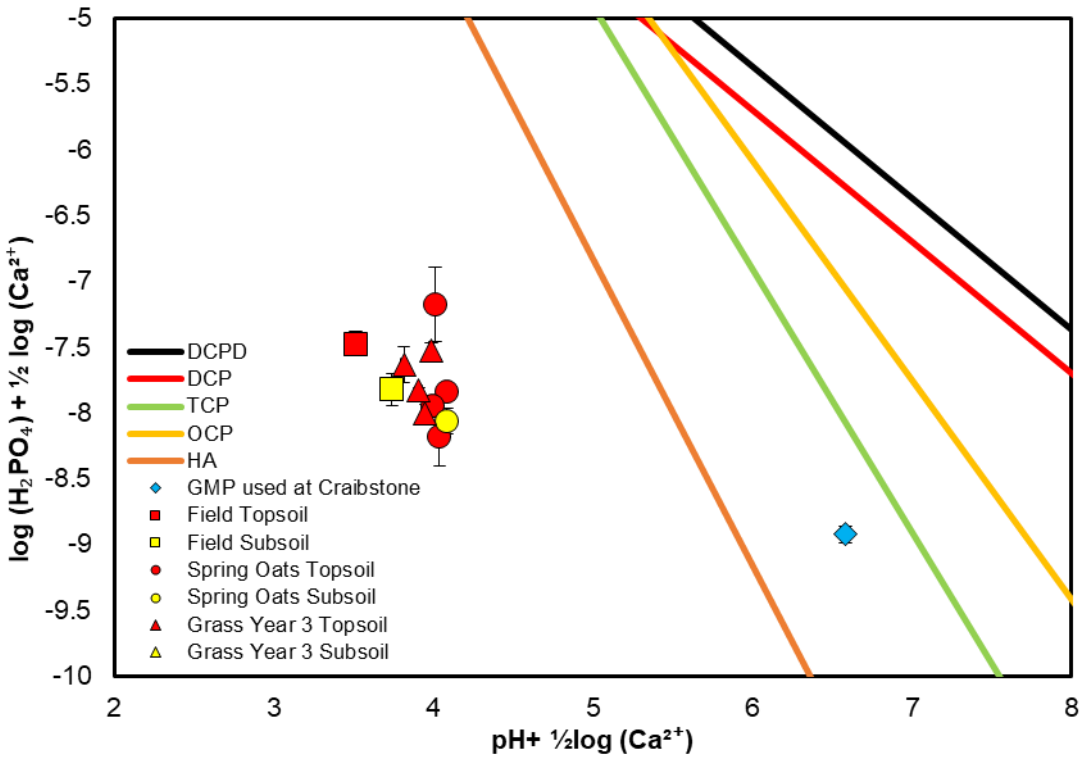


Figure 5.15. Solubility phase diagram for the topsoils and subsoils of the Old Rotation using $P_{Soln-Col}$ to estimate PO_4 activity for the grass year 3 and spring oats phases in the rotation: each point represents one of the fertiliser management strategies (± SEM 3 auger borings). Included are the Field topsoil and subsoil and the GMP fertiliser as reference values.

5.5 Conclusions

The effect of crop phase, fertiliser management strategy and soil pH control on the concentration of soil solution P, and the main factors controlling PO_4^{3-} solubility in the two long-term experiments based at SRUC's Craibstone Estate Aberdeen, were investigated. The use of lime to control the soil pH in the pH Rotation showed that topsoil and subsoil pH values were similar to the target pH values set for the topsoils, indicating that uniformity had been achieved through long-term pH management across the pH gradient. There was no apparent effect of soil pH on inorganic soil solution PO_4^{3-} as determined by colorimetry which was unexpected, and low P concentrations in the fertiliser management experiment made it difficult to conclude an effect of fertiliser use on soil solution inorganic PO_4^{3-} levels. The total P in the soil solution as determined by ICP-MS was thought to be more reliable but estimates using the C: P ratio derived by Tipping, *et al*., (2016) suggested that P associated with dissolved organic matter may have contributed to the total P concentration which meant that inferring PO_4^{3-} activity using total P concentrations was not strictly valid. Soil pH influenced soil solution total P concentrations, indicating that soil processes such as adsorption with Fe and Al oxides (< pH 5.5) and dissolution/precipitation with calcium phosphates (> pH 6) were influencing the concentration of P in solution. The results for the soil in the uncultivated field surrounding the long-term experiments showed that adsorption to Fe and Al oxides were likely controlling soil solution P. The main factors controlling PO_4^{3-} solubility were adsorption to Fe and Al oxides in all treatments with measured soil pH values < pH 6 where the soils were under-saturated with respect to hydroxyapatite (HA). Regardless of fertiliser treatment (NK with GMP, NK with TSP, NK without P and zero fertiliser application), HPO_4^{2-} and $H_2PO_4^-$ interactions with Fe/ Al hydroxide surfaces was the main factor in the Old Rotation. The pH, (Ca^{2+}) and $H_2PO_4^-$ data were consistent with forms of HA controlling the PO_4^{3-} solubility in the topsoils and subsoils of plots maintained at pH 6.5 and greater in the pH Rotation. The key conclusion is that residual P in the long-term experiments is highly insoluble- either as HA, or under-saturated with respect to HA, and adsorbed on to Fe and Al oxide surfaces. These results provide field-based evidence and insight into the long-term effects of pH management on topsoil and subsoil P dynamics over an established pH gradient, along with fertiliser use, on PO_4^{3-} solubility and contribute to the ongoing discussions regarding the underlying mechanisms controlling PO_4^{3-} release in soil solution. The practical insight for farmers is that long-term liming can alter underlying mechanisms controlling P fertiliser availability to crops (which is dependent on soil texture) and that residual P which accumulates in the soil may be transformed in to unavailable forms over the long-term.

6 Assessing Labile Soil Phosphorus Using the 'Diffusive-Gradients in Thin-Films' Technique

6.1 Abstract

Topsoil and subsoil labile phosphorus was investigated in long-term experiments using the Diffusive Gradients in Thin-Films technique. The hypothetical concentration of phosphate in solution resolved by the DGT device (P_{DGT}, μg L^{-1}) was positively correlated with P_{Total}, P_{Olsen}, $P_{MMorgan}$ and P_{Soln}. However, soil pH significantly influenced P_{DGT} indicating a pH-dependence to the phosphate buffering capacity of soil. In the pH Rotation trial, topsoil and subsoil P_{DGT} increased linearly from pH 4.5 to 7.5, reflecting strong adsorption of P to the surface of Fe and Al oxides < pH 5.5 and a change in solubility control at pH > 6 to dissolution and precipitation of calcium phosphates. Equilibrium distribution coefficients (e.g. P_{Olsen}/P_{DGT}, mL g^{-1}) decreased from a maximum at pH 4.5 to a minimum around pH 6 before rising slightly towards pH 7.5, again supporting the conclusion of two contrasting P buffering systems across the pH range of the pH Rotation. The distribution coefficients of the subsoils were greater than those of the topsoils suggesting intrinsically stronger adsorption of labile P in the subsoil – possibly reflecting the lower available P content and so occupancy of stronger sites. Furthermore, the buffering capacity of soil (R_{DGT}) in plots with pH > 6 showed that soil was able to respond faster to depletion of soil solution P (by the DGT device) than in plots with pH < 5.5. The continuous application of reactive P fertiliser to the topsoil of the pH Rotation likely encouraged migration of labile P to the subsoil where it was adsorbed. Despite an apparently high concentration of 'plant-available P' (P_{Olsen} and $P_{MMorgan}$) at pH < 5.5, the lability and speed of resupply of P to the soil solution (as determined by P_{DGT}) was least throughout the soil profile across the pH gradient. This highlights a weakness in traditional methods, based on chemical extraction, used to predict P availability in the soil solid phase. In plots which had not received P fertiliser in the Old Rotation P_{DGT} was depleted in the topsoils and subsoils relative to the (uncultivated) Field. If it is assumed that the Field is unaffected by proximity to the long-term experiments, then this suggests that crops have actually depleted native pools of labile P in plots receiving zero P during the period of the trials. Labile P (P_{DGT}) was greater in the topsoils and subsoils of the TSP plot than the GMP plot reflecting differences in the solubility of the two fertilisers.

6.2 Introduction

Phosphorus (P) fertilisers are used in agriculture to sustain critical concentrations of plant-available P in soils in order to maintain crop production and yield (Johnston, *et al*., 2013; Poulton, *et al*., 2013). However, over-application of P fertilisers in excess of crop requirements is inefficient and results in the accumulation of residual P in the topsoil and an increased risk of leaching to the wider environment (Khan, *et al*., 2018). The demand on global stocks of phosphate rock, the main sources of P fertiliser is estimated to peak around 2030 and reserves could become low in the next 50 to 100 years (Cordell, *et al*., 2009). One strategy to reduce global demand on P fertilisers is to quantify the amount of residual P in soils and investigate methods to utilise the 'legacy' P stocks currently in soil systems in order to 'feed the crop' (Withers, *et al*., 2014). Utilising legacy P in soils would also have an additional benefit of reducing P pollution to river catchments (Haygarth, *et al*., 2014). This requires an understanding of labile phosphorus dynamics i.e. the ability of the soil to re-supply P to the soil solution through processes such as desorption from the solid phase following removal by crop uptake (Menezes-Blackburn, *et al*., 2016). Phosphorus fertiliser may be strongly adsorbed to Fe and Al oxides and/or precipitated as calcium phosphates which reduces the extent of P diffusion in soil and affects the lability and plant-availability of P (Degryse & McLaughlin, 2014). Plant-available P is usually estimated using soil P tests such as Olsen (Olsen, *et al*., 1954) or Modified Morgan (McIntosh, 1969 Ideally, these tests provide an indication of the capacity of the soil to provide sufficient P from the solid phase to meet plant demand. However, all 'available P extractions' take the form of a simple *quantity* of P in the soil (Pypers, *et al*., 2006). They do not provide any indication of speed of response, or of P concentration, immediately in contact with plant roots. Furthermore, traditional soil P tests may overestimate plant-available P by dissolving both labile and non-labile forms of P from the solid phase (Six, *et al*., 2012). Therefore, other tests which attempt to measure the *intensity* of P in the soil solution, such as phosphate extractable with dilute calcium nitrate or water may have greater validity. However, the limitation with such tests are that they do not provide information on the ability of the soil to re-supply P that is removed from solution by crop uptake. The Diffusive Gradients in Thin-Films Technique (DGT) is an alternative method which can be used to study the labile P species in soil (Zhang & Davison, 2015). This method is thought to mimic the uptake of nutrients by roots in soil, extracting the pool of labile P which is accessible to arable crops such as wheat (Mason, *et al*., 2013). In theory, DGT can provide information on P dynamics between soil solid and solution phases and the potential to resupply P to soil solution (Harper, *et al*., 1998).

The DGT method was originally developed to measure trace-metals in situ in water (Davison & Zhang, 1994) and was then used to quantify labile Cd, Cu, Fe and Mn in natural waters (Zhang & Davison, 1995) before being adapted for the measurement of P (Zhang, *et al*., 1998). Briefly, a plastic device with a window containing a filter membrane, diffusive gel and a ferrihydrite (Fe-oxide) binding gel is deployed on to a saturated soil surface which induces the diffusion of soil solution P through the device towards the Fe-oxide gel which acts as an infinite-sink for P (Menezes-Blackburn, *et al*., 2016). This depletes the P in the soil solution at the device window and creates a concentration gradient which then induces diffusive re-supply of P from soil solid-phases in order to maintain an equilibrium between the solid and solution phases (Harper, *et al*., 1998). Diffusion is the sole mechanism transporting P to the device and so by applying Fick's first law of diffusion (Zhang & Davison, 1995) the mass of P accumulated on the Fe-oxide gel (M) is used to calculate a time-averaged concentration (P_{DGT}) (Menezes-Blackburn, *et al*., 2016). In the situation where a solution containing a known concentration of P is well mixed, the ratio (R_{DGT}) of P_{DGT} to the solution P concentration (P_{Soln}) will be 1, indicating that the resupply of P to the device surface was rapid and sustained. Solution pH (pH 3 to 9) and increasing concentrations of chloride, sulfate, nitrate and bicarbonate have no effect on the ratio (R_{DGT}) of P_{DGT} to P_{Soln} in stirred solutions (Mason, *et al*., 2008). However, where diffusion is limited by the effects of tortuosity and adsorption to a solid phase, such as in a soil, the ratio of C_{DGT} to P_{soln} is between 0 and 1, providing information on the ability of the soil to resupply and buffer the soil solution P following removal (Harper, *et al*., 1998). Thus, the DGT method provides information on the *dynamics* of 'labile P' that is reversibly exchangeable between the soil solid and solution phases. The value of R_{DGT} where only diffusion of P from the pore water contributes to the resupply of P to the DGT device with no solid phase resupply (R_{diff}) can be calculated using the 'DGT induced fluxes in soils and sediments model' (DIFS) (Harper, *et al*., 2000; Menezes-Blackburn, *et al*., 2016). However, by simply comparing the ratio (R_{DGT}) of P_{DGT} to P_{Soln} across experimental treatments, factors that influence solution concentration at the interface of the DGT surface can be investigated. Finally, solid-solution equilibrium distribution coefficients (K_d) can also be determined using the DGT method (Degryse, *et al*., 2009). The soil K_d and the response time of the soil to depletion of soil solution P (T_c) can be estimated using the DIFS model (Lehto, *et al*., 2008) by deploying DGT devices at different times in the soil (DGT guide, 2003). However, a simple comparison of K_d values across experimental treatments using estimates of the labile solid phase pool (such as P_{Olsen} or $P_{MMorgan}$) against P_{DGT} (Menezes-Blackburn, *et al*., 2016) would provide some insights in to how the size of the exchangeable P pool changes depending on soil factors or experimental treatments. For example, at low pH it may be expected that much of the P associated with the solid-phase is adsorbed to Fe and Al oxide surfaces but

as the pH rises and P becomes more soluble in solution, P may become precipitated as calcium phosphates (Weng, *et al*., 2011). The desorption of P from Fe and Al oxides in response to a disturbance in the equilibrium with the soil solution may be slower than the dissolution of calcium phosphates which may be in a more dynamic equilibrium with the soil solution particularly between pH 6 and 6.5 where several calcium phosphates co-exit to control phosphate solubility (Linsday, 1979). This is particularly important for agricultural crops because pH 6 to 6.5 is the range considered optimum for phosphate acquisition (Goulding, 2016).

The DGT method could potentially be used to predict plant-available P in soil systems when plant uptake is limited by diffusion (Degryse, *et al*., 2009) and when the uptake flux of P by DGT and plants is similar (Zhang & Davison, 2015). In soils amended with both mineral and organic fertilisers, maize dry matter yield correlated best with DGT compared to Olsen extractable-P and anion exchange membrane-P (Six, *et al*., 2014). Mason, *et al*., (2010) showed that under a variety of field-based conditions, climatic conditions and soil types, DGT provided a more accurate prediction of wheat dry matter and grain response to P fertiliser use than traditional soil P extraction tests. The authors labelled soils with ^{32}P and found that much of the P in soil extracts was non-labile. Six, *et al*., (2012) also compared P measured by DGT to conventional soil extracts in addition to ^{33}P labelling in their study investigating P uptake by maize. They too, found that traditional soil P tests extracted significant amounts of both labile and non-labile (non-plant available) P and concluded that their DGT measurements sampled only P fractions that were accessible to plants. In contrast, Burkitt, *et al*., (2016) found pasture response to P was better predicted by traditional soils P tests compared to DGT because (they hypothesised) the soil P tests likely mimicked the action of perennial pasture roots to solubilise less labile forms of P. Thus, DGT did not fully account for P which could be accessed by crops. In temperate soils across Europe, no single test (such as DGT or Olsen) was superior to another in predicting the crop response to soil P (Nawara, *et al*., 2017). This was thought to be because the soils included in the study did not have high P retention strengths; the authors conceded that soils with high Fe, Al and Ca were under-represented. The exchange of P between soil solid and solution phases is hypothesised to be the main process in soil that controls plant-available P and further research is required in to the dynamic mechanisms controlling labile P in soils (Menezes-Blackburn, *et al*., 2016).

Improving our understanding of the soil mechanisms affecting labile P dynamics would provide meaningful information on why there should be correlations between P_{DGT} and plant uptake of P

(Degryse, *et al*., 2009). For example, Menezes-Blackburn, *et al*., (2016) did not observe a positive correlation between soil pH and P desorption or mobility indicators, despite their expectations given that P speciation and solubility in solution is mainly controlled by pH (Lindsay. 1979). However, Menezes-Blackburn, *et al*., (2016) noted that experimental conditions did not force soil pH changes which could then be used to investigate the effect. Six, *et al*. (2014) investigated DGT as a predictor for plant-available P in soils amended with organic matter, TSP fertilisers and plant residues. They concluded that further research was needed to elucidate the effect that soil pH had on correlations between plant relative yields and P_{DGT}. Thus, the long-term pH Rotation experiment in Woodlands Field, which consists of a pH gradient of 4.5 to 7.5 (0.5-unit increments), provides an invaluable opportunity to apply the DGT technique in the investigation of the lability of P, and the distribution of P between the soil solid and solution phases as a function of soil pH. In addition, the Old Rotation could provide further insights into the effect of long-term fertiliser management on the lability of P, particularly as these plots have generally low P status. The DGT method would allow the lability of P stocks in low P status (Old Rotation) and high P status plots (pH Rotation) to be evaluated. Long-term experiments with known management and fertiliser use histories, and thus known P balances, can be used to study the dynamics of P in agricultural soil profiles (Johnston & Poulton, 2018). it would also be useful to know more about labile phosphorus dynamics in *subsoils* as well as topsoils, to gain an insight in to the long-term factors that influence the distribution of labile P between the solid and solution phases throughout the soil profile, should crops access and supplement requirements using subsoil P reserves. Deficiencies of P in the subsoils are cited as one of the main challenges for deep rooting crops (Lynch & Wojciechowski, 2015). However, subsoils can have large P sorption capacities and may intercept and retain (or release) P leaching from topsoils on soil surfaces (Andersson, *et al*., 2013). Thus, the equilibrium and dynamics of labile P in the subsoil between soil surfaces and the solution phase can be investigated using the DGT method to show whether subsoil solution P can be replenished by surface P, following removal by crop uptake. Subsoils may contain up to 70% of crop nutrient requirements (Kautz, *et al*., 2013) and so research in to subsoil lability for crops will provide further insight in to the potential of the subsoil to contribute to crop P demands.

6.2.1 Aims and Objectives

The aims of this chapter were (i) to investigate factors controlling the lability of P in the topsoils and subsoils of the Woodland's Field long-term experiments using the Diffusive Gradients in Thin-Films (DGT) Technique and (ii) assess DGT against more traditional extraction methods. The hypothesis was that topsoil and subsoil P is more labile in plots receiving soluble P fertiliser (TSP) compared to insoluble P fertiliser (GMP). Furthermore, the lability and resupply of P from soil surfaces to solution is controlled by pH and underlying solubility mechanisms. For example, strong adsorption responsible for controlling P dynamics in acidic soils decreases P lability whereas dissolution of calcium phosphates results in increased lability. The experimental objectives are listed below.

1. Determine the DGT parameters (P_{DGT} and R_{DGT}) in topsoils and subsoils of the Old Rotation and pH Rotation.
2. Determine the distribution coefficient (K_d) of labile P between the solid and solution phase throughout the soil profile in both long-term experiments using P_{Olsen} and $P_{MMorgan}$ as 'capacity terms' (numerators in K_d) and P_{DGT} as the 'intensity term' (denominator).

6.3 Materials and Methods

6.3.1 Sample Site, Trial Description, Sample Selection and Preparation

The full details of the long-term experiments used in this study are described in **Chapter 2 Materials and Methods** which outlines the sample site and description of the trials (**section 2.1**), trial management (**section 2.1.1**), soil sampling and preparation (**section 2.2**) and various soil analysis such as soil pH (**section 2.4**), total element analysis (**section 2.6**), Olsen and Modified Morgan phosphate extractions (**section 2.7**) and the colorimetric determination of P (**section 2.7.3**). Briefly for this study, air-dried, sieved (< 2 mm) topsoil and subsoil samples from all three auger borings were selected from all seven target pH plots (pH 4.5 to 7.5 in 0.5 unit increments) that had been under spring oats (pH Rotation) and also from all four fertiliser treatment plots (NK with GMP, NK with TSP, NK without P and zero fertiliser) that had been under grass year 3 (Old Rotation). Three topsoil and subsoil samples from the uncultivated field surrounding the trials (the Field) were also selected. Samples from four plots, but only one soil layer (i.e. topsoil or subsoil) were selected to undergo additional DGT deployment and were analysed in triplicate to determine the repeatability of the DGT measurement (i.e. 12 individual soil samples, 3 DGT deployments per sample, 24 total repeat deployments). These samples covered a range of P_{Olsen} from 5.87 to 79.3 mg kg^{-1} assuming that the concentration of P accumulated by the DGT device (P_{DGT}) would increase with P_{Olsen} thus providing some indication of the repeatability over a range of P_{DGT}.

6.3.2 Diffusive Gradients in Thin-Films Technique

6.3.2.1 Water Holding Capacity

The soil water holding capacity (WHC) was pre-determined prior to the experiment. Air dried, sieved (< 2mm) soil (c. 10 g) was weighed into a pre-weighed wetted filter paper and funnel. The soil was continuously wetted with de-ionised water, until saturated, then left to drain. The weight of water in the soil was then determined by subtracting the weight of the wet filter paper and funnel from the combined weight of the wet funnel, filter paper and soil. This was then used to calculate the water holding capacity (WHC) (g g^{-1}) of each soil sample by dividing the weight of water in the soil by the dry soil weight. The moisture content at 50% and 100% WHC for 40 g of soil was determined for each sample individually.

6.3.2.2 DGT Deployment and Temperature Control

Soil samples (c. 40 g) were wetted to an average WHC of 47.1% (SD = 4.93%, SEM = 0.503%, *n* = 96), mixed, and left to equilibrate for 24 hr at room temperature. Samples were then wetted to an average WHC of 97.8% (SD = 7.05%, SE = 0.72%, *n* = 96), mixed, and left for a further 24 hr. Sub-samples of the Milli-Q water used to wet the soils to WHC were retained for P analysis by ICP-MS. The DGT devices were removed from the fridge (4^{o}C) at least 6 hr before the beginning of the experiment and stored at room temperature. The wetted soil was then mixed thoroughly into a paste before filling a petri dish (50 mm diameter x 20 mm height) to the brim, ensuring no air gaps by tapping the petri dish on the bench top before smoothing the soil surface. The DGT device was then removed from its individual plastic bag using clean gloves and the deployment window was gently rinsed with Milli-Q water taking care not to touch the membrane. Some of the excess soil paste was smeared on to the device window which was then gently pushed and twisted on to the soil surface, ensuring full contact. The time of contact with the soil paste ('the deployment') was recorded to the nearest minute. The petri dish was immediately placed in a plastic box with wet paper inside to maintain 100% humidity in the atmosphere so that the soil surface did not dry out. The plastic box was stored in a temperature-controlled incubator with a target temperature of 20^{o}C. To obtain an accurate record of the temperature inside the incubator, a Tinytag™ Data Logger was placed in a plastic container inside the incubator next to the box containing the samples. The temperature was continuously recorded every 5 minutes for the duration of the entire experiment without interruption; the data showed an average temperature of 20.037^{o}C (± SD = 0.451 ^{o}C, ± SE = 0.014 ^{o}C, n = 1101 measurements).

6.3.2.3 Recovery of the Fe-oxide Gel

The DGT device was removed from the soil surface (c. 24 hours) and the time was recorded to the nearest minute. Adhering soil particles were removed from the device window with a steady stream of Milli-Q water and the surface was gently blotted with tissue to remove excess water. The seal of the device cap was broken with a screwdriver. The filter and diffusive gel layers were removed and discarded using clean plastic tweezers before recovering the orange Fe-oxide gel, which was transferred to a clean 8 mL tube containing 5 mL of 0.25 M H_2SO_4 eluent and left to dissolve (c. 24 hours). Sub-samples of the 0.25 M H_2SO_4 eluent were retained for P analysis by ICP-MS. Between each sample the tweezers were rinsed with Milli-Q water and clean 0.25 M H_2SO_4 and then dried to prevent cross contamination between samples. Background concentrations of P on the Fe-oxide gels were determined on 3 unused DGT

devices, treated in the same way as deployed sample gels. After 24 hours the orange Fe-oxide had dissolved in the eluent to leave a clear and colourless gel behind, which was transferred to a clean 8 mL tube for further elution if required. The 5 mL eluent for the samples, the 3 DGT Fe-oxide gel 'blanks', the sub-samples of 0.25 M H_2SO_4 and the Milli-Q sub-samples from the WHC step were syringe-filtered (0.22 µm, PES membrane) into clean 8 mL tubes for analysis of P.

6.3.2.4 Determining the Concentration of P in the Fe-oxide Gels (Ce)

The concentration of P in the eluent of the sample Fe-oxide gels was measured by colorimetry (see **section 2.7.3**) and by ICP-MS (see **section 2.6.3**). The colorimetric determination of molybdate-reactive P was not successful despite the method being adapted to a reduced total volume (6.25 mL) because sample P was non-detectable, and the P standard range was non-linear. The ICP-MS analysis was therefore used to determine the concentration of P (µg mL^{-1}) that had accumulated on the DGT device (Ce) for each sample (see **Equation 6.1**, next **section 6.3.3**). The sample eluent (2.5 mL) was diluted with 3 mL of Milli-Q water. Calibration standards containing 5, 10 and 20 mg L^{-1} P in 0.125 M H_2SO_4 (containing 5 ppb Rh as the internal standard) showed total P recoveries of 97.7%, 96.7% and 95.7% respectively at the beginning of the analysis, and 93.8%, 93.6% and 91.6% respectively at the end. There was a consistent 10% drift in the repeated P calibration standard towards the end of the analysis which was not corrected by the Rh internal standard, which was comparable to levels of drift normally found in P_{Total} analysis on the ICP-MS in 2% HNO_3 which is acceptable. Nine operational blanks were analysed: 3 sub-samples of Milli-Q used to saturate the soils to water holding capacity, 3 sub-samples of the 0.25 M H_2SO_4 eluent and finally 3 sub-samples of the 'blank' DGT Fe-oxide gel eluents (0.25 M H_2SO_4). The blanks returned negligible concentrations of P.

The total P determined by ICP-MS may result in an overestimation of inorganic P on the Fe-oxide gels if organic P species had also accumulated on the gel (van Moorleghem, *et al*., 2011). However, other studies have used ICP-MS as the main technique for analysing P in DGT (Nawara, *et al*., 2017). It is recommended that ICP-MS determined P concentrations are not used to calculate because organic P compounds have their own unique diffusive coefficients in the DGT device (Menezes-Blackburn, *et al*., 2016). The difference between ICP-MS and colorimetric determined P is used to estimate the amount of organic P that was bound to the gel and it could be between 6.7% and 60.3% of the total P (Menezes-Blackburn, *et al*., 2016). Therefore, in this study, the use of the ICP-MS data as the only measure of P must be treated with caution, bearing in mind the potential effect of organic P on the results.

6.3.3 Calculating the Concentration of Phosphate-P Measured by DGT (P_{DGT})

The mass of P in the Fe-oxide gel (M) was calculated (µg) according to **Equation 6.1**:

$$M = \frac{Ce\,.\,(V_{eluent} + V_{gel})}{fe} \qquad \textit{Equation 6.1}$$

where Ce is the measured concentration of P in the 0.25 M H_2SO_4 elution solution (µg L^{-1}) determined by ICP-MS, V_{eluent} is the volume of the 0.25 M H_2SO_4 solution which elutes the Fe-oxide gel (5 mL), V_{gel} is the volume of the Fe-oxide gel based on a window size of 3.14 cm^2 and a gel thickness of 0.06 cm (0.1884 mL) and *fe* is the elution factor for P, which is 1.

The concentration of P measured by the DGT device (P_{DGT}) (normally denoted as C_{DGT} in the literature) was calculated using **Equation 6.2** as seen in Zhang & Davison, (1995):

$$P_{DGT} = \frac{M.\Delta g}{(D.t.A)} \qquad \textit{Equation 6.2}$$

where Δg (0.092 cm) is the thickness of the diffusive gel (0.0780 cm) plus the thickness of the filter membrane (0.0140 cm), D is the diffusion coefficient of P in the diffusive layer at the average temperature (20.0^oC) throughout the experiment which is 5.27 x 10^{-6} cm^2 sec^{-1} (DGT guide, 2003), t is the deployment time in seconds, and A is the device window exposure area (3.14 cm^2).

6.3.4 Equilibrium Distribution Coefficient Between Solid and Solution phases (K_d)

If it is assumed that P_{Olsen} and $P_{MMorgan}$ (mg kg^{-1}) are estimates of labile P in the solid phase, then the distribution coefficient (K_d) of P between the solid and solution phase (mL g^{-1}) can be calculated using **Equation 6.3** or **Equation 6.4** (Menezes-Blackburn, *et al*., 2016):

$$K_{d(Olsen)} = \frac{P_{Olsen}}{P_{DGT}} \qquad \textit{Equation 6.3}$$

$$K_{d(MMorgan)} = \frac{P_{MMorgan}}{P_{DGT}} \qquad \textit{Equation 6.4}$$

6.3.5 Buffering Capacity (R_{DGT})

The concentration of P in the soil solution (P_{Soln}) measured by colorimetry ($P_{Soln\text{-}Col}$) and ICP-MS ($P_{Soln\text{-}ICP}$) from **Chapter 5** were used to investigate the extent to which P_{DGT} was sustained by the concentration in the soil solution alone. The application of **Equation 6.5** gives a ratio (R_{DGT}) which indicates the buffering capacity and contribution of the solid phase to maintain the dynamic with the P in the solution at the interface between the soil and DGT device (Harper, *et al*., 1998; Menezes-Blackburn, *et al*., 2016):

$$\mathrm{R_{DGT}} = \frac{\mathrm{P_{DGT}}}{\mathrm{P_{Soln}}}, \;\; 0 < \mathrm{R_{DGT}} < 1 \qquad \textit{Equation 6.5}$$

The interpretation of R_{DGT} is summarised (as follows) from the DGT Guide (2003, p. 36) supplied by Hao Zhang: When $R_{DGT} > 0.95$ the re-supply of P in the soil solution at the DGT device window is sustained by the bulk soil solution. This can be because the rate of resupply from the solid phase is fast compared to the rate at which the DGT removes P from solution and thus indicates that the solid phase has a large enough buffering capacity to maintain the soil pore water P following removal. When R_{DGT} is closer to 0, the soil pore water P has been depleted and there is no resupply of P from the solid phase and it indicates that the major factor controlling P in soil solution is the resupply from solid phases. Normally R_{DGT} is between 0 and 1, indicating the relative ability of the solid-phase to resupply P to the solution-phase following removal of P by the DGT device. The theoretical value of 1 cannot be achieved because an instant and infinite supply of P is required which is not possible.

6.4 Results and Discussion

6.4.1 Repeatability of the DGT Deployment

The repeatability of the DGT deployment for the 12 soil samples is shown in **Figure 6.1**. There were 24 re-deployments in total, but three Fe-oxide gels had to be discarded due to contamination because soil had accessed the device window and come into direct contact with the Fe-oxide gel. This could be because the diffusive layer at the device window had dried out during storage prior to deployment. The second and third deployments both showed strong agreement with the first deployment: slopes = 0.99 and 0.97 respectively (**Figure 6.1**). There was better agreement at low P concentrations and increased scatter when P concentrations were > 80 µg L^{-1}. Overall the repeatability was acceptable however the 'gold-standard' would have been to run all soil samples in triplicate DGT deployments. Instead, three replicate soil samples per treatment plot were analysed to account for variation in the plot.

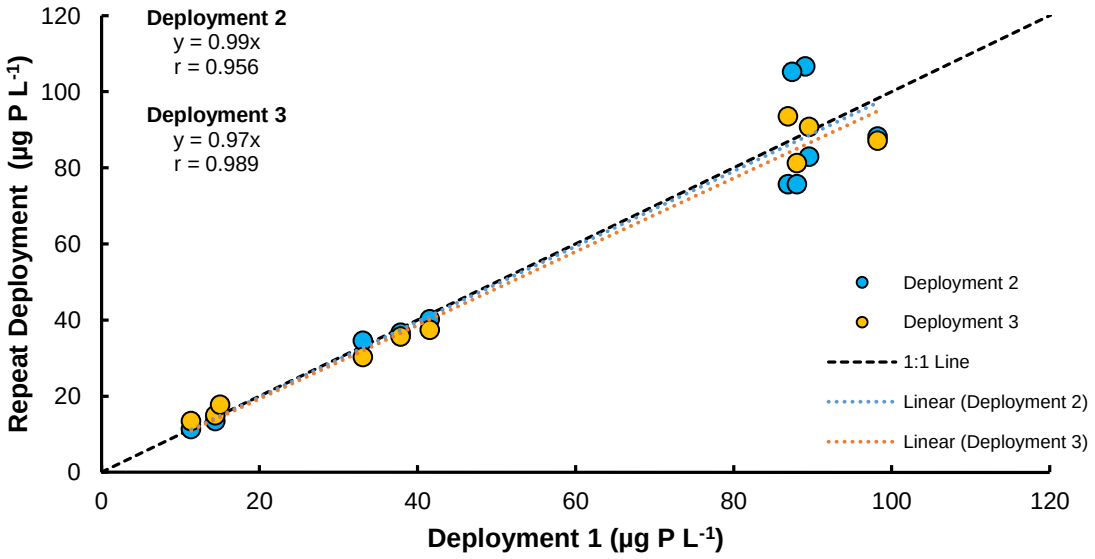


Figure 6.1. Agreement between P concentrations for repeated DGT deployments compared to a 1:1 (broken) line; intercepts are forced through zero.

6.4.2 Relationships Between P_{DGT}, P_{Total} and Soil P Extractions

P_{Total} vs P_{DGT}

The relationship between P_{Total} and P_{DGT} in the topsoils and subsoils of the Field, pH Rotation and the Old Rotation is shown in **Figure 6.2**. Overall P_{DGT} appeared to positively correlate with P_{Total} across the six datasets. However, a subset of data from the pH Rotation topsoils (red circles) displayed a considerable range of P_{DGT} from 57.1 and 111 µg L^{-1} over a very restricted range of P_{Total} between 1940 to 2160 mg kg^{-1}. This suggested that P_{DGT} was not simply a function of P_{Total} in these plots but was related to soil pH control. There was a strong, positive correlation between P_{DGT} and P_{Total} in the subsoils of the pH Rotation ($r = 0.695$) with a spread of P_{DGT} values (10.9 to 78.1 µg L^{-1}) across the subsoil P_{Total} range (923 to 1780 mg kg^{-1}) indicating that there was a more consistent relationship between P_{Total} and P_{DGT} in the subsoils. The scatter in P_{DGT} for the Old Rotation topsoils (25.8 to 67.6 µg L^{-1}), which were positively correlated with P_{Total} ($r = 0.612$), reflects differences in P fertiliser management (highly soluble TSP, insoluble GMP or no P fertiliser applied). The Old Rotation subsoils showed a narrow P_{DGT} range (11.3 to 24.9 µg L^{-1}), with a positive correlation with P_{Total} ($r = 0.541$) and less scatter in the data compared to P_{DGT} in the topsoils. The P_{DGT} in the Field soil profile was on average 42.9 (± SD 9.57 µg L^{-1}, $n = 9$) and was within the P_{Total} range of 1270 to 1450 mg kg^{-1}. There was a positive correlation between P_{DGT} and P_{Total} in the topsoils ($r = 0.370$) and a strong, positive correlation in the subsoils ($r = 0.981$). If the Field P_{DGT} data is taken to be the native P_{DGT} in the soil (assuming no effect caused by their proximity to the trials) then the experimental treatments have resulted in changes to the P_{DGT} in the pH Rotation and Old Rotation and are worth investigating further.

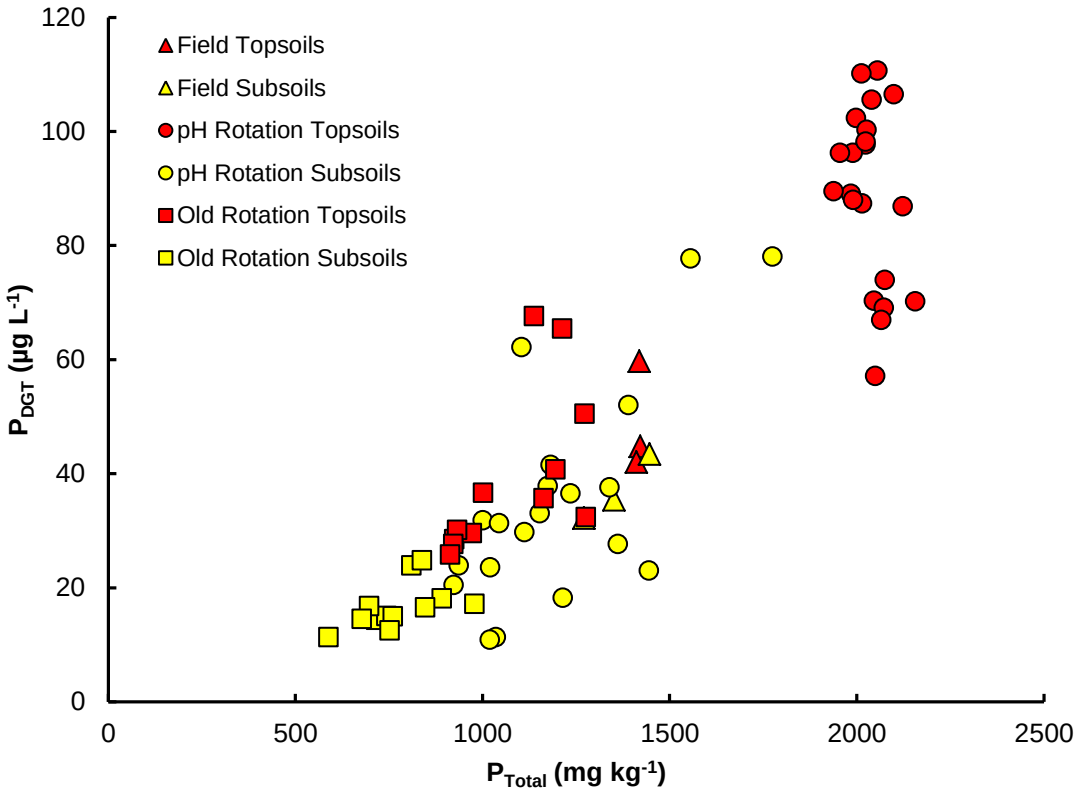


Figure 6.2. Relationships between P_{Total} and P_{DGT} in the Field topsoils (r = 0.370) and subsoil (r = 0.981), pH Rotation topsoils (r = -0.340) and subsoils (r = 0.695) and the Old Rotation topsoils (r = 0.612) and subsoils (r = 0.541). One outlier with suspected P_{DGT} contamination is excluded from the pH Rotation subsoil data.

P_{DGT} vs P_{Olsen}

The relationships between P_{DGT} and P_{Olsen} for the soil samples in the topsoils and subsoils of the Field, pH Rotation and Old Rotation are shown in **Figure 6.3**. There were mostly positive correlations between P_{DGT} and P_{Olsen} across the entire dataset suggesting that P_{Olsen} increased with rising P_{DGT}, particularly in the Old Rotation topsoils (r = 0.911) and subsoils (r = 0.691). There was a weak, positive correlation in the subsoils of the Field (r = 0.263) but a strong, negative correlation in the topsoils (r = -0.997). There was considerable variation between the subsets of samples, such as topsoils and subsoils, which suggested other influences on P_{DGT} such as pH control and fertiliser management strategy. In particular, the scatter in the pH Rotation topsoils for P_{Olsen} suggests pH is an important factor influencing the lability and resupply of P to the soil solution. A strong, negative correlation was observed between P_{DGT} and P_{Olsen} in the pH Rotation topsoils (r = -0.748) and a relatively weak, positive correlation in the subsoils (r = 0.302). Burkitt, *et al*., (2016) found significant, positive correlations between P_{Olsen} (4 to 32 mg kg^{-1}) and P_{DGT} (6 to 1565 µg L^{-1}) in 25 sites treated with mineral fertilisers over a narrow soil pH range of pH 4 to 5. The soils in Burkitt, *et al*., (2016) covered a range of soil textures across Australia which suggested that soil pH

may not be the only influence on the lability of P as their values of P_{Olsen} were relatively small, and P_{DGT} relatively large, compared to the data presented in **Figure 6.3**.

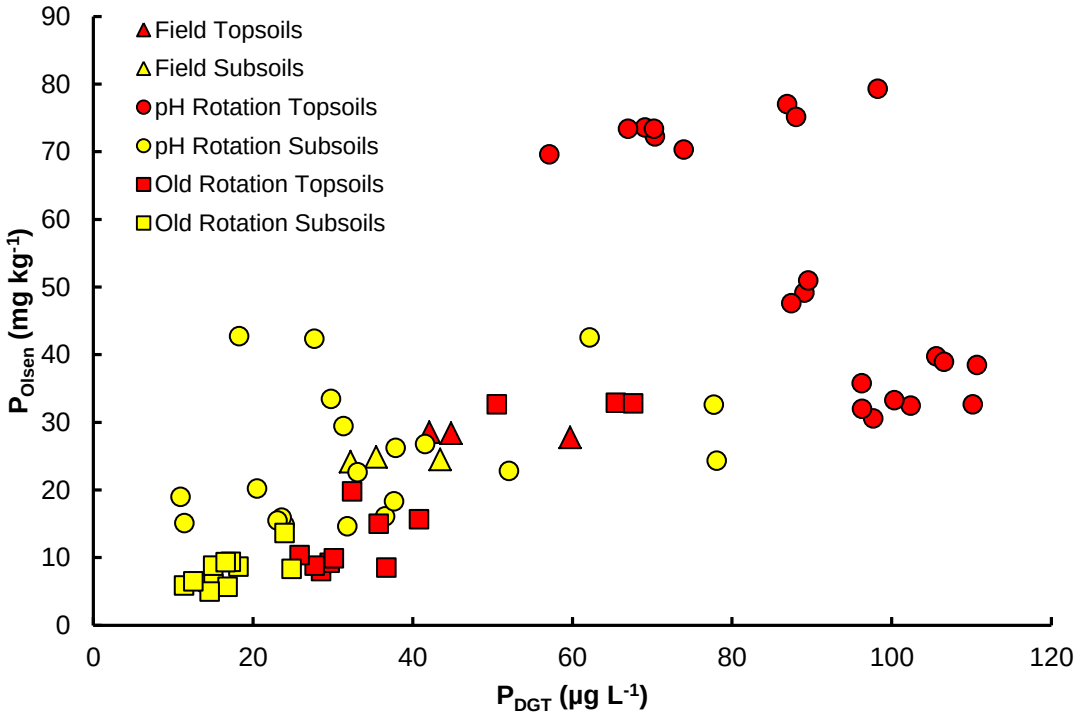


Figure 6.3. Relationship between P_{DGT} and P_{Olsen} in the Field topsoils (r = -0.997) and subsoils (r = 0.263), pH Rotation topsoils (r = -0.748) and subsoils (r = 0.302) and the Old Rotation topsoils (r = 0.911) and subsoils (r = 0.691).

$P_{MMorgan}$ vs P_{DGT}

The relationships between P_{DGT} and $P_{MMorgan}$ for the soil samples in the topsoils and subsoils of the Field, pH Rotation and Old Rotation are shown in **Figure 6.4**. In contrast to the P_{Olsen} data, the correlation between P_{DGT} and $P_{MMorgan}$ in the pH Rotation topsoils was weak and negative (r = -0.024) and strong and positive in the subsoils (r = 0.593). This suggests there are differences between the two extraction methods in their assessments of available P in the pH Rotation, which appeared to be significantly influenced by soil pH management, due to the large scatter in the data throughout the soil profile. The correlations between P_{DGT} and $P_{MMorgan}$ in the (uncultivated) Field were positive in both topsoils (r = 0.232) and subsoils (r = 0.433). Finally, strong, positive correlations were found between P_{DGT} and $P_{MMorgan}$ in the topsoils (r = 0.840) and subsoils (r = 0.700) of the Old Rotation. These strong, positive correlations throughout the soil profile between P_{DGT} and $P_{MMorgan}$ in the Old Rotation suggest that the relationship between P_{DGT} and $P_{MMorgan}$ is positively affected by the restriction of P fertiliser, or the application of P as TSP and GMP.

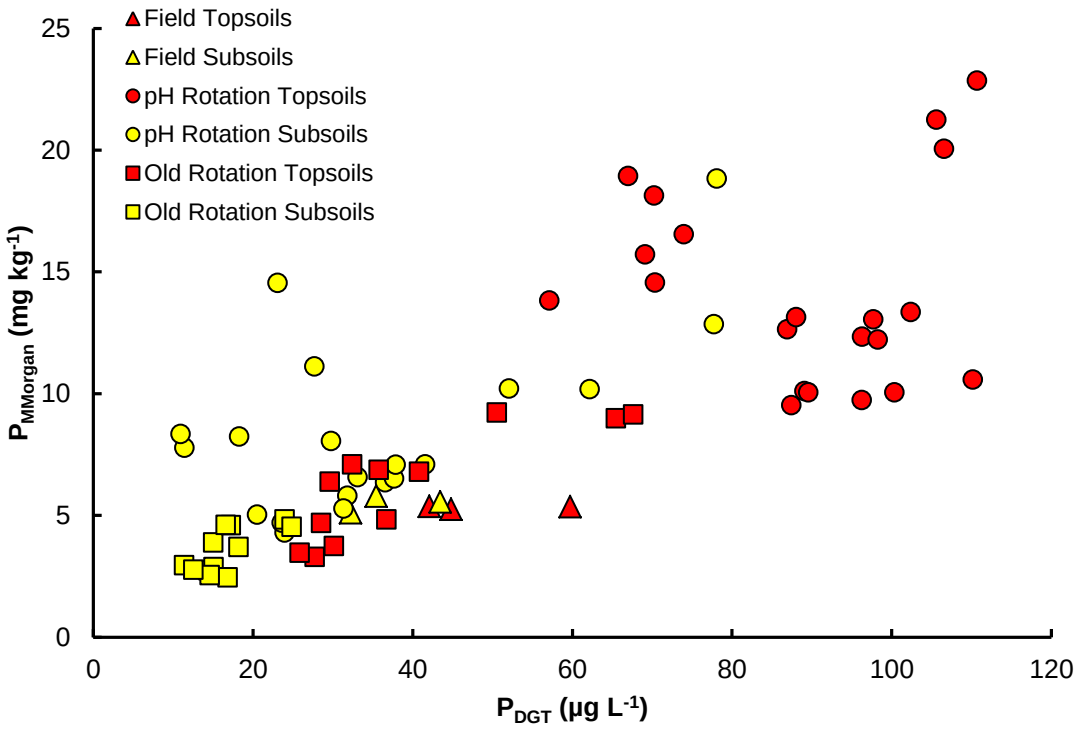


Figure 6.4. Relationship between P_{DGT} and $P_{MMorgan}$ in the Field topsoils (r = 0.232) and subsoils (r = 0.433), pH Rotation topsoils (r = -0.024) and subsoils (r = 0.593) and the Old Rotation topsoils (r = 0.840) and subsoils (r = 0.700).

The target P_{Olsen} in agricultural soils is 16 to 25 mg kg^{-1} (Index is '2A/B') (AHDB, 2017) and the target $P_{MMorgan}$ is 4.4 to 13.4 mg kg^{-1} (designated 'M±') (Edwards, *et al*., 2016). Most samples shown in **Figure 6.3** and **Figure 6.4** were within, or above, the optimum P_{Olsen} and $P_{MMorgan}$ target ranges for arable crops in rotations, which would suggest that the soils contained at least sufficient quantities of plant-available P. However, it was clear that while the soil had a large capacity of 'plant-available P' as observed in relatively high P_{Olsen} and $P_{MMorgan}$, the lability of the solid phase P as measured by the DGT method varied. This may highlight the main flaw in traditional soil P tests such as Olsen and Modified Morgan's as estimates of the 'capacity' of plant-available P on the solid-phase because not all the soil P extracted may be labile and accessible to crops during the course of a growing season. Phosphate dissolved in the Olsen and Morgan extractants may not be able to respond kinetically to simple depletion of P in soil solution caused by plant uptake or adsorption on to a DGT gel. These results suggested that there were significant factors influencing the ability of the soil to resupply P to solution measured as P_{DGT} such as differences due to soil pH control, fertiliser management strategy and soil depth (topsoil or subsoil).

6.4.3 Relationship Between Topsoil and Subsoil P_{DGT}

The relationships between topsoil and subsoil P_{DGT} in the Field, pH Rotation and Old Rotation are shown in **Figure 6.5**. One soil core was excluded from the pH Rotation due to suspected contamination during the assay of P_{DGT} for the subsoil. There was a significant, strong correlation between topsoil and subsoil P_{DGT} in the Field (r = 0.991) which suggested that the field had reached a steady-state, with comparable P_{DGT} values in the topsoils (48.9 µg L^{-1}) and subsoils (37.0 µg L^{-1}). In contrast, P_{DGT} in the topsoil exceeded subsoil values within both Rotations due to treatment effects including P fertiliser use in most topsoils. The positive correlation between topsoil and subsoil P_{DGT} in the pH Rotation (r = 0.451) was similar to that in the Old Rotation (r = 0.424). Topsoil P_{DGT} in the Old Rotation ranged from 25.8 to 67.6 µg L^{-1} - similar to values of P_{DGT} the Field topsoil. However, P_{DGT} in the Old Rotation subsoils ranged from 12.5 to 24.9 µg L^{-1} which fell below values of P_{DGT} the Field subsoils; this suggests depletion of subsoil P_{DGT} which is not renewed in the Old Rotation compared to the Field. In the pH Rotation, topsoil P_{DGT} values (57.1 to 110 µg L^{-1}) were greater than those in the Field, reflecting the positive balance of P fertiliser inputs in the pH plot topsoils. Subsoil P_{DGT} values (10.9 to 78.1 µg L^{-1}) covered a greater range than those in the Field suggesting a pH-dependent relationship between topsoil and subsoil P_{DGT}.

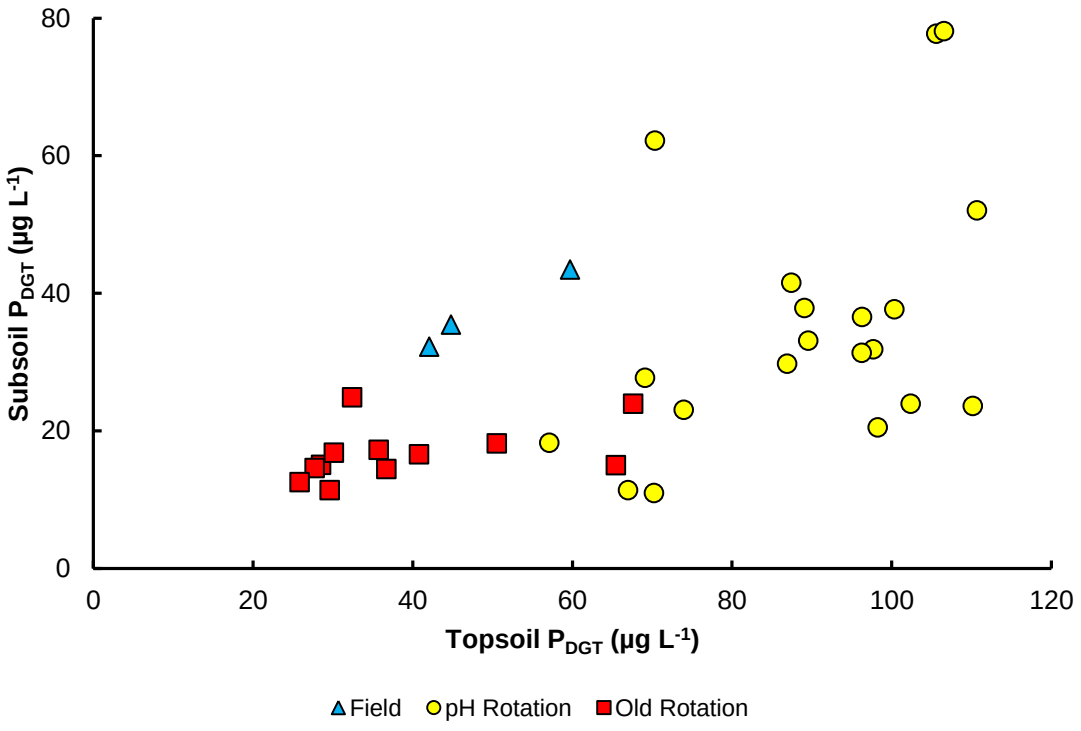


Figure 6.5. Relationship between topsoil and subsoil P_{DGT} in the Field (r = 0.991), pH Rotation (r = 0.451) and Old Rotation (r = 0.424). One soil core with suspected P_{DGT} contamination in the pH Rotation subsoil was excluded.

6.4.4 Relationship Between P_{DGT} and Soil Solution P

The relationships between P_{DGT} and soil solution P concentration (P_{Soln}) for the topsoils and subsoils of the Field, pH Rotation and the Old Rotation, measured either by (i) colorimetry ($P_{Soln\text{-}Col}$) or (ii) ICP-MS ($P_{Soln\text{-}ICP}$), are shown in **Figure 6.6** and **Figure 6.7** and respectively. The two measures of P_{Soln} are taken from **Chapter 5**; $P_{Soln\text{-}Col}$ may underestimate the inorganic P_{Soln} due to analytical limitations caused by low P concentrations. Values of $P_{Soln\text{-}ICP}$ may overestimate inorganic P_{Soln} because the total P in the solution is assayed and so dissolved organic phosphorus may have contributed to the results. Furthermore, P_{DGT} in these samples may also include labile organic P species which have been collected by the DGT device. Positive correlations are expected between P_{DGT} and P_{Soln} because P_{DGT} results from diffusion of solution P towards the device sustained by re-supply of soil solution P by desorption of P from labile solid phase fractions.

Generally, P_{DGT} increased linearly with $P_{Soln\text{-}Col}$ (**Figure 6.6**) with strong, positive correlations for most of the datasets. Correlation coefficients (r) ranged from 0.550 (Old Rotation Topsoils) to 0.926 (Field Subsoils), with an average r value of 0.680 across the five data subsets. The values for the Field P_{DGT} and $P_{Soln\text{-}Col}$ topsoils and subsoils fell within the same range as most of the other data subsets (< 80 µg L^{-1} for P_{DGT} and < 40 µg L^{-1} for $P_{Soln\text{-}Col}$) except for the pH Rotation topsoils which showed high levels of P_{DGT} (57.1 to 110 µg L^{-1}) and $P_{Soln\text{-}Col}$ (45.5 to 97.0 µg L^{-1}), suggesting a strong effect of pH on the labile P species in the topsoils. Relationships between P_{DGT} and $P_{Soln\text{-}ICP}$ (**Figure 6.7**) showed mostly positive correlations. In the Old Rotation, there was a strong, positive correlation between P_{DGT} and $P_{Soln\text{-}ICP}$ in the topsoil (r = 0.949) and a weak, positive correlation in the subsoil (r = 0.285) which may reflect the direct application of P fertilisers to the topsoils in half of the plots resulting in a relatively higher solution P in the topsoil, and the lack of replenishment of solution and labile P in the subsoils. There was a strong, positive correlation in the Field subsoil (r = 0.920) but a strong, negative correlation in the topsoil (r = -0.820). Finally, there was no correlation between P_{DGT} and $P_{Soln\text{-}ICP}$ in the pH Rotation topsoil (r = 0.010) but a strong, positive correlation in the subsoil (r = 0.838) which suggests there may be a pH effect on subsoil solution and labile P, which is not seen in the topsoil. As some of the P was un-detectable in the $P_{Soln\text{-}Col}$ analysis, the $P_{Soln\text{-}ICP}$ results may be a better indicator of P_{Soln} notwithstanding the presence of organic P which may also be collected by the DGT device (Menezes-Blackburn, *et al*., 2016).

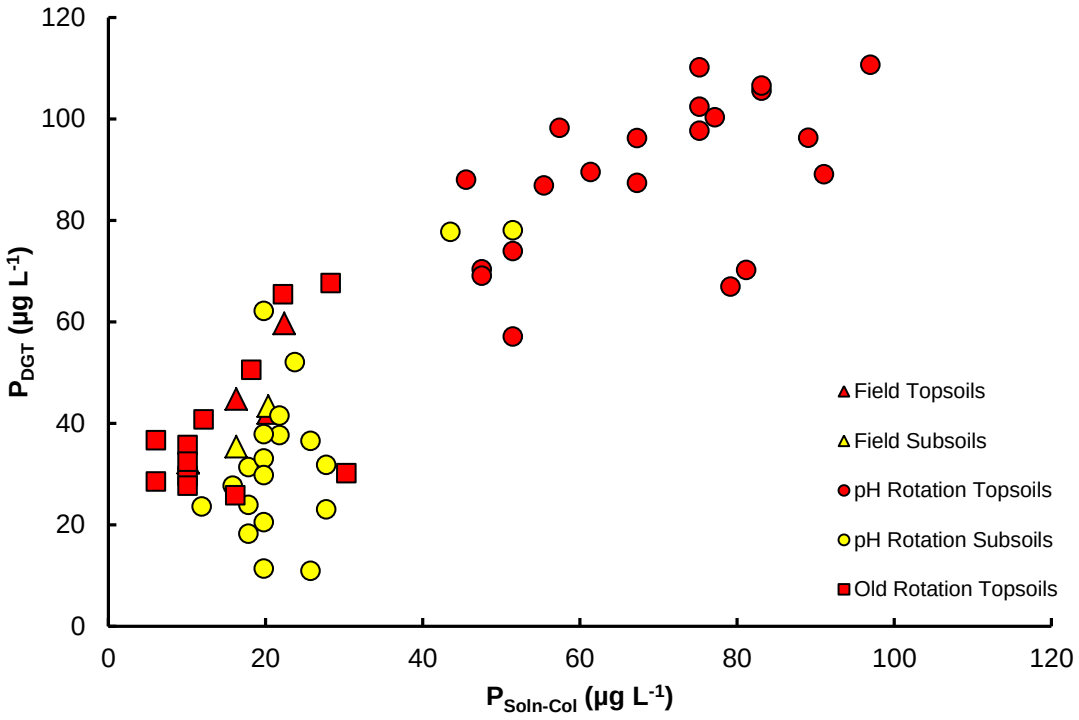


Figure 6.6. Relationship between P_{DGT} and $P_{Soln-CoI}$ in Field topsoils (r = 0.653) and subsoils (r = 0.936), pH Rotation topsoils (r = 0.552) and subsoils (r = 0.709) and Old Rotation topsoils (r = 0.550) except (i) one outlier in the pH Rotation subsoils and (ii) Old Rotation subsoils have been excluded due to un-detectable $P_{Soln-CoI}$.

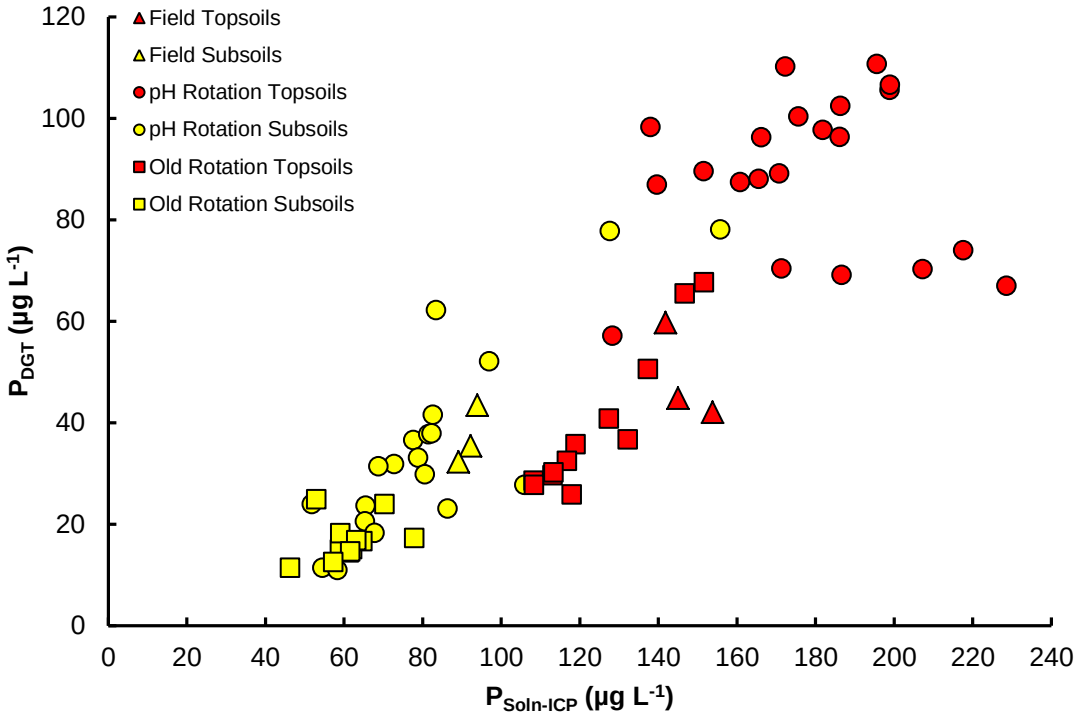


Figure 6.7. Relationship between P_{DGT} and $P_{Soln-ICP}$ in the Field topsoils (r = -0.801) and subsoils (r = 0.920), pH Rotation topsoils (r = 0.010) and subsoils (r = 0.838) and the Old Rotation topsoils (r = 0.949) and subsoils (r = 0.285). One outlier has been excluded.

6.4.5 Effect of Soil pH Management on P_{DGT} in the pH Rotation

Topsoil

The relationship between the measured soil pH values and P_{DGT} in the topsoil and subsoil of the pH Rotation is shown in **Figure 6.8**. Topsoil P_{DGT} increased linearly with soil pH values (r = 0.904) from 70.4 µg L^{-1} (± SEM 2.05 µg L^{-1}) at pH 4.5 to 108 µg L^{-1} (± SEM 1.58 µg L^{-1}) at pH 7.5. Relative to the Field topsoil, all pH plots were elevated in labile P_{DGT} likely due to the application of TSP fertilisers. In the topsoil, P may be strongly bound to Fe and Al oxides at pH 4.5, reducing the lability of P. However, as pH increases towards pH 6 and the strength of adsorption between P and oxide surfaces decreases due to an increase in negative surfaces charges and greater competition with organic matter further weakening the adsorption strength for phosphate (Weng, *et al*., 2011), labile P increases in solution and so may explain the rise in topsoil P_{DGT}. The continued rise in topsoil P_{DGT} above pH 6 may indicate that the concentration of P in soil solution was greater possibly due to increased solubility of P from calcium phosphates or it may indicate a greater rate of dissolution in response to depletion of the solution phase. The resupply of P to the DGT device from the solid phase may be maintained by more rapid processes at high pH, such as dissolution, or the diffusion coefficient may be higher due to weaker adsorption. The linear increase in the topsoil P_{DGT} from pH 4.5 to 7.5 is in contrast to the trends in P_{Olsen} and $P_{MMorgan}$ (**Chapter 4**) which show that 'plant-available P' estimates are greatest at pH 4.5 and decline with pH to a minimum at pH 6 before showing rising towards pH 7.5. This suggests that, although the soil has a large quantity of plant-available P adsorbed on the solid-phase at pH 4.5, it is relatively slow to react (desorb) following depletion of P in solution by crop uptake. However, it should be acknowledged that the short contact period of 24 hours may not reflect long-term uptake by crops and may be unreliable for predicting quantity of P which can be taken up during the period of crop growth (Santner, *et al*., 2015).

Subsoil

Subsoil P_{DGT} also increased with soil pH (r = 0.687), from a minimum of 15.1 µg L^{-1} (± SEM 4.02 µg L^{-1}) at pH 4.5 to a maximum P_{DGT} of 69.3 µg L^{-1} (± SEM 8.72 µg L^{-1}) at pH 7.5, displaying a relatively flat trend between pH 5.2 and 7.0. The variation in subsoil P_{DGT} appears to be related to topsoil P_{DGT} as both rise with pH which suggests that the re-distribution of reactive P fertiliser from the topsoil is likely the main source of labile P in the subsoil (see **Chapter 4**). The relatively lower concentration of P in the subsoil may be more strongly adsorbed to Fe oxide surfaces rendering subsoil P less labile than P in the topsoil. This may explain why the subsoil P_{DGT} is lowest at this point because P is strongly retained < pH 5.5 and

therefore any P that does migrate in the solution within the pH 4.5 plot to the subsoil is probably strongly retained by surface adsorption. The subsoil P_{DGT} in the Field was similar to the P_{DGT} in the pH plots at similar pH values which indicate similar mechanisms controlling P lability.

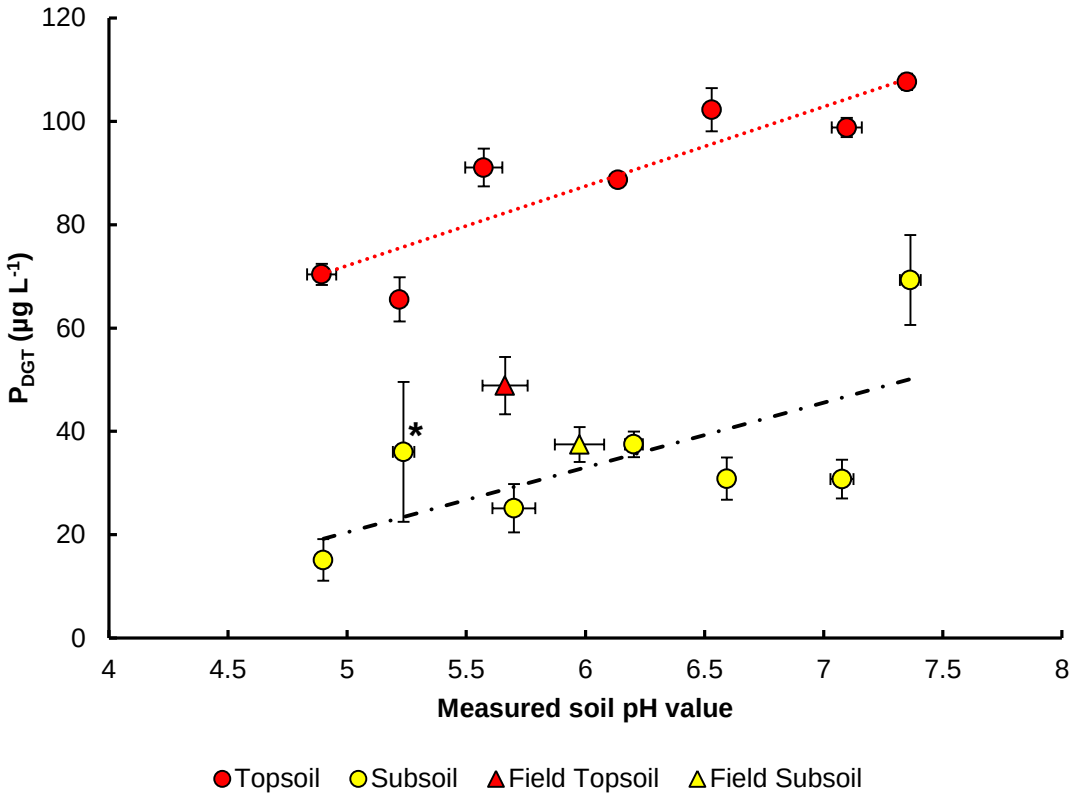


Figure 6.8. Relationship between P_{DGT} and measured soil pH in topsoils (r = 0.904) and subsoils (r = 0.687) of the pH Rotation; points are mean of 3 replicates ± SEM (except * where 1 replicate was excluded due to suspected contamination).

6.4.6 Effect of Soil pH on the Equilibrium Distribution Coefficient (K_d) in the pH Rotation

The effect of soil pH on labile P $K_{d(Olsen)}$ (**Equation 6.3**) in topsoils and subsoils of the pH Rotation is shown in **Figure 6.9**. Topsoil and subsoil $K_{d(Olsen)}$ values showed similar trends across the pH gradient. Subsoil $K_{d(Olsen)}$ was greatest in the pH 5.0 plot at 1520 mL g^{-1} (± SEM 479 mL g^{-1}) and decreased to a minimum through the pH range to 390 mL g^{-1} (± SEM 39.6 mL g^{-1}) at pH 7.5. Topsoil values also peaked at pH 5.0 (1100 mL g^{-1} ± SEM 58.6 mL g^{-1}) and decreased through the pH gradient to a minimum of 363 mL g^{-1} (± SEM 8.49 mL g^{-1}) in the pH 7.5 plot, where topsoil and subsoil $K_{d(Olsen)}$ were near identical in value. The trend with pH suggests that P is more strongly adsorbed to Fe and Al oxide surfaces in the acidic pH range (< pH 5.5). With rising pH, labile P is less strongly bound to oxide surfaces due to an increase in negative charges which lower the adsorption strength resulting in a release of labile P (Weng, *et al*., 2011) and therefore $K_{d(Olsen)}$ decreases as a result. Below pH 5.5 topsoil P_{Olsen} is greatest but $K_{d(Olsen)}$ reveals that it is strongly bound to the solid phase and therefore it may not necessarily be easily available for crop uptake. The higher $K_{d(Olsen)}$ observed in the subsoils suggests that P is more strongly bound than in the topsoils which may be due to a relatively lower concentration of P in the subsoil which is distributed across strong adsorbing sites. Leaching of labile P from the topsoils to subsoils may be an important source of labile P which is then rapidly and strongly adsorbed (De Bolle, *et al*., 2013). In the topsoil data reported by Menezes-Blackburn, *et al*., (2016) and Stutter, *et al*., (2015), $K_{d(Olsen)}$ values covered the range of 16 to 1090 mL g^{-1} between soil pH values of 4.03 to 4.99 reflecting differences in sites, land use and P fertiliser treatments. The greatest $K_{d(Olsen)}$ value of 1090 mL g^{-1} was found in a soil at pH 4.2 which is comparable to the results shown in **Figure 6.9** at pH 4.5 (1030 mL g^{-1}). Between pH 6 and 6.5 in the pH Rotation (**Figure 6.9**) $K_{d(Olsen)}$ was 333 to 555 mL g^{-1} which was similar to the range of 269 to 727 mL g^{-1} reported by Menezes-Blackburn, *et al*., (2016) between pH 6.07 and 6.57 (Stutter, *et al*., 2015). However, soil pH is not the only factor which influences the adsorption strength in soils. The P_{DGT} and P_{Olsen} data reported by Burkitt, *et al*., (2016) was used to calculate $K_{d(Olsen)}$ of their soils (**Equation 6.3**); the soils were sampled across Australia and covered a restricted range of pH values (4.0 to 5.0) and varied in soil textural class. The results produced $K_{d(Olsen)}$ values ranging from a minimum of 12.2 mL g^{-1} in a ‘sand’ soil to 1830 mL g^{-1} in a ‘sandy loam’ soil suggesting that texture is also a factor influencing the P adsorption strength in soils.

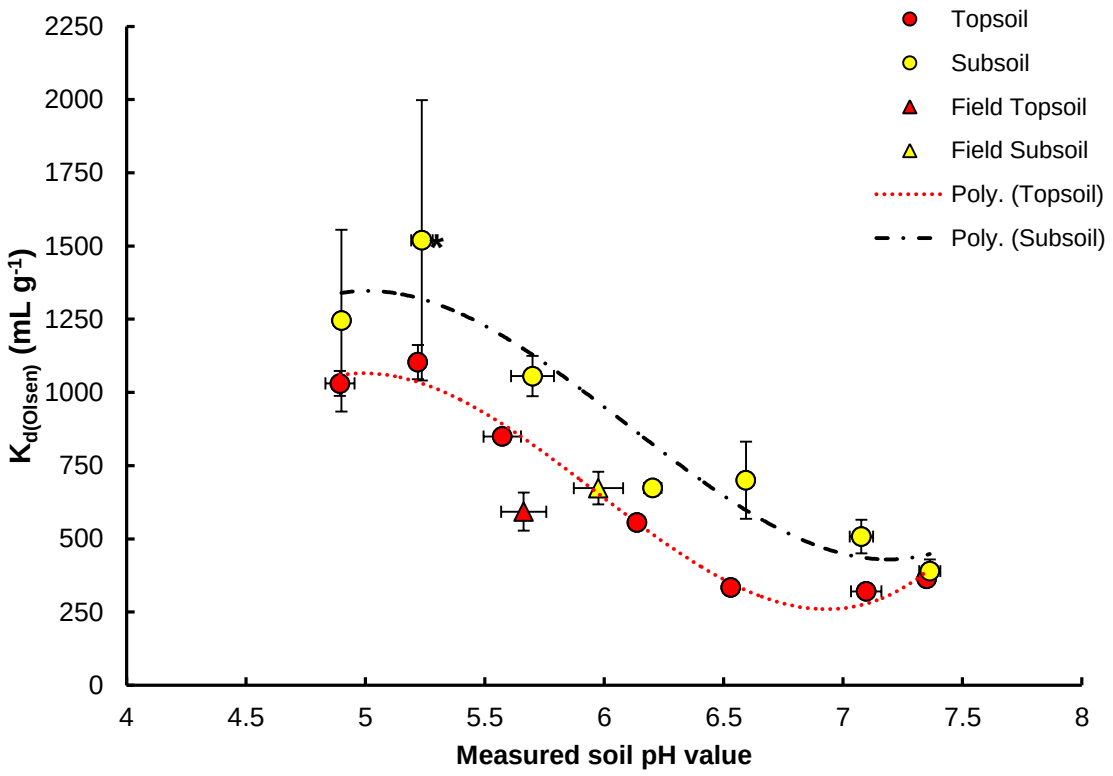


Figure 6.9. Relationship between measured soil pH and $K_{d(Olsen)}$ in the pH Rotation and the Field (mean 3 replicates ± SEM except * were mean 2 replicates ± SEM); 3rd order polynomials are fitted to the data.

The effect of soil pH on $K_{d(MMorgan)}$ in the topsoils and subsoil of the pH plots in the pH Rotation and compared the Field is shown in **Figure 6.10** and was calculated using **Equation 6.4**. The topsoil and subsoil trends are similar for $K_{d(MMorgan)}$ with the distribution coefficients larger in the subsoil than the topsoil, suggesting the adsorption strength is stronger in the subsoils. Topsoil and subsoil $K_{d(MMorgan)}$ were within the same scale and show a decrease in $K_{d(MMorgan)}$ with rising soil pH. At pH 4.5, $K_{d(MMorgan)}$ in the subsoil decreased from a maximum of 693 mL g^{-1} (± SEM 38.6 mL g^{-1}) to a minimum of 179 mL g^{-1} (± SEM 2.49 mL g^{-1}) between pH 7 and 7.5, with a slight upturn to 201 mL g^{-1} (± SEM 22.0 mL g^{-1}) in the pH 7.5 plot. Topsoil $K_{d(MMorgan)}$ declined from 255 mL g^{-1} (± SEM 17.2 mL g^{-1}) at pH 4.5 to a minimum at pH 6.5 of 99.2 mL g^{-1} (± SEM 1.58 mL g^{-1}) before showing a similar upturn to 199 mL g^{-1} (± SEM 5.44 mL g^{-1}) at pH 7.5. As with $K_{d(Olsen)}$, $K_{d(MMorgan)}$ for topsoil and subsoil at pH 7.5 were close in value which suggests that the adsorption strength throughout the soil profile was the same. This is possibly due to a change in solubility control as P is associated with calcium phosphates throughout the soil profile above pH 6 (**Chapter 5**). Similarly, higher $K_{d(MMorgan)}$ was found below pH 5.5 suggesting a high adsorption strength throughout the soil profile likely associated with Al and Fe oxides which is larger in the subsoil due to a lower concentration of P.

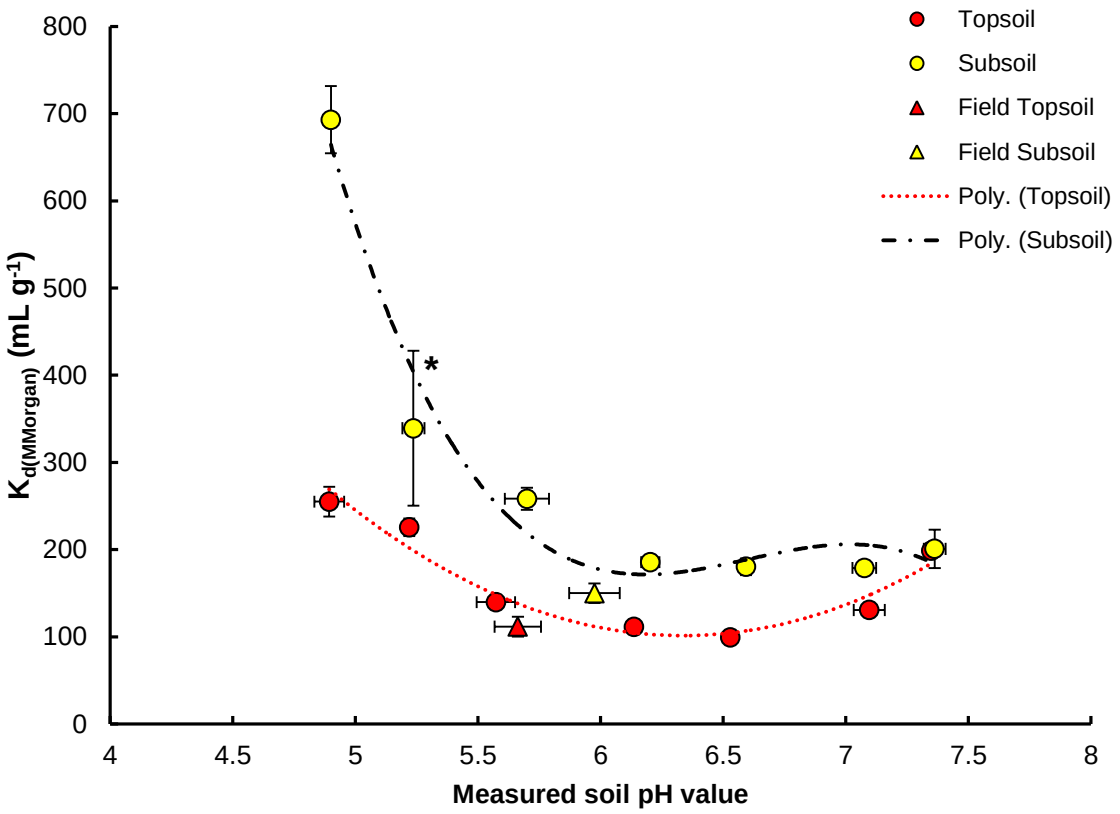


Figure 6.10. Relationship between measured soil pH and $Kd_{(MMorgan)}$ in the pH Rotation and the Field (mean 3 replicates ± SEM except * were mean 2 replicates ± SEM); 2nd (topsoil) and 3rd (subsoil) order polynomials are fitted to the data.

6.4.6.1 The Effect of pH Management on the Ratio (R_{DGT}) of P_{DGT}: P_{Soln} in the pH Rotation

The ratios of P_{DGT} to $P_{Soln\text{-}Col}$ (**Figure 6.11**) and $P_{Soln\text{-}ICP}$ (**Figure 6.12**) in the topsoils and subsoils of the pH Rotation differ by a factor of 3 or 4 but show similar trends with pH. The ratios should not exceed 1 (DGT Guide, 2003) because the P_{DGT} measures the flux of P_{Soln} to the device therefore the results using the $P_{Soln\text{-}Col}$ data clearly reflect the analytical errors associated with the results which underestimate the value of P_{Soln}. The lack of variation in $P_{Soln\text{-}Col}$ with pH in the topsoils ($r = 0.001$) further suggests inaccuracies. The ratio of P_{DGT}: $P_{Soln\text{-}ICP}$ (R_{DGT}) provide more promising results although the ratios may be overestimated due to the presence of organic P in both P_{DGT} and $P_{Soln\text{-}ICP}$ (**Figure 6.12**).

The $P_{Soln\text{-}ICP}$ results (**Figure 6.12**) show that all pH plots have higher R_{DGT} than the Field topsoil (0.335) and subsoil (0.403), probably due to the application of P fertiliser to the treatment plots. The topsoil R_{DGT} value increases with pH ($r = 0.640$) rising from a minimum of 0.324 at pH 4.5 to a final value of 0.544 at pH 7.5. The subsoil R_{DGT} values also increased with rising pH from a minimum of 0.221 (pH 4.5) to 0.549 (pH 7.5) where it converged to a near identical value to the topsoil. These results suggest that as the soil pH increases, the rate of resupply of P from the solid phase to the solution concentration increases following depletion by the DGT device. The rate of desorption was greater in the topsoil than the subsoil which suggests P is more strongly held in the subsoil, possibly due a lower concentration of P in the subsoil layer. Topsoil P is likely adsorbed to a weaker range of adsorption sites because of the higher concentration of P due to the direct application of fertilisers. As the soil pH rises, competition with organic matter for binding sites weakens the adsorption strength of P as does the decrease in positive surface charge on Fe and Al oxides (Antelo, *et al*., 2005), resulting in faster desorption of P (Weng, *et al*., 2011). The rise in both topsoil and subsoil R_{DGT} with pH suggests a possible link between the two layers in terms of distribution of labile P species throughout the soil profile.

Assuming that R_{DGT} reflects the intrinsic speed of desorption and the magnitude of the reservoir of adsorbed labile P able to respond to a depletion of the soil solution P, the results show that the speed of desorption is much lower at acidic pH values despite the high reservoir of P_{Olsen} and $P_{MMorgan}$ at pH 4.5, the lowest R_{DGT} is found in the topsoil and subsoil of this plot. This indicates a weakness in soil P tests to predict plant-available P based on chemical extraction. Although there was an apparently high available-P content in the soil at low pH, the response of the soil and desorption of surface P to resupply the soil solution following crop uptake may be limited. In this chapter, the underlying mineralogy that controls P solubility, and soil pH, are likely to be the significant factors. Furthermore, the R_{DGT} reported in the data

shown by Menezes-Blackburn, *et al*., (2016) and Stutter, *et al*., (2015), ranged from 0.08 to 0.360 between the pH range 3.28 and 7.05 in soils covering a range of textures and treatments. The highest topsoil R_{DGT} (0.622), which was observed at pH 5.5 in the pH Rotation, was 1.72x the maximum R_{DGT} in the range reported by Menezes-Blackburn, *et al*., (2016) which was 0.360 at pH 5.56.This suggests that soil pH control is not the only factor influencing the rate of P desorption from soils and other factors such as soil textures and treatments can also influence the speed of desorption.

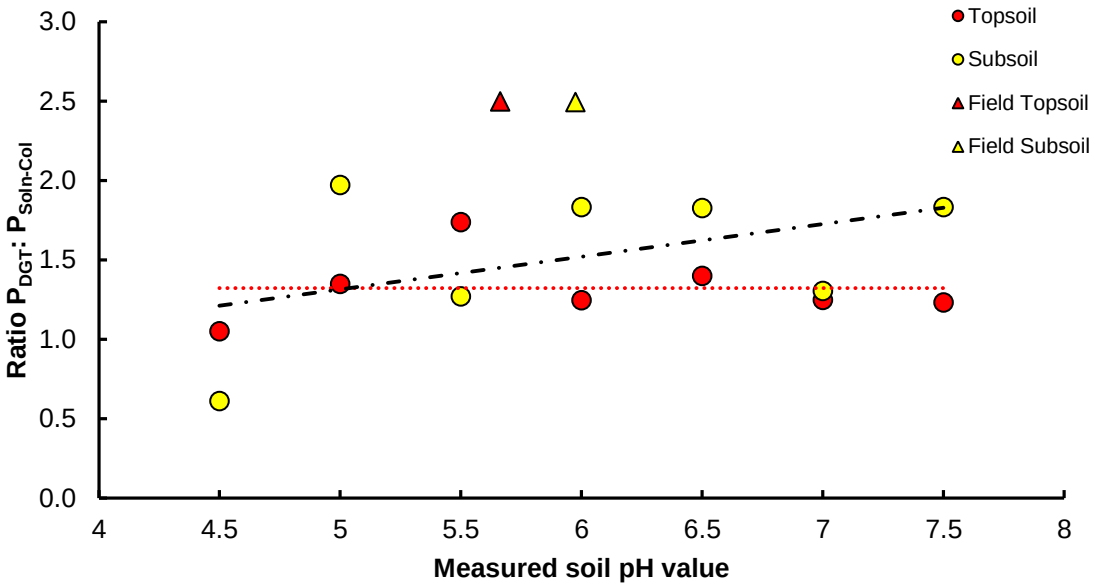


Figure 6.11. Ratio of P_{DGT}: $P_{Soln-Col}$ with soil pH in the topsoils (r = 0.001) and subsoils (r = 0.456) of the pH Rotation.

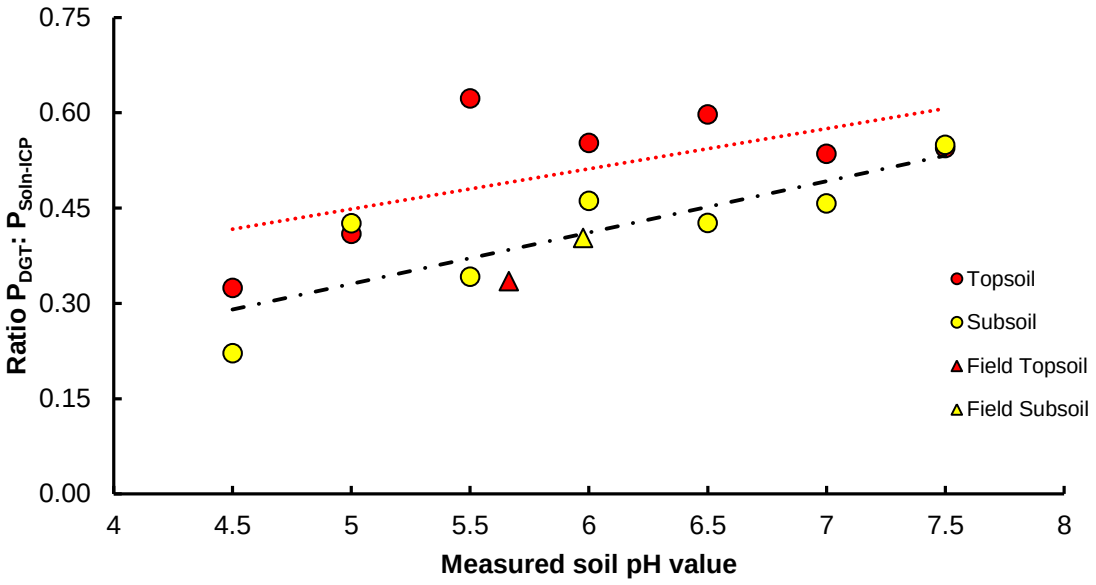


Figure 6.12. Ratio (R_{DGT}) of P_{DGT}: $P_{Soln-ICP}$ with soil pH in the topsoils (r = 0.640) and subsoils (r = 0.839) of the pH Rotation.

6.4.7 Effect of Fertiliser Management on P_{DGT} in the Old Rotation

A comparison of topsoil and subsoil P_{DGT} between fertiliser treatments in the Old Rotation and the Field is shown in **Figure 6.13**. Topsoil P_{DGT} in the Field (48.8 µg L^{-1} ± SEM 5.55 µg L^{-1}) was greater than the subsoil (37.5 µg L^{-1} ± SEM 3.38 µg L^{-1}). In most cases the treatment plots P_{DGT} did not exceed that of the Field, except for the NK with TSP topsoil, where the P_{DGT} was 61.2 µg L^{-1} (± SEM 5.44 µg L^{-1}). This is due to the input of highly soluble reactive P which is more labile than P from GMP fertilisers. The GMP topsoil P_{DGT} was 36.3 µg L^{-1} (± SEM 2.46 µg L^{-1}) and the subsoil P_{DGT} was 19.8 µg L^{-1} (± SEM 2.69 µg L^{-1}). The GMP topsoil was depleted relative to the Field and was comparable to the P_{DGT} in the topsoils of the zero fertiliser (31.6 µg L^{-1} ± SEM 2.59 µg L^{-1}) and NK without P (27.9 µg L^{-1} ± SEM 1.27 µg L^{-1}) treatment plots. This could be because GMP is relatively insoluble and may persist in the topsoil, releasing P slowly over time which can then become adsorbed to the soil surfaces as opposed to the rapid dissolution and adsorption of TSP to the solid phase in a labile form which contributes to the P_{DGT} assay. Subsoil P_{DGT} was comparable between TSP and GMP fertiliser use at 19.8 µg L^{-1} (± SEM 2.69 µg L^{-1}) and 19.3 µg L^{-1} (± SEM 2.65 µg L^{-1}) respectively. Furthermore, without P fertiliser use, subsoil P_{DGT} was similar in the NK without P and zero fertiliser treatment plots at 14.8 µg L^{-1} (± SEM 1.25 µg L^{-1}) and 13.8 µg L^{-1} (± SEM 1.16 µg L^{-1}) respectively. This suggests that a similar amount of labile P is possibly transferred from the topsoil to the subsoil under both P fertiliser treatments which is then adsorbed to the solid phase. Overall subsoil P_{DGT} was lower relative to the Field which may suggest crops acquire labile P from the subsoils in the treatment plots, depleting the amount available to resupply the soil solution (assuming that the Field has not been affected by inputs of P fertiliser due to the proximity to the experiments). The plant-available P estimates for the TSP plot were greatest for P_{Olsen} and $P_{MMorgan}$ (**Chapter 4**) and so the lability of the P_{DGT} in these plots suggest that TSP rapidly dissolves in solution and is either retained by surface adsorption in the topsoil or leached via soil solution to the subsoil where reactive P becomes adsorbed.

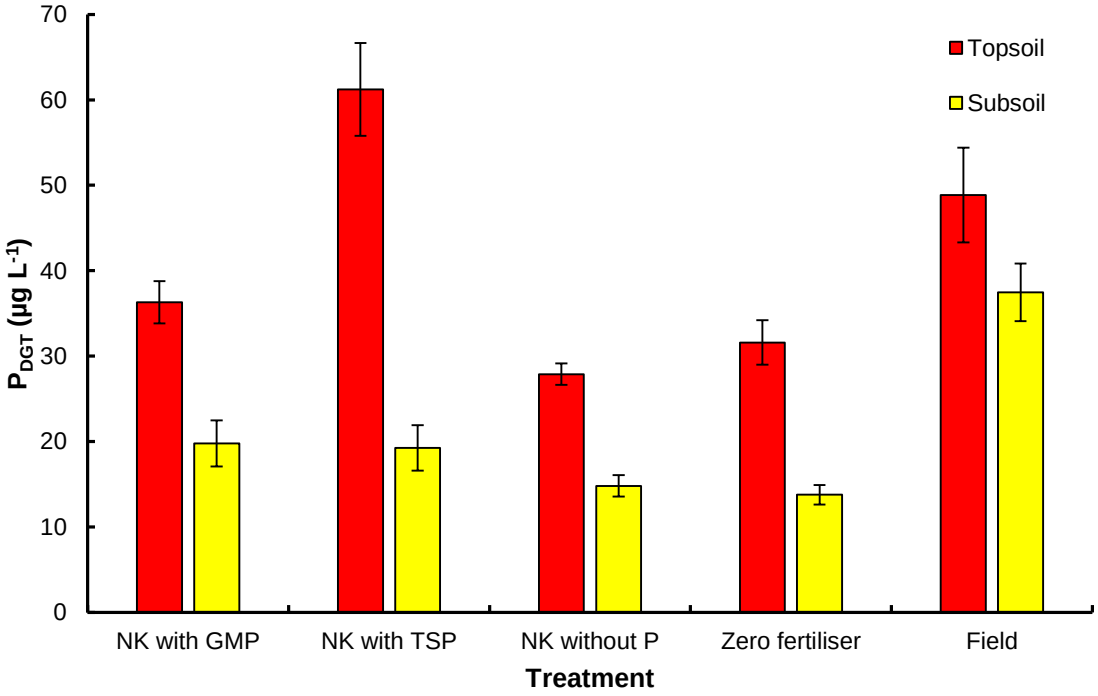


Figure 6.13. Effect of fertiliser treatment (and Field) on topsoil and subsoil P_{DGT} in the Old Rotation; results are mean of 3 replicates ± SEM.

6.4.8 Effect of Fertiliser Management on the Equilibrium Distribution Coefficient (K_d) in the Old Rotation

The effects of fertiliser treatment on $K_{d(Olsen)}$ and $K_{d(MMorgan)}$ for the Old Rotation and the Field are shown in **Figure 6.14** and **Figure 6.15**. The fertiliser treatment topsoil $K_{d(Olsen)}$ ranged from a minimum of 275 mL g^{-1} (± 23.3 SEM mL g^{-1}) in the zero fertiliser plot to a maximum of 544 mL g^{-1} (± SEM 51.0 mL g^{-1}) in the NK with TSP treatment. The NK with GMP was 472 mL g^{-1} (± SEM 69.9 mL g^{-1}) and the NK without P was 349 mL g^{-1} (± SEM 26.4 mL g^{-1}) while the Field topsoil was 593 mL g^{-1} (± SEM 65.0 mL g^{-1}). Values of K_d in the fertiliser treatment subsoils ranged from 400 mL g^{-1} (± SEM 58.6 mL g^{-1}) (NK without P) to 545 mL g^{-1} (± SEM 33.8 mL g^{-1}) (NK with TSP), with the highest $K_{d(Olsen)}$ in the Field at 673 mL g^{-1} (± SEM 55.8 mL g^{-1}). The NK with GMP plot was 480 mL g^{-1} (± SEM 72.7 mL g^{-1}) and the zero fertiliser trial was 455 mL g^{-1} (± SEM 32.9 mL g^{-1}). The topsoils and subsoils $K_{d(Olsen)}$ directly overlapped in the NK with GMP and the TSP treatment which showed that the soil profile had uniform $K_{d(Olsen)}$ whereas the the subsoil $K_{d(Olsen)}$ in the zero-fertiliser plot was greater than the topsoil which suggested that more P was distributed on the solid phase in the subsoil than the topsoil. The topsoil and subsoil $K_{d(Olsen)}$ partially overlapped (in error bars) in the NK without P treatment plot. When P fertilisers are restricted, $K_{d(Olsen)}$ values which are greater in the subsoil than the topsoil may suggest that crops have accessed and depleted labile topsoil P

from the solid-phase due to the lack of labile P inputs from fertilisers. However, P restricted plots do receive FYM inputs once during the crop rotation cycle and so it is possible that labile forms of P have leached rapidly from the topsoil to the subsoil and have become adsorbed to the subsoil solid phase. Pizzeghello, *et al*., (2014) showed that leaching of labile P from topsoils amended with farm yard manure and mineral fertilisers had resulted in subsoils to become enriched in P in a variety of soil textures. The range of $K_{d(Olsen)}$ valuesin the Old Rotation (275 to 545 mL g^{-1}) matched the range reported by Menezes-Blackburn, *et al*., (2016) which was reported to be 269 to 519 mL g^{-1} between pH 6.07 and 6.57, which is similar to the pH target of the Old Rotation plots are maintained. However, in the Old Rotation, the adsorption to Fe and Al oxides likely control the solubility as opposed to calcium phosphate mineralogy (**Chapter 5**) however it is possible for a combination of interactions of P with Al, Fe and Ca can simultaneously control the release of P in soil (McDowell & Sharpley, 2003).

The separation between subsoils and topsoils was greater for $K_{d(MMorgan)}$ and all treatments showed subsoils with greater distribution coefficients than the topsoil (**Figure 6.15**) however the values were much lower compared to $K_{d(Olsen)}$. Topsoil $K_{d(MMorgan)}$ increased in the order of 112 mL g^{-1} (± SEM 11.4 mL g^{-1}) (Field), 126 mL g^{-1} (± SEM 4.52 mL g^{-1}) (NK without P), 152 mL g^{-1} (± SEM 15.4 mL g^{-1}) (NK with TSP), 171 mL g^{-1} (± SEM 24.6 mL g^{-1}) (zero fertiliser) and finally 193 mL g^{-1} (± SEM 15.2 mL g^{-1}) (NK with GMP). Subsoil $K_{d(MMorgan)}$ increased in a similar order treatments from 150 mL g^{-1} (± SEM 11.2 mL g^{-1}) (Field), 181 mL g^{-1} (± SEM 22.0 mL g^{-1}) (NK without P), 215 mL g^{-1} (± SEM 23.4 mL g^{-1}) (zero fertiliser), 222 mL g^{-1} (± SEM 18.9 mL g^{-1}) (NK with TSP) and finally 243 mL g^{-1} (± SEM 30.2 mL g^{-1}). The clear separation between subsoils and topsoils $K_{d(MMorgan)}$ suggested that the subsoil contains more labile P than the topsoil possibly due to leaching of reactive P from fertiliser and farm yard manure. The differences in the value of the distribution coefficient between $K_{d(Olsen)}$ and $K_{d(MMorgan)}$ is likely due to differences in the P pools which are extracted by the acidic Modified Morgan and alkaline Olsen reagents. The alkaline Olsen P may be removing a larger proportion of potentially non-labile P than the Modified Morgan reagent. As the Old Rotation is maintained around pH 6, and the solubility of P is mainly controlled by Fe and Al oxides (**Chapter 5**), it could be that the Olsen reagent overestimates the labile P fraction due to alkaline hydrolysis of organic matter in the plots. Modified Morgan is closer in pH to the conditions in the plots and so may extract less non-labile P from the solid phase than the Olsen P and thus be more comparable to the labile species measured by P_{DGT}. Regardless, both methods are showing that the subsoils have a larger solid phase distribution of P compared to the topsoils.

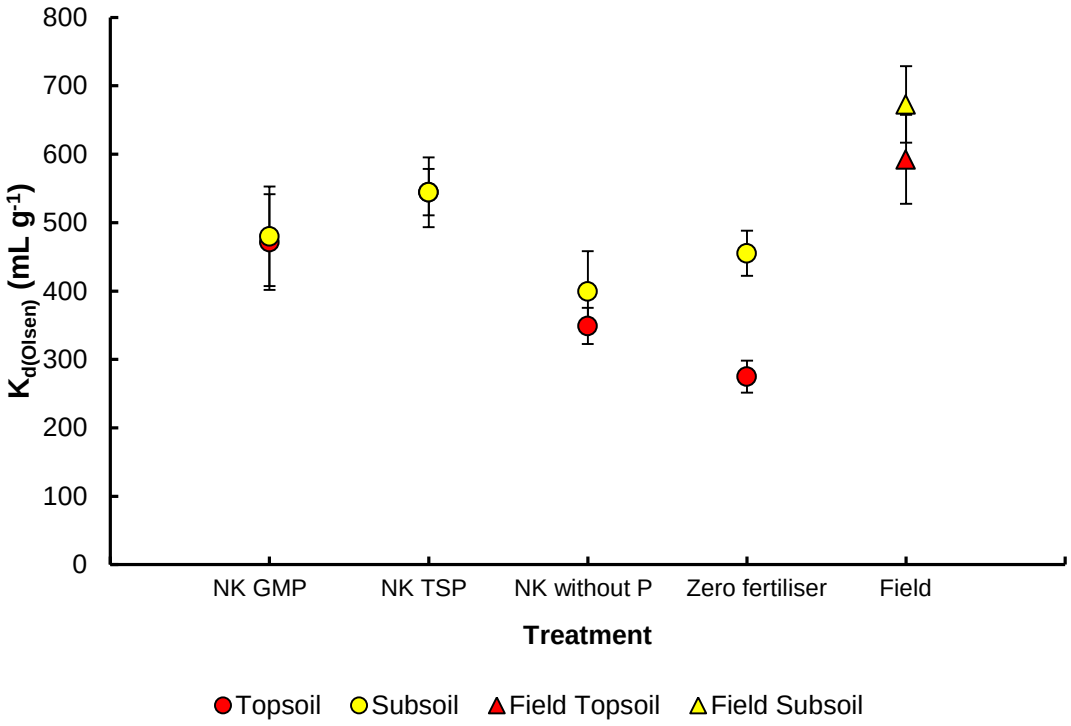


Figure 6.14. Relationship between fertiliser treatments and $K_{d(Olsen)}$ in the Old Rotation plots and the Field (mean 3 replicates ± SEM).

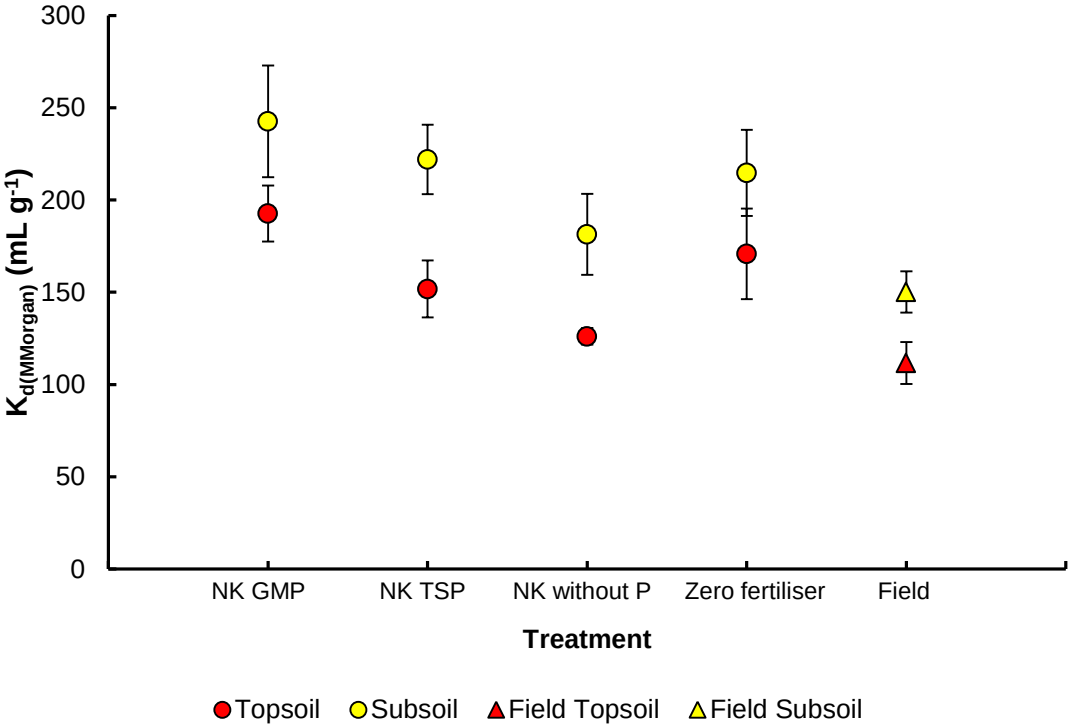


Figure 6.15. Relationship between fertiliser treatments and $Kd_{(MMorgan)}$ in the Old Rotation plots and the Field (mean 3 replicates ± SEM).

6.4.9 Effect of Fertiliser Management on the Ratio (R_{DGT}) of P_{DGT} to P_{Soln}

The ratios of P_{DGT}: $P_{Soln\text{-}Col}$ (**Figure 6.16**) and P_{DGT}: $P_{Soln\text{-}ICP}$ (**Figure 6.17**) in the topsoils and subsoils of the fertiliser treatment plots in the Old Rotation and the Field show differences in magnitude. The $P_{Soln\text{-}Col}$ ratios are greater than 1 which is not a valid result as this suggests that the P_{Soln} is greater than the P accumulated by the P_{DGT}, which is a direct measure of the flux from the soil solution. Again, this highlights the uncertainty surrounding the $P_{Soln\text{-}Col}$ which was explored previously in **Chapter 5**. The ratio (R_{DGT}) of P_{DGT}: $P_{Soln\text{-}ICP}$ (R_{DGT}) shows more promising results as the values are between 1 and 0 but again both may contain organic P species which could be contributing to the results (**Figure 6.17**). The R_{DGT} in the NK without P treatment overlap with the topsoil (0.247) slightly greater than the subsoil (0.241) but in the zero fertiliser treatment the topsoil (0.268) and subsoil (0.241) R_{DGT} separate, with R_{DGT} equal between the two treatments in the subsoil. The Field topsoil R_{DGT} (0.335) is less than the subsoil (0.403) which is also the case in the NK with GMP treatment plot where the topsoil (0.299) and subsoil (0.316) R_{DGT} marginally overlap and are similar in value. The biggest contrast is in the NK with TSP treated plot where the topsoil R_{DGT} is much higher than most treatments at 0.420 (although comparable to the Field subsoil result) with a subsoil R_{DGT} of 0.301 which is similar to the other plots. This is expected as the application of highly reactive TSP fertiliser would rapidly dissolve in soil solution and adsorb on to soil surfaces where it may be labile for maintaining the equilibrium between the solid and solution phases. The lack of P application, or the use of relatively insoluble GMP fertiliser, results in lower R_{DGT} values, indicating that those solid phases respond more slowly to a depletion in solution P by the DGT device possibly due to a stronger bond between P and the solid phase if the P represents much older, mineral P in the P restricted plots. The relatively insoluble GMP fertiliser may persist in soil but has a slow response rate in comparison to the TSP fertiliser. These plots are maintained around pH 6 and the R_{DGT} are between 0.241 and 0.420 with an average of 0.307. At pH 6 in the pH Rotation the R_{DGT} are much higher at 0.552 (topsoil) and 0.461 (subsoil) however the pH Rotation receives highly soluble TSP fertiliser and so a direct comparison on the effect of pH between the pH Rotation and Old Rotation does not seem to reflect a common pH effect except for the R_{DGT} in the NK with TSP plot were the topsoil (0.420) is somewhat comparable to the pH 6 plot in the pH Rotation. Instead, the resupply of P from the solid surfaces in the Old Rotation is likely influenced by the adsorption of P on Fe and Al oxides and also the P fertiliser management strategy. The main factor controlling P solubility in the Old Rotation was thought to be P interactions with Fe and Al oxide mineralogy (**Chapter 5**). Menezes-Blackburn, *et al*., (2016) reported R_{DGT} values between 0.08 and 0.360 for soils with pH values ranging from 3.28 and 7.05 using some previous data from the Appendices

of Stutter, *et al*., (2015). Therefore, the Old Rotation R_{DGT} values, which are concentrated mainly around pH 6, are partially within this range but the fertiliser management strategies have resulted in higher R_{DGT} in the Old Rotation.

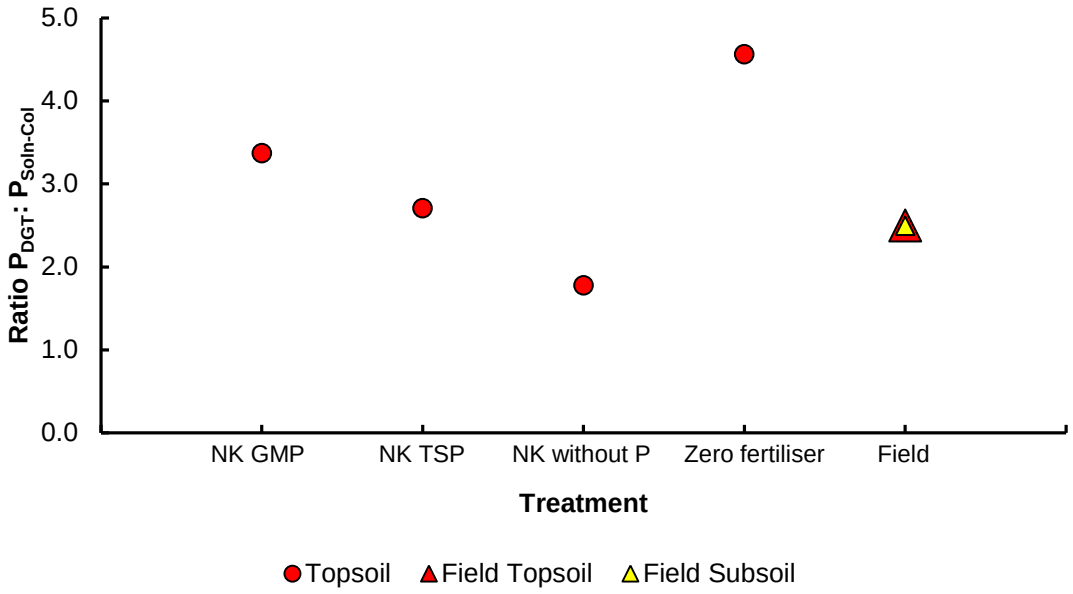


Figure 6.16. Ratio of P_{DGT}: $P_{Soln-Col}$ in the topsoils of the fertiliser treatments in the Old Rotation compared to the Field. No $P_{Soln-Col}$ was obtained for the subsoils.

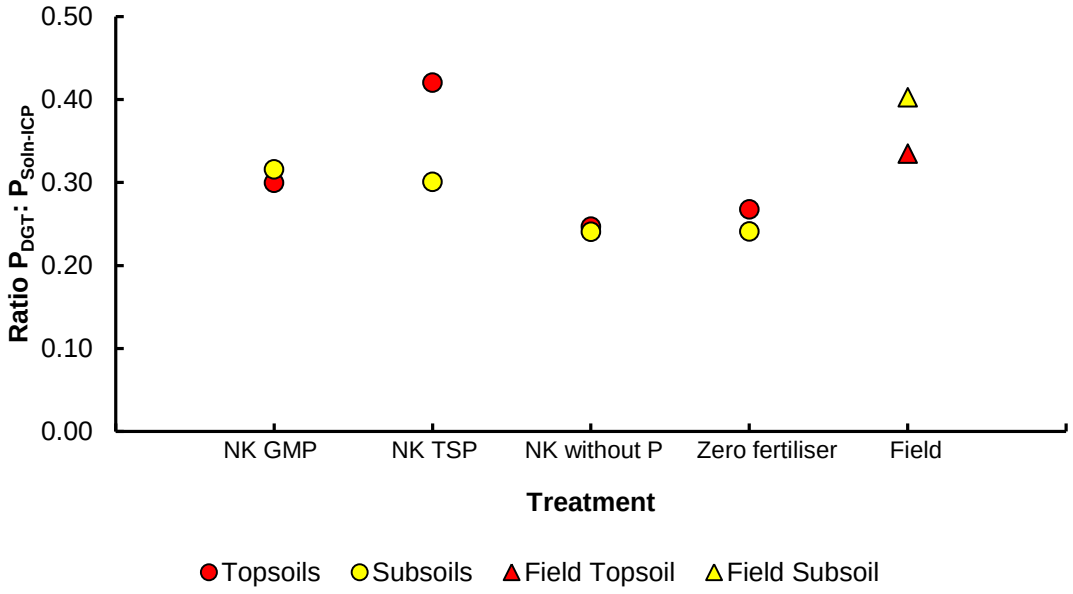


Figure 6.17. Ratio (R_{DGT}) of P_{DGT}: $P_{Soln-ICP}$ in the topsoils and subsoils of the fertiliser treatments in the Old Rotation compared to the Field.

6.5 Conclusions

The aim of this chapter was to investigate the factors controlling the lability of P, and the distribution of P between the solid and solution phases, in the topsoils and subsoils of the Woodland's long-term experiments. The effect of soil pH management across a gradient from pH 4.5 to 7.5, and the effect of fertiliser management strategy on the intensity (P_{DGT}) and quantity (P_{Olsen} and $P_{MMorgan}$) of labile P, was investigated. It was found that P_{DGT} was positively correlated with P_{Total} throughout the soil profile except in the pH Rotation where P_{DGT} showed variation over a narrow P_{Total} range in the topsoils depending on the target pH of the plot. P_{DGT} was also positively correlated with P_{Olsen} and $P_{MMorgan}$ throughout the soil profile. Furthermore, P_{DGT} was strongly correlated with increasing $P_{Soln\text{-}ICP}$ which was expected because the DGT device measures the flux of P in soil solution to the device interface. Topsoil and subsoil P_{DGT} increased linearly from pH 4.5 to 7.5 which showed that P was more labile as the soil pH increased; this was thought to reflect the desorption of P from Al and Fe oxides as negative surface charges increased and a change in solubility controls of P above pH 6, when the dissolution and precipitation of calcium phosphates become important in these plots (**Chapter 5**). However, the capacity of the topsoil to supply plant available P (i.e. P_{Olsen} and $P_{MMorgan}$) did not necessarily coincide with an increase in the lability of P_{DGT} or rate of desorption. The equilibrium distribution coefficients of labile P between the solid and solution phases (K_d) in the topsoils and subsoils decreased from a maximum at pH 4.5 to a minimum around pH 6 before rising slightly towards pH 7.5. This shows that labile P is more strongly held on the solid phase by adsorption at low pH (< 5.5) in the topsoils and subsoils, with limited evidence that the adsorption strength of the solid phase increases as pH values rise greater than 7. The subsoil K_d was higher than in the topsoil across the pH range because the concentration of P was lower in the subsoil and was adsorbed on to stronger (labile) adsorbing sites. This is due to two main factors: (i) there is more solution P in the topsoil due to the direct application of fertilisers which results in labile P being bound to both strong and weak adsorption sites and (ii) there is a higher organic matter content in the topsoils (i.e. humic and fulvic acids) which compete with phosphate for adsorption sites on Fe oxides thus rendering the Fe oxides more negatively charged and the phosphate more weakly bound (Weng, *et al*., 2011).

The ratio of P_{DGT}: P_{Soln} (R_{DGT}) provided an indication of the solution P buffering capacity of the soil. In plots > pH 6 the soil was able to respond faster to a depletion in soil solution P by the DGT as indicated by a maximum ratio at pH 6 in the topsoil and at pH 7.5 in the subsoil. The buffering capacity of the soil < pH 5.5 was least throughout the soil profile. This further supported the conclusion that strong retention mechanisms were controlling the lability of P at acid pH values as influenced by soil pH management.

Therefore, despite apparently high 'plant-available P' and a large capacity of the soil to supply P < pH 5.5, strong retention processes were preventing the 'available' P from being rapidly resupplied to the soil solution phase following depletion. As the DGT method simulates removal of P from soil solution by crops this has important implications for crop productivity and fertiliser management strategies because it shows the importance of maintaining optimal soil pH levels for the crop or crop rotation in the field, as sub-optimal pH levels may be rendering applied P fertiliser unavailable for crops in systems where liming is not routinely carried out. The results have also shown that subsoil P_{DGT} is influenced by soil pH; between pH 6 and 6.5, which is optimum for crop production, P_{DGT} was greatest, suggesting maximum solubility of P in the soil solution. Therefore, subsoil P reserves may be plant-available and an important additional source of P although further research is required. The direct application of labile, reactive P from TSP, and possibly farm yard manure, temporarily increased the P concentration in the solution; this would encourage migration by leaching to the subsoil and would be the main input of solution P to the subsoil. Therefore, it is important to consider the type of P fertiliser applied whilst also considering the farming system in place (arable vs grassland) and the potential for losses to the subsoil and the wider environment.

The restriction of P fertilisers in the Old Rotation appeared to have resulted in a depletion of P_{DGT} in the topsoils and subsoils relative to the Field 'control' where P_{DGT} was relatively uniform throughout the profile. This suggested that crops have accessed native pools of labile P over the 94-year duration of the experiment. It also shows that fertilisers are required to maintain labile P concentrations in the soil which are accessible and available to plant roots. The application of TSP and GMP fertiliser seems to have maintained labile P levels relative to the Field to some degree but were overall depleted in P_{DGT} in comparison suggesting that the fertiliser application rates are inadequate for this crop rotation and consideration should be given to increase inputs of P in order to secure future crop yields. The Old Rotation is maintained around pH 6 however, the lability of P in the TSP and GMP plots was lower than the pH 6 plot in the pH Rotation which could be because the fertiliser application rates do not seem to be adequate to maintain soil P levels suitable for crops in rotation. The solubility of P in the Old Rotation plots is controlled by P adsorption to Fe and Al oxide surfaces (**Chapter 5**) which would explain why P_{DGT} and thus labile P, and the ability of the solid phase to respond and buffer depletions in the soil solution, was lower in these plots compared to the pH Rotation plots at similar pH values (pH 5 to 6). This work may be of interest to those developing guidelines which take in to consideration the soil texture and also the ability of the soil to sorb P and regulate plant-available P in solution (Sinclair, *et al*., 2015).

7 Topsoil and Subsoil $\delta^{18}O_P$ Signatures Following Historical P Fertiliser Use and pH Control

7.1 Abstract

The processes affecting topsoil and subsoil phosphate dynamics were investigated through analysis of $\delta^{18}O_P$ signatures of HCl-extractable phosphate using two long-term experiments: one with a pH gradient ranging from pH 4.5 to 7.5 in 0.5 increments and a second fertiliser management trial, where the use of two phosphate fertilisers were contrasted. The HCl-extractable P made up approximately 49.1% of the total P concentration in both the topsoil and the subsoil. Hydrolysis and incorporation of organic P compound oxygen during extraction with HCl was minimal across the dataset (< $2^0/_{00}$) with O: P ratios in the isolated silver phosphate (Ag_3PO_4) of approximately 4.0. The $\delta^{18}O_P$ signatures of soil phosphate in the dataset were constrained between $18.1^0/_{00}$ and $23.0^0/_{00}$. Isotopic signatures within the soil profiles suggested that relatively insoluble GMP fertiliser underwent slow biological processing in the topsoil before being leached down to the subsoil creating a uniform $\delta^{18}O_P$ signature tending towards equilibrium with the soil pore water. By contrast, the $\delta^{18}O_P$ signature of highly soluble TSP fertiliser was partially retained in soil phosphate and had apparently been rendered un-available through abiotic processes in the topsoil and was shown to be moving towards equilibrium. Subsoil signatures were close to equilibrium suggesting leaching of highly processed P or continued microbial processing in the subsoil. Soil pH had a strong influence on P cycling. Topsoil and subsoil $\delta^{18}O_P$ signatures at pH 4.5 were close to the original TSP $\delta^{18}O_P$ suggesting rapid leaching of fertiliser to the subsoil and strong abiotic processes rendering the fertiliser unavailable for biological processing. Maximum solubility of phosphate between pH 6 and 7 revealed close to uniform $\delta^{18}O_P$ signatures across the topsoil and subsoil which were close to equilibrium with the soil pore water. Results in the long-term experiments were similar to the $\delta^{18}O_P$ signature of the 'native' P in the field surrounding the trials; however, these values were not in equilibrium with the soil pore water as calculated for the field, suggesting the field may represent older, more highly processed P.

7.2 Introduction

Phosphate rock is the main source of P in agricultural fertilisers; global stocks are finite, and the quality and availability of existing resources is in decline (Cordell & White, 2015). Therefore, reducing P demand and improving P use efficiency in agriculture is important for long-term food security (George *et al*., 2016). Crop production could benefit from the utilisation and mobilisation of residual P fertiliser in agricultural soils (Sattari, *et al*., 2012; Menezes-Blackburn, *et al*., 2017) and subsoils can store a significant proportion of the P in soil profiles (Bauke, *et al*., 2018; Barej, *et al*., 2014; Kautz, *et al*., 2013). The extent, rate and mechanisms of P fertiliser transport into the subsoil are currently very difficult to trace. However, there is potential to discriminate between cycling and transfer processes of soil phosphate by examining the ratio of oxygen isotopes (i.e. ^{18}O: ^{16}O) in phosphate extracted by acid dissolution of inorganic P with HCl ($\delta^{18}O_P$). This techniqueisolates and purifies soil inorganic phosphate as Ag_3PO_4 which can then be assayed by mass spectrometry (Tamburini, *et al*., 2010). The HCl-extractable P (P_{HCl}) can make up a significant proportion of the total P in agricultural soils (Granger, *et al*., 2017b) and it is thought to consist of mainly apatite minerals (Hedley, *et al*., 1982) but can also contain other forms of P such as those bound to Fe or Al oxides (Helfenstein, *et al*., 2018). Stable oxygen isotope analysis of soil phosphates can also be performed on operationally defined pools in sequential extractions of resin, microbial, sodium hydroxide (inorganic), sodium hydroxide (organic) and then HCl extractable P to trace biological cycling of P (Helfenstein, *et al*., 2018). The method of Tamburini, *et al*., (2010) has also been adapted for analysing the stable oxygen isotope ratios in river sediments (Pistocchi, *et al*., 2017). Agricultural sites that receive mineral fertilisers may have a higher proportion of total P existing as P_{HCl} than those where organic fertilisers are applied (Amelung, *et al*., 2015). Measured $\delta^{18}O_P$ values in P_{HCl} can provide information on the degree of biological transformation and can be used to trace P dynamics in the environment (Tamburini, *et al.*, 2014; McLaughlin, *et al*., 2006b).

The movement and cycling of phosphate throughout the environment may be traced if the $\delta^{18}O_P$ signature of the source phosphate is known. Gruau, *et al.*, (2005) suggested that the oxygen isotope composition of phosphate in inorganic fertilisers such as TSP is controlled by that of the original phosphate rock deposit - despite the dissolution and re-precipitation processes associated with TSP production. Furthermore, the oxygen atoms of the phosphate molecule are non-labile in response to *abiotic* soil processes such as adsorption and precipitation (Gross & Angert, 2015). By contrast, Paytan, *et al*., (2002) and Blake, *et al.*, (2005) showed that biological processes, such as intra-cellular enzymatic hydrolysis, can cause the P-O bond to break, rendering the oxygen labile and subject to rapid exchange with oxygen in water. The

overall result of enzymatic processing is isotopic depletion, resulting in lower $\delta^{18}O_P$ values. Thus Gruau, *et al.*, (2005) found that $\delta^{18}O_P$ values for inorganicfertilisers fell in broadly the same range as phosphorite source materials (c. $19.6^0/_{00}$ to $23.1^0/_{00}$) whereas values for phosphate from waste water treatments plants were isotopically depleted and the $\delta^{18}O_P$ fell in a more confined range at $17.7^0/_{00}$ to $18.1^0/_{00}$. Organic fertilisers such as farmyard manure tend to have lower $\delta^{18}O_P$ values for example $12^0/_{00}$ to $15^0/_{00}$ (Amelung, *et al*., 2015; Granger, *et al*., 2017a). Pfahler, *et al*., (2013) showed that P taken up by soybean crops from a hydroponic solution ($12.4^0/_{00}$) was altered within the plant as leaves were isotopically enriched up to a $\delta^{18}O_P$ of $68.0^0/_{00}$. Elsbury, *et al*., (2009) were able to conclude that multiple sources contributed to the $\delta^{18}O_P$ of dissolved phosphate in Lake Erie because the measured values ranged from $10^0/_{00}$ to $17^0/_{00}$ while the expected equilibrium value was $14^0/_{00}$. Elsbury, *et al*., (2009) also concluded that there were sources of P that were uncharacterised thus highlighting the importance of knowing source values as a reference for tracing the fate of P in the environment. Tamburini, *et al*., (2018) recently published a method for analysing the oxygen isotope ratios of organic-P in soils and plants and the reported $\delta^{18}O_P$ ranges for soil organic-P was 12.7 to $20.3^0/_{00}$ and for plants it was 17 to $27^0/_{00}$. Slowly exchangeable soil phosphates may have $\delta^{18}O_P$ signatures in the range of 10 to $25^0/_{00}$ (Tamburini, *et al*., 2014). Agricultural topsoil $\delta^{18}O_P$ signatures may be between 14 and $18^0/_{00}$ (Bauke, *et al*., 2018; Amelung, *et al*., 2015) while subsoil $\delta^{18}O_P$ values have been reported between 12 and $16^0/_{00}$ (Bauke, *et al*., 2018) at depths of 40 to 90 cm. Values between 14 and $17^0/_{00}$ were found between depths of 40 and 80 cm which decreased to $12^0/_{00}$ and $13^0/_{00}$ at depths of 80 and 120 cm, reflecting the influence of parent material on $\delta^{18}O_P$ (Amelung, *et al*., 2015). Angert, *et al*., (2012) found some soils to have $\delta^{18}O_P$ values ranging from 8.2 to $10.9^0/_{00}$ and suggested that this could be because the HCl-extractable P was in the form of primary minerals. Phosphate in solution may reach isotopic equilibrium with water rapidly and theoretical ranges can be calculated (Longinelli & Nuti, 1973; Chang & Blake, 2015); these ranges then serve as another useful reference to the extent of P cycling in the environment. Measured $\delta^{18}O_P$ values close to, or within, equilibrium ranges indicate intensive cycling of P through biological processes whereas $\delta^{18}O_P$ values closer to source materials indicate a lack of biological cycling due to abiotic soil processes (Gross & Angert, 2015). Values of $\delta^{18}O_P$ between source materials and equilibrium ranges may be transitioning towards equilibrium and indicate the effects of partial biological cycling (Amelung, *et al*., 2015). It is also useful to know the extent to which the isotopic signature may be altered by other sources of P.

Forms of P other than phosphate (i.e. condensed phosphate, pyro- and polyphosphate, phosphate mono- and diester, or phosphonate) can be present in soil extracts (Frossard, *et al*., 2011) and the hydrolysis of

these compounds through microbial action can lead to the incorporation of oxygen from water which would change the isotopic signature in part or in full (Blake, *et al*., 1997). Therefore, duplicate HCl extractions are performed with ^{18}O-enriched and non-enriched HCl as the incorporation of ^{18}O from the enriched extraction would be evident from differences in the isotopic signatures between the paired extractions (Frossard, *et al*., 2011). A 'true' $\delta^{18}O_P$ can be determined using the differences between the two extractions through mass-balancing and the degree of incorporation can be interpreted by analysing the degree of incorporation and the O: P ratio (which should be 4 for pure phosphate) (McLaughlin, *et al*., 2006a). However, significant differences between ^{18}O-enriched and non-enriched extractions are not usually observed in soil extracts (Tamburini, *et al*., 2010) with reports of differences no greater than $1^0/_{00}$ (Granger, *et al*., 2017a). Gross & Angert (2015) reported a $2^0/_{00}$ difference between ^{18}O-enriched and non-enriched in the decomposition of RNA and less than 1% exchange between water and phosphate oxygen. A recent study did not perform the duplicate extraction with ^{18}O-enriched reagents with the assumption (using evidence from the literature) that hydrolysis and exchange of oxygen from organic P does not occur during the extraction, even in samples containing small amounts of organic P (Bauke, *et al*., 2018). The HCl-extractable P fraction (P_{HCl}) is generally free from organic P sources and is also a fraction of the total P in soils that is relatively stable and not liable to short-term changes in isotopic composition (Amelung, *et al*., 2015).

The *primary hypothesis* of this study was that the relatively abiotic subsoil (Taylor, *et al*., 2002) may contain phosphate which has rapidly leached down the soil profile (De Bolle, *et al*., 2013) after application of highly soluble mono-calcium phosphate (TSP) to the topsoil. Subsoil phosphate would therefore have $\delta^{18}O_P$ values which more closely reflect those of the original fertiliser (e.g. GMP and TSP in the case of the Woodland's Rotations) than the natural soil profile, provided the fertiliser material $\delta^{18}O_P$ values were sufficiently different from the native soil $\delta^{18}O_P$ values. This was expected to be seen from comparisons of topsoil and subsoil in treatment plots which produce differences in P solubility. For example, relatively insoluble phosphate rock fertiliser application is more slowly leached from the topsoil and so may be more likely to be biologically processed prior to leaching. In such a case, P_{HCl} in the subsoil would have a $\delta^{18}O_P$ signature closer to equilibrium with soil water. The second hypothesis was that, because leaching rates are likely to be pH-dependent, differences in $\delta^{18}O_P$ values in P_{HCl} are also likely to be seen comparing the Woodland's pH Rotation plots (4.5 to 7.5 in 0.5 increments). Differences in P solubility across this range have already been verified (see **Chapter 5**) with maximum solubility around pH 6, between the zones of Ca-phosphate precipitation (pH > 6.5) and strong adsorption on Fe/Al hydrous oxides (pH < 5.5). Thus,

TSP may be strongly retained as apatite (high pH) or adsorption to Fe and Al oxides (low pH) in the *topsoil* and thus be rendered both unavailable for microbial processing (Gross & Angert, 2015), and leaching, and the $\delta^{18}O_P$ in the *topsoil* may be closer to that of the TSP. The *counter hypothesis* is that biological processing (and equilibrium with soil water oxygen) is faster than topsoil-subsoil transfer processes and/or that biological processing continues to some extent within the subsoil (Amelung, *et al*., 2015). This would be indicated if $\delta^{18}O_P$ values in P_{HCl} for topsoil and subsoil fell within the same range, and that of theoretical soil pore water equilibrium ranges. Thus, the Woodland's Rotations provide an excellent opportunity to further develop the measurement of $\delta^{18}O_P$ values as an analytical tool which reveals the 'pathway origin' of P transferred to subsoil pools.

7.2.1 Aim and Objectives

The aim of this chapter was to investigate processes influencing the cycling and transfer of P in the topsoil to subsoil of long-term experiments using measurement of $\delta^{18}O_P$ in P_{HCl} from HCl extractions of soil (Tamburini, *et al*., 2010). The hypothesis was that rapid leaching of reactive fertiliser P from topsoil to subsoil would result in fertiliser P bypassing biological mixing in the topsoil and becoming adsorbed in the subsoil. Subsoil $\delta^{18}O_P$ would therefore be similar to original fertiliser $\delta^{18}O_P$. Furthermore, P fertiliser retained in acidic topsoil (< pH 5.5) by adsorption is subject to less biological cycling than soils at pH > 6, where solubility of P is greater, and therefore closer to the theoretical soil pore water equilibrium $\delta^{18}O_P$. Soluble TSP fertiliser would be more highly processed and distributed throughout the soil profile than insoluble P fertilisers such as GMP, which persists in the topsoil and undergoes long-term cycling and equilibration. The counter hypothesis was that microbial cycling of fertiliser P in the topsoil would be so fast that equilibrium would be reached with the soil pore water before transfer to the subsoil occurred, resulting in uniform $\delta^{18}O_P$ values throughout the soil profile. The experimental objectives are listed below.

1. Complete a pilot-study to investigate the viability of the method on a sub-set of soil samples collected from the Woodland's Field long-term experiments.
2. Determine values of $\delta^{18}O_P$ in appropriate reference materials, including: GMP and TSP fertilisers, the uncultivated native soil surrounding the field trials, and the soil pore water equilibrium using local rainfall and topsoil and subsoil pore water and temperature data.
3. Investigate the effect of fertiliser treatment and pH management on topsoil and subsoil values of $\delta^{18}O_P$ in P_{HCl} to reveal, where possible, the underlying mechanisms controlling P dynamics in the Woodland's Field long-term experiments.

7.3 Materials and Methods

7.3.1 Sample Site, Trial Descriptions, Sample Selection and Preparation

The full details of the long-term experiments used in this study are described in **Chapter 2 Materials and Methods** for the sample site and description of the trials (**section 2.1**), trial management (**section 2.1.1**), soil sampling and preparation (**section 2.2**) and various soil analysis such as soil pH (**section 2.4**) and total element analysis (**section 2.6**). Briefly for this study, air-dried, sieved (< 2 mm) soil samples from all three auger borings in each treatment were selected from all seven target pH plots that had been under Grass Year 2 (pH Rotation) and four fertiliser treatment plots (NK with GMP, NK with TSP, NK without P and zero fertiliser) that had been under Grass Year 3 (Old Rotation). Sub-samples of the GMP and TSP fertilisers applied to these trials were also taken for analysis and three un-managed field topsoil and subsoil samples were selected to compare soils subject to treatment effects with the 'native' field soil profile conditions. Grass years 2 and 3 in the crop phases of both rotations do not receive fertiliser or FYM additions and were chosen on the assumption that $\delta^{18}O_P$ values may be more stable than in soil from (i) cereal phases which would have received fertiliser additions at the beginning of the growing season, and (ii) the root crop phase which would have received fertiliser and FYM additions at the start of the growing season.

A pilot study was conducted on a sub-sample chosen from the treatments (**Table 7.1**). Topsoil and subsoil samples of 6 unique auger borings were chosen from the range of treatments and P_{Total} concentrations across both long-term experiments. In addition, soil from one field auger boring and two fertiliser materials (TSP and GMP) were included to obtain reference values against which to compare the treatments.

Table 7.1. Summary of the sub-group of soil samples in the pilot study. The topsoil and subsoil of one out of three augers per plot were selected and processed and samples were chosen to reflect a range of treatments and P_{Total} concentrations. In addition, one sub-sample of GMP and TSP fertilisers were processed.

Source	Crop	Treatment	Layer	Auger	P_{Total} (mg kg^{-1})
pH Rotation	Grass Year 2	7.5	Topsoil	1	1780
pH Rotation	Grass Year 2	6	Topsoil	1	1730
pH Rotation	Grass Year 2	4.5	Topsoil	1	1930
pH Rotation	Grass Year 2	7.5	Subsoil	1	1160
pH Rotation	Grass Year 2	6	Subsoil	1	1290
pH Rotation	Grass Year 2	4.5	Subsoil	1	877
Old Rotation	Grass Year 3	TSP	Topsoil	1	1210
Old Rotation	Grass Year 3	GMP	Topsoil	1	1160
Old Rotation	Grass Year 3	TSP	Subsoil	1	760
Old Rotation	Grass Year 3	GMP	Subsoil	1	978
Uncultivated field	Grass	Control	Topsoil	1	1420
Uncultivated field	Grass	Control	Subsoil	1	1450

7.3.2 Rainfall, Soil Pore Water and Soil Temperature Sampling and Processing

Rainfall and soil samples were collected every month from March to November 2017 in Woodland's Field adjacent to the long-term experiments and the Craibstone Meteorological Office weather station following a rainfall event. Data for daily precipitation and soil temperatures at depths of 10, 30 and 100 cm has been available since 2009. A copper collection vessel was used to collect rainfall and sub-samples were decanted into plastic containers, filled to the brim to minimise air space and exchange with atmospheric oxygen, sealed with Parafilm™, and stored at 4^{o}C. At the same time, topsoil (< 20 cm) and subsoil (20 to 40 cm) samples were collected using a hand auger, sealed inside three air tight plastic sample bags to minimise oxygen exchange with the surrounding atmosphere, and stored at 4^{o}C to minimise biological cycling of P. Samples were sent to the University of Nottingham and stored at 4^{o}C before processing. Rainfall samples were syringe-filtered (< 0.22 μm, PES membrane) and a sub-sample transferred to a 2 mL septum-cap chromatography vial (zero headspace), the top sealed with Parafilm™ and stored at 4^{o}C. The topsoil and subsoil samples were sieved (< 2 mm) while still field-moist and a sub-sample was transferred to a gas chromatography glass vial, stored at 4^{o}C, then frozen at the British Geological Survey laboratory, Keyworth.

7.3.3 Soil Pore Water Extraction

Soil pore water was cryogenically extracted from the frozen topsoil and subsoil samples by NIGL, BGS using a bespoke vacuum line (borosilicate glass). Samples were transferred to borosilicate glass tubes which were then partially immersed in liquid N to ensure complete freezing of the soil pore water. The atmosphere within the tube was removed by vacuum (< 10^{-2} bar); the tube was then sealed and removed from the line. To achieve full soil pore water extraction, one side of the tube (containing the soil) was rapidly heated (> 100^{o}C) to evaporate the soil pore water while the opposite side was immersed in liquid N to force condensation of the water; the extraction process was continued for at least 1 hour to ensure full extraction. The soil pore water was stored in 1.5 mL septum-cap chromatography vials (zero headspace) at 4^{o}C prior to analysis.

7.3.4 Experimental Procedure for Soil Phosphate Extraction, Purification and Analysis

7.3.4.1 Pilot study, training and method development

A two-week pilot study was conducted, with Dr Andrew Smith (British Geological Survey, Keyworth), to test the methods for extraction, purification and analysis of soil phosphate developed by Tamburini, *et al*., (2010). The methodology for the main study was then adapted following a week-long training visit to Dr Pfahler and colleagues (Rothamsted Research, North Wyke), and a recommendation was made to follow the more detailed instructions of the method which was published by the International Atomic Energy Agency (Aigner, *et al*., 2016). This procedure is presented herein and, where relevant, differences from the pilot study method are described. Finally, the experience gained from the pilot study and training visit was used to set up the method locally at the University of Nottingham. This involved the procurement of equipment and reagents, the development of a standard operating and work flow procedure and a risk assessment for the methodology.

7.3.4.2 Extraction of soil phosphate with 1M HCl

Air-dried, sieved (< 2 mm) topsoil and subsoil samples from all three auger borings in each treatment plot (c. 6 g), and sub-samples of TSP and GMP fertilisers (c. 0.2 g) were weighed in duplicate into 50 mL blue-screw cap centrifuge tubes to which 30 mL of 1M HCl extractant was added. Two HCl stock solutions were used, one of which was ^{18}O-labelled (97% ^{18}O $H_2{}^{18}$O, OLM-240-91-1, LOT #:16A-002, Cambridge Isotope Laboratories Inc., Andover, MA, USA) in order to test for possible hydrolysis of

organic-P during which ^{18}O would be incorporated into the PO_4 molecule. Samples were shaken overnight (c. 16 hours) end-over-end (26 rpm) before centrifugation (3500 *g*, 15 minutes). Supernatant solutions were syringe-filtered (< 0.22 µm PES membrane) into universal tubes. An aliquot of 1 mL supernatant solution was diluted 1 in 6 with 5 mL of 2 % HNO_3 for P_{HCl} analysis by ICP-MS, to determine the concentration of P extracted from the soil sample. The remaining solution was stored at 4°C until required for phosphate isolation through a series of precipitation steps. In the pilot study, 4 samples were analysed by ICP-MS to determine P_{HCl} contents and the volume of sample required to produce 30 µmol PO_4 for Ag_3PO_4 precipitation was determined. The volumes calculated (between 3 and 15 mL) were used in the first half of the pilot study but in the second week all of the supernatant solution was used to maximize the yield of Ag_3PO_4 for analysis.

7.3.4.3 Batch processing and quality assurance

Throughout the precipitation stages of the sample preparation, samples were processed in batches of 14 to reduce experimental errors, check the reproducibility and increase the reliability of the results. For each individual topsoil or subsoil sample, the three auger boring replicates were run in separate batches. However, within each batch, the sample HCl solutions (^{18}O enriched and non-enriched) were run as a pair making a total of 7 individual 'auger boring' samples per batch. Topsoil and subsoil from the same auger were not necessarily run together. By running the pairs together, and the auger replicates separately, the reliability of the results within a batch and between batches could be assessed.

7.3.4.4 Precipitation of ammonium phospho-molybdate (APM)

The sample supernatant solution was pipetted (recording c. 20 to 25 mL) into a conical flask to which 25 mL of 4.2 M ammonium nitrate and 40 mL of ammonium heptamolybdate solution 10% w/v was added which resulted in the precipitation of yellow ammonium phospho-molybdate (APM). Concentrated H_2SO_4 was added (max. 1 mL) to acidify solutions to pH 1 and induce precipitation when necessary. The flasks were then covered with Parafilm™ with a small hole and placed in a temperature-controlled water bath set to 50°C and left to agitate gently overnight (min. 16 hours). The APM precipitate was recovered by vacuum filtration (< 0.22 µm cellulose acetate filter membrane) and rinsed with 100 to 200 mL of 0.6 M ammonium nitrate solution which was collected for safe disposal. The filter membrane and APM precipitate were then transferred to a new conical flask for the next stage of the experiment (dissolution and precipitation as MAP). Between samples, the vacuum filter apparatus was thoroughly rinsed with Milli-Q water and wiped dry to remove any residual APM.

Several procedural problems became apparent at this stage in the pilot study. First, there was a failure to precipitate APM with sample supernatants < 10 mL because the solutions were not acidic enough; the addition of H_2SO_4 to acidify was a strategy adopted later. Thus, for some samples, the procedure failed at the beginning to carry any PO_4 through and resulted in a negligible yield of Ag_3PO_4 at the end of the experiment. Following advice, H_2SO_4 was used to acidify the samples, the maximum amount of sample available (> 15 mL) was used, except for fertiliser samples, where < 10 mL was used due to the high PO_4 content. A secondary issue was that the APM precipitate was (i) initially re-suspended in the wash solution which was discovered to be inefficient and (ii) washed with an insufficient volume of 0.6 M ammonium nitrate (< 50 mL) which would have allowed nitrate (NO_3) (a source of oxygen) to be carried through to the next stage of the procedure. Once realised, the precipitate was allowed to settle during filtration and washed with between 100 and 200 mL solution. These changes resulted in successful APM precipitation from the remaining samples in the pilot study.

7.3.4.5 Precipitation of magnesium ammonium phosphate (MAP)

The APM was dissolved by adding a maximum quantity of citric acid-NH_4OH solution between 20 and 25 mL before removing the filter membrane with clean, plastic tweezers. The solutions were magnetically stirred and the APM was left to fully dissolve before slowly adding 22.5 mL of 'magnesia solution' (50 g $MgCl_2.6H_2O$ + 100 g NH_4Cl dissolved in 500 mL Milli-Q water, acidified to pH 1 with concentrated HCl and made up to 1000 mL). The first few batches in the experiment were pH-adjusted using up to 7 mL of 1:1 NH_4OH: Milli-Q (17.5%) solution to bring the pH above pH 9 so that it may decrease overnight into the ideal range for MAP precipitation (pH 8 to 9). However, in later batches the pH was checked first and it was observed that the optimum range of pH 8 to 9 was achieved after adding 22.5 mL magnesia solution and so the pH adjustment step was not necessary in most cases. After the magnesia solution addition, a white precipitate (MAP) was observed to form after a few minutes of mixing. The flasks were covered with Parafilm™ with a small hole in the top and left to stir overnight. The following day, the MAP precipitate was vacuum-filtered (< 0.22 µm cellulose nitrate membrane). It was observed that there was a range of precipitate colours from different soil samples, including white, green, grey and dark yellow, whereas fertiliser sample precipitates were typically white. This was not considered unusual, and simply reflects the fact that fertiliser samples had a greater purity than the soil samples which was expected. The MAP was rinsed 3 times, without agitation or resuspension, with a maximum 100 mL of 1:20 v/v NH_4OH/Milli-Q (1.7%) solution which was collected for safe disposal.

The MAP was dissolved out of the filter membrane in 20 mL of 0.5 M HNO_3 in a 50 mL centrifuge tube and the filter was removed with plastic tweezers, which was rinsed with Mill-Q water between samples. A spatula-tip of $AgNO_3$ crystals were added to the sample solutions to check for the presence of AgCl (formation of a white precipitate) and the solution was gently shaken for 15 minutes. All solutions were then syringe-filtered (< 0.22 µm PES membrane) into a clean 50 mL screw cap centrifuge tube and stored at 4^{o}C until all samples were brought to this stage of the procedure, ready for the removal of cations and precipitation of Ag_3PO_4. An aliquot of 1 mL from each sample was then diluted 1 in 6 with 5 mL 2% HNO_3 and analysed by ICP-MS, to determine how much PO_4^{3-} had reached this stage (assuming the isolation of PO_4^{3-} was successful and that total P is in the PO_4^{3-} form). The potential amount of Ag_3PO_4 that could be precipitated was then estimated.

In the pilot study, the main problems with this stage of the experiment arose from problems in the APM formation stage. First there was difficulty in dissolving the (presumed) APM precipitate in the citric acid-NH_4OH solution- varying amounts were used (25 to 200 mL) and samples were vacuum-filtered to remove unidentified solids that formed following the citric-acid solution addition. This issue may have affected the formation of MAP and thus the amount of PO_4^{3-} carried to the end of the experiment but this effect could not be determined. For all samples, the precipitate that formed (presumed to be MAP) was a range of colours as described in the main study and dissolved easily in 0.5 M HNO_3.

7.3.4.6 Cation removal

New BioRad AG50 X8 cation resin (H^+ form, 100 – 200 mesh) was pre-conditioned in advanced with 7 M HNO_3. When required, the resin was thoroughly rinsed with Milli-Q water until the pH of the wash solution reached the pH of the Milli-Q used. The tip of a 10 mL pipette was cut off and used to transfer the resin slurry (c. 6 mL) to the sample solutions. The tubes caps were sealed, secured with Parafilm™, and left to agitate overnight (c. 16 hours). The sample solution was syringe-filtered (< 0.22 µm PES membrane) and collected in a clean centrifuge tube. The cation resin was retained in the syringe and rinsed with 2 mL Milli-Q which was filtered and collected with the sample solution. The cation resin was recovered for re-use and stored in 1M HNO_3 prior to reconditioning. In the pilot study, the cation resin was removed by vacuum-filtration and discarded.

7.3.4.7 Silver phosphate precipitation and recovery

Silver-ammine solution was produced by dissolving 10.3 g of $AgNO_3$ (crystalline, 99.9+% (metal basis). Alfa Aesar, Heysham, England) and 9.6 g of NH_4OH in 18.5 mL of NH_4OH (35%) and 81.5 mL of Milli-Q. To precipitate yellow Ag_3PO_4, 5 mL of silver-ammine was mixed with the sample solution. In the pilot study, and the first few batches of the main experiment, the pH of the sample was adjusted above pH 10 using concentrated ammonia solution (35%) to dissolve the precipitate. The samples were left for a few days in a water bath (50^oC) covered with Parafilm™ with a small hole to allow ammonia to volatilise from the solution and reduce the pH slowly into the optimum range (pH 8 to 9) for Ag_3PO_4 precipitation. In the pilot study only, the volume was topped up with Milli-Q water over the course of a few days. This method yielded Ag_3PO_4 in most samples for the pilot study, and in nearly all in the main experiment (except those in which sample PO_4^{3-} content was too low such as samples where fertiliser management strategy in the field excluded P fertiliser application). However, in the main experiment, the amount of solids recovered was not considered optimal, and so for the remaining batches of the experiment, once the 5 mL silver-ammine was added, the precipitate was left overnight at 50^oC and filtered in the morning, under the advice given during training.

The Ag_3PO_4 crystals were vacuum-filtered (< 0.22 µm polycarbonate filter membrane) and rinsed three times with Milli-Q water (50 to 100 mL) to remove traces of NO_3. The filter membrane and the Ag_3PO_4 crystals were transferred to individually labelled petri dishes and left to oven-dry overnight at 50^oC. The next day, the petri dishes were removed from the oven, sealed with tape and stored in a box in the dark at room temperature. Once all of the samples had reached this stage, the crystals were scraped from the filter paper on to clean weighing paper using a clean scalpel, transferred to a 1.5 mL micro-centrifuge tube, labelled, and stored in a box in the dark at room temperature, until required for mass spectrometry analysis. A small number of samples (16) did not yield enough Ag_3PO_4 for analysis due to errors in the methodology and these were re-processed through the extraction and purification stages. For the repeat samples, P contents in the 1M HCl extracts and the 0.5 M HNO_3 dissolution stage were not re-analysed by ICP-MS.

In the pilot study, only 16 extractions (out of 28) successfully yielded Ag_3PO_4 due to the range of issues highlighted throughout. The method described by Tamburini, *et al*., (2010) suggested that samples may be treated with hydrogen peroxide (H_2O_2) to remove any organic compounds that had persisted

throughout the experiment although there may be a risk of incorporation of oxygen from the hydrogen peroxide in to samples which would affect the results. In the pilot study, three soil samples were selected where Ag_3PO_4 crystals were recovered from both sets of extraction ($H_2{}^{18}O$ enriched and non-enriched 1 M HCl). The Ag_3PO_4 crystals were transferred to a glass container and several drops of hydrogen peroxide were added to cover the crystals before being left overnight to react (which was indicated by the formation of CO_2 bubbles). The following day, several more drops were added to test for a further reaction and when no more bubbles were released, the samples were rinsed thoroughly with Milli-Q water and then filtered and dried as before, ready for oxygen analysis. Samples from the main study were not treated with hydrogen peroxide to test for the presence of organics.

7.3.5 Mass Spectrometry Analysis

7.3.5.1 Silver phosphate $\delta^{18}O_P$ analysis

Sample silver phosphate was weighed (c. 0.285 to 0.320 mg) into silver capsules (pressed 5 x 3.5 mm, light weight) (Elemental Microanalysis, Okehampton, UK) on a 6 d.p. microbalance (Mettler Toledo MT/UMT) and stored in 98 well plates. A set number of standards were weighed (c. 0.270 to 0.340 mg) per run to check the reliability and accuracy of the results to established values and included 5x "Ag_3PO_4 precipitate" (precipitated locally at BGS), 15x "Alfa-2" (Alfa Aesar, Ag_3PO_4, 99%) and 6x "B2207" (Elemental Microanalysis, Ltd., Okehampton, U.K.). The ratio of ^{18}O:^{16}O was determined (1400^{o}C thermal conversion to CO gas) using an elemental analyser (TC−EA) linked to mass spectrometer (Delta Plus XL, ThermoFinnigan, Bremen, Germany). The N peaks and O % yield compared to "the Alfa-2" standard was also determined. The $\delta^{18}O_P$ values in parts per thousand (‰) were determined with respect to Vienna Standard Mean Ocean Water (VSMOW) using the following equation:

$$\delta^{18}\mathrm{O_P}(‰) = 1000 \cdot \left(\frac{R_{Sample}}{R_{Standard}}\right) - 1 \qquad \textit{Equation 7.1}$$

Where 'Ratio' is ^{18}O: ^{16}O ratio of the sample, and standard, respectively (Tamburini, *et al*., 2010). The $\delta^{18}O_P$ for the established laboratory standard "Alfa-2" was corrected back to 14.2‰ ± SD 0.3‰ and the inter-laboratory certified "B2207" was run as an unknown with an expected value of 21.7‰ ± SD 0.3‰. The values returned for "Ag_3PO_4 precipitate" were compared (for information only) to the life-time average of the standard (14.3‰ ± 0.3‰).

7.3.5.2 Rainfall and soil pore water $\delta^{18}O_W$ and $\delta^{2}H_W$ analysis

Values for soil pore water and rainfall $\delta^{18}O_W$ were determined through headspace CO_2 equilibration with sample water with an Isoprime Aquaprep (Isoprime Ltd., Cheadle, England) coupled to an Isoprime 100 dual-inlet stable isotope mass spectrometer (Isoprime Ltd., Cheadle, England). Laboratory standards were calibrated against International Atomic Energy Agency (IAEA) standards VSMOW and Standard Light Antarctic Precipitation (SLAP) (SD ≤ 0.05‰) and the isotope ratio results were expressed as $\delta^{18}O_W$ with respect to VSMOW compared to the laboratory standards. Water sample $\delta^{2}H_W$ was determined by online Cr reduction using a EuroPyrOH-3110 coupled to a Micromass Isoprime stable isotope mass spectrometer (Isoprime Ltd., Cheadle, England) with internal standard calibrated against international standards Vienna Standard Mean Ocean Water 2 (VSMOW2) and Standard Light Antarctic Precipitation 2 (SLAP2) (SD ± 1.0‰). The rainfall and soil pore water $\delta^{18}O_W$ and $\delta^{2}H_W$ showed good agreement to the Global Meteoric Water Line (GMWL) (**Figure 7.1**) which confirmed that the soil pore water extraction went to completion.

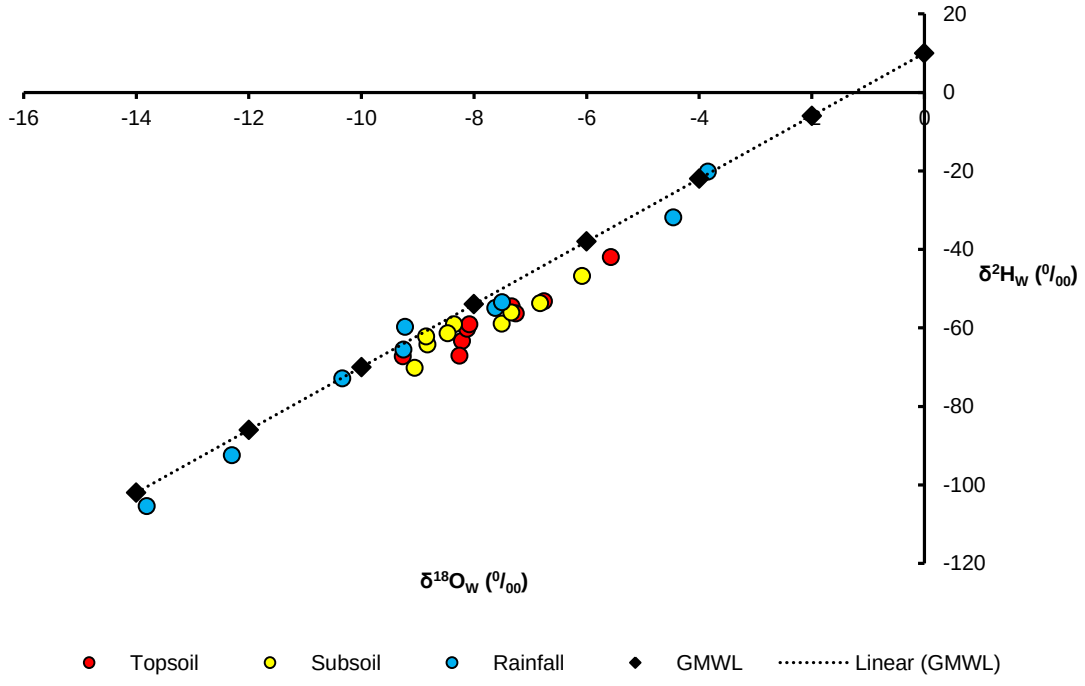


Figure 7.1. Comparison of $\delta^{18}O_W$ and $\delta^{2}H_W$ values for the monthly rain water samples and the topsoil and subsoil pore waters against the GMWL line.

7.3.6 Calculating Extent of Organic-P Hydrolysis and ^{18}O Incorporation in to Soil Phosphate

Soils were extracted with $H_2{}^{18}O$ enriched and non-enriched HCl solutions to investigate whether the HCl reagent oxygen (from H_2O) was incorporated into the soil PO_4^{3-}; this is used as an indicator of hydrolysis of organic-P compounds (Frossard, *et al*., 2011) as this would affect the sample $\delta^{18}O_P$ which would be revealed in the analysis of Ag_3PO_4 precipitates. In order to correct for potential incorporation of reagent ^{18}O into P_{HCl}, the equation of McLaughlin, *et al*., (2006a), which was later corrected (for an error of ± in the equations presented) in Pistocchi, *et al*., (2017), was used:

$$\delta^{18}O_P = \frac{\delta^{18}O_{PHI}.\delta^{18}O_{WLO} - \delta^{18}O_{PLO}.\delta^{18}O_{WHI}}{\delta^{18}O_{PHI} - \delta^{18}O_{PLO} - \delta^{18}O_{WHI} + \delta^{18}O_{WLO}} \qquad \textit{Equation 7.2}$$

where $\delta^{18}O_P$ is the 'corrected' value if hydrolysis had not occurred, $\delta^{18}O_{PHI}$ is the soil sample $\delta^{18}O_P$ value from the ^{18}O-enriched HCl, $\delta^{18}O_{PLO}$ is the soil sample $\delta^{18}O_P$ value from the non-enriched HCl extraction, $\delta^{18}O_{WHI}$ is the average $\delta^{18}O_W$ of the ^{18}O-enriched water (41.16‰ ± SEM 0.51‰, n = 3) before HCl dilution, and $\delta^{18}O_{WLO}$ was the average $\delta^{18}O_W$ of the non-enriched water (-7.32‰ ± SEM 0.11‰, n = 3) before HCl dilution. The pilot study $\delta^{18}O_{WHI}$ (41.56‰) and $\delta^{18}O_{WLO}$ (-7.46‰) were representative of one sub-sample analysis.

7.3.7 Calculating % of phosphate *not* exchanged during hydrolysis and O:P ratios

The proportion (%) of PO_4^{3-} not exchanged during the hydrolysis and incorporation of ^{18}O during the ^{18}O-enriched HCl extraction was calculated using the equation:

$$\%\ \text{Not exchanged} = \frac{\delta^{18}O_{PLO} - \delta^{18}O_{PHI} - \delta^{18}O_{WLO} + \delta^{18}O_{WHI}}{(\delta^{18}O_{WHI} - \delta^{18}O_{WLO})}.\ 100 \qquad \textit{Equation 7.3}$$

where 100% not exchanged is the target and equates to zero incorporation of ^{18}O reagent from hydrolysis in the HCl extraction step.

The O: P ratios for samples were calculated using the following equation:

$$\text{O: P ratio} = 4\,.\,\frac{100-\left(\delta^{18}O_{PHI}-\delta^{18}O_{PLO}\right)}{100} \qquad \textit{Equation 7.4}$$

where $\delta^{18}O_{PHI}$ is the soil sample, $\delta^{18}O_P$ value from the ^{18}O-enriched HCl, $\delta^{18}O_{PLO}$ is the soil sample $\delta^{18}O_P$ value from the non-enriched HCl extraction. The O:P ratio is expected to be close to 4.0 if no organic phosphorus compounds are extracted and incorporated in to the Ag_3PO_4 precipitate (McLaughlin, *et al*., 2006a). Standard deviations of ± 0.2 were considered to be acceptable and likely a result of experimental errors in the $\delta^{18}O_P$ analysis.

7.3.8 Calculating theoretical soil pore water equilibrium

Theoretical soil pore water phosphate equilibrium ranges were calculated separately for the topsoil and subsoil in the long-term experiments using the two main equations applied in soil studies:

The Longinelli & Nuti (1973) equation:

$$\delta^{18}O_P = \frac{111.4-T}{4.3} + \delta^{18}O_W \qquad \textit{Equation 7.5}$$

The Chang & Blake (2015) equation:

$$\delta^{18}O_P = (\delta^{18}O_W + 10^3)\,.\,e^{\frac{\left[\left(14.43\,.\,\frac{10^3}{T}\right)-26.54\right]}{10^3}} - 10^3 \qquad \textit{Equation 7.6}$$

Where $\delta^{18}O_P$ is the theoretical soil pore water equilibrium value, T is the average temperature (^oC) of the topsoil (10 cm) or subsoil (30 cm) over the 9 months sampled in 2017 (recorded by the on-site Craibstone Meteorological Office weather station), and $\delta^{18}O_W$ is the average soil pore water oxygen isotopic composition for the 9 months sampled. In this study, the two equations are compared in **section 7.4.3** and ultimately the Chang & Blake (2015) equation was used to calculate the soil pore water equilibrium ranges as a reference to compare the effects of treatments on soil $\delta^{18}O_P$ in the long-term experiments.

7.4 Results and Discussion

7.4.1 Pilot Study results

7.4.1.1 Ag_3PO_4 mass vs oxygen yield

The relationships between the mass of Ag_3PO_4 precipitate used and the total CO peak area (oxygen yield) for standards, samples and samples treated with H_2O_2 in the pilot study are shown in **Figure 7.2** but samples with which there were issues with Ag_3PO_4 purification were excluded (see pilot study issues described throughout **section 7.3.4** for more details). There was a strong, positive correlation between the mass of the Alfa-2 standards and the oxygen yield (r = 0.856). This was expected because the Alfa-2 Ag_3PO_4 is the main source of oxygen due to its purity (Tamburini, *et al*., 2010). The oxygen yield produced by the samples treated and un-treated with H_2O_2 were offset slightly above the standard line, but similar to the samples, which suggested that the purification and isolation of soil phosphate to remove additional sources of oxygen (i.e. from organic sources) was largely successful (Tamburini, *et al*., 2010). This was supported by the O: P ratios of c. 4.0 for all samples shown in **Table 7.2**, which summaries the $\delta^{18}O_P$ values and O: P ratios of the samples for which the phosphate purification and isolation were successful. Further details of the calculation of O: P ratios (**Equation 7.4**) can be found in **section 7.3.7**. The O: P ratios of 4.0 further suggested that there was no isotope fractionation of the PO_4^{3-} molecule during the HCl extraction (McLaughlin, *et al*., 2006a). Additionally, the O: P ratio was 4.0 for all Ag_3PO_4 samples that were reacted with H_2O_2 which indicated that additional oxygen was not incorporated in to the precipitate during this extra treatment of the samples. The use of H_2O_2 did not appear to have a significant effect on the sample $\delta^{18}O_P$ which suggested that there were no residual organics in the Ag_3PO_4 contributing to the sample oxygen yield (Tamburini, *et al*., 2010).

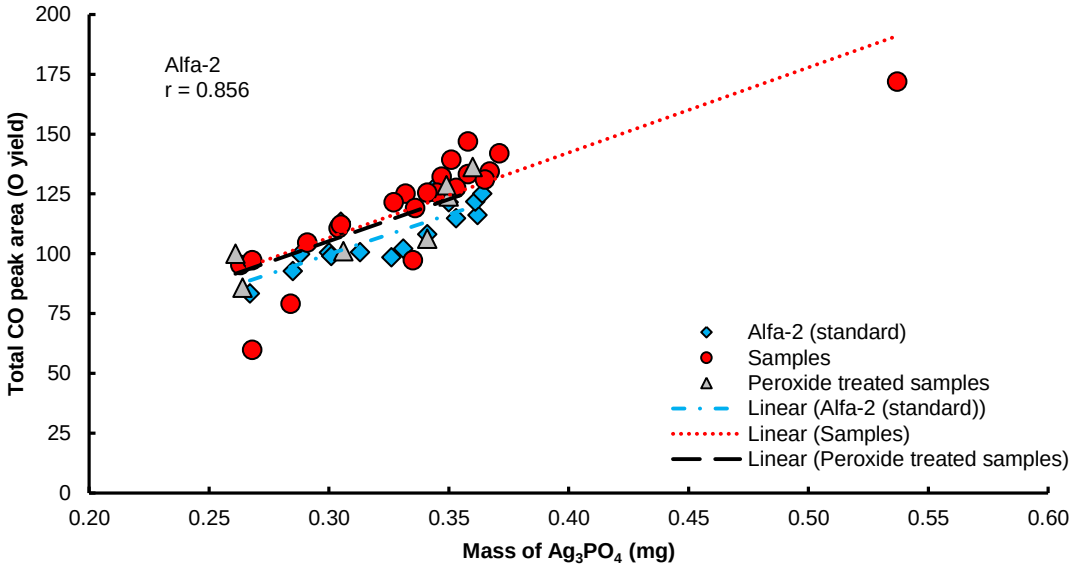


Figure 7.2. Relationship between the mass of Ag_3PO_4 crystals and total CO peak area (oxygen yield) for the Alfa-2 standards and a selection of samples (H_2O_2 treated and non-treated) in the pilot study. Linear trend lines shown are forced through zero. Samples were the purification process was unsuccessful are excluded.

7.4.1.2 Pilot study soil sample $\delta^{18}O_P$ results

There were mixed results in the pilot study, with the ^{18}O-enriched, non-enriched and corrected $\delta^{18}O_P$ values for successful samples shown in **Table 7.2** and samples that were deemed unreliable in the pilot study shown in **Table 7.3**. The results in **Table 7.3** should be treated with caution because (i) they deviated largely from the Alfa-2 standard Ag_3PO_4 oxygen yield line (**Figure 7.1**) or (ii) only one $\delta^{18}O_P$ value was obtained for the ^{18}O-enriched and non-enriched HCl paired extractions (both are required to correct for the incorporation of reagent ^{18}O in to the sample PO_4^{3-} (**Equation 7.2**) and calculation of the O:P ratio (**Equation 7.4**) (see **section 7.3.6** and **section 7.3.7** respectively) or (iii) when $\delta^{18}O_P$ values for both of the paired HCl extractions *were* obtained, there was evidence of ^{18}O incorporation between the two extractions in the corrected $\delta^{18}O_P$ value (which indicates hydrolysis of organic P at the HCl stage). Samples that were considered 'successful' (**Table 7.2**) therefore (i) showed good fit to the Alfa-2 standard Ag_3PO_4 oxygen yield line (**Figure 7.1**) and (ii) $\delta^{18}O_P$ values were obtained for the HCl pairs and (iii) there was no evidence of isotope fractionation in the corrected $\delta^{18}O_P$. The 'corrected' $\delta^{18}O_P$ values and the O: P ratios are used in the interpretation of the treatment effects on soil $\delta^{18}O_P$ because these results convey whether isotope fractionation that may have occurred due to the incorporation of ^{18}O due to organic P hydrolysis in the ^{18}O-enriched HCl extraction. The calculation of the 'corrected' $\delta^{18}O_P$ value is described in **Equation 7.2** (**section 7.3.6**) and the calculation of the O: P ratios is described in **Equation 7.4** (**section 7.3.7**). For the successful samples shown in **Table 7.2**, topsoil and subsoil sample corrected $\delta^{18}O_P$ values

fell within a narrow range between a minimum of 17.9‰ to a maximum of 20.8‰ (excluding the aforementioned subsoil at 8.3‰) and were within the expected range of 10‰ and 25‰ (Tamburini, *et al*., 2014). The topsoil of the uncultivated Field surrounding the long-term experiments had a corrected $\delta^{18}O_P$ value of 20.7‰ and the subsoil was 20.5‰. The Field values serve as a reference for the effect of treatments on topsoil and subsoil $\delta^{18}O_P$.

The soil samples in the plot treated with NK and GMP as the main source of P had a topsoil $\delta^{18}O_P$ value of 20.2‰ and subsoil $\delta^{18}O_P$ value of 18.4‰ (**Table 7.2**). No reliable result was obtained for the GMP fertiliser for comparison (i) due to the mixture of unidentified white and yellow precipitate that was produced in the purification of the GMP fertiliser and (ii) due to the issues with the purification steps in the pilot study as highlighted throughout **section 7.3.4**. The greatest contrast in sample corrected $\delta^{18}O_P$ was seen in the plot fertilised with NK and TSP as the source of P, where the topsoil (19.7‰), subsoil (8.3‰) and TSP fertiliser material (20.8‰) were significantly different. The TSP fertiliser material was similar to the TSP sample analysed by Amelung, *et al*., (2015) of 20.2‰ (± SD 0.49‰) and the result also fell within the range of 19.6 to 23.1‰ for commercial fertilisers (Gruau, *et al*., 2005). However, the subsoil result (8.3‰) was thought to be erroneous because soil P pools are thought to be typically constrained to between 10‰ and 25‰ (Tamburini, *et al*., 2014). In a sequential soil extraction Zohar, *et al*., (2010) found HCl-extractable measured $\delta^{18}O_P$ values of 6.3‰ and 7.7‰ in soils but these were irrigated with reclaimed wastewater and fresh water amended with fertiliser respectively and so are potentially not comparable to this study. Subsoil $\delta^{18}O_P$ values of long-term agricultural field experiments in Amelung, *et al*., (2015) ranged from 18‰ (40 cm depth) and 12‰ (120 cm depth). In 2018, Bauke, *et al*., reported average subsoil $\delta^{18}O_P$ values in long-term field trials constrained between 12‰ and 16‰ in one trial, and between 15‰ and 18‰ in another. The subsoil results of Amelung, *et al*., (2015) and Bauke, *et al*., (2018) fall within the range reported by Tamburini, *et al*., (2014) and therefore it can be reasonably expected that subsoils in the long-term experiments studied here would also fall within the range of 10‰ and 25‰. However, the sequential extraction of topsoils in a long-term fertilisation experiment in China revealed HCl-extractable $\delta^{18}O_P$ values of 8.72‰ in a control treatment and 8.49‰ in an NK without P treatment and values of 10.96‰ (PK no N), 11.83‰ (NP no K) and 11.55‰ (NPK) in treatments receiving calcium superphosphate fertiliser treatments which had a $\delta^{18}O_P$ value of 17.6‰ (Bi, *et al*., 2018) and so there remains some doubt whether to discard the subsoil result in this pilot study. Finally, the result from the subsoil of the pH 4.5 plot had a corrected $\delta^{18}O_P$ value of 20.6‰ which was close to the subsoil $\delta^{18}O_P$ value of 20.5‰ in the field surrounding the trials. However, these are both comparable

to the TSP fertiliser result of $20.8^{0}/_{00}$ which suggests that differentiating between TSP and native signatures may be difficult. Overall these results in **Table 7.2** suggested that the effect of treatments resulted in minor deviations from values of $\delta^{18}O_P$ in the field surrounding the trials. The pilot study results presented here require further validation through the analysis of the soil from the replicate auger borings extracted with both $H_2{}^{18}O$ enriched and non-enriched HCl solutions before interpreting treatment effects.

The main reasons for discounting some $\delta^{18}O_P$ results in **Table 7.3** were that the isolation and purification of the PO_4^{3-} in the HCl extracts through the precipitation steps were considered incomplete (see **section 7.3.4**), or because the paired HCl extractions were not successful. In the latter case it could not be determined whether there was an effect of organic P hydrolysis by the HCl or if there was any incorporation of reagent ^{18}O in to the sample PO_4^{3-} if there was no $\delta^{18}O_P$ value for the $H_2{}^{18}O$ enriched HCl extraction. For example, the $\delta^{18}O_P$ value of the non-enriched extraction of the subsoil in the pH 7.5 plot was $17.2^{0}/_{00}$ but no $\delta^{18}O_P$ value was obtained for the ^{18}O-enriched extraction. Although the value of $17.2^{0}/_{00}$ was close to the range of the successful samples ($17.9^{0}/_{00}$ to $20.8^{0}/_{00}$) shown in **Table 7.2**, and within the range expected for agricultural soils of $10^{0}/_{00}$ to $25^{0}/_{00}$ (Tamburini, *et al*., 2014), alone this was not reliable as the extent of incorporation of ^{18}O could not be determined without the paired ^{18}O-enriched $\delta^{18}O_P$. No reliable result could be obtained for the GMP fertiliser sample because there was a mixture of white and yellow precipitate formed at the end of the purification. These were separated as thoroughly as possible and analysed as Ag_3PO_4. It was thought that the yellow precipitate was Ag_3PO_4 due to the colour and the $\delta^{18}O_P$ of $20.4^{0}/_{00}$ is within the expected range for commercial fertilisers (Tamburini, *et al*., 2014) but the data produced was not considered reliable. The white precipitate was initially thought to be AgCl, which is formed when excess Cl- is present when Ag-solutions (such as the Ag-ammine reagent) are added, however the $\delta^{18}O_P$ result obtained suggested that the sample included compounds containing oxygen. The final composition was not determined but the sample was unlikely to contain organic compounds because of the H_2O_2 treatment.

Overall the pilot study was successful as a training exercise for the application of the HCl-extractable P method (Tamburini, *et al*., 2010) on the soils from Woodland's Field long-term experiments. The results provided some indication of the $\delta^{18}O_P$ values that might be expected and problem areas in the methodology were identified and rectified for the main study.

Table 7.2. Summary of the pilot study results for samples for which enough Ag_3PO_4 was produced for analysis and the data was considered reliable.

Treatment	Layer	Non-enriched HCl $\delta^{18}O_P$ ($^0/_{00}$)	Enriched HCl $\delta^{18}O_P$ ($^0/_{00}$)	Corrected HCl $\delta^{18}O_P$ ($^0/_{00}$)	O:P Ratio	Non-enriched HCl $\delta^{18}O_P$ ($^0/_{00}$) after H_2O_2	Enriched HCl $\delta^{18}O_P$ ($^0/_{00}$) after H_2O_2	Corrected HCl $\delta^{18}O_P$ ($^0/_{00}$) after H_2O_2	O:P Ratio
NK with GMP	Topsoil	20.1	20.2	20.1	4.00				4.00
	Subsoil	17.4	18.4	17.9	3.96				
TSP fertiliser (5mL)		21.2	20.6	20.8	4.02	21.2	20.8	21.0	4.01
NK with TSP	Topsoil	20.4	19.0	19.7	4.05	21.3	21.3	21.3	4.00
	Subsoil	8.6	7.6	8.3	4.04				
Field	Topsoil	20.8	20.7	20.7	4.01	20.9	20.4	20.6	4.02
	Subsoil	20.3	20.6	20.5	3.99				
pH 4.5	Subsoil	20.4	20.8	20.6	3.99				

Table 7.3. Summary of the pilot study results for samples for which the purification stage and precipitate of Ag_3PO_4 was considered unsuccessful and results unreliable. Samples marked * must be treated with caution because only one result was produced from the paired HCl extractions.

Treatment	Layer	Non-enriched HCl $\delta^{18}O_P$ ($^0/_{00}$)	Enriched HCl $\delta^{18}O_P$ ($^0/_{00}$)	Corrected HCl $\delta^{18}O_P$ ($^0/_{00}$)	O:P Ratio	Non-enriched HCl $\delta^{18}O_P$ ($^0/_{00}$) after H_2O_2	Enriched HCl $\delta^{18}O_P$ ($^0/_{00}$) after H_2O_2	Corrected HCl $\delta^{18}O_P$ ($^0/_{00}$) after H_2O_2	O:P Ratio
*GMP fertiliser (yellow)		20.4				21.0			
GMP fertiliser (white)		15.7	13.9	18.5	3.79	19.7	17.6	18.6	4.08
*TSP fertiliser (2mL)			20.9						
pH 7.5	Topsoil	1.1	9.1	2.8	3.68				
*pH 7.5	Subsoil	17.2							
pH 6	Topsoil	1.2	10.1	3.2	3.64				
*pH 6	Subsoil		10.1						

7.4.1.3 Main study vs pilot study corrected $\delta^{18}O_P$ values

A summary of the corrected $\delta^{18}O_P$ values for individual samples in the pilot compared to the average $\delta^{18}O_P$ of the sample from the main study is shown in **Table 7.4** and the comparison between pilot and main study is shown in **Figure 7.3** compared to a 1:1 line. The pilot vs main study ratio ranged from 0.14 to 1.03 indicating the issues encountered during the isolation and purification of P_{HCl} in the pilot study; most samples were not comparable (see issues highlighted throughout **section 7.3.4**). For example, there was poor agreement between the pilot vs main $\delta^{18}O_P$ values where the ratio was 0.14 in the topsoil of the 'pH 7' plot and 0.15 in the topsoil of the 'pH 6' plot. However, some samples showed good agreement between the two studies in which the ratios of $\delta^{18}O_P$ values were close to 1.0. The topsoil and subsoil from the 'NK with GMP' treatment plot had pilot vs main study $\delta^{18}O_P$ ratios of 1.05 and 0.99 respectively and for the topsoil and subsoil of the Field the pilot vs main study $\delta^{18}O_P$ ratios were 1.00 and 1.03 respectively. These indicated that the issues of the pilot study were resolved for the samples isolated and purified towards the end of the study.

Table 7.4. Comparison of the pilot study vs main study $\delta^{18}O_P$ values and the ratio between the studies. The pilot study result was of one individual sample; the main study result was the mean of three samples collected per treatment.

Treatment	Layer	Pilot $\delta^{18}O_P$ ($^0/_{00}$)	Main $\delta^{18}O_P$ ($^0/_{00}$)	Ratio
NK with GMP	Topsoil	20.1	19.1	1.05
NK with GMP	Subsoil	17.9	18.1	0.99
TSP fertiliser		20.8	23.9	0.87
NK with TSP	Topsoil	19.7	21.3	0.92
NK with TSP	Subsoil	8.3	19.1	0.43
Field	Topsoil	20.7	20.7	1.00
Field	Subsoil	20.5	20.0	1.03
pH 4.5	Subsoil	20.6	22.5	0.92
GMP fertiliser (white)		18.5	21.2	0.87
pH 7.5	Topsoil	2.8	20.6	0.14
pH 6	Topsoil	3.2	21.9	0.15

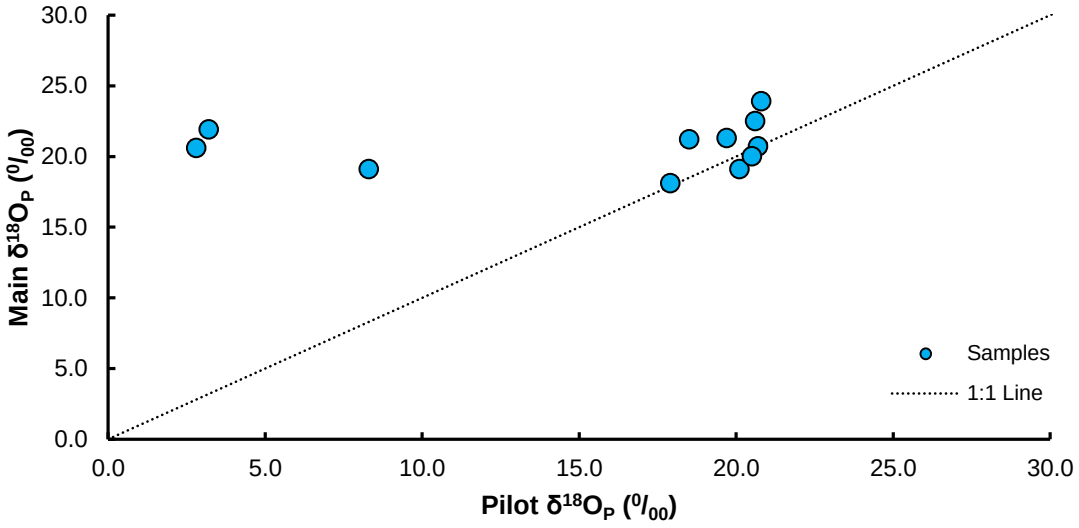


Figure 7.3. Pilot vs main study $\delta^{18}O_P$ values compared to a 1:1 line.

7.4.2 Rain and Soil Pore Eater Analysis results for Woodland's Field Rxperimental Site

The total amount of rainfall and the $\delta^{18}O_W$ and $\delta^{2}H_W$ analysis for the rain water, and topsoil and subsoil pore waters, is shown in **Table 7.5**. The average monthly total rainfall was 79.5 mm (± SD 34.3 mm), with the least amount of rain falling in May (25.6 mm) and the most falling in June (146 mm). The average $\delta^{18}O_W$ for the rain water over the 9 months was -8.7$^0/_{00}$ (± SD 3.29$^0/_{00}$) and the topsoil and subsoils were -7.6$^0/_{00}$ (± SD 1.07$^0/_{00}$) and -7.9$^0/_{00}$ (± SD 1.03$^0/_{00}$) respectively. The topsoil: subsoil $\delta^{18}O_W$ ratio was on average 1.0 (± SD 0.1$^0/_{00}$) which indicated that the $\delta^{18}O_W$ was uniform throughout the soil profile. This suggested that there was not an evaporation gradient in the soil profile which would have resulted in isotopic enrichment of topsoil water compared to the subsoil which could then affect soil $\delta^{18}O_P$ values. Amelung, *et al*., (2015) suspected that isotopic enrichment of topsoils due to an evaporation gradient may have increased topsoil $\delta^{18}O_P$ values.

Table 7.5. Summary of results for the 2017 rainfall and soil pore water analysis for topsoils and subsoils.

Month (2017)	Total rainfall (mm)	Rain water		Topsoil		Subsoil		Topsoil: Subsoil $\delta^{18}O_W$ Ratio
		$\delta^{18}O_W$ ($^0/_{00}$)	$\delta^{2}H_W$ ($^0/_{00}$)	$\delta^{18}O_W$ ($^0/_{00}$)	$\delta^{2}H_W$ ($^0/_{00}$)	$\delta^{18}O_W$ ($^0/_{00}$)	$\delta^{2}H_W$ ($^0/_{00}$)	
March	62.8	-10.34	-72.92	-9.26	-67.24	-8.35	-59.09	1.11
April	49.0	-4.46	-31.85	-8.21	-63.34	-8.83	-64.21	0.93
May	25.6	-13.81	-105.39	-8.12	-60.22	-8.47	-61.40	0.96
June	146	-7.62	-54.95	-8.08	-59.11	-8.85	-62.25	0.91
July	78.2	-7.50	-53.48	-7.33	-54.52	-9.05	-70.17	0.81
August	81.4	-12.30	-92.49	-8.26	-67.12	-7.50	-58.94	1.10
September	84.2	-9.25	-65.58	-6.76	-53.24	-7.34	-56.10	0.92
October	79.2	-3.84	-20.23	-7.26	-56.30	-6.83	-53.72	1.06
November	110	-9.22	-59.73	-5.57	-41.99	-6.08	-46.83	0.92

The variation in $\delta^{18}O_W$ values for the rainfall, topsoil and subsoil pore water samples that were collected throughout the year (2017) is shown in **Figure 7.4**. There was significant variation in the rainfall $\delta^{18}O_W$, ranging between -3.84 and -13.8$^0/_{00}$, with an average of -8.71$^0/_{00}$ (± SD 3.29$^0/_{00}$). There was a steady increase in topsoil and subsoil pore water $\delta^{18}O_W$, rising from -9.26 and -8.35$^0/_{00}$ (March) to -5.57 and -6.08$^0/_{00}$ (November) respectively. The $\delta^{18}O_W$ for the topsoil and subsoil pore waters were similar with a combined average $\delta^{18}O_W$ of -7.79$^0/_{00}$ ± SD 1.03$^0/_{00}$ (n = 18). **Figure 7.5** shows that the topsoil: subsoil $\delta^{18}O_W$ ratio was uniform and that there was good agreement between the topsoil: subsoil $\delta^{18}O_W$ ratio to the 1:1 relationship line. These results suggested rapid infiltration of rainwater throughout the soil profile and further suggested that there was not an evaporation gradient throughout the profile which would enrich the topsoil with heavier $H_2{}^{18}O$ as $H_2{}^{16}O$ preferentially evaporated. This was expected because the average annual rainfall was 878 mm (2013 to 2017) and it was unlikely that an evaporation gradient would develop in these soils due to the amount and frequency of precipitation.

There is significant daily variation in rainfall $\delta^{18}O_W$ measurements throughout the UK which are possibly linked to certain weather types and in the NE of Scotland it is likely that the amount of rainfall and the location of the long-term field experiments near to the North Sea coast are contributing factors to the rainfall $\delta^{18}O_W$ values (Tyler, *et al*., 2016). Rainfall was sampled once per month after single rainfall events and so samples were not the result of a monthly bulked collection of rainwater and therefore do not capture the daily variation in $\delta^{18}O_W$ through the month. Therefore, the rainfall $\delta^{18}O_W$ values are expected to have a strong dependence on the nature of the rainfall event that preceded the sampling, which may be influenced by the direction of the prevailing wind, the original source of precipitation and the dominant weather system that day (Tyler, *et al*., 2016).

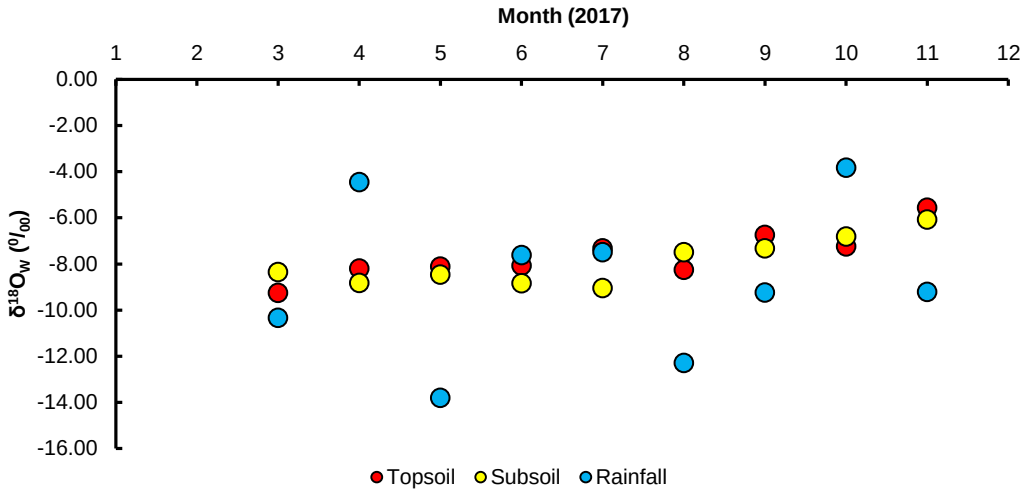


Figure 7.4. The variation in $\delta^{18}O_W$ ($^0/_{00}$) results for rainfall, topsoil pore water and subsoil pore water throughout 2017.

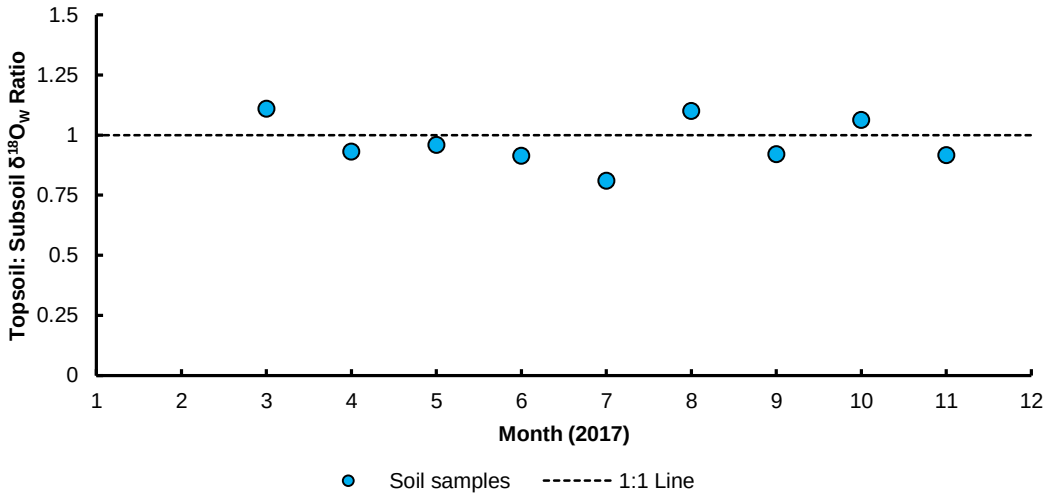


Figure 7.5. Monthly topsoil: subsoil $\delta^{18}O_W$ ratios throughout 2017 compared to a 1:1 line.

There was no correlation between monthly rainfall $\delta^{18}O_W$ and topsoil (r = 0.182) or subsoil (r = 0.050) pore water $\delta^{18}O_W$ values (**Figure 7.6**) which was expected as the incoming rain water $\delta^{18}O_W$ would become completely and rapidly equilibrated with the $\delta^{18}O_W$ signature of soil pore water, which is the larger pool of water, mediated by microbial enzymes such as inorganic pyrophosphatase (Chang & Blake, 2015). Paytan, *et al*., (2002) showed that the $\delta^{18}O_P$ of dissolved inorganic phosphate (DIP) from added fertiliser ($6^0/_{00}$) was rapidly equilibrated with the DIP of seawater ($20.6^0/_{00}$) in less than 48 hours in the presence of algae. Therefore, the isotopic composition of relatively small and variable inputs of H_2O from rainfall is unlikely to have a significant impact on the soil pore water isotopic composition, because the soil contains the larger pool of H_2O (Chang & Blake, 2015).

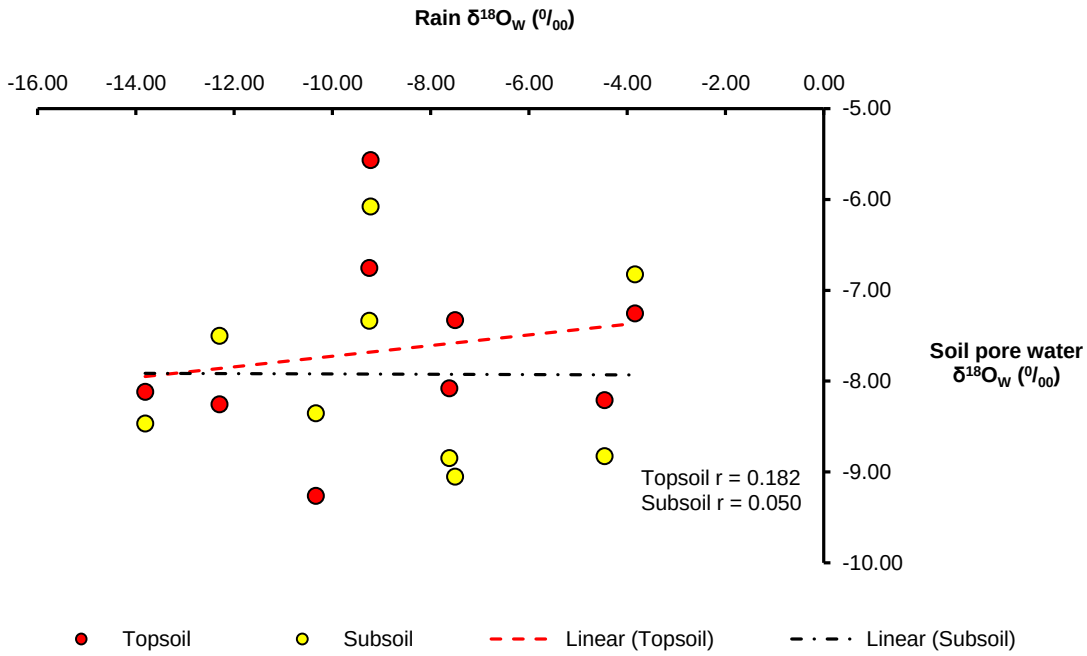


Figure 7.6. The relationship between rainfall and the topsoil and subsoil soil pore waters $\delta^{18}O_W$.

7.4.3 Comparing Equations to Calculate Soil Pore Water Equilibrium $\delta^{18}O_P$ Ranges

Two alternative equations may be used to calculate theoretical temperature-dependent values of $\delta^{18}O_P$ in soil pore water (Tamburini, *et al*., 2010) assuming equilibrium has been established and complete fractionation of the phosphate molecule by microbial processes has occurred (**section 7.3.8**). Longinelli & Nuti (1973) presented a revised water-phosphate isotopic equilibrium equation (**Equation 7.5**) by measuring $\delta^{18}O_P$ in phosphate from fish teeth and bones isolated as $BiPO_4$. The revision assumed temperatures ranges in which the biogenic apatite in the teeth and bones might have formed. Chang & Blake (2015) presented a further revised equation (**Equation 7.6**) for the equilibration of dissolved inorganic phosphate with water, catalysed by the enzyme inorganic pyrophosphatase. The equation was thoroughly calibrated in a controlled laboratory environment over a range of temperatures by analysing dissolved inorganic phosphates isolated as Ag_3PO_4 to determine $\delta^{18}O_P$. This equation considers the complete fractionation of dissolved inorganic phosphate with water mediated by the inorganic pyrophosphatase enzyme which is usually present in natural systems (Blake, *et al*., 2005) and can be assumed to be present in the long-term experiments. Both equations are frequently used in soil and water $\delta^{18}O_P$ studies and so, in this section, a comparison is made between the two equations to determine (i) whether they produce significant differences in theoretical values of $\delta^{18}O_P$ in topsoils and subsoils and (ii) which equation is most appropriate for the current study. The equation by Chang & Blake (2015) is being increasingly employed in $\delta^{18}O_P$ studies and was recently used by Bauke, *et al*., (2018) in a similar study

investigating the effect of fertiliser management strategy on topsoil and subsoil $\delta^{18}O_P$ in long-term field trials.

Summaries of topsoil and subsoil $\delta^{18}O_W$ and temperature data measured at 10 cm and 30 cm soil depths for the uncultivated grassland area in Woodland's Field, along with the results of the soil pore water $\delta^{18}O_P$ equilibrium calculations for the average, minimum and maximum temperature parameters, are shown in **Table 7.6** (topsoil) and **Table 7.7** (subsoil). Data was recorded daily using the Craibstone Meteorological Weather Station situated in Woodland's Field adjacent to the long-term experiments and the monthly results are the average of five years' worth of data for each month from January 2013 to December 2017 (inclusive). The $\delta^{18}O_W$ and temperature data are used to calculate the soil pore water equilibrium value using both the Longinelli & Nuti ("L&N") (1973) equation and the more recent equation by Chang & Blake ("C&B") (2015). The average difference between the two equations in both topsoil and subsoil were small. In the topsoil $\delta^{18}O_P$ differences in values were $1.01^0/_{00}$ (± SD $0.19^0/_{00}$), $1.13^0/_{00}$ (± SD $0.19^0/_{00}$) and $0.91^0/_{00}$ (± SD $0.19^0/_{00}$) using the average, maximum and minimum soil temperatures (**Table 7.6**). Differences in the subsoil $\delta^{18}O_P$ values were similar at $1.01^0/_{00}$ (± SD $0.18^0/_{00}$), $1.10^0/_{00}$ (± SD $0.16^0/_{00}$) and $0.93^0/_{00}$ (± SD $0.19^0/_{00}$) for the average, maximum and minimum temperatures (**Table 7.7**). The similarity was confirmed by the ratio of the two equations which ranged from 0.93 to 0.95 in the topsoil and 0.93 to 0.94 in the subsoil. Both equations appear to be suitable for estimating the theoretical soil pore water equilibrium value. For both the topsoil and the subsoil, soil pore water equilibrium limits would be set using the $\delta^{18}O_P$ calculated using the average $\delta^{18}O_W$, and average temperature for the 9 months in 2017 (± 1 SD). This would allow the interpretation of the effect of experimental treatments on soil $\delta^{18}O_P$ to be treated with the most caution.

Table 7.6. Topsoil $\delta^{18}O_P$ equilibrium calculations: Summary of the monthly topsoil pore water $\delta^{18}O_W$ values, the soil temperatures at 10 cm depth (Av, Max Min), the $\delta^{18}O_P$ calculated by both L&N (1973) and C&B (2015) equations for each month using the temperature data. The ratio of the two equations is presented and the difference (multiplied by -1) is also summarised. The average and standard deviation $\delta^{18}O_P$ with the upper and lower limits (average ± 1 SD) of the monthly results combined are shown.

Month	$\delta^{18}O_W$ ($^0/_{00}$)	Soil Temperature 10cm (^oC)			Equations $\delta^{18}O_P$ ($^0/_{00}$) Results						Ratio (L&N):(C&B)			($^0/_{00}$) Difference (L&N)-(C&B)*-1		
					L&N			C&B								
		Av	Max	Min	Av	Max	Min	Av	Max	Min	Av	Max	Min	Av	Max	Min
March	-9.26	5.19	8.30	2.80	15.4	14.7	16.0	16.1	15.5	16.6	0.96	0.95	0.96	0.69	0.83	0.59
April	-8.21	7.67	9.30	6.10	15.9	15.5	16.3	16.7	16.4	17.0	0.95	0.94	0.96	0.83	0.90	0.76
May	-8.12	11.5	15.8	8.60	15.1	14.1	15.8	16.1	15.4	16.7	0.94	0.92	0.95	1.01	1.25	0.87
June	-8.08	14.2	16.7	11.6	14.5	13.9	15.1	15.7	15.2	16.1	0.93	0.91	0.94	1.16	1.30	1.02
July	-7.33	15.2	16.8	13.5	15.0	14.7	15.4	16.3	16.0	16.6	0.92	0.92	0.93	1.23	1.33	1.14
August	-8.26	15.0	16.1	13.7	14.2	13.9	14.5	15.4	15.2	15.6	0.92	0.92	0.93	1.20	1.26	1.13
September	-6.76	13.0	14.7	11.5	16.1	15.7	16.5	17.3	17.0	17.5	0.93	0.93	0.94	1.13	1.22	1.05
October	-7.26	10.8	11.7	8.60	16.1	15.9	16.7	17.1	17.0	17.5	0.94	0.94	0.95	1.00	1.05	0.89
November	-5.57	5.88	9.60	3.40	19.0	18.1	19.5	19.8	19.1	20.3	0.96	0.95	0.96	0.81	0.98	0.71
				Average	15.7	15.2	16.2	16.7	16.3	17.1	0.94	0.93	0.95	1.01	1.13	0.91
				SD	1.40	1.34	1.43	1.31	1.26	1.33	0.01	0.01	0.01	0.19	0.19	0.19
				Upper Limit (Average + 1 SD)	17.1	16.5	17.6	18.0	17.6	18.4						
				Lower Limit (Average - 1 SD)	14.3	13.8	14.8	15.4	15.1	15.8						

Abbreviations: Average (Av), Maximum (Max), Minimum (Min), Longinelli & Nuti (1973) equation (L&N), Chang & Blake (2015) equation (C&B), Standard Deviation (SD).
Five years of soil temperature data was available between January 2013 and December 2017 therefore each temperature parameter is the average of five years for each month.

Table 7.7. Subsoil $\delta^{18}O_P$ equilibrium calculations: Summary of the monthly subsoil pore water $\delta^{18}O_W$ values, the soil temperatures at 30 cm depth (Av, Max Min), the $\delta^{18}O_P$ calculated by both L&N (1973) and C&B (2015) equations for each month using the temperature data. The ratio of the two equations is presented and the $\delta^{18}O_P$ difference (multiplied by -1) is also summarised. The average and standard deviation $\delta^{18}O_P$ with the upper and lower limits (average ± 1 SD) of the monthly results combined are shown.

Month	$\delta^{18}O_W$ ($^0/_{00}$)	Soil Temperature 30cm (^oC)			Equations $\delta^{18}O_P$ ($^0/_{00}$) Results						Ratio (L&N):(C&B)			($^0/_{00}$) Difference (L&N)-(C&B)*-1		
					L&N			C&B								
		Av	Max	Min	Av	Max	Min	Av	Max	Min	Av	Max	Min	Av	Max	Min
March	-8.35	5.34	8.00	3.40	16.3	15.7	16.8	17.0	16.5	17.4	0.96	0.95	0.96	0.72	0.84	0.64
April	-8.83	7.85	9.10	6.70	15.3	15.0	15.5	16.1	15.8	16.3	0.95	0.94	0.95	0.82	0.88	0.77
May	-8.47	11.2	14.7	8.80	14.8	14.0	15.4	15.8	15.2	16.3	0.94	0.92	0.95	0.99	1.18	0.87
June	-8.85	14.2	15.9	12.2	13.8	13.4	14.2	14.9	14.6	15.3	0.92	0.92	0.93	1.14	1.24	1.04
July	-9.05	15.1	16.0	13.8	13.4	13.1	13.6	14.5	14.4	14.8	0.92	0.91	0.92	1.19	1.24	1.12
August	-7.50	15.0	15.8	14.1	14.9	14.7	15.1	16.1	16.0	16.3	0.92	0.92	0.93	1.22	1.27	1.17
September	-7.34	13.3	14.5	12.2	15.5	15.2	15.7	16.6	16.4	16.8	0.93	0.93	0.94	1.13	1.20	1.07
October	-6.83	11.3	12.2	9.40	16.5	16.2	16.9	17.5	17.3	17.8	0.94	0.94	0.95	1.04	1.08	0.94
November	-6.08	6.84	10.0	4.30	18.2	17.5	18.8	19.1	18.5	19.6	0.96	0.95	0.96	0.84	0.99	0.73
				Average	15.4	15.0	15.8	16.4	16.1	16.7	0.94	0.93	0.94	1.01	1.10	0.93
				SD	1.48	1.39	1.55	1.37	1.31	1.43	0.01	0.01	0.01	0.18	0.16	0.19
				Upper Limit (Average + 1 SD)	16.9	16.4	17.3	17.8	17.4	18.1						
				Lower Limit (Average - 1 SD)	13.9	13.6	14.2	15.0	14.8	15.3						

Abbreviations: Average (Av), Maximum (Max), Minimum (Min), Longinelli & Nuti (1973) equation (L&N), Chang & Blake (2015) equation (C&B), Standard Deviation (SD).
Five years of soil temperature data was available between January 2013 and December 2017 therefore each temperature parameter is the average of five years for each month.

The relationships between the two equations for the monthly $\delta^{18}O_P$ in the topsoils and subsoils of the uncultivated area of Woodland's Field calculated using maximum, minimum and average temperatures for each month and compared to a 1:1 line are shown in **Figure 7.7**. The temperatures for each parameter were within a constrained range of 15.0 and 16.7°C across both layers (**Table 7.6** and **Table 7.7**) and in all temperature scenarios, there were strong, positive correlations (topsoils = 0.991, 0.992 and subsoils = 0.995) between the equations. Values of $\delta^{18}O$ were offset by +2.14 to 2.20 $^0/_{00}$ in all cases by the Chang & Blake (2015) equation which is in close agreement with the offset in their study of 2.3 $^0/_{00}$ at 37°C in which Ag_3PO_4 was used to determine $\delta^{18}O_P$ rather than fluorination of $BiPO_4$ (Longinelli & Nuti, 1974). Therefore, the equation by Chang & Blake (2015) ist most appropriate for this study where soil phosphate was isolated as Ag_3PO_4.

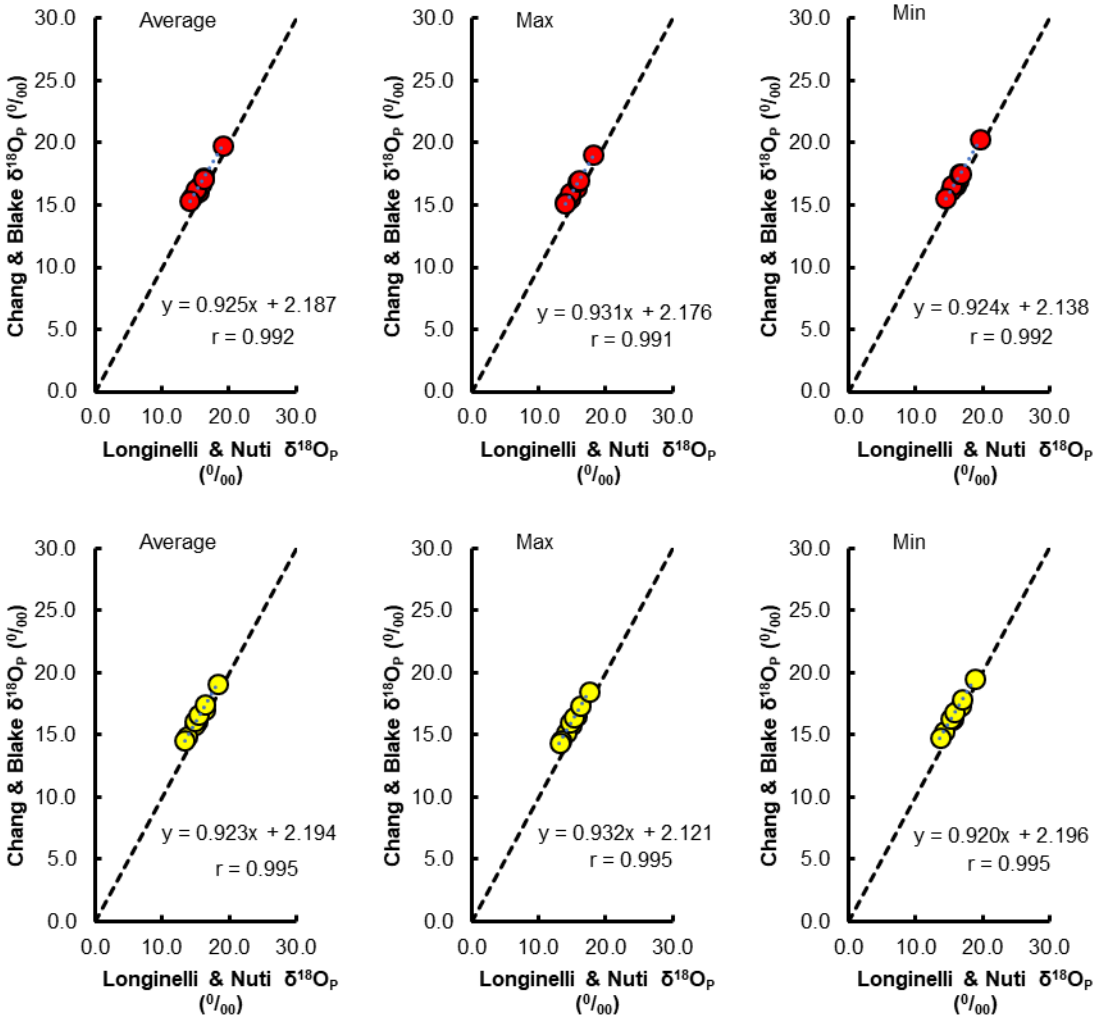


Figure 7.7. Relationship between the monthly $\delta^{18}O_P$ calculated by the two equations in the 9 additional topsoils (red circles) and subsoils (yellow circles) of the uncultivated feld, using maximum, minimum and average temperatures for each month.

7.4.4 Oxygen Yields from Standards and Soil Sample Ag_3PO_4 Precipitates

The relationship between the mass (mg) of samples and standard Ag_3PO_4 and the total CO peak area (representing oxygen yield) is shown in **Figure 7.8**. The average total CO peak area is expected to be 100% ± SD 20% for pure Ag_3PO_4. The average total CO peak area for Alfa-2 standard (97.8% ± 22.9%, n = 104) and B2207 (98.8% ± SD 18.7%, n = 35) were within acceptable limits, and the linear trend-lines overlapped which showed that the standards agreed. If Ag_3PO_4 isolated from a soil sample was pure then analytical data would fall close to that of the Alfa-2 standard and would indicate that Ag_3PO_4 was the source of oxygen (Tamburini, *et al*., 2014). Most samples were similar to the Alfa-2 standard however, on average, the total CO peak area was 114 ± SD 28.1% (n = 349) which suggested the presence of impurities in the Ag_3PO_4 produced from the samples in this study. Furthermore, there was a clear sub-set of samples which had total CO peak areas much higher than the main sample group (> 150%, highlighted in yellow). Although some Alfa-2 standards also showed a similar off-set with total CO peak areas (~ 150%) the Alfa-2 standards $\delta^{18}O_P$ across all seven runs were corrected back to $14.2^0/_{00}$ ± SD $0.27^0/_{00}$ (n = 104) through inter-laboratory calibration. The 'B2207' standards are used to determine the success of each run as they are presented as 'unknowns' with an expected value of $21.7^0/_{00}$ ± 1 SD $0.3^0/_{00}$. In the main study, over all runs, the average B2207 result was $21.41^0/_{00}$ ± 1 SD $0.32^0/_{00}$ (n = 35) which was $0.29^0/_{00}$ less than expected but within the expected standard deviation of the inter-laboratory result of $21.7^0/_{00}$ which confirmed that the analysis was good. Samples with raised total CO peak areas were not excluded in this study and accepted within random analytical errors and experimental errors associated with the precipitation procedure. However, Tonderski, *et al*., (2017) excluded samples in their study with total CO peak ranges out with a minimum and maximum range of 75 and 115%, defined by the lower and upper limits of peak area of their standards ± an additional 10%. Generally, few studies have reported the limits they have adopted (if any) on acceptable total CO peak areas. In this study, the limits would have been between 74.9 and 121% based on the Alfa-2 standard average total CO peak area ± 1 SD but would have been between 66 and 150% if based on the maximum and minimum Alfa-2 standard values, which is the range into which most of the samples fall. Further analysis showed that the elevated total CO peak areas were from samples analysed in one specific run- but not all samples in this run were elevated. This suggested that the oxygen yield from these samples may have been affected by the presence of other sources of oxygen such as organic compounds (Tamburini, *et al*., 2010) or from NO_3 from incomplete washing during the Ag_3PO_4 precipitation and isolation stages of the experiment.

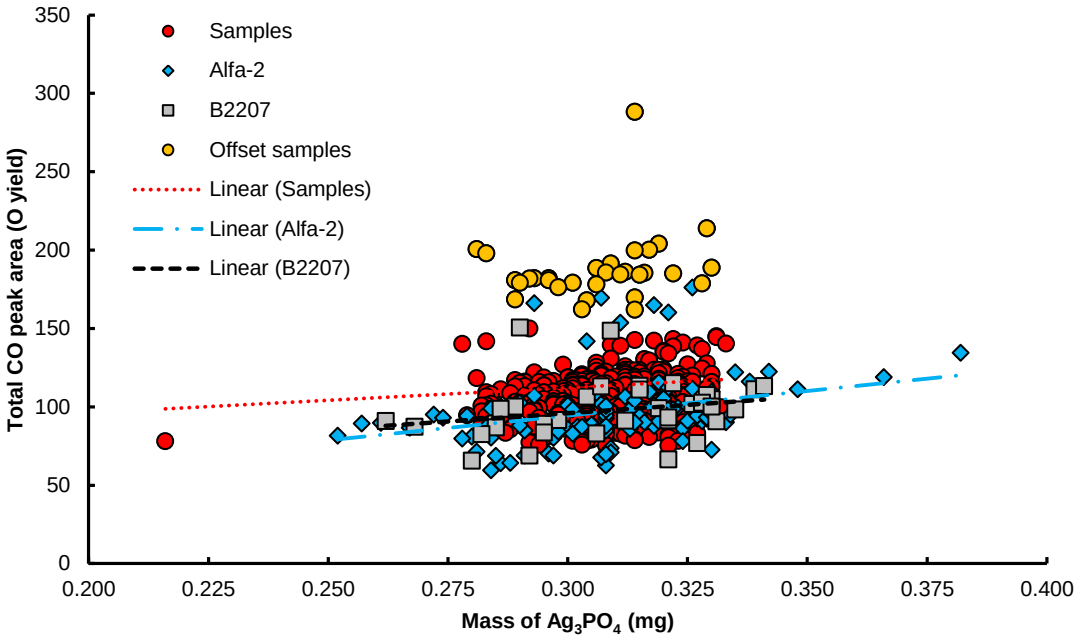


Figure 7.8. Relationship between the mass of Ag_3PO_4 and total CO peak area (oxygen yield) for the samples, Alfa-2 standard (r = 0.356) and B2207 standard.

The relationship between the total nitrogen peak area and the sample % oxygen yield relative to the Alfa-2 standard for samples where both data sets were available (n = 236) is shown in **Figure 7.9**. There was a weak positive correlation between the % oxygen yields relative to the Alfa-2 standard and the total nitrogen peak area (r = 0.325) which may suggest that oxides of nitrogen (such as NO_3) were a contributing factor to the elevated oxygen yields observed. However, the majority of % oxygen yields in samples were relatively constrained between 100 and 150% at a nitrogen peak area of 1 or less. Samples with a nitrogen yield greater than 1 showed elevated oxygen yields greater than 100% but were invariant with the N peak area which suggested that oxides of nitrogen (i.e. NO_3) were not contributing to the elevated oxygen yields.

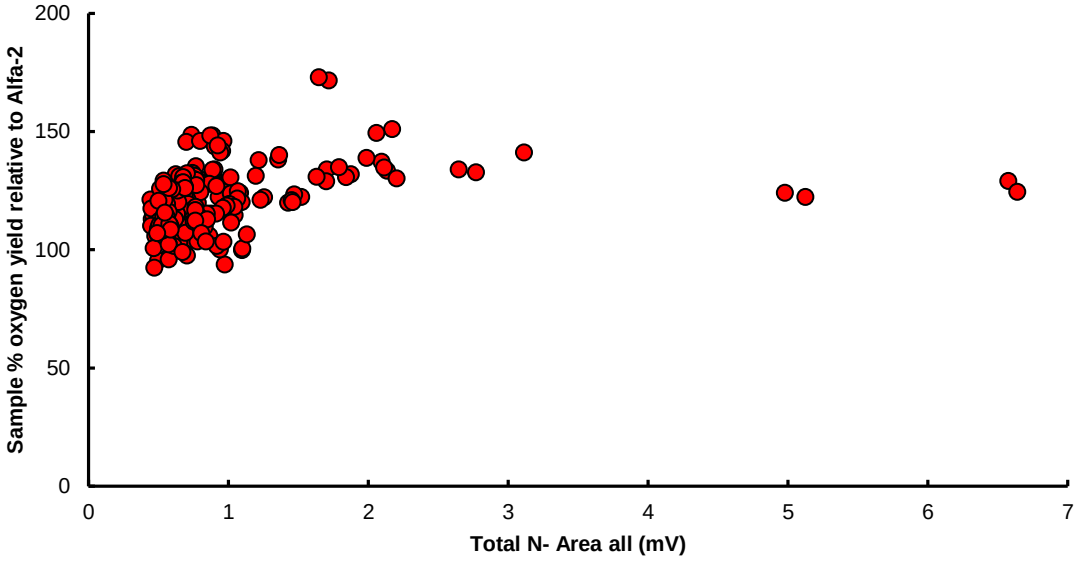


Figure 7.9. Relationship between the total nitrogen peak area and the sample % oxygen yield relative to the Alfa-2 standard for 236 analyses (r = 0.325) where both data sets were available.

7.4.5 The HCl-Extractable P (P_{HCl}) in the Long-Term Experiments

The relationship between P_{HCl} extracted by the non-enriched and the ^{18}O-enriched HCl solution for all soil samples is shown in **Figure 7.10**. There was a strong correlation between the results from both extractions (r = 0.994), with sample values of P_{HCl} ranging from 200 to 1200 mg kg^{-1} likely due to the differences in the experimental treatments of the soil samples that were extracted. The strong correlation between the two extractions for the soil samples was expected because there should be no effect of ^{18}O enrichment on the concentration of P_{HCl} extracted. The slope (0.939) shown in **Figure 7.10** suggests 6% less P in the ^{18}O-enriched HCl solutions.

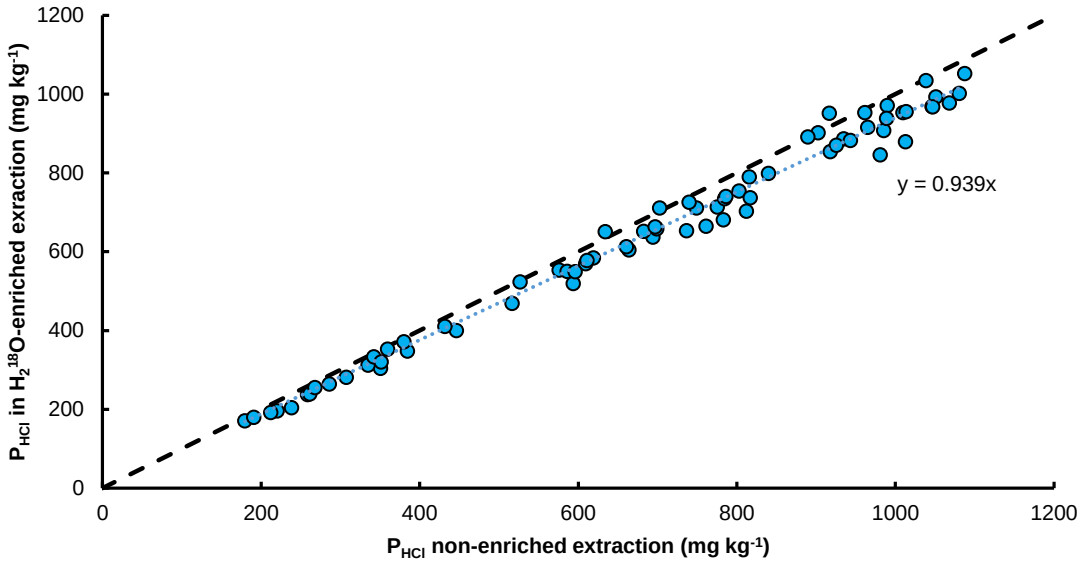


Figure 7.10. Relationship between sample P_{HCl} extracted by the non-enriched HCl vs $H_2{}^{18}O$ enriched HCl solutions: data is forced through zero and compared to a 1:1 (dashed) line.

The relationship between P_{Total} and P_{HCl} in the individual topsoil and subsoil samples in the long-term experiments and the uncultivated field is shown in **Figure 7.11**. As P_{Total} increased throughout the soil profile P_{HCl} also increased with strong, positive correlations between P_{Total} and P_{HCl} in the topsoils (r = 0.987) and subsoils (r = 0.964) across the entire dataset. Topsoil P_{Total} ranged between 913 and 1950 mg kg^{-1} with an average of 1520 mg kg^{-1} (± SD 352 mg kg^{-1}) whereas subsoil P_{Total} ranged from 589 to 1520 mg kg^{-1} with an average of 1090 mg kg^{-1} (± SD 269 mg kg^{-1}). In their phosphate stable oxygen isotope study, Granger, *et al*., (2017a) also reported strong, positive correlations (r = 0.91) between soil P_{Total} and P_{HCl} in an agricultural field with a known 25-year history of intensive grassland management at Rothamsted Research's North Wyke Farm Platform in south-west England.

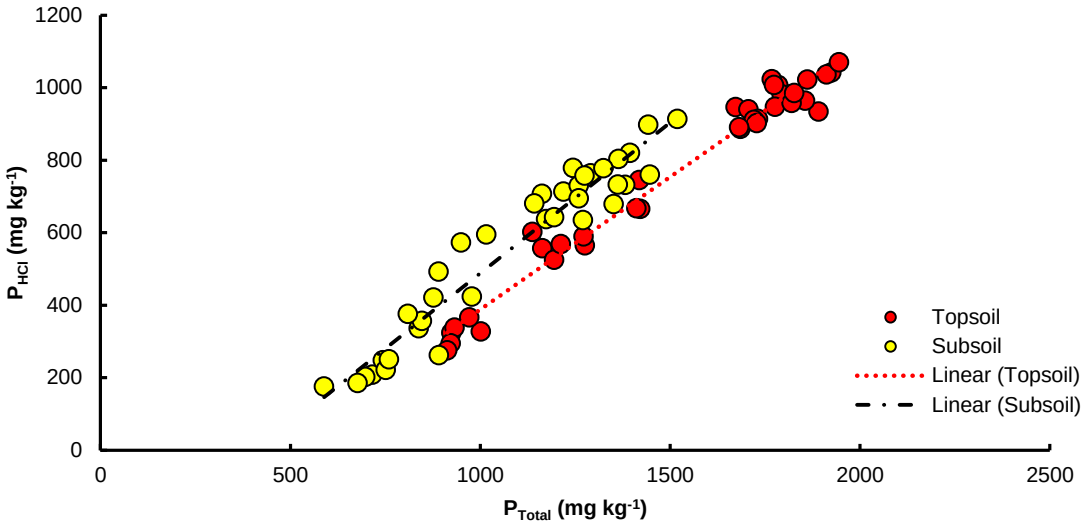


Figure 7.11. Relationship between P_{Total} and P_{HCl} in the topsoils (r = 0.987) and subsoils (r = 0.964) of the long-term experiments.

7.4.5.1 P speciation

Average values of measured soil pH, P_{Total} and P_{HCl} in each of the treatments across both long-term experiments and the uncultivated field are summarised in **Table 7.8**. Average values of P_{HCl} as a proportion (%) of P_{Total} across the dataset were 49.1% (± SD 7.76%) in the topsoil and 49.1% (± SD 11.8%) in the subsoil. Across the entire dataset, a minimum of 28.6% was found in the subsoil of the NK without P plot in the Old Rotation and a maximum of 65% was found in the subsoil of the pH 7 plot in the pH Rotation. The range of P_{Total} that was P_{HCl} ($\%P_{HCl}$) was reflective of the treatment effects: pH control and P fertiliser management.

After 94 years of fertiliser restriction the soil profile which received either NK without P, or zero fertiliser treatments (with the exception of FYM inputs once every six years) had $\%P_{HCl}$ values between 28.6% (NK-P, subsoil) and 35.1% (zero fertiliser, topsoil) (**Table 7.8**). The soil profiles of treatments with mineral P fertilisers had higher values of $\%P_{HCl}$: 48.6% in topsoil from the NK with TSP plot and 36.1% in the subsoil; 45.3% in topsoil from the NK with GMP plot and 41.8% in the subsoil. These high proportions were likely the result of accumulation of inorganic P forms from continuous annual applications of phosphate fertilisers over the 94-year duration of the long-term experiment. These ranges were higher than those found by Amelung, *et al*., (2015) where topsoils of experimental sites, to which no fertiliser was added for more than 20 years, had $\%P_{HCl}$ values between 17.9% and 26.6%. These authors also reported that topsoil in experiments which received mineral fertilisers for over 30 years had $\%P_{HCl}$ values of 20.9 to 23.5%. Finally, Amelung, *et al*., (2015) found that experiments which received organic fertilisers (> 12 years) had a much smaller % P_{HCl} values, between 13.3 and 18.9%. Within a single field $\%P_{HCl}$ can also vary greatly, as reported in Granger *et al*., (2017a) where values of 12 to 48% were reported in an agricultural field which was under intensive grassland management strategies for 25 years. Although the HCl extraction is operationally defined, it is generally accepted that the P_{HCl} pool is made up of slowly exchangeable inorganic phosphates existing partially as poorly soluble calcium phosphate minerals (Tamburini, *et al*., 2014) and also bound to Al and Fe oxides (Helfenstein, *et al*., 2018) and so can be found to represent a greater proportion of the P_{Total} content in soils subject to prolonged P fertiliser application.

In the pH Rotation, it was expected that at low pH (< 5.5) P_{HCl} would be from phosphate strongly adsorbed to Fe and Al oxides, whereas above pH 6, calcium phosphates were likely the main source of P_{HCl}. Regardless, across both topsoils and subsoils and across all pH treatments, a high proportion of the P_{Total} was accounted for by P_{HCl} (between 48.8 to 61.6%) with an average of 55.8% (± SD 2.72%) and no significant trend with soil pH or soil layer. Proportions of $\%P_{HCl}$ of P_{Total} between 48 and 88% were reported by Tian, *et al*., (2016) in soils sampled from two areas of intensive agriculture in Beijing, China.

Table 7.8. Summary of the average (± SEM) measured soil pH values, P_{Total}, P_{HCl} and % P_{HCl} of P_{Total} for the topsoils and subsoil in all treatments in the long-term experiments and the uncultivated area of the Field.

Experiment	Treatment	Layer	Measured pH	P_{Total} (mg kg^{-1})	P_{HCl} (mg kg^{-1})	% P_{HCl} of P_{Total}
Old Rotation	NK with GMP	Topsoil	5.90 ± 0.02	1210 ± 33.5	549 ± 12.1	45.3
Old Rotation	NK with TSP	Topsoil	6.13 ± 0.01	1210 ± 39.0	586 ± 9.87	48.6
Old Rotation	NK without P	Topsoil	5.95 ± 0.02	923 ± 5.55	302 ± 18.6	32.7
Old Rotation	Zero fertiliser	Topsoil	6.11 ± 0.03	966 ± 22.5	339 ± 13.7	35.1
Old Rotation	NK with GMP	Subsoil	6.16 ± 0.01	887 ± 45.3	371 ± 26.4	41.8
Old Rotation	NK with TSP	Subsoil	6.08 ± 0.01	820 ± 38.3	296 ± 40.2	36.1
Old Rotation	NK without P	Subsoil	6.17 ± 0.07	708 ± 22.2	203 ± 10.4	28.6
Old Rotation	Zero fertiliser	Subsoil	6.27 ± 0.03	683 ± 47.7	210 ± 21.1	30.8
pH Rotation	7.5	Topsoil	7.18 ± 0.01	1820 ± 22.2	1000 ± 12.2	55.1
pH Rotation	7	Topsoil	6.97 ± 0.01	1780 ± 8.05	1000 ± 12.1	56.4
pH Rotation	6.5	Topsoil	6.56 ± 0.03	1720 ± 30.4	944 ± 2.01	54.9
pH Rotation	6	Topsoil	6.14 ± 0.04	1710 ± 14.0	903 ± 8.79	52.7
pH Rotation	5.5	Topsoil	5.56 ± 0.07	1770 ± 63.5	909 ± 13.0	51.4
pH Rotation	5	Topsoil	5.22 ± 0.05	1830 ± 10.9	968 ± 8.27	52.8
pH Rotation	4.5	Topsoil	4.90 ± 0.01	1930 ± 9.56	1049 ± 10.4	54.4
pH Rotation	7.5	Subsoil	7.33 ± 0.02	1230 ± 80.9	735 ± 42.7	59.6
pH Rotation	7	Subsoil	7.17 ± 0.03	1400 ± 81.9	863 ± 42.5	61.6
pH Rotation	6.5	Subsoil	6.90 ± 0.04	1320 ± 51.6	749 ± 27.3	56.7
pH Rotation	6	Subsoil	6.40 ± 0.04	1240 ± 35.1	710 ± 37.9	57.2
pH Rotation	5.5	Subsoil	5.81 ± 0.06	1160 ± 135	655 ± 84.6	56.5
pH Rotation	5	Subsoil	5.54 ± 0.05	1050 ± 73.1	603 ± 20.6	57.3
pH Rotation	4.5	Subsoil	5.21 ± 0.05	1170 ± 149	637 ± 108	54.4
Field	Field	Topsoil	5.94 ± 0.04	1420 ± 3.04	692 ± 26.0	48.8
Field	Field	Subsoil	6.18 ± 0.07	1360 ± 50.9	691 ± 39.7	50.9

7.4.5.2 Effect of fertiliser management on P_{HCl} in the Old Rotation

The effect of fertiliser treatment on the P_{HCl} in the topsoils and subsoils of the Old Rotation compared to the Field is shown in **Figure 7.12**. Values of P_{HCl} were greatest in the soil profile of the Field (outside the experimental plots). The Field topsoil and subsoil P_{HCl} were 692 mg kg^{-1} and 691 mg kg^{-1} respectively (topsoil: subsoil P_{HCl} ratio was 1.00). Values of P_{HCl} in topsoils treated with NK and GMP or TSP were 549 and 586 mg kg^{-1} respectively, which equated to 143 and 106 mg kg^{-1} less than in the Field topsoil respectively. The P_{HCl} in the NK without P and the zero fertiliser treatments with P_{HCl} were almost half that of the P treated plots at 302 and 339 mg kg^{-1} respectively. Compared to the Field topsoil, there was 353 mg kg^{-1} less in the zero fertiliser treatment and 390 mg kg^{-1} less in the NK without P treatment. Subsoils were significantly depleted relative to the Field subsoil. Subsoil P_{HCl} was 371 mg kg^{-1} under the NK with GMP treatment and this was 319 mg kg^{-1} less than the Field subsoil. The subsoil of the NK with TSP treatment was lower, with an average of 296 mg kg^{-1}, which was 395 mg kg^{-1} less than the Field subsoil. The subsoil P_{HCl} of the NK without P and zero fertiliser treatments were similar, at 202 and 210 mg kg^{-1} respectively. Both were significantly depleted relative to the Field subsoil, by 488 mg kg^{-1} in the NK without P treatment and by 481 mg kg^{-1} for the zero fertiliser treatment.

The reduction in topsoil and subsoil P_{HCl} as a result of the long-term experiment was evident across all fertiliser treatments, with the effect being greater where P fertiliser was restricted, or zero mineral fertilisers were applied, when compared to the values in the surrounding Field. Whilst the effect of crop phase was not tested in this study, these results may suggest that long-term rotational cropping and fertiliser use for 94 years resulted in the depletion of P_{HCl} stores, relative to the Field not under agricultural management, due to removal in harvested crops. Subsoil P_{HCl} was significantly reduced by between 320 and 490 mg kg^{-1} which suggested that crops may have accessed native subsoil P_{HCl} stocks over the duration of the experiment. Particularly in the NK with GMP or TSP treatments, topsoils were less depleted than subsoils possibly due to re-supply from fertiliser application. In the NK with TSP plot there was almost double the amount of P_{HCl} in the topsoil as the subsoil (topsoil: subsoil ratio of 1.98). The ratio was 1.48 and 1.49 in the NK with GMP and NK without P treatments respectively. Where P fertiliser was restricted, the topsoil: subsoil ratio was 1.61. These results suggested that fertiliser management had increased topsoil P_{HCl} relative to subsoil P_{HCl} and the topsoil: subsoil ratios suggested that continuous inputs of P fertiliser may have been retained in the topsoil and contributed to P_{HCl} and any leaching of fertiliser P to the subsoil may not have been sufficient to counter crop removal rates. These results are in

contrast to Bauke, *et al*., (2018) who found that subsoil P_{HCl} stocks were greater in plots were N and K were applied but P was restricted when compared to plots receiving N, K and P likely due to poor crop productivity resulting in less efficient utilisation of subsoil stable-P stocks such as HCl-extractable P pools.

It is entirely possible that P_{HCl} in the surrounding Field was affected by the proximity to the long-term experiments were high inputs of P fertiliser are applied. The accidental deposition of P fertiliser in the surrounding Field may increase native levels of P_{HCl} in the uncropped areas and margins of the Field. Furthermore, aerial deposition of excrement from wildlife may enrich the topsoils of the Field with P following the consumption of crop grain by birds or the consumption of root crops by wildlife such as deer. Consumption of grain and roots has been observed in the trial and there is a woodland area adjacent to the trials which has been extensively felled in recent years for the construction of the Aberdeen Western Peripheral Route bypass. This is evident in woodland soils adjacent to arable fields were long-term deposition by birds can lead to minor topsoil enrichment of P (Ahmed, *et al*., 2014). Although the grass is cut in the Field, no grass is removed and instead left to mulch, and so the mechanisms of slow accumulation in the topsoil are possible.

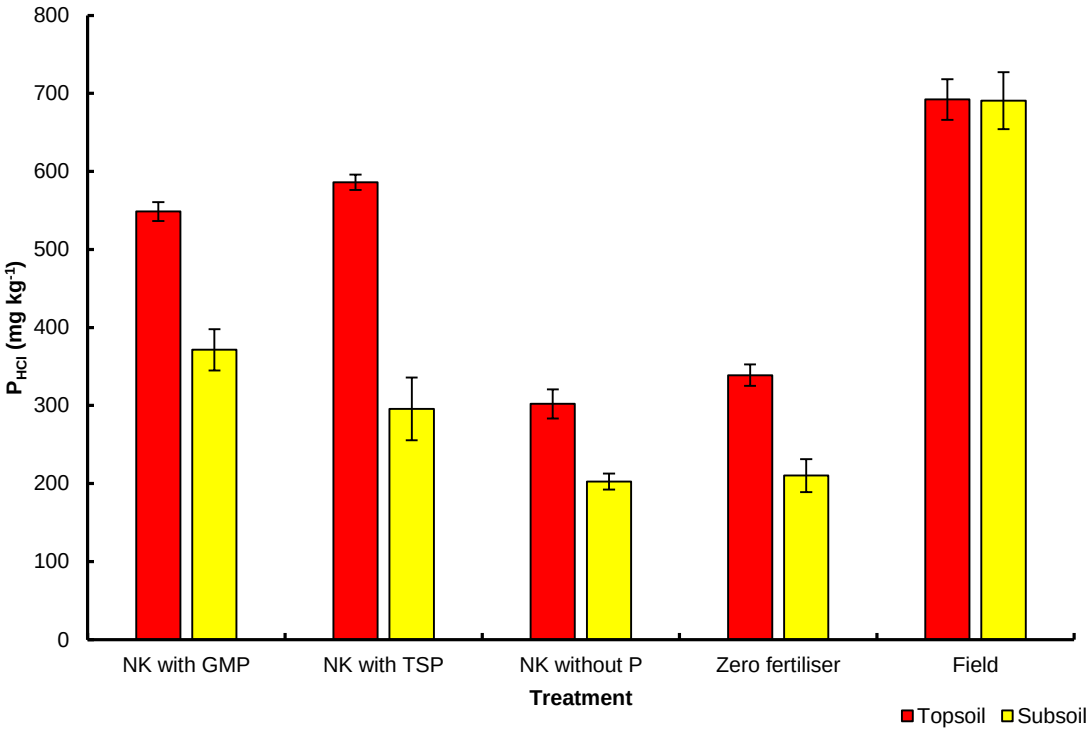


Figure 7.12. The effect of fertiliser treatment on the average (± SEM) P_{HCl} in the topsoils and subsoils of the Old Rotation compared with the soil profile of the Field (uncultivated grassland).

7.4.5.3 Effect of pH control on P_{HCl} in the pH Rotation

The effect of soil pH on topsoil and subsoil P_{HCl} in the pH Rotation and the Field is shown in **Figure 7.13**. There was some variation in topsoil P_{HCl} which decreased from 1050 mg kg^{-1} at pH 4.5 towards a minimum of 903 mg kg^{-1} at pH 6.5 before rising to 1003 mg kg^{-1} at pH 7.5. Across the pH plots the average topsoil P_{HCl} was 969 mg kg^{-1} (± SD 53.8 mg kg^{-1}). Subsoil P_{HCl} increased from a minimum of 603 mg kg^{-1} at pH 5 to a maximum of 863 mg kg^{-1} at pH 7 with an average of 707 mg kg^{-1} (± SD 87.0 mg kg^{-1}) across the pH plots. The topsoil: subsoil ratios decreased from 1.65 at pH 4.5 to 1.16 around pH 7 which suggested that more P was retained in the topsoil at pH 4.5. As the pH increased, desorption of P from Fe and Al oxides such as desorption from goethite (Antelo, *et al*., 2005), and leaching to the subsoil may explain the redistribution of P from topsoil to subsoil. The 3rd order polynomial regression models used to describe the trends in the topsoil and subsoil (**Appendix 4**, **Table 10.30**) were used to predict whether the P_{HCl} across the target soil pH values were significantly elevated compared to the native Field (**section 2.8**). The topsoil P_{HCl} was significantly elevated across all target pH plots than the Field topsoil (pH = 5.94, P_{HCl} = 692 mg kg^{-1}) whereas the pH plot subsoil was not significantly different to the Field subsoil (pH = 6.18, P_{HCl} = 691 mg kg^{-1}) (**Appendix 4**, **Table 10.31**). The pH plots did not show significant depletion relative to the Field; the topsoil appears to be elevated while subsoils appear unchanged. However, in the Old Rotation, plots appeared to be depleted relative to the Field and the annual application of P fertilisers do not account for the differences between the two experiments. The main differences could be due to the differences in the length of the trials, with the Old Rotation lasting 93 years whereas the pH Rotation was only 54 years. Historically, the Old Rotation received less P fertiliser between 1922 and 1991 than it has done since 1991 to the present day (see **section 2.1.1**). Furthermore, the pH Rotation has received consistently higher applications of P since 1991 and has more crop phases (and thus more P fertiliser applied over one rotation cycle) which could also explain why the pH Rotation had higher P_{HCl} levels than the Old Rotation.

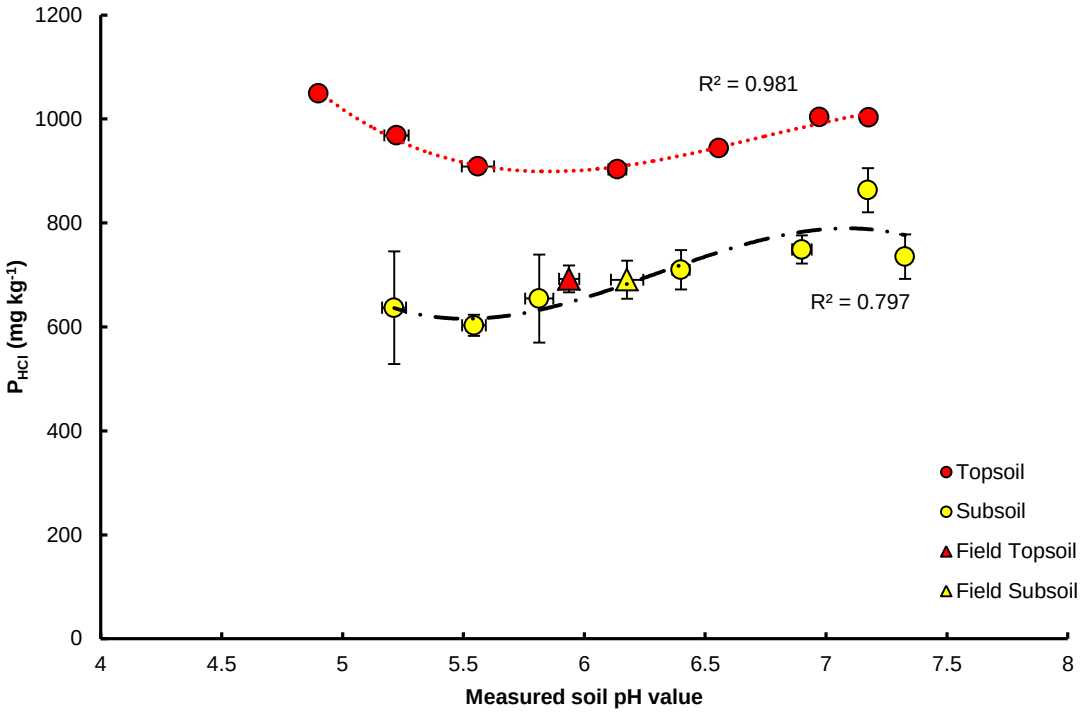


Figure 7.13. Effect of soil pH control on the mean (± SEM) topsoil and subsoil P_{HCl} in the pH Rotation compared to the soil profile of the Field (uncultivated grassland). Topsoil and subsoils are fitted with 3rd order polynomials.

7.4.6 Topsoil and Subsoil $\delta^{18}O_P$ in the Long-Term Experiments

7.4.6.1 Non-enriched vs ^{18}O-enriched HCl $\delta^{18}O_P$ values

The comparison between the $\delta^{18}O_P$ values of the non-enriched and enriched HCl extraction $\delta^{18}O_P$ values for all treatments in topsols (red circles) and subsoils (yellow circles) in the study are compared to a 1:1 line and shown in **Figure 7.14**; the labels indicate the experimental treatment (i.e. 5.0 = pH 5.0 plot). The standard errors of the $\delta^{18}O_P$ data were generally less than $0.5^0/_{00}$, with most < $1^0/_{00}$ and a few exceptions between 1 and $2^0/_{00}$ which reflected spatial variability likely arising from variation within treatment plots and random error throughout the precipitation and isolation stages of the HCl-extractable soil phosphate. There did not appear to be a particular treatment effect however topsoil $\delta^{18}O_P$ tended to be greater in the enriched extractant more than in the subsoils which suggested that hydrolysis of organic P may have occurred during the extraction with 1M HCl causing incorporation of enriched ^{18}O from the reagent into the isolated phosphate (McLaughlin, *et al*., 2006a). This was expected to be greater in the topsoil simply because of the greater concentration of organic matter.

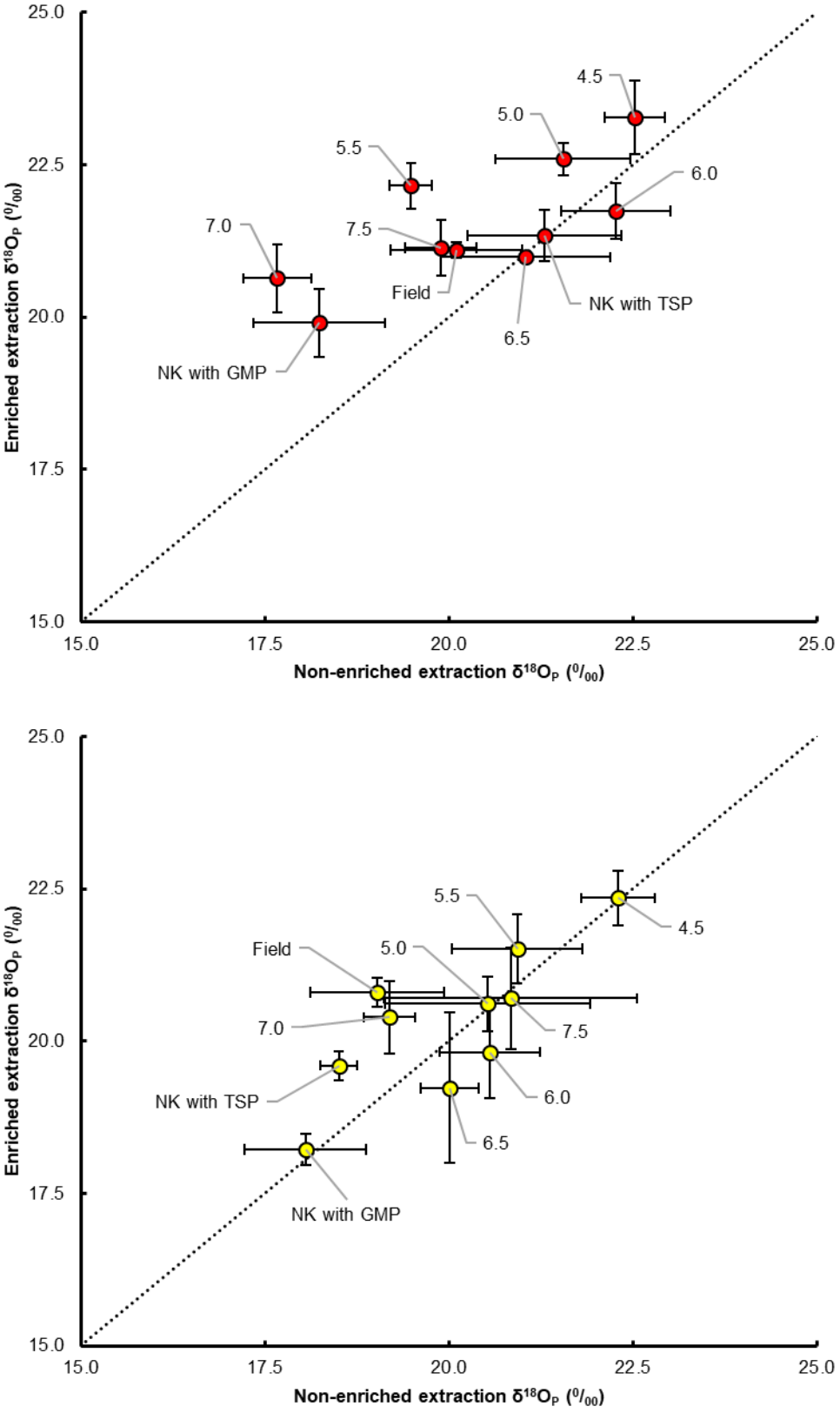


Figure 7.14. Comparison of the non-enriched and enriched HCl extractable $\delta^{18}O_P$ for the plots compared to a 1:1 line in topsoils (red circles) and subsoils (yellow circles).

7.4.6.2 Reference $\delta^{18}O_P$ values for fertiliser materials, native soils and theoretical soil pore water equilibrium ranges

Two 'reference' $\delta^{18}O_P$ values were obtained to characterise the effect of fertiliser treatment: (i) soil samples taken from the Field surround the trials were assumed to represent 'native' $\delta^{18}O_P$ values without agricultural management and (ii) the fertiliser material $\delta^{18}O_P$ for TSP and GMP. The theoretical soil water phosphate equilibrium ranges were used as a third reference (**section 7.3.8**). The $\delta^{18}O_P$ values for the fertiliser materials used in the long-term experiments and the topsoil and subsoil of the Field are summarised in **Table 7.9**. The 'enriched' and 'non-enriched' $\delta^{18}O_P$ values represent the $\delta^{18}O_P$ from the PO_4^{3-} extracted by the ^{18}O-enriched HCl and non-enriched HCl respectively. The corrected $\delta^{18}O_P$ value accounts for the incorporation of ^{18}O from hydrolysis during the HCl extraction and the O: P ratio is used to identify whether the isolation of PO_4^{3}- was successful (ideal value 4.0 ± SD 0.2) (see **section 7.3.6** and **7.3.7**).

The analysis of the fertiliser materials revealed isotopically distinct signatures between the TSP and GMP applied to the field trials (**Table 7.9**). There was a difference of $0.204^0/_{00}$ between the $\delta^{18}O_P$ of the ^{18}O-enriched and non-enriched HCl extraction of the GMP fertiliser. The enriched extraction of GMP had an average $\delta^{18}O_P$ of $21.3^0/_{00}$ (± SEM $0.215^0/_{00}$) and the non-enriched extraction resulted in an average $\delta^{18}O_P$ of $21.2^0/_{00}$ (± SEM $0.329^0/_{00}$). The isolation of PO_4^{3-} from the GMP fertiliser was successful with 99.6% (±SEM 1.09%) of the PO_4^{3-} unaffected by the incorporation of ^{18}O due to hydrolysis of organic P, confirmed by the O: P ratio of 3.99 ± SEM 0.02. This was expected because the fertiliser materials should be purely inorganic PO_4^{3-} and free from organic sources of PO_4^{3-}. The corrected $\delta^{18}O_P$ for the GMP fertiliser was therefore $21.2^0/_{00}$ (± SEM $0.064^0/_{00}$). The TSP fertiliser was also unaffected by the ^{18}O extraction with a difference of -0.537 between the average $\delta^{18}O_P$ of the^{18}O-enriched ($23.8^0/_{00}$ ± SEM $0.432^0/_{00}$) and non-enriched ($24.3^0/_{00}$ ± SEM $0.491^0/_{00}$) HCl extractions. The negative value shown was due to analytical error. The percentage not exchanged (**Equation 7.3**) was 101% (± SEM 2.25%) and the O: P ratio was 4.02 (± SEM 0.04) indicating the successful isolation of PO_4^{3-} subject to minor errors in the analysis as the fertiliser materials are expected to be pure and free from other sources of PO_4^{3-}. The corrected $\delta^{18}O_P$ value and thus the reference value for the TSP was $23.9^0/_{00}$ (± SEM $0.074^0/_{00}$). The results for both fertiliser materials were within around the expected range of 19.6 to $23.1^0/_{00}$ for commercial fertilisers (Gruau, *et al*., 2005).

In the field surrounding the trials (Field) there was a difference of $1^0/_{00}$ between the topsoil $\delta^{18}O_P$ of the ^{18}O-enriched HCl and non-enriched HCl extractions which indicated a minor effect of hydrolysis and incorporation of organic P (**Table 7.9**). The non-enriched $\delta^{18}O_P$ value was $20.1^0/_{00}$ (± SEM $0.895^0/_{00}$) and the ^{18}O-enriched extraction $\delta^{18}O_P$ value was $21.1^0/_{00}$ (± SEM $0.131^0/_{00}$). The O: P ratio was 3.96 (± SEM 0.03, n = 3) and 97.9% (± SEM 1.71%, n = 3) of the PO_4^{3-} was not exchanged with the reagent water oxygen. Therefore, the topsoil reference value for the Field i.e. the 'corrected' $\delta^{18}O_P$ value accounting for the minor incorporation was $20.7^0/_{00}$ (± SEM $0.439^0/_{00}$). There was a difference of $1.77^0/_{00}$ between the ^{18}O-enriched HCl and non-enriched HCl extractions in the subsoil of the Field, with an average non-enriched extraction $\delta^{18}O_P$ value of $19.0^0/_{00}$ (± SEM $0.916^0/_{00}$) and ^{18}O-enriched extraction $\delta^{18}O_P$ value of $20.8^0/_{00}$ (± SEM $0.239^0/_{00}$). The O: P ratio in the subsoil was 3.93 (± 0.04) and up to 96.3% (± SEM 1.89%) of the isolated soil PO_4^{3-} was not exchanged with ^{18}O during the HCl extraction indicating again minor (negligible) effect of hydrolysis and incorporation of reagent ^{18}O. The corrected $\delta^{18}O_P$ in the subsoil was therefore $20.0^0/_{00}$ (± SEM $0.457^0/_{00}$). The assumption that the uncultivated Field results respresent native $\delta^{18}O_P$ may be flawed because it is possible that P in the Field is affected by the proximity to the long-term experiments which receive annual P fertiliser inputs. Deposition of P fertiliser transferred across the Field to the plots may alter the $\delta^{18}O_P$ signature in the Field towards that of the fertiliser. Deposition of crop and grain residues post-harvest may also influence native levels because the $\delta^{18}O_P$ signature may be altered within the plant (Pfahler, *et al*., 2013; Pfahler, *et al*., 2017). Furthermore, native $\delta^{18}O_P$ in topsoils in particular may be affected by the deposition of P from the excrement of wildlife such as birds (Ahmed, *et al*., 2014) or grazers such as rabbits. Although it might be expected that animals deposit P with lower $\delta^{18}O_P$ values due to the internal equilibration of P with body water (Amelung, *et al*., 2015). However, assuming that the Field is unaltered from aerial deposits of P from other sources, it was expected that the Field topsoil and subsoil would fall within the equilibrium $\delta^{18}O_P$ range for the topsoil ($15.4^0/_{00}$ to $18.0^0/_{00}$) and subsoil ($15.0^0/_{00}$ to $17.8^0/_{00}$). This is because the theoretical equilibrium ranges are calculated using Field $\delta^{18}O_P$. They are also calculated using an average of the soil pore water $\delta^{18}O_W$ values taken from fresh topsoil and subsoil samples over a period of 9 months. The corrected $\delta^{18}O_P$ for the Field topsoil (20.7 ± SEM $0.439^0/_{00}$) and subsoil (20.0 ± SEM $0.457^0/_{00}$) were outwith the theoretical soil pore water equilibrium ranges and were isotopically enriched in comparison. Angert, *et al*., (2011) showed in their study, average $\delta^{18}O_P$ values of soil P_{HCl} ($16.5^0/_{00}$) which were within the calculated soil pore water equilibrium range of 16 to $19.5^0/_{00}$ and concluded that the P_{HCl} had been thoroughly processed by soil microorganisms. Therefore, it is possible that the Field has become isotopically enriched due to long-term inputs from other sources arising from the proximity to the trials; the fertilisers that are applied

to the trials have higher $\delta^{18}O_P$ values; TSP ($23.9^0/_{00}$) and GMP ($21.2^0/_{00}$). Thus, the Field $\delta^{18}O_P$ shall be used, with some caution, to represent the native $\delta^{18}O_P$ (unchanged due to agricultural management), alongside the soil pore water equilibrium $\delta^{18}O_P$ values, with the understanding that the Field $\delta^{18}O_P$ values may have been affected by external sources of P.

Table 7.9. Summary of $\delta^{18}O_P$ values of the GMP and TSP fertiliser materials and the topsoil and subsoil of the Field (uncultivated grassland); values are mean ± SEM.

Sample	Layer	Non-enriched $\delta^{18}O_P$ ($^0/_{00}$)	Enriched $\delta^{18}O_P$ ($^0/_{00}$)	Corrected $\delta^{18}O_P$ ($^0/_{00}$)	Enriched - non-enriched $\delta^{18}O_P$ ($^0/_{00}$)	% Not exchanged	O:P ratio
Field	Topsoil	20.1 ± 0.895	21.1 ± 0.131	20.7 ± 0.439	1.00	97.9 ± 1.71	3.96 ± 0.03
	Subsoil	19.0 ± 0.916	20.8 ± 0.239	20.0 ± 0.457	1.77	96.3 ± 1.89	3.93 ± 0.04
GMP fertiliser		21.1 ± 0.329	21.3 ± 0.215	21.2 ± 0.064	0.204	99.6 ± 1.09	3.99 ± 0.02
TSP fertiliser		24.3 ± 0.491	23.8 ± 0.432	23.9 ± 0.074	-0.537	101 ± 2.25	4.02 ± 0.04

7.4.6.3 Effect of soil pH control on topsoil and subsoil $\delta^{18}O_P$ values in the pH Rotation

The results of the $\delta^{18}O_P$ analysis for the target pH plots in the pH Rotation are shown in **Table 7.10** along with the Field topsoil and subsoil and the TSP fertiliser material for reference. The $\delta^{18}O_P$ for the non-enriched and ^{18}O-enriched HCl extractions and also the $\delta^{18}O_P$ corrected for exchange (**Equation 7.2**) and incorporation of the HCl reagent oxygen (**Equation 7.3**) are summarised (see **section 7.3.6** and **7.3.7** for calculations). Differences between the enriched and non-enriched $\delta^{18}O_P$ data for all samples across the pH plots was an average of $0.596^0/_{00}$ (± SD $1.16^0/_{00}$, n = 14) which suggested that hydrolysis of organic P and the incorporation of ^{18}O from the HCl reagent was minimal. This was further supported by the calculation of 'average percentage of oxygen *not* being exchanged' which was 98.6% (± SD 2.44%). Finally, O: P ratios were on average 3.98 ± (SD 0.05, n = 14), effectively 4.0, which confirmed that there was a minimal effect of fractionation and incorporation of oxygen from organic P compounds with lower O: P ratios into the Ag_3PO_4 precipitate (Tamburini, *et al*., 2010). Corrected $\delta^{18}O_P$ values for topsoil and subsoils were, on average, $21.3^0/_{00}$ (± SD $1.20^0/_{00}$) and $20.7^0/_{00}$ (± SD $0.99^0/_{00}$) respectively with a minimal difference of $0.6^0/_{00}$ between the average of the two layers. The minimum $\delta^{18}O_P$ value was found in the subsoil of the pH 7 plot at $19.3^0/_{00}$ (± SEM $0.270^0/_{00}$) and the maximum value was $23.0^0/_{00}$ (± SEM $0.500^0/_{00}$) found in the topsoil of the pH 4.5 plot. Overall, it can be expected that soil $\delta^{18}O_P$ may range between $5^0/_{00}$ and $25^0/_{00}$ (Tamburini, *et al*., 2014) and these results are closer to the upper limit. The results across the pH gradient were slightly higher than the topsoil $\delta^{18}O_P$ values in long-term experiments where no fertiliser was applied ($21.6^0/_{00}$) or where mineral fertiliser was applied ($19.8^0/_{00}$) (Amelung, *et al*., 2015). Subsoil $\delta^{18}O_P$ signatures between $12^0/_{00}$ and $16^0/_{00}$ (Bauke, *et al*., 2018) at depths of 40 to 90 cm have been reported. Amelung, *et al*., (2015) reported subsoil values between $14^0/_{00}$ and $17^0/_{00}$ at depths of 40 to 80 cm and also $12^0/_{00}$ and $13^0/_{00}$ at depths between 80 and 120 cm (Amelung, *et al*., 2015). Values between $10^0/_{00}$ and $20^0/_{00}$ were observed in the chronosequence of a glacier forefield (Tamburini, *et al*., 2012).

Table 7.10. Summary of the $\delta^{18}O_P$ analysis for the target soil pH plots in the pH Rotation and also the Field soil profile and TSP fertiliser material for reference. Results are mean of 3 replicates ± SEM except (^{o}) n = 2 and (^{x}) n = 4.

Treatment	Layer	Non-enriched $\delta^{18}O_P$ ($^{0}/_{00}$)	Enriched $\delta^{18}O_P$ ($^{0}/_{00}$)	Corrected $\delta^{18}O_P$ ($^{0}/_{00}$)	Enriched - non-enriched $\delta^{18}O_P$ ($^{0}/_{00}$)	% Not exchanged	O:P ratio
Field	Topsoil	20.1 ± 0.895	21.1 ± 0.131	20.7 ± 0.439	1.00	97.9 ± 1.71	3.96 ± 0.03
	Subsoil	19.0 ± 0.916	20.8 ± 0.239	20.0 ± 0.457	1.77	96.3 ± 1.89	3.93 ± 0.04
TSP fertiliser		24.3 ± 0.491 ^{x}	23.8 ± 0.432	23.9 ± 0.074	-0.537	101 ± 2.25	4.02 ± 0.04
4.5	Topsoil	22.5 ± 0.410	23.3 ± 0.597	23.0 ± 0.500	0.748	98.5 ± 0.844	3.97 ± 0.016
4.5	Subsoil	22.3 ± 0.500	22.4 ± 0.451 ^{o}	22.5 ± 0.309 ^{o}	1.038	101 ± 0.742	4.02 ± 0.014
5	Topsoil	21.6 ± 0.917	22.6 ± 0.264	22.2 ± 0.413	2.67	97.9 ± 1.929	3.96 ± 0.037
5	Subsoil	20.5 ± 1.397	20.6 ± 0.456	20.5 ± 0.873	-0.531	99.8 ± 1.941	4.00 ± 0.038
5.5	Topsoil	19.5 ± 0.288	22.2 ± 0.374	21.1 ± 0.152	-0.06	94.5 ± 1.300	3.89 ± 0.025
5.5	Subsoil	20.9 ± 0.883	21.5 ± 0.564	21.3 ± 0.299	2.970	98.8 ± 2.712	3.98 ± 0.053
6	Topsoil	22.3 ± 0.737	21.7 ± 0.454	21.9 ± 0.397	1.242	101 ± 1.753	4.02 ± 0.034
6	Subsoil	20.6 ± 0.678	19.8 ± 0.753	20.1 ± 0.701	0.049	102 ± 0.403	4.03 ± 0.008
6.5	Topsoil	21.0 ± 1.151	21.0 ± 0.095	21.0 ± 0.418	0.082	100 ± 2.556	4.00 ± 0.050
6.5	Subsoil	20.0 ± 0.392	19.2 ± 1.233	19.6 ± 0.820	0.581	102 ± 1.848	4.03 ± 0.036
7	Topsoil	17.7 ± 0.466	20.6 ± 0.560	19.3 ± 0.270	-0.73	93.9 ± 1.869	3.88 ± 0.036
7	Subsoil	19.2 ± 0.343	20.4 ± 0.595	19.9 ± 0.336	-0.78	97.5 ± 1.585	3.95 ± 0.031
7.5	Topsoil	19.9 ± 0.488	21.1 ± 0.462	20.6 ± 0.454	1.20	97.4 ± 0.681	3.95 ± 0.013
7.5	Subsoil	20.8 ± 1.721	20.7 ± 0.833	20.7 ± 1.129	-0.140	100 ± 2.327	4.01 ± 0.045

The effects of target soil pH on the topsoil and subsoil $\delta^{18}O_P$ are shown in **Figure 7.15**. The Field topsoil and subsoil $\delta^{18}O_P$ are plotted against the measured soil pH values to compare to the treatment plots. The upper and lower limits of the average $\delta^{18}O_P$ for the TSP fertiliser ($23.9^0/_{00}$ ± SEM $0.07^0/_{00}$) which is applied to these plots is also shown for reference. Finally, the upper and lower limits (based on the average ± 1 SD) of the theoretical pore water equilibrium $\delta^{18}O_P$ ranges for the topsoil ($15.4^0/_{00}$ to $18.0^0/_{00}$) and subsoil ($15.0^0/_{00}$ to $17.8^0/_{00}$) are also shown for comparison. There were various expected outcomes in this experiment and these are summarised here prior to discussion.

1. The original (first) hypothesis was that freshly applied highly soluble TSP fertiliser may move rapidly to the subsoil, bypassing microbial processing in the topsoil, and become fixed as apatite at high pH (< pH 6) and oxide-bound P at low pH (> pH 6), thus retaining a $\delta^{18}O_P$ signature close to the TSP assuming the subsoil is relatively abiotic (Taylor, *et al*., 2002).

2. A second hypothesis was that the solubility (and therefore the rate of leaching) was also expected to be pH-dependent and so TSP may be strongly retained as apatite (high pH) or adsorbed to Fe and Al oxides (low pH) in the *topsoil* and thus be rendered both unavailable for microbial processing and leaching. Thus, the $\delta^{18}O_P$ in the *topsoil* may be closer to that of the TSP, especially at acid and alkaline pH values. Maximum solubility and therefore availability of P in soil solution for microbial processing and potential leaching to the subsoil was expected to occur around pH 6.5. Therefore, topsoil $\delta^{18}O_P$ may be closer to the soil pore water equilibrium range between pH 6 and pH 7.

3. A third hypothesis was that biological processing and the equilibration of fertiliser phosphate with the soil pore water may be faster than the topsoil-to-subsoil transfer of P. If biological processing continued in the subsoil, then phosphate throughout the soil profile may be closer to equilibrium with the soil pore water oxygen. This may be the case if the topsoil and subsoil $\delta^{18}O_P$ are relatively similar as highly processed $\delta^{18}O_P$ becomes evenly distributed throughout the soil profile.

The average topsoil $\delta^{18}O_P$ in the pH 4.5 plot was $23.0^0/_{00}$ (± SEM $0.500^0/_{00}$) and the average subsoil $\delta^{18}O_P$ was $22.5^0/_{00}$ (± SEM $0.309^0/_{00}$) in the subsoil (**Figure 7.15**). There was a small difference of $0.5^0/_{00}$ between the topsoil and subsoil. Both the topsoil and subsoil average $\delta^{18}O_P$ were close to the TSP

signature which was 23.9‰ (± SEM 0.074‰). This suggested that TSP was retained in the topsoil, by abiotic processes (Gross & Angert, 2015) such as fixation to Al and Fe oxides and so were unavailable for exchange with soil pore water oxygen. These results also suggested that TSP was rapidly leached to the subsoil where it was fixed and retained its $\delta^{18}O_P$ signature and did not undergo biological processing which is rapid (Paytan, *et al*., 2002; Blake, *et al*., 2005) and so it appeared that biological processing of TSP fertiliser and soil water was minimal in this plot. In the pH 5 plot the topsoil $\delta^{18}O_P$ was 22.2‰ (± SEM 0.413‰) and the subsoil $\delta^{18}O_P$ was 20.5 (± SEM 0.873‰) with a difference of 1.7‰ between the two layers. This suggested that topsoil P was more available for processing, perhaps due to weaker adsorption strength with rising pH, and was partially processed by microorganisms before leaching to the subsoil where it may have continued to be processed towards equilibrium. Furthermore, the topsoil $\delta^{18}O_P$ remained closer to the TSP fertiliser signature reflecting retention of TSP possibly through adsorption. In the pH 5.5 treatment, topsoil and subsoil $\delta^{18}O_P$ were almost identical at 21.1‰ (± SEM 0.152‰) and 21.3‰ (± SEM 0.299‰) respectively. The further decrease in the $\delta^{18}O_P$ of the topsoil may have been due to greater solubility of P as the adsorption with Fe and Al oxides decreased and interactions with Ca increased with rising pH (Weng, *et al*., 2011). It also suggested that the third (counter) hypothesis may hold true where biological mixing surpassed topsoil to subsoil transfer of P and so the $\delta^{18}O_P$ throughout the soil profile was more even. As both layers had not yet reached the theoretical soil pore water equilibrium this suggested that equilibration was not complete and that both layers were still moving towards full exchange with soil pore water oxygen. However, in comparison to the Field soil profile, the results were fairly similar and if these were taken as reference values than perhaps the pH 5.5 treatment was almost at the expected $\delta^{18}O_P$.

The topsoil and subsoil $\delta^{18}O_P$ in the pH 6 and 6.5 plot showed a similar pattern, with topsoils closer to the TSP signature and the subsoils apparently moving closer towards soil pore water equilibrium. This was the pH range where maximum P solubility (and the minimum $\delta^{18}O_P$) was expected and it was also expected that relatively insoluble calcium phosphates would be the main control of this process which was shown in **Chapter 5**. However, minimal values of topsoil and subsoil $\delta^{18}O_P$ across the pH gradient were found in the pH 7 treatment. The subsoil $\delta^{18}O_P$ (19.9‰ ± SEM 0.336‰) was 0.6‰ greater than the topsoil $\delta^{18}O_P$ (19.3‰ ± SEM 0.270‰). Both were close to the soil pore water equilibrium $\delta^{18}O_P$ ranges which suggested that a large degree of biological processing had occurred to alter the original

TSP $\delta^{18}O_P$ signature throughout the soil profile. Finally, at pH 7.5 there was a very small difference of $0.1^0/_{00}$ topsoil and subsoil $\delta^{18}O_P$ of $20.6^0/_{00}$ (± SEM $0.454^0/_{00}$) and $20.7^0/_{00}$ (± SEM $1.129^0/_{00}$) respectively. The slight increase in $\delta^{18}O_P$ at pH 7.5 suggested that biological processing was declining with rising pH, possibly due to the precipitation of calcium phosphates such as hydroxyapatite removing the amount of P available in solution for equilibration.

Overall the results suggested that the second hypothesis held true: topsoil-to-subsoil transfer of fertiliser P increased with soil pH where a maximum distribution and equilibration was reached in the pH 7 plot. Strong adsorption of TSP fertiliser to Fe and Al oxides likely explained why topsoil and subsoil $\delta^{18}O_P$ signatures were approximate to the fertiliser $\delta^{18}O_P$ particularly at pH 4.5 which suggested that the first hypothesis was in part, also true. Generally, P_{HCl} in subsoils were highly processed and closer to the soil pore water equilibrium than topsoils which suggested that P was retained in the topsoil, and leached to the subsoil and the additions of fresh TSP almost every year might have caused the topsoil $\delta^{18}O_P$ to remain closer to the TSP. In this crop phase, no TSP fertiliser had been applied for 2 years and so this suggested that complete equilibration of P had not occurred in this timeline if referring to the theoretical soil pore water equilibrium $\delta^{18}O_P$. If considering the Field topsoil and subsoil are considered the true background $\delta^{18}O_P$ then it appeared that the treatment subsoils $\delta^{18}O_P$ were unchanged > pH 5.5 but whether this was because highly processed P from the topsoil had moved to the subsoil or whether the subsoil represented older stocks of mineral P is unclear. Subsoils < pH 5.5 may have become $\delta^{18}O_P$ enriched either (i) by processed P leaching from the topsoil or (ii) from rapid leaching of topsoil P which is then slowly processed in the subsoil, thus possibly indicating that biological processing increases in the subsoil with rising pH towards 6.5.

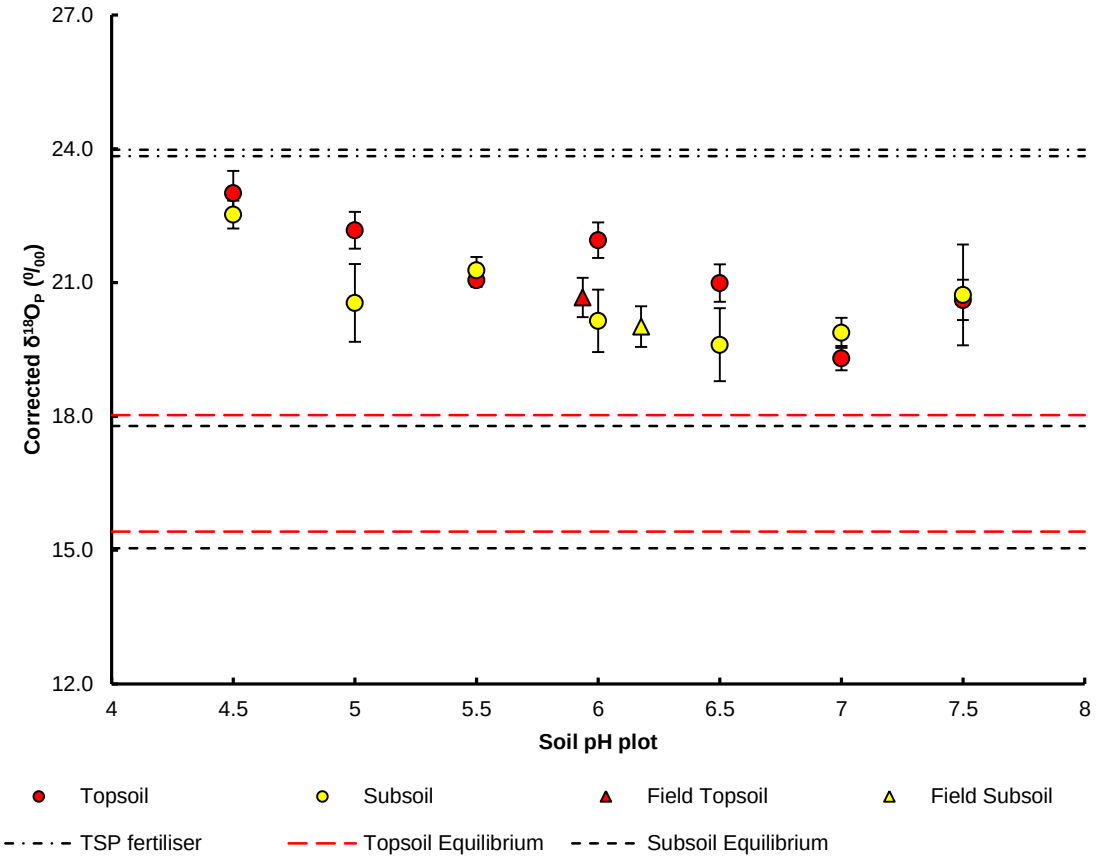


Figure 7.15. Effect of soil pH target on the corrected $\delta^{18}O_P$ for topsoils and subsoils in the pH Rotation (n = 3, mean ± SEM except for pH 4.5 subsoil (n=2)). Upper and lower soil pore water equilibrium ranges for topsoil and subsoil are calculated using the mean temperature (± 1 SD). TSP fertiliser corrected $\delta^{18}O_P$ is included for reference (mean ± 1 SD). Field topsoil and subsoil corrected $\delta^{18}O_P$ values are plotted against their measured soil pH values.

7.4.6.4 The effect of P fertilisers on topsoil and subsoil $\delta^{18}O_P$ values in the Old Rotation

The results of the $\delta^{18}O_P$ analysis for the non-enriched and ^{18}O-enriched HCl extractions and the $\delta^{18}O_P$ values corrected for the enrichment (**Equation 7.2**) in the fertiliser treatments of the Old Rotation are summarised in **Table 7.11**. Enriched $\delta^{18}O_P$ values were from samples extracted with ^{18}O-enriched HCl and the non-enriched $\delta^{18}O_P$ values were for samples extracted with non-enriched HCl. The extent of the effect of ^{18}O incorporation into the P_{HCl} due to hydrolysis with the reagent is expressed as '% not exchanged' (**Equation 7.3**) and also in the O: P ratio (**Equation 7.4**). The greatest difference between the ^{18}O-enriched and non-enriched values of $\delta^{18}O_P$ occurred in the topsoil of the plot treated with NK and GMP ($1.67^0/_{00}$) and there was a minimal difference in the topsoil of the NK with TSP treatment ($0.040^0/_{00}$) which are acceptable differences. Overall, the differences between enriched and non-enriched $\delta^{18}O_P$ values for the dataset were small at an average of $0.68^0/_{00}$ (± SD $0.83^0/_{00}$) which suggested that hydrolysis of organic-P was minimal. Granger, *et al*., (2017a) reported differences no greater than $1^0/_{00}$ between duplicate soil extractions. This conclusion was further supported by the high percentage that was not exchanged, which was on average 98.6% (± SD 1.65%). Finally, the O: P ratios were, on average, 3.97 (± SEM 0.03), effectively 4.0, which confirmed that the effect of fractionation and incorporation of oxygen from organic P in to the Ag_3PO_4 was minimal.

Table 7.11. Summary of the topsoil and subsoil mean $\delta^{18}O_P$ (± SEM) for the fertiliser treatments, Field soil profile and the TSP and GMP fertiliser materials used in the Old Rotation.

Sample	Layer	Non-enriched $\delta^{18}O_P$ ($^0/_{00}$)	Enriched $\delta^{18}O_P$ ($^0/_{00}$)	Corrected $\delta^{18}O_P$ ($^0/_{00}$)	Enriched - non-enriched $\delta^{18}O_P$ ($^0/_{00}$)	% Not exchanged	O:P ratio
Field	Topsoil	20.1 ± 0.895	21.1 ± 0.131	20.7 ± 0.439	1.00	97.9 ± 1.71	3.96 ± 0.03
	Subsoil	19.0 ± 0.916	20.8 ± 0.239	20.0 ± 0.457	1.77	96.3 ± 1.89	3.93 ± 0.04
GMP fertiliser		21.1 ± 0.329	21.3 ± 0.215	21.2 ± 0.064	0.204	99.6 ± 1.09	3.99 ± 0.02
NK with GMP	Topsoil	18.2 ± 0.888	19.9 ± 0.557	19.1 ± 0.615	1.67	96.6 ± 1.70	3.93 ± 0.03
	Subsoil	18.1 ± 0.827	18.2 ± 0.263	18.1 ± 0.326	0.17	99.7 ± 2.08	3.99 ± 0.04
TSP fertiliser		24.3 ± 0.491	23.8 ± 0.432	23.9 ± 0.074	-0.537	101 ± 2.25	4.02 ± 0.04
NK with TSP	Topsoil	21.3 ± 1.05	21.3 ± 0.414	21.3 ± 0.445	0.040	99.9 ± 2.51	4.00 ± 0.05
	Subsoil	18.5 ± 0.254	19.6 ± 0.239	19.1 ± 0.242	1.09	97.7 ± 0.29	3.96 ± 0.01

The effects of fertiliser treatments, NK with GMP or TSP, on topsoil and subsoil $\delta^{18}O_P$ in the Old Rotation, corrected for hydrolysis effects, are shown in **Figure 7.16**. Unfortunately, no results were obtained for the treatments 'zero fertiliser' and 'NK without P' to compare the restriction of P fertiliser to the use of P fertilisers on $\delta^{18}O_P$ values in the Old Rotation. These plots did not yield any Ag_3PO_4 for $\delta^{18}O_P$ analysis because not enough PO_4^{3-} was present in the HCl extraction. In order to explore the $\delta^{18}O_P$ values in the Old Rotation and the effect of fertiliser treatment, it is first necessary to summarise the references used to characterise the effects of treatments on topsoil and subsoil $\delta^{18}O_P$ in the plots. The $\delta^{18}O_P$ for the (uncultivated grassland) Field, the GMP and TSP fertiliser materials and the theoretical soil pore water-phosphate equilibrium ranges for both layers are included in **Figure 7.16** as three references with which to compare the effects of the fertiliser treatments (see **section 7.4.6.2**). The uncultivated Field topsoil and subsoil provide a possible 'native' $\delta^{18}O_P$ value for the local soil to investigate the cycling and transfer of P fertiliser throughout the soil profile in the long-term experiments - although this may not be strictly valid as $\delta^{18}O_P$ measured in the uncultivated margin may be affected by other inputs. The theoretical soil pore water equilibrium ranges provide a third reference for comparison as discussed previously. The corrected Field topsoil $\delta^{18}O_P$ ($20.7^0/_{00}$) and subsoil $\delta^{18}O_P$ ($20.0^0/_{00}$) did not fall within the theoretical $\delta^{18}O_P$ ranges for the topsoil (15.4 to $18.0^0/_{00}$) or subsoil (15.0 to $17.8^0/_{00}$) as discussed in **section 7.4.6.2**. The two fertiliser materials had distinct 'corrected' $\delta^{18}O_P$ values: the average $\delta^{18}O_P$ for the TSP fertiliser was $23.9^0/_{00}$ and the GMP fertiliser was $21.2^0/_{00}$ and both of these values fell within the expected range for chemical fertilisers (Tamburini, *et al*., 2014).

The original hypothesis for this experiment was that phosphate may be rapidly leached to the subsoil after the application of highly soluble mono-calcium phosphate (TSP) (bypassing rapid processing in the topsoil) where it might become fixed as a relatively insoluble Ca phosphate (apatite) or perhaps adsorbed to Fe and Al oxides and so would retain a $\delta^{18}O_P$ value closer to the original fertiliser signature. It might be reasonable to expect that subsoil $\delta^{18}O_P$ would be moving towards soil-pore water equilibration if relatively slower biological processing continued in the subsoil. Continued processing of P in the subsoil was observed in $\delta^{18}O_P$ signatures reported by Bauke, *et al*., (2018) for example. For the GMP fertiliser, which is relatively insoluble, following application it may be expected to persist longer in the topsoil, become more highly biologically processed, and leach slowly to the subsoil over time and therefore have a $\delta^{18}O_P$ value closer to the theoretical soil pore water equilibrium $\delta^{18}O_P$ throughout the soil profile. The counter hypothesis was that the biological processing of soluble TSP in the topsoil was rapid and faster than topsoil to subsoil transfer processes thus a relatively uniform $\delta^{18}O_P$ signature would develop throughout

the profile in line with the soil equilibrium $\delta^{18}O_P$ values. The hypothesis is explored and discussed throughout this section.

Cycling of GMP fertiliser in the topsoil and subsoil

The $\delta^{18}O_P$ in the topsoil receiving NK with GMP as the source of P was on average $19.1^0/_{00}$ (± SEM $0.615^0/_{00}$, n = 3) and the subsoil was $18.1^0/_{00}$ (± SEM $0.326^0/_{00}$, n = 3) with a difference of $1^0/_{00}$ between the two layers (**Figure 7.16**). These topsoil and subsoil $\delta^{18}O_P$ values were much lower than the GMP fertiliser $\delta^{18}O_P$ ($21.2^0/_{00}$) and also lower than the Field topsoil and subsoil $\delta^{18}O_P$ of $20.7^0/_{00}$ and $20.0^0/_{00}$ respectively, whilst being near to the upper limits of the theoretical soil equilibrium $\delta^{18}O_P$ in the topsoil ($18.0^0/_{00}$) and subsoil ($17.8^0/_{00}$) of the Field. This suggested that the GMP fertiliser applied to the plots underwent biological processing in the topsoil as the $\delta^{18}O_P$ was lowered throughout the soil profile towards equilibrium. The isotopic signature in both the topsoil and subsoil was close to the upper limits of the theoretical soil pore water equilibrium ranges calculated for both layers suggesting that the GMP was highly processed in the soil. The small difference between the topsoil and subsoil suggested that either (i) P was rapidly equilibrated in the topsoil and leached to the subsoil maintaining a uniform signature in the profile above the indurated layer (40 cm) or (ii) the P was partially cycled in the topsoil and leached to the subsoil where biological processing continued. Thus, the hypothesis for the GMP fertiliser appeared to be proven in that topsoil and subsoil signatures were relatively similar suggesting persistence in the topsoil with slower biological processing due to the insolubility of the fertiliser and thus slower leaching of P with $\delta^{18}O_P$ in equilibration with the soil pore water.

Cycling of TSP fertiliser in the topsoil and subsoil

In contrast to the GMP plot, the plot treated with NK and TSP as the main source of P showed that the topsoil $\delta^{18}O_P$ was $21.3^0/_{00}$ (± SEM $0.445^0/_{00}$, n = 3) and the subsoil was $19.1^0/_{00}$ (± SEM $0.242^0/_{00}$, n = 3) with a difference of $2.2^0/_{00}$ between the two layers (**Figure 7.16**). The topsoil $\delta^{18}O_P$ was closer to the TSP fertiliser $\delta^{18}O_P$ signature ($23.9^0/_{00}$) than the upper limit of the topsoil pore water equilibrium ($18.0^0/_{00}$) whereas the subsoil was closer to the upper limit of the subsoil pore water equilibrium range ($17.8^0/_{00}$). This suggests that fresh TSP may be cycled rapidly and leached to the subsoil where the TSP $\delta^{18}O_P$ signature then continues to be processed towards equilibrium and the application of TSP directly to the topsoil maintains a $\delta^{18}O_P$ signature closer to the fertiliser. However, these plots have not received TSP applications for 3 years and so for the topsoils to retain a signature closer to the TSP $\delta^{18}O_P$ suggests that biological cycling and equilibration in the topsoil is slow which is not expected because biological

processing results in rapid exchange with water (Paytan, *et al*., 2002; Blake, *et al*., 2005) and P is more actively cycled in topsoils than subsoils (Joshi, *et al*., 2016). The soil pH in these plots is between pH 5 and 6, and so it is more likely that the highly soluble TSP fertiliser dissolves quickly and becomes adsorbed to Fe and Al oxides and thus becomes less labile due to abiotic soil processes (Gross & Angert, 2015) and is un-available for exchange with water. It is also possible that P is desorbed from Fe and Al oxides, partially cycled and is re-adsorbed which would explain why the topsoil $\delta^{18}O_P$ has moved towards equilibrium. Some of this desorbed P may become fully processed and leached to the subsoil, or partially processed and leached to the subsoil were biological mixing continues (Bauke, *et al*., 2018) thus explaining why the subsoil $\delta^{18}O_P$ values was closer to equilibrium. It is also possible that the internal equilibration of $\delta^{18}O_P$ signatures and subsequent deposition of P in to the subsoil from decaying roots could alter the isotopic signature in the subsoil however more research is required to understand the contribution of plant processes to soil $\delta^{18}O_P$ values (Pfahler, *et al*., 2017; Frossard, *et al*., 2011). Finally, it is important to mention the possibility of subsoil $\delta^{18}O_P$ values being affected by historical application of farm yard manure to the plots. Rapid leaching between the topsoil and subsoil of highly processed P from farmyard manure in previous crop phases may also contribute to a lower subsoil $\delta^{18}O_P$ values because calculated $\delta^{18}O_P$ values of farm yard manure tend to be lower due to internal equilibration with body water at 37^{o}C (Amelung, *et al*., 2015). The main conclusion from this analysis therefore, is that the original hypothesis is not supported: subsoil $\delta^{18}O_P$ values were closer to equilibrium $\delta^{18}O_P$ values and *not* to the fertiliser $\delta^{18}O_P$ values signature which suggested rapid leaching and bypassing of biological equilibration *did not occur*. However, the counter hypothesis is also unsupported in that the NK with TSP plot topsoil and subsoil $\delta^{18}O_P$ values were not uniform, nor in line with soil pore water equilibrium values, suggesting that rapid biological processing and subsequent leaching of highly processed TSP did not occur. The evidence suggests that highly soluble TSP fertiliser was rapidly fixed in the topsoil following application and retained a $\delta^{18}O_P$ signature closer to the source fertiliser due to abiotic controls (Gross & Angert, 2015). The main control of solubility in these plots is thought to be adsorption to Fe and Al oxides due to the pH of the plots < pH 6 (see chapter 5) and so the relatively rapid adsorption of fertiliser P to Fe and Al oxides would mean that P was fixed and un-available for biological processing thus retaining the isotopic signature of the fertilisers. The recent cropping history of these plots (grass for 3 years) meant that a minimal amount of P fertiliser was applied at the beginning of the three-year grass phases and so if the TSP fertiliser was available for biological processing, the signature would be closer to equilibrium due to rapid equilibrium by microorganisms (Paytan, *et al*., 2002; Blake, *et al*., 2005). Apart from one harvest of hay in the first year, P is not removed the plots although the grass is cut monthly and left to mulch on the

surface during years 2 and 3 which may encourage biological mixing and equilibration of P in the topsoil. However, under grass for three years, cycling of P fertiliser through microbial action appears to have been slow; the topsoil was closer to the TSP signature than the Field topsoil or the topsoil equilibrium range. Over time, the slow desorption and migration of P towards the subsoil could explain why the subsoil is more closely aligned to the soil pore water equilibrium, if the processing of P continues in the subsoil. If the subsoil in the plots consisted of much older, processed P, perhaps it would match the Field subsoil $\delta^{18}O_P$ unless the subsoil has been impacted from aerial inputs of P in to the topsoil which have then significantly altered the 'native' $\delta^{18}O_P$ in the subsoil. This does not support the hypothesis that freshly applied P fertiliser bypasses the topsoil and is fixed in the subsoil where the $\delta^{18}O_P$ would more closely resemble that of the fertiliser $\delta^{18}O_P$. Instead, it is likely that P is retained in the topsoil where it is processed slowly before migrating into the subsoil.

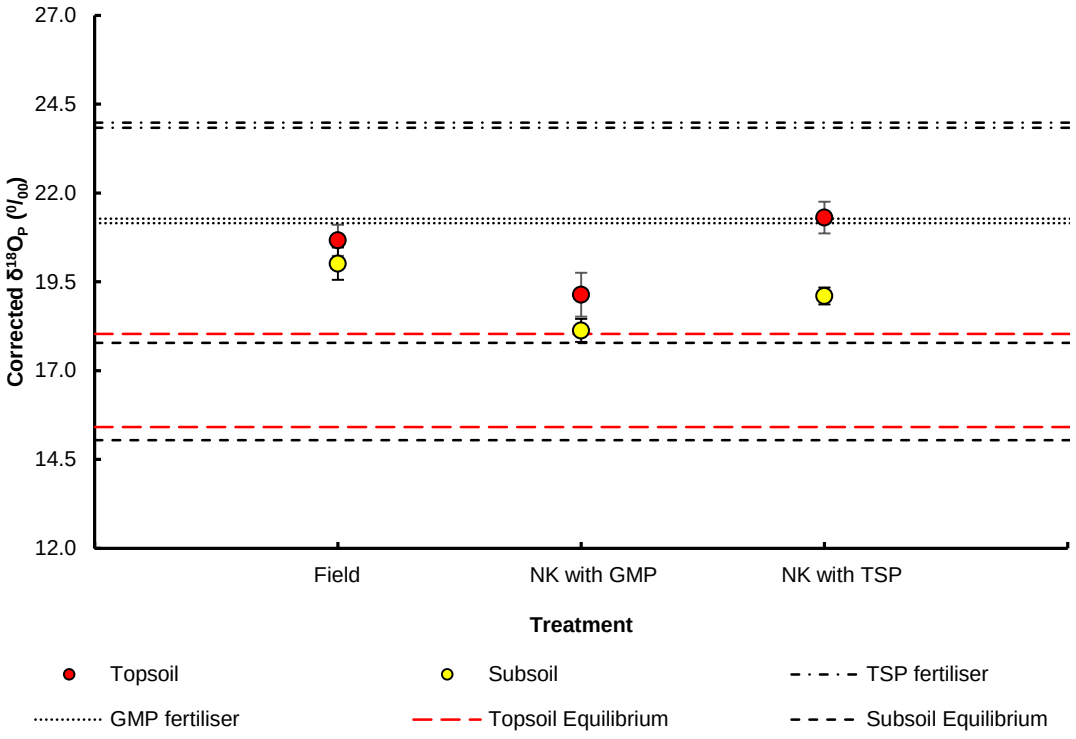


Figure 7.16. Effect of fertiliser treatment on corrected $\delta^{18}O_P$ in the topsoil and subsoil compared to the uncultivated grassland (Field), the TSP and GMP $\delta^{18}O_P$ and the topsoil and subsoil $\delta^{18}O_P$ equilibrium ranges. The upper and lower limits of the $\delta^{18}O_P$ equilibrium ranges, TSP and GMP fertilisers, are set as the mean ± 1 SD.

7.5 Conclusions

The processes influencing the cycling and transfer of P in the topsoil to subsoil of long-term experiments were investigated using measurement of $\delta^{18}O_P$ in soil P_{HCl} (Tamburini, *et al*., 2010) from a pH-controlled experiment (pH 4.5 to 7.5 in increments of 0.5 pH units) and a fertiliser management experiment contrasting the use of TSP and GMP fertilisers.

The hypothesis that relatively insoluble GMP fertiliser would persist in the topsoil and undergo biological processing before leaching to the subsoil appeared proven in that topsoil and subsoil $\delta^{18}O_P$ signatures were relatively similar and appeared to move towards equilibration with the soil pore water $\delta^{18}O_P$. Highly soluble TSP fertiliser appeared to be partially biologically cycled in the topsoil because the $\delta^{18}O_P$ value was between that of the fertiliser and the soil pore water equilibrium value. It seems likely that abiotic soil processes retained TSP in the topsoil rendering it relatively unavailable for isotopic exchange. If P is retained on soil surfaces, and unavailable in the soil pore water for microbial uptake and processing, then this suggests that the P fertiliser is also not available to plants which obtain P from the soil solution through their roots. Slow leaching of processed TSP to the subsoil and continued cycling in the subsoil may have contributed to the movement of subsoil $\delta^{18}O_P$ towards equilibrium. This evidence does not support the initial hypothesis that freshly applied, highly soluble TSP fertiliser would bypass biological mixing in the topsoil through rapid leaching to the subsoil where it would become fixed and so the value of $\delta^{18}O_P$ would more closely resemble that of the fertiliser $\delta^{18}O_P$. Instead, it seemed likely that P was retained in the topsoil by abiotic soil processes where it was partially equilibrated and migrated slowly into the subsoil where biological mixing may have continued. Furthermore, the counter hypothesis also appeared unlikely: biological mixing in the topsoil was not faster than topsoil to subsoil transfer because topsoil and subsoil $\delta^{18}O_P$ signatures were not uniform. This suggests that the rate movement of P from the topsoil and subsoil varies with pH and this is important to consider in arable agricultural systems as soil pH naturally buffers towards the natural pH over time following alteration by lime.

In the pH Rotation plots there was evidence of both retention of relatively non-biologically cycled TSP in the topsoil and rapid leaching of TSP into the subsoil (< pH 5.5) as $\delta^{18}O_P$ signatures in both layers were closer to the $\delta^{18}O_P$ of TSP than to the soil pore water equilibrium values. By contrast, the maximum solubility and availability of P between pH 6 and 7 was reflected in greater processing of P towards the soil pore water equilibrium $\delta^{18}O_P$ values. This shows that microbial activity is more efficient at turning over fertiliser P within an optimal pH range for crop productivity and this is important for overall soil health.

Results across the pH gradient suggested that the second hypothesis held true: topsoil to subsoil solubility and rate of transfer of fertiliser P was pH-dependent and TSP was strongly retained within Fe and Al oxides (low pH), and partially as apatite at high pH in the *topsoil*. Thus, the $\delta^{18}O_P$ in the *topsoil* was closest to that of the TSP at pH 4.5 due to abiotic processes. The retention of the TSP $\delta^{18}O_P$ signature in the subsoil at pH 4.5 supported the original hypothesis that TSP might be rapidly transferred without undergoing biological transformation in the topsoil. Maximum solubility and therefore availability of P in the soil solution for microbial processing and potential leaching to the subsoil did occur around pH 6.5 and the topsoil and subsoil $\delta^{18}O_P$ were relatively uniform and closer to the soil pore water equilibrium range between pH 6 and pH 7.

Future work may consider investigating the effect of each of the crop phases on the $\delta^{18}O_P$ and applying the P_{HCl} isolation procedure to a wider range of samples. In the absence of a crop effect this may verify the results presented here. In the presence of a crop effect, this would provide insights in to the cycling of P under different crop regimes within a rotational setting. Furthermore, investigating the $\delta^{18}O_P$ of crop material could also provide further insights into the uptake of fertiliser P by crops and how this is processed internally within the plant thus providing a wider overview of the crop-soil system (Pfahler, *et al*., 2013). Finally, and most importantly, characterising a wider range of operationally defined compartments of soil $\delta^{18}O_P$ (especially organic forms) may provide useful insights in to the cycling of P through different soil biological and chemical processes (Helfenstein, *et al*., 2018). Through greater understanding of the processes controlling the fate and cycling of fertiliser P, fertiliser use efficiency can be improved on farm as decisions regarding the solubility of P fertiliser can be made in order to maximise Pavailability. For example, whether to apply TSP or GMP inorganic fertilisers, compared to applying farm yard manure which may contain more labile forms of P but can also increase the soil organic matter content.

8 Conclusions

The aim of this project was to understand topsoil and subsoil phosphorus (P) dynamics in long-term experiments and this aim was achieved using SRUC's Woodland's Field Rotations. The Old Rotation is a fertiliser management trial established in 1922. The pH Rotation was established in 1961 and consists of plots with a range of target pH values from pH 4.5 to 7.5 in 0.5 increments. The effect of fertiliser management, soil pH control and cropping on P dynamics in topsoils and subsoils was investigated using a range of traditional and innovative analytical techniques. The unique contribution of this work has been to our understanding of topsoil and also *subsoil* P dynamics under sustained management regimes. Crucially, insights into the nature, and potential agronomic significance, of subsoil P have been revealed and the implications will be discussed within this section.

In Chapter 3, the effects of soil pH control, cropping and fertiliser management on the accumulation and distribution of P fertiliser and associated contaminants (As, Cd and U) were investigated. It was found that, in the pH Rotation, subsoil pH values matched topsoil target pH values due to long-term liming creating a virtually zero pH gradient from 0 – 40 cm depth. The Ca_{Total} increased with rising pH from 7000 at pH 4.5 to 13,000 mg kg^{-1} at pH 7.5 with topsoil: subsoil ratios rising from less than 1.00 at pH 4.5 to 1.75 at pH 7.5. Topsoil P_{Total} (1770 to 1930 mg kg^{-1}) was significantly enriched relative to the Field P_{Total} (1380 mg kg^{-1}) due to long-term TSP application regardless of soil pH but there was no significant P_{Total} accumulation in the pH plot subsoils (1050 to 1260 mg kg^{-1}) compared to the Field subsoil (1100 mg kg^{-1}). The topsoil: subsoil ratio at pH 4.5 was 1.84 and the near convergence of both layers at pH 6 (ratio 1.40) showed greater redistribution of P_{Total} as a result of pH control. The net annual P_{Total} accumulation rates (relative to the Field P_{Total}) across all pH plots show that they are apparently accumulating between 0.86 to 51.5 kg ha^{-1} yr^{-1} of fertiliser P but was not specific to a particular pH. The results show that P in P_{Total} is strongly retained in the topsoil at acid pH values (pH < 5.5) by adsorption to Fe and Al oxides. Between pH 6 and 7, P_{Total} re-distribution from topsoil to subsoil is greatest where P is most soluble.

In the Old Rotation, topsoil and subsoil P_{Total} under all fertiliser management strategies (NK with TSP or GMP or without P and zero fertilisers) were *depleted* relative to the Field due to long-term cropping. The most severe depletion was found in the plots where P fertiliser was withheld, and the reduction in subsoil P_{Total} (compared to the uncultivated Field) suggested crops had acquired native P stocks over the lifetime of the trials with net annual soil profile P_{Total} depletion rates ranging from -0.9 to -22.2 kg ha^{-1} yr^{-1}.

The accumulation of contaminants As, Cd and U were associated with P fertiliser in both trials with Cd particularly associated with GMP and U with TSP use. The maximum concentrations of As_{Total} (7.75 mg kg^{-1}) and Cd_{Total} (0.295 mg kg^{-1}) in the soils were five and ten times less, respectively, than the permissible limits in soils which have had sewage sludge applied. Therefore, the build-up of P fertiliser associated contaminants is of minor concern in these long-term experiments.

In Chapter 4, the plant-availability of topsoil and subsoil P was assessed using the Olsen (P_{Olsen}) and Modified Morgan ($P_{MMorgan}$) extraction methods. On average across the entire dataset of the pH Rotation and Old Rotation, topsoil P_{Olsen} was 2.53% and $P_{MMorgan}$ was 0.60% of P_{Total} whereas in the subsoil, P_{Olsen} was 1.84% and $P_{MMorgan}$ was 0.59% of the P_{Total}. Subsoil P_{Olsen} ranged from 21.7 to 35.2 mg kg^{-1} and $P_{MMorgan}$ ranged from 7.03 to 10.2 mg kg^{-1}; both sets of results show subsoil available-P to be at a level assumed to be optimal for crop P requirements in most cases (AHDB, 2015; Sinclair, *et al*., 2010). The plots had become significantly enriched compared to the Field P_{Olsen} topsoil (25.3 mg kg^{-1}) and subsoil (18.5 mg kg^{-1}) and $P_{MMorgan}$ topsoil (4.67 mg kg^{-1}) and subsoil (3.95 mg kg^{-1}). The high subsoil levels coupled with high topsoil P_{Olsen} (36.4 to 74.5 mg kg^{-1}) and $P_{MMorgan}$ (8.73 to 17.1 mg kg^{-1}) suggest adequate P supplies for crops throughout the soil profile. The topsoil: subsoil ratios for P_{Olsen} and $P_{MMorgan}$ at pH 4.5 were 3.0 and 2.0 respectively and were a minimum at pH 6 where the ratios decreased to 1.5 and close to 1.0 respectively. This shows greatest P solubility and movement from the topsoil to the subsoil at pH values within the preferred agronomic range. The high P_{Olsen} and $P_{MMorgan}$ levels in all pH plot subsoils show that fertiliser P moves to the subsoil and remains reactive regardless of pH. In the Old Rotation, P_{Olsen} in the topsoil was depleted relative to the Field except when TSP was applied (34.2 mg kg^{-1}), compared to GMP (16.2 mg kg^{-1}), and least when no fertilisers were used (between 10 and 12 mg kg^{-1}). Subsoil P_{Olsen} was depleted under TSP (17.4 mg kg^{-1}), GMP (16.2 mg kg^{-1}) and restriction of P fertilisers (10.2 to 11.3 mg kg^{-1}). There were similarities in $P_{MMorgan}$ where the topsoil under TSP (7.49 mg kg^{-1}) and GMP (5.96 mg kg^{-1}) were enriched compared to the Field and the plots not receiving P fertilisers (3.52 to 4.72 mg kg^{-1}). Subsoil $P_{MMorgan}$ was elevated under TSP (4.96 mg kg^{-1}) and GMP (4.21 mg kg^{-1}) compared to zero P fertiliser plots (2.82 to 3.16 mg kg^{-1}) which confirms that available-P moves to the subsoil when P fertilisers are used. Although plots were generally depleted in plant-available P in the Old Rotation, the use of TSP and GMP seemed to maintain the soil P concentrations compared to those of the uncultivated Field. This work shows that the subsoils contain significant concentrations of available-P for crops regardless of soil pH. However, the most significant elevations in subsoil were seen between pH 6 and 7 which is the optimum range for arable crops. The use of TSP fertiliser has a greater impact on

available P than GMP. However, these extraction techniques only measure the capacity of the soils to provide plant-available P and do not say anything about the underlying mineralogy that controls the solubility of P in solution or the labile P which is reversibly exchangeable between the solid and solution phases.

In Chapter 5, geochemical speciation modelling using WHAM-VII to resolve free ion activities and a phosphate potential vs lime potential stability plot, revealed the dominant mineralogy controlling P solubility across both the long-term experiments. Analysis of the pH gradient in the pH Rotation showed that the dominant mineralogy controlling P solubility changed with rising soil pH. In all plots with a topsoil and subsoil pH > 6, hydroxyapatite was the dominant calcium-phosphate mineral controlling P solubility whereas below pH 5.5, plots were under-saturated with respect to hydroxyapatite. In the Old Rotation, the solubility of HPO_4^{2-} and $H_2PO_4^-$ was mainly controlled by adsorption reactions with Fe/ Al oxide surfaces, as these plots were all under-saturated with respect to hydroxyapatite regardless of fertiliser treatment (NK with GMP, TSP or without P, and zero fertiliser application). Hydroxyapatite is the least soluble calcium phosphate mineral and so the solubility of P in solution is likely to be low in these agricultural soils. This finding is significant because the solubility of P minerals can improve crop yield and production. Further work in the Old Rotation and pH Rotation may consider evaluating the role of the dominant minerals in the topsoil and subsoil on crop yields and production.

In Chapter 6, the lability and distribution of P between the solid and solution phase was investigated using the Diffusive Gradients in Thin-Films (DGT) technique to determine the 'effective' P concentration in solution (P_{DGT}) and P distribution coefficient (K_d). The main findings from the pH Rotation were (i) P_{DGT} increased between pH 4.5 and 7.5 in topsoils (70.4 to 108 µg L^{-1}) and subsoils (15.1 to 69.3 µg L^{-1}), (ii) the equilibrium distribution coefficient (K_d) between the solid and solution phases decreased with rising pH for P_{Olsen} topsoils (1100 to 363 mL g^{-1}) and subsoils (1520 to 390 mL g^{-1}) and $P_{MMorgan}$ topsoils (693 to 179 mL g^{-1}) and subsoils (255 to 99.2 mL g^{-1}) and (iii) the rate at which the soil could resupply P to the solution (R_{DGT}) increased with soil pH in both topsoils (0.324 to 0.544) and subsoils (0.221 to 0.549). Despite apparently high P_{Olsen} and $P_{MMorgan}$ in topsoil and subsoil at pH 4.5, the lability of P as determined by DGT (P_{DGT}), was least at this pH across the pH range. This suggests strong adsorption of *labile* P to the solid-phase at acid pH values, limiting the kinetics of P release into solution and highlighting the limitation of traditional extraction techniques in assessing the availability of P to crops. This work is important because it shows the lability of P over a pH gradient relevant to agricultural soils where many

soils in the UK are acidic and sub-optimal to the recommended range of pH 6 to 7 (Goulding, 2016). The Old Rotation showed that labile P is greater when soluble fertilisers such as TSP are applied compared to insoluble GMP fertilisers or when P is restricted. This research shows that studying soils across a consistent and broad range pH gradient under field conditions has demonstrated clear differences between (i) tests such as P_{Olsen} and $P_{MMorgan}$ which measure only a static reservoir of P in the soil and (ii) tests such as DGT which treat the labile P pool as a dynamic supply in which kinetics of desorption are an integral part of the measurement.

In Chapter 7, the extent of biological mixing and transfer of P throughout the soil profile was investigated through the analysis of stable oxygen isotope ratios in soil phosphate ($\delta^{18}O_P$) extracted by HCl (P_{HCl}). The main comparisons were between topsoils and subsoils across a pH gradient (pH 4.5 to 7.5) and in two contrasting P fertiliser management plots (NK with TSP or GMP). Across the dataset, P_{HCl} increased with rising P_{Total} in the topsoils (r = 0.987) and subsoils (r = 0.964). The P_{HCl} was, on average, in both layers, 49.1% of the P_{Total} but ranged from 28.6% to 65%. Reference $\delta^{18}O_P$ values were obtained for the fertilisers TSP ($23.9^0/_{00}$) and GMP ($21.2^0/_{00}$), the (uncultivated) Field topsoil ($20.7^0/_{00}$) and subsoil ($20.0^0/_{00}$) and the soil pore water equilibrium ranges for the topsoil (15.4 to $18.0^0/_{00}$) and subsoil (15.0 to $17.8^0/_{00}$). Near uniform $\delta^{18}O_P$ signatures in the topsoil ($23.0^0/_{00}$) and subsoil ($22.5^0/_{00}$) of the pH 4.5 plot, which were close to the TSP fertiliser $\delta^{18}O_P$, suggested two mechanisms were occurring; (i) TSP had become rapidly adsorbed to Fe and Al oxides in the topsoil, rendering the phosphate unavailable for biological processing thus allowing it to retain the fertiliser signature and (ii) rapid leaching of TSP to the subsoil had also occurred, with phosphate bypassing biological processing in the topsoil and becoming rapidly adsorbed in the subsoil. As the soil pH increased to pH 5.5, topsoil and subsoil $\delta^{18}O_P$ values were almost identical at 21.1 and $21.3^0/_{00}$ respectively, suggesting that as P became less strongly held by adsorption to Fe and Al oxides (due to decreasing positive surface charges), more P was available in solution for cycling through microorganisms and thus the $\delta^{18}O_P$ signatures were closer to equilibrium with the soil pore water and the Field topsoil and subsoil $\delta^{18}O_P$. Biological cycling and turnover in the topsoil was greatest around pH 7 and the near identical $\delta^{18}O_P$ signatures in the topsoil ($20.6^0/_{00}$) and subsoil ($20.7^0/_{00}$), which were the closest values across the pH range to the soil pore water equilibrium $\delta^{18}O_P$, suggested P was biologically cycled in the topsoil before migrating to the subsoil, creating a uniform soil profile $\delta^{18}O_P$. Thus, soil pH has a strong influence on the mechanisms controlling P distribution in the soil profile, the extent to which TSP may be biologically cycled, and the rate at which P may be transferred to the subsoil. The $\delta^{18}O_P$ results from the Old Rotation showed that GMP fertiliser was processed in the

topsoil (19.1$^{0}/_{00}$) before moving to the subsoil (18.1$^{0}/_{00}$) where biological cycling may have continued as the $\delta^{18}O_P$ values were closer to soil pore water equilibrium. The TSP subsoil (19.1$^{0}/_{00}$) was more highly processed than the topsoil (21.3$^{0}/_{00}$) which indicated slow leaching of topsoil P to the subsoil where it may continue to be processed; this was also suggested by Amelung, *et al*., (2015). Therefore, the solubility of P fertilisers also influences the extent of biological cycling and transfer of P in the soil profile, with less soluble fertilisers persisting in the topsoil for longer, undergoing a higher degree of transformation than more soluble TSP, which dissolves rapidly and becomes adsorbed or precipitated and is apparently less available for biological cycling. It would have been useful in this study to compare the $\delta^{18}O_P$ of the NK plus TSP or GMP treatment to plots where P was restricted, and so future work could include isolating soil phosphate from these two treatment plots. In addition, it would be useful to determine $\delta^{18}O_P$ in plots that were not soil sampled in this thesis (PK without N and PN without K) in order to obtain a wider range of field-based comparisons. Finally, this study also showed that the incorporation of oxygen into the soil phosphate originating from organic sources, due to hydrolysis during the extraction stage, was minimal across a soil pH gradient and between topsoil and subsoil layers (< 2$^{0}/_{00}$). This possibly validates the decision of Bauke, *et al*. (2018) to exclude the duplicate HCl extraction with ^{18}O-enriched water to test for the incorporation of phosphate derived from the hydrolysis of organic p.

In summary, this project used evidence from long-term experiments which provide unique insights into the effect of soil pH management, cropping and fertiliser use strategy on topsoil and subsoil P dynamics in field-based settings through comparison to the (uncultivated, grassland) Field surrounding the plots. An assessment of accumulation, availability, solubility, lability and the cycling and transfer of P throughout the soil was undertaken. This work revealed that while highly reactive P accumulates in topsoils, underlying mineralogy and soil pH has an important influence on the distribution of available P throughout the soil profile. This highlights the importance of not only maintaining the correct soil pH but also the importance of considering soil texture and soil sorption capacities for controlling P fertiliser dynamics in soil (Sinclair, *et al*., 2015). Furthermore, the ability of a soil to resupply P following uptake by crops is also significantly impacted by pH and soil processes such as adsorption/desorption and dissolution/precipitation reactions. Soluble TSP fertilisers undergo biological cycling and move slowly to the subsoil but can also leach rapidly to the subsoil, bypassing biological mixing in the topsoil, and becoming more strongly adsorbed than in the topsoil. Fertiliser use is also important in determining long term P status; insoluble fertilisers such as GMP persist longer in the topsoil than soluble fertilisers such as TSP. Therefore, the use of insoluble P fertilisers which persist in the topsoil may be important for

reducing P transfer to the subsoil. Overall, the effect of crop rotation appeared to have a minimal impact on P dynamics although poor crop performance was linked to a higher residual P content in the soil. Taking in to consideration annual P balances between fertiliser inputs and crop offtakes would help a farmer to identify whether the fertiliser rate is appropriate, or if the crop is able to efficiently utilise the P applied. A key finding of this research is the potential agronomic significance of subsoil P: the concentrations of plant-available P in the subsoils in the pH Rotation are optimal for crop production and are labile to varying degrees (depending on pH), so the subsoil should have the ability to resupply P to the solution following uptake by crops. This knowledge would help improve P fertiliser management strategies by reducing the amount of P fertiliser needed through modelling of the contribution of subsoil P reserves to crop nutrition to create new fertiliser application strategies.

The next step for soil phosphorus research would be to improve our understanding of the contribution of *subsoil* P to crop nutrition. It would be useful to understand this contribution as it could mean less fertiliser application is required if a significant contribution can be made from the subsoil. This could be achieved by analysis of topsoil and subsoil contributions under controlled conditions using methods such as dual-isotopic labelling combining $^{32/33}$P radioactive tracing with stable oxygen isotope analysis in hydroponic studies by Pfahler, *et al*., (2017). This would show the proportional contribution from topsoil and subsoil P pools. It would also be interesting to analyse the stable oxygen isotope ratios in soil and crop phosphate from a wider range of treatments in the long-term experiments to assess the effect of crop rotation on the cycling and transfer of P throughout the soil profile. Different crops require different P fertiliser application rates and the utilisation of P will depend on the ability of the crops to root in to the subsoil and acquire P. Finally, it would be useful to understand *organic-P* dynamics in topsoils and subsoils because organic P can be up to 50% of the total P concentration in the soil (Nash, *et al*., 2014). This thesis supports the suggestion of Johnston & Poulton (2018), that future research studies should consider the value of long-term experiments and their unique role in improving our understanding of the impact of historical agricultural management on soil health and crop production. Long-term field experiments are relevant to modern agricultural systems because these are usually long-standing, historical sites which have been farmed through several generations of farmers. Therefore, utilising long-term field experiments is important to provide insights in to the effects of historical agricultural practice on soil health.

9 References

Abdi, D., Cade-Menun, B.J., Ziadi, N. & Parent, L.E., (2014). Long-Term Impact of Tillage Practices and Phosphorus Fertilization on Soil Phosphorus Forms as Determined by 31P Nuclear Magnetic Resonance Spectroscopy. *Journal of Environmental Quality*, 43(4): 1431 – 1441

Adesanwo, O.O., Ige, D.V., Thibault, L., Flaten, D. & Akinremi, W., (2013). Comparison of Colorimetric and ICP Methods of Phosphorus Determination in Soil Extracts. *Communications in Soil Science and Plant Analysis*, 44(21): 3061 – 3075.

Agriculture and Horticulture Development Board (AHDB), (2017). Nutrient Management Guide (RB209) Sections 1- 7. AHDB, Stoneleigh Park, Kenilworth, Warwickshire, UK

Ahmed, H., Young, S.D. & Shaw, G., (2014). Factors affecting uranium and thorium fractionation and profile distribution in contrasting arable and woodland soils. *Journal of Geochemical Exploration*, 145: 98 – 105.

Aigner, M., Tamburini, F., Heiling, M. & Dercon, G., (2016). Method for the Purification of Inorganic Phosphate in Soil- and Sediment Samples Prior to Analysis of the δ18O Isotopic Abundance in Phosphate. In: IAEA-TECDOC-1783, Supporting Sampling and Sample Preparation Tools for Isotope and Nuclear Analysis. International Atomic Energy Agency, Vienna, ISBN 978-92-0-100416-1.

Al-Tameemi, H.J., Ashoor, N.I. & Omer, L.A., (2015). Solubility and Movement of Calcium Phosphate Minerals in Some Calcareous Soils as Influenced by Application of Phosphate Fertilizer and Water Potential (ISSN: 2350-2274). *Merit Research Journal of Agricultural Science and Soil Sciences*, 3(7): 98 – 105.

Alvarez, R., Evans, L.A., Milham, P.J. & Wilson, M.A., (2004). Effects of humic material on the precipitation of calcium phosphate. *Geoderma*, 118(3-4): 245 – 260.

Amelung, W., Antar, P., Kleeberg, I., Oelmann, Y., Lücke, A., Alt, F., Lewandowski, H., Pätzold, S. & Barej, J.A.M., (2015). The delta O-18 signatures of HCl-extractable soil phosphates: methodological challenges and evidence of the cycling of biological P in arable soil. *European Journal of Soil Science*, 66(6): 965 – 972.

Andersson, H., Bergström, L., Djodjic, F., Ulén, B. & Kirchmann, H., (2013). Topsoil and Subsoil Properties Influence Phosphorus Leaching from Four Agricultural Soils. *Journal of Environmental Quality*, 42(2): 455 – 463.

Andersson, H., Bergström, L., Ulén, B., Djodjic, F. & Kirchmann, H., (2015). The Role of Subsoil as a Source or Sink for Phosphorus Leaching. *Journal of Environmental Quality*, 44(2): 535 – 544.

Angert, A., Weiner, T., Mazeh, S., Tamburini, F., Frossard, E., Bernasconi, S.M. & Sternberg, M., (2011). Seasonal variability of soil phosphate stable oxygen isotopes in rainfall manipulation experiments. *Geochimica et Cosmochimica Acta*, 75(15): 4216 – 4227.

Angert, A., Weiner, T., Mazeh, S. & Sternberg, M., (2012). Soil Phosphate Stable Oxygen Isotopes across Rainfall and Bedrock Gradients. *Environmental Science & Technology*, 46(4): 2156 – 2162.

Antelo, J., Avena, M., Fiol, S., López, R. & Arce, F., (2005). Effects of pH and ionic strength on the adsorption of phosphate and arsenate at the goethite-water interface. *Journal of Colloid and Interface Science*, 285(2): 476 – 486.

Baken, S., Moens, C., van der Grift, B. & Smolders, E., (2016). Phosphate binding by natural iron-rich colloids in streams. *Water Research*, 98: 326 – 333.

Barej, J.A.M., Pätzold, S., Perkons, U. & Amelung, W., (2014). Phosphorus fractions in bulk subsoil and its biopore systems. *European Journal of Soil Science*, 65(4): 553 – 561.

Barraclough, P.B., Bollons, H.M., Chambers, B.J., Hatley, D. & Moss, D.P., (1997). Planting Testing to Determine the P and K Status of Wheat. HGCA Report No. 137

Barrow, N.J., (2017). The effects of pH on phosphate uptake from soil. *Plant Soil*, 410(1-2): 401 – 410.

Bauke, S.L., von Sperber, C., Tamburini, F., Gocke, M.I., Honermeier, B., Schweitzer, K., Baumecker, M., Don, A., Sandhage-Hofmann, A. & Amelung, W., (2018). Subsoil phosphorus is affected by fertilization regime in long-term agricultural experimental trials. *European Journal of Soil Science*, 69(1): 103 – 112.

Bi, Q.F., Zheng, B.X., Lin, X.Y., Li, K.J., Liu, X.P., Hao, X.L., Zhang, H., Zhang, J.B., Jaisi, D.P. & Zhu, Y.G., (2018). The microbial cycling of phosphorus on long-term fertilized soil: Insights from phosphate oxygen isotope ratios. *Chemical Geology*, 483: 56 – 64.

Bigalke, M., Ulrich, A., Rehmus, A. & Keller, A., (2017). Accumulation of cadmium and uranium in arable soils in Switzerland. *Environmental Pollution*, 221: 85 – 93.

Blake, R.E., O'Neil, J.R. & Garcia, G.A., (1997). Oxygen isotope systematics of biologically mediated reactions of phosphate: 1. Microbial degradation of organophosphorus compounds. *Geochimica et Cosmochimica Acta*, 61(20): 4411 – 4422.

Blake, R.E., O'Neil, J.R. & Surkov, A.V., (2005). Biogeochemical cycling of phosphorus: Insights from oxygen isotope effects of phosphoenzymes. *America Journal of Science*, 305(6-8, SI): 596 – 620.

Bolan, N.S., Naidu, R., Mahimairaja, S. & Baskaran, S., (1994). Influence of low-molecular-weight organic-acids on the solubilization of phosphates. *Biology and Fertility of Soils*, 18(4): 311 – 319.

Bollons, H.M. & Barraclough, P.B., (1999). Assessing the phosphorus status of winter wheat crops: inorganic orthophosphate in whole shoots. *Journal of Agricultural Science*, 133 (Part 3): 285 – 295.

The British Survey of Fertiliser Practice, Fertiliser Use on Farm Crops for Crop Year 2017, (2018). British Library Cataloguing in Publication Data, ISBN 978-0-99297-353-7 Available at: https://www.gov.uk/government/statistics/british-survey-of-fertiliser-practice-2017

Burkitt, L.L., Mason, S.D., Dougherty, W.J. & Sale, P.W.G., (2016). The ability of the DGT soil phosphorus test to predict pasture response in Australian pasture soils – a preliminary assessment. *Soil Use and Management*, 32(1): 27 – 35.

Burns, R.G., (1976). Uptake of cobalt into ferromanganese nodules, soils, and synthetic manganese (IV) oxides. *Geochimica et Cosmochimica Acta*, 40(1): 95 – 102.

Campbell, C.A., Lafond, G.P., Biederbeck, V.O. & Winkleman, G.E., (1993). Influence of legumes and fertilization on deep distribution of available phosphorus (Olsen-P) in a thin Black Chernozemic soil. *Canadian Journal of Soil Science*, 73(4): 555 – 565.

Cao, X., Harris, W.G., Josan, M.S. & Nair, V.D., (2007). Inhibition of calcium phosphate precipitation under environmentally-relevant conditions. *Science of the Total Environment*, 383(1-3): 205 – 215.

Cao, X. & Harris, W.G., (2008). Carbonate and Magnesium Interactive Effect on Calcium Phosphate Precipitation. *Environmental Science & Technology*, 42(2): 436 – 442.

Capo, R.C., Stewart, B.W. & Chadwick, O.A., (1998). Strontium isotopes as tracers of ecosystem processes: theory and methods. *Geoderma*, 82(1-3): 197 – 225.

Chang, S.J. & Blake, R.E., (2015). Precise calibration of equilibrium oxygen isotope fractionations between dissolved phosphate and water from 3 to 37oC. *Geochimica et Cosmochimica Acta*, 150: 314 – 329.

Chen, D.J., Hu, M.P., Guo, Y., Wang, J.H., Huang, H. & Dahlgren, R.A., (2017). Long-term (1980–2010) changes in cropland phosphorus budgets, use efficiency and legacy pools across townships in the Yongan watershed, eastern China. *Agriculture, Ecosystems and Environment*, 236: 166 – 176.

Cooper, J., Lombardi, R., Boardman, D. & Carliell-Marquet, C., (2011). The future distribution and production of global phosphate rock reserves. *Resources, Conservation and Recycling*, 57: 78 – 86.

Cordell, D., Drangert, J.-O. & White, S., (2009). The story of phosphorus: Global food security and food for thought. *Global Environmental Change*, 19(2): 292 – 305.

Cordell, D. & White, S., (2011). Peak Phosphorus: Clarifying the Key Issues of a Vigorous Debate about Long-Term Phosphorus Security. *Sustainability*, 3(10): 2027 – 2049.

Cordell, D. & White, S., (2015). Tracking phosphorus security: indicators of phosphorus vulnerability in the global food system. *Food Security*, 7(2): 337 – 350.

Darch, T., Blackwell, M.S.A., Hawkins, J.M.B., Haygarth, P.M. & Chadwick, D., (2014). A Meta-Analysis of Organic and Inorganic Phosphorus in Organic Fertilizers, Soils, and Water: Implications for Water Quality. *Critical Reviews in Environmental Science and Technology*, 44(19): 2172 – 2202.

Davison, W. & Zhang, H., (1994). In situ speciation measurements of trace components in natural waters using thin-film gels. *Nature*, 367(6463): 546 – 548.

De Bolle, S., De Neve, S. & Hofman, G., (2013). Rapid redistribution of P to deeper soil layers in P saturated acid sandy soils. *Soil Use and Management*, 29(Suppl.1, SI): 76 – 82.

de Miranda, L.N. & Rowell, D.L., (1987). The effects of lime and phosphorus on the function of wheat roots in acid topsoils and subsoils. *Plant and Soil*, 104(2): 253 – 262.

Degryse, F., Smolders, E., Zhang, H. & Davison, W., (2009). Predicting availability of mineral elements to plants with the DGT technique: a review of experimental data and interpretation by modelling. *Environmental Chemistry*, 6(3): 198 – 218.

Degryse, F. & McLaughlin, M.J., (2014). Phosphorus Diffusion from Fertilizer: Visualization, Chemical Measurements, and Modeling. *Soil Science Society of America Journal*, 78(3): 832 – 842.

Deng, Y.X., Li, Y.T., Li, X.J., Sun, Y., Ma, J., Lei, M. & Weng, L.P., (2018). Influence of calcium and phosphate on pH dependency of arsenite and arsenate adsorption to goethite. *Chemosphere*, 199: 617 – 624.

DGT Guide (2003). DGT Research Ltd., Skelmorlie, Bay Horse Rd, Quernmore, Lancaster, Lancashire, LA2 0QJ.

Dodd, R.J. & Sharpley, A.N., (2015). Recognizing the role of soil organic phosphorus in soil fertility and water quality. *Resources, Conservation and Recycling*, 105(Part B): 282 – 293.

Echevarria, G., Sheppard, M.I. & Morel, J.-L., (2001). Effect of pH on the sorption of uranium in soils. *Journal of Environmental Radioactivity*, 53(2): 257 – 264.

Edwards, A.C., Sinclair, A.H., Coull, M., Crooks, W., Rees, R.M. & Lumsdon, D.G., (2016). Regional trends in Scottish advisory soil acidity and phosphorus results: significance of management history, land use and soil attributes. *Soil Use and Management*, 32(Suppl. 1, SI): 44 – 53.

Elless, M.P. & Lee, S.Y., (1998). Uranium solubility of carbonate-rich uranium-contaminated soils. *Water, Air and Soil Pollution*, 107(1-4): 147 – 162.

Elsbury, K.E., Paytan, A., Ostrom, N.E., Kendall, C., Young, M.B., McLaughlin, K., Rollog, M.E. & Watson, S., (2009). Using Oxygen Isotopes of Phosphate To Trace Phosphorus Sources and Cycling in Lake Erie. *Environmental Science & Technology*, 43(9): 3108 – 3114.

Elser, J.J. (2012). Phosphorus: a limiting nutrient for humanity? *Current Opinion in Biotechnology*, 23(6): 833 – 838.

Eriksson, A.K., Gustafsson, J.P. & Hesterberg, D., (2015). Phosphorus speciation of clay fractions from long-term fertility experiments in Sweden. *Geoderma*, 241: 68 – 74.

Esmail, A.O., (2012). Effect of Soil Phosphorus Chemical Equilibrium on P-availability for Wheat using Solubility Diagram and (DRIS-Chart) Methods. *Journal of Kirkuk University for Agricultural Sciences*, 3(2): 43 – 51.

Evans, L.J., Sengdy, B., Lumsdon, D.G. & Stanbury, D.A., (2003). Cadmium adsorption by an organic soil: a comparison of some humic – metal complexation models. *Chemical Speciation and Bioavailability*, 15(4): 93 – 100.

Fisher, E., Thornton, B., Hudson, G. & Edwards, A.C., (1998). The variability in total and extractable soil phosphorus under a grazed pasture. *Plant and Soil*, 203(2): 249 – 255.

Fortune, S., Lu, J., Addiscott, T.M. & Brookes, P.C., (2005). Assessment of phosphorus leaching losses from arable land. *Plant and Soil*, 269(SI:1-2): 99 – 108.

Frossard, E., Achat, D.L., Bernasconi, S.M., Bünemann, E.K., Fardeau, J.-C., Jansa, J, Morel, C., Rabeharisoa, L., Randriamanantsoa, L., Sinaj, S., Tamburini, F. & Oberson, A., (2011). The Use of Tracers to Investigate Phosphate Cycling in Soil–Plant Systems. In: Phosphorus in Action: Biological Processes in Soil Phosphorus Cycling (editors: Bünemann, E., Oberson, A. & Frossard, E.), pp. 59–91. Springer, Berlin.

Gallet, A., Flisch, R., Ryser, J.P., Frossard, E. & Sinaj, S., (2003). Effect of phosphate fertilization on crop yield and soil phosphorus status. *Journal of Plant Nutrition and Soil Science*, 166(5): 568 – 578.

George, T.S., Hinsinger, P. & Turner, B.L., (2016). Phosphorus in soil and plants- facing phosphorus scarcity. *Plant and Soil*, 401(1-2): 1- 6.

Glæsner, N., Bælum, J., Jacobsen, C.S., Ritz, C., Rubæk, G.H., Kjaergaard, C. & Magid, J., (2016). Bacteria as transporters of phosphorus through soil. *European Journal of Soil Science*, 67(1, SI): 99 – 108.

Glentworth, R. & Muir, J.W., (1963). The Soils of the Country Round Aberdeen, Inverurie and Fraserburgh (Sheets 77, 76 and 87/97). Macaulay Institute of Land Use Research. Memoirs of the Soil Survey of Great Britain. Edinburgh: HMSO.

Gregory, A.S., Dungait, J.A.J., Watts, C.W., Bol, R., Dixon, E.R., White, R.P. & Whitmore, A.P., (2016). Long-term management changes topsoil and subsoil organic carbon and nitrogen dynamics in a temperate agricultural system. *European Journal of Soil Science*, 67(4): 421 – 430.

Gross, A. & Angert, A., (2015). What processes control the oxygen isotopes of soil bio-available phosphate? *Geochimica et Cosmochimica Acta*, 159: 100 – 111.

Gruau, G., Legeas, M., Riou, C., Gallacier, E., Martineau, F. & Hénin, O., (2005). The oxygen isotope composition of dissolved anthropogenic phosphates: a new tool for eutrophication research? *Water Research*, 39(1): 232 – 238.

Gustafsson, J.P., (2011). Visual MINTEQ version 3.1 (https://vminteq.lwr.kth.se/)

Hamdan, R., El-Rifai, H.M., Cheesman, A.W., Turner, B.L., Reddy, K.R. & Cooper, W.T., (2012). Linking Phosphorus Sequestration to Carbon Humification in Wetland Soils by P-31 and C-13 NMR Spectroscopy. *Environmental Science & Technology*, 46(9): 4775 – 4782.

Hao, H.Z., Jin, M.G., Chen, T.B., Lei, M., Liu, C.W. & Zu, W.P., (2011). The distribution and bioavailability of Cd and Zn in cultivated soil of Henan Province. *Chemical Speciation and Bioavailability*, 23(3): 155 – 162.

Harper, M.P., Davison, W., Zhang, H. & Tych, W., (1998). Kinetics of metal exchange between solids and solutions in sediments and soils interpreted from DGT measured fluxes. *Geochimica et Cosmochimica Acta*, 62(16): 2757 – 2770.

Harper, M.P., Davison, W. & Tych, W., (2000). DIFS – a modelling and simulation tool for DGT induced trace metal remobilisation in sediments and soils. *Environmental Modelling & Software*, 15(1): 55 – 66.

Hartikainen, H., Rasa, K. & Withers, P.J.A., (2010). Phosphorus exchange properties of European soils and sediments derived from them. *European Journal of Soil Science*, 61(6): 1033 – 1042.

Hartley, T.N., Macdonald, A.J., McGrath, S.P. & Zhao, F.-J., (2013). Historical arsenic contamination of soil due to long-term phosphate fertiliser applications. *Environmental Pollution*, 180: 259 – 264.

Haygarth, P.M., Jarvie, H.P., Powers, S.M., Sharpley, A.N., Elser, J.J., Shen, J.B., Peterson, H.M., Chan, N.I., Howden, N.J.K., Burt, T., Worrall, F., Zhang, F.S. & Liu, X.J., (2014). Sustainable Phosphorus

Management and the Need for a Long-Term Perspective: The Legacy Hypothesis. *Environmental Science & Technnology*, 48(15, SI): 8417 – 8419.

Haygarth, P.M., Harrison, A.F. & Turner, B.L., (2018). On the history and future of soil organic phosphorus research: a critique across three generations. *European Journal of Soil Science*, 69(1): 86 – 94.

Hedley, M.J., Stewart, J.W.B. & Chauhan, B.S., (1982). Changes in Inorganic and Organic Soil-Phosphorus Fractions Induced by Cultivation Practices and by Laboratory Incubations. *Soil Science Society of America Journal*, 46(5): 970 – 976.

Helfenstein, J., Tamburini, F., von Sperber, C., Massey, M.S., Pistocchi, C., Chadwick, O.A., Vitousek, P.M., Kretzschmar, R. & Forssard, E., (2018). Combining spectroscopic and isotopic techniques gives a dynamic view of phosphorus cycling in soil. *Nature Communications*, 9: 3326.

Hinsinger, P., (2001). Bioavailability of soil inorganic P in the rhizosphere as affected by root-induced chemical changes: a review. *Plant and Soil*, 237(2): 173 – 195.

Holland, J.E., Bennet, A.E., Newton, A.C., White, P.J., McKenzie, B.M., George, T.S., Pakeman, R.J., Bailey, J.S., Fornara, D.A. & Hayes, R.C., (2018). Liming impacts on soils, crops and biodiversity in the UK: A review. *Science of the Total Environment*, 610: 316 – 322.

Ivanov, K., Zaprjanova, P., Petkova, M., Stefanova, V., Kmetov, V., Georgieva, D. & Angelova, V., (2012). Comparison of inductively coupled plasma mass spectrometry and colorimetric determination of total and extractable phosphorus in soils. *Spectrochimica Acta Part B – Atomic Spectroscopy*, 71-72: 117 – 122.

Jalali, M. & Jalali, M., (2016). Minerals control phosphorus solubility in long-term-cultivated calcareous soils. *Soil Research*, 55(2): 182 – 190.

Johnston, A.E., Poulton, P.R. & White, R.P., (2013). Plant-available soil phosphorus. Part II: the response of arable crops to Olsen P on a sandy clay loam and a silty clay loam. *Soil Use and Management*, 29(1): 12 – 21.

Johnston, A.E. & Poulton, P.R., (2018). The importance of long-term experiments in agriculture: their management to ensure continued crop production and soil fertility; the Rothamsted experience. *European Journal of Soil Science*, 69(1): 113 – 125.

Joshi, S.R., Li, X.N. & Jaisi, D.P., (2016). Transformation of Phosphorus Pools in an Agricultural Soil: An Application of Oxygen-18 Labelling in Phosphate. *Soil Science Society of America Journal*, 80(1): 69 – 78.

Kautz, T., Amelung, W., Ewert, F., Gaiser, T., Horn, R., Jahn, R., Javaux, M., Kemna, A., Kuzyakov, Y., Munch, J.C., Pätzold, S., Peth, S., Scherer, H.W., Schloter, M., Schneider, H., Vanderborght, J., Vetterlein, D., Walter, A., Wiesenberg, G.L.B. & Kopke, U., (2013). Nutrient acquisition from arable subsoils in temperate climates: a review. *Soil Biology & Biochemistry*, 57: 1003–1022.

Khan, A., Lu, G.Y., Ayaz, M., Zhang, H.T., Wang, R.J., Lv, F.L., Yang, X.Y., Sun, B.H. & Zhang, S.L., (2018). Phosphorus efficiency, soil phosphorus dynamics and critical phosphorus level under long-term fertilization for single and double cropping systems. *Agriculture, Ecosystems & Environment*, 256: 1 – 11.

Kleinman, P.J.A., Church, C., Saporito, L.S., McGrath, J.M., Reiter, M.S., Allen, A.L. Tingle, S., Binford, G.D., Han, K. & Joern, B.C., (2015). Phosphorus Leaching from Agricultural Soils of the Delmarva Peninsula, USA. *Journal of Environmental Quality*, 44(2): 524 – 534.

Kruse, J., Abraham, M., Amelung, W., Baum, C., Bol, R., Kühn, O., Lewandowski, H., Niederberger, J., Oelmann, Y., Rüger, C., Santner, J., Siebers, M., Siebers, N., Spohn, M., Vestergren, J., Vogts, A. & Leinweber, P., (2015). Innovative methods in soil phosphorus research: A review. *Journal of Plant Nutrition and Soil Science*, 178(1): 43 – 88.

Kuhlmann, H. & Baumgärtel, G., (1991). Potential importance of the subsoil for the P and Mg nutrition of wheat. *Plant and Soil*, 137(2): 259 – 266.

Kuo, S., Huang, B. & Bembenek, R., (2007). Release of cadmium from a triple superphosphate and a phosphate rock in soil. *Soil Science Technical Articles*, 172(4): 257 – 265.

Larsen, S. & Court, M.N., (1961). Soil Phosphate Solubility. *Nature*, 189(475): 164 – 165.

Larsson, M.A., Hadialhejazi, G. & Gustafsson, J.P., (2017). Vanadium sorption by minerals soils: Development of a predictive model. *Chemosphere*, 168: 925 – 932.

Lehto, N.J., Sochaczewski, L., Davison, W., Tych, W. & Zhang, H., (2008). Quantitative assessment of soil parameter (K-D and Tc) estimation using DGT measurements and the 2D DIFS model. *Chemosphere*, 71(4): 795 – 801.

Leinweber, P., Bathmann, U., Buczko, U., Douhaire, C., Eichler-Löbermann, B., Frossard, E., Ekardt, F., Jarvie, H., Krämer, I., Kabbe, C., Lennartz, B., Mellander, P.E., Nausch, G., Ohtake, H. & Tränckner, J., (2018). Handling the phosphorus paradox in agriculture and natural ecosystems: Scarcity, necessity, and burden of P. *Ambio*, 47(Suppl. 1, SI): S3 – S19.

Li, J.Y., Bai, Y.G., Bear, K., Joshi, S. & Jaisi, D., (2017). Phosphorus availability and turnover in the Chesapeake Bay: Insights from nutrient stoichiometry and phosphate oxygen isotope ratios. *Journal of Geophysical Research-Biogeosciences*, 122(4): 811 – 824.

Lindsay, W.L., (1979). Chemical Equilibria in Soils. Wiley-Interscience, John Wikey & Sons, NY, USA.

Liu, K., Lv, J.L., He, W.X., Zhang, H., Cao, Y.F. & Dai, Y.C., (2015). Major factors influencing cadmium uptake from the soil into wheat plants. *Ecotoxicology and Environmental Safety*, 113: 207 – 213.

Longinelli, A. & Nuti, S., (1973). Oxygen isotope measurements of phosphate from fish teeth and bones. *Earth and Planetary Science Letters*, 20(3): 337 – 340.

Lynch, J.P. & Wojciechowski, T., (2015). Opportunities and challenges in the subsoil: pathways to deeper rooted crops. *Journal of Experimental Botany*, 66(8 SI): 2199 – 2210.

Manning, B.A. & Goldberg, S., (1996). Modeling Competitive Adsorption of Arsenate with Phosphate and Molybdate on Oxide Minerals. *Soil Science Society of America Journal*, 60(1): 121 – 131.

Mason, S., Harnon, R., Zhang, H. & Anderson, J., (2008). Investigating chemical constraints to the measurement of phosphorus in soils using diffusive gradients in thin films (DGT) and resin methods. *Talanta*, 74(4): 779 – 787.

Mason, S., McNeill, A., McLaughlin, M.J. & Zhang, H., (2010). Prediction of wheat response to an application of phosphorus under field conditions using diffusive gradients in thin-films (DGT) and extraction methods. *Plant and Soil*, 337(1-2): 243 – 258.

Mason, S.D., McLaughlin, M.J., Johnston, C. & McNeill, A., (2013). Soil test measures of available P (Colwell, resin and DGT) compared with plant P uptake using isotope dilution. *Plant and Soil*, 373 (1-2): 711 – 722.

Matthieux, F., Ardente, F., Bobba, S., Nuss, P., Blengini, G., Alves Dias, P., Blagoeva, D., Torres De Matos, C., Wittmer, D., Pavel, C., Hamor, T., Saveyn, H., Gawlik, B., Orveillon, G., Huygens, D., Garbarino, E., Tzimas, E., Bouraoui, F. and Solar, S., Critical Raw Materials and the Circular Economy – Background report. JRC Science-for-policy report, EUR 28832 EN, Publications Office of the European Union, Luxembourg, 2017, ISBN:978-92-79-74282-8

McDowell, R.W. & Sharpley, A.N., (2003). Phosphorus solubility and release kinetics as a function of soil test P concentration. *Geoderma*, 112(1-2): 143 – 154.

McDowell, R.W., (2012). The rate of accumulation of cadmium and uranium in a long-term grazed pasture: implications for soil quality. *New Zealand Journal of Agricultural Research*, 55(2, SI): 133 – 146.

McIntosh, J.L., (1969). Bray and Morgan Soil Extractants Modified for Testing Acid Soils from Different Parent Materials. *Agronomy Journal*, 61(2): 259 – 265.

McLaren, T.I., Smernik, R.J., Simpson, R.J., McLaughlin, M.J., McBeath, T.M., Guppy, C.N. & Richardson, A.E., (2017). The chemical nature of organic phosphorus that accumulates in fertilized soils of a temperate pasture as determined by solution P-31 NMR spectroscopy. *Journal of Plant Nutrition and Soil Science*, 180(1): 27 – 38.

McLaughlin, K., Paytan, A., Kendall, C. & Silva, S., (2006a). Oxygen isotopes of phosphatic compounds – Application for marine particulate matter, sediments and soils. *Marine Chemistry*, 98(2-4): 148 – 155.

McLaughlin, K., Cade-Menun, B.J. & Paytan, A., (2006b). The oxygen isotopic composition of phosphate in Elkhorn Slough, California: A tracer for phosphate sources. *Estuarine, Coastal and Shelf Science*, 70(3): 499 – 506.

Menezes-Blackburn, D., Zhang, H., Stutter, M.I., Giles, C.D., Darch, T., George, T.S., Shand, C.A., Lumsdon, D., Blackwell, M., Wearing, C., Cooper, P., Wendler, R., Brown, L. & Haygarth, P.M., (2016). A Holistic Approach to Understanding Desorption of Phosphorus in Soils. *Environmental Science & Technology*, 50(7): 3371 – 3381.

Menezes-Blackburn, D., Giles, C., Darch, T., George, T.S., Blackwell, M., Stutter, M., Shand, C., Lumsdon, D., Cooper, P., Wendler, R., Brown, L., Almeida, D.S., Wearing, C., Zhang, H. & Haygarth, P.M., (2017). Opportunities for mobilizing recalcitrant phosphorus from agricultural soils: a review. *Plant and Soil*, 427(1-2): 5 – 16, Special Issue.

Metson, G.S., Bennet, E.M. & Elser, J.J., (2012). The role of diet in phosphorus demand. *Environmental Research Letters*, 7(4): Article Number 044043.

Murphy, J. & Riley, I.P. (1962). A modified single solution method for the determination of phosphate in natural waters. *Analytica Chimica Acta*, 27: 31 – 36.

Nash, D.M., Haygarth, P.M., Turner, B.L., Condron, L.M., McDowell, R.W., Richardson, A.E., Watkins, M. & Heaven, M.W., (2014). Using organic phosphorus to sustain pasture productivity: A perspective. *Geoderma*, 221: 11 – 19.

Nawara, S., Van Dael, T., Merckx, R., Amery, F., Elsen, A., Odeurs, W., Vandendriessche, H., Mcgrath, S., Roisin, C., Jouany, C., Pellerin, S., Denoroy, P., Eichler-Lobermann, B., Borjesson, G., Goos, P., Akkermans, W. & Smolders, E., (2017). A comparison of soil tests for available phosphorus in long-term field experiments in Europe. *European Journal of Soil Science*, 68(6): 873 – 885.

Neyroud, J.A. & Lischer, P., (2003). Do different methods used to estimate soil phosphorus availability across Europe give comparable results? *Journal of Plant Nutrition and Soil Science*, 166(4): 422 – 431.

Olsen, S.R., Cole, C.V., Watanabe, F.S. & Dean, L.A., (1954). Estimation of available phosphorus in soils by extraction with sodium bicarbonate. United States Department of Agriculture, Circular 939.

Oxmann, J.F. & Schwendenmann, L., (2015). Authigenic apatite and octacalcium phosphate formation due to adsorption-precipitation switching across estuarine salinity gradients. *Biogeosceinces*, 12(3): 723 – 738.

Paterson, E. & (Eds.) Campbell, C., Coull, M. & Shand, C., (2011). Geochemical Atlas for Scottish Topsoils. Macaulay Land Use Research Institute, Craigiebuckler, Aberdeen, AB15 8QH. ISBN:978-0-902701-00-7

Paytan, A., Kolodny, Y., Neori, A. & Luz, B., (2002). Rapid biologically mediated oxygen isotope exchange between water and phosphate. *Global Biogeochemical Cycles*, 16(1): Article Number 1013.

Perassi, I. & Borgnino, L., (2014). Adsorption and surface precipitation of phosphate onto CaCO3-montmorillonite: effect of pH, ionic strength and competition with humic acid. *Geoderma*, 232: 600 – 608.

Pfahler, V., Dürr-Auster, T., Tamburini, F., Bernasconi, S. & Frossard, E., (2013). 18O enrichment in phosphorus pools extracted from soybean leaves. *New Phytologist*, 197(1): 186 – 193.

Pfahler, V., Tamburini, F., Bernasconi, S.M. & Frossard, E., (2017). A dual isotopic approach using radioactive phosphorus and the isotopic composition of oxygen associated to phosphorus to understand plant reaction to a change in P nutrition. *Plant Methods*, 13: Article Number 75.

Pistocchi, C., Tamburini, F., Gruau, G., Ferhi, A., Trevisan, D. & Dorioz, J.M., (2017). Tracing the sources and cycling of phosphorus in river sediments using oxygen isotopes: Methodological adaptations and first results from a case study in France. *Water Research*, 111: 346 – 356.

Pizzeghello, D., Berti, A., Nardi, S. & Morari, F., (2011). Phosphorus forms and P-sorption properties in three alkaline soils after long-term mineral applications in north-eastern Italy. *Agriculture, Ecosystems and Environment*, 141(1-2): 58 – 66.

Pizzeghello, D., Berti, A., Nardi, S. & Morari, F., (2014). Phosphorus-related properties in the profiles of three Italian soils after long-term mineral and manure applications. *Agriculture, Ecosystems and Environment*, 189: 216 – 228.

Poulton, P.R., Johnston, A.E. & White, R.P., (2013). Plant-available soil phosphorus. Part I: the response of winter wheat and spring barley to Olsen P on a silty clay loam. *Soil Use and Management*, 29(1): 4 – 11.

Poulton, P., Johnston, J., Macdonald, A., White, R. & Powlson, D., (2018). Major limitations to achieving "4 per 1000" increases in soil organic carbon stock in temperate regions: Evidence from long-term experiments at Rothamsted Research, United Kingdom. *Global Change Biology*, 24(6): 2563 – 2584.

Pypers, P., Delrue, J., Diels, J., Smolders, E. & Merckx, R., (2006). Phosphorus intensity determines short-term P uptake by pigeon pea (Cajanus cajan L.) grown in soils with differing P buffering capacity. *Plant and Soil*, 284(1-2): 217 – 227.

Rahnemaie, R., Hiemstra, T. & van Riemsdijk. W.H., (2007). Carbonate adsorption on goethite in competition with phosphate. *Journal of Colloid and Interface Science*, 315(2): 415 – 425.

Regelink, I.C., Weng, L., Lair, G.J. & Comans, R.N.J., (2015). Adsorption of phosphate and organic matter on metal (hydr)oxides in arable and forest soil: a mechanistic modelling study. *European Journal of Soil Science*, 66(5): 867 – 875.

Richards, J.E., Bates, T.E. & Sheppard, S.C., (1995). Changes in the forms and distribution of soil phosphorus due to long-term corn production. *Canadian Journal of Soil Science*, 75(3): 311 – 318.

Ross, S.M., Wood M.D., Copplestone, D., Warriner, M. and Crook, P., (2007). UK Soil and Herbage Pollutant Survey, UKSHS Report No. 7: Environmental concentrations of heavy metals in UK soil and herbage. Bristol, UK: The Environment Agency ISBN:978-1-84432-772-0.

Rubæk, G.H., Kristensen, K., Olesen, S.E., Østergaard, H.S. & Heckrath, G., (2013). Phosphorus accumulation and spatial distribution in agricultural soils in Denmark. *Geoderma*, 209: 241 – 250.

Sade, H., Meriga, B., Surapu, V., Gadi, J., Sunita, M.S.L., Suravajhala, P. & Kishor, P.B.K., (2016). Toxicity and tolerance of aluminium in plants: tailoring plants to suit to acid soils. *Biometals*, 29(2): 187 – 210.

Santner, J., Mannel, M., Burrell, L.D., Hoefer, C., Kreuzeder, A. & Wenzel, W.W., (2015). Phosphorus uptake by Zea mays L. quantitatively predicted by infinite sink extraction of soil P. *Plant and Soil*, 386(1-2): 371 – 383.

Sattari, S.Z., Bouwman, A.F., Giller, K.E. & van Ittersum, M.K., (2012). Residual soil phosphorus as the missing piece in the global phosphorus crisis puzzle. *Proceedings of the National Academy of Sciences of The United States of America*, 109(16): 6348 – 6353.

Schipper, L.A., Sparling, G.P., Fisk, L.M., Dodd, M.B., Power, I.L. & Littler, R.A., (2011). Rates of accumulation of cadmium and uranium in a New Zealand Hill farm soil as a result of long-term use of phosphate fertilizer. *Agriculture, Ecosystems and Environment*, 144(1): 95 – 101.

Schwertmann, U. & Pfab, G., (1996). Structural vanadium and chromium in lateritic iron oxides: Genetic implications. *Geochimica et Cosmochimica Acta*, 60(21): 4279 – 4283.

Sharpley, A., Jarvie, H.P., Buda, A., May, L., Spears, B. & Kleinman, P., (2013). Phosphorus legacy: overcoming the effects of past management practices to mitigate future water quality impairment. *Journal of Environmental Quality*, 42(5): 1308 – 1326.

Sharpley, A.N., Bergström, L., Aronsson, H., Bechmann, M., Bolster, C.H., Börling, K., Djodjic, F., Jarvie, H.P., Schoumans, O.F., Stamm, C., Tonderski, K.S., Ulén, B., Uusitalo, R. & Withers, P.J.A., (2015). Future agriculture with minimized phosphorus losses to waters: Research needs and direction. *Ambio*, 44(Suppl. 2, SI): S163 – S179.

Simonsson, M., Östlund, A., Renfjäll, L., Sigtryggsson, C., Börjesson, G. & Kätterer, T., (2018). Pools and solubility of soil phosphorus as affected by liming in long-term agricultural field experiments. *Geoderma*, 315: 208 – 219.

Sinclair, A., Shipway, P. & Wale, S., (2013). Technical Note TN633: Phosphorus, potassium, sulphur and magnesium recommendations for cereals, oilseed rape and potatoes. The Scottish Agricultural College, Edinburgh, EH9 3JG.

Sinclair, A., Crooks, W., Edwards, A.C. & Coull, M. (2015). Technical Note TN668: Managing Soil Phosphorus. The Scottish Agricultural College, Edinburgh, EH9 3JG.

Six, L., Pypers, P., Degryse, F., Smolders, E. & Merckx, R., (2012). The performance of DGT versus conventional soil phosphorus tests in tropical soils – An isotope dilution study. *Plant and Soil*, 359(1-2): 267 – 279.

Six, L., Smolders, E. & Merckx, R., (2014). Testing phosphorus availability for maize with DGT in weathered soils amended with organic materials. *Plant and Soil*, 376(1-2): 177 – 192.

Six, L. & Smolders, E., (2014). Future trends in soil cadmium concentration under current cadmium fluxes to European agricultural soils. *Science of the Total Environment*, 485: 319 – 328.

Sorn-srivichai, P., Tillman, R.W., Syers, J.K. & Cornforth, I.S., (1984). The Effect of Soil pH on Olsen Bicarbonate Phosphate Values. *Journal of the Science of Food and Agriculture*, 35(3): 257 – 264.

Stutter, M. I., Shand, C.A., George, T.S., Blackwell, M.S.A., Bol, R., MacKay, R.L., Richardson, A.E., Condron, L.M., Turner, B.L. & Haygarth, P.M., (2012). Recovering Phosphorus from Soil: A Root Solution? *Environmental Science & Technology*, 46(4): 1977 – 1978.

Stutter, M.I., Shand, C.A., George, T.S., Blackwell, M.S.A., Dixon, L., Bol, R., MacKay, R.L., Richardson, A.E., Condron, L.M. & Haygarth, P.M., (2015). Land use and soil factors affecting accumulation of phosphorus species in temperate soils. *Geoderma*, 257(SI): 29 – 39.

Tamburini, F., Bernasconi, S. M., Angert, A., Weiner, T. & Frossard, E., (2010). A method for the analysis of the delta O-18 of inorganic phosphate extracted from soils with HCl. *European Journal of Soil Science*, 61(6): 1025 – 1032.

Tamburini, F., Pfahler, V., Bünemann, E.K., Guelland, K., Bernasconi, S.M. & Frossard, E., (2012). Oxygen Isotopes Unravel the Role of Microorganisms in Phosphate Cycling in Soils. *Environmental Science & Technology*, 46(11): 5956 – 5962.

Tamburini, F., Pfahler, V., von Sperber, C., Frossard, E. & Bernasconi, S.M., (2014). Oxygen Isotopes for Unraveling Phosphorus Transformations in the Soil-Plant System: A Review. *Soil Science Society of America Journal*, 78(1): 38 – 46.

Tamburini, F., Pistocchi, C., Helfenstein, J. & Frossard, E., (2018). A method to analyse the isotopic composition of oxygen associated with organic phosphorus in soil and plant material. *European Journal of Soil Science*, 69(5): 816 – 826.

Taylor, J.P., Wilson, B., Mills, M.S. & Burns, R.G., (2002). Comparison of microbial numbers and enzymatic activities in surface soils and subsoils using various techniques. *Soil Biology & Biochemistry*, 34(3): 387 – 401. Article Number: PII S0038-0717(01)00199-7.

The Sludge (Use in Agriculture) Regulations (1989). Statutory Instruments 1989 No. 1263: Public Health, England and Wales & Public Health, Scotland. Available at http://www.legislation.gov.uk/uksi/1989/1263/introduction/made

Tian, L.Y., Guo, Q.J., Zhu, Y.G., He, H.J., Lang, Y.C., Hu, J., Zhang, H., Wei, R.F., Han, X.K., Peters, M. & Yang, J.X., (2016). Research and application of method of oxygen isotope of inorganic phosphate in Beijing agricultural soils. *Environmental Science and Pollution Research*, 23(23): 23406 – 23414.

Tipping, E., Lofts, S. & Sonke, J.E., (2011). Humic Ion-Binding Model VII: a revised parameterisation of cation-binding by humic substances. *Environmental Chemistry*, 8(3): 225 – 235.

Tipping, E., Somerville, C.J. & Luster, J., (2016). The C:N:P:S stoichiometry of soil organic matter. *Biogeochemistry*, 130(1-2): 117 – 131.

Tonderski, K., Andersson, L., Lindström, G., St Cyr, R., Schönberg, R. & Taubald, H., (2017). Assessing the use of $\delta^{18}O$ in phosphate as a tracer for catchment phosphorus sources. *Science of the Total Environment*, 607: 1 – 10.

Tóth, G., Hermann, T., Da Silva, M.R. & Montanarella, L., (2016). Heavy metals in agricultural soils of the European Union with implications for food safety. *Environment International*, 88: 299 – 309.

Tunesi, S., Poggi, V. & Gessa, C., (1999). Phosphate adsorption and precipitation in calcareous soils: the role of calcium ions in solution and carbonate minerals. *Nutrient Cycling in Agroecosystems*, 53(3): 219 – 227.

Turner, B.L. & Haygarth, P.M., (2003). Changes in Bicarbonate-extractable Inorganic and Organic Phosphorus by Drying Pasture Soils. *Soil Science Society of America Journal*, 67(1): 344 – 350.

Turner, B.L., Cade-Menun, B.J., Condron, L.M. & Newman, S., (2005). Extraction of soil organic phosphorus. *Talanta*, 66(2): 294 – 306.

Turner, B.L. & Blackwell, M.S.A. (2013). Isolating the influence of pH on the amounts and forms of soil organic phosphorus. *European Journal of Soil Science*, 64(2): 249 – 259.

Tyler, J.J., Jones, M., Arrowsmith, C., Allot, T. & Leng, M.J. (2016). Spatial patterns in the oxygen isotope composition of daily rainfall in the British Isles. *Climate Dynamics*, 47(5-6): 1971 – 1987.

Ulrich, A.E., (2019). Cadmium governance in Europe's phosphate fertilisers: Not so fast? *Science of the Total Environment*, 650(Part 1): 541 – 545.

United Nations, Department of Economic and Social Affairs, Population Division (2017). World Population Prospects: The 2017 Revision, Key Findings and Advance Tables. ESA/P/WP/248.

van Dijk, K.C., Lesschen, J.P. & Oenema, O., (2016). Phosphorus flows and balances of the European Union Member States. *Science of Total Environment*, 542(SI Part B): 1078 – 1093.

van Hees, P.A.W., Vinogradoff, S.I., Edwards, A.C., Godbold, D.L. & Jones, D.L., (2003). Low molecular weight organic acid adsorption in forest soils: effects on soil solution concentrations and biodegradation rates. *Soil Biology & Biochemistry*, 35(8): 1015 – 1026.

Van Moorleghem, C., Six, L., Degryse, F., Smolders, E. & Merckx, R., (2011). Effect of Organic P Forms and P Present in Inorganic Colloids on the Determination of Dissolved P in Environmental Samples by the Diffusive Gradients in Thin Films Technique, Ion Chromatography, and Colorimetry. *Analytical Chemistry*, 83(13): 5317 – 5323.

Vanden Nest, T., Ruysschaert, G., Vandecasteele, B., Houot, S., Baken, S., Smolders, E., Cougnon, M., Reheul, D. & Merckx, R., (2016). The long term use of farmyard manure and compost: Effects on P availability, orthophosphate sorption strength and P leaching. *Agriculture, Ecosystems and Environment*, 216: 23 – 33.

Verbeeck, M., Hiemstra, T., Thiry, Y. & Smolders, E., (2017). Soil organic matter reduces the sorption of arsenate and phosphate: a soil profile study and geochemical modelling. *European Journal of Soil Science*, 68(5): 678 – 688.

Vieillard, P., Blanc, P., Fialips, C.I., Gailhanou, H. & Gaboreau, S., (2011). Hydration thermodynamics of the SWy-1 montmorillonite saturated with alkali and alkaline-earth cations: A predictive model. *Geochimica et Cosmochimica Acta*, 75(19): 5664 – 5685.
von Tucher, S., Hörndl, D. & Schmidhalter, U., (2018). Interaction of soil pH and phosphorus efficacy: Long-term effects of P fertilizer and lime applications on wheat, barley and sugar beet. *Ambio*, 47(Suppl. 1, SI): S41 – S49.

Walker, R.L., Watson, C.A. & Edwards, A.C., (2011). The long-term effects of widely differing soil pH on the yields of an eight course crop rotation established in 1961. *Aspects of Applied Biology*, 113: 111 – 115.

Walker, R.L., Watson, C.A. & Edwards, A.C., (2015). Aspects of pH gradient effect on crop productivity and crop quality parameters in an eight course ley-arable rotation started in 1961. *Aspects of Applied Biology*, 128: 63 – 68.

Weng, L.P., Vega, F.A. & van Riemsdijk, W.H., (2011). Competitive and Synergistic Effects in pH Dependent Phosphate Adsorption in Soils: LCD Modeling. *Environmental Science & Technology*, 45(19): 8420 – 8428.

Wisawapipat, W. & Kretzschmar, R., (2017). Solid Phase Speciation and Solubility of Vanadium in Highly Weathered Soils. *Environmental Science & Technology*, 51(15): 8254 – 8262.

Withers, P.J.A., Edwards, A.C. & Foy, R.H., (2001). Phosphorus cycling in UK agriculture and implications for phosphorus loss from soil. *Soil Use and Management*, 17(3): 139 – 149.

Withers, P.J.A., Sylvester-Bradley, R., Jones, D.L., Healey, J.R. & Talboys, P.J., (2014). Feed the Crop Not the Soil: Rethinking Phosphorus Management in the Food Chain. *Environmental Science & Technology*, 48(12): 6523 – 6530.

Withers, P.J.A., Hodgkinson, R.A., Rollett, A., Dyer, C., Dils, R., Collins, A.L., Bilsborrow, P.E., Bailey, G. & Sylvester-Bradley, R., (2017). Reducing soil phosphorus fertility brings potential long-term environmental gains: A UK analysis. *Environmental Research Letters*, 12(6): Article Number:063001.

Wuenscher, R., Unterfrauner, H., Peticzka, R. & Zehetner, F., (2015). A comparison of 14 soil phosphorus extraction methods applied to 50 agricultural soils from Central Europe. *Plant, Soil and Environment*, 61(2): 86 – 96.

Zaunbrecher, L.K., Cygan, R.T. & Elliott, W.C., (2015). Molecular Models of Cesium and Rubidium Adsorption on Weathered Micaceous Minerals. *Journal of Physical Chemistry A*, 119(22): 5691 – 5700.

Zhang, H. & Davison, W., (1995). Performance Characteristics of Diffusion Gradients in Thin Films for the in Situ Measurement of Trace Metals in Aqueous Solution. *Analytical Chemistry*, 67(19): 3391 – 3400.

Zhang, M., Li, C.L., Li, Y.C. & Harris, W.G., (2014). Phosphate minerals and solubility in native agricultural calcareous soils. *Geoderma*, 232: 164 – 171.

Zhang, H. & Davison, W., (2015). Use of diffusive gradients in thin-films for studies of chemical speciation and bioavailability. *Environmental Chemistry*, 12(2): 85 – 101.

Ziadi, N., Belanger, G., Gagnon, B. & Mongrain, D., (2009). Mehlich 3 Soil Phosphorus as Determined by Colorimetry and Inductively Coupled Plasma. *Communications in Soil Science and Plant Analysis*, 40(1-6, SI): 132 – 140 Article Number:PII 909554998.

Zohar, I., Shaviv, A., Klass, T., Roberts, K. & Paytan, A., (2010). Method for the Analysis of Oxygen Isotopic Composition of Soil Phosphate Fractions. *Environmental Science & Technology*, 44(19, SI): 7583 – 7588.

10 Appendices

Appendix 1 – Pearson Correlation Coefficient Matrices

Table 10.1. The Old Rotation Topsoil Pearson Correlation Coefficient Matrix and *p* values

	pH	N	C	Na	Mg	P	S	K	Ca	Al	Li	Be	V	Cr	Mn	Fe	Co	Ni	Cu	Zn	As	Se	Rb	Sr	Mo	Ag	Cd	Cs	Ba	Tl	Pb
N	-0.452																														
	0.000																														
C	-0.474	0.613																													
	0.000	0.000																													
Na	0.438	-0.379	-0.380																												
	0.000	0.003	0.003																												
Mg	0.539	-0.281	-0.285	0.862																											
	0.000	0.030	0.027	0.000																											
P	0.112	0.173	0.057	-0.148	-0.073																										
	0.395	0.187	0.663	0.258	0.582																										
S	-0.141	0.292	0.344	0.031	0.104	0.045																									
	0.284	0.024	0.007	0.813	0.428	0.731																									
K	-0.111	-0.115	0.086	0.502	0.253	-0.271	0.277																								
	0.398	0.381	0.513	0.000	0.051	0.036	0.032																								
Ca	0.425	0.011	-0.115	0.504	0.549	0.575	0.302	0.124																							
	0.001	0.933	0.381	0.000	0.000	0.000	0.019	0.346																							
Al	0.109	-0.012	0.065	0.404	0.471	0.068	0.369	0.399	0.592																						
	0.405	0.929	0.621	0.001	0.000	0.603	0.004	0.002	0.000																						
Li	0.409	-0.339	-0.409	0.708	0.803	-0.302	-0.126	0.142	0.211	0.181																					
	0.001	0.008	0.001	0.000	0.000	0.019	0.338	0.279	0.106	0.167																					
Be	0.307	-0.381	-0.296	0.396	0.313	-0.146	-0.160	0.154	0.070	-0.022	0.494																				
	0.017	0.003	0.022	0.002	0.015	0.265	0.223	0.241	0.593	0.869	0.000																				
V	0.437	-0.220	-0.172	0.839	0.921	-0.054	0.236	0.417	0.584	0.548	0.725	0.311																			
	0.000	0.092	0.189	0.000	0.000	0.680	0.069	0.001	0.000	0.000	0.000	0.016																			
Cr	0.516	-0.295	-0.264	0.848	0.935	0.082	0.124	0.288	0.633	0.417	0.749	0.377	0.920																		
	0.000	0.022	0.041	0.000	0.000	0.532	0.343	0.025	0.000	0.001	0.000	0.003	0.000																		
Mn	0.412	-0.370	-0.190	0.717	0.830	-0.190	0.181	0.360	0.412	0.553	0.739	0.318	0.837	0.805																	
	0.001	0.004	0.146	0.000	0.000	0.147	0.165	0.005	0.001	0.000	0.000	0.013	0.000	0.000																	
Fe	0.378	-0.147	-0.184	0.778	0.921	-0.077	0.266	0.338	0.581	0.689	0.703	0.195	0.920	0.838	0.842																
	0.003	0.264	0.160	0.000	0.000	0.560	0.040	0.008	0.000	0.000	0.000	0.135	0.000	0.000	0.000																
Co	0.464	-0.397	-0.352	0.794	0.863	-0.148	0.054	0.326	0.394	0.361	0.829	0.381	0.834	0.843	0.861	0.810															
	0.000	0.002	0.006	0.000	0.000	0.259	0.682	0.011	0.002	0.005	0.000	0.003	0.000	0.000	0.000	0.000															
Ni	0.133	-0.330	-0.159	0.449	0.501	-0.134	0.035	0.205	0.188	0.159	0.479	0.298	0.552	0.567	0.437	0.434	0.519														
	0.311	0.010	0.224	0.000	0.000	0.306	0.789	0.115	0.149	0.225	0.000	0.021	0.000	0.000	0.000	0.001	0.000														
Cu	-0.304	0.072	0.308	-0.199	-0.188	-0.171	-0.044	0.180	-0.294	0.089	-0.128	-0.039	-0.049	-0.186	0.007	-0.103	-0.089	0.067													
	0.018	0.587	0.017	0.128	0.151	0.193	0.738	0.169	0.023	0.499	0.331	0.769	0.708	0.154	0.960	0.431	0.498	0.613													
Zn	0.342	-0.239	-0.165	0.419	0.543	0.096	0.014	-0.028	0.320	0.198	0.497	0.347	0.531	0.602	0.519	0.434	0.492	0.381	0.040												
	0.008	0.066	0.208	0.001	0.000	0.467	0.916	0.832	0.013	0.130	0.000	0.007	0.000	0.000	0.000	0.001	0.000	0.003	0.759												
As	0.317	-0.271	-0.100	0.487	0.510	0.165	-0.022	0.244	0.237	0.306	0.226	0.266	0.566	0.526	0.386	0.463	0.391	0.378	0.133	0.413											
	0.014	0.036	0.448	0.000	0.000	0.208	0.865	0.061	0.068	0.017	0.082	0.040	0.000	0.000	0.002	0.000	0.002	0.003	0.313	0.001											
Se	0.126	0.195	0.100	0.297	0.413	0.421	0.219	0.074	0.656	0.566	0.19	0.019	0.541	0.489	0.368	0.527	0.299	0.246	0.112	0.264	0.315										
	0.336	0.136	0.445	0.021	0.001	0.001	0.093	0.576	0.000	0.000	0.146	0.884	0.000	0.000	0.004	0.000	0.020	0.058	0.394	0.042	0.014										
Rb	0.026	-0.108	0.139	0.558	0.472	-0.289	0.428	0.831	0.266	0.652	0.308	0.181	0.592	0.457	0.588	0.609	0.501	0.317	0.098	0.115	0.294	0.234									
	0.841	0.413	0.289	0.000	0.000	0.025	0.001	0.000	0.040	0.000	0.017	0.166	0.000	0.000	0.000	0.000	0.000	0.014	0.458	0.382	0.022	0.072									
Sr	0.270	-0.096	-0.103	0.696	0.661	0.172	0.334	0.494	0.807	0.820	0.398	0.136	0.725	0.665	0.648	0.795	0.589	0.273	-0.169	0.220	0.260	0.566	0.685								
	0.037	0.465	0.434	0.000	0.000	0.190	0.009	0.000	0.000	0.000	0.002	0.300	0.000	0.000	0.000	0.000	0.000	0.035	0.196	0.091	0.045	0.000	0.000								
Mo	-0.282	-0.000	0.195	-0.146	-0.091	0.002	0.219	0.130	-0.111	0.141	-0.09	-0.054	0.064	0.011	0.208	0.029	0.037	0.179	0.324	0.157	0.126	0.104	0.157	0.002							
	0.029	0.999	0.136	0.265	0.490	0.986	0.093	0.322	0.396	0.282	0.494	0.684	0.629	0.933	0.111	0.827	0.777	0.170	0.012	0.231	0.339	0.429	0.231	0.990							
Ag	0.014	-0.022	-0.098	0.070	-0.106	0.171	-0.091	0.082	0.103	-0.137	-0.122	0.008	-0.085	-0.017	-0.240	-0.154	-0.172	-0.115	-0.359	-0.224	-0.061	-0.098	-0.066	0.027	-0.098						
	0.915	0.868	0.456	0.597	0.421	0.193	0.489	0.535	0.432	0.298	0.353	0.950	0.518	0.900	0.065	0.239	0.188	0.380	0.005	0.085	0.645	0.459	0.619	0.835	0.455						
Cd	0.062	0.177	-0.030	-0.208	-0.095	0.681	0.043	-0.354	0.408	-0.037	-0.197	-0.036	-0.146	0.000	-0.265	-0.127	-0.254	-0.160	-0.246	0.252	-0.041	0.199	-0.376	0.010	-0.109	0.134					
	0.635	0.176	0.818	0.110	0.472	0.000	0.743	0.006	0.001	0.777	0.131	0.785	0.266	0.998	0.041	0.335	0.050	0.221	0.058	0.052	0.755	0.127	0.003	0.942	0.406	0.307					
Cs	0.010	-0.003	0.329	0.276	0.360	-0.072	0.517	0.537	0.330	0.758	0.129	-0.000	0.496	0.349	0.544	0.556	0.354	0.280	0.213	0.141	0.262	0.443	0.839	0.624	0.331	-0.164	-0.229				
	0.940	0.984	0.010	0.033	0.005	0.587	0.000	0.000	0.010	0.000	0.327	0.998	0.000	0.006	0.000	0.000	0.006	0.031	0.102	0.281	0.043	0.000	0.000	0.000	0.010	0.209	0.078				
Ba	-0.167	-0.041	0.094	0.415	0.214	-0.228	0.203	0.908	0.120	0.379	0.076	-0.010	0.360	0.243	0.314	0.314	0.250	0.162	0.194	-0.023	0.199	0.072	0.719	0.460	0.134	0.094	-0.254	0.485			
	0.202	0.754	0.474	0.001	0.101	0.080	0.119	0.000	0.360	0.003	0.562	0.937	0.005	0.062	0.015	0.015	0.054	0.218	0.138	0.863	0.128	0.586	0.000	0.000	0.308	0.474	0.050	0.000			
Tl	0.229	-0.326	-0.075	0.701	0.593	-0.184	0.163	0.636	0.190	0.334	0.474	0.379	0.664	0.623	0.566	0.526	0.572	0.435	0.143	0.398	0.644	0.205	0.594	0.377	0.070	0.106	-0.218	0.397	0.514		
	0.078	0.011	0.569	0.000	0.000	0.159	0.214	0.000	0.147	0.009	0.000	0.003	0.000	0.000	0.000	0.000	0.000	0.001	0.275	0.002	0.000	0.116	0.000	0.003	0.597	0.421	0.094	0.002	0.000		
Pb	0.006	-0.108	0.038	-0.113	-0.210	-0.221	0.098	0.146	-0.242	-0.042	-0.147	0.135	-0.164	-0.195	-0.029	-0.221	-0.065	-0.046	0.120	-0.090	0.123	-0.183	0.037	-0.220	0.038	-0.071	-0.196	-0.013	0.021	0.231	
	0.961	0.410	0.775	0.392	0.107	0.089	0.456	0.266	0.063	0.750	0.262	0.304	0.212	0.136	0.827	0.089	0.621	0.727	0.359	0.496	0.347	0.161	0.781	0.091	0.775	0.591	0.134	0.921	0.875	0.076	
U	0.276	0.021	0.036	0.231	0.338	0.613	0.151	0.014	0.601	0.448	-0.004	0.040	0.309	0.380	0.218	0.339	0.137	0.058	-0.005	0.265	0.444	0.587	0.113	0.430	0.094	0.035	0.353	0.331	0.010	0.223	-0.226
	0.033	0.875	0.786	0.075	0.008	0.000	0.248	0.915	0.000	0.000	0.977	0.764	0.016	0.003	0.094	0.008	0.298	0.658	0.968	0.041	0.000	0.000	0.390	0.001	0.473	0.792	0.006	0.010	0.942	0.086	0.082

Table 10.2. The Old Rotation Subsoil Pearson Correlation Coefficient Matrix and *p* values

	pH	N	C	Na	Mg	P	S	K	Ca	Al	Li	Be	V	Cr	Mn	Fe	Co	Ni	Cu	Zn	As	Se	Rb	Sr	Mo	Ag	Cd	Cs	Ba	Tl	Pb
N	0.049																														
	0.709																														
C	-0.231	0.590																													
	0.076	0.000																													
Na	0.233	-0.365	-0.645																												
	0.073	0.004	0.000																												
Mg	0.039	-0.281	-0.387	0.396																											
	0.765	0.030	0.002	0.002																											
P	-0.022	0.517	0.423	-0.001	-0.034																										
	0.870	0.000	0.001	0.994	0.797																										
S	0.031	0.429	0.355	-0.179	0.027	0.231																									
	0.814	0.001	0.005	0.171	0.836	0.076																									
K	0.110	-0.421	-0.506	0.428	0.309	-0.449	0.107																								
	0.404	0.001	0.000	0.001	0.016	0.000	0.417																								
Ca	-0.062	0.027	-0.147	0.517	0.553	0.358	0.327	0.190																							
	0.637	0.838	0.261	0.000	0.000	0.005	0.011	0.146																							
Al	-0.409	-0.067	0.054	0.043	0.321	-0.124	0.365	0.170	0.638																						
	0.001	0.613	0.684	0.746	0.012	0.343	0.004	0.193	0.000																						
Li	0.080	-0.077	-0.313	0.289	0.621	0.064	-0.198	0.013	0.182	-0.005																					
	0.542	0.560	0.015	0.025	0.000	0.625	0.130	0.924	0.163	0.967																					
Be	0.056	-0.002	-0.163	0.421	-0.214	0.071	-0.284	0.035	0.116	-0.085	0.308																				
	0.671	0.988	0.212	0.001	0.101	0.591	0.028	0.792	0.377	0.518	0.017																				
V	-0.090	0.007	0.018	0.055	0.814	0.081	0.269	0.145	0.485	0.450	0.456	-0.337																			
	0.496	0.956	0.891	0.678	0.000	0.540	0.038	0.269	0.000	0.000	0.000	0.008																			
Cr	0.056	-0.140	-0.231	0.393	0.915	0.176	0.053	0.251	0.618	0.288	0.574	-0.132	0.814																		
	0.671	0.286	0.075	0.002	0.000	0.177	0.689	0.053	0.000	0.026	0.000	0.314	0.000																		
Mn	-0.086	-0.128	-0.232	0.438	0.711	0.178	0.104	0.182	0.630	0.362	0.564	0.117	0.699	0.725																	
	0.514	0.329	0.075	0.000	0.000	0.174	0.429	0.164	0.000	0.004	0.000	0.372	0.000	0.000																	
Fe	-0.113	-0.174	-0.196	0.145	0.858	-0.001	0.194	0.243	0.532	0.529	0.404	-0.406	0.900	0.766	0.673																
	0.391	0.184	0.134	0.269	0.000	0.991	0.137	0.061	0.000	0.000	0.001	0.001	0.000	0.000	0.000																
Co	-0.122	-0.262	-0.345	0.253	0.438	-0.006	-0.270	0.149	0.172	0.064	0.442	0.099	0.261	0.423	0.389	0.356															
	0.351	0.043	0.007	0.051	0.000	0.962	0.037	0.256	0.188	0.628	0.000	0.450	0.044	0.001	0.002	0.005															
Ni	0.062	-0.257	-0.419	0.422	0.866	0.009	-0.040	0.295	0.482	0.213	0.656	-0.015	0.713	0.830	0.753	0.745	0.502														
	0.638	0.047	0.001	0.001	0.000	0.948	0.762	0.022	0.000	0.102	0.000	0.908	0.000	0.000	0.000	0.000	0.000														
Cu	-0.182	0.064	0.229	-0.013	0.072	0.204	0.206	-0.105	0.218	0.266	-0.066	-0.029	0.168	0.138	0.242	0.162	0.266	0.135													
	0.165	0.626	0.078	0.920	0.583	0.118	0.114	0.426	0.094	0.040	0.614	0.825	0.199	0.293	0.062	0.216	0.040	0.305													
Zn	-0.051	0.164	0.040	0.211	0.542	0.496	0.168	-0.164	0.393	0.079	0.616	0.048	0.586	0.563	0.717	0.548	0.390	0.614	0.340												
	0.696	0.211	0.760	0.106	0.000	0.000	0.198	0.211	0.002	0.548	0.000	0.715	0.000	0.000	0.000	0.000	0.002	0.000	0.008												
As	-0.213	0.362	0.441	-0.017	-0.029	0.527	0.339	-0.407	0.266	0.258	0.132	0.123	0.265	0.083	0.379	0.141	0.097	0.076	0.524	0.636											
	0.102	0.004	0.000	0.896	0.829	0.000	0.008	0.001	0.040	0.047	0.314	0.349	0.041	0.530	0.003	0.282	0.461	0.564	0.000	0.000											
Se	-0.241	0.360	0.671	-0.477	0.107	0.303	0.317	-0.362	0.177	0.305	-0.097	-0.339	0.410	0.245	0.035	0.236	-0.201	0.037	0.252	0.143	0.313										
	0.063	0.005	0.000	0.000	0.417	0.019	0.014	0.004	0.177	0.018	0.460	0.008	0.001	0.059	0.792	0.069	0.125	0.782	0.052	0.276	0.015										
Rb	-0.117	-0.243	-0.272	0.056	0.463	-0.405	0.272	0.640	0.282	0.584	0.121	-0.264	0.511	0.386	0.301	0.571	0.186	0.357	0.094	0.059	-0.039	0.057									
	0.375	0.061	0.036	0.670	0.000	0.001	0.036	0.000	0.029	0.000	0.357	0.041	0.000	0.002	0.019	0.000	0.154	0.005	0.474	0.653	0.770	0.664									
Sr	-0.063	-0.143	-0.349	0.641	0.435	0.083	0.285	0.387	0.887	0.707	0.132	0.211	0.333	0.446	0.570	0.453	0.190	0.431	0.231	0.245	0.215	-0.078	0.412								
	0.632	0.275	0.006	0.000	0.001	0.530	0.027	0.002	0.000	0.000	0.314	0.106	0.009	0.000	0.000	0.000	0.146	0.001	0.076	0.059	0.099	0.554	0.001								
Mo	-0.036	0.041	0.023	-0.120	-0.018	0.160	0.070	-0.197	0.074	0.015	-0.111	-0.067	0.024	0.009	0.038	0.047	-0.038	0.095	0.156	0.069	0.074	0.239	-0.069	0.025							
	0.786	0.754	0.864	0.361	0.890	0.221	0.596	0.131	0.574	0.908	0.399	0.613	0.857	0.947	0.775	0.722	0.774	0.469	0.232	0.602	0.574	0.066	0.601	0.847							
Ag	-0.066	0.117	0.323	-0.011	0.014	0.295	0.240	-0.122	0.124	0.081	0.12	0.026	0.178	0.129	0.173	0.022	-0.029	0.139	0.294	0.304	0.537	0.184	-0.017	0.086	0.062						
	0.614	0.372	0.012	0.931	0.916	0.022	0.064	0.352	0.344	0.538	0.362	0.847	0.174	0.327	0.186	0.867	0.827	0.291	0.023	0.018	0.000	0.160	0.899	0.516	0.639						
Cd	-0.106	0.564	0.607	-0.170	-0.163	0.902	0.254	-0.463	0.195	-0.131	0.022	0.050	0.040	0.042	0.038	-0.098	-0.094	-0.117	0.169	0.401	0.535	0.362	-0.408	-0.059	0.051	0.456					
	0.420	0.000	0.000	0.194	0.212	0.000	0.050	0.000	0.136	0.317	0.869	0.706	0.760	0.751	0.773	0.458	0.473	0.375	0.197	0.002	0.000	0.004	0.001	0.655	0.698	0.000					
Cs	-0.237	0.096	0.229	-0.431	0.328	-0.238	0.379	0.176	0.167	0.635	0.006	-0.443	0.591	0.286	0.134	0.549	-0.022	0.151	0.093	0.025	0.081	0.497	0.770	0.122	0.004	-0.003	-0.183				
	0.068	0.466	0.078	0.001	0.011	0.068	0.003	0.179	0.203	0.000	0.963	0.000	0.000	0.027	0.306	0.000	0.868	0.249	0.481	0.850	0.538	0.000	0.000	0.352	0.977	0.984	0.162				
Ba	0.131	-0.208	-0.435	0.520	0.216	-0.183	0.208	0.837	0.393	0.188	-0.063	0.138	0.083	0.231	0.241	0.151	0.180	0.286	0.069	-0.064	-0.203	-0.293	0.488	0.574	-0.140	-0.057	-0.268	0.037			
	0.317	0.111	0.001	0.000	0.097	0.162	0.111	0.000	0.002	0.151	0.634	0.291	0.526	0.075	0.063	0.251	0.168	0.027	0.600	0.628	0.119	0.023	0.000	0.000	0.286	0.663	0.038	0.777			
Tl	-0.019	0.002	0.094	0.019	0.491	0.010	0.145	0.341	0.092	0.142	0.486	-0.087	0.623	0.518	0.436	0.479	0.321	0.503	0.236	0.477	0.262	0.179	0.537	0.059	-0.138	0.409	0.115	0.436	0.208		
	0.886	0.987	0.474	0.887	0.000	0.940	0.270	0.008	0.486	0.280	0.000	0.510	0.000	0.000	0.001	0.000	0.012	0.000	0.070	0.000	0.043	0.172	0.000	0.652	0.293	0.001	0.381	0.000	0.111		
Pb	-0.091	0.417	0.422	-0.078	-0.136	0.308	0.407	-0.076	0.127	0.086	-0.014	0.124	0.214	0.012	0.293	-0.015	-0.003	0.044	0.504	0.394	0.667	0.238	0.050	0.119	0.096	0.496	0.393	0.073	0.146	0.370	
	0.489	0.001	0.001	0.551	0.301	0.017	0.001	0.564	0.334	0.515	0.915	0.346	0.100	0.927	0.023	0.910	0.981	0.738	0.000	0.002	0.000	0.067	0.702	0.365	0.464	0.000	0.002	0.580	0.266	0.004	
U	-0.245	0.034	0.202	0.233	0.297	0.473	0.011	-0.033	0.583	0.314	0.113	0.170	0.350	0.527	0.507	0.255	0.209	0.307	0.460	0.364	0.400	0.414	0.050	0.422	0.217	0.379	0.417	0.051	0.137	0.242	0.324
	0.059	0.796	0.122	0.073	0.021	0.000	0.932	0.803	0.000	0.014	0.391	0.194	0.006	0.000	0.000	0.050	0.109	0.017	0.000	0.004	0.002	0.001	0.703	0.001	0.097	0.003	0.001	0.696	0.298	0.062	0.012

Table 10.3. The pH Rotation Topsoil Pearson Correlation Coefficient Matrix and *p* values

	pH	N	C	Na	Mg	P	S	K	Ca	Al	Li	Be	V	Cr	Mn	Fe	Co	Ni	Cu	Zn	As	Se	Rb	Sr	Mo	Ag	Cd	Cs	Ba	Tl	Pb
N	0.207																														
	0.034																														
C	0.197	0.372																													
	0.044	0.000																													
Na	-0.159	-0.218	-0.377																												
	0.105	0.026	0.000																												
Mg	0.383	0.024	-0.150	0.749																											
	0.000	0.805	0.126	0.000																											
P	-0.129	0.236	0.454	0.122	0.079																										
	0.191	0.015	0.000	0.217	0.421																										
S	0.147	0.067	0.142	0.703	0.676	0.514																									
	0.134	0.499	0.149	0.000	0.000	0.000																									
K	-0.218	-0.162	-0.374	0.855	0.590	0.116	0.620																								
	0.026	0.098	0.000	0.000	0.000	0.238	0.000																								
Ca	0.945	0.228	0.237	-0.024	0.545	-0.022	0.301	-0.062																							
	0.000	0.019	0.015	0.810	0.000	0.825	0.002	0.527																							
Al	-0.032	0.104	-0.132	0.542	0.486	0.057	0.539	0.613	0.128																						
	0.746	0.291	0.180	0.000	0.000	0.563	0.000	0.000	0.192																						
Li	-0.143	-0.041	-0.195	0.559	0.540	0.053	0.482	0.449	-0.014	0.417																					
	0.146	0.679	0.046	0.000	0.000	0.594	0.000	0.000	0.887	0.000																					
Be	0.091	0.059	-0.038	0.472	0.568	0.137	0.574	0.372	0.227	0.447	0.92																				
	0.358	0.552	0.699	0.000	0.000	0.164	0.000	0.000	0.020	0.000	0.000																				
V	-0.330	0.047	0.100	0.708	0.528	0.543	0.703	0.690	-0.137	0.549	0.468	0.416																			
	0.001	0.636	0.311	0.000	0.000	0.000	0.000	0.000	0.162	0.000	0.000	0.000																			
Cr	-0.213	0.029	-0.096	0.828	0.724	0.343	0.742	0.728	-0.020	0.577	0.72	0.655	0.875																		
	0.029	0.767	0.329	0.000	0.000	0.000	0.000	0.000	0.842	0.000	0.000	0.000	0.000																		
Mn	0.470	0.163	0.181	0.028	0.219	0.329	0.266	-0.018	0.388	0.117	-0.09	0.047	0.152	0.063																	
	0.000	0.097	0.065	0.777	0.025	0.001	0.006	0.853	0.000	0.235	0.361	0.637	0.123	0.526																	
Fe	-0.172	0.234	-0.013	0.373	0.344	0.212	0.372	0.434	-0.024	0.657	0.372	0.345	0.586	0.614	0.136																
	0.079	0.016	0.894	0.000	0.000	0.030	0.000	0.000	0.808	0.000	0.000	0.000	0.000	0.000	0.168																
Co	-0.122	-0.007	-0.324	0.757	0.700	0.183	0.551	0.679	0.024	0.413	0.646	0.560	0.635	0.805	0.069	0.529															
	0.215	0.943	0.001	0.000	0.000	0.062	0.000	0.000	0.806	0.000	0.000	0.000	0.000	0.000	0.484	0.000															
Ni	0.032	0.061	-0.116	0.651	0.707	0.215	0.647	0.565	0.212	0.501	0.707	0.711	0.590	0.763	0.059	0.437	0.709														
	0.744	0.534	0.238	0.000	0.000	0.028	0.000	0.000	0.030	0.000	0.000	0.000	0.000	0.000	0.550	0.000	0.000														
Cu	-0.083	0.180	0.270	0.191	0.080	0.461	0.414	0.168	0.010	0.175	0.075	0.130	0.366	0.275	-0.026	0.294	0.129	0.161													
	0.400	0.067	0.005	0.051	0.418	0.000	0.000	0.086	0.919	0.074	0.445	0.186	0.000	0.005	0.793	0.002	0.191	0.101													
Zn	0.628	0.141	0.123	0.400	0.726	0.216	0.646	0.255	0.684	0.323	0.422	0.582	0.300	0.430	0.540	0.152	0.382	0.528	0.177												
	0.000	0.151	0.213	0.000	0.000	0.027	0.000	0.009	0.000	0.001	0.000	0.000	0.002	0.000	0.000	0.121	0.000	0.000	0.071												
As	0.154	0.248	0.244	0.162	0.348	0.010	0.420	0.151	0.292	0.477	0.681	0.773	0.291	0.443	-0.050	0.421	0.266	0.483	0.196	0.438											
	0.116	0.011	0.012	0.098	0.000	0.920	0.000	0.124	0.003	0.000	0.000	0.000	0.003	0.000	0.610	0.000	0.006	0.000	0.045	0.000											
Se	-0.305	0.049	0.516	-0.039	-0.159	0.489	0.062	-0.053	-0.255	0.016	-0.246	-0.256	0.451	0.115	0.122	0.159	-0.079	-0.141	0.330	-0.122	-0.112										
	0.002	0.621	0.000	0.690	0.105	0.000	0.533	0.588	0.009	0.874	0.012	0.008	0.000	0.241	0.217	0.105	0.426	0.152	0.001	0.215	0.254										
Rb	-0.538	-0.077	-0.413	0.575	0.264	-0.124	0.213	0.744	-0.390	0.671	0.477	0.309	0.523	0.568	-0.310	0.560	0.522	0.391	0.079	-0.146	0.254	-0.021									
	0.000	0.433	0.000	0.000	0.007	0.208	0.029	0.000	0.000	0.000	0.000	0.001	0.000	0.000	0.001	0.000	0.000	0.000	0.421	0.138	0.009	0.833									
Sr	0.858	0.231	0.086	-0.010	0.528	-0.183	0.178	0.035	0.935	0.275	-0.019	0.188	-0.157	-0.026	0.271	0.103	0.065	0.198	-0.062	0.544	0.283	-0.327	-0.158								
	0.000	0.018	0.384	0.921	0.000	0.061	0.069	0.720	0.000	0.005	0.851	0.055	0.109	0.795	0.005	0.297	0.512	0.043	0.531	0.000	0.003	0.001	0.107								
Mo	-0.449	0.067	0.185	0.054	-0.142	0.496	0.289	0.066	-0.381	0.205	0.54	0.507	0.371	0.363	0.026	0.304	0.170	0.300	0.270	0.016	0.459	0.163	0.232	-0.449							
	0.000	0.496	0.059	0.586	0.148	0.000	0.003	0.502	0.000	0.036	0.000	0.000	0.000	0.000	0.792	0.002	0.082	0.002	0.005	0.869	0.000	0.096	0.017	0.000							
Ag	-0.059	0.039	0.032	0.285	0.170	0.197	0.237	0.206	-0.045	0.062	0.021	-0.010	0.301	0.252	0.076	0.033	0.102	0.146	0.132	0.160	-0.015	0.209	0.045	-0.093	-0.052						
	0.551	0.694	0.742	0.003	0.082	0.044	0.015	0.035	0.647	0.528	0.832	0.919	0.002	0.010	0.440	0.739	0.301	0.136	0.180	0.104	0.880	0.032	0.645	0.344	0.598						
Cd	0.436	0.180	0.230	0.091	0.401	0.095	0.273	0.077	0.507	0.113	0.045	0.194	0.131	0.123	0.120	-0.000	0.145	0.276	0.107	0.459	0.261	0.062	-0.153	0.453	-0.193	0.136					
	0.000	0.065	0.018	0.354	0.000	0.334	0.005	0.434	0.000	0.251	0.652	0.048	0.184	0.210	0.225	0.999	0.141	0.004	0.280	0.000	0.007	0.532	0.118	0.000	0.048	0.166					
Cs	-0.534	0.078	-0.194	0.261	0.083	-0.174	0.027	0.384	-0.381	0.589	0.479	0.338	0.387	0.433	-0.420	0.568	0.329	0.298	0.087	-0.247	0.467	0.052	0.860	-0.156	0.365	-0.106	-0.166				
	0.000	0.429	0.047	0.007	0.402	0.077	0.785	0.000	0.000	0.000	0.000	0.000	0.000	0.000	0.000	0.000	0.001	0.002	0.376	0.011	0.000	0.601	0.000	0.112	0.000	0.282	0.090				
Ba	-0.128	-0.018	-0.171	0.043	0.042	-0.196	-0.127	0.300	-0.055	0.138	0.032	-0.013	0.119	0.100	-0.146	0.194	0.161	0.087	-0.034	-0.144	0.032	0.027	0.380	0.115	-0.113	-0.008	0.096	0.336			
	0.194	0.858	0.082	0.662	0.670	0.045	0.197	0.002	0.580	0.162	0.746	0.899	0.225	0.308	0.137	0.047	0.102	0.377	0.730	0.144	0.745	0.787	0.000	0.241	0.252	0.935	0.329	0.000			
Tl	-0.141	-0.067	-0.211	0.721	0.664	-0.159	0.460	0.755	0.048	0.546	0.591	0.494	0.592	0.734	-0.271	0.446	0.674	0.615	0.063	0.237	0.454	-0.089	0.708	0.160	-0.021	0.130	0.177	0.582	0.264		
	0.152	0.499	0.031	0.000	0.000	0.105	0.000	0.000	0.629	0.000	0.000	0.000	0.000	0.000	0.005	0.000	0.000	0.000	0.522	0.015	0.000	0.365	0.000	0.104	0.834	0.186	0.071	0.000	0.006		
Pb	-0.037	0.120	0.139	0.281	0.327	0.260	0.529	0.248	0.098	0.390	0.813	0.873	0.389	0.557	-0.025	0.414	0.418	0.585	0.265	0.428	0.846	-0.133	0.281	0.047	0.715	-0.075	0.115	0.409	-0.032	0.363	
	0.706	0.223	0.158	0.004	0.001	0.007	0.000	0.011	0.321	0.000	0.000	0.000	0.000	0.000	0.800	0.000	0.000	0.000	0.006	0.000	0.000	0.176	0.004	0.631	0.000	0.448	0.242	0.000	0.749	0.000	
U	-0.466	0.286	0.085	0.143	0.009	0.223	0.037	0.243	-0.344	0.357	0.088	0.015	0.504	0.369	-0.139	0.557	0.203	0.081	0.174	-0.217	0.154	0.425	0.477	-0.225	0.211	0.081	-0.105	0.569	0.245	0.352	0.113
	0.000	0.003	0.386	0.146	0.931	0.022	0.710	0.013	0.000	0.000	0.370	0.883	0.000	0.000	0.157	0.000	0.037	0.409	0.076	0.026	0.118	0.000	0.000	0.021	0.031	0.412	0.287	0.000	0.012	0.000	0.249

Table 10.4. The pH Rotation Subsoil Pearson Correlation Coefficient Matrix and *p* values

	pH	N	C	Na	Mg	P	S	K	Ca	Al	Li	Be	V	Cr	Mn	Fe	Co	Ni	Cu	Zn	As	Se	Rb	Sr	Mo	Ag	Cd	Cs	Ba	Tl	Pb
N	0.208																														
	0.033																														
C	0.289	0.593																													
	0.003	0.000																													
Na	-0.155	-0.361	-0.754																												
	0.115	0.000	0.000																												
Mg	-0.198	-0.384	-0.468	0.443																											
	0.043	0.000	0.000	0.000																											
P	0.347	0.458	0.605	-0.489	-0.406																										
	0.000	0.000	0.000	0.000	0.000																										
S	0.034	0.247	0.276	-0.168	0.130	0.416																									
	0.734	0.011	0.004	0.086	0.186	0.000																									
K	-0.187	-0.305	-0.644	0.822	0.321	-0.339	-0.099																								
	0.056	0.002	0.000	0.000	0.001	0.000	0.314																								
Ca	0.918	0.120	0.147	-0.027	0.011	0.338	0.165	-0.095																							
	0.000	0.222	0.134	0.785	0.909	0.000	0.093	0.333																							
Al	-0.217	-0.099	-0.352	0.392	0.546	-0.195	0.357	0.368	0.034																						
	0.026	0.315	0.000	0.000	0.000	0.047	0.000	0.000	0.732																						
Li	-0.497	-0.301	-0.418	0.271	0.755	-0.436	0.138	0.205	-0.363	0.494																					
	0.000	0.002	0.000	0.005	0.000	0.000	0.162	0.036	0.000	0.000																					
Be	-0.173	-0.134	-0.387	0.524	0.147	-0.089	0.016	0.517	-0.106	0.154	0.223																				
	0.077	0.172	0.000	0.000	0.135	0.367	0.869	0.000	0.280	0.117	0.022																				
V	-0.276	-0.151	-0.014	-0.083	0.702	-0.115	0.219	-0.072	-0.143	0.401	0.55	-0.208																			
	0.004	0.125	0.885	0.397	0.000	0.244	0.025	0.467	0.145	0.000	0.000	0.033																			
Cr	-0.341	-0.245	-0.266	0.248	0.905	-0.297	0.161	0.149	-0.175	0.468	0.734	0.020	0.809																		
	0.000	0.012	0.006	0.011	0.000	0.002	0.101	0.129	0.074	0.000	0.000	0.837	0.000																		
Mn	0.175	0.216	-0.002	0.196	-0.114	-0.195	-0.138	0.071	0.134	0.126	-0.216	-0.131	-0.046	-0.106																	
	0.074	0.027	0.981	0.046	0.247	0.047	0.160	0.469	0.172	0.201	0.027	0.181	0.641	0.282																	
Fe	-0.105	-0.171	-0.120	0.044	0.706	-0.161	0.131	-0.062	0.059	0.501	0.441	-0.344	0.859	0.774	0.090																
	0.288	0.082	0.223	0.657	0.000	0.102	0.183	0.533	0.548	0.000	0.000	0.000	0.000	0.000	0.361																
Co	-0.203	-0.326	-0.475	0.511	0.861	-0.343	0.065	0.371	-0.042	0.479	0.604	0.184	0.629	0.829	0.132	0.685															
	0.038	0.001	0.000	0.000	0.000	0.000	0.510	0.000	0.672	0.000	0.000	0.060	0.000	0.000	0.179	0.000															
Ni	-0.395	-0.283	-0.302	0.294	0.742	-0.168	0.185	0.249	-0.233	0.391	0.634	0.161	0.621	0.785	-0.197	0.577	0.721														
	0.000	0.003	0.002	0.002	0.000	0.087	0.059	0.010	0.017	0.000	0.000	0.101	0.000	0.000	0.044	0.000	0.000														
Cu	0.255	0.246	0.443	-0.349	-0.095	0.592	0.289	-0.272	0.256	-0.077	-0.221	-0.182	0.089	0.041	-0.150	0.117	-0.036	0.087													
	0.009	0.011	0.000	0.000	0.336	0.000	0.003	0.005	0.008	0.435	0.023	0.063	0.366	0.675	0.128	0.234	0.716	0.378													
Zn	-0.027	0.014	0.124	-0.152	0.463	0.429	0.500	-0.118	0.144	0.310	0.378	-0.012	0.549	0.533	-0.330	0.503	0.418	0.611	0.470												
	0.782	0.888	0.206	0.122	0.000	0.000	0.000	0.230	0.144	0.001	0.000	0.902	0.000	0.000	0.001	0.000	0.000	0.000	0.000												
As	0.407	0.421	0.597	-0.497	-0.321	0.848	0.473	-0.270	0.367	-0.154	-0.366	-0.064	0.003	-0.235	-0.203	-0.122	-0.307	-0.163	0.557	0.364											
	0.000	0.000	0.000	0.000	0.001	0.000	0.000	0.005	0.000	0.117	0.000	0.514	0.974	0.016	0.038	0.214	0.001	0.097	0.000	0.000											
Se	-0.170	0.093	0.467	-0.508	0.211	0.075	0.275	-0.546	-0.135	0.108	0.268	-0.360	0.663	0.419	-0.075	0.548	0.087	0.223	0.199	0.415	0.108										
	0.083	0.347	0.000	0.000	0.030	0.445	0.005	0.000	0.171	0.274	0.006	0.000	0.000	0.000	0.447	0.000	0.375	0.022	0.042	0.000	0.271										
Rb	-0.468	-0.268	-0.508	0.485	0.493	-0.446	0.010	0.648	-0.334	0.644	0.568	0.244	0.371	0.448	0.228	0.315	0.491	0.377	-0.340	0.026	-0.335	-0.08									
	0.000	0.006	0.000	0.000	0.000	0.000	0.919	0.000	0.000	0.000	0.000	0.012	0.000	0.000	0.019	0.001	0.000	0.000	0.000	0.789	0.000	0.415									
Sr	0.596	-0.011	-0.270	0.457	0.182	0.048	0.113	0.339	0.775	0.451	-0.127	0.163	-0.195	-0.063	0.237	0.106	0.178	-0.094	0.005	0.061	0.052	-0.373	0.101								
	0.000	0.915	0.005	0.000	0.063	0.628	0.253	0.000	0.000	0.000	0.197	0.096	0.046	0.523	0.015	0.284	0.070	0.340	0.959	0.538	0.601	0.000	0.306								
Mo	-0.233	0.041	0.124	-0.163	-0.153	0.285	-0.007	-0.071	-0.258	-0.131	-0.129	-0.103	0.120	0.018	-0.097	0.056	0.050	0.111	0.295	0.165	0.077	0.106	-0.075	-0.336							
	0.017	0.679	0.208	0.097	0.120	0.003	0.946	0.469	0.008	0.183	0.188	0.296	0.223	0.855	0.327	0.570	0.610	0.261	0.002	0.092	0.432	0.283	0.444	0.000							
Ag	-0.202	0.059	0.113	-0.066	0.179	0.065	0.325	-0.016	-0.173	0.155	0.328	0.199	0.232	0.244	-0.165	0.007	0.062	0.218	-0.007	0.269	0.225	0.283	0.123	-0.164	-0.070						
	0.038	0.550	0.251	0.501	0.068	0.510	0.001	0.873	0.077	0.113	0.001	0.042	0.017	0.012	0.092	0.946	0.529	0.025	0.940	0.006	0.021	0.003	0.212	0.094	0.475						
Cd	0.251	0.236	0.333	-0.263	-0.252	0.578	0.147	-0.122	0.195	-0.155	-0.232	0.015	-0.072	-0.226	-0.182	-0.126	-0.227	-0.061	0.283	0.252	0.567	-0.012	-0.251	0.057	0.050	0.153					
	0.010	0.015	0.001	0.007	0.010	0.000	0.134	0.215	0.046	0.115	0.017	0.878	0.468	0.020	0.063	0.201	0.020	0.539	0.003	0.010	0.000	0.905	0.010	0.563	0.612	0.118					
Cs	-0.512	-0.200	-0.159	-0.009	0.509	-0.348	0.113	0.163	-0.406	0.469	0.674	-0.005	0.656	0.582	0.030	0.440	0.401	0.413	-0.227	0.209	-0.188	0.386	0.779	-0.258	-0.027	0.308	-0.175				
	0.000	0.041	0.106	0.930	0.000	0.000	0.249	0.097	0.000	0.000	0.000	0.962	0.000	0.000	0.764	0.000	0.000	0.000	0.020	0.033	0.055	0.000	0.000	0.008	0.784	0.001	0.075				
Ba	-0.251	-0.318	-0.588	0.599	0.188	-0.377	-0.164	0.692	-0.135	0.412	0.264	0.302	-0.099	0.061	0.152	-0.013	0.222	0.032	-0.437	-0.189	-0.326	-0.398	0.696	0.370	-0.200	0.035	-0.147	0.311			
	0.010	0.001	0.000	0.000	0.055	0.000	0.095	0.000	0.170	0.000	0.006	0.002	0.317	0.536	0.123	0.895	0.023	0.744	0.000	0.053	0.001	0.000	0.000	0.000	0.041	0.721	0.136	0.001			
Tl	-0.203	-0.088	-0.139	0.210	0.494	0.083	0.385	0.491	-0.107	0.377	0.512	0.365	0.446	0.471	-0.212	0.216	0.457	0.508	0.099	0.452	0.322	0.031	0.573	0.012	-0.040	0.442	0.173	0.560	0.287		
	0.038	0.372	0.157	0.031	0.000	0.399	0.000	0.000	0.278	0.000	0.000	0.000	0.000	0.000	0.030	0.027	0.000	0.000	0.317	0.000	0.001	0.756	0.000	0.900	0.686	0.000	0.078	0.000	0.003		
Pb	0.269	0.262	0.367	-0.326	-0.392	0.589	0.266	-0.180	0.251	-0.210	-0.429	-0.032	-0.209	-0.394	-0.170	-0.271	-0.365	-0.197	0.265	0.122	0.610	-0.062	-0.360	0.049	0.115	0.061	0.365	-0.312	-0.178	0.092	
	0.006	0.007	0.000	0.001	0.000	0.000	0.006	0.066	0.010	0.032	0.000	0.748	0.032	0.000	0.084	0.005	0.000	0.044	0.006	0.216	0.000	0.527	0.000	0.619	0.244	0.537	0.000	0.001	0.070	0.349	
U	0.327	0.317	0.421	-0.219	-0.257	0.784	0.407	-0.069	0.355	0.066	-0.368	0.094	-0.096	-0.176	-0.120	-0.114	-0.153	-0.137	0.522	0.337	0.745	-0.007	-0.192	0.237	0.259	0.150	0.472	-0.204	-0.079	0.217	0.460
	0.001	0.001	0.000	0.025	0.008	0.000	0.000	0.486	0.000	0.502	0.000	0.340	0.332	0.072	0.222	0.246	0.119	0.162	0.000	0.000	0.000	0.940	0.050	0.015	0.008	0.126	0.000	0.037	0.423	0.026	0.000

Appendix 2 – Plot P_{Total} Balances and Net Annual Accumulation Rates

Table 10.5. P_{Total} Balance (2015) in the Old Rotation with P fertiliser inputs, crop yields, crop P concentrations and total P offtakes- the (*) roots are in one single split plot.

Crop	Treatment	$P_{fertiliser}$ input (kg ha^{-1})	Crop yields (kg ha^{-1})	Average P_{Crop} (mg kg^{-1})	P_{Crop} removal (mg ha^{-1})	Plot P_{Crop} offtake (kg ha^{-1})	Annual P Balance Input - Offtake P (kg ha^{-1})
Grass Y1 (Hay)	**Zero fertiliser**	0	1360	1979	2691853	2.69	-2.69
	NK TSP	20	5041	1877	9458740	9.46	10.5
	NK GMP	20	5347	1943	10385907	10.4	9.61
	NK without P	0	4089	1393	5694833	5.69	-5.69
	PK without N	20	1896	2383	4516564	4.52	15.5
	PN without K	20	5287	1938	10244332	10.2	9.76
Grass Y2	**Zero fertiliser**	0	0	3791	0	0.00	0.00
	NK TSP	0	0	4272	0	0.00	0.00
	NK GMP	0	0	3648	0	0.00	0.00
	NK without P	0	0	3648	0	0.00	0.00
	PK without N	0	0	4866	0	0.00	0.00
	PN without K	0	0	4943	0	0.00	0.00
Barley	**Zero fertiliser**	0	1326	2648	3510774	3.51	-3.51
	NK TSP	20	4106	2741	11251408	11.3	8.75
	NK GMP	20	2193	2646	5802442	5.80	14.2
	NK without P	0	1573	2388	3755139	3.76	-3.76
	PK without N	20	2406	2354	5662128	5.66	14.3
	PN without K	20	3817	2810	10725403	10.7	9.27
Potato*	**Zero fertiliser**	42	8120	1573	12769915	12.8	29.2
	NK TSP	108	15940	1621	25837310	25.8	82.2
	NK GMP	108	10820	1655	17901809	17.9	90.1
	NK without P	42	8380	1896	15890049	15.9	26.1
	PK without N	108	15260	1760	26855423	26.9	81.1
	PN without K	108	15420	1828	28191104	28.2	79.8
Swede*	**Zero fertiliser**	42	1980	1688	3342200	3.34	38.7
	NK TSP	108	2210	1884	4164670	4.16	103.8
	NK GMP	108	570	1710	974519	0.97	107.0
	NK without P	42	650	1536	998419	1.00	41.0
	PK without N	108	3560	2450	8722192	8.72	99.3
	PN without K	108	1260	2454	3091735	3.09	104.9
Turnip*	**Zero fertiliser**	42	860	1907	1640136	1.64	40.4
	NK TSP	108	1100	2657	2922198	2.92	105.1
	NK GMP	108	400	1966	786395	0.79	107.2
	NK without P	42	340	1694	575982	0.58	41.4
	PK without N	108	2230	3927	8757758	8.76	99.2
	PN without K	108	1530	3585	5484550	5.48	102.5
Oats	**Zero fertiliser**	0	3392	3700	12548947	12.5	-12.5
	NK TSP	20	5168	3887	20088333	20.1	-0.09
	NK GMP	20	4803	3928	18862733	18.9	1.14
	NK without P	0	4029	4022	16204178	16.2	-16.2
	PK without N	20	5177	4091	21178407	21.2	-1.18
	PN without K	20	3995	3923	15671941	15.7	4.33

Table 10.6. Net Soil Profile P_{Total} Accumulation Rates in the Old Rotation over 94 years.

Crop	Treatment	Topsoil P_{Total} (mg kg^{-1})	Topsoil P_{Total} (kg ha^{-1})	Subsoil P_{Total} (mg kg^{-1})	Subsoil P_{Total} (kg ha^{-1})	Soil Profile P_{Total} (mg kg^{-1})	Soil Profile P_{Total} (kg ha^{-1})	Net Soil Profile P_{Total} Accumulation (Plot – Field) (kg ha^{-1})	Net Soil Profile P_{Total} Annual Accumulation Rate (kg ha^{-1} yr^{-1})
-	Field	1378	3308	1101	2643	2480	5951	-	-
Grass Y1 (Hay)	Zero fertiliser	951	2281	818	1964	1769	4245	-1706	-18.3
	NK TSP	1271	3051	980	2351	2251	5402	-549	-5.90
	NK GMP	1279	3069	997	2394	2276	5462	-489	-5.26
	NK without P	935	2244	841	2018	1776	4262	-1689	-18.2
Grass Y2	Zero fertiliser	1065	2556	811	1947	1876	4503	-1448	-15.6
	NK TSP	1228	2948	987	2370	2216	5318	-633	-6.81
	NK GMP	1436	3446	962	2308	2397	5754	-198	-2.12
	NK without P	957	2298	730	1752	1687	4049	-1902	-20.5
Grass Y3	Zero fertiliser	966	2318	683	1638	1648	3956	-1995	-21.5
	NK TSP	1207	2898	820	1969	2028	4866	-1085	-11.7
	NK GMP	1211	2907	887	2130	2099	5037	-915	-9.83
	NK without P	923	2214	708	1700	1631	3914	-2037	-21.9
Barley	Zero fertiliser	905	2172	715	1716	1620	3888	-2063	-22.2
	NK TSP	1415	3396	1030	2472	2445	5867	-83.8	-0.90
	NK GMP	1255	3012	1168	2804	2423	5815	-136	-1.46
	NK without P	884	2122	857	2058	1741	4179	-1772	-19.1
Oats	Zero fertiliser	993	2383	740	1777	1733	4160	-1791	-19.3
	NK TSP	1312	3150	1093	2622	2405	5772	-179	-1.93
	NK GMP	1289	3094	1099	2638	2388	5732	-219	-2.36
	NK without P	955	2293	827	1986	1783	4279	-1672	-18.0

Table 10.7. P_{Total} Balance (2015) in the pH Rotation with P fertiliser inputs, crop yields, crop P concentrations and total P offtakes.

Crop	Treatment	$P_{fertiliser}$ input (kg ha^{-1})	Crop yields (kg ha^{-1})	Crop yields 2014 Straw (kg ha^{-1})	Average P_{crop} (mg kg^{-1})	Average P_{crop} Straw (mg kg^{-1})	P_{Crop} removal (mg ha^{-1})	P_{Crop} removal Straw (mg ha^{-1})	P_{Crop} removal (kg ha^{-1})	P_{Crop} removal Straw (kg ha^{-1})	Plot P_{Crop} offtake (kg ha^{-1})	Annual P Balance Input - Offtake (kg ha^{-1})
Grass Y1 (Hay)	**4.5**	13	4760	0	1850	0	8807078	0	8.81	0	8.81	4.19
	5	13	5810	0	2041	0	11859053	0	11.9	0	11.9	1.14
	5.5	13	5920	0	1927	0	11408136	0	11.4	0	11.4	1.59
	6	13	7360	0	1968	0	14481275	0	14.5	0	14.5	-1.48
	6.5	13	6150	0	2026	0	12459576	0	12.5	0	12.5	0.54
	7	13	5460	0	2205	0	12041062	0	12.0	0	12.0	0.96
	7.5	13	5950	0	2456	0	14612823	0	14.6	0	14.6	-1.61
Grass Y2	**4.5**	0	0	0	4914	0	0	0	0	0	0	0
	5	0	0	0	4805	0	0	0	0	0	0	0
	5.5	0	0	0	4895	0	0	0	0	0	0	0
	6	0	0	0	4634	0	0	0	0	0	0	0
	6.5	0	0	0	4590	0	0	0	0	0	0	0
	7	0	0	0	4211	0	0	0	0	0	0	0
	7.5	0	0	0	4214	0	0	0	0	0	0	0
Wheat	**4.5**	28	0	1800	0	1460	0	2627144	0	2.63	2.63	25.4
	5	28	3579	1560	2694	757	9640865	1180510	9.64	1.18	10.8	17.2
	5.5	28	7327	5330	2643	750	19368308	4000065	19.4	4.00	23.4	4.63
	6	28	7565	4400	2576	1025	19489327	4508831	19.5	4.51	24.0	4.00
	6.5	28	6086	3440	2814	1266	17128562	4354029	17.1	4.35	21.5	6.52
	7	28	4361	3310	0	1509	0	4995919	0	5.00	5.00	23.0
	7.5	28	1547	1100	0	1965	0	2161002	0	2.16	2.16	25.8
Potato	**4.5**	108	10150	0	1547	0	15701903	0	15.7	0	15.7	92.3
	5	108	11176	0	2403	0	26861006	0	26.9	0	26.9	81.1
	5.5	108	11342	0	1905	0	21610420	0	21.6	0	21.6	86.4
	6	108	11308	0	1658	0	18743851	0	18.7	0	18.7	89.3
	6.5	108	10994	0	1804	0	19835089	0	19.8	0	19.8	88.2
	7	108	11076	0	1550	0	17168003	0	17.2	0	17.2	90.8
	7.5	108	10728	0	1703	0	18268901	0	18.3	0	18.3	89.7
Barley	**4.5**	22	0	0	0	0	0	0	0	0	0	22.0
	5	22	0	930	0	1172	0	1090081	0	1.09	1.09	20.9
	5.5	22	3706	3240	2665	887	9875203	2872264	9.88	2.87	12.7	9.25
	6	22	5058	3670	2946	834	14898741	3060447	14.9	3.06	18.0	4.04
	6.5	22	4310	2210	3250	1166	14006558	2576828	14.0	2.58	16.6	5.42
	7	22	2746	2730	3505	1570	9622591	4284963	9.62	4.28	13.9	8.09
	7.5	22	1998	1020	3634	1668	7258347	1701323	7.26	1.70	8.96	13.0
Swede	**4.5**	77	6440	0	2447	0	15755934	0	15.8	0	15.8	61.2
	5	77	6870	0	2558	0	17575822	0	17.6	0	17.6	59.4
	5.5	77	8000	0	2912	0	23297689	0	23.3	0	23.3	53.7
	6	77	7480	0	3186	0	23829110	0	23.8	0	23.8	53.2
	6.5	77	8660	0	3181	0	27547005	0	27.5	0	27.5	49.5
	7	77	8020	0	3282	0	26317751	0	26.3	0	26.3	50.7
	7.5	77	6430	0	3426	0	22031792	0	22.0	0	22.0	55.0
Oats	**4.5**	22	2661	3730	3703	629	9850512	2347435	9.85	2.35	12.2	9.80
	5	22	3579	4040	3558	668	12732749	2698506	12.7	2.70	15.4	6.57
	5.5	22	4701	3640	3553	753	16699097	2739268	16.7	2.74	19.4	2.56
	6	22	3995	3600	3135	836	12524099	3009249	12.5	3.01	15.5	6.47
	6.5	22	2771	4330	3459	803	9585734	3478694	9.59	3.48	13.1	8.94
	7	22	527	960	3399	1836	1791370	1762617	1.79	1.76	3.55	18.4
	7.5	22	0	0	0	0	0	0	0	0	0	22.0

Table 10.8. Net Soil Profile P_{Total} Annual Accumulates Rates in the pH Rotation over 53 years.

Crop	Treatment	Topsoil P_{Total} (mg kg^{-1})	Topsoil P_{Total} (kg ha^{-1})	Subsoil P_{Total} (mg kg^{-1})	Subsoil P_{Total} (kg ha^{-1})	Soil Profile P_{Total} (mg kg^{-1})	Soil Profile P_{Total} (kg ha^{-1})	Net Soil Profile P_{Total} Accumulation (Plot – Field) (kg ha^{-1})	Net Soil Profile P_{Total} Annual Accumulation Rate (kg ha^{-1} yr^{-1})
-	**Field**	1378	3308	1101	2643	2480	5951	-	-
Grass Y1 (Hay)	**4.5**	1954	4689	1075	2581	3029	7270	1318	24.4
	5	1801	4321	1225	2939	3025	7260	1309	24.2
	5.5	1768	4242	1371	3290	3138	7532	1581	29.3
	6	1745	4187	1224	2937	2969	7124	1173	21.7
	6.5	1807	4337	1336	3206	3143	7543	1592	29.5
	7	1808	4338	1284	3081	3091	7419	1468	27.2
	7.5	1889	4533	1138	2730	3026	7263	1312	24.3
Grass Y2	**4.5**	1927	4625	1171	2811	3098	7436	1485	27.5
	5	1834	4402	1053	2527	2887	6930	978	18.1
	5.5	1767	4241	1158	2779	2925	7020	1069	19.8
	6	1712	4109	1241	2979	2954	7089	1137	21.1
	6.5	1718	4124	1322	3172	3040	7296	1345	24.9
	7	1778	4268	1402	3365	3180	7633	1681	31.1
	7.5	1821	4370	1233	2960	3054	7330	1378	25.5
Wheat	**4.5**	1756	4215	934	2242	2690	6457	506	9.36
	5	1655	3972	844	2026	2499	5998	47	0.86
	5.5	1556	3734	1271	3049	2827	6784	833	15.4
	6	1583	3800	1280	3072	2863	6871	920	17.0
	6.5	1545	3708	1228	2948	2773	6656	705	13.1
	7	1609	3863	1103	2648	2713	6510	559	10.4
	7.5	1755	4213	1280	3071	3035	7284	1333	24.7
Barley	**4.5**	1893	4543	890	2137	2783	6680	729	13.5
	5	1806	4334	1100	2640	2906	6974	1023	18.9
	5.5	1822	4373	1341	3218	3163	7591	1639	30.4
	6	1815	4355	1371	3290	3186	7645	1694	31.4
	6.5	1794	4307	1207	2896	3001	7202	1251	23.2
	7	1792	4300	1244	2986	3036	7285	1334	24.7
	7.5	1824	4377	1168	2803	2992	7180	1229	22.8
Oats	**4.5**	2099	5037	1167	2800	3265	7837	1886	34.9
	5	2056	4934	1227	2944	3282	7878	1927	35.7
	5.5	2045	4908	997	2393	3042	7301	1350	25.0
	6	1979	4749	1170	2807	3148	7555	1604	29.7
	6.5	1998	4795	1135	2723	3133	7518	1567	29.0
	7	2004	4809	1057	2538	3061	7347	1396	25.8
	7.5	2065	4955	1573	3776	3638	8731	2780	51.5

Appendix 3 – Analysis of Variance Tables

Table 10.9. Old Rotation P_{Total} Analysis of Variance

Crop x Treatment X Layer						(Crop + Treatment) x Layer					
Source of variation	d.f.	s.s.	m.s.	v.r.	F pr.	Source of variation	d.f.	s.s.	m.s.	v.r.	F pr.
Plot stratum						Plot stratum					
Crop	4	199061	49765			Crop	4	199061	49765	3.67	0.036
Treatment	3	2412976	804325			Treatment	3	2412976	804325	59.4	<.001
Crop.Treatment	12	162551	13546			Residual	12	162551	13546	4.22	
Plot.Auger stratum	40	128298	3207	0.96		Plot.Auger stratum	40	128298	3207	0.61	
Plot.Auger.*Units* stratum						Plot.Auger.*Units* stratum					
Layer	1	1644415	1644415	490	<.001	Layer	1	1644415	1644415	315	<.001
Crop.Layer	4	91045	22761	6.78	<.001	Crop.Layer	4	91045	22761	4.36	0.004
Treatment.Layer	3	118089	39363	11.7	<.001	Treatment.Layer	3	118089	39363	7.53	<.001
Crop.Treatment.Layer	12	137397	11450	3.41	0.002						
Residual	40	134258	3356			Residual	52	271655	5224		
Total	119	5028091				Total	119	5028091			

Table 10.10. Old Rotation As_{Total} Analysis of Variance

Crop x Treatment X Layer						(Crop + Treatment) x Layer					
Source of variation	d.f.	s.s.	m.s.	v.r.	F pr.	Source of variation	d.f.	s.s.	m.s.	v.r.	F pr.
Plot stratum						Plot stratum					
Crop	4	5.99	1.50			Crop	4	5.99	1.50	7.35	0.003
Treatment	3	6.69	2.23			Treatment	3	6.69	2.23	10.9	<.001
Crop.Treatment	12	2.45	0.204			Residual	12	2.45	0.204	2.64	
Plot.Auger stratum	40	3.09	0.077	0.86		Plot.Auger stratum	40	3.09	0.077	0.61	
Plot.Auger.*Units* stratum						Plot.Auger.*Units* stratum					
Layer	1	32.8	32.8	365	<.001	Layer	1	32.8	32.8	261	<.001
Crop.Layer	4	2.77	0.69	7.72	<.001	Crop.Layer	4	2.774	0.693	5.51	<.001
Treatment.Layer	3	1.05	0.35	3.89	0.016	Treatment.Layer	3	1.048	0.349	2.78	0.050
Crop.Treatment.Layer	12	2.95	0.25	2.74	0.008	Residual	52	6.544	0.126		
Residual	40	3.59	0.09								
Total	119	61.4				Total	119	61.4			

Table 10.11. Old Rotation Cd_{Total} Analysis of Variance

Crop x Treatment X Layer						(Crop + Treatment) x Layer					
Source of variation	d.f.	s.s.	m.s.	v.r.	F pr.	Source of variation	d.f.	s.s.	m.s.	v.r.	F pr.
Plot stratum						Plot stratum					
Crop	4	0.033	0.008			Crop	4	0.033	0.008	2.64	0.087
Treatment	3	0.201	0.067			Treatment	3	0.201	0.067	21.7	<.001
Crop.Treatment	12	0.037	0.003			Residual	12	0.037	0.003	2.34	
Plot.Auger stratum	40	0.053	0.001	0.97		Plot.Auger stratum	40	0.053	0.001	0.92	
Plot.Auger.*Units* stratum						Plot.Auger.*Units* stratum					
Layer	1	0.157	0.157	115	<.001	Layer	1	0.157	0.157	110	<.001
Crop.Layer	4	0.011	0.003	1.97	0.118	Crop.Layer	4	0.011	0.003	1.87	0.129
Treatment.Layer	3	0.019	0.006	4.64	0.007	Treatment.Layer	3	0.019	0.006	4.41	0.008
Crop.Treatment.Layer	12	0.020	0.002	1.23	0.299						
Residual	40	0.055	0.001			Residual	52	0.075	0.001		
Total	119	0.586				Total	119	0.586			

Table 10.12. Old Rotation U_{Total} Analysis of Variance

Crop x Treatment X Layer						(Crop + Treatment) x Layer					
Source of variation	d.f.	s.s.	m.s.	v.r.	F pr.	Source of variation	d.f.	s.s.	m.s.	v.r.	F pr.
Plot stratum						Plot stratum					
Crop	4	0.207	0.052			Crop	4	0.207	0.052	5.94	0.007
Treatment	3	0.813	0.271			Treatment	3	0.813	0.271	31.09	<.001
Crop.Treatment	12	0.105	0.009			Residual	12	0.105	0.009	0.78	
Plot.Auger stratum	40	0.448	0.011	0.86		Plot.Auger stratum	40	0.448	0.011	0.89	
Plot.Auger.*Units* stratum						Plot.Auger.*Units* stratum					
Layer	1	0.546	0.546	42	<.001	Layer	1	0.546	0.546	43.11	<.001
Crop.Layer	4	0.139	0.035	2.66	0.046	Crop.Layer	4	0.139	0.035	2.74	0.038
Treatment.Layer	3	0.030	0.010	0.77	0.519	Treatment.Layer	3	0.030	0.010	0.79	0.506
Crop.Treatment.Layer	12	0.138	0.012	0.88	0.569						
Residual	40	0.520	0.013			Residual	52	0.658	0.013		
Total	119	2.945				Total	119	2.945			

Table 10.13. Old Rotation Ca_{Total} Analysis of Variance

Crop x Treatment X Layer						(Crop + Treatment) x Layer					
Source of variation	d.f.	s.s.	m.s.	v.r.	F pr.	Source of variation	d.f.	s.s.	m.s.	v.r.	F pr.
Plot stratum						Plot stratum					
Crop	4	4289365	1072341			Crop	4	4289365	1072341	4.55	0.018
Treatment	3	6547260	2182420			Treatment	3	6547260	2182420	9.27	0.002
Crop.Treatment	12	2825257	235438			Residual	12	2825257	235438	1.05	
Plot.Auger stratum	40	8982141	224554	1.21		Plot.Auger stratum	40	8982141	224554	1.20	
Plot.Auger.*Units* stratum						Plot.Auger.*Units* stratum					
Layer	1	7347	7347	0.04	0.843	Layer	1	7347	7347	0.04	0.844
Crop.Layer	4	623786	155946	0.84	0.509	Crop.Layer	4	623786	155946	0.83	0.509
Treatment.Layer	3	2816774	938925	5.05	0.005	Treatment.Layer	3	2816774	938925	5.03	0.004
Crop.Treatment.Layer	12	2272966	189414	1.02	0.451						
Residual	40	7441897	186047			Residual	52	9714863	186824		
Total	119	35806793				Total	119	35806793			

Table 10.14. Old Rotation P_{Olsen} Analysis of Variance

Crop x Treatment X Layer						(Crop + Treatment) x Layer					
Source of variation	d.f.	s.s.	m.s.	v.r.	F pr.	Source of variation	d.f.	s.s.	m.s.	v.r.	F pr.
Plot stratum						Plot stratum					
Crop	4	324	81.0			Crop	4	324	81.0	3.26	0.05
Treatment	3	6026	2009			Treatment	3	6026	2009	80.8	<.001
Crop.Treatment	12	298	24.9			Residual	12	298	24.9	2.68	
Plot.Auger stratum	40	370	9.26	1.5		Plot.Auger stratum	40	370	9.26	0.96	
Plot.Auger.*Units* stratum						Plot.Auger.*Units* stratum					
Layer	1	1894	1894	306	<.001	Layer	1	1894	1894	196	<.001
Crop.Layer	4	212	53.1	8.57	<.001	Crop.Layer	4	212	53.1	5.51	<.001
Treatment.Layer	3	796	265	42.9	<.001	Treatment.Layer	3	796	265	27.5	<.001
Crop.Treatment.Layer	12	254	21.1	3.41	0.002						
Residual	40	248	6.20			Residual	52	501	9.64		
Total	119	10422				Total	119	10422			

Table 10.15. Old Rotation $P_{MMorgan}$ Analysis of Variance

Crop x Treatment X Layer						(Crop + Treatment) x Layer					
Source of variation	d.f.	s.s.	m.s.	v.r.	F pr.	Source of variation	d.f.	s.s.	m.s.	v.r.	F pr.
Plot stratum						Plot stratum					
Crop	4	119	29.7			Crop	4	119	29.7	9.99	<.001
Treatment	3	160	53.5			Treatment	3	160	53.5	18.0	<.001
Crop.Treatment	12	35.7	2.97			Residual	12	35.7	2.97	10.7	
Plot.Auger stratum	40	11.1	0.278	1.41		Plot.Auger stratum	40	11.1	0.278	0.69	
Plot.Auger.*Units* stratum						Plot.Auger.*Units* stratum					
Layer	1	80.5	80.5	410	<.001	Layer	1	80.5	80.5	200	<.001
Crop.Layer	4	34.4	8.61	43.8	<.001	Crop.Layer	4	34.4	8.61	21.4	<.001
Treatment.Layer	3	12.6	4.21	21.4	<.001	Treatment.Layer	3	12.6	4.21	10.4	<.001
Crop.Treatment.Layer	12	13.1	1.09	5.55	<.001						
Residual	40	7.9	0.197			Residual	52	21.0	0.403		
Total	119	475				Total	119	475			

Table 10.16. pH Rotation P_{Total} Analysis of Variance

Crop x Treatment X Layer						(Crop + Treatment) x Layer					
Source of variation	d.f.	s.s.	m.s.	v.r.	F pr.	Source of variation	d.f.	s.s.	m.s.	v.r.	F pr.
Plot stratum						Plot stratum					
Crop	4	1.1E+06	2.8E+05			Crop	4	1.1E+06	2.8E+05	9.23	<.001
Treatment	6	2.2E+05	3.6E+04			Treatment	6	2.2E+05	3.6E+04	1.2	0.339
Crop.Treatment	24	7.2E+05	3.0E+04			Residual	24	7.2E+05	3.0E+04	1.73	
Plot.Auger stratum	70	1.2E+06	1.7E+04	1.18		Plot.Auger stratum	70	1.2E+06	1.7E+04	0.91	
Plot.Auger.*Units* stratum						Plot.Auger.*Units* stratum					
Layer	1	2.1E+07	2.1E+07	1409	<.001	Layer	1	2.1E+07	2.1E+07	1086	<.001
Crop.Layer	4	7.2E+05	1.8E+05	12.2	<.001	Crop.Layer	4	7.2E+05	1.8E+05	9.4	<.001
Treatment.Layer	6	8.0E+05	1.3E+05	9.13	<.001	Treatment.Layer	6	8.0E+05	1.3E+05	7.03	<.001
Crop.Treatment.Layer	24	7.6E+05	3.2E+04	2.17	0.007	Residual	94	1.8E+06	1.9E+04		
Residual	70	1.0E+06	1.5E+04								
Total	209	2.7E+07				Total	209	2.7E+07			

Table 10.17. pH Rotation As_{Total} Analysis of Variance

Crop x Treatment X Layer						(Crop + Treatment) x Layer					
Source of variation	d.f.	s.s.	m.s.	v.r.	F pr.	Source of variation	d.f.	s.s.	m.s.	v.r.	F pr.
Plot stratum						Plot stratum					
Crop	4	64.06	16.01			Crop	4	64.06	16.01	22.02	<.001
Treatment	6	24.64	4.11			Treatment	6	24.64	4.11	5.7	<.001
Crop.Treatment	24	17.46	0.727			Residual	24	17.46	0.727	0.77	
Plot.Auger stratum	70	65.72	0.939	1.27		Plot.Auger stratum	70	65.72	0.939	1	
Plot.Auger.*Units* stratum						Plot.Auger.*Units* stratum					
Layer	1	194	194	262	<.001	Layer	1	194	194	206	<.001
Crop.Layer	4	1.951	0.488	0.66	0.623	Crop.Layer	4	1.951	0.488	0.52	0.722
Treatment.Layer	6	14.197	2.366	3.19	0.008	Treatment.Layer	6	14.197	2.366	2.52	0.027
Crop.Treatment.Layer	24	36.532	1.522	2.05	0.011	Residual	94	88.437	0.941		
Residual	70	51.905	0.742								
Total	209	470.7				Total	209	470.7			

Table 10.18. pH Rotation Cd_{Total} Analysis of Variance

Crop x Treatment X Layer						(Crop + Treatment) x Layer					
Source of variation	d.f.	s.s.	m.s.	v.r.	F pr.	Source of variation	d.f.	s.s.	m.s.	v.r.	F pr.
Plot stratum						Plot stratum					
Crop	4	0.06	0.02			Crop	4	0.06	0.02	5.83	0.002
Treatment	6	0.06	0.01			Treatment	6	0.06	0.01	3.9	0.008
Crop.Treatment	24	0.07	0.003			Residual	24	0.07	0.003	1.56	
Plot.Auger stratum	70	0.12	0.002	1		Plot.Auger stratum	70	0.12	0.002	0.88	
Plot.Auger.*Units* stratum						Plot.Auger.*Units* stratum					
Layer	1	0.4	0.4	206	<.001	Layer	1	0.4	0.4	181	<.001
Crop.Layer	4	0.009	0.002	1.22	0.310	Crop.Layer	4	0.009	0.002	1.08	0.373
Treatment.Layer	6	0.027	0.004	2.54	0.028	Treatment.Layer	6	0.027	0.004	2.24	0.046
Crop.Treatment.Layer	24	0.064	0.003	1.53	0.086	Residual	94	0.187	0.002		
Residual	70	0.122	0.002								
Total	209	0.9				Total	209	0.9			

Table 10.19. pH Rotation U_{Total} Analysis of Variance

Crop x Treatment X Layer						(Crop + Treatment) x Layer					
Source of variation	d.f.	s.s.	m.s.	v.r.	F pr.	Source of variation	d.f.	s.s.	m.s.	v.r.	F pr.
Plot stratum						Plot stratum					
Crop	4	0.08	0.02			Crop	4	0.08	0.02	1.6	0.207
Treatment	6	0.08	0.01			Treatment	6	0.08	0.01	1.2	0.365
Crop.Treatment	24	0.29	0.012			Residual	24	0.29	0.012	1.06	
Plot.Auger stratum	70	0.81	0.012	0.96		Plot.Auger stratum	70	0.81	0.012	1	
Plot.Auger.*Units* stratum						Plot.Auger.*Units* stratum					
Layer	1	3.0	3.0	248	<.001	Layer	1	3.0	3.0	257	<.001
Crop.Layer	4	0.046	0.012	0.96	0.433	Crop.Layer	4	0.046	0.012	1	0.412
Treatment.Layer	6	0.566	0.094	7.9	<.001	Treatment.Layer	6	0.566	0.094	8.18	<.001
Crop.Treatment.Layer	24	0.247	0.010	0.86	0.647	Residual	94	1.084	0.012		
Residual	70	0.836	0.012								
Total	209	5.9				Total	209	5.9			

Table 10.20. pH Rotation Ca_{Total} Analysis of Variance

Crop x Treatment X Layer						(Crop + Treatment) x Layer					
Source of variation	d.f.	s.s.	m.s.	v.r.	F pr.	Source of variation	d.f.	s.s.	m.s.	v.r.	F pr.
Plot stratum						Plot stratum					
Crop	4	6.8E+06	1.7E+06			Crop	4	6.8E+06	1.7E+06	3.82	0.015
Treatment	6	6.9E+08	1.2E+08			Treatment	6	6.9E+08	1.2E+08	259	<.001
Crop.Treatment	24	1.1E+07	4.4E+05			Residual	24	1.1E+07	4.4E+05	1.89	
Plot.Auger stratum	70	1.6E+07	2.3E+05	1.07		Plot.Auger stratum	70	1.6E+07	2.3E+05	1.04	
Plot.Auger.*Units* stratum						Plot.Auger.*Units* stratum					
Layer	1	7.0E+06	7.0E+06	31.6	<.001	Layer	1	7.0E+06	7.0E+06	30.9	<.001
Crop.Layer	4	6.5E+06	1.6E+06	7.39	<.001	Crop.Layer	4	6.5E+06	1.6E+06	7.23	<.001
Treatment.Layer	6	2.0E+07	3.3E+06	14.9	<.001	Treatment.Layer	6	2.0E+07	3.3E+06	14.6	<.001
Crop.Treatment.Layer	24	5.7E+06	2.4E+05	1.08	0.386	Residual	94	2.1E+07	2.3E+05		
Residual	70	1.5E+07	2.2E+05								
Total	209	7.8E+08				Total	209	7.8E+08			

Table 10.21. pH Rotation P_{Olsen} Analysis of Variance

Crop x Treatment X Layer						(Crop + Treatment) x Layer					
Source of variation	d.f.	s.s.	m.s.	v.r.	F pr.	Source of variation	d.f.	s.s.	m.s.	v.r.	F pr.
Plot stratum						Plot stratum					
Crop	4	3541	885			Crop	4	3541	885	8.74	<.001
Treatment	6	18512	3085			Treatment	6	18512	3085	30.5	<.001
Crop.Treatment	24	2431	101			Residual	24	2431	101	4.05	
Plot.Auger stratum	70	1751	25.0	1.25		Plot.Auger stratum	70	1751	25.0	0.53	
Plot.Auger.*Units* stratum						Plot.Auger.*Units* stratum					
Layer	1	32639	32639	1626	<.001	Layer	1	32639	32639	697	<.001
Crop.Layer	4	875	219	10.9	<.001	Crop.Layer	4	875	219	4.67	0.002
Treatment.Layer	6	8189	1365	68.0	<.001	Treatment.Layer	6	8189	1365	29.1	<.001
Crop.Treatment.Layer	24	2998	125	6.23	<.001	Residual	94	4403	46.8		
Residual	70	1405	20.1								
Total	209	72340				Total	209	72340			

Table 10.22. pH Rotation $P_{MMorgan}$ Analysis of Variance

Crop x Treatment X Layer						(Crop + Treatment) x Layer					
Source of variation	d.f.	s.s.	m.s.	v.r.	F pr.	Source of variation	d.f.	s.s.	m.s.	v.r.	F pr.
Plot stratum						Plot stratum					
Crop	4	275	68.8			Crop	4	275	68.8	6.51	0.001
Treatment	6	851	142			Treatment	6	851	142	13.4	<.001
Crop.Treatment	24	254	10.6			Residual	24	254	10.6	4.8	
Plot.Auger stratum	70	154	2.20	1.13		Plot.Auger stratum	70	154	2.20	0.76	
Plot.Auger.*Units* stratum						Plot.Auger.*Units* stratum					
Layer	1	858	858	440	<.001	Layer	1	858	858	297	<.001
Crop.Layer	4	266	66.5	34.09	<.001	Crop.Layer	4	266	66.5	23	<.001
Treatment.Layer	6	307	51.2	26.26	<.001	Treatment.Layer	6	307	51.2	17.7	<.001
Crop.Treatment.Layer	24	135	5.63	2.89	<.001	Residual	94	272	2.89		
Residual	70	136	1.95								
Total	209	3237				Total	209	3237			

Appendix 4 – pH Rotation Polynomial Regression Models and Predictions

Table 10.23. P_{Total} topsoil and subsoil Polynomial Regression Models

Topsoil						Subsoil					
2nd order						*2nd order*					
Change	d.f.	s.s.	m.s.	v.r.	F pr.	Change	d.f.	s.s.	m.s.	v.r.	F pr.
+ POL(pH; 2)	2	113689	56844.5	79.78	<.001	+ POL(pH; 2)	2	200625	100312	7.59	0.004
+ Crop	4	541908.6	135477.1	190.14	<.001	+ Crop	4	39084	9771	0.74	0.576
+ POL(pH; 2).Crop	8	22499.6	2812.5	3.95	0.006	+ POL(pH; 2).Crop	8	243966	30496	2.31	0.062
Residual	20	14250	712.5			Residual	20	264186	13209		
Total	34	692347.2	20363.2			Total	34	747861	21996		

Table 10.24. As_{Total} topsoil and subsoil Polynomial Regression Models

Topsoil						Subsoil					
2nd order						*2nd order*					
Change	d.f.	s.s.	m.s.	v.r.	F pr.	Change	d.f.	s.s.	m.s.	v.r.	F pr.
+ POL(pH; 2)	2	0.89808	0.44904	11.98	<.001	+ POL(pH; 2)	2	8.8588	4.4294	13.91	<.001
+ Crop	4	7.79306	1.94827	51.99	<.001	+ Crop	4	9.4677	2.3669	7.44	<.001
+ POL(pH; 2).Crop	8	0.25566	0.03196	0.85	0.570	+ POL(pH; 2).Crop	8	5.097	0.6371	2	0.100
Residual	20	0.74947	0.03747			Residual	20	6.367	0.3183		
Total	34	9.69627	0.28518			Total	34	29.7905	0.8762		

Table 10.25. Cd_{Total} topsoil and subsoil Polynomial Regression Models

Topsoil						Subsoil					
2nd order						*3rd order*					
Change	d.f.	s.s.	m.s.	v.r.	F pr.	Change	d.f.	s.s.	m.s.	v.r.	F pr.
+ POL(pH; 2)	2	0.01240	0.00620	19.95	<.001	+ POL(pH; 3)	3	0.00951	0.00317	5.64	0.009
+ Crop	4	0.01038	0.00260	8.35	<.001	+ Crop	4	0.00563	0.00141	2.5	0.087
+ POL(pH; 2).Crop	8	0.00200	0.00025	0.8	0.607	+ POL(pH; 3).Crop	12	0.01072	0.00089	1.59	0.197
Residual	20	0.00622	0.00031			Residual	15	0.00843	0.00056		
Total	34	0.03100	0.00091			Total	34	0.03428	0.00101		

Table 10.26. U_{Total} topsoil and subsoil Polynomial Regression Models

Topsoil						Subsoil					
2nd order						*3rd order*					
Change	d.f.	s.s.	m.s.	v.r.	F pr.	Change	d.f.	s.s.	m.s.	v.r.	F pr.
+ POL(pH; 2)	2	0.07290	0.03645	51.65	<.001	+ POL(pH; 3)	3	0.13354	0.04451	16.83	<.001
+ Crop	4	0.01064	0.00266	3.77	0.019	+ Crop	4	0.02542	0.00636	2.4	0.096
+ POL(pH; 2).Crop	8	0.03515	0.00439	6.23	<.001	+ POL(pH; 3).Crop	12	0.10611	0.00884	3.34	0.015
Residual	20	0.01412	0.00071			Residual	15	0.03968	0.00265		
Total	34	0.13281	0.00391			Total	34	0.30474	0.00896		

Table 10.27. Ca_{Total} topsoil and subsoil Polynomial Regression Models

Topsoil						Subsoil					
2nd order						*2nd order*					
Change	d.f.	s.s.	m.s.	v.r.	F pr.	Change	d.f.	s.s.	m.s.	v.r.	F pr.
+ POL(pH; 2)	2	1.5.E+08	7.6.E+07	508	<.001	+ POL(pH; 2)	2	8.1.E+07	4.1.E+07	549	<.001
+ Crop	4	5.1.E+06	1.3.E+06	8.54	<.001	+ Crop	4	1.6.E+06	3.9.E+05	5.3	0.004
+ POL(pH; 2).Crop	8	5.0.E+05	6.3.E+04	0.42	0.897	+ POL(pH; 2).Crop	8	1.5.E+06	1.8.E+05	2.48	0.048
Residual	20	3.0.E+06	1.5.E+05			Residual	20	1.5.E+06	7.4.E+04		
Total	34	1.6.E+08	4.7.E+06			Total	34	8.6.E+07	2.5.E+06		

Table 10.28. P_{Olsen} topsoil and subsoil Polynomial Regression Models

Topsoil						Subsoil					
3rd order						*3rd order*					
Change	d.f.	s.s.	m.s.	v.r.	F pr.	Change	d.f.	s.s.	m.s.	v.r.	F pr.
+ POL(pH; 3)	3	8062.258	2687.419	286.76	<.001	+ POL(pH; 3)	3	839.08	279.69	7.26	0.003
+ Crop	4	545.611	136.403	14.55	<.001	+ Crop	4	946.04	236.51	6.14	0.004
+ POL(pH; 3).Crop	12	433.922	36.16	3.86	0.008	+ POL(pH; 3).Crop	12	636.99	53.08	1.38	0.275
Residual	15	140.574	9.372			Residual	15	577.51	38.5		
Total	34	9182.366	270.07			Total	34	2999.62	88.22		

Table 10.29. $P_{MMorgan}$ topsoil and subsoil Polynomial Regression Models

Topsoil						Subsoil					
3rd order						*3rd order*					
Change	d.f.	s.s.	m.s.	v.r.	F pr.	Change	d.f.	s.s.	m.s.	v.r.	F pr.
+ POL(pH; 3)	3	362.461	120.82	109.65	<.001	+ POL(pH; 3)	3	31.555	10.52	6.04	0.007
+ Crop	4	43.111	10.78	9.78	<.001	+ Crop	4	131.402	32.85	18.85	<.001
+ POL(pH; 3).Crop	12	48.317	4.03	3.65	0.010	+ POL(pH; 3).Crop	12	36.417	3.04	1.74	0.154
Residual	15	16.528	1.10			Residual	15	26.143	1.74		
Total	34	470.418	13.836			Total	34	225.518	6.633		

Table 10.30. P_{HCl} topsoil and subsoil Polynomial Regression Models

Topsoil						Subsoil					
3rd order						*3rd order*					
Source	d.f.	s.s.	m.s.	v.r.	F pr.	Source	d.f.	s.s.	m.s.	v.r.	F pr.
Regression	3	16434.8	5478.3	17.66	0.021	Regression	3	40878	13626	9.11	0.051
Residual	3	930.8	310.3			Residual	3	4490	1497		
Total	6	17365.6	2894.3			Total	6	45368	7561		
Percentage variance accounted for 89.3						*Percentage variance accounted for 80.2*					
Standard error of observations is estimated to be 17.6.						*Standard error of observations is estimated to be 38.7.*					

Table 10.31. Prediction of Field concentration (Model output) using the fitted polynomial models using 'pH value Input'. If the 'True Value' of the Field was within the range of x3 SEM of the Model Output then the conclusion was Not Different; out-with this range is 'Significantly (Sig.) Different' to the fitted model.

Element	Layer	Model	pH Value Input	True Value	Model Output	SEM	True within x3 ±SEM range?	Conclusion
P_{Total}	Topsoil	2nd order	5.663	1378	1785	33.24	Yes	Not Different
	Subsoil	2nd order	5.975	1101	1197	34.28	No	Sig. Different
As_{Total}	Topsoil	2nd order	5.663	6.69	7.698	0.0478	Yes	Not Different
	Subsoil	2nd order	5.975	5.94	5.771	0.212	No	Sig. Different
Cd_{Total}	Topsoil	2nd order	5.663	0.227	0.246	0.006	Yes	Not Different
	Subsoil	3rd order	5.975	0.169	0.181	0.008	No	Sig. Different
U_{Total}	Topsoil	2nd order	5.663	1.89	2.364	0.0107	No	Sig. Different
	Subsoil	3rd order	5.975	1.90	2.151	0.02104	No	Sig. Different
Ca_{Total}	Topsoil	2nd order	5.663	7876	8161	128.5	Yes	Not Different
	Subsoil	3rd order	5.975	8240	8311	171.9	Yes	Not Different
P_{Olsen}	Topsoil	3rd order	5.663	25.3	59.36	1.918	Yes	Not Different
	Subsoil	3rd order	5.975	18.5	32.75	2.364	Yes	Not Different
$P_{MMorgan}$	Topsoil	3rd order	5.663	4.67	10.29	0.4806	No	Sig. Different
	Subsoil	3rd order	5.975	3.95	7.975	0.7083	No	Sig. Different
P_{HCl}	Topsoil	3rd order	5.940	692	914.3	20.36	No	Sig. Different
	Subsoil	3rd order	6.180	691	745.4	45.02	Yes	Not Different